GENETICS AND EPIGENETICS OF RNA METHYLATION SYSTEM IN HUMAN CANCERS

EDITED BY: Shicheng Guo, Shenying Fang, Dingyuan Luo, Xiang Shu, Zhifu Sun and Xiangqian Zheng

PUBLISHED IN: Frontiers in Oncology and Frontiers in Genetics

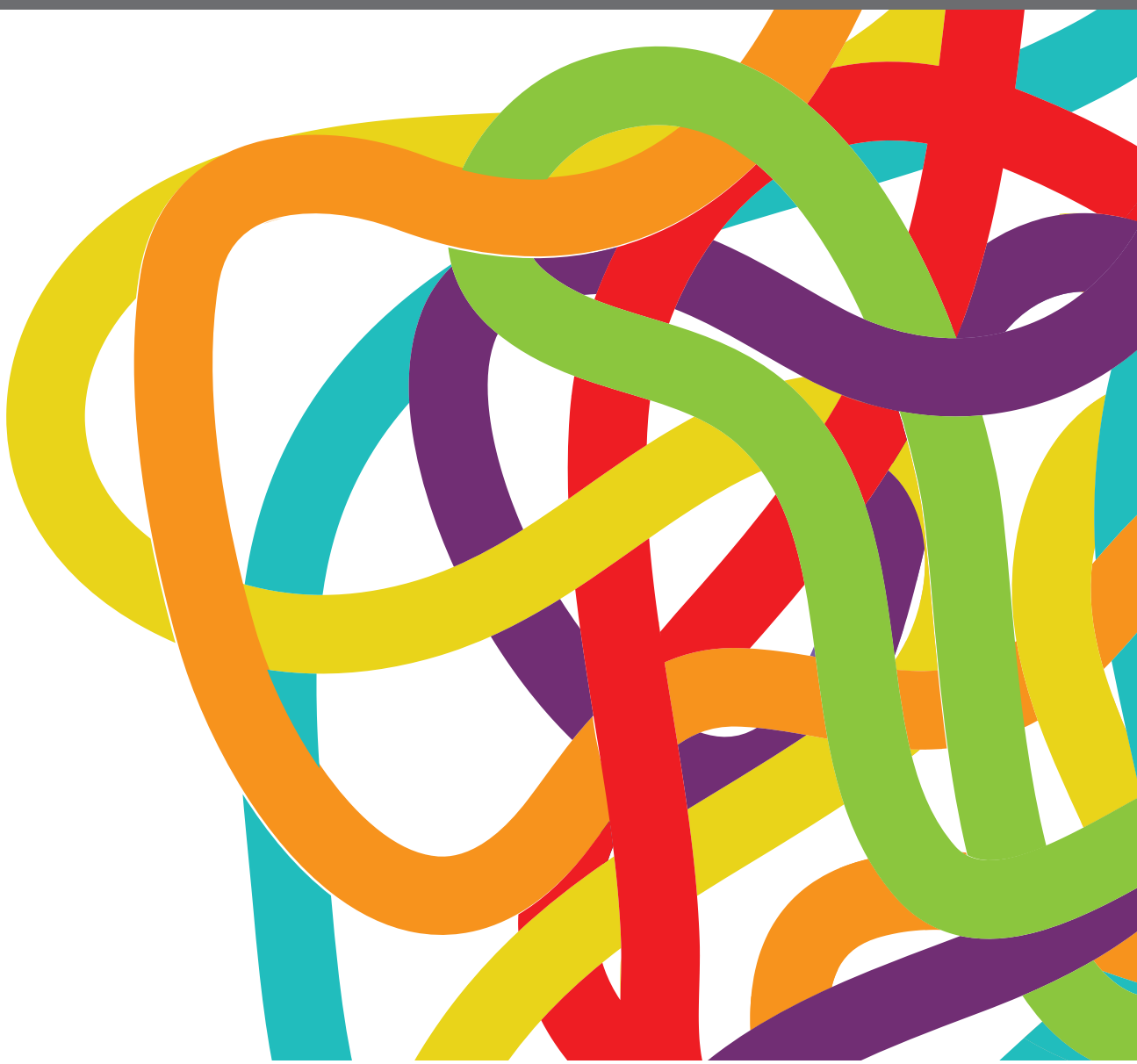

frontiers Research Topics

frontiers

ISSN 1664-8714
ISBN 978-2-88971-447-6
DOI 10.3389/978-2-88971-447-6

About Frontiers

Frontiers is more than just an open-access publisher of scholarly articles: it is a pioneering approach to the world of academia, radically improving the way scholarly research is managed. The grand vision of Frontiers is a world where all people have an equal opportunity to seek, share and generate knowledge. Frontiers provides immediate and permanent online open access to all its publications, but this alone is not enough to realize our grand goals.

Frontiers Journal Series

The Frontiers Journal Series is a multi-tier and interdisciplinary set of open-access, online journals, promising a paradigm shift from the current review, selection and dissemination processes in academic publishing. All Frontiers journals are driven by researchers for researchers; therefore, they constitute a service to the scholarly community. At the same time, the Frontiers Journal Series operates on a revolutionary invention, the tiered publishing system, initially addressing specific communities of scholars, and gradually climbing up to broader public understanding, thus serving the interests of the lay society, too.

Dedication to Quality

Each Frontiers article is a landmark of the highest quality, thanks to genuinely collaborative interactions between authors and review editors, who include some of the world's best academicians. Research must be certified by peers before entering a stream of knowledge that may eventually reach the public - and shape society; therefore, Frontiers only applies the most rigorous and unbiased reviews.
Frontiers revolutionizes research publishing by freely delivering the most outstanding research, evaluated with no bias from both the academic and social point of view. By applying the most advanced information technologies, Frontiers is catapulting scholarly publishing into a new generation.

What are Frontiers Research Topics?

Frontiers Research Topics are very popular trademarks of the Frontiers Journals Series: they are collections of at least ten articles, all centered on a particular subject. With their unique mix of varied contributions from Original Research to Review Articles, Frontiers Research Topics unify the most influential researchers, the latest key findings and historical advances in a hot research area! Find out more on how to host your own Frontiers Research Topic or contribute to one as an author by contacting the Frontiers Editorial Office: frontiersin.org/about/contact

GENETICS AND EPIGENETICS OF RNA METHYLATION SYSTEM IN HUMAN CANCERS

Topic Editors:
Shicheng Guo, University of Wisconsin-Madison, United States
Shenying Fang, University of Texas MD Anderson Cancer Center, United States
Dingyuan Luo, Department of Thyroid Surgery, Sun Yat-sen Memorial Hospital, China
Xiang Shu, Vanderbilt University Medical Center, United States
Zhifu Sun, Mayo Clinic, United States
Xiangqian Zheng, Tianjin Medical University Cancer Institute and Hospital, China

Citation: Guo, S., Fang, S., Luo, D., Shu, X., Sun, Z., Zheng, X., eds. (2022). Genetics and Epigenetics of RNA Methylation System in Human Cancers.
Lausanne: Frontiers Media SA. doi: 10.3389/978-2-88971-447-6

Table of Contents

frontiers in Oncology

ORIGINAL RESEARCH
published: 14 July 2020
doi: 10.3389/fonc.2020.01126

Reduced Expression of *METTL3* Promotes Metastasis of Triple-Negative Breast Cancer by m6A Methylation-Mediated *COL3A1* Up-Regulation

Yu Shi[1,2,3†], *Chunlei Zheng*[1,2,3†], *Yue Jin*[1,2,3], *Bowen Bao*[1,2,3], *Duo Wang*[1,2,3], *Kezuo Hou*[1,2,3], *Jing Feng*[1,2,3], *Shiying Tang*[1,2,3], *Xiujuan Qu*[1,2,3], *Yunpeng Liu*[1,2,3], *Xiaofang Che*[1,2,3*] and *Yuee Teng*[1,2,3*]

[1] Department of Medical Oncology, The First Hospital of China Medical University, Shenyang, China, [2] Key Laboratory of Anticancer Drugs and Biotherapy of Liaoning Province, The First Hospital of China Medical University, Shenyang, China, [3] Liaoning Province Clinical Research Center for Cancer, China Medical University, Shenyang, China

The abnormal m6A modification caused by m6A modulators is a common feature of various tumors; however, little is known about which m6A modulator plays the most important role in triple-negative breast cancer (TNBC). In this study, when analyzing the influence of m6A modulators (*METTL3*, *METTL14*, *WTAP*, *FTO*, and *ALKBH5*) on the prognosis of breast cancer, especially in TNBC using several on-line databases, methyltransferase-like 3 (*METTL3*) was found to have low expression in breast cancer, and was closely associated with short-distance-metastasis-free survival in TNBC. Further investigation showed that knockdown of *METTL3* could enhance the ability of migration, invasion, and adhesion by decreasing m6A level in TNBC cell lines. Collagen type III alpha 1 chain (*COL3A1*) was identified and verified as a target gene of *METTL3*. *METTL3* could down-regulate the expression of *COL3A1* by increasing its m6A methylation, ultimately inhibiting the metastasis of TNBC cells. Finally, with immunohistochemistry staining in breast cancer tissues, it was proved that *METTL3* expression was negatively correlated with *COL3A1* in TNBC, but not in non-TNBC. This study demonstrated the potential mechanism of m6A modification in metastasis and provided potential targets for treatment in TNBC.

Keywords: *METTL3*, m6A, triple-negative breast cancer, metastasis, *COL3A1*

OPEN ACCESS

Edited by:
Xiangqian Zheng,
Tianjin Medical University Cancer Institute and Hospital, China

Reviewed by:
Tong Wei-Min,
Chinese Academy of Medical Sciences and Peking Union Medical College, China
Guo-Jun Zhang,
Xiamen University, China

****Correspondence:***
Xiaofang Che
xfche@cmu.edu.cn
Yuee Teng
yeteng@cmu.edu.cn

[†]These authors have contributed equally to this work

Specialty section:
This article was submitted to Cancer Genetics, a section of the journal Frontiers in Oncology

Received: *26 March 2020*
Accepted: *04 June 2020*
Published: *14 July 2020*

Citation:
Shi Y, Zheng C, Jin Y, Bao B, Wang D, Hou K, Feng J, Tang S, Qu X, Liu Y, Che X and Teng Y (2020) Reduced Expression of METTL3 Promotes Metastasis of Triple-Negative Breast Cancer by m6A Methylation-Mediated COL3A1 Up-Regulation. Front. Oncol. 10:1126. doi: 10.3389/fonc.2020.01126

INTRODUCTION

Breast cancer, the most common cancer in women, poses a serious threat to the health of women (1). Despite the improvement of treatment strategies, the prognosis of breast cancer, especially triple-negative breast cancer (TNBC), remains poor due to metastasis. In recent years, epigenetic regulation, such as DNA methylation, histone acetylation, and non-coding RNAs, has been reported to play a critical role in the development of breast cancer including TNBC. Especially, as a new emerging epigenetic modification, RNA methylation has attracted much attention due to its non-negligible function in cancer development; however, current studies of

RNA methylation-related cancer development are just the tip of the iceberg in this cognate area. It is necessary to clarify the mechanisms underlying RNA methylation-involved metastasis in TNBC.

As the most prevalent RNA methylation modification, N6-methyladenosine (m6A) infers that the nitrogen-6 position of adenosine base in RNA is methylated by the regulation of m6A methyltransferases and m6A demethylases. Methyltransferase, including methyltransferase-like 3 (*METTL3*), methyltransferase-like 14 (*METTL14*), and Wilms tumor 1-associated protein (*WTAP*) can form into complexes and mediate the cellular deposition of m6A on mammalian mRNAs, whereas demethylases including *FTO* and its homolog AlkB family member 5 (*ALKBH5*) can selectively reverse m6A to adenosine (2–5). RNA m6A methylation is known to be involved in various biological processes, such as stem cell differentiation and pluripotency, circadian periods, embryogenesis, and DNA damage response (2, 3). Cumulative studies have proved that the change of RNA m6A modification caused by the aberrant expression of m6A modulators can also influence the development of cancers. The methyltransferase *METTL14* can inhibit tumor metastasis in HCC by positively regulating the m6A level of *DGCR8* and promoting the binding of *DGCR8* to pri-miRNAs (6); similarly, the demethylase *FTO* can promote cell proliferation via down-regulating the m6A level of *USP7* in advanced non-small cell lung cancer, indicating the repression role of m6A in cancer development (7), however, other studies obtained contradictory results wherein *METTL3* could promote the proliferation of prostate cancer cell via enhancing the m6A level of *GLI15* (8); similarly, *ALKBH5* was found to be able to inhibit pancreatic cancer metastasis by down-regulating *KCNK15-AS1*, suggesting that m6A modification of RNA plays an oncogenic role in cancer (9). Therefore, it seems that an m6A modulator might play both promotional, and inhibitory roles in different types of cancers by regulating different specific target genes. To date, the role of RNA m6A methylation in the development of breast cancer remains unclear. The only studies of breast cancer have shown that *METTL3*-mediated enhancement of m6A level could promote the proliferation of breast cancer cells (10), while the high level of m6A caused by *FTO* knockdown could inhibit the proliferation and metastasis of breast cancer (11). Therefore, it seems that, although the changes in m6A level are consistent, the effects of different modulators on breast cancer differ because the specific target genes are different. The underlying role and epigenetic regulation of m6A modulators in breast cancer, especially in TNBC, still needs to be investigated.

Abbreviations: *ALKBH5*, AlkB family member 5; *COL3A1*, collagen type III alpha 1 chain; DMFS, the distance-metastasis-free survival; ECM, cell-extracellular matrix; FC, fold change; GO, Gene Ontology; GTEx, the Genotype Tissue Expression; IHC, Immunohistochemistry; KD, knockdown; *METTL3*, methyltransferase-like 3; *METTL14*, methyltransferase-like 14; *MYH11*, myosin heavy chain 11; NC, negative control; OE, overexpression; PVDF, polyvinylidene difluoride; qRT-PCR, quantitative real-time; TCGA, the Cancer Genome Atlas; TNBC, triple-negative breast cancer; TMA, The tissue microarray; *WTAP*, Wilms tumor 1-associated protein.

In this study, we analyzed the prognostic role of m6A modulators in TNBC using several online databases and found that the low expression of *METTL3* was associated with the poor prognosis of TNBC. Further molecular mechanism investigation indicated that silence of *METTL3* could up-regulate the expression of Collagen type III alpha 1 chain (*COL3A1*) by increasing m6A-levels, ultimately promoting metastasis of TNBC cells. This study revealed the important role of m6A modification mediated by *METTL3* in TNBC and suggests that *METTL3* might act as a novel therapeutic target in TNBC metastasis.

MATERIALS AND METHODS

Data Sources: On-Line Databases

KM plotter (http://kmplot.com/analysis/) is a website used for on-line analysis, which is capable of assessing 54k genes on the survival of 21 cancer types, including breast cancer. The association between the distance-metastasis-free survival (DMFS) and the expression of m6A modulators (*METTL3*, *METTL14*, *WTAP*, *FTO*, and *ALKBH5*), *COL3A1* was analyzed using KM plotter, respectively. GEPIA (http://gepia.cancer-pku.cn) is an on-line database including the RNA sequencing expression data of 9,736 tumors and 8,587 normal tissue samples from the Cancer Genome Atlas (TCGA) and the Genotype Tissue Expression (GTEx). The transcriptional levels of five m6A modulators above in breast cancer tissues and normal breast tissues were obtained from GEPIA. The mRNA expression data of 91 patients with TNBC were downloaded from TCGA (https://www.cancer.gov/) for analysis of the correlation between the m6A modulators and target genes.

Cell Culture

The human breast cancer cell lines, MDA-MB-231, and MDA-MB-468, were acquired from the Cell Bank of the Chinese Academy of Sciences (Shanghai, China). All the cells were incubated in L15 culture medium (Gibco, NY, USA) supplemented with 10% FBS at 37°C under 5% CO_2 and saturated humidity.

Antibodies

The primary antibodies for western blot, anti-*METTL3* (#96391) were sourced from Cell Signaling Technology (MA, USA), anti-*COL3A1* (sc-514601) was sourced from Santa Cruz (CA, USA), anti-α-tubulin (ab7291) was sourced from Abcam (CA, USA). HRP-conjugated goat anti-mouse/rabbit secondary antibodies (ZDR-5306/5307) were sourced from ZSBIO (Beijing, China). The antibodies for immunohistochemistry, anti-*METTL3* (ab195352) were sourced from Abcam (CA, USA), and anti-*COL3A1* (sc-166316) was sourced from Santa Cruz (CA, USA).

Trans-well Migration and Invasion Assays

For the migration assay, $\sim 2 \times 10^4$ cells were suspended in 200 μl serum-free L15 medium and added into the upper chamber of a trans-well plate (Corning, USA) with an 8-μm pore size polycarbonate filter, and 500 μl L15 medium with 10% FBS were dispensed into the lower chambers, and incubated for 24 h.

Then the upper chambers were fixed in 75% ethanol, and the cells on the upper surface of the filter were removed manually with a cotton swab. Then the migrating cells were stained with Wright–Giemsa stain.

The invasion assay was similar to the migration assay except that 3% matrigel was dispensed into the upper chamber before seeding 3×10^4 cells into the culture system. Migrating and invading cells were observed under an optical microscope. The cells from three fields were counted with Image J (https://imagej.nih.gov/ij/download.html).

Cell Adhesion Assay

The cells were seeded at 3×10^4 per well into 96-well-plates pre-coated with 10% matrigel overnight. After 30 min-incubation at 37 °C, the non-adherent cells were removed by PBS washing. Then the cells were fixed with 75% ethanol for 10 min and stained with Wright–Giemsa stain. Images were acquired by microscope and the quantities of cells were counted with Image J.

RNA Isolation and Quantitative Real-Time PCR Assay

RNA was isolated with TRIzol reagent (Invitrogen, CA, USA) and identified using a NanoDrop spectrophotometer (Thermo Scientific, Rockford, IL, USA). The Reverse Transcription Kit (Promega, WI, USA) was used for mRNA reverse transcription. Quantitative real-time PCR (qRT-PCR) assay was then performed using the SYBR Green kit (Promega, WI, USA) on the ABI7500 instrument (Thermofisher, IL, USA). All the reactions were conducted for triplicates. 18S RNA was used as the internal control. Primers of *METTL3*, *COL3A1*, *MYH11*, and 18S were used as follows:

METTL3 forward: 5′-TTGTCTCCAACCTTCCGTAGT-3′
METTL3 reverse: 5′-CCAGATCAGAGAGGTGGTGTAG-3′
COL3A1 forward: 5′-CCCACTATTATTTTGGCACAACAG-3′
COL3A1 reverse: 5′-AACGGATCCTGAGTCACAGACA-3′
MYH11 forward: 5′-AGTTCGAAAGGGATCTCCA-3′
MYH11 reverse: 5′-CATACTCGTGAAGCTGTCTC-3′
18S forward: 5′CCCGGGGAGGTAGTGACGAAAAAT-3′
18S reverse: 5′-CGCCCGCCCGCTCCCAAGAT-3′.

Methylated RNA Immunoprecipitation-qRT-PCR

The methylated RNA immunoprecipitation-qRT-PCR (MeRIP-qRT-PCR) assay was conducted according to the standard protocol of Magna MeRIP m6A Kit (Millipore, MA, USA, 17-10499) with a slight modification. The total RNA (300 μg) was isolated with TRIzol reagent and fragmented. Except for 3 μg of the total RNA as input, the remaining RNA was used for m6A-immunoprecipitation with m6A antibody. The Protein A/G Magnetic Beads were prepared by 30 min-incubation with m6A-specific antibody in immunoprecipitation buffer at room temperature, then incubated with the MeRIP reaction mixture and RNA for 2h at 4°C. Finally, the MeRIPed-RNA was cleaned up and concentrated with RNeasy MinElute Clean-up Kit (Qiagen, Hilden, Germany). The enriched RNA level of *COL3A1* was analyzed by qRT-PCR. The primers were as same as the primers used in real-time PCR assay.

Transfection

For the knockdown of *METTL3* and *COL3A1*, the cells were seeded at 10^5 cells/well in a 6-well-plate and the siRNAs targeted to *METTL3* and *COL3A1* (GENEWIZ, Beijing, China) at a final concentration of 50 nM were transfected using JetPRIME Transfection Reagent (Polyplus, Illkirch, France) according to the manufacturer's instructions. Negative control (NC) siRNA was used as a control. For the overexpression of *METLL3*, the cells were seeded at 10^5 per 6-well-plate and transfected with plasmids pcDNA3.1-FLAG and pcDNA3.1-*METTL3* (Obio, Shanghai, China) at a final concentration of 1 μg/ml using JetPRIME Transfection Reagent. The siRNA sequences of NC, *METTL3*, and *COL3A1* were used as follows:

si-*METTL3*-1126 (KD1): 5′-CCUGCAAGUAUGUUCACUATT-3′
si-*METTL3*-1400 (KD2): 5′-GCUCAACAUACCCGUACUATT-3′
si-*METTL3*-1604 (KD3): 5′-GGUUGGUGUCAAAGGAAAUTT-3′
si-*COL3A1*-1 (KD1): 5′-GGAUGCAAAUUGGAUGCUAtt-3′
si-*COL3A1*-2 (KD2): 5′-CCCUCCUAAUGGUCAAGGAtt-3′
si-NC: 5′-UUCUCCGAACGUGUCACGUtt-3′.

Western Blot

The harvested cells were lysed in a lysis buffer (50 mM Tris, pH 7.4, 150 mM NaCl, 10 mM EDTA, 50 mM NaF, 1 mM NaVanadate, 1% Triton X-100, 1 mM PMSF, and 0.5% aprotin) and the protein concentration was quantified according to the Coomassie blue G250 staining technique. Equivalent protein was electrophoresed on 8–10% SDS-PAGE gels and transferred to polyvinylidene difluoride (PVDF) membranes (Perkin-Elmer, Waltham, MA, USA). Then the membranes were blocked with 5% skimmed milk in TBST for 1 h and incubated with the primary antibodies overnight (more than 6 h). The concentration of anti-*METTL3* (#96391) was 1:1,000, the concentration of anti-*COL3A1* (sc-514601) was 1:200, the concentration of anti-α-tubulin (ab7291) was 1:1,000. After being immunoblotted with HRP-conjugated goat anti-mouse/rabbit antibody (1:2,000) for 40 min, the signal strength of revealed protein bands could be detected with enhanced chemiluminescence reagent (SuperSignal Western Pico Chemiluminescent Substrate; Pierce, Rockford, IL, USA) and visualized with the Electrophoresis Gel Imaging Analysis System (DNR Bio-Imaging Systems, Jerusalem, Israel). The blots were scanned and the abundance assessed quantitatively using ImageJ.

ELISA

Cells at a density of 1×10^5/well in a 6-well-plate were incubated for 72 h, and Collagen α1(III) levels in cell culture medium and cell lysate were measured, respectively, using a commercially available Collagen α1(III) ELISA kit at 450 nm by a microplate spectrophotometer (CSB-E13446h, Cusabio, Wuhan,

China). The experiment process was carried out according to the instructions of the kit. The samples were added into wells and incubated 2 h in 37°C. After removing the liquid of each well, Biotin-antibody was added into each well. After incubated 1 h in 37°C, HRP-avidin and TMB Substrate were used for color rendering. The standard curve was constructed by the mean absorbance of each standard and the concentration. The concentration of each sample was determined according to standard curve. To acquire the total amount of Collagen α1(III) in each sample, the concentration was multiplied by the total volume. Then the amount of Collagen α1(III) in each sample was normalized to the amount of Collagen α1(III) in 10^7 cells. All samples and standards were detected in duplicate.

Immunohistochemistry

The tissue microarray (TMA) sections (HBreD140Su06) and the relevant clinical data were obtained from Shanghai Outdo Biotechnology Company. This study was approved by the Ethics Committee of Shanghai Outdo Biotechnology Company (YB M-05-02), and all patients have given their informed consent. The TMA sections were deparaffinized and rehydrated with an ethanol gradient. Then antigen retrieval was performed with citrate buffer (MXB, Fuzhou, China, MVS-0066) and the TMA sections were blocked with endogenous peroxidases in UltraSensitive™ SP (Mouse/Rabbit) IHC Kit (MXB, Fuzhou, China, KIT-9730-A&B). The concentration of anti-*METTL3* (ab195352) was 1:500, the concentration of anti-*COL3A1* (sc-166316) was 1:50. After overnight incubation with primary antibody, the TMA sections were incubated with biotinylated secondary antibody for 10 min in UltraSensitive™ SP (Mouse/Rabbit) IHC Kit (MXB, Fuzhou, China, KIT-9730-C&D) and developed with DAB Kit (MXB, China, DAB-0031). Finally, the TMA sections were counterstained with hematoxylin (Solarbio, Beijing, China), and dehydrated with an ethanol gradient and mounted with neutral balsam (Solarbio, Beijing, China). *METTL3* expression was evaluated by two independent reviewers by calculating the average positively stained tumor cells at 400× magnification. The positive signal of *COL3A1* was quantified as integrate optical density (IOD) value using ImageJ software.

Statistical Analysis

Statistical analyses were carried out using SPSS (version 16.0) and R (V.3.2.5). Limma package analysis was conducted to explore the correlations between *METTL3* and other genes. One-way ANOVA and Student's *t*-test were used to determine statistical significance. Statistical significance was identified as *P*-values of <0.05.

RESULTS

Low Expression of *METTL3* Was Associated With Poor Prognosis in TNBC

To investigate which m6A modulator plays an important role in breast cancer, especially in TNBC, the mRNA expressions of m6A methyltransferases (*METTL3*, *METTL14*, and *WTAP*) and demethylases (*FTO* and *ALKBH5*) were first compared between breast cancer tissues and normal breast tissues using the RNA sequencing expression data in GEPIA (http://gepia.cancer-pku.cn) on-line database. The result showed that the expression of *METTL3* ($T = 4.8$, $N = 5.4$) and *FTO* ($T = 4.9$, $N = 5.3$) was significantly lower, whereas that of *METTL14* ($T = 4.2$, $N = 3.8$) was higher in breast cancer tissues than that in normal tissues, but the difference in the expression of *WTAP* ($T = 5.9$, $N = 6.2$) and *ALKBH5* ($T = 5.7$, $N = 5.5$) was not very significant (**Figure 1A**). Next, the effects of *METTL3*, *METTL14*, and *FTO* on distant metastasis free survival (DMFS) of total breast cancer patients and TNBC patients were analyzed using KM-plotter on-line database, respectively. For overall patients, the analysis result indicated that no significant difference of DMFS was obtained between the patients with all three modulators in high-expression groups and low-expression groups (**Figure 1B**); however, for the TNBC patients, although no significant difference was found between the DMFS of the *METTL14* high-expression group and low-expression group, the DMFS of *METTL3* high expression group was shown to be longer than that in the *METTL3* low-expression group, whereas the DMFS of the *FTO* high-expression group was shorter than that of the *FTO* low-expression group, indicating that *METTL3* is a protective factor, but *FTO* is a risk factor for DMFS of TNBC (**Figure 1C**). As the result, the low expression of *FTO* in TNBC tissues was contradictory to its role as a risk factor (**Figures 1A,E**) and only *METTL3* was shown to play an important inhibitory role in the metastasis of TNBC (**Figures 1A,D**), indicating that *METTL3* might contribute to the metastasis of TNBC. Therefore, the role of *METTL3* in TNBC metastasis was focused on in the following investigation.

METTL3 Suppressed Metastasis of TNBC Cells by Enhancing m6A Modification

For the knockdown of *METTL3*, three siRNAs targeted to *METTL3* were transfected according to the manufacturer's instructions (**Figures 2A,B**). Two sequences, si-*METTL3*-1604 (KD2) and si-*METTL3*-1126 (KD3), were selected for subsequent experiments. To investigate whether *METTL3* could inhibit TNBC metastasis, the effect of *METTL3* on migration, invasion, and adhesion to cell-extracellular matrix (ECM) was detected by trans-well assay or adhesion assay in TNBC cell lines, MDA-MB-231, and MDA-MB-468. The results showed that *METTL3* knockdown (KD) significantly increased the ability of migration and invasion, as well as the adhesion capability to ECM in both MDA-MB-231 and MDA-MB-468 cells (**Figures 2C–E**), indicating that *METTL3* could inhibit the potential of cell mobility of TNBC cells. Then, to determine whether *METTL3*-inhibited potential of cell mobility was related to m6A modification or not, *METTL3* was transiently overexpressed in MDA-MB-231 and MDA-MB-468 cells followed by the treatment with cycloleucine, a small molecule inhibitor of m6A modification. The results of trans-well assays demonstrated that *METTL3* overexpression (OE)-suppressed migration, invasion, and adhesion were significantly recovered by cycloleucine (**Figures 3A–D**). These results strongly suggested that *METTL3* inhibited the potential of cell mobility of TNBC cells by enhancing m6A modification.

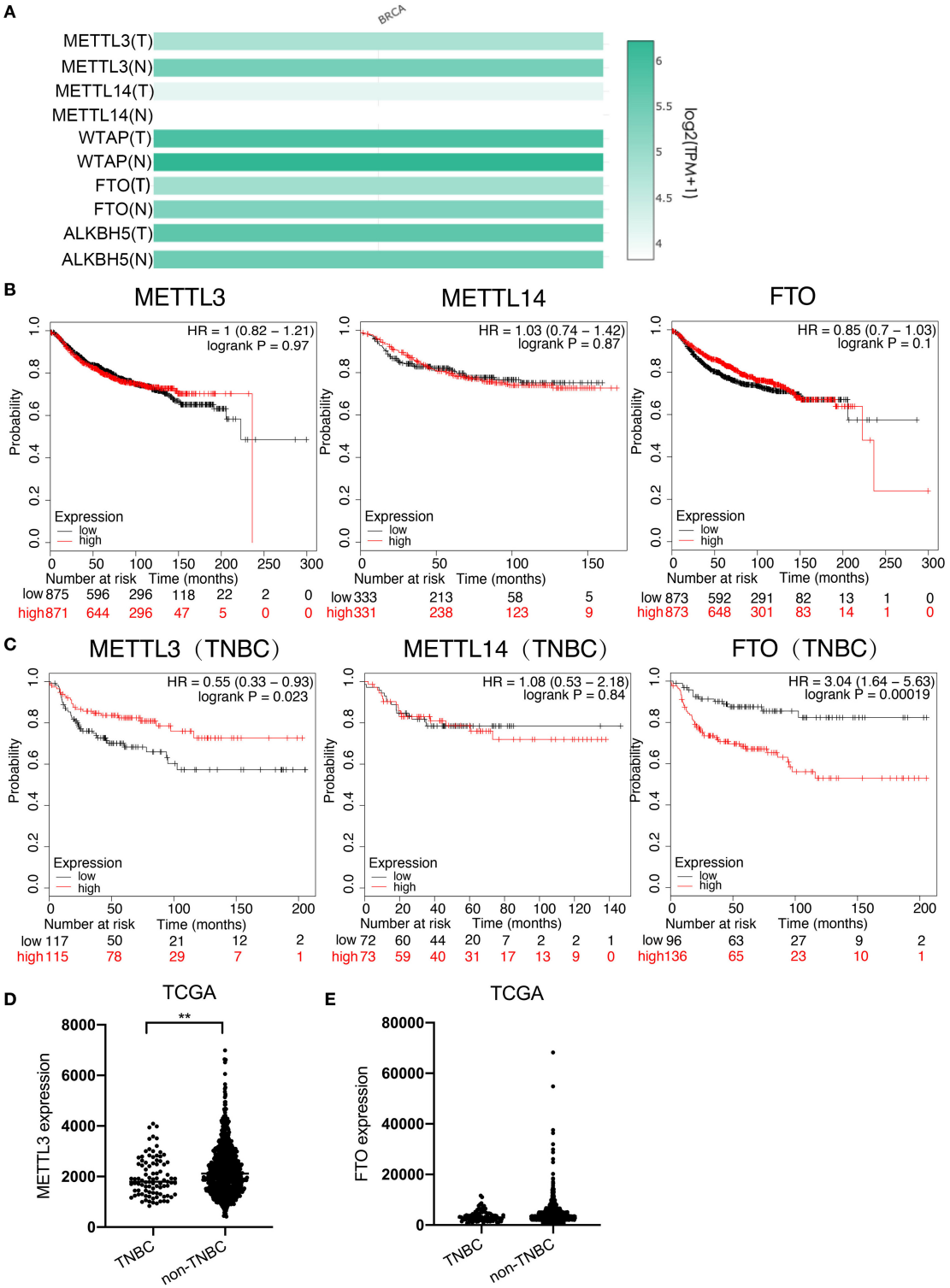

FIGURE 1 | Low expression of *METTL3* was associated with poor prognosis in TNBC. **(A)** Expression analysis of *METTL3*, *METTL14*, *WTAP*, *FTO*, and *ALKBH5* in BC tissue (1085) and normal tissue (291) using TCGA and GTEx online database. **(B)** Kaplan–Meier analysis for the DMFS of *METTL3*, *METTL14*, and *FTO* in overall BC patients using KM-plotter online database. **(C)** Kaplan–Meier analysis for the DMFS of *METTL3*, *METTL14*, and *FTO* in TNBC patients using KM-plotter online database. **(D)** *METTL3* expression analysis in TNBC patients ($n = 91$) and non-TNBC patients ($n = 1,005$) using TCGA. **(E)** *FTO* expression analysis in TNBC patients ($n = 1,005$) and non-TNBC patients ($n = 584$) using TCGA. $^{**}P < 0.01$.

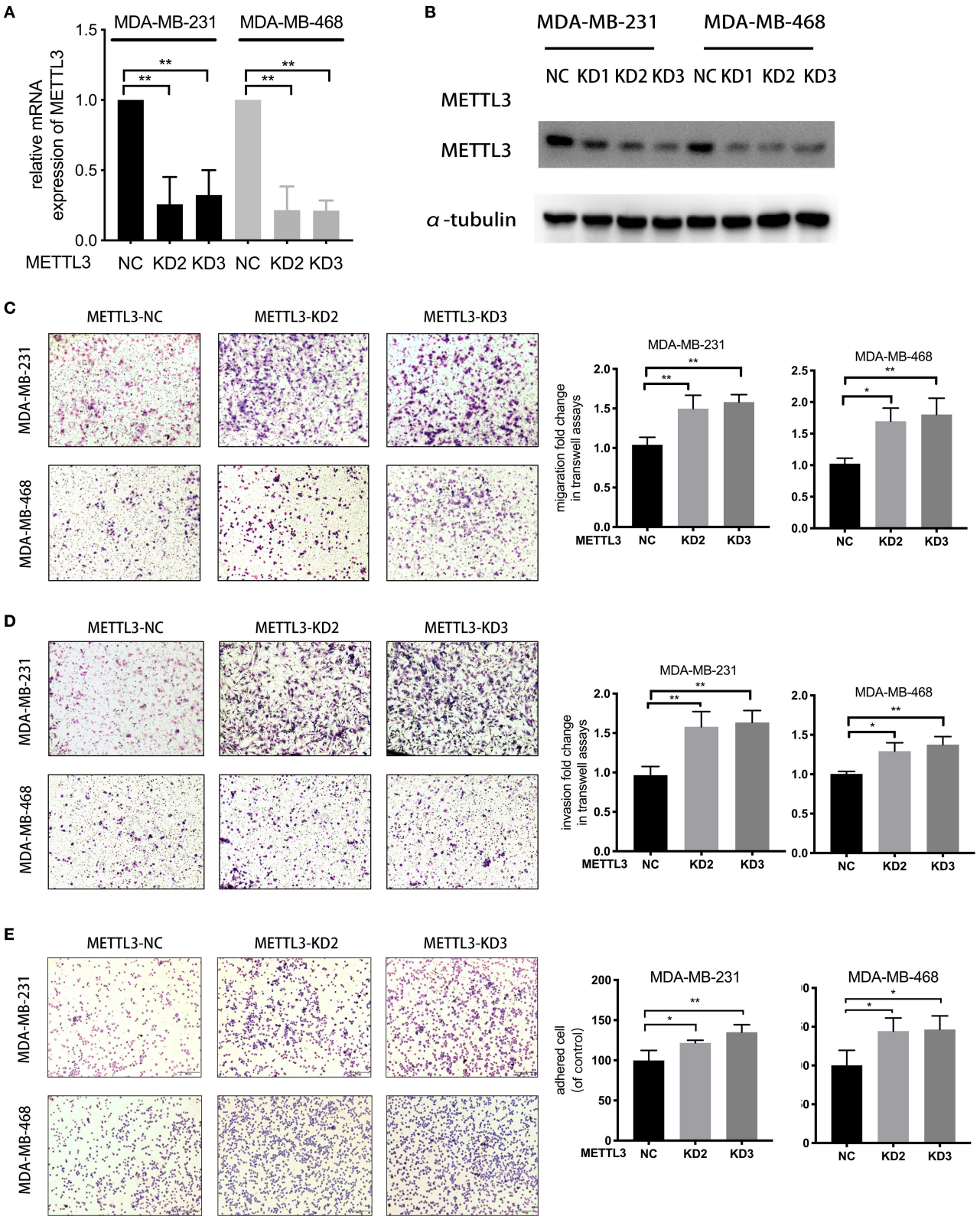

FIGURE 2 | *METTL3* suppressed metastatic ability in TNBC cells. **(A)** qRT-PCR was used to detect *METTL3* expression in MDA-MB-231 and MDA-MB-468 cells transfected with si-NC or si-*METTL3*. 18S was used as an internal control. **(B)** Western blot was used to detect *METTL3* expression in MDA-MB-231 and

(Continued)

FIGURE 2 | MDA-MB-468 cells transfected with si-NC or si-*METTL3*. α-tubulin was used as a loading control. **(C,D)** Transwell assay was used to detect the migration and invasion ability in MDA-MB-231 and MDA-MB-468 cells with *METTL3* transient knockdown (left panels). Relative fold change was shown as the proportion of the number of control cells transfected with si-NC (right panels). Original magnification, 100×. **(E)** Adhesion assay was used to detect the adhesion ability of MDA-MB-231 and MDA-MB-468 cells with *METTL3* transient knockdown (left panels). Relative fold change was shown as the proportion of the number of control cells transfected with si-NC (right panels). Original magnification, 100×. $^{*}P < 0.05$, $^{**}P < 0.01$. Error bars represent the mean ± SD of three independent experiments.

COL3A1 Was Identified as a Potential Target of *METTL3* in TNBC

It was known that m6A modification could down-regulate gene expression by accelerating RNA degradation (12–14). Therefore, to identify the target gene of *METTL3* involved in *METTL3*-inhibited metastasis, multi-step screening was performed as summarized in **Figure 4A**. Firstly, mRNA expression profiles of 91 TNBC patients in the TCGA dataset were downloaded, and the differentially expressed genes (DEG) were screened to identify those with $P < 0.05$ and log fold change (FC) using the "limma" package in R. The Log FC of DEG genes more than 0 was identified as representing positive related genes, whereas that <0 represented negative related genes. Among the genes for which mRNA expression was negatively related to *METTL3*, the top 100 genes according to the correlation coefficient were selected for further m6A methylation analysis using the m6Avar database (http://m6avar.renlab.org). All these genes and related information were listed in **Table S1**. As a result, 51 genes, which were verified to be able to be modified by m6A, were screened. Then, with the KEGG pathway enrichment analysis by DAVID (https://david.ncifcrf.gov), 18 genes were shown to be associated with the focal adhesion pathway, metabolism pathway, and so on, suggesting close involvement with metastasis in breast cancer. Subsequently, the association of 18 genes with the DMFS of TNBC patients was further analyzed using KM-plotter, and six alternative genes were found to have shorter DMFS at high levels in TNBC (**Table 1**). In particular, *COL3A1* and *MYH11* aroused our attention, because, according to the Gene Ontology (GO) analysis in DAVID, it was shown that *COL3A1* was involved in the biological process of skeletal system development and cell-matrix adhesion, and *MYH11* was involved in the biological process of elastic fiber assembly, which were similar to the findings of previous studies that they could promote metastasis in breast cancer. Therefore, the two genes were chosen as target gene candidates for *METTL3*. The further verification result of qRT-PCR detection showed that *METTL3*-KD only up-regulated the mRNA expression of *COL3A1*, but not *MYH11* in MDA-MB-231 and MDA-MB-468 cells (**Figures 4B,C**). Similarly, the result of western blot assay also confirmed that *METTL3*-KD increased the protein level of *COL3A1* in TNBC cells (**Figure 4D**). All of the above data strongly suggested that *COL3A1* might be the target gene of *METTL3*.

METTL3 Down-Regulated the Expression of *COL3A1* by Increasing m6A Level

To investigate whether *COL3A1* was regulated by *METTL3*-mediated m6A methylation or not, the relative m6A enrichment level change of *COL3A1* before and after *METTL3*-KD was detected by MeRIP-qRT-PCR in MDA-MB-231 and MDA-MB-468 cells. As shown in **Figure 5A**, *METTL3*-KD significantly reduced m6A-methylated *COL3A1* mRNA expression. Furthermore, with qRT-PCR detection, it was shown that *METTL3*- OE decreased the mRNA expression of *COL3A1*, while cycloleucine partially recovered *METTL3*-OE-down-regulated *COL3A1* (**Figure 5B**). As shown in **Figure 5C**, the results of ELISA showed that the secretion level of Collagen α1(III) in supernatant decreased by *METTL3*-OE could be recovered by cycloleucine while the *METTL3*-OE decreased the intracellular level of Collagen α1(III), the cycloleucine could not recover the reduction of the intracellular level of Collagen α1(III). Considering the amount of Collagen α1(III) secreted into the supernatant is greater than the amount in the cell, the total levels of Collagen α1(III) which were decreased by *METTL3*-OE could be recovered by cycloleucine after normalizing (**Figure 5C**). These results proved that *COL3A1* was down-regulated by *METTL3*-mediated m6A modification on *COL3A1* (**Figure 5C**).

COL3A1 Promoted the Metastatic Ability of TNBC Cells

The role of *COL3A1* in TNBC metastasis was further investigated. The influence of *COL3A1* on DMFS of TNBC patients analyzed by KM-plotter is shown in **Figure 6B**, the DMFS of TNBC patients with high-expression *COL3A1* was shorter than in those with a low expression thereof. There was no significant difference in the expression level of *COL3A1* and DMFS in the overall patients (**Figure S1**). In addition, when *COL3A1* was knocked-down in MDA-MB-231 and MDA-MB-468 cells (**Figure 6A**), the migration, invasion, and adhesion to ECM were significantly suppressed (**Figures 6C–E**). These data indicated that *COL3A1* played an important role in promoting metastasis in TNBC.

Reduced *COL3A1* m6A Modification by *METTL3* Inhibition Leads to Poor Prognosis in TNBC Patients

In order to verify the effects of *METTL3* and *COL3A1* on the prognosis of breast cancer patients *in vivo*, the expression of *METTL3* and *COL3A1* was investigated by immunohistochemistry using TMA sections containing 31 TNBC patients and 109 Non-TNBC patients. The results of survival analysis showed that low *METTL3* expression was related to short overall survival (OS) (**Figure 7A**) in TNBC but not in non-TNBC (**Figure S2A**). The OS of TNBC with *COL3A1*-high expression was shorter than that with low expression (**Figure 7B**), which may not be statistically significant because of the small number of TNBC cases. In non-TNBC, *COL3A1* has the opposite trend, and patients with high expression have longer OS (**Figure S2B**). Finally, the relationship between *METTL3* and *COL3A1* in breast cancer was analyzed with

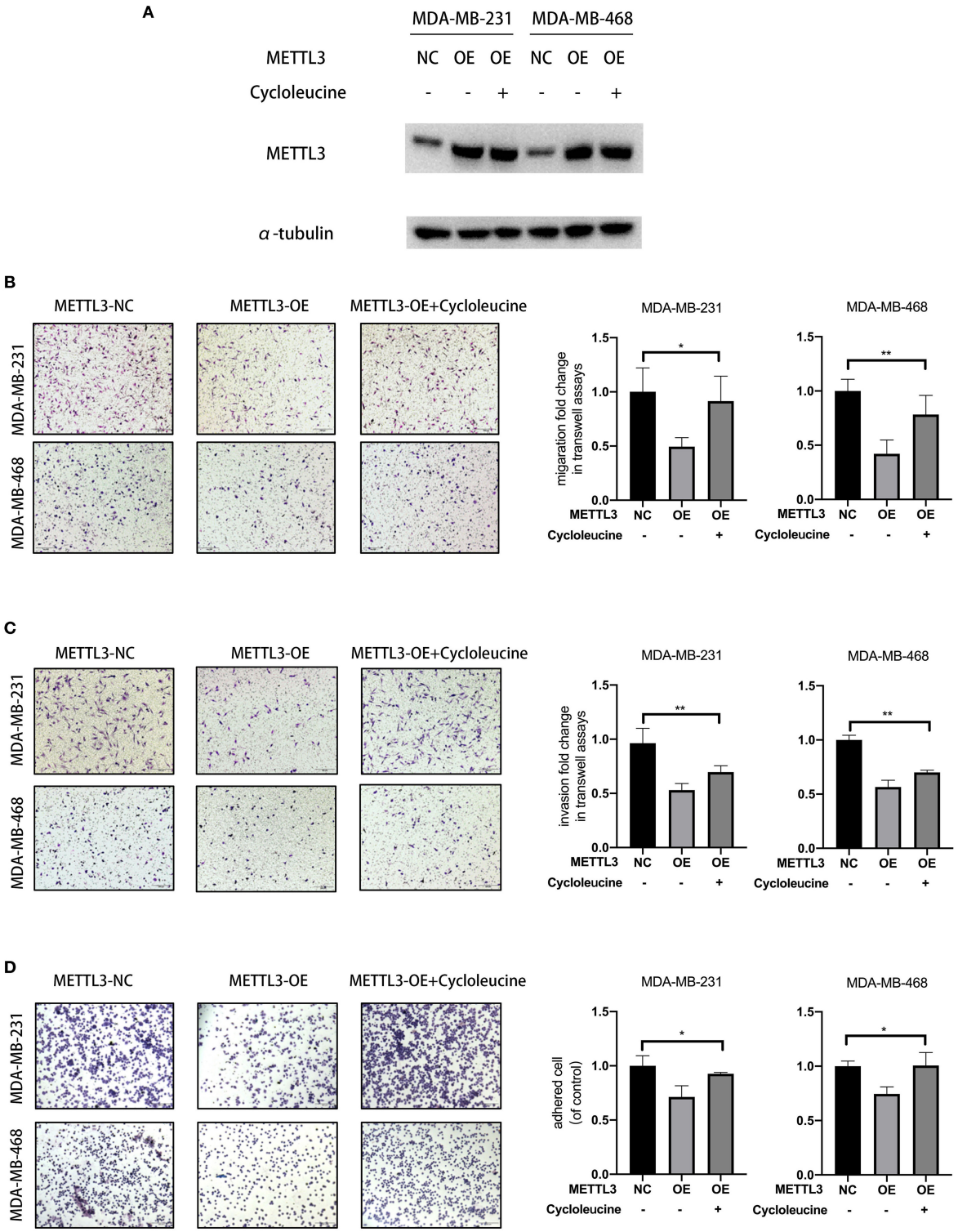

FIGURE 3 | *METTL3* overexpression-suppressed migration, invasion, and adhesion were significantly rescued by cycloleucine. **(A)** Western blot was used to detect *METTL3* expression in MDA-MB-231 and MDA-MB-468 cells in rescued assay. α-tubulin was used as a loading control. **(B,C)** Transwell assay was used to detect the migration and invasion ability in MDA-MB-231 and MDA-MB-468 cells with *METTL3* transient overexpression and *METTL3* overexpression rescued with cycloleucine (left panels). Relative fold change was shown as the proportion of the number of control cells transfected with pcDNA3.1-FLAG (right panels). Original magnification, 100×. **(D)** Adhesion assay was used to detect the adhesion ability of MDA-MB-231 and MDA-MB-468 cells with *METTL3* transient overexpression (left panels). Relative fold change was shown as the proportion of the number of control cells transfected with pcDNA3.1-FLAG (right panels). Original magnification, 100×. $^{*}P < 0.05$, $^{**}P < 0.01$. Error bars represent the mean ± SD of three independent experiments.

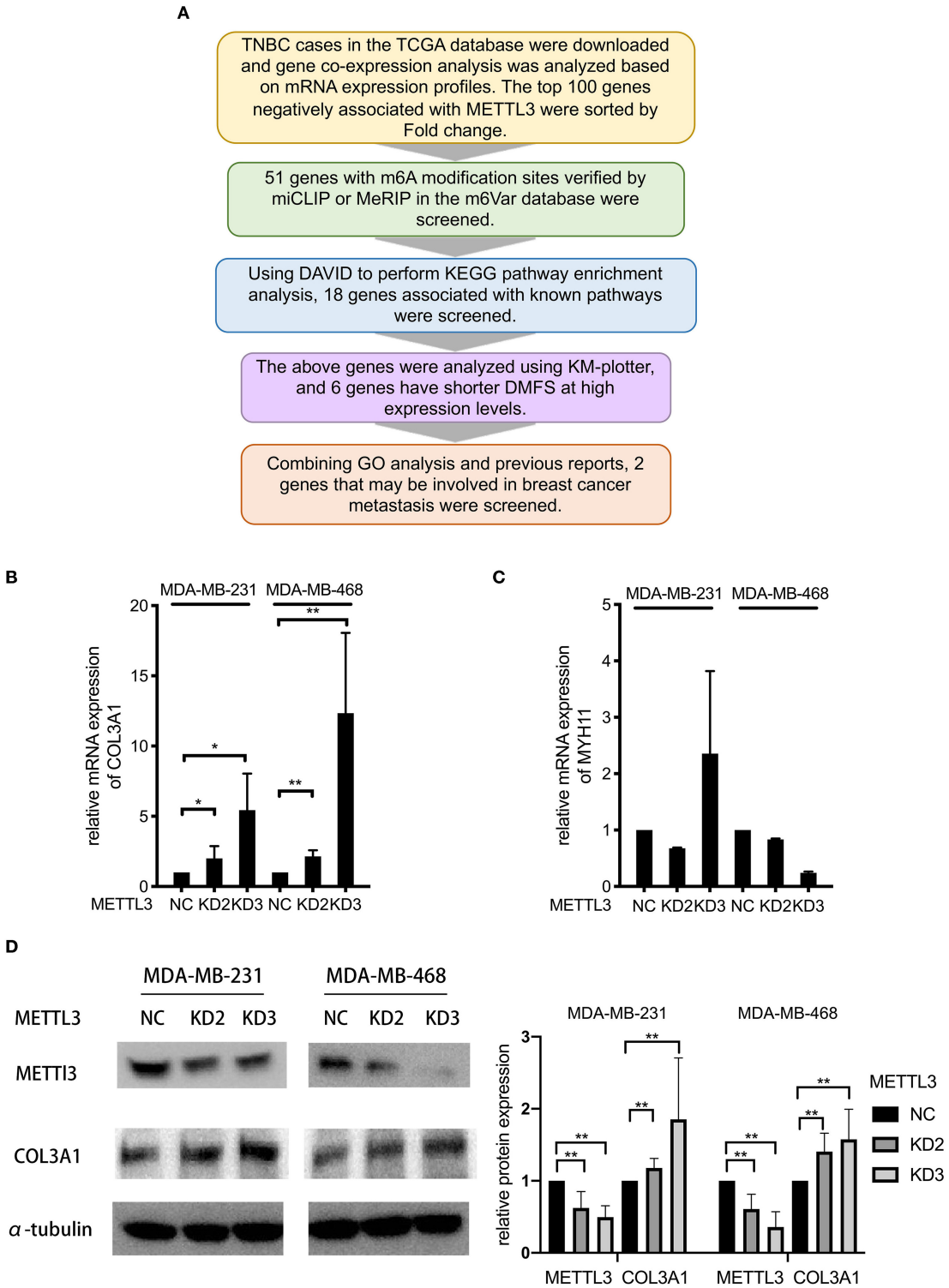

FIGURE 4 | *COL3A1* was identified as a potential target of *METTL3* in TNBC. **(A)** Flowchart for screening potential target genes. **(B,C)** qRT-PCR was used to detect *COL3A1* and *MYH11* expression in MDA-MB-231 and MDA-MB-468 cells transfected with the si-NC or the si-*METTL3*. 18S was used as an internal control. **(D)** Western blot was used to detect *COL3A1* expression in MDA-MB-231 and MDA-MB-468 cells transfected with the si-NC or the si-*METTL3*. α-tubulin was used as a loading control (left panel). The blots were scanned and the abundance assessed quantitatively using ImageJ (right panel). $^{*}P < 0.05$, $^{**}P < 0.01$. Error bars represent the mean ± SD of three independent experiments.

TABLE 1 | 18 genes which were associated with pathways involved in metastasis and relative KEGG pathway, and DMFS analysis.

	Gene name	KEGG Pathway enrichment analysis	DMFS analysis HR (*P*)
1	*FZD4*	Wnt signaling pathway, Hippo signaling pathway, signaling pathways regulating pluripotency of stem cells, melanogenesis, HTLV-I infection, pathways in cancer, proteoglycans in cancer, basal cell carcinoma	0.47 (0.034)
2	*UTS2R*	Neuroactive ligand-receptor interaction	1.42 (0.350)
3	*PTPRJ*	Adherens junction	1.66 (0.048)
4	*CPSF3*	mRNA surveillance pathway	0.50 (0.088)
5	*MTHFD2L*	One carbon pool by folate, Metabolic pathways	1.77 (0.035)
6	*MYH11*	Tight junction	2.06 (0.033)
7	*LPGAT1*	Glycerophospholipid metabolism	1.57 (0.270)
8	*LAPTM4B*	Lysosome	1.36 (0.230)
9	*IL1R1*	MAPK signaling pathway, cytokine–cytokine receptor interaction, NF-kappa B signaling pathway, osteoclast differentiation, hematopoietic cell lineage, inflammatory mediator regulation of TRP channels, amoebiasis, HTLV-I infection	1.59 (0.160)
10	*COL3A1*	PI3K-Akt signaling pathway, focal adhesion, ECM-receptor interaction, platelet activation, protein digestion and absorption, amoebiasis	1.74 (0.041)
11	*ALG10B*	N-Glycan biosynthesis, metabolic pathways	2.14 (0.033)
12	*GMPPB*	Fructose and mannose metabolism, amino sugar and nucleotide sugar metabolism, metabolic pathways	1.43 (0.190)
13	*RNASEH1*	DNA replication	1.53 (0.100)
14	*UBE4B*	Ubiquitin mediated proteolysis, protein processing in endoplasmic reticulum	2.46 (0.007)
15	*NCOA1*	Thyroid hormone signaling pathway	1.47 (0.200)
16	*SNRPE*	Spliceosome	1.45 (0.160)
17	*TGM2*	Huntington's disease	0.54 (0.043)
18	*FDFT1*	Steroid biosynthesis, metabolic pathways, biosynthesis of antibiotics	1.28 (0.340)

Pearson correlation analysis (**Figures 7C,D**). The results showed that the expression level of *COL3A1* was negatively correlated with *METTL3* expression in TNBC patients ($R = -0.564$, $P = 0.001$; **Figure 7E**); however, the expression level of *METTL3* and *COL3A1* had no significant relationship in the 109 NTNBC patients ($R = -0.132$, $P = 0.170$; **Figure 7F**). This result further confirmed that the metastasis-inhibition function of *METTL3* by negatively regulating *COL3A1* expression was TNBC specific.

DISCUSSION

In this study, by analyzing the prognostic role of m6A modulators (*METTL3*, *METTL14*, *WTAP*, *FTO*, and *ALKBH5*) in breast cancer using on-line databases, we found that only *METTL3* played an important role in TNBC metastasis. The expression of *METTL3* in breast cancer tissues was lower than that in normal tissues, and *METTL3* was a protective factor of DMFS in TNBC. Using TNBC cell lines, it was confirmed that *METTL3* could inhibit metastasis by increasing the level of m6A modification, and *COL3A1* was identified as one of the possible target genes of *METTL3*. Furthermore, reduced expression of *METTL3* was proved to be able to contributes the potential of mobility of triple-negative breast cancer cells by m6A methylation-mediated *COL3A1* up-regulation.

The role of m6A modification that is mainly regulated by methyltransferases and demethylases, is complicated and specific in various cancers. A bioinformatics analysis study involving 33 cancers showed that m6A modulators are closely related to both the activation pathway and inhibition pathway of cancer; the distribution of m6A modifications varies widely among different cancers; even for the same type of cancer, the prognostic function of m6A was not consistent within each subtype (15). Several studies also exhibit the complicated roles of m6A modulators in the development of breast cancer. It was reported that *FTO*, a key m6A demethylase, was up-regulated and significantly associated with poor prognosis in breast cancer (8); *FTO*-reduced m6A modification could promote breast cancer cell proliferation and metastasis by inhibiting BNIP3 expression (11). Similarly, *METTL14* overexpression or *ALKBH5* silence could also inhibit the growth and migration of breast cancer cell line, MDA-MB-231 (16). The opposite result was also reported such that the deficiency of *METTL3* could inhibit the proliferation of breast cancer cell line MCF-7, by m6A-level-decreasing-mediated Bcl-2 up-regulation (10). In this study, using online database, we analyzed the prognostic role of five m6A modulators in breast cancer, especially in TNBC, the subtype with the worst prognosis and the greatest potential for metastasis, and found that *METTL3* is the most critical in TNBC, that *METTL3* occurred at low expression in TNBC, and was a protective factor of DMSF. The results of the TMA section also confirm the protective effect of *METTL3* on the overall survival of TNBC patients. These results are consistent with some previous researches (16), while contradictory to the other researches focused on proliferation (10, 17). This difference might be due to the different subtypes of the breast cancer cell lines used. It should be taken into consideration that those previous study had mainly used non-TNBC cell lines.

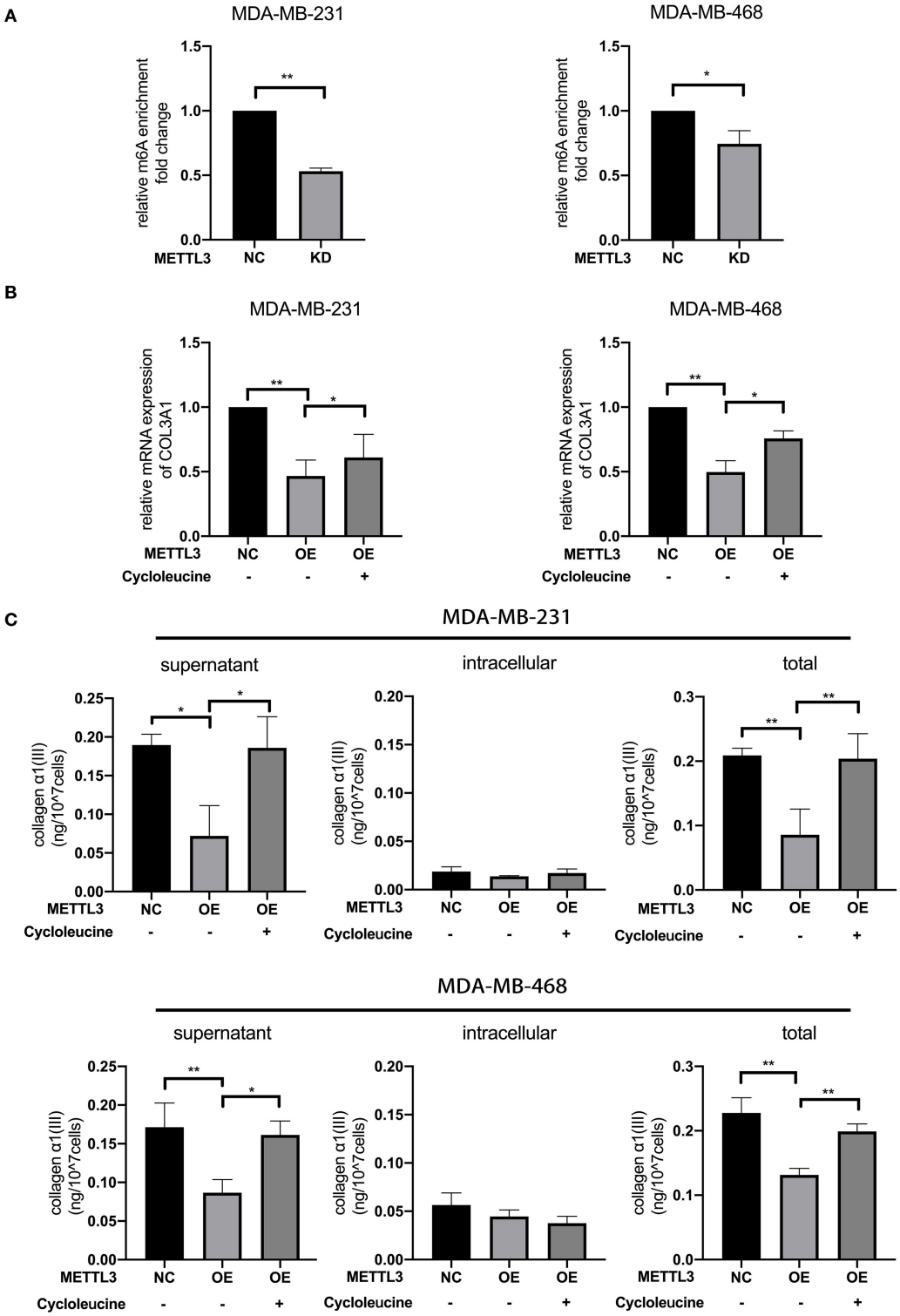

FIGURE 5 | *METTL3* down-regulated the expression of *COL3A1* by increasing m6A levels. **(A)** MeRIP-qRT-PCR was used to detect the m6A modification level of *COL3A1* in MDA-MB-231 and MDA-MB-468 cells transfected with si-NC or si-*METTL3*. The relative enrichment fold changes were shown as proportions of control cells enrichment. **(B)** qRT-PCR was used to detect *COL3A1* expression in MDA-MB-231 and MDA-MB-468 cells with *METTL3* transient overexpression or the combination of *METTL3* overexpression with cycloleucine. 18S was used as an internal control. **(C)** ELISA was used to detect the secretion level of collagen α1 (III) of the supernatant (left panels), intracellular (middle panels) and total secreted protein (right panels) in MDA-MB-231 and MDA-MB-468 cells with *METTL3* transient overexpression or the combination of *METTL3* overexpression with cycloleucine. $^{*}P < 0.05$, $^{**}P < 0.01$. Error bars represent the mean ± SD of three independent experiments.

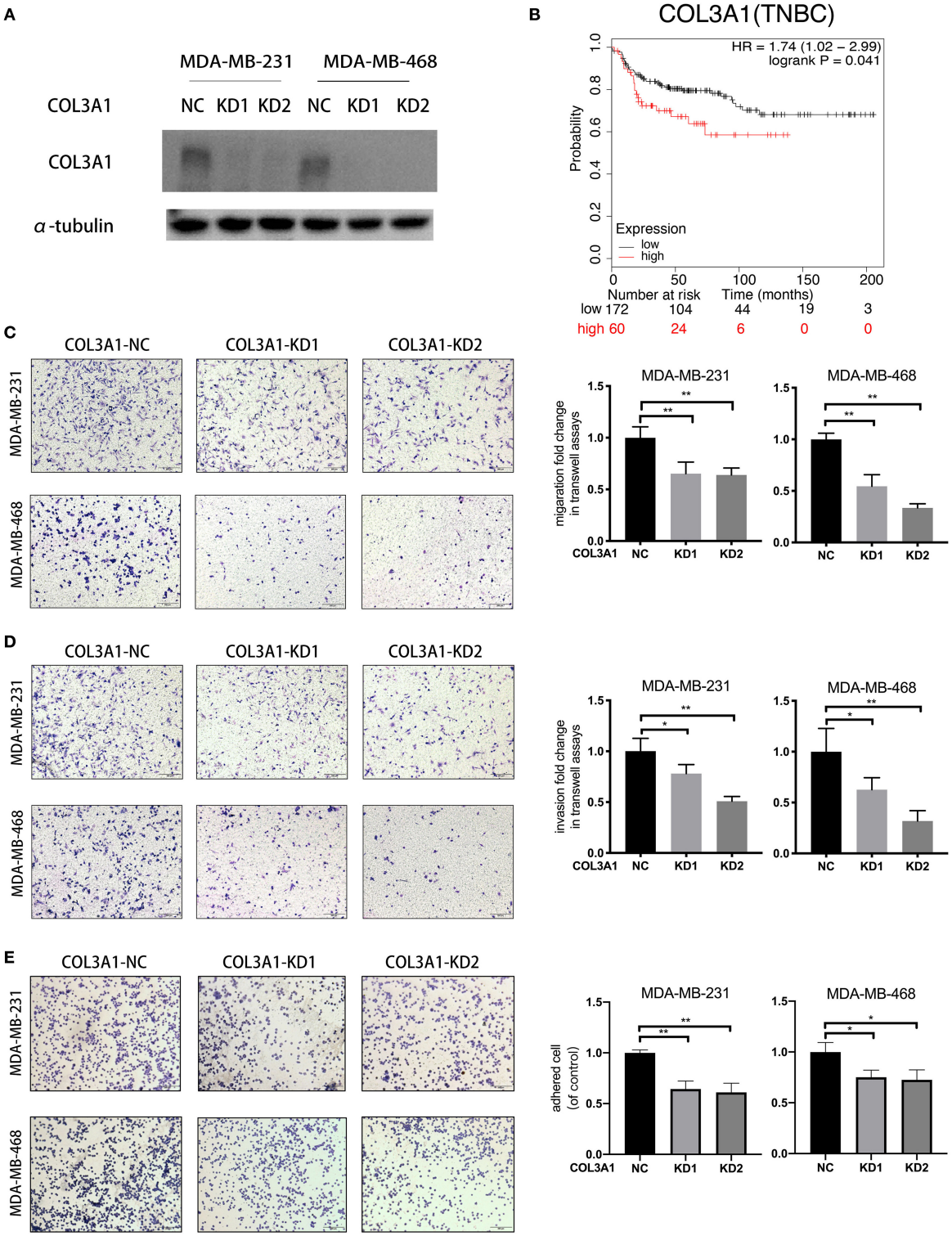

FIGURE 6 | *COL3A1* promoted the metastatic ability of TNBC cells. **(A)** Western blot was used to detect *COL3A1* expression in MDA-MB-231 and MDA-MB-468 cells transfected with the si-NC or the si-*COL3A1*. α-tubulin was used as a loading control. **(B)** Kaplan–Meier analysis for the DMFS of *COL3A1* in TNBC patients using KM-plotter online database. **(C,D)** The migration and invasion of MDA-MB-231 and MDA-MB-468 with transient *COL3A1*-KD was detected by transwell assays (left panels). Relative fold change was shown as the proportion of the number of control cells transfected with si-NC (right panels). Original magnification, 100×. **(E)** The adhesion ability of MDA-MB-231 and MDA-MB-468 after transient *COL3A1*-KD was evaluated by adhesion assay (left panels). Relative fold change was shown as the proportion of the number of control cells transfected with si-NC (right panels). Original magnification, 100×. $^{*}P < 0.05$, $^{**}P < 0.01$. Error bars represent the mean ± SD of three independent experiments.

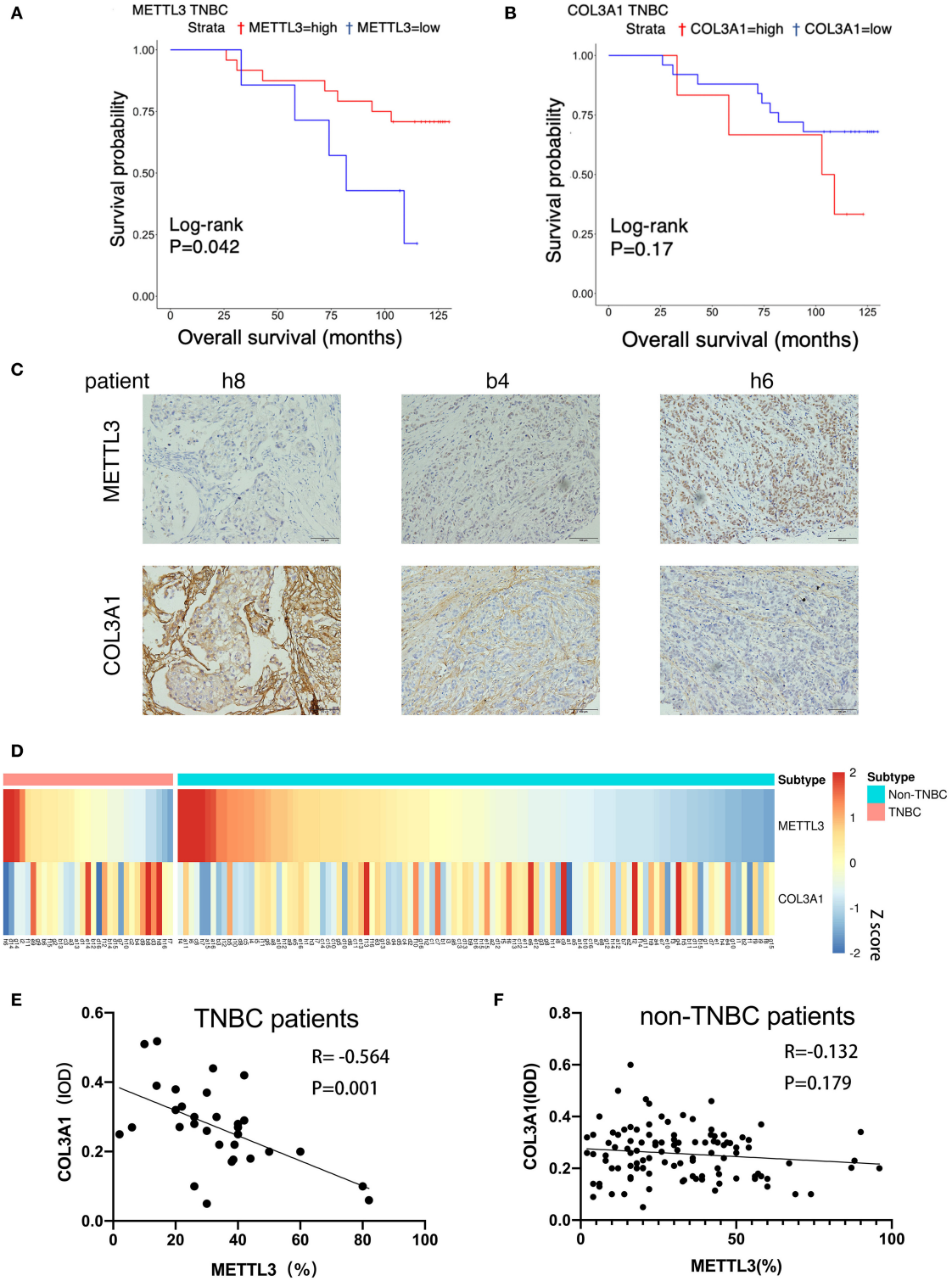

FIGURE 7 | The correlation between *METTL3* and *COL3A1* in breast cancer patients. **(A,B)** Kaplan–Meier analysis for the OS of *METTL3* and *COL3A1* in TNBC patients of the TMA sections. **(C)** The expression of *METTL3* and *COL3A1* detected by IHC in the representative samples of breast cancer. h8, low expression of *METTL3* and high expression of *COL3A1*. b4, middle expression of *METTL3* and *COL3A1*. h6, high expression of *METTL3* and low expression of *COL3A1*. Original magnification, 200×. **(D)** Heatmap of the expression level of *METTL3* and *COL3A1* protein in breast cancer patients. **(E,F)** Correlation of *METTL3* and *COL3A1* in human TNBC patients ($n = 31$) and non-TNBC patients ($n = 109$), respectively, in TMA sections.

Meanwhile, the conclusion of previous studies was based on the result of cellular level investigation and lack of clinical specimen validation. Therefore, although the trend in m6A modification levels was consistent, different regulators might eventually cause opposite effects by regulating different target genes; an m6A modulator might also execute different functions in each sub-type due to the heterogeneity of cancer. The function of *METTL3* and other m6A modulators in other sub-types of breast cancer warrants further investigation in the future.

Widely distributed in eukaryotes, RNA methylation modification occurs in thousands of genes (18). *METTL3* is known to achieve its biological effects by increasing the m6A modification level of target genes, which leads to various effects on target genes, such as faster degradation of target gene mRNA, increase in target gene translation efficiency, or accurate cell localization of target genes (2–5). Among them, the mechanism of accelerating the rate of degradation of target gene mRNA is most widely investigated. Therefore, *METTL3* might have many target genes in TNBC, and the inhibitory effect of *METTL3* on TNBC metastasis might also be achieved by affecting multiple target genes together. In this study, by expression correlation analysis and methylation search, *COL3A1* was identified as the target gene candidate of *METTL3*. Collagen type III alpha 1 chain (*COL3A1*), which encodes the pro-alpha 1 chains of type III collagen, previously was reported to be associated with malignant potential of breast cancer (19). To date, no specific mechanism has been reported for *COL3A1* regulation. In this study, we proved that knocking down *METTL3*, while reducing the methylation of m6A, also eventually up-regulated the expression level of *COL3A1*. Validation of clinical specimens indicated that this relationship appears to be only in TNBC patients. Thus, this study demonstrated that *METTL3* and *COL3A1* might only play a significant role in the TNBC subtype. Certainly, there must be multiple target genes of *METTL3* that play the same role. *COL3A1* may also have modification sites different from those provided by online databases. Further MeRIP-sequence is needed to clarify the mechanisms of *METTL3* in metastasis inhibition of TNBC in the future and the specific modified sites of *COL3A1*. Considering that the mRNA level of *COL3A1* has changed, we speculate that the change of m6A level may affect the degradation rate of *COL3A1* mRNA in TNBC cells. In this case, the position of m6A seems to be more likely to be distributed in the 3′UTR region of mRNA (2). But this speculation still needs further experimental proof.

Collagen, the most abundant component of extracellular matrix (ECM) in the tumor micro-environment, is known to be able to contribute to tumor progression (20). Collagen could promote the metastasis and proliferation of cancer by increasing the accumulation of integrin, which leads to phosphorylation of focal adhesion kinase and activation of extracellular signal-regulated kinase (21). *COL3A1*, which encodes pro-alpha1 chains of type III collagen, could form homotrimeric fibrils to play its role. Except for normal localization in connective tissues, *COL3A1* was also found to be highly expressed in various cancers including bladder cancer, glioblastoma, and gastric cancer (22–24). In breast cancer, it was reported that stromal *COL3A1* expression was significantly increased from benign breast tumors to malignant breast tumors (18). Another study has shown that when Pirfenidone, an anti-fibrotic drug, was applied to breast cancer to investigate its possible role on tumor microenvironment normalization, the level of *COL3A1* was down-regulated, thereby inhibiting the *TGFβ* signaling pathway. That causes the reduction of extracellular matrix components, which significantly increases vascular function and perfusion, and increases the anti-tumor efficacy of doxorubicin (25). Therefore, these studies showed that *COL3A1* played an important role in the development of breast cancer. In addition, it was reported that *COL3A1* up-regulation cause extracellular matrix changes and reduced tumor perfusion, while the hypoxic micro-environment caused by hypoperfusion was considered to be the main reason for forcing cancer cells to metastasize (26). Therefore, the reduction of tumor perfusion caused by up-regulation of *COL3A1* was likely to be one of the reasons for the increased ability of TNBC cells to metastasis. In this study, we demonstrated that *COL3A1*, which was up-regulated by the reduced expression of *METTL3*, could contribute to TNBC metastasis. The molecular mechanism of *COL3A1* in promoting TNBC metastasis warrants further investigation.

In summary, this study not only revealed that, among m6A modulators, only *METTL3* played an important role in TNBC metastasis, but also demonstrated that the low expression of *METTL3*-reduced m6A modification could promote TNBC metastasis by up-regulating its target gene, *COL3A1*. Our results provided sufficient evidence of the important epigenetic role in the development of TNBC and allowed a more comprehensive understanding of the mechanism of tumor metastasis. *METTL3* and its target gene *COL3A1* might have the potential to become novel biomarkers for TNBC prognostic prediction and new targets for TNBC therapy.

DATA AVAILABILITY STATEMENT

Publicly available datasets were analyzed in this study. This data can be found here: https://www.cancer.gov/?TCGA-BRCA</b&gt.

ETHICS STATEMENT

This study was approved by the Ethics Committee of Shanghai Outdo Biotechnology Company (YB M-05-02), and all patients have signed informed consent. The patients/participants provided their written informed consent to participate in this study.

AUTHOR CONTRIBUTIONS

YS and CZ analyzed and interpreted the data regarding the m6A modulators and DMFS of breast cancer patients, performed most experiments and were major contributor in writing the manuscript and contributed equally to this work. YJ and DW performed partial qRT-PCR experiment. BB analyzed the correlation analysis between *METTL3*

and other genes. JF helped evaluated the expression of *METTL3* in IHC. ST helped with the making of heatmap. XQ and YL provided guidance on interpreting the results. XC and YT designed the study and revised the manuscript. All authors read and approved the final manuscript.

FUNDING

This research was supported by National Natural Science Foundation of China (No. 81672605), The Key Research and Development Program of Liaoning Province (2018225060), Science and Technology Plan Project of Liaoning Province (2019-ZD-777), Science and Technology Plan Project of Shenyang city (19-112-4-099), and Science and Technology Plan Project of Liaoning Province (No. 2013225585).

SUPPLEMENTARY MATERIAL

The Supplementary Material for this article can be found online at: https://www.frontiersin.org/articles/10.3389/fonc.2020.01126/full#supplementary-material

REFERENCES

1. DeSantis CE, Bray F, Ferlay J, Lortet-Tieulent J, Anderson BO, Jemal A. International variation in female breast cancer incidence and mortality rates. *Cancer Epidemiol Biomark Prev.* (2015) 24:1495–506. doi: 10.1158/1055-9965.EPI-15-0535
2. Lan Q, Liu PY, Haase J, Bell JL, Hüttelmaier S, Liu T. The critical role of RNA m^6a methylation in cancer. *Cancer Res.* (2019) 79:1285–92. doi: 10.1158/0008-5472.CAN-18-2965
3. Deng X, Su R, Weng H, Huang H, Li Z, Chen J. RNA N^6-methyladenosine modification in cancers: current status and perspectives. *Cell Res.* (2018) 28:507–17. doi: 10.1038/s41422-018-0034-6
4. Zhang J, Guo S, Piao HY, Wang Y, Wu Y, Meng XY, et al. ALKBH5 promotes invasion and metastasis of gastric cancer by decreasing methylation of the lncRNA NEAT1. *J Physiol Biochem.* (2019) 75:379–89. doi: 10.1007/s13105-019-00690-8
5. Wang Y, Zhao JC. Update: mechanisms underlying N^6-Methyladenosine modification of eukaryotic mRNA. *Trends Genet*. (2016) 32:763–73. doi: 10.1016/j.tig.2016.09.006
6. Li Z, Li F, Peng Y, Fang J, Zhou J. Identification of three m6A-related mRNAs signature and risk score for the prognostication of hepatocellular carcinoma. *Cancer Med.* (2020) 9:1877–89. doi: 10.1002/cam4.2833
7. Li J, Han Y, Zhang H, Qian Z, Jia W, Gao Y, et al. The m6A demethylase FTO promotes the growth of lung cancer cells by regulating the m6A level of USP7 mRNA. *Biochem Biophys Res Commun.* (2019) 512:479–85. doi: 10.1016/j.bbrc.2019.03.093
8. Cai J, Yang F, Zhan H, Situ J, Li W, Mao Y, et al. RNA m6A Methyltransferase METTL3 promotes the growth of prostate cancer by regulating hedgehog pathway. *Onco Targets Ther.* (2019) 12:9143–52. doi: 10.2147/OTT.S226796
9. He Y, Hu H, Wang Y, Yuan H, Lu Z, Wu P, et al. ALKBH5 inhibits pancreatic cancer motility by decreasing long non-coding RNA KCNK15-AS1 methylation. *Cell Physiol Biochem.* (2018) 48:838–46. doi: 10.1159/000491915
10. Wang H, Xu B, Shi J. N6-methyladenosine METTL3 promotes the breast cancer progression via targeting Bcl-2. *Gene.* (2020) 722:144076. doi: 10.1016/j.gene.2019.144076
11. Niu Y, Lin Z, Wan A, Chen H, Liang H, Sun L, et al. RNA N6-methyladenosine demethylase FTO promotes breast tumor progression through inhibiting BNIP3. *Mol Cancer.* (2019) 18:46. doi: 10.1186/s12943-019-1004-4
12. Wang X, Lu Z, Gomez A, Hon GC, Yue Y, Han D, et al. N6-methyladenosine-dependent regulation of messenger RNA stability. *Naure.* (2014) 505:117–20. doi: 10.1038/nature12730
13. Xiao W, Adhikari S, Dahal U, Chen YS, Hao YJ, Sun BF, et al. Nuclear m^6a reader YTHDC1 regulates mRNA splicing. *Mol Cell.* (2016) 61:507–19. doi: 10.1016/j.molcel.2016.01.012
14. Ma J-Z, Yang F, Zhou C-C, Liu F, Yuan Y-H, Wang F, et al. METTL14 suppresses the metastatic potential of hepatocellular carcinoma by modulating N^6-methyladenosine-dependent primary MicroRNA processing. *Hepatology.* (2017) 65:529–43. doi: 10.1002/hep.28885
15. Li Y, Xiao J, Bai J, Tian Y, Qu Y, Chen X, et al. Molecular characterization and clinical relevance of m6A regulators across 33 cancer types. *Mol Cancer.* (2019) 18:137. doi: 10.1186/s12943-019-1066-3
16. Wu L, Wu D, Ning J, Liu W, Zhang D. Changes of N^6-methyladenosine modulators promote breast cancer progression. *BMC Cancer.* (2019) 19:326. doi: 10.1186/s12885-019-5538-z
17. Cai X, Wang X, Cao C, Gao Y, Zhang S, Yang Z, et al. HBXIP-elevated methyltransferase METTL3 promotes the progression of breast cancer via inhibiting tumor suppressor let-7g. *Cancer letter.* (2018) 415:11–9. doi: 10.1016/j.canlet.2017.11.018
18. Dominissini D, Moshitch-Moshkovitz S, Schwartz S, Salmon-Divon M, Ungar L, Osenberg S, et al. Topology of the human and mouse m6A RNA methylomes revealed by m6A-seq. *Nature.* (2012) 485:201–6. doi: 10.1038/nature11112
19. Wang Y, Resnick MB, Lu S, Hui Y, Brodsky AS, Yang D, et al. Collagen type III α1 as a useful diagnostic immunohistochemical marker for fibroepithelial lesions of the breast. *Hum Pathol.* (2016) c57:176–81. doi: 10.1016/j.humpath.2016.07.017
20. Hasebe T. Tumor-stromal interactions in breast tumor progression–significance of histological heterogeneity of tumor-stromal fibroblasts. *Expert Opin Ther Targets.* (2013) 17:449–60. doi: 10.1517/14728222.2013.757305
21. Paolillo M, Schinelli S. Extracellular matrix alterations in metastatic processes. *Int J Mol Sci.* (2019) 20:4947. doi: 10.3390/ijms20194947
22. Shi S, Tian B. Identification of biomarkers associated with progression and prognosis in bladder cancer via co-expression analysis. *Cancer Biomark.* (2019) 24:183–93. doi: 10.3233/CBM-181940
23. Gao YF, Zhu T, Chen J, Liu L, Ouyang R. Knockdown of collagen α-1(III) inhibits glioma cell proliferation and migration and is regulated by miR128-3p. *Oncol Lett.* (2018) 16:1917–23. doi: 10.3892/ol.2018.8830
24. Nie K, Shi L, Wen Y, Pan J, Li P, Zheng Z, et al. Identification of hub genes correlated with the pathogenesis and prognosis of gastric cancer via bioinformatics methods. *Minerva Med.* (2020) 111:213–25. doi: 10.23736/S0026-4806.19.06166-4
25. Polydorou C, Mpekris F, Papageorgis P, Voutouri C, Stylianopoulos T. Pirfenidone normalizes the tumor microenvironment to improve chemotherapy. *Oncotarget.* (2017) 8:24506–17. doi: 10.18632/oncotarget.15534
26. Christner PJ, Ayitey S. Extracellular matrix containing mutated fibrillin-1 (Fbn1) down regulates Col1a1, Col1a2, Col3a1, Col5a1, and Col5a2 mRNA levels in Tsk/+ and Tsk/Tsk embryonic fibroblasts. *Amino Acids.* (2006) 30:445–51. doi: 10.1007/s00726-005-0265-y

Conflict of Interest: The authors declare that the research was conducted in the absence of any commercial or financial relationships that could be construed as a potential conflict of interest.

frontiers in Oncology

ORIGINAL RESEARCH
published: 21 August 2020
doi: 10.3389/fonc.2020.01444

Development and Validation of an m6A RNA Methylation Regulator-Based Signature for Prognostic Prediction in Cervical Squamous Cell Carcinoma

Jingxin Pan[1†], *Lichao Xu*[2,3†] *and Hongda Pan*[3*†]

[1] Department of Internal Medicine, The Second Affiliated Hospital of Fujian Medical University, Quanzhou, China, [2] Department of Interventional Radiology, Fudan University Shanghai Cancer Center, Shanghai, China, [3] Department of Oncology, Shanghai Medical College, Fudan University, Shanghai, China

OPEN ACCESS

Edited by:
Xiangqian Zheng,
Tianjin Medical University Cancer Institute and Hospital, China

Reviewed by:
Xiaocheng Weng,
University of Chicago, United States
Ye Fu,
Harvard University, United States
Lin Zhang,
China University of Mining and Technology, China

***Correspondence:**
Hongda Pan
panhongda@shca.org.cn

[†]These authors have contributed equally to this work

Specialty section:
This article was submitted to Cancer Genetics, a section of the journal Frontiers in Oncology

Received: 23 March 2020
Accepted: 08 July 2020
Published: 21 August 2020

Citation:
Pan J, Xu L and Pan H (2020) Development and Validation of an m6A RNA Methylation Regulator-Based Signature for Prognostic Prediction in Cervical Squamous Cell Carcinoma. Front. Oncol. 10:1444. doi: 10.3389/fonc.2020.01444

Background: Cervical squamous cell carcinoma (CESC) is one of the most common causes of cancer-related death worldwide. N6-methyladenosine (m6A) plays an important role in various cellular responses by regulating mRNA biology. This study aimed to develop and validate an m6A RNA methylation regulator-based signature for prognostic prediction in CESC.

Methods: Clinical and survival data as well as RNA sequencing data of 13 m6A RNA methylation regulators were obtained from The Cancer Genome Atlas (TCGA) CESC database. Consensus clustering was performed to identify different CESC clusters based on the differential expression of the regulators. LASSO Cox regression analysis was used to generate a prognostic signature based on m6A RNA methylation regulator expression. The effect of the signature was further explored by univariate and multivariate Cox analyses.

Results: Four regulators (RBM15, METTL3, FTO, and YTHDF2) were identified to be aberrantly expressed in CESC tissues. A prognostic signature that includes ZC3H13, YTHDC1, and YTHDF1 was developed, which can act as an independent prognostic indicator. Significant differences of survival rate and clinicopathological features were found between the high- and low-risk groups. The results of bioinformatics analysis were then validated in the clinical CESC cohort by qRT-PCR and immunohistochemistry staining.

Conclusion: In the present study, we developed and validated an m6A RNA methylation regulator-based prognostic signature, which might provide useful insights regarding the development and prognosis of CESC.

Keywords: m6A, RNA methylation, cervical squamous cell carcinoma, prognosis, experimental validation

INTRODUCTION

Cervical squamous cell carcinoma (CESC) is the fourth most commonly diagnosed cancer and the fourth leading cause of cancer-associated mortality in women worldwide (1). Persistent infection with human papillomavirus (HPV) is the predominant cause of CESC (2). The development of accurate prognostic predictors in order to establish personalized treatment for CESC patients is crucial.

N6-methyladenosine (m6A) modification is one of the most prevalent modification in mRNA in eukaryotic cells. m6A RNA modification plays crucial roles in many processes of gene regulation such as mRNA stability, splicing, and translation (3). m6A RNA modification can be installed enzymatically by various methyltransferases, termed m6A "writers" (METTL3, METTL14, WTAP, KIAA1429, RBM15, and ZC3H13). m6A in RNA can be removed by demethylases, termed m6A "erasers" (FTO and ALKBH5). Proteins that selectively bind m6A can be defined as m6A "readers" (HNRNPC, YTHDF1, YTHDF2, YTHDC2, and YTHDC1) that exert regulatory functions by selective recognition of methylated RNA (4). Emerging evidence has revealed the cancer promoter or suppressor role of m6A regulators in the development of various malignancies (5–7), whereas the correlation between prognosis of CESC and m6A RNA methylation regulators is still unclear.

In this study, the differential expression of m6A RNA methylation regulators was analyzed using the RNA sequencing data from the TCGA-CESC dataset. The interactions among these regulators and their correlation with clinicopathological features were evaluated. Consensus clustering was used to identify two clusters of CESC patients to predict clinical outcome. By LASSO Cox analysis, a three-gene prognostic signature was generated. Moreover, the bioinformatics prediction was experimentally validated in a clinical CESC cohort (**Figure 1**). The m6A RNA methylation regulator-based prognostic signature can act as a useful tool for predicting the survival outcomes of CESC patients.

MATERIALS AND METHODS

TCGA Data Acquisition

RNA transcriptome data in the Fragments Per Kilobase per Million (FPKM) format and the clinical and survival data of CESC patients were downloaded from TCGA database (https://cancergenome.nih.gov/). All analyses were performed according to the publication guidelines of TCGA. After duplicate samples from the same patients were excluded, a total of 304 CESC samples and three normal tissue samples were enrolled for subsequent analysis. Thirteen well-acknowledged m6A RNA methylation regulators (YTHDC1, YTHDC2, YTHDF1, YTHDF2, ALKBH5, FTO, METTL3, METTL14, HNRNPC, WTAP, RBM15, KIAA1429, and ZC3H13) were selected for further analysis according to previously published literature (8).

Bioinformatics Analysis

Differential expressions of 13 m6A methylation regulators between different sample groups were identified by "limma" package in R software. Gene expression levels, as well as their correlation with clinicopathological features, were visualized by heatmaps generated with "pheatmap" package. The "corrplot" package was employed to reveal the correlation among m6A RNA methylation regulators. Interactions among m6A RNA methylation regulators were analyzed and a protein–protein interaction network was established and visualized by the STRING and Cytoscape 3.6.0. The genetic alterations of the m6A methylation regulators were analyzed by cBioPortal using data from TCGA. The CESC cohort was clustered into different groups by consensus expression of m6A RNA methylation regulators with "ConsensusClusterPlus" package. A "survminer" package in R software was used to determine the best cutoff of the expression value for survival analysis. Gene ontology (GO) annotation were performed by "clusterProfiler" package and visualized using circos plots generated by the "ggplot2" package.

Construction of the Prognostic Signature

All m6A methylation regulators were included in the Least Absolute Shrinkage and Selection Operator (LASSO) Cox regression model to construct the powerful prognostic signature and calculate a coefficient for each gene. A risk score for each patient was calculated as the sum of each gene's score, which was obtained by multiplying the expression of each gene and its coefficient. The sensitivity and specificity of the prognostic signature were accessed by receiver operating characteristic (ROC) curves and area under the ROC curves (AUC values).

Experimental Validation

One hundred twenty CESC tissues and paired normal tissues were obtained from Outdo Biotech (Shanghai, China). The mRNA and protein expression of ZC3H13, YTHDC1, and YTHDF1 were quantified by immunohistochemistry (IHC) staining and quantitative real-time PCR (qRT-PCR), as per previously described methods (9, 10). GAPDH was used as internal standard for normalization in qRT-PCR. Primer sequences of genes measured in this study were listed in **Table S1**. The validation cohort was grouped into low- and high-risk groups according to the risk scores calculated by the TCGA cohort. Written informed consent was obtained from all the patients. The validation study was approved by the Ethics Committee of Fudan University.

Statistical Analysis

The chi-square test was used to compare the clinicopathological features between different groups. The Student's *t*-test (two-tailed) was applied to compare the differences between groups. Univariate and multivariate Cox regression analyses were used to identify the independent prognostic factors for patients with CESC. Kaplan–Meier method and log-rank test were used to compare the overall survival (OS) difference between different groups. Data analysis was performed with either GraphPad Prism 7.0 (GraphPad, San Diego, CA, USA) or SPSS v23.0 (IBM Corp., Armonk, NY, USA). All statistical tests were two-sided. A $P < 0.05$ was considered statistically significant.

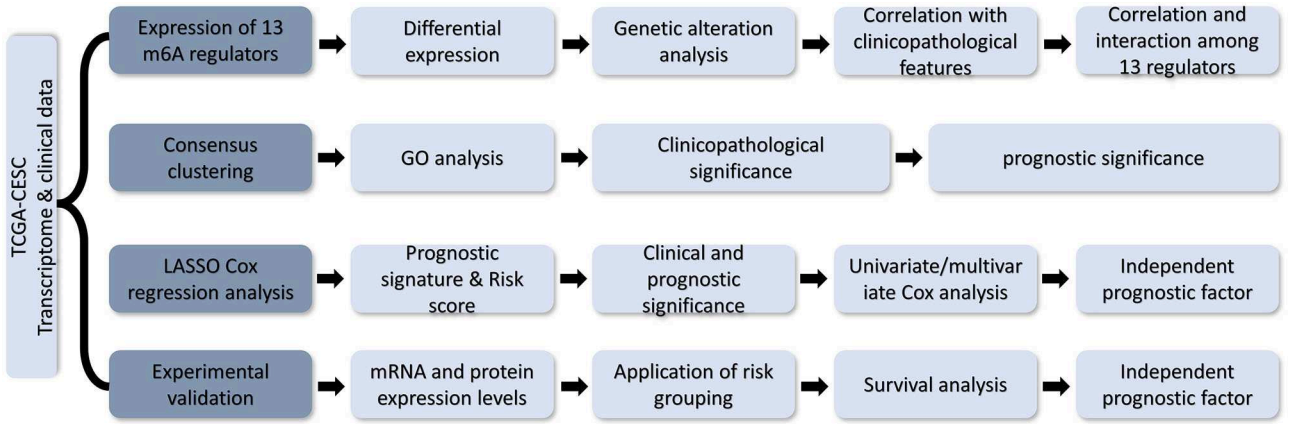

FIGURE 1 | Flow chart of development and validation of an m6A RNA methylation regulator-based prognostic signature for CESC.

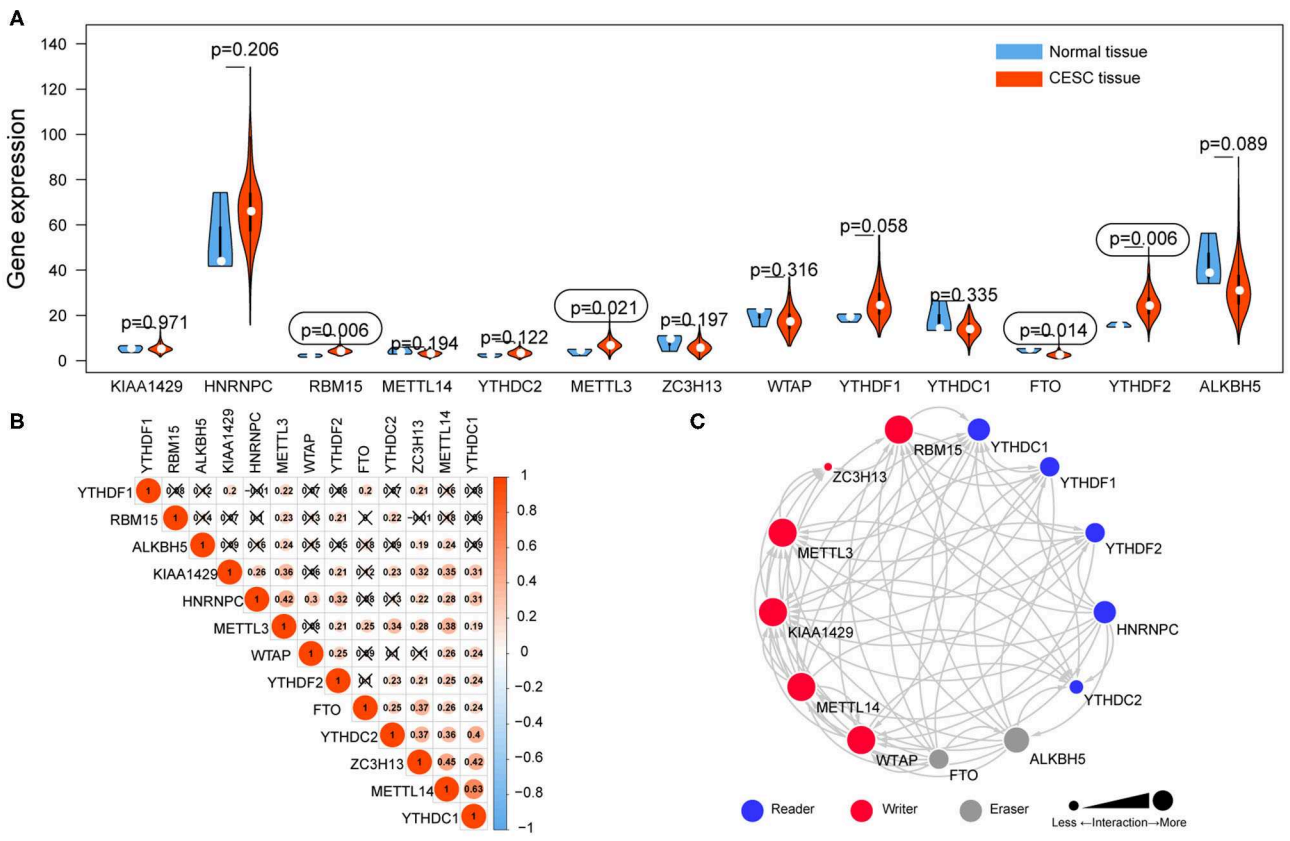

FIGURE 2 | The expression of 13 m6A RNA methylation regulators in TCGA-CESC cohort. **(A)** The violin plot showed the significantly differentially expressed m6A RNA methylation regulators between CESC tissues and the normal tissues. **(B)** The correlations among m6A RNA methylation regulators were analyzed by Pearson correlation. **(C)** PPI network showed the interactions among m6A RNA methylation regulators.

RESULTS

Expression Profile of m6A RNA Methylation Regulators in CESC

The mRNA expression levels of m6A RNA methylation regulators were analyzed using transcriptome data in FPKM format. The differential expression of 13 regulators between CESC and normal tissues was demonstrated by a violin plot (**Figure 2A**). The mRNA expression levels of three regulators (RBM15, METTL3, and YTHDF2) were significantly increased, and FTO was decreased in CESC compared with normal tissues. No significant difference was found for the other nine regulators.

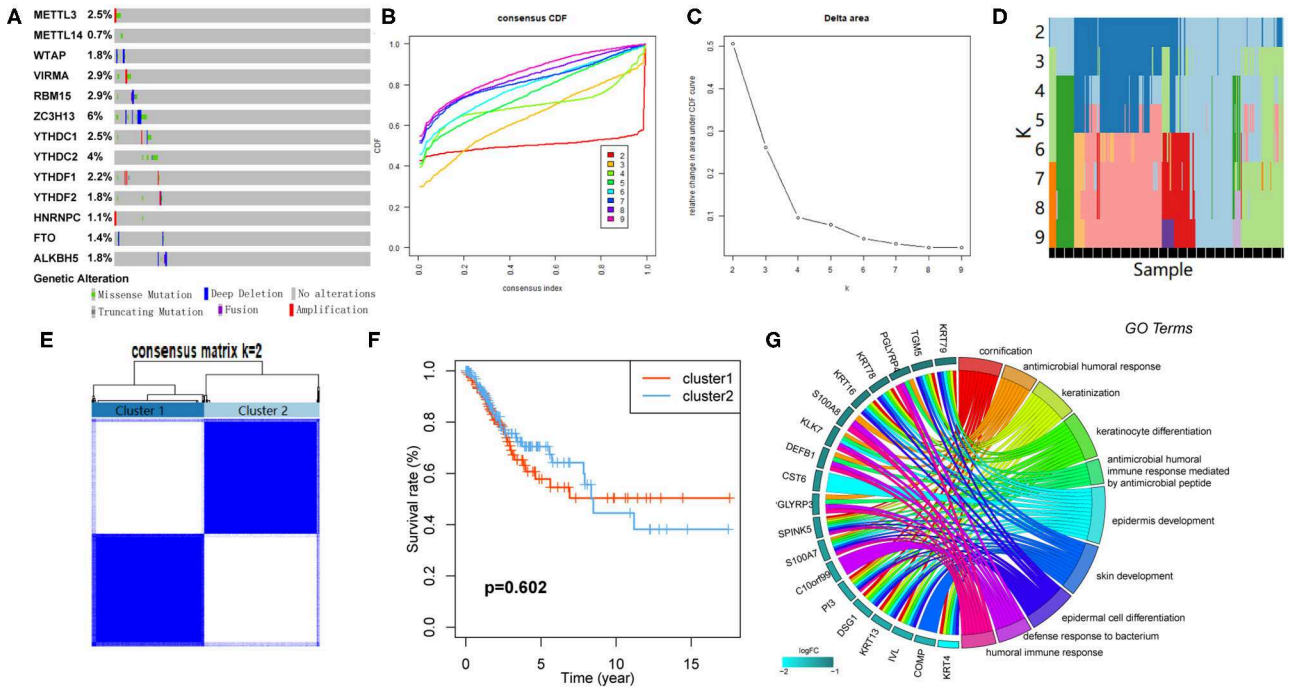

FIGURE 3 | Consensus clustering based on the expression of m6A RNA methylation regulators. **(A)** Genetic alteration was analyzed *via* cBioPortal database. **(B)** Area under cumulative distribution function (CDF) curve when index *k* ranges from 2 to 10. **(C)** Changes of length and slope of CDF curve when index *k* ranges from 2 to 10. **(D)** Distribution of each sample in different clusters when *k* ranges from 2 to 10. **(E)** The overlap between clusters when $k = 2$. **(F)** The Kaplan–Meier survival analysis for Clusters 1 and 2. **(G)** GO analysis for the DEGs between Clusters 1 and 2.

Correlation and Interaction Among m6A RNA Methylation Regulators in CESC

Correlations among the mRNA expression levels of 13 m6A RNA methylation regulators were analyzed by Pearson correlation analysis (**Figure 2B**), and the protein–protein interactions (PPIs) were retrieved via String database (**Figure 2C**). The results showed that all the regulators were positively correlated with each other. Notably, YTHDC1 was significantly correlated with METTL14 ($r = 0.63$). The PPI network revealed that five writers (METTL3, METTL14, RBM15, KIAA1429, and WTAP) were all significantly correlated with each other, as well as readers and erasers. Interactions were founded to be few among the two erasers and five readers in the PPI network.

Genetic Alteration of m6A RNA Methylation Regulators in CESC

The CNV and mutation of m6A RNA methylation regulators were analyzed via the cBioPortal database using TCGA data to investigate the effects of genetic alteration on the gene expression (**Figure 3A**). The results revealed that the frequencies of genetic alteration for ZC3H13 were 6%, and the most frequent alteration was deep deletion. Frequencies for other regulators were <3%, indicating that changes in the expression levels of these regulators were not caused by genetic alteration.

Consensus Clustering Identified Two Clusters of Patients With CESC

CESC cohort could be divided into several clusters according to the consensus of mRNA expression of the 13 m6A RNA methylation regulators. When the clustering index "*k*" increased from 2 to 9, $k = 2$ was demonstrated to be the optimal point to obtain the largest differences between clusters (**Figures 3B,C**). Besides, the interference between clusters was minimal when $k = 2$ (**Figures 3D,E**). Subsequently, the CESC cohort was divided into two clusters, namely, Cluster 1 and Cluster 2 (**Figure 3E**). However, no survival difference between the two clusters was found by Kaplan–Meier survival analysis (**Figure 3F**).

GO Analysis for Differentially Expressed Genes (DEGs) Between Clusters

One hundred ten DEGs between clusters were identified to investigate the differences of biological roles between these clusters. GO analyses for biological processes were conducted and showed that DEGs were mainly enriched in biological processes associated with the development of the immune system (**Figure 3G**).

Clinicopathological Differences Between the Clusters

Correlation between the clustering and clinicopathological characteristics was then analyzed between the two clusters. As

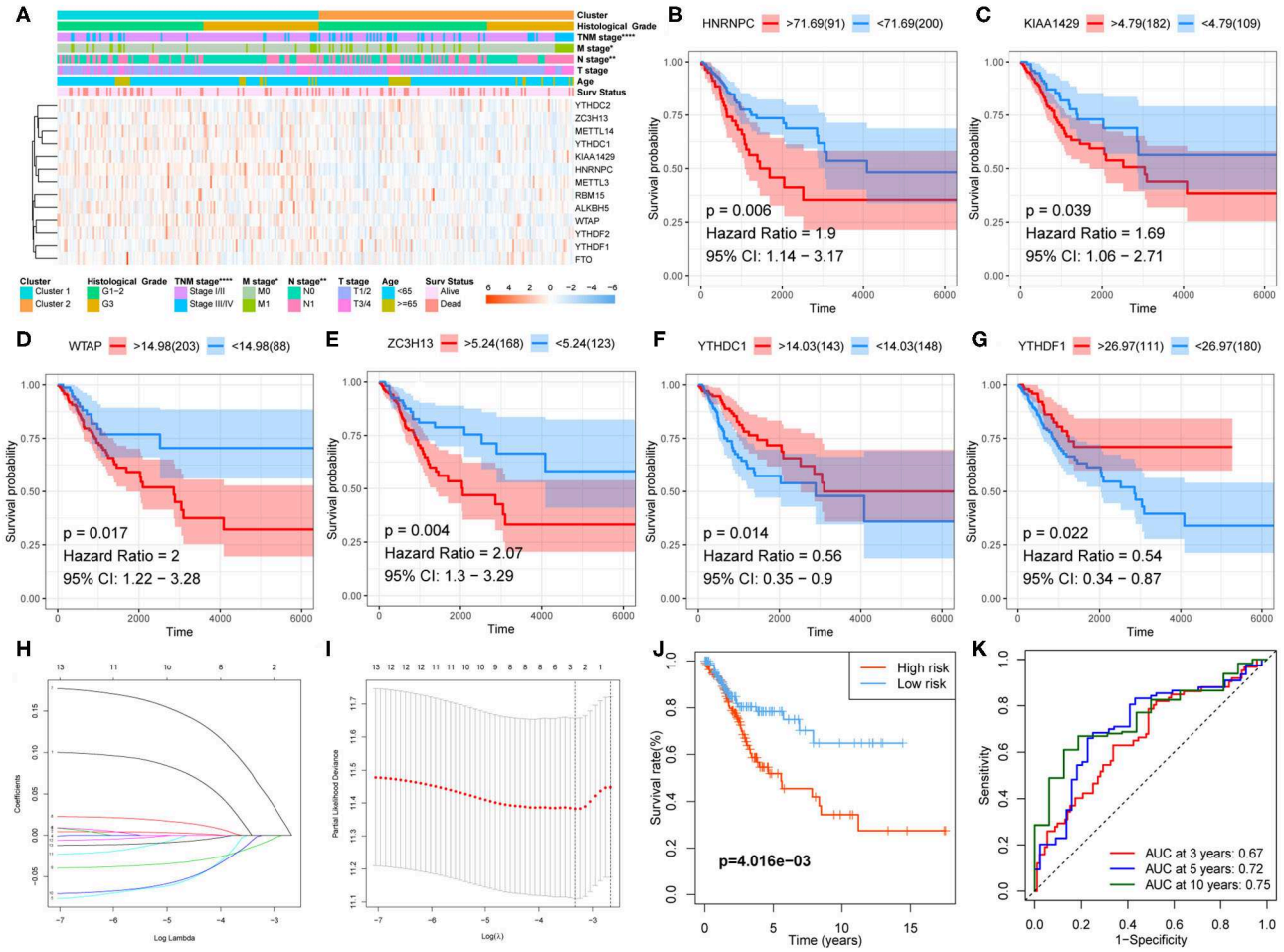

FIGURE 4 | Clinical significance of clustering and construction of the prognostic signature. **(A)** The clinicopathological differences between the two clusters. **(B–G)** Kaplan–Meier survival curve for HNRNPC, KIAA1429, WTAP, ZC3H13, YTHDC1, and YTHDF1. **(H,I)** The prognostic signature constructed by the minimum criterion of LASSO Cox regression algorithm. **(J)** The Kaplan–Meier survival analysis for high- and low-risk groups. **(K)** ROC curve was used to evaluate the prediction efficiency of the prognostic signature.

shown in **Figure 4A**, Cluster 1 was significantly associated with advanced N stage, M stage, and TNM stage.

Development of a Prognostic Signature

Kaplan–Meier survival analysis was conducted for these 13 regulators to explore the prognostic significance of the m6A RNA methylation regulators in CESC. The results showed that high expression levels of HNRNPC, KIAA1429, WTAP (**Figures 4B–E**), and ZC3H13 were correlated with poor survival, whereas high expression levels of YTHDC1 and YTHDF1 were associated with longer OS (**Figures 4F,G**).

A prognostic signature, including ZC3H13, YTHDC1, and YTHDF1, was developed using the LASSO Cox regression model according to the minimum criterion (**Figures 4H,I**). The coefficients of ZC3H13, YTHDC1, and YTHDF1 were 0.0644, −0.0016, and −0.012, respectively. The risk score for each CESC patient was therefore calculated with the following formula: Risk Score = 0.0644 * ZC3H13 – 0.0016 * YTHDC1 – 0.012 * YTHDF1. Then, the CESC cohort was divided into low- and high-risk groups on the basis of the median risk score.

Prognostic and Clinicopathological Differences Between Low- and High-Risk Groups

Kaplan–Meier survival analysis was conducted to validate the prognostic value of risk grouping. The results revealed that the high-risk group had a worse overall survival than the low-risk group ($P = 4.016e{-}03$) (**Figure 4J**). Time-dependent ROC curve was used to assess the specificity and sensitivity of the prognostic signature. The area under the curve (AUC) at 3, 5, and 10 years was 0.67, 0.72, and 0.75, respectively, suggesting good prediction performances (**Figure 4K**). The high-risk group was significantly associated with advanced N stage ($P < 0.05$), M stage ($P < 0.0001$), TNM stage ($P < 0.0001$), and poor survival ($P < 0.01$) (**Figure 5A**).

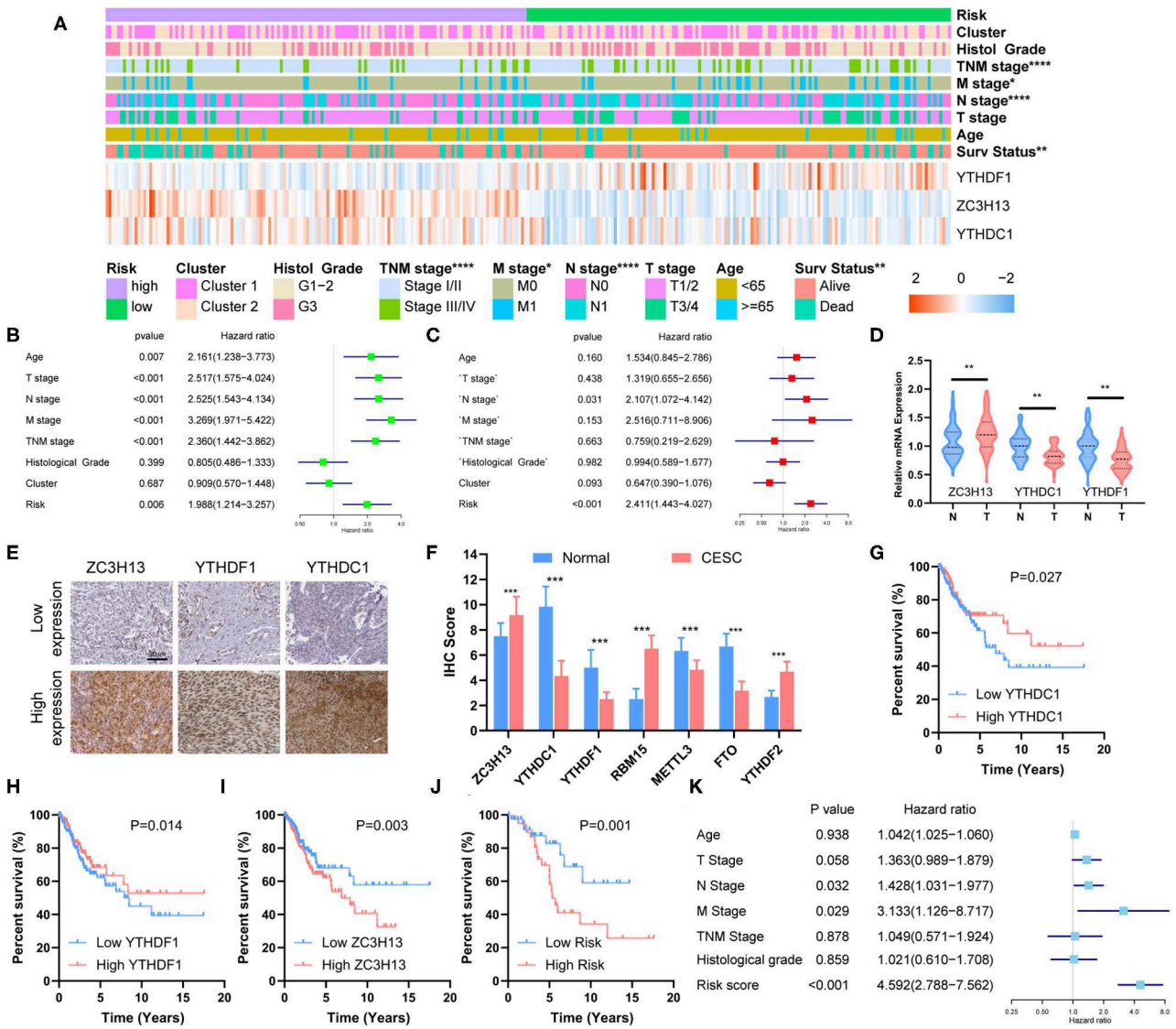

FIGURE 5 | Clinical significance of risk grouping and experimental validation. **(A)** The clinicopathological differences between the high- and low-risk groups. **(B)** Univariate Cox analysis of the clinicopathological features and risk score. **(C)** Multivariate Cox analysis identified the independent prognostic predictors. **(D)** mRNA levels of ZC3H13, YTHDC1, and YTHDF1 in CESC and normal tissues were measured by qRT-PCR. **(E)** Representative IHC staining for ZC3H13, YTHDC1, and YTHDF1 in CESC and normal tissues (scale bar: 50 μm). **(F)** Protein expression of RBM15, METTL3, FTO, YTHDF2, ZC3H13, YTHDC1, and YTHDF1 was measured by IHC. **(G–I)** Kaplan–Meier survival analysis for patients with high or low expression levels of YTHDC1, YTHDF1, and ZC3H13. **(J)** Kaplan–Meier survival analysis for patients in low- or high-risk groups. **(K)** Multivariate COX analysis identified the independent prognostic predictors in the clinical CESC cohort.

The Prognostic Signature Acts as an Independent Prognostic Predictor

Univariate and multivariate Cox analyses were performed to identify the independent prognostic predictors for CESC patients. The univariate Cox analysis showed that the Age, T stage, N stage, M stage, TNM stage, and Risk Score were significantly associated with the survival (**Figure 5B**). The multivariate Cox regression model showed that only Risk Score ($P < 0.001$, HR = 2.411, 95% CI = 1.443–4.027) and N stage ($P = 0.031$, HR = 2.107, 95% CI = 1.072–4.142) were the independent prognostic factors for CESC (**Figure 5C**).

Experimental Validation

The mRNA expression of ZC3H13, YTHDC1, and YTHDF1 was measured with qRT-PCR, and the results showed that ZC3H13 was significantly upregulated in CESC tissues, whereas YTHDC1 and YTHDF1 were significantly downregulated in CESC tissues (**Figure 5D**). The differential expressions were also confirmed by IHC staining (**Figures 5E,F**). Low YTHDC1 and YTHDF1 expression was associated with poor survival (**Figures 5G,H**), and high level of ZC3H13 was correlated with lower survival rate (**Figure 5I**). Risk score was calculated for each patient in the validation cohort according to the formula

and coefficient obtained from the TCGA cohort. Fifty-seven patients were identified as a high-risk group, and the rest of the 63 patients were categorized into a low-risk group. The survival rate was significantly lower in the high-risk group in comparison with that in the low-risk group (**Figure 5J**). Multivariate Cox analysis showed that the risk score, along with the N stage and M stage, was an independent prognostic factor for the overall survival of CESC patients in the validation cohort (**Figure 5K**). The prognostic significance of the three-gene signature in the validation cohort was in accordance with that of TCGA cohort.

DISCUSSION

Globally, CESC is one of the most common types of cancer and exists as a major therapeutic challenge (8, 11). One major cause of high mortality of CESC is high levels of patient relapse and mortality after treatment. The carcinogenesis of CESC is a complex multistep process characterized by a broad spectrum of molecular abnormalities that offers numerous potential therapeutic targets (12). Understanding the mechanisms of action of these molecules is crucial for their potential therapeutic use. Human papillomavirus (HPV) infection plays an important role in cervical cancer (13). m6A is the most abundant internal modification of RNA in eukaryotic cells (14). Emerging evidence suggests that aberrant m6A RNA methylation plays a critical role in cancer through various mechanisms (15, 16).

The level of m6A methylation is regulated by methyltransferases (writers), demethylases (erasers), and binding proteins (readers). Previous studies have demonstrated that m6A RNA methylation regulators were aberrantly expressed in various types of cancers and exert roles of promoter or suppressor of cancers (17). Zhang et al. demonstrated m6A regulator-mediated methylation modification patterns and tumor microenvironment infiltration characterization in gastric cancer (5). METTL3 is significantly upregulated in hepatoblastoma, and it regulates β-catenin to promote tumor proliferation (17). Yang et al. revealed that FTO promoted melanoma tumorigenesis and anti-PD-1 resistance and suggest that the combination of FTO inhibition with anti-PD-1 blockade may reduce the resistance to immunotherapy in melanoma (18). However, the roles of m6A methylation regulators in CESC are unclear.

In the present study, a three-gene prognostic signature, consisting of ZC3H13, YTHDC1, and YTHDF1, was developed and demonstrated good performance for predicting the survival outcome of CESC. Additionally, we validated the results of bioinformatics analysis with a clinical CESC cohort. The protein and mRNA expression of ZC3H13, YTHDC1, and YTHDF1 were measured by IHC and qRT-PCR. The results of experimental validation are consistent with those of bioinformatics prediction, suggesting that the prognostic signature might serve as a useful tool for predicting survival outcomes of CESC.

ZC3H13 is a canonical CCCH zinc finger protein and plays an important role in modulating RNA m6A methylation in the nucleus (19). Zhu et al. reported that ZC3H13 might be an upstream regulator of Ras-ERK signaling pathway and suppressed invasion and proliferation of colorectal cancer (20). Xiao et al. reported that the nuclear m6A reader protein YTHDC1 impacts mRNA splicing, providing a transcriptome-wide glance of splicing changes affected by this mRNA methylation reader protein (21, 22). YTHDF1 is a core factor in RNA methylation modification. Bai et al. demonstrated that knocking down the expression of YTHDF1 significantly inhibited the colorectal cell progression, and silencing YTHDF1 significantly inhibited Wnt/β-catenin pathway activity in colorectal cells (23). Han et al. reported that loss of YTHDF1 in classical dendritic cells enhanced the cross-presentation of tumor antigens and the cross-priming of CD8+ T cells *in vivo*. The therapeutic efficacy of PD-L1 checkpoint blockade is enhanced in Ythdf1$^{-/-}$ mice, implicating YTHDF1 as a potential therapeutic target in anticancer immunotherapy (24).

In conclusion, our study revealed that the aberrant expression of m6A RNA methylation regulators is significantly correlated with the survival and clinicopathological characteristics of patients with CESC. The m6A RNA methylation regulator-based prognostic signature can effectively predict the prognosis of CESC patients.

DATA AVAILABILITY STATEMENT

Publicly available datasets were analyzed in this study, these can be found in The Cancer Genome Atlas (https://portal.gdc.cancer.gov/).

ETHICS STATEMENT

The studies involving human participants were reviewed and approved by the Ethics Committee of Fudan University. The patients/participants provided their written informed consent to participate in this study.

AUTHOR CONTRIBUTIONS

HP, LX, and JP conceived and designed the experiments. JP analyzed the data and drafted the manuscript. LX discussed, contributed to the data analysis, and contributed to the sampling. All authors read and approved the final manuscript.

FUNDING

This study was supported by National Natural Science Foundation of China (No. 81902424) and Beijing Natural Science Foundation (No. 7184240).

ACKNOWLEDGMENTS

The authors thank Profs. Zhiyi Pan and Xuan Zhang for their help in clinical data collection.

SUPPLEMENTARY MATERIAL

The Supplementary Material for this article can be found online at: https://www.frontiersin.org/articles/10.3389/fonc.2020.01444/full#supplementary-material

REFERENCES

1. Sawaya G, Smith-Mccune K, Kuppermann M. Cervical cancer screening: more choices in 2019. *JAMA*. (2019) 321:2018–9. doi: 10.1001/jama.2019.4595
2. Cohen P, Jhingran A, Oaknin A, Denny L. Cervical cancer. *Lancet*. (2019) 393:169–82. doi: 10.1016/S0140-6736(18)32470-X
3. Lee Y, Choe J, Park O, Kim Y. Molecular mechanisms driving mRNA degradation by mA modification. *Trends Genetics*. (2020) 36:177–88. doi: 10.1016/j.tig.2019.12.007
4. Luo J, Liu H, Luan S, He C, Li Z. Aberrant regulation of mRNA m6A modification in cancer development. *Int J Mol Sci*. (2018) 19:92515. doi: 10.3390/ijms19092515
5. Zhang B, Wu Q, Li B, Wang D, Wang L, Zhou Y. mA regulator-mediated methylation modification patterns and tumor microenvironment infiltration characterization in gastric cancer. *Mol Cancer*. (2020) 19:53. doi: 10.1186/s12943-020-01170-0
6. Li H, Su Q, Li B, Lan L, Wang C, Li W, et al. High expression of WTAP leads to poor prognosis of gastric cancer by influencing tumour-associated T lymphocyte infiltration. *J Cell Mol Med*. (2020) 24:4452–65. doi: 10.1111/jcmm.15104
7. Yang D, Chen Z, Yu K, Lu J, Wu Q, Wang Y, et al. METTL3 promotes the progression of gastric cancer via targeting the MYC pathway. *Front Oncol*. (2020) 10:115. doi: 10.3389/fonc.2020.00115
8. Bray F, Ferlay J, Soerjomataram I, Siegel RL, Torre LA, Jemal A. Global cancer statistics 2018: GLOBOCAN estimates of incidence and mortality worldwide for 36 cancers in 185 countries. *CA Cancer J Clin*. (2018) 68:394–424. doi: 10.3322/caac.21492
9. Pan H, Pan J, Ji L, Song S, Lv H, Yang Z, et al. Carboxypeptidase A4 promotes cell growth via activating STAT3 and ERK signaling pathways and predicts a poor prognosis in colorectal cancer. *Int J Biol Macromol*. (2019) 138:125–34. doi: 10.1016/j.ijbiomac.2019.07.028
10. Zhang J, Hou L, Liang R, Chen X, Zhang R, Chen W, et al. CircDLST promotes the tumorigenesis and metastasis of gastric cancer by sponging miR-502-5p and activating the NRAS/MEK1/ERK1/2 signaling. *Mol Cancer*. (2019) 18:80. doi: 10.1186/s12943-019-1015-1
11. Mayadev J, Enserro D, Lin Y, Da Silva D, Lankes H, Aghajanian C, et al. Sequential ipilimumab after chemoradiotherapy in curative-intent treatment of patients with node-positive cervical cancer. *JAMA Oncol*. (2019) 6:92–9. doi: 10.1001/jamaoncol.2019.3857
12. Lin C, Slama J, Gonzalez P, Goodman M, Xia N, Kreimer A, et al. Cervical determinants of anal HPV infection and high-grade anal lesions in women: a collaborative pooled analysis. *Lancet Infect Dis*. (2019) 19:880–91. doi: 10.1016/S1473-3099(19)30164-1
13. Brisson M, Kim J, Canfell K, Drolet M, Gingras G, Burger E, et al. Impact of HPV vaccination and cervical screening on cervical cancer elimination: a comparative modelling analysis in 78 low-income and lower-middle-income countries. *Lancet*. (2020) 395:575–90. doi: 10.1016/S0140-6736(20)30068-4
14. Huang H, Weng H, Chen J. The biogenesis and precise control of RNA mA methylation. *Trends Genetics*. (2020) 36:44–52. doi: 10.1016/j.tig.2019.10.011
15. Chen M, Wong C. The emerging roles of N6-methyladenosine (m6A) deregulation in liver carcinogenesis. *Mol Cancer*. (2020) 19:44. doi: 10.1186/s12943-020-01172-y
16. Zhao W, Qi X, Liu L, Ma S, Liu J, Wu J. Epigenetic regulation of mA modifications in human cancer. *Mol Ther Nucl Acids*. (2020) 19:405–12. doi: 10.1016/j.omtn.2019.11.022
17. Liu L, Wang J, Sun G, Wu Q, Ma J, Zhang X, et al. mA mRNA methylation regulates CTNNB1 to promote the proliferation of hepatoblastoma. *Mol Cancer*. (2019) 18:188. doi: 10.1186/s12943-019-1119-7
18. Su M, Xiao Y, Ma J, Tang Y, Tian B, Zhang Y, et al. Circular RNAs in Cancer: emerging functions in hallmarks, stemness, resistance and roles as potential biomarkers. *Mol Cancer*. (2019) 18:90. doi: 10.1186/s12943-019-1002-6
19. Wen J, Lv R, Ma H, Shen H, He C, Wang J, et al. Zc3h13 regulates nuclear RNA mA methylation and mouse embryonic stem cell self-renewal. *Mol Cell*. (2018) 69:1028–38.e1026. doi: 10.1016/j.molcel.2018.02.015
20. Zhu D, Zhou J, Zhao J, Jiang G, Zhang X, Zhang Y, et al. ZC3H13 suppresses colorectal cancer proliferation and invasion via inactivating Ras-ERK signaling. *J Cell Physiol*. (2019) 234:8899–907. doi: 10.1002/jcp.27551
21. Roundtree IR, He C. Nuclear m(6)A reader YTHDC1 regulates mRNA splicing. *Trends Genetics*. (2016) 32:320–1. doi: 10.1016/j.tig.2016.03.006
22. Xiao W, Adhikari S, Dahal U, Chen Y, Hao Y, Sun B, et al. Nuclear m(6)A reader YTHDC1 regulates mRNA splicing. *Mol Cell*. (2016) 61:507–19. doi: 10.1016/j.molcel.2016.01.012
23. Bai Y, Yang C, Wu R, Huang L, Song S, Li W, et al. YTHDF1 regulates tumorigenicity and cancer stem cell-like activity in human colorectal carcinoma. *Front Oncol*. (2019) 9:332. doi: 10.3389/fonc.2019.00332
24. Han D, Liu J, Chen C, Dong L, Liu Y, Chang R, et al. Anti-tumour immunity controlled through mRNA m(6)A methylation and YTHDF1 in dendritic cells. *Nature*. (2019) 566:270–4. doi: 10.1038/s41586-019-0916-x

Conflict of Interest: The authors declare that the research was conducted in the absence of any commercial or financial relationships that could be construed as a potential conflict of interest.

frontiers in Oncology

ORIGINAL RESEARCH
published: 29 September 2020
doi: 10.3389/fonc.2020.553045

m^{6}A Reader HNRNPA2B1 Promotes Esophageal Cancer Progression via Up-Regulation of ACLY and ACC1

Huimin Guo[1†], Bei Wang[2†], Kaiyue Xu[3†], Ling Nie[4], Yao Fu[4], Zhangding Wang[1], Qiang Wang[5], Shouyu Wang[5,6,7*] and Xiaoping Zou[1*]*

[1] Department of Gastroenterology, The Affiliated Drum Tower Hospital of Nanjing University Medical School, Nanjing, China, [2] Yancheng First Hospital, Affiliated Hospital of Nanjing University Medical School, Yancheng, China, [3] Department of Radiotherapy, The First Affiliated Hospital of Nanjing Medical University, Nanjing, China, [4] Department of Pathology, The Affiliated Drum Tower Hospital of Nanjing University Medical School, Nanjing, China, [5] Department of Hepatobiliary Surgery, The Affiliated Drum Tower Hospital of Nanjing University Medical School, Nanjing, China, [6] Jiangsu Key Laboratory of Molecular Medicine, Medical School of Nanjing University, Nanjing, China, [7] Center for Public Health Research, Medical School of Nanjing University, Nanjing, China

OPEN ACCESS

Edited by:
Xiangqian Zheng,
Tianjin Medical University Cancer Institute and Hospital, China

Reviewed by:
Shengli Li,
Shanghai Jiao Tong University, China
Jianfeng Huang,
Sanford Burnham Prebys Medical Discovery Institute, United States

***Correspondence:**
Qiang Wang
njmuwangqiang@163.com
Shouyu Wang
sywang@nju.edu.cn
Xiaoping Zou
13770771661@163.com

[†] These authors have contributed equally to this work

Specialty section:
This article was submitted to Cancer Genetics, a section of the journal Frontiers in Oncology

Received: 17 April 2020
Accepted: 17 August 2020
Published: 29 September 2020

Citation:
Guo H, Wang B, Xu K, Nie L, Fu Y, Wang Z, Wang Q, Wang S and Zou X (2020) m^{6}A Reader HNRNPA2B1 Promotes Esophageal Cancer Progression via Up-Regulation of ACLY and ACC1. Front. Oncol. 10:553045. doi: 10.3389/fonc.2020.553045

N6-methyladenosine (m^{6}A) modification is the most abundant modification on eukaryotic RNA. In recent years, lots of studies have reported that m^{6}A modification and m^{6}A RNA methylation regulators were involved in cancer progression. However, the m^{6}A level and its regulators in esophageal cancer (ESCA) remain poorly understood. In this study, we analyzed the expression of m^{6}A regulators using The Cancer Genome Atlas data and found 14 of 19 m^{6}A regulators are significantly increased in ESCA samples. Then we performed a univariate Cox regression analysis and LASSO (least absolute shrinkage and selection operator) Cox regression model to investigate the prognostic role of m^{6}A regulators in ESCA, and the results indicated that a two-gene prognostic signature including ALKBH5 and HNRNPA2B1 could predict overall survival of ESCA patients. Moreover, HNRNPA2B1 is higher expressed in high-risk scores subtype of ESCA, indicating that HNRNPA2B1 may be involved in ESCA development. Subsequently, we confirmed that the level of m^{6}A and HNRNPA2B1 was significantly increased in ESCA. We also found that HNRNPA2B1 expression positively correlated with tumor diameter and lymphatic metastasis of ESCA. Moreover, functional study showed that knockdown of HNRNPA2B1 inhibited the proliferation, migration, and invasion of ESCA. Mechanistically, we found that knockdown of HNRNPA2B1 inhibited the expression of *de novo* fatty acid synthetic enzymes, ACLY and ACC1, and subsequently suppressed cellular lipid accumulation. In conclusion, our study provides critical clues to understand the role of m^{6}A and its regulators in ESCA. Moreover, HNRNPA2B1 functions as an oncogenic factor in promoting ESCA progression via up-regulation of fatty acid synthesis enzymes ACLY and ACC1, and it may be a promising prognostic biomarker and therapeutic target for human ESCA.

Keywords: m^{6}A, esophageal cancer, HNRNPA2B1, fatty acid synthesis, ACLY, ACC1

INTRODUCTION

Esophageal cancer (ESCA) is one of the major malignant cancers that threatened human health worldwide (1, 2). Esophageal squamous cell carcinoma (ESCC) and esophageal adenocarcinoma (EAC) are the two common subtypes of ESCA, especially the ESCC accounting for 80% in China (3). Over the last several decades, improved treatments have prolonged the survival of ESCA patients diagnosed at an early stage; however, most ESCA patients are first diagnosed at an advanced stage with malignant proliferation and metastasis (4). Surgical resection combined with radiotherapy and chemotherapy has improved the prognosis of ESCA patients, but the overall 5-year survival rate remains extremely poor (5). Therefore, identifying novel biomarkers and therapeutic targets for ESCA patients is an urgent need.

It is well-known that lots of chemical modifications on human RNA were involved in the development of human diseases, including cancer (6, 7). Recent studies reveal that N6-methyladenosine (m^{6}A) modification is the most abundant modification involved in the progression of different cancers (6, 8–10). The m^{6}A modification accounts for ∼0.1–0.4% of adenosine on isolated mammals RNA (6, 11). The level of m^{6}A is reversible and dynamic, which could be installed by m^{6}A methyltransferases (writers) or removed by m^{6}A demethylases (erasers). In addition, the specific RNA-binding proteins (readers) could recognize and bind to m^{6}A motif, regulating RNA metabolism, including RNA stability, degradation, splicing, transport, localization, translation, and others (9, 12). Lots of studies have shown that the writers, erasers, and readers are closely associated with the characteristics of cancer, including tumor proliferation, apoptosis, metastasis, angiogenesis, drug resistance, energy metabolism, and cancer stem cell (6, 8, 13–16). Despite the function of m^{6}A modification and its regulators in different malignant cancers have been reported, its role in ESCA has not been studied so far.

Abbreviations: HR, hazard ratio; CI, confidence interval; ESCA, esophageal cancer; m^{6}A, N6-methyladenosine; TCGA, The Cancer Genome Atlas; METTL3, methyltransferase-like 3; METTL14, methyltransferase-like 14; METTL16, methyltransferase-like 16; WTAP, WT1 associated protein; KIAA1429, VIRMA, vir like m^{6}A methyltransferase associated; RBM15, RNA binding motif protein 15; ZC3H13, zinc finger CCCH-type containing 13; FTO, FTO alpha-ketoglutarate dependent dioxygenase; ALKBH5, alkB homolog 5, RNA demethylase; YTHDC1/2, YTH domain-containing protein 1/2; YTHDF1/2/3, YTH N6-methyladenosine RNA binding protein 1/2/3; IGF2BP1/2/3, insulin like growth factor 2 mRNA binding protein 1/2/3; HNRNPA2B1, heterogeneous nuclear ribonucleoprotein A2/B1; HNRNPC, heterogeneous nuclear ribonucleoprotein C. OS, overall survival; ESCC, Esophageal squamous cell carcinoma; EAC, esophageal adenocarcinoma; PPI, protein-protein interaction; OS, overall survival; LASSO, least absolute shrinkage and selection operator; ROC, Receiver operating characteristic; TMA, tissue microarray; IHC, Immunohistochemistry; AUC, area under the ROC curve; MKI67, marker of proliferation Ki-67; PCNA, proliferating cell nuclear antigen; SOX4, SRY-box transcription factor 4; BRAP, BRCA1 associated protein; FASN, fatty acid synthase; ACLY, ATP citrate lyase; SCD1, stearoyl-Coenzyme A desaturase 1; ACC1, acetyl-CoA carboxylase alpha; MCAD, acyl-CoA dehydrogenase medium chain; CD36, CD36 molecule; FABP5, fatty acid binding protein 5; KEGG, Kyoto Encyclopedia of Genes and Genomes; qRT-PCR, Quantitative real-time RT-PCR; OA, oleate.

In the present study, we systematically analyzed the expression of 19 m^{6}A RNA regulators in ESCA using The Cancer Genome Atlas (TCGA) dataset, as well as their association with the clinicopathological characteristics. After a comprehensive analysis, we found that HNRNPA2B1 may play a key role in ESCA development. Subsequently, we found that the levels of m^{6}A and its regulator HNRNPA2B1 were significantly increased in ESCA, and HNRNPA2B1 acts an oncogenic role in the progression of ESCA cells, indicating that it may be a promising prognostic biomarker and therapeutic target for human ESCA.

MATERIALS AND METHODS

Selection of m^{6}A RNA Methylation Regulators

Previous studies have reported the bioinformatics analysis of total 13 m^{6}A-related genes in gastric cancer (17), bladder cancer (18), and other cancers (19, 20). In our study, a total of 19 m^{6}A RNA methylation regulators were included for systematically analysis based on the recent the m^{6}A review (9).

Bioinformatics Analysis

The RNA-seq transcriptome data and clinical information of ESCA patients were obtained from TCGA (https://cancergenome.nih.gov/). All 19-gene expression data are downloaded via the R package "TCGA-Assembler." The expression of 19 m^{6}A-related genes in 160 ESCA tissues and 11 normal esophageal tissues was analyzed via limma package. Next, the violin map was used to visualize the expression of 19 genes in 160 ESCA tissues and 11 normal tissues. We then used the STRING database (http://string-db.org) to analyze the protein–protein interaction (PPI) among 19 m^{6}A regulators. The correlation analysis of 19 m^{6}A regulators was further analyzed by Pearson correlation analysis. To evaluate the association between the expression of m^{6}A regulators and prognosis of ESCA patients, the ESCA cohort was clustered into different groups through consensus clustering analysis with "ConsensusClusterPlus" in R (21). The overall survival (OS) difference was calculated by the Kaplan–Meier method and log-rank test. A χ^2-test was used to compare the distribution of age, gender, grade, and stage between different clusters. Univariate Cox analysis was performed to evaluate the correlation between m^{6}A regulators and OS of ESCA patients using survival analysis in R. Two m^{6}A genes were selected for further analysis, and a risk signature was developed using the least absolute shrinkage and selection operator (LASSO) Cox regression algorithm. The formula of the risk score for ESCA patients' prognosis prediction was as follows: risk score = the sum of each multivariate cox regression coefficient ratio of mRNA multiple each expression of mRNA. Based on the median risk score, we divided the patients into high- and low-risk subgroups. Each patient's survival status, death time, and gene expression profile in two subgroups were presented via "heatmap" and "survival" R packages (22). Besides, the Kaplan–Meier curve analysis was performed, and the receiver operating characteristic (ROC) curve was drawn to estimate the sensitivity and specificity of the prognostic signature. The ESCA cohort was divided into high-

and low-risk group based on the median value of the risk scores. OS between different clusters or groups was calculated by the Kaplan–Meier method. ROC curve was constructed to evaluate the prediction accuracy of ESCA prognosis (22). The distribution of clinicopathological parameters between high- and low-risk group was analyzed through χ^2-test. Univariate and multivariate Cox regression analyses were used to identify the independent prognostic factors.

ESCC Tissue, Tissue Microarray, and Cell Culture

Eighteen pathologically confirmed ESCC tissues from recent patients at the Nanjing Drum Tower Hospital, the Affiliated Hospital of Nanjing University Medical School (Nanjing, Jiangsu, China), were obtained after signed informed consent. The ESCC tissue microarray (TMA, 34 cases) was obtained from servicebio (Wuhan, Hubei, China). Immunohistochemistry (IHC) was performed according to standard procedures as described previously (8, 23). Institutional approval was obtained from the Review Board of Nanjing Drum Tower Hospital prior to this study. Human esophageal epithelial cell line HEEpiC and ESCC cell lines (ECA109 and TE10) were purchased from the Type Culture Collection of the Chinese Academy of Sciences (Shanghai, China). All cells were cryopreserved at −80°C using CELLSAVING (C40100, New Cell & Molecular Biotech, China). All cell lines were cultured in RPMI-1640 medium supplemented with 100 μg/mL streptomycin, 100 U/mL penicillin, and 10% fetal bovine serum (FBS). Oleate (OA) was obtained from Sigma.

siRNA Constructs and Transfection

The two specific HNRNPA2B1 siRNAs were designed and synthesized by RiboBio (Guangzhou, China): the sequence of si-HNRNPA2B1#1: GGAGAGTAGTTGAGCCAAA and the sequence of si-HNRNPA2B1#2: GCTACGGAGGTGGTTATGA. The HNRNPA2B1 siRNAs and corresponding control siRNA were transfected into the ESCC cells by DharmaFECT4 (Dharmacon, Chicago, IL).

Dot Blot Assay

The dot blot assay was performed according to the bio-protocol database (https://en.bio-protocol.org/e2095). The experiments procedures have been described previously (8).

Western Blot Assay

Western blot assays were performed as previously reported (23). The following antibodies were used: anti-GAPDH (1:2,000; Beyotime, Shanghai, China) and anti-HNRNPA2B1 (1:1,000, Proteintech Group, Rosemont, IL, USA). Phenylmethylsulfonyl fluoride used in Western blot assay was from Selleck (Houston, TX, USA).

Quantitative Real-Time Reverse Transcription–Polymerase Chain Reaction Assay

Total RNA was extracted from cells or tissues using TRIzol reagent (Invitrogen, Carlsbad, CA, USA). Reverse transcription (RT) was performed with HiScript Q RT SuperMix for qPCR (Vazyme, Jiangsu, China). RT–polymerase chain reaction (PCR) was performed with an SYBR Green PCR Kit (Vazyme, Jiangsu, China) on an Applied Biosystems 7900HT sequence detection system (Applied Biosystems), with triplicate reactions. The primers used are listed in **Supplementary Table 1**.

Proliferation Assay

For CCK8 assay, after the cells were transfected for 48 h, the cells were plated at a density of 2,000 cells per well in 96-well-plates. After 72 h, cell viability was determined using CCK-8 assay according to the manufacturer's instructions (APExBIO, Houston, TX, USA).

For clonogenic assay, after the cells were transfected for 48 h, the cells were seeded at a density of 500 cells per well in 12-well-plates and incubated at 37°C for 10–14 days. Then, cells were fixed with methanol for 30 min and stained with crystal violet (Beyotime, Shanghai, China) for 30 min.

For EdU assay, the cells were plated at a density of 10,000 cells per well in 96-well-plates, and the cells were transfected for 48 h. The cell immunofluorescence was determined by the EdU kit according to the manufacturer's instructions (RiboBio, Guangzhou, China). Images of the cells were acquired with a Leica DMi8 system.

Cell Mobility Assay

For wound-healing assay, the transfected cells were grown to confluence in a 12-well-plate. Next, the cells were cultured in RPMI-1640 with 1% FBS for 12 h. The confluent monolayer was then disrupted with a cell scraper and filmed at the indicated hours via Leica DMi8 system. The rate of wound closure was calculated as the ratio of the average distance between the two wound edges and the total cell duration of migration.

For Transwell assay, the transfected cells in 100 μL of serum-free medium were seeded in the upper chambers coated with or without 50 μL of Matrigel (BD Biosciences), and 600 μL of culture medium containing 10% FBS was placed in the lower chambers. After 12 h of incubation at 37°C, cells that migrated to the bottom of the membrane were fixed with 4% paraformaldehyde for 30 min, stained with crystal violet (Beyotime, Shanghai, China) for 30 min, and imaged.

Nile Red Staining

The transfected cells were fixed in 4% paraformaldehyde solution on the 12-well-plates, stained with 0.05 μg/mL Nile red (Sigma, USA) for 10 min, washed with phosphate-buffered saline twice, and then stained with DAPI (Beyotime, Shanghai, China). Images of the cells were acquired with a Leica DMi8 system.

Statistical Analyses

The expression of 19 m^{6}A-related genes in ESCA tissues and normal tissues from TCGA dataset was analyzed via one-way analysis of variance. Kolmogorov–Smirnov test was used to analyze the relationship between m^{6}A-related genes and clinicopathological characteristics. The median risk score was used as a cutoff value to divide into a high- and a low-risk group. OS was analyzed between different groups through the Kaplan–Meier method. The relationship between the risk score

and clinicopathological variables was analyzed through χ^2-test. Functional experiments were performed at least three times. The representative data shown are means ± SD; $P < 0.05$ was considered statistically significant.

RESULTS

The Expression and Correlation of m^{6}A RNA Methylation Regulators in ESCA

First, we analyzed the level of 19 m^{6}A RNA methylation regulators (7 writers, 2 erasers, and 10 readers) in ESCA tissues and normal tissues from TCGA dataset (**Figure 1A**). We found that 14 of 19 m^{6}A-related genes were significantly increased in ESCA tissues compared with the normal tissues through heatmap visualization (**Figure 1B**). The expression levels of five writers (METTL16, WTAP, METTL3, KIAA1429, and RBM15) and nine readers (YTHDF1/2/3, YTHDC1, IGF2BP1/2/3, HNRNPC, and HNRNPA2B1) were significantly up-regulated in ESCA tissues, whereas no significant difference was found for the two erasers (FTO and ALKBH5) (**Figure 1C**). We further analyzed the interaction among the 19 m^{6}A-related genes using PPI network, and KIAA1429 and METTL14 seemed to be the center in the interaction network (**Supplementary Figure 1A**). Using Pearson correlation analysis, we found the correlation between 19 m^{6}A-related genes was weak, and it was shown that KIAA1429 is most correlated with YTHDF3 (**Supplementary Figure 1B**).

Identification of Prognostic Signature Among m^{6}A Regulators in ESCA

Next, the consistent clustering analysis was carried out based on the expression similarity of m^{6}A-related genes in ESCA from TCGA dataset. The $k = 2$ seemed to be the most appropriated selection to cluster the patients into two subgroups (cluster 1 and cluster 2) (**Supplementary Figures 2A–D**). Moreover, we analyzed the clustering result and clinical outcomes, and the results showed that cluster 1 subgroup had a shorter OS than cluster 2 subgroup, although it showed a borderline statistical significance ($P = 0.064$) (**Supplementary Figure 2E**).

To better understand the role of the 19 m^{6}A regulators in the prognosis of ESCA patients, univariate Cox regression was used to analyze the expression of m^{6}A-related genes associated with OS in ESCA TCGA dataset. The results demonstrated that high expression of ALKBH5 was significantly correlated with good OS [$P = 0.005$, hazard ratio (HR) = 0.949, 95% confidence interval (CI) = 0.915–0.984], but high expression of HNRNPA2B1 was associated with poor OS ($P = 0.013$, HR = 1.012, 95% CI = 1.002–1.022) (**Figure 2A**). Furthermore, we applied the LASSO Cox regression algorithm to establish the risk signature, and two genes (low of ALKBH5 and high of HNRNPA2B1) were selected to build the risk signature according to the minimum criteria and the coefficients (**Supplementary Figures 3A,B**). Then, we analyzed the correlation of HNRNPA2B1 expression with ALKBH5 via online bioinformatics tool (http://gepia.cancer-pku.cn/). The results showed that the expression of HNRNPA2B1 was significantly positively correlated with the expressions of ALKBH5 (**Supplementary Figure 3C**). In order to analyze the prognostic role of the two-gene risk signature, the ESCA patients in TCGA dataset were separated into low- and high-risk groups based on the median risk score, and the results indicated that the high-risk group has a worse survival compared to low-risk groups, although it showed a borderline statistical significance ($P = 0.05501$) (**Figure 2B**). However, the risk score of the signature of ALKBH5 and HNRNPA2B1 was more significantly associated with poor OS ($P < 0.001$, HR = 10.239, 95% CI = 3.737–28.053) than individual ALKBH5 or HNRNPA2B1 by univariate Cox regression, suggesting that the risk signature of them is more reliable for OS prognosis (**Figure 2C**). Furthermore, we found that patients with low level of ALKBH5 suffer a poor OS ($P = 0.016$), whereas whose with a high level of HNRNPA2B1 suffer a poor OS ($P = 0.027$; **Figure 2D**). When combining ALKBH5 and HNRNPA2B1 as a new variable, ESCA patients were divided into three subgroups according to the median of each expressed value: high level of ALKBH5 and low level of HNRNPA2B1, low level of ALKBH5 and high level of HNRNPA2B1, and both of high ALKBH5/ HNRNPA2B1 expression and low ALKBH5/ HNRNPA2B1 expression. Kaplan–Meier curves demonstrated that the subgroup of high level of ALKBH5 and low level of HNRNPA2B1 was much more favorable to the OS than the subgroup of low level of ALKBH5 and high level of HNRNPA2B1 ($P = 0.002$; **Figure 2E**). Moreover, ROC curve was applied to predict the survival rates for ESCA patients using two-gene signature risk scores in different years (**Supplementary Figures 3D–H**); the results indicated that it has a good predictive efficiency with the area under the ROC curve within 2, 4, or 5 years (**Supplementary Figures 3E, G–H**), whereas the result did not show robust prediction within 4 and 5 years (**Supplementary Figures 3G,H**).

Validation of the Clinical Relevance of Two-Gene Signature

To better understand the clinical relevance of two-gene signature in ESCA, we first selected the patients with clinical characteristic variables and divided these patients into low- and high-risk groups, which were assessed by two-gene expression and clinical characteristic variables (**Figure 3A**). Interestingly, we found the most individuals with relative lower expression of ALKBH5 and higher expression of HNRNPA2B1 in the high-risk group, suggesting the risk was associated with the gene expression (**Figure 3A**). Simultaneously, univariate Cox regression analysis revealed that N stage, stage, and risk score (ALKBH5/HNRNPA2B1 signature) were significantly related with OS of ESCA, and multivariate Cox regression analysis showed that only risk score were an independent prognostic factor for OS of ESCA patients (**Figures 3B,C**).

The Correlation Between HNRNPA2B1 and Clinicopathological Features

Considering that the expression of HNRNPA2B1 is significantly increased in ESCA, while ALKBH5 had no significant difference between ESCA tissues and normal control tissues (**Figure 1C**), which suggest that HNRNPA2B1 may be involved in ESCA

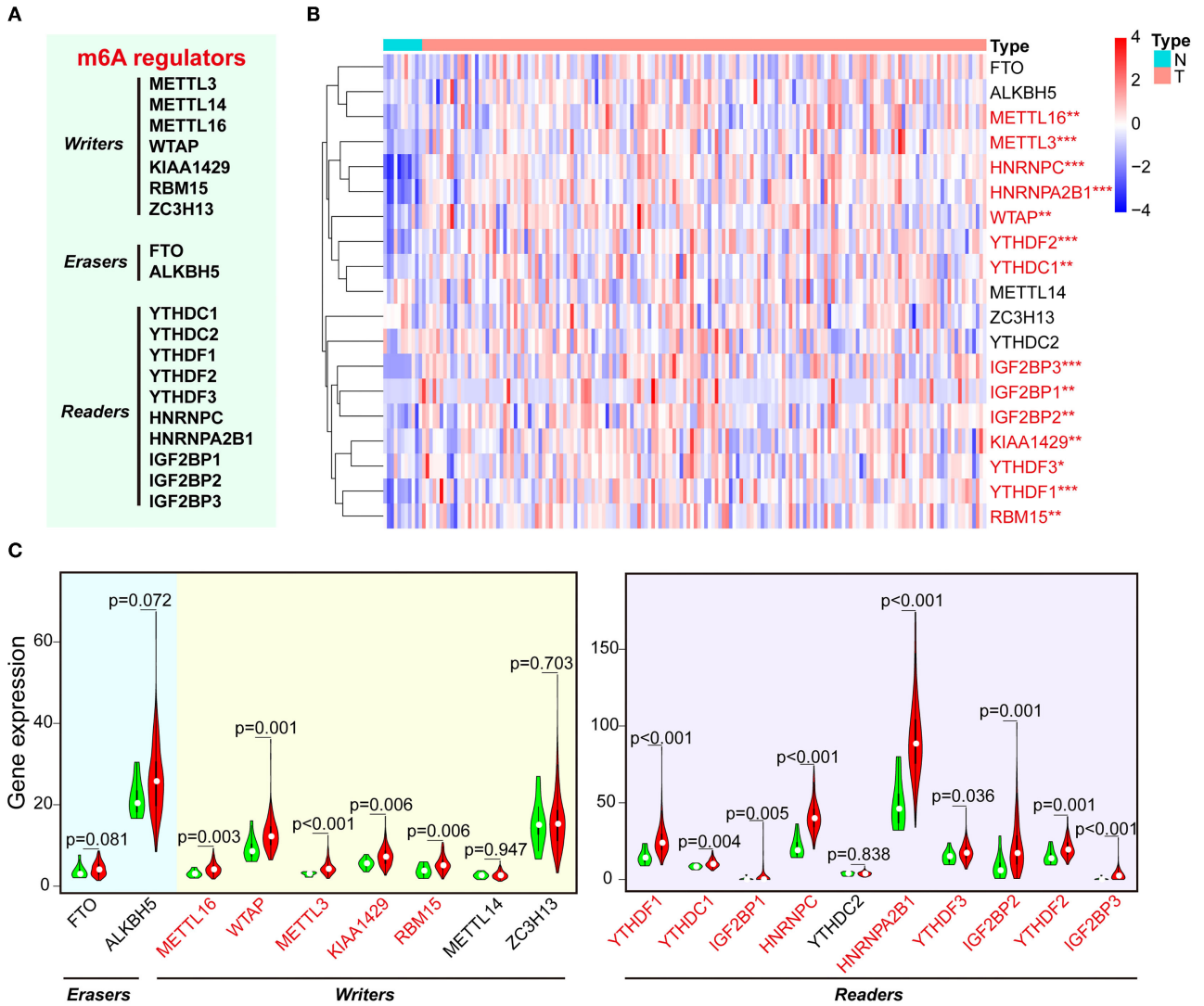

FIGURE 1 | The expression of m^{6}A-related regulators in ESCA and normal control samples of TCGA. **(A)** The list of m^{6}A RNA methylation–related writers, erasers, and readers. **(B)** The expression levels of 19 m^{6}A-related genes in ESCA were displayed via heatmap. N, non-tumor tissues; T, tumor tissues. **(C)** Violplot visualizing the expression of m^{6}A-related genes in ESCA. Green color represents non-tumor tissues, and the red color represents tumor tissues. $^*P < 0.05$, $^{**}P < 0.01$, and $^{***}P < 0.001$.

development. We then perform a comprehensive analysis the HNRNPA2B1 expression in different subgroups based on relative clinical characteristics including tumor histology, cancer stage, tumor grade, gender, age, and patient's weight via online bioinformatics tool (http://ualcan.path.uab.edu/index.html). Compared with the normal subgroup, the HNRNPA2B1 expression was significantly up-regulated ($P < 0.05$) in cancer patients with different clinical characteristics (**Figures 4A–F**). In the ESCA patients, it showed that the HNRNPA2B1 expression between ESCC and EAC had no significant difference (**Figure 4A**). It also showed that the HNRNPA2B1 expression was not related with gender in ESCA patients (**Figure 4D**). However, the expression of HNRNPA2B1 significantly increased in the advanced stage and grade (**Figures 4B,C**). Interestingly, the expression of HNRNPA2B1 was dramatically increased in the young ESCA patients (**Figure 4E**). Meanwhile, the expression level of HNRNPA2B1 was significantly higher in extreme obese subgroup than other subgroups (**Figure 4F**), indicating that HNRNPA2B1 may be associated with fatty acid metabolism in ESCA cells.

The m^{6}A Level and HNRNPA2B1 Expression Are Increased in ESCC

To elucidate the m^{6}A modification in ESCC, we first examined the m^{6}A RNA levels in 18 ESCC tissues and paired normal tissues. We found that the m^{6}A RNA levels were significantly higher in ESCC tissues via dot blot assay (**Figure 5A**). Next, we compared the mRNA levels of HNRNPA2B1 in 18 pairs

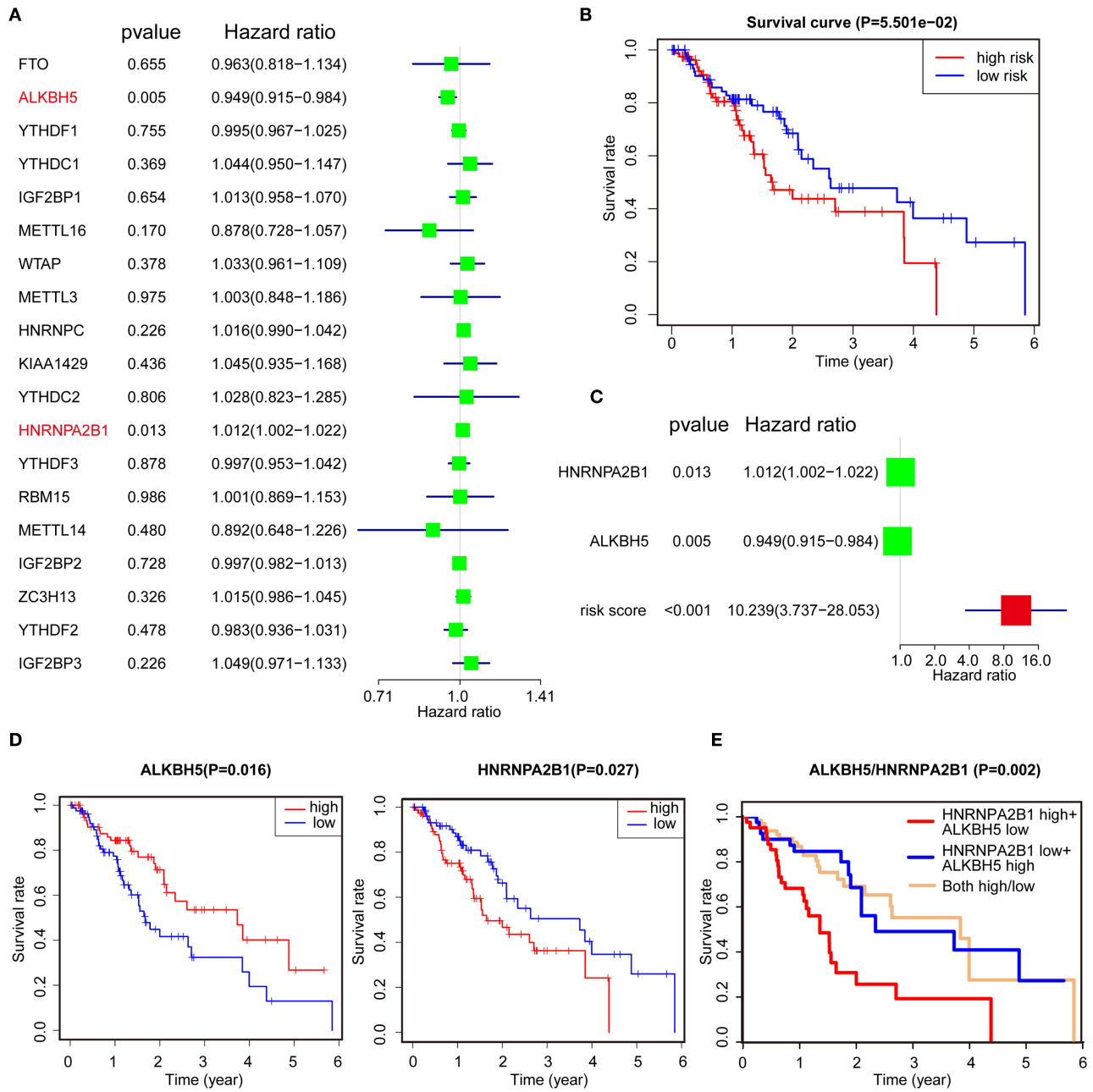

FIGURE 2 | Identification of prognostic signature among m^{6}A regulators. **(A)** Identification of the m^{6}A-related genes that significantly correlated with OS via univariate analysis. **(B)** Kaplan–Meier OS curves for ESCA patients assigned to high- and low-risk groups. **(C)** The risk signature of ALKBH5 + HNRNPA2B1 is more reliable for OS prognosis via univariate analysis. **(D,E)** Kaplan–Meier curves depicting OS according to the expression ALKBH5 or HNRNPA2B1 **(D)** and combined with ALKBH5/HNRNPA2B1 **(E)** based on TCGA data.

of ESCC and paired normal tissues. The results showed that the mRNA level of HNRNPA2B1 was significantly up-regulated in ESCC (**Figure 5B**). In addition, the HNRNPA2B1 mRNA and protein level were significantly increased in ESCC cell lines compared with that in normal esophageal epithelial cell lines (**Figures 5C,D**). To investigate the clinical implication of HNRNPA2B1 with ESCC, we performed IHC staining for HNRNPA2B1 in ESCC TMA. The results indicated that the HNRNPA2B1 level was increased in the tumor diameter of ESCC tissues $\geq$5 cm compared with that <5 cm (**Figure 5E**). Similarly, the levels of HNRNPA2B1 protein were also significantly elevated in ESCC tissues with lymph node metastasis than those without lymph node metastasis (**Figure 5F**). Moreover, we analyzed the correlation of HNRNPA2B1 expression with the

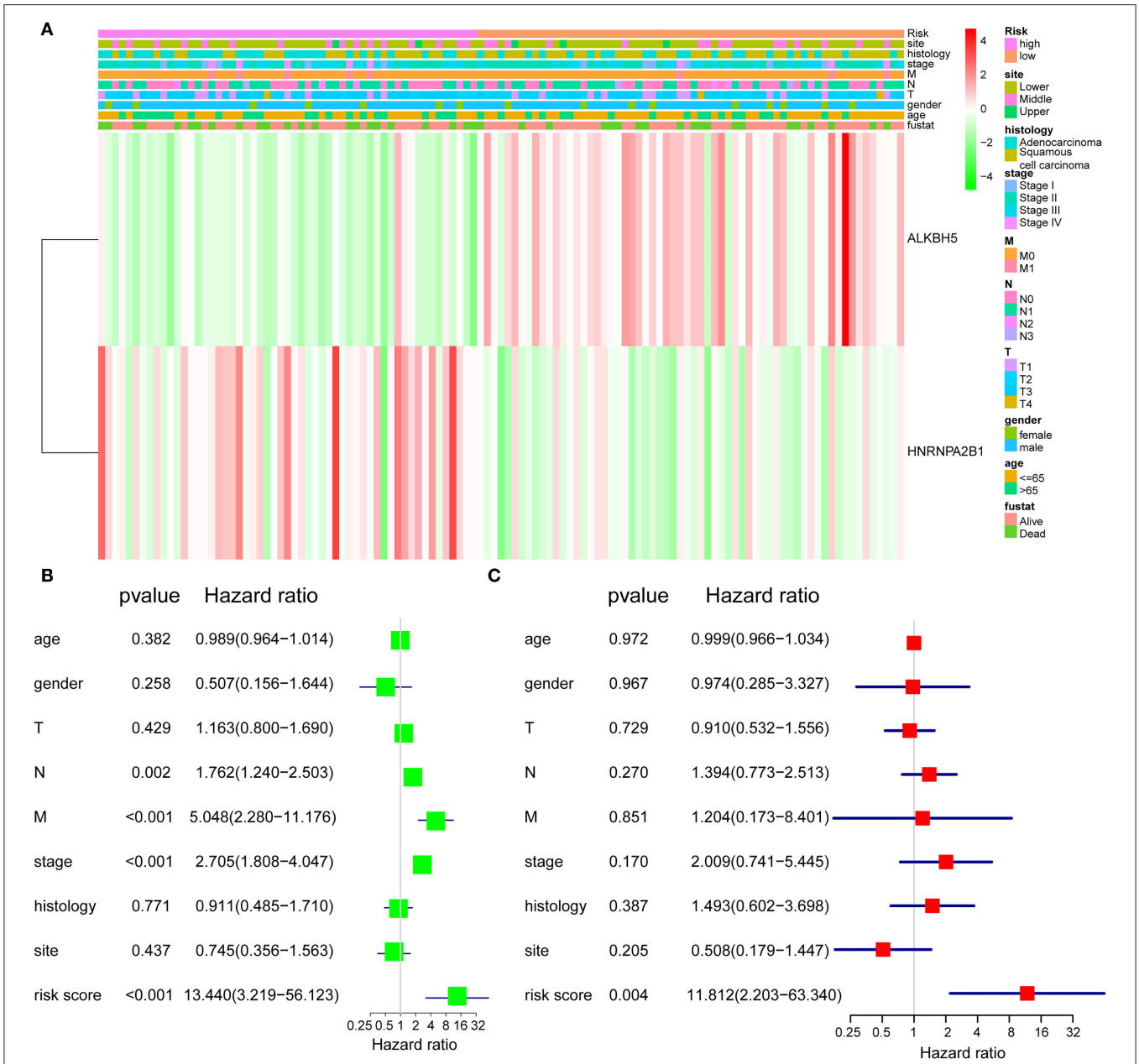

FIGURE 3 | Validation of the prognostic signature. **(A)** The expression levels of the HNRNPA2B1 and ALKBH5 in low- and high-risk ESCA patients. **(B)** Univariate Cox regression analyses of the association between clinicopathological factors and OS of ESCA patients. **(C)** Multivariate Cox regression analyses of the association between clinicopathological factors and OS of ESCA patients.

markers of proliferation and metastasis via online bioinformatics tool (http://gepia.cancer-pku.cn/). The results showed that the expression of HNRNPA2B1 was significantly positively correlated with the expressions of MKI67 and PCNA, which were the classic biomarkers of proliferative cancer cells (**Figure 5G**). The expression of HNRNPA2B1 was also significantly positively correlated with SOX4 and BRAP expressions, which were the biomarkers of ESCA metastasis (24, 25) (**Figure 5G**). Taken together, these results indicated that the levels of m^{6}A modification and its regulator HNRNPA2B1 are increased in ESCC, and HNRNPA2B1 may play a critical role in tumor growth and metastasis of ESCC.

HNRNPA2B1 Promotes ESCC Cell Proliferation

To further characterize the role of HNRNPA2B1 in ESCC, we designed and constructed two specific siRNAs to target HNRNPA2B1. The knockdown efficiency was confirmed

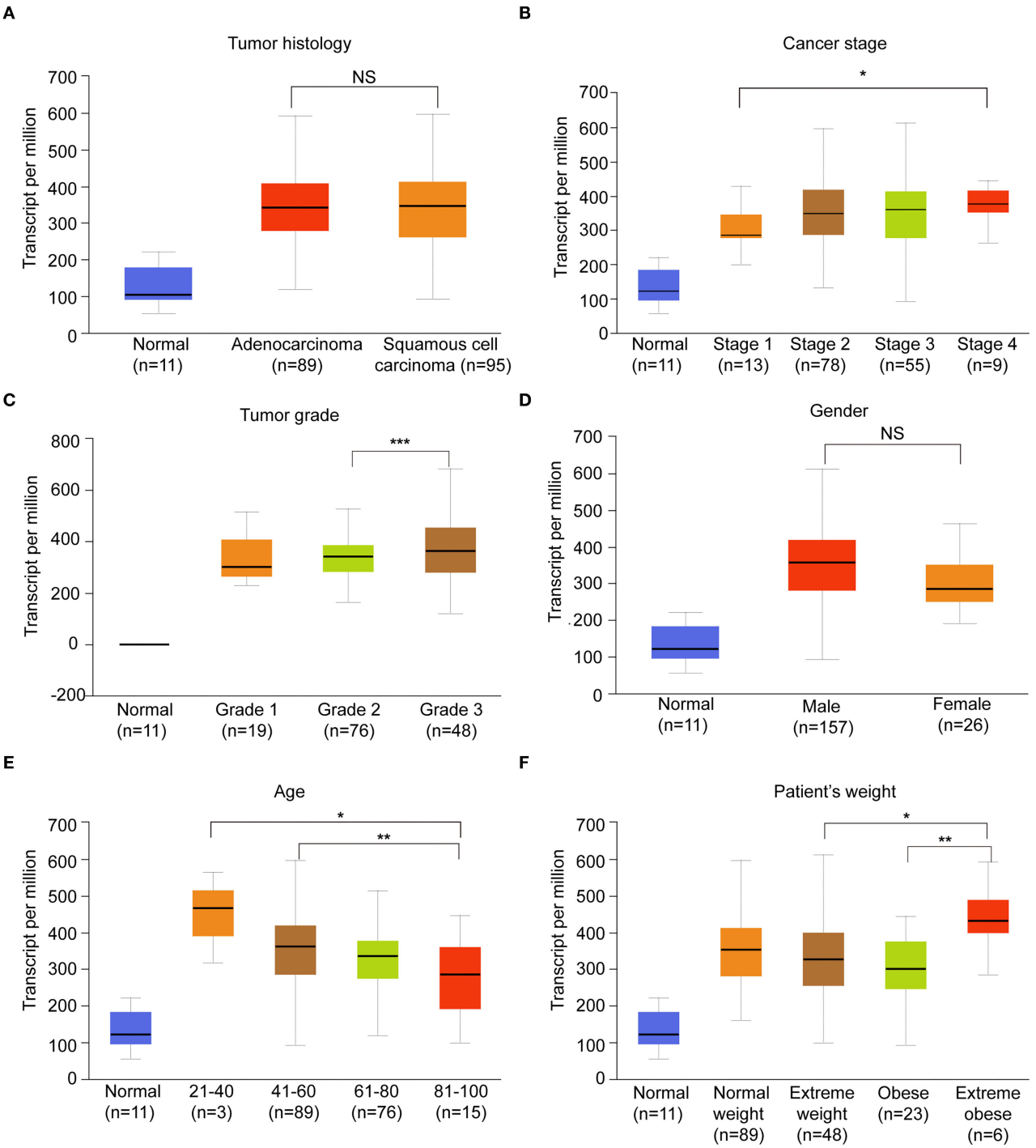

FIGURE 4 | The correlation between HNRNPA2B1 and clinicopathological features. **(A)** The expression of HNRNPA2B1 in ESCA patients of different tumor histology. **(B)** The expression of HNRNPA2B1 in ESCA patients of different cancer stage. **(C)** The expression of HNRNPA2B1 in ESCA patients of different tumor grade. **(D)** The expression of HNRNPA2B1 in ESCA patients of different gender. **(E)** The expression of HNRNPA2B1 in ESCA patients of different age. **(F)** The expression of HNRNPA2B1 in ESCA patients of different weight. *$P < 0.05$, **$P < 0.01$, and ***$P < 0.001$.

by qRT-PCR and Western blotting in two ESCC cells (**Figures 6A,B**). Knockdown of HNRNPA2B1 dramatically suppressed ESCC cell proliferation via CCK8 assay (**Figure 6C**). As shown in **Figure 6D**, knockdown of HNRNPA2B1 also significantly inhibited the ESCC cells colony formation. In addition, the EdU assay results also indicated that down-regulation of HNRNPA2B1 could inhibit cell proliferation in ESCC cells (**Figure 6E**).

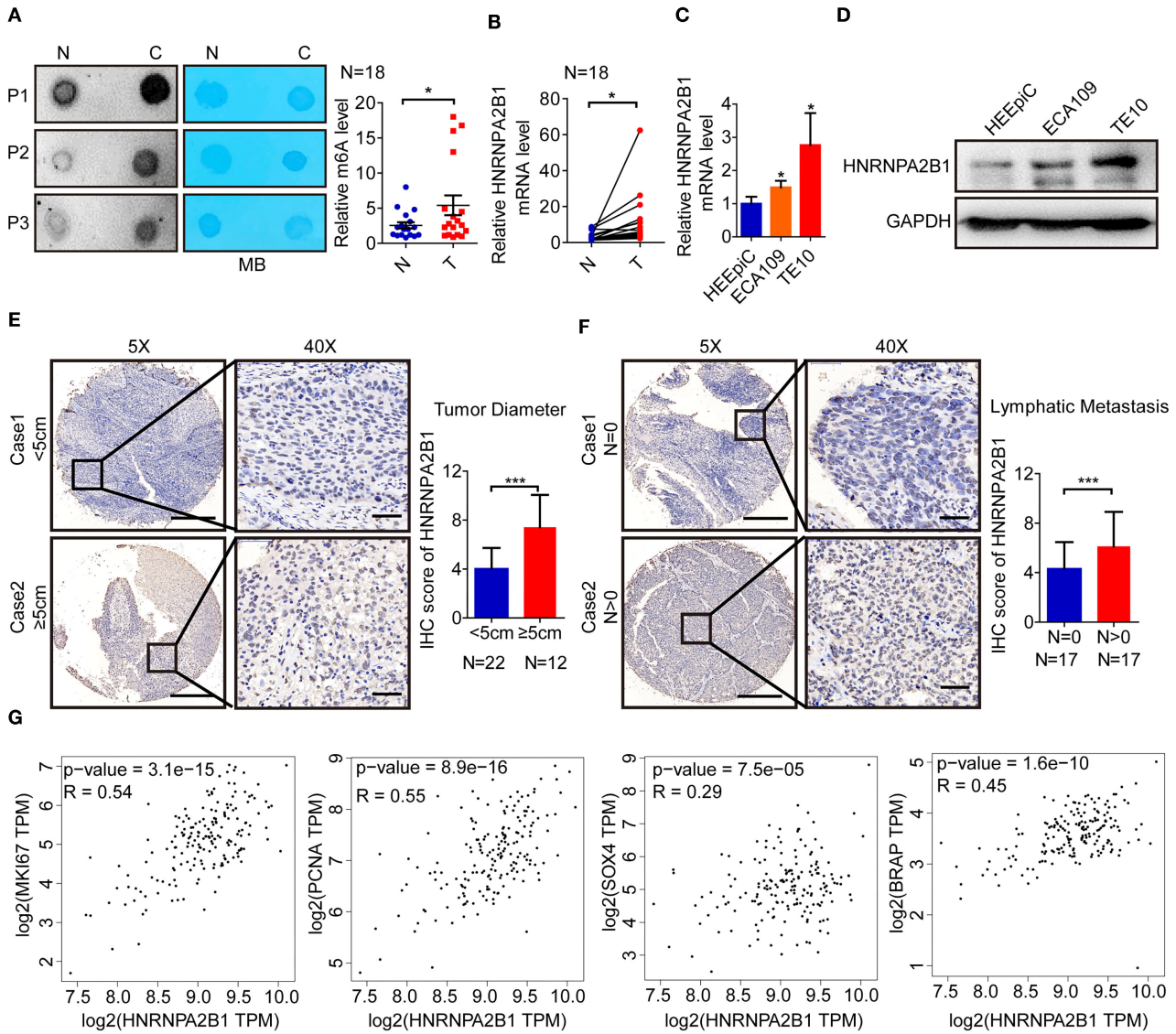

FIGURE 5 | The m^{6}A level and HNRNPA2B1 expression are increased in ESCC. **(A)** The mRNAs isolated from ESCC tissues and paired normal tissues were used in dot blot analyses with an anti-m^{6}A antibody, and methylene blue (MB) staining served as the loading control (left panel). The relative m^{6}A contents on mRNA in ESCC tissues and paired normal tissues were calculated (right panel, $N = 18$). **(B)** The levels of HNRNPA2B1 expression in ESCC and paired normal tissues were measured by qRT-PCR ($N = 18$). **(C)** The levels of HNRNPA2B1 expression in esophageal epithelial cell line (HEEpiC) and ESCC cell lines (ECA109 and TE10) were measured by qRT-PCR. **(D)** The levels of HNRNPA2B1 expression in esophageal epithelial cell line and ESCC cell lines were measured by Western blotting. **(E)** Representative IHC images on the TMA probed with the anti-HNRNPA2B1 antibody (scale bars = 500 or 50 μm, respectively, left panel) are shown. The IHC score of HNRNPA2B1 in ESCC tissues with tumor diameter <5 cm ($N = 22$) and ≥5 cm ($N = 12$) were calculated (right panel). **(F)** Representative IHC images on the TMA probed with the anti-HNRNPA2B1 antibody (scale bars = 500 or 50 μm, respectively, left panel) are shown. The IHC score of HNRNPA2B1 in ESCC tissues with lymphatic metastasis ($N = 17$) or without lymphatic metastasis ($N = 17$) were calculated (right panel). **(G)** The correlation of HNRNPA2B1 expression with the markers of proliferation and metastasis via online bioinformatics tool (http://gepia.cancer-pku.cn/) is analyzed. *$P < 0.05$, **$P < 0.01$, and ***$P < 0.001$.

HNRNPA2B1 Promotes ESCC Cell Migration and Invasion

Subsequently, we investigated the role of HNRNPA2B1 in mobility capacity of ESCC cells. The wound healing results showed that knockdown of HNRNPA2B1 suppressed the migration ability of ESCC cells (**Figures 7A,B**). In addition, the Transwell chamber assays also demonstrated that knockdown of HNRNPA2B1 significantly reduced the migration and invasion of ESCC cells (**Figures 7C,D**).

HNRNPA2B1 Accelerates Fatty Acid Synthesis in ESCC

To identify the molecular mechanism involved in HNRNPA2B1 promoting ESCC progression, we first analyzed the genes

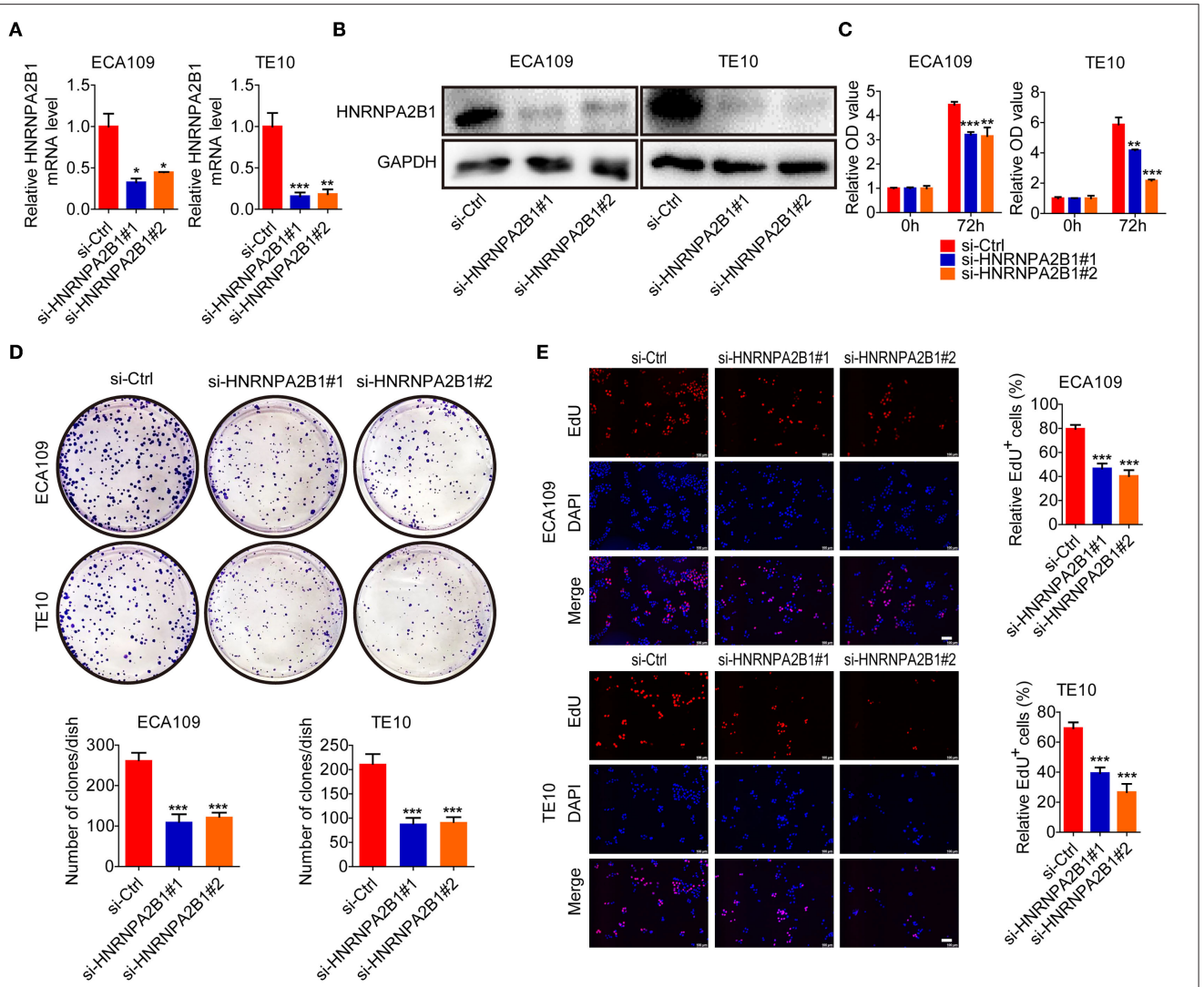

FIGURE 6 | HNRNPA2B1 promotes ESCC cell proliferation. **(A)** The HNRNPA2B1 knockdown efficiency was verified at the mRNA levels in ECA109 and TE10 cells by qRT-PCR assay. **(B)** The HNRNPA2B1 knockdown efficiency was verified at the protein levels in ECA109 and TE10 cells by Western blot assay. **(C)** CCK8 assays showed the growth of ECA109 and TE10 cells upon HNRNPA2B1 knockdown. **(D)** Knockdown of HNRNPA2B1 impaired the colony formation ability of ECA109 and TE10 cells (upper panel). Quantification of the colony formation assay results (bottom panel). **(E)** EdU assays showed the growth of ECA109 and TE10 cells upon HNRNPA2B1 knockdown (left panel). Quantification of the EdU-positive cell results (right panel). Scale bars, 100 μm. $^*P < 0.05$, $^{**}P < 0.01$, and $^{***}P < 0.001$.

correlated with HNRNPA2B1 expression in ESCA patients using TCGA data (**Supplementary Table 2**). Then we analyzed the pathway of these related genes via the Kyoto Encyclopedia of Genes and Genomes (KEGG) enrichment, which showed the pathways included Peroxisome Proliferator-Activated Receptors (PPAR) signaling pathway and fat digestion and absorption (**Figure 8A**). As shown in **Figure 4F**, it was suggested that the HNRNPA2B1 level was significantly higher in extreme obese subgroup than other subgroups. Therefore, we investigated whether HNRNPA2B1 could regulate fatty acid metabolism to promote ESCC malignant process. Next, we detected the major enzymes involved in *de novo* fatty acid synthesis, fatty acid β-oxidation and fatty acid uptake, revealing that *de novo* fatty acid synthetic enzymes ACLY, and ACC1 were markedly decreased when knockdown of HNRNPA2B1 in both two ESCC cells (**Figure 8B**). Moreover, we also found that the expression of HNRNPA2B1 was positively correlated with the expressions of ACLY and ACC1 in ESCA TCGA data via online bioinformatics tool (http://gepia.cancer-pku.cn/, **Figure 8C**). Meanwhile, knockdown of HNRNPA2B1 suppressed cellular lipid accumulation by staining Nile red in ESCC cells (**Figure 8D**). Further, we added OA (oleate) into ESCC cells (**Supplementary Figure 4A**), and the results showed that OA promoted ESCC cell proliferation, migration, and invasion, whereas knockdown of HNRNPA2B1 inhibited OA-induced the malignant process (**Figures 8E,F**). Collectively, the results reveal that HNRNPA2B1 functions as an oncogenic factor promoting ESCC progression via acceleration of fatty acid synthesis.

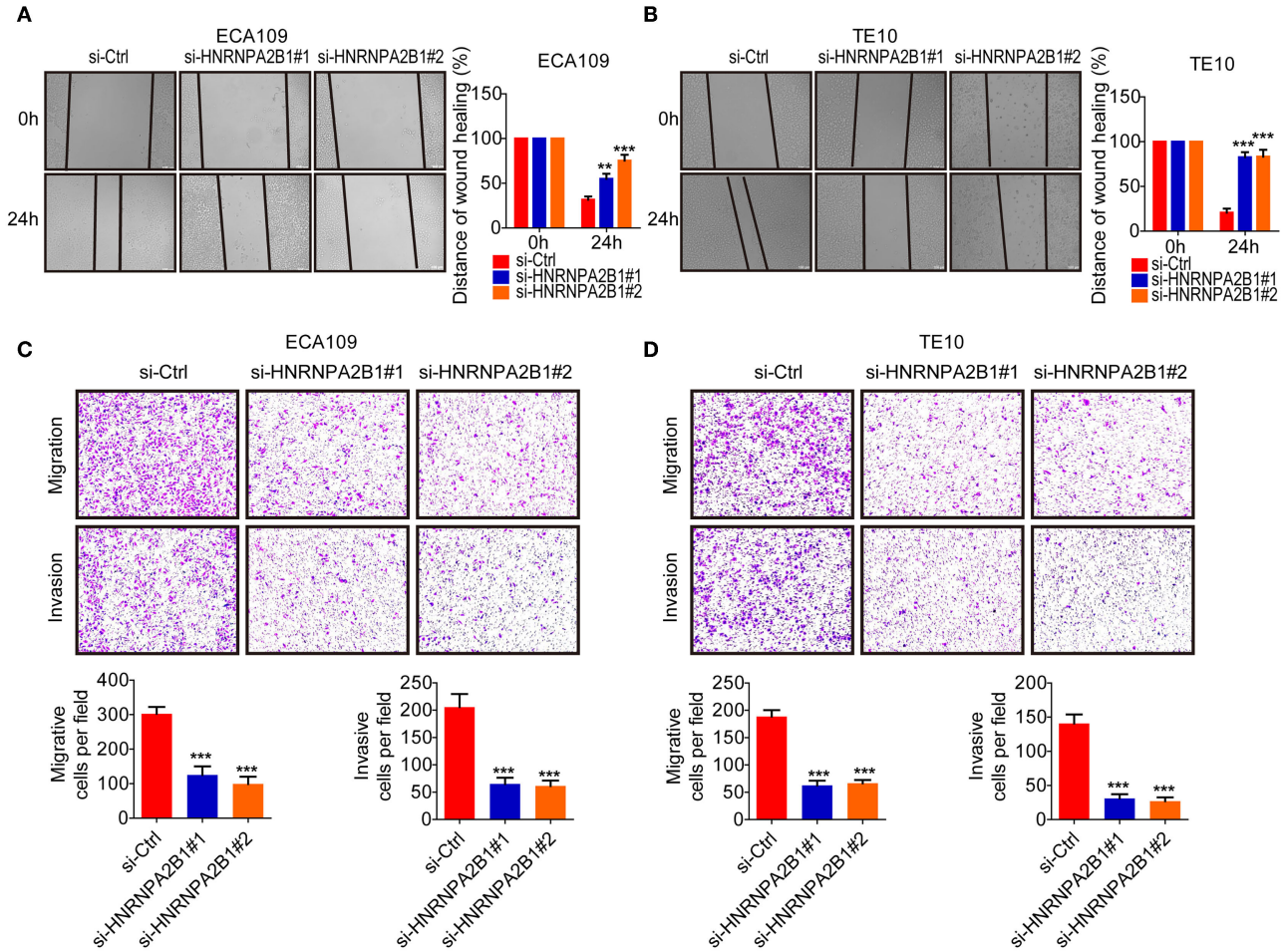

FIGURE 7 | HNRNPA2B1 promotes ESCC cell migration and invasion. **(A,B)** Knockdown of HNRNPA2B1 impaired the migration ability of ECA109 cells **(A)** and TE10 cells **(B)** via wound healing assay (left panel). Quantification of the wound healing assay results (right panel). **(C,D)** Knockdown of HNRNPA2B1 impaired the migration ability of ECA109 cells **(C)** and TE10 cells **(D)** via Transwell assay (upper panel). Quantification of the Transwell assay results (bottom panel). $^*P < 0.05$, $^{**}P < 0.01$, and $^{***}P < 0.001$.

DISCUSSION

ESCA, as a common digestive tract tumor, is a serious threat to human health and contributes to poor prognosis (2, 26). The significant regional difference is the main epidemiological characteristic of ESCA (27). There are two main subtypes in ESCA, called ESCC and EAC, respectively (27, 28). ESCC is mainly in the East Asian population, whereas EAC mainly occurs in Western countries (29). About half of the newly diagnosed ESCA cases in the world occur in China every year (30, 31). ESCA is considered to be a multifactor, multigene, and multistage complicated disease (27). Its occurrence is closely related to chronic nitrosamine stimulation, inflammation and trauma, genetic and epigenetic modification, and other factors (29, 32). Operation, radiotherapy, and chemotherapy are still the main treatment methods for ESCA, but inoperableness and radiochemotherapy resistance limit the clinical effect (29). Therefore, identification of new molecular markers and therapeutic targets is still an urgent need.

The m^{6}A modification has become a hot research topic in RNA modification–mediated epigenetic regulation, which was associated with the expression of gene and disease development, including cancer (33, 34). The m^{6}A modification is dynamically regulated via the methyltransferases and demethylases (12, 35). Meanwhile, the m^{6}A "readers" could recognize m^{6}A-modified sites and regulate RNA function. Recent studies have shown that m^{6}A modification and its regulators play an important role in various cancers (33). Previous study has systematically characterized the molecular alterations and clinical relevance of 20 m^{6}A RNA regulators across 33 cancer types, and they found that m^{6}A regulators were found to be potentially useful for prognostic stratification and identified IGF2BP3 as a potential oncogene across multiple cancer types (36). However, the m^{6}A level and its regulators in ESCA have not been systematically reported yet. In the present study, we demonstrated that the expression levels of five writers (METTL16, WTAP, METTL3, KIAA1429, and RBM15) and nine readers (YTHDF1/2/3, YTHDC1, IGF2BP1/2/3, HNRNPC, and HNRNPA2B1) were

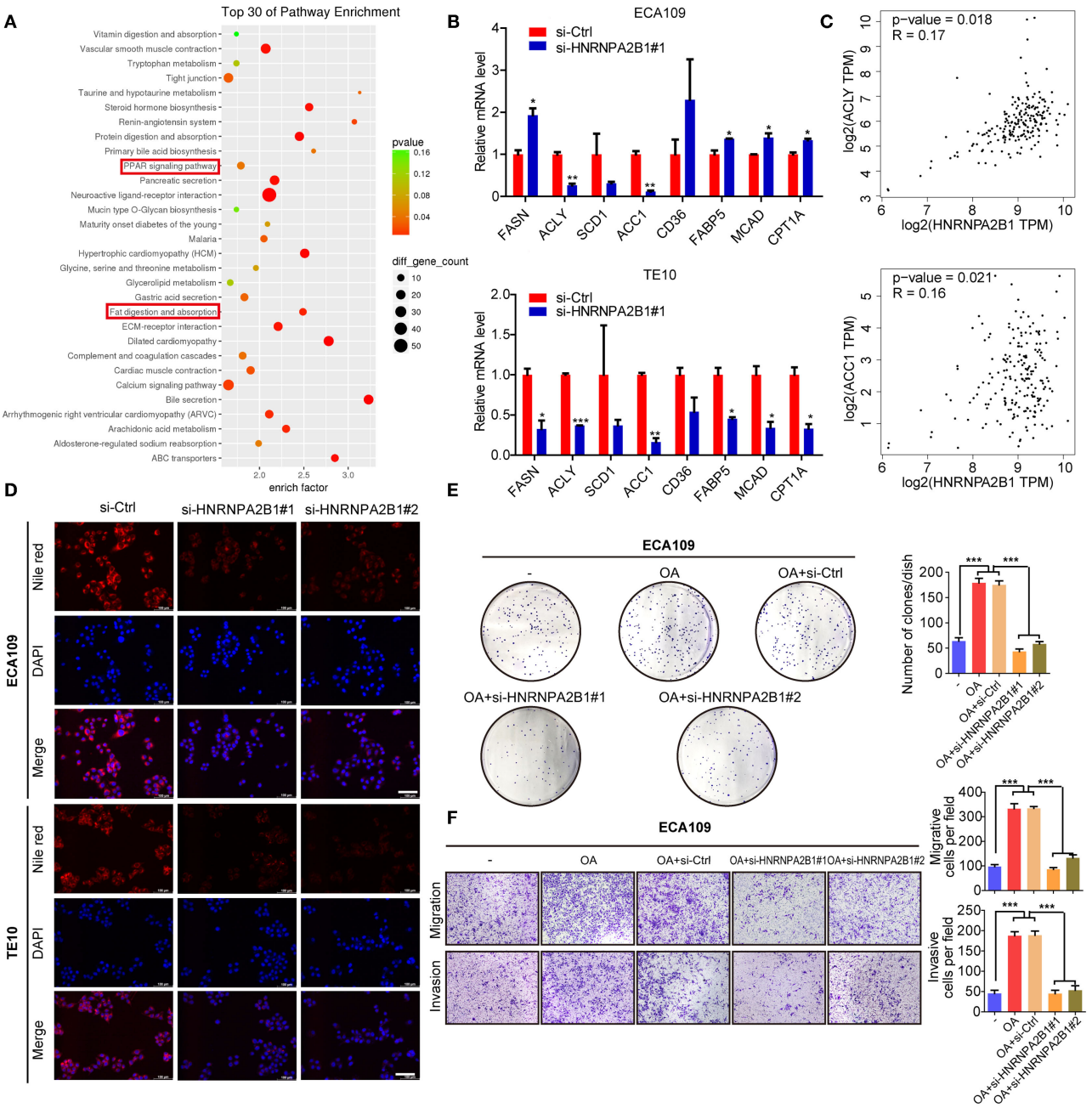

FIGURE 8 | HNRNPA2B1 promotes ESCC progression by regulation of fatty acid metabolism. **(A)** The genes correlated with HNRNPA2B1 expression in ESCA patients were analyzed using TCGA dataset and then the pathway of these genes via KEGG enrichment. **(B)** The mRNA levels of major enzymes in *de novo* fatty acid synthesis (FASN, ACLY, SCD1, and ACC1), fatty acid β-oxidation (MCAD and CPT1A), and fatty acid uptake (CD36 and FABP5) were detected in ECA109 and TE10 cells upon HNRNPA2B1 knockdown. **(C)** The correlations of HNRNPA2B1 expression with ACLY and ACC1 via online bioinformatics tool (http://gepia.cancer-pku.cn/) are analyzed. **(D)** Cellular neutral lipids were measured in ECA109 cells and TE10 cells upon HNRNPA2B1 knockdown by Nile red staining, Scale bars, 100 μm. **(E,F)** OA promoted ESCC cell proliferation, migration, and invasion, whereas knockdown of HNRNPA2B1 inhibited OA-induced ESCC cell proliferation, migration, and invasion. $^*P < 0.05$, $^{**}P < 0.01$, and $^{***}P < 0.001$.

significantly increased in ESCA tissues, whereas no significant difference was found for the two erasers (FTO and ALKBH5), and most of RNA m^{6}A regulators in our study were overlapped with the previous study (36). Meanwhile, we analyzed the PPI among 19 m^{6}A regulators, which could be systematically and directly helpful to analyze the interaction between these regulators. Herein, we found there are direct or indirect interactions among the 19 m^{6}A regulators, and the writers METTL3, METTL14, WTAP, and KIAA1429 and the erasers FTO and ALKBH5 may localized in the center of regulatory network. It was also

demonstrated that the relationship between most of the m^{6}A RNA methylation regulators is positively correlated, and the KIAA1429 and YTHDF3 genes are most relevant. Subsequently, we confirmed that the RNA m^{6}A levels were significantly higher in 18 cancerous tissues than corresponding normal tissues in ESCC patients via a dot blot assay. These results suggest that RNA m^{6}A modification may be involved in the ESCA development.

We then analyzed the relationship between RNA m^{6}A regulators and OS in ESCA via the consistent clustering analysis, and the results showed that cluster 1 had a shorter OS than cluster 2. In addition, the univariate Cox regression analysis and LASSO Cox regression data indicated that a two-gene prognostic signature including ALKBH5 and HNRNPA2B1 could predict OS of ESCA patients. Moreover, high expression of HNRNPA2B1 and low expression of ALKBH5 were indicated as the risk factor for the survival of ESCA, and the combination of these two factors showed more predictive potential than the alone, although the ROC curve did not show robust prediction within 4 and 5 years, which because of that there are too few patients in the fourth and fifth years, which may lead to the instability of the ROC curve. It is reported that HNRNPA2B1 could selectively bind to m^{6}A-containing transcripts via the "m^{6}A-switch," a mechanism in which m^{6}A weakens Watson–Crick base pairing to destabilize the RNA hairpin structure and thereby exposes the single stranded hnRNP binding motif (37). HNRNPA2B1 has been reported to be a RNA-binding protein involved in different cancer progression (38–40). HNRNPA2B1 could interact with LINC01234 to promote lung cancer progression (38). It also reported that HNRNPA2B1 promoted malignant capability and inhibited apoptosis via down-regulation of Lin28B expression in ovarian cancer (39). In this study, we also found that HNRNPA2B1 was significantly increased in cancerous tissues of ESCC using TCGA data, which was confirmed in our own samples. Furthermore, we found that HNRNPA2B1 expression positively correlated with tumor diameter and lymphatic metastasis of ESCC. Intriguingly, it was shown that knockdown of HNRNPA2B1 inhibited the proliferation, migration, and invasion of ESCC cell lines, which suggest that HNRNPA2B1 may be critical in the development and progression of ESCA.

Further, we analyzed the KEGG enrichment of genes, which were correlated with HNRNPA2B1 expression in ESCA patients using TCGA data. The data indicated that HNRNPA2B1 may be involved in fatty acid metabolism of ESCA. We also found that the HNRNPA2B1 level was significantly higher in extreme obese subgroup than other subgroups. The abnormal lipid metabolism of tumor cells is mainly manifested in the activation of *de novo* synthesis and oxidative metabolism of fatty acids, which provide the necessary raw materials for tumor cell proliferation (41, 42). The key enzymes related to lipid metabolism play a key role in the abnormal lipid metabolism of tumor cells (43, 44). Subsequently, we detected the expression of major enzymes involved in *de novo* fatty acid synthesis, fatty acid β-oxidation, and fatty acid uptake, revealing that *de novo* fatty acid synthetic enzymes ACLY and ACC1 were markedly positively regulated by HNRNPA2B1. However, the expression of FASN, fatty acid uptake, and fatty acid oxidation genes is inconsistent in the two ESCC cell lines with HNRNPA2B1 deficiency, which may be due to the heterogeneity of the two different ESCC cells. In addition, knockdown of HNRNPA2B1 suppressed cellular lipid accumulation. Collectively, the results reveal that HNRNPA2B1 could accelerate fatty acid synthesis via up-regulation of *de novo* fatty acid synthetic enzymes ACLY and ACC1.

In summary, our findings reveal that the levels of m^{6}A and its regulator HNRNPA2B1 were significantly increased in cancerous tissues of ESCA, and overexpression of HNRNPA2B1 promotes ESCA progression via up-regulation of *de novo* fatty acid synthetic enzymes ACLY and ACC1. Therefore, HNRNPA2B1 may be a promising prognostic biomarker and therapeutic target for human ESCA.

DATA AVAILABILITY STATEMENT

The raw data supporting the conclusions of this article will be made available by the authors, without undue reservation.

ETHICS STATEMENT

This study was approved by the Ethical Committee of Nanjing Drum Tower Hospital. Written informed consent to participate in this study was provided by the patients.

AUTHOR CONTRIBUTIONS

SW, QW, and XZ provided the direction of this manuscript. HG, BW, and KX collected and analyzed the data. LN and YF analyzed and evaluated the IHC of TMA. KX and ZW performed the experiments. QW wrote the manuscript. SW revised this manuscript. All authors read and approved the final manuscript.

FUNDING

This study was supported by the National Natural Science Foundation of China (81773383, 81370078, and 81903085); the Science Foundation for Distinguished Young Scholars of Jiangsu Province (BK20170047); the Fundamental Research Funds for the Central Universities (021414380439); and the Project funded by China Postdoctoral Science Foundation (2019M651808 and 2020T130291).

SUPPLEMENTARY MATERIAL

The Supplementary Material for this article can be found online at: https://www.frontiersin.org/articles/10.3389/fonc.2020.553045/full#supplementary-material

REFERENCES

1. Buckley AM, Lynam-Lennon N, O'Neill H, O'Sullivan J. Targeting hallmarks of cancer to enhance radiosensitivity in gastrointestinal cancers. *Nat Rev Gastroenterol Hepatol.* (2020) 17:298–313. doi: 10.1038/s41575-019-0247-2
2. Smyth EC, Lagergren J, Fitzgerald RC, Lordick F, Shah MA, Lagergren P, et al. Oesophageal cancer. *Nat Rev Dis Primers.* (2017) 3:17048. doi: 10.1038/nrdp.2017.48
3. Arnold M, Soerjomataram I, Ferlay J, Forman D. Global incidence of oesophageal cancer by histological subtype in 2012. *Gut.* (2015) 64:381–7. doi: 10.1136/gutjnl-2014-308124
4. Mannath J, Ragunath K. Role of endoscopy in early oesophageal cancer. *Nat Rev Gastroenterol Hepatol.* (2016) 13:720–30. doi: 10.1038/nrgastro.2016.148
5. van Rossum PSN, Mohammad NH, Vleggaar FP, van Hillegersberg R. Treatment for unresectable or metastatic oesophageal cancer: current evidence and trends. *Nat Rev Gastroenterol Hepatol.* (2018) 15:235–49. doi: 10.1038/nrgastro.2017.162
6. Huang H, Weng H, Chen J. m6A modification in coding and non-coding RNAs: roles and therapeutic implications in cancer. *Cancer Cell.* (2020) 37:270–88. doi: 10.1016/j.ccell.2020.02.004
7. Lee Y, Choe J, Park OH, Kim YK. Molecular mechanisms driving mRNA degradation by m6A modification. *Trends Genet.* (2020) 36:177–88. doi: 10.1016/j.tig.2019.12.007
8. Wang Q, Chen C, Ding Q, Zhao Y, Wang Z, Chen J, et al. METTL3-mediated m6A modification of HDGF mRNA promotes gastric cancer progression and has prognostic significance. *Gut.* (2019) 69:1193–205. doi: 10.1136/gutjnl-2019-319639
9. He L, Li H, Wu A, Peng Y, Shu G, Yin G. Functions of N6-methyladenosine and its role in cancer. *Mol Cancer.* (2019) 18:176. doi: 10.1186/s12943-019-1109-9
10. Wang Q, Geng W, Guo H, Wang Z, Xu K, Chen C, et al. Emerging role of RNA methyltransferase METTL3 in gastrointestinal cancer. *J Hematol Oncol.* (2020) 13:57. doi: 10.1186/s13045-020-00895-1
11. Desrosiers R, Friderici K, Rottman F. Identification of methylated nucleosides in messenger RNA from Novikoff hepatoma cells. *Proc Natl Acad Sci USA.* (1974) 71:3971–5. doi: 10.1073/pnas.71.10.3971
12. Yang Y, Hsu PJ, Chen YS, Yang YG. Dynamic transcriptomic m(6)A decoration: writers, erasers, readers and functions in RNA metabolism. *Cell Res.* (2018) 28:616–24. doi: 10.1038/s41422-018-0040-8
13. Zhu S, Wang JZ, Chen. He YT, Meng N, Chen M, Lu RX, et al. An oncopeptide regulates m(6)A recognition by the m(6)A reader IGF2BP1 and tumorigenesis. *Nat Commun.* (2020) 11:1685. doi: 10.1038/s41467-020-15403-9
14. Shen C, Xuan B, Yan T, Ma Y, Xu P, Tian X, et al. Hong, m6A-dependent glycolysis enhances colorectal cancer progression. *Mol Cancer.* (2020) 19:72. doi: 10.1186/s12943-020-01190-w
15. Jin D, Guo J, Wu Y, Yang L, Wang X, Du J, et al. Sun, m6A demethylase ALKBH5 inhibits tumor growth and metastasis by reducing YTHDFs-mediated YAP expression and inhibiting miR-107/LATS2-mediated YAP activity in NSCLC. *Mol Cancer.* (2020) 19:40. doi: 10.1186/s12943-020-01161-1
16. Liu T, Wei Q, Jin J, Luo Q, Liu Y, Yang Y, et al. The m6A reader YTHDF1 promotes ovarian cancer progression via augmenting EIF3C translation. *Nucleic Acids Res.* (2020) 48:3816–3831. doi: 10.1093/nar/gkaa048
17. Su Y, Huang J, Hu J. m6A RNA methylation regulators contribute to malignant progression and have clinical prognostic impact in gastric cancer. *Front Oncol.* (2019) 9:1038. doi: 10.3389/fonc.2019.01038
18. Chen M, Nie ZY, Wen XH, Gao YH, Cao H, Zhang SF. m6A RNA methylation regulators can contribute to malignant progression and impact the prognosis of bladder cancer. *Biosci Rep.* (2019) 39:BSR20192892. doi: 10.1042/BSR20192892
19. Zhao Y, Tao Z, Chen X. Identification of a three-m6A related gene risk score model as a potential prognostic biomarker in clear cell renal cell carcinoma. *PeerJ.* (2020) 8:e8827. doi: 10.7717/peerj.8827
20. Du J, Hou K, Mi S, Ji H, Ma S, Ba Y, et al. Malignant evaluation and clinical prognostic values of m6A RNA methylation regulators in glioblastoma. *Front Oncol.* (2020) 10:208. doi: 10.3389/fonc.2020.00208
21. Wilkerson MD, Hayes DN. ConsensusClusterPlus: a class discovery tool with confidence assessments and item tracking. *Bioinformatics.* (2010) 26:1572–3. doi: 10.1093/bioinformatics/btq170
22. Zhao X, Cui L. Development and validation of a m6A RNA methylation regulators-based signature for predicting the prognosis of head and neck squamous cell carcinoma. *Am J Cancer Res.* (2019) 9:2156–69.
23. Wang S, Wu X, Zhang J, Chen Y, Xu J, Xia X, et al. CHIP functions as a novel suppressor of tumour angiogenesis with prognostic significance in human gastric cancer. *Gut.* (2013) 62:496–508. doi: 10.1136/gutjnl-2011-301522
24. Koumangoye RB, Andl T, Taubenslag KJ, Zilberman ST, Taylor CJ, Loomans HA, et al. SOX4 interacts with EZH2 and HDAC3 to suppress microRNA-31 in invasive esophageal cancer cells. *Mol Cancer.* (2015) 14:24. doi: 10.1186/s12943-014-0284-y
25. Zhao Y, Wei L, Shao M, Huang X, Chang J, Zheng J, et al. BRCA1-associated protein increases invasiveness of esophageal squamous cell carcinoma. *Gastroenterology.* (2017) 153:1304–19.e5. doi: 10.1053/j.gastro.2017.07.042
26. Morrisey EE, Rustgi AK. The lung and esophagus: developmental and regenerative overlap. *Trends Cell Biol.* (2018) 28:738–48. doi: 10.1016/j.tcb.2018.04.007
27. Palumbo A, Meireles Da Costa N, Pontes B, Leite de Oliveira F, Lohan Codeço M, Ribeiro Pinto LF, et al. Esophageal cancer development: crucial clues arising from the extracellular matrix. *Cells.* (2020) 9:455. doi: 10.3390/cells9020455
28. Kumarasinghe MP, Bourke MJ, Brown I, Draganov PV, McLeod D, Streutker C, et al. Pathological assessment of endoscopic resections of the gastrointestinal tract: a comprehensive clinicopathologic review. *Mod Pathol.* (2020) 33:986–1006. doi: 10.1038/s41379-020-0460-0
29. Lin L, Lin DC. Biological significance of tumor heterogeneity in esophageal squamous cell carcinoma. *Cancers.* (2019) 11:1156. doi: 10.3390/cancers11081156
30. Zhou M, Wang H, Zeng X, Yin P, Zhu J, Chen W, et al. Mortality, morbidity, and risk factors in China and its provinces, 1990-2017: a systematic analysis for the global burden of disease study 2017. *Lancet.* (2019) 394:1145–58. doi: 10.1016/S0140-6736(19)30427-1
31. Chen W, Zheng R, Baade PD, Zhang S, Zeng H, Bray F, et al. Cancer statistics in China, 2015. *CA Cancer J Clin.* (2016) 66:115–32. doi: 10.3322/caac.21338
32. Fatehi Hassanabad. Chehade R, Breadner D, Raphael J. Esophageal carcinoma: towards targeted therapies. *Cell Oncol.* (2020) 43:195–209. doi: 10.1007/s13402-019-00488-2
33. Zhao Y, Shi Y, Shen H, Xie W. m6A-binding proteins: the emerging crucial performers in epigenetics. *J Hematol Oncol.* (2020) 13:35. doi: 10.1186/s13045-020-00872-8
34. Huang H, Weng H, Chen J. The biogenesis and precise control of RNA m6A methylation. *Trends Genet.* (2020) 36:44–52. doi: 10.1016/j.tig.2019.10.011
35. Chen XY, Zhang J, Zhu JS. The role of m6A RNA methylation in human cancer. *Mol Cancer.* (2019) 18:103. doi: 10.1186/s12943-019-1033-z
36. Li Y, Xiao J, Bai J, Tian Y, Qu Y, Chen X, et al. Molecular characterization and clinical relevance of m(6)A regulators across 33 cancer types. *Mol Cancer.* (2019) 18:137. doi: 10.1186/s12943-019-1066-3
37. Chen M, Wong CM. The emerging roles of N6-methyladenosine (m6A) deregulation in liver carcinogenesis. *Mol Cancer.* (2020) 19:44. doi: 10.1186/s12943-020-01172-y
38. Chen Z, Chen X, Lei T, Gu Y, Gu J, Huang J, et al. Integrative analysis of NSCLC identifies LINC01234 as an oncogenic lncRNA that interacts with HNRNPA2B1 and regulates miR-106b biogenesis. *Mol Ther.* (2020) 28:1479–93. doi: 10.1016/j.ymthe.2020.03.010
39. Yang Y, Wei Q, Tang Y, Yuanyuan W, Luo Q, Zhao H, et al. Loss of hnRNPA2B1 inhibits malignant capability and promotes apoptosis via down-regulating Lin28B expression in ovarian cancer. *Cancer Lett.* (2020) 475:43–52. doi: 10.1016/j.canlet.2020.01.029
40. Chen C, Luo Y, He W, Zhao Y, Kong Y, Liu H, et al. Exosomal long noncoding RNA LNMAT2 promotes lymphatic metastasis in bladder cancer. *J Clin Invest.* (2020) 130:404–21. doi: 10.1172/JCI130892

41. Snaebjornsson MT, Janaki-Raman S, Schulze A. Greasing the wheels of the cancer machine: the role of lipid metabolism in cancer. *Cell Metab.* (2020) 31:62–76. doi: 10.1016/j.cmet.2019.11.010
42. Counihan JL, Grossman EA, Nomura DK. Cancer metabolism: current understanding and therapies. *Chem Rev.* (2018) 118:6893–923. doi: 10.1021/acs.chemrev.7b00775
43. Martinez-Outschoorn UE, Peiris-Pages M, Pestell RG, Sotgia F, Lisanti MP. Cancer metabolism: a therapeutic perspective. *Nat Rev Clin Oncol.* (2017) 14:11–31. doi: 10.1038/nrclinonc.2016.60
44. Rohrig F, Schulze A. The multifaceted roles of fatty acid synthesis in cancer. *Nat Rev Cancer.* (2016) 16:732–49. doi: 10.1038/nrc.2016.89

Conflict of Interest: The authors declare that the research was conducted in the absence of any commercial or financial relationships that could be construed as a potential conflict of interest.

frontiers in Oncology

ORIGINAL RESEARCH
published: 30 September 2020
doi: 10.3389/fonc.2020.572708

Hematopoietic Gene Expression Regulation Through m^{6}A Methylation Predicts Prognosis in Stage III Colorectal Cancer

Zheng Zhou[1,2†], Shaobo Mo[1,2†], Ruiqi Gu[1,2†], Weixing Dai[1,2], Xinhui Zou[3], Lingyu Han[1,2], Long Zhang[1,4], Renjie Wang[1,2*] and Guoxiang Cai[1,2*]*

[1] Department of Colorectal Surgery, Fudan University Shanghai Cancer Center, Shanghai, China, [2] Department of Oncology, Shanghai Medical College, Fudan University, Shanghai, China, [3] School of Public Health, Shanghai Medical College, Fudan University, Shanghai, China, [4] Department of Cancer Institute, Fudan University Shanghai Cancer Center, Fudan University, Shanghai, China

OPEN ACCESS

Edited by:
Xiang Shu,
Vanderbilt University Medical Center, United States

Reviewed by:
Guochong Jia,
Vanderbilt University, United States
Shu-Hong Lin,
National Cancer Institute (NCI), United States

***Correspondence:**
Guoxiang Cai
gxcaifuscc@163.com
Renjie Wang
oncosurgeonli@sohu.com;
wangbladejay@sina.com
Long Zhang
caisanjun_sh@163.com;
longzhangcrc@yeah.net

† These authors have contributed equally to this work

Specialty section:
This article was submitted to Cancer Genetics, a section of the journal Frontiers in Oncology

Received: *15 June 2020*
Accepted: *08 September 2020*
Published: *30 September 2020*

Citation:
Zhou Z, Mo S, Gu R, Dai W, Zou X, Han L, Zhang L, Wang R and Cai G (2020) Hematopoietic Gene Expression Regulation Through m^{6}A Methylation Predicts Prognosis in Stage III Colorectal Cancer. Front. Oncol. 10:572708. doi: 10.3389/fonc.2020.572708

Background: Methylation of N6 adenosine (m^{6}A) plays important regulatory roles in diverse biological processes. The purpose of this research was to explore the potential mechanism of m^{6}A modification level on the clinical outcome of stage III colorectal cancer (CRC).

Methods: Gene set variation analysis (GSVA) and gene set enrichment analysis (GSEA) were adopted to reveal the signal pathway which was most likely affected by m^{6}A methylation. The linear models for microarray data (LIMMA) method and the least absolute shrink-age and selection operator (LASSO) Cox regression model were used to identify the signature. The signature can sensitively separate the patients into high and low risk indicating the relapse-free survival (RFS) time based on time-dependent receiver operating characteristic (ROC) analysis. Then, the multi-gene signature was validated in GSE14333 and the Cancer Genome Atlas (TCGA) cohort. The number of the samples in GSE14333 and TCGA cohort are 63 and 150. Finally, two nomograms were set up and validated to predict prognosis of patients with stage III CRC.

Results: The hematopoietic cell lineage (HCL) signaling pathway was disclosed through GSEA and GSVA. Seven HCL-related genes were determined in the LASSO model to construct signature, with AUC 0.663, 0.708, and 0.703 at 1-, 3-, and 5-year RFS, respectively. Independent datasets analysis and stratification analysis indicated that the HCL-related signature was reliable in distinguishing high- and low-risk stage III CRC patients. Two nomograms incorporating the signature and pathological N stage were set up, which yielded good discrimination and calibration in the predictions of prognosis for stage III CRC patients.

Conclusions: A novel HCL-related signature was developed as a predictive model for survival rate of stage III CRC patients. Nomograms based on the signature were advantageous to facilitate personalized counseling and treatment in stage III CRC.

Keywords: colorectal cancer, stage III, m^{6}A, signature, prognosis

BACKGROUND

In 2019, the nation's 14.8 million new colorectal cancer (CRC) cases made it the most common cancer of digestive tract, with 146 deaths per day ranking third among all malignant tumors in the United States (1). Closely related to economic developments, CRC has emerged as a critical public health problem in China as the living standard of its people improves, and the incidence of CRC was about 37.6/100,000 in 2016, ranking third likewise (2). More than 50% of patients with CRC are diagnosed at or beyond stage III. Therefore, distant metastasis occurred and their 5-year survival rate drops to 10%. Adjuvant chemotherapy (ACT) combined with surgery is the prominent treatment to enhance survival for stage III CRC patients (3). Many variables contribute to the prognosis of stage III CRC patients. For instance, the number of negative lymph nodes is a significant prognostic factor for patients with stage III CRC (4). Perineural invasion (PNI) is also a prognostic factor. Stage III CRC patients with PNI are more likely to have metastasis and recrudesce (5).

According to current NCCN guidelines, FOLFOX (fluorouracil, leucovorin, and oxaliplatin) or CAPOX (capecitabine and oxaliplatin) has become the first-line ACT for stage III CRC patients. It has been proved that stage III CRC patients with proper ACT have a survival advantage compared to those without ACT (6). Based on the results carried out by the International Duration Evaluation of Adjuvant Therapy (IDEA) collaboration, for low-risk (T1-3, N1) stage III CRC patients, the optimal ACT options are 3 months of CAPOX or 3 to 6 months of FOLFOX. 6 months of FOLFOX or 3 to 6 months of CAPOX is suitable for the high risk (T4, N1-2 or T any, N2) stage III patients (7). However, there is a lack of effective molecular markers for the prognosis of stage III CRC.

N6-methyladenosine (m^6A) is one form of RNA modifications. M^6A RNA methylation, which are widely found in the various types of RNA, is recognized as the most prominent and abundant form of internal modifications in eukaryotic cells. M^6A modification is regulated by methyltransferases, demethylases and binding proteins, which can be also called "writers," "erasers" and "readers." It has been reported that the m^6A regulators play a crucial role in a variety of biological functions in post-transcriptional regulation of gene expression (8). Increasing evidence demonstrated that dysregulated expression and genetic changes of m^6A regulators were correlated with the disorders of multiple biological process including abnormal cell death and proliferation, developmental defects, tumor malignant progression, and immunomodulatory abnormality. Previously, researchers unraveled the correlation between the genetic alterations of m^6A regulatory genes and TP53 pathway in the processing of acute myeloid leukemia (9). Recently, research into the gastric carcinoma proved that m^6A modification in cancer tissue had a close relationship with tumor microenvironment (10). Certain single-nucleotide polymorphisms (SNPs) in m^6A modification genes were also proved to have correlation with the formation of CRC (11). To conclude, m^6A modifications not only correlated with the hematologic tumor, but it might also provide novel insight into the classification and precise treatment toward gastrointestinal carcinoma.

Hematopoietic stem cells (HSCs) are self-renewing and have the potential to become different progenitor cells. The differentiation mainly follows two pathways, which are lymphoid and myeloid pathways. In the lymphoid pathway, the common lymphoid progenitor cells differentiate into immune cells and in myeloid pathway, the progenitor cells differentiate into granulocytes, monocytes, erythrocytes and platelets. Hematopoietic cell lineage (HCL) pathway has both intercellular and extracellular factors via transcription as well as post transcription level. DNA methylation, histone modifications, small non-coding RNAs are involved in post transactional regulation (12). However, the correlation between HCL pathway and CRC still needs further investigation.

In this research, CRC patients' gene expression microarray data and clinicopathological information were adopted from the Gene Expression Omnibus (GEO) for identifying different m^6A modification patterns mediated by m^6A regulators (13). Using principal component analysis (PCA), Gene Set Variation Analysis (GSVA) and Gene Set Enrichment Analysis (GSEA), a seven-HCL related regulators was identified from the GSE39582 and GSE14333, downloaded from GEO. The GSVA is a non-parametric unsupervised method for assessing gene set enrichment (GSE) in gene expression microarray and RNA-seq data. In contrast to most GSE methods, GSVA performs a change in coordinate systems, transforming the data from a gene by sample matrix to a gene set by sample matrix. Thereby allowing for the evaluation of pathway enrichment for each sample. This transformation is done without the use of a phenotype, thus facilitating very powerful and open-ended analyses in a now pathway centric manner (14). Then, we constructed a predictive gene signature and verified the results in GSE14333 and the Cancer Genome Atlas (TCGA) cohorts. Eventually, nomograms based on the prognostic signature and clinicopathological characteristics was constructed to assess prognosis in stage III CRC patients.

Abbreviations: CRC, colorectal cancer; ACT, adjuvant chemotherapy; PNI, perineural invasion; m^6A, N6-methyladenosinel; SNPs, single-nucleotide polymorphisms; HSCs, Hematopoietic stem cells; HCL, Hematopoietic cell lineage; PCA, principal component analysis; GEO, Gene Expression Omnibus; TCGA, the Cancer Genome Atlas; DCA, decision curve analysis; GSVA, Gene Set Variation Analysis; GSEA, Gene Set Enrichment Analysis; KEGG, Kyoto encyclopedia of genes and genomes; AUC, the area under the curve; ROC, receiver operating characteristic; LIMMA, linear models for microarray data; DEGs, differentially expressed genes; LASSO, least absolute shrink-age and selection operator; RFS, relapse-free survival; OS, overall survival; K-M, Kaplan–Meier; DEHG, discrepantly expressed HCL-related genes.

MATERIALS AND METHODS

Data Selection

A total of 21 m^6A regulators were extracted from two independent GSE datasets, GSE39582 and GSE14333, downloaded from the GEO database[1], for identifying different m^6A modification patterns mediated by 21 m^6A regulators. These

[1]http://www.ncbi.nlm.nih.gov/geo/

21 m^6A regulators included 8 writers (*METTL3, METTL14, RBM15, RBM15B, WTAP, KIAA1429, CBLL1, ZC3H13*), 2 erasers (*ALKBH5, FTO*) and 11 readers (*YTHDC1, YTHDC2, YTHDF1, YTHDF2, YTHDF3, IGF2BP1, HNRNPA2B1, HNRNPC, FMR1, LRPPRC, ELAVL1*) (**Supplementary Table 1**) (10). The 87 genes in **Supplementary Table 2** were derived from "KEGG_HEMATOPOIETIC_CELL_LINEAGE" gene list within 186 Kyoto encyclopedia of genes and genomes (KEGG) gene sets of canonical pathways, download from the MSigDB of GSEA database[2]. Expression data and clinical information were downloaded from GEO database and robust multichip average method was applied in normalizing the raw microarray data (13). UCSC Xena[3] were the source of the TCGA clinical information and genome data. GSE39582 is the largest, most comprehensive and most complete data series in the GEO dataset. It contains 23495 genes' expression information of 585 patients. The GSE14333 data series contains genes expression information of 290 patients sequenced by same measuring method as GSE39582. In this research, we only extracted the stage III CRC patients' data, which are 205 and 91, respectively. The detailed and demographical information is listed in the **Supplementary Table 3**.

PCA, GSVA, and GSEA

To quantify the m^6A modification patterns of individual tumor, the m^6Ascore, a set of scoring system was constructed to evaluate the m^6A modification pattern of individual patients with CRC. This research performed PCA on the expression levels of 21 m^6A regulators, which were identified as principal components, in GSE39582 and GSE14333 to reduce the number of dimensions and construct m^6Ascore. This method had advantage of focusing the score on the set with the largest block of well-correlated (or anticorrelated) genes in the set, while down-weighting contributions from genes that do not track with other set members. The median of sums of 21 principal components in 296 samples was calculated as the cut-off points to divide patients into two m^6A clusters. Using the KEGG gene sets as the reference gene set and setting the p value < 0.05, we conducted GSVA to measure the signaling pathway variation score for each sample in stage III CRC by using "GSVA" R package (14). In this research, enrichment score was calculated as the magnitude difference between the largest positive and negative random walk deviations. GSEA was also performed to analyze difference between CRC patients' m^6A subgroups via "javaGSEA" to obtain GSEA result with the same data sets (15). Then, linear models for microarray data (LIMMA) method was used to sort out the pathway with the most positive correlation. The detailed workflow is shown in **Figure 1**.

Construction of the Predictive Gene Signature

Patients suffering from early recurrence within 1 year after primary resection was classified as early relapsing group. Based on the "glmnet" package in R, we searched optimum predictive genes for GSE39582 CRC samples by applying pathway brought from the results of GSVA and GSEA (16), and using least absolute shrink-age and selection operator (LASSO) Cox regression analysis. In LASSO regression, recurrence-free survival, which was also used to determine the ACT response, was identified as patients' outcomes. Besides, LIMMA method was introduced to conduct an analysis of differentially expressed genes (DEGs) between early recurrence and long-term survival patients (no relapse after at least 5 years after the surgery) (17), with $p < 0.05$ and fold change $\geq$1.1. The number of patients in the early relapsing group in the GSE39582 was 26 while the number of patients in the long-term survival group was 56. Considering the results of LASSO and LIMMA analysis simultaneously, genes with best fold change or λ was defined as a valuable biomarker. The samples used in signature building and validation must have adopted ACT, with clear RFS time and the gene expression information we needed. Thus, the sample size of the constructing is 146. The detailed demographical information is listed in **Supplementary Table 3**.

Statistics for Classification, Prediction and Validation in the GEO and TCGA Series

We built a risk score using the formula of *CD36*, *ITGA3*, *FLT3*, *CR2*, *IL7*, *CD2*, and *CD55* expression by the method of LASSO Cox regression. Then, Patients were divided into high-risk and low-risk groups according to this specific risk score formula. Time-dependent receiver operating characteristic (ROC) analysis was implemented to calculate the area under the curve (AUC) for 1-, 3-, and 5-year overall survival (OS) and relapse-free survival (RFS) in order to confirm the accuracy of predicted response by signature using the "survivalROC" R package (18). Using the Kaplan-Meier (K-M) survival curve analyses and log-rank test, this research evaluated the prognostic significance of this signature. Then, we plotted the distribution of patients' risk score, survival and recurrence status to show the relationship between the risk score and patients' response. A heatmap was constructed with cluster analysis in view of the gene expression difference, according to the risk score in the help of the "ComplexHeatmap" R package. To further investigate the classification reliability of the identified genes signature, this research verified it in GSE14333 and TCGA in the same protocol. The samples used in signature building and validation must have adopted ACT, with clear RFS time and the gene expression information we needed. Thus, the sample sizes were 63 and 150 for signature building and validation, respectively. The detailed demographical information is listed in **Supplementary Table 3**.

Functional Enrichment Analysis

Functional enrichment analysis of KEGG pathway was performed to determine significantly enriched KEGG pathways of genes correlated with the signature using the ClueGO plugin (version 2.5.6) in Cytoscape limited in biological processes (19) and R software. The results of functional map and clusters of KEGG enrichment were obtained and visualized using a two-sided hypergeometric test with Bonferroni

[2]http://software.broadinstitute.org/gsea/index.jsp

[3]https://tcga.xenahubs.net

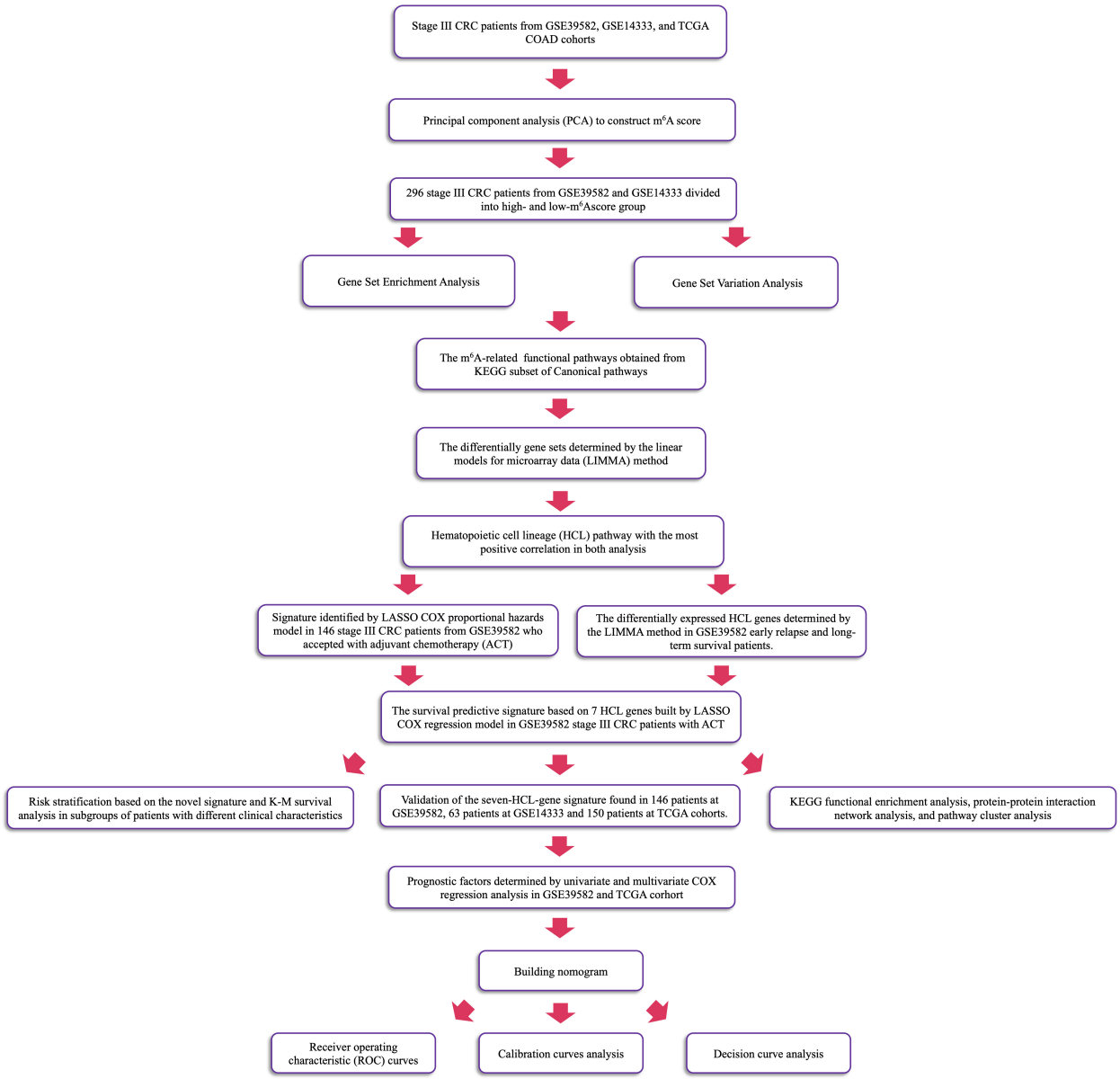

FIGURE 1 | The workflow of identification of CRC ACT-related seven-HCL signature.

step down correction and kappa score threshold of 0.4, and limited in the level intervals 3–8 with $p \leq 0.05$. Biological pathways with $p < 0.05$ was considered as significant using functional annotation chart options with the whole human genome as background.

Correlation Between the Prognostic Signature and Other Clinicopathological Characteristics and Clinical Usefulness

The K-M survival analysis was performed on designated subtypes of different clinicopathological features, including gender, age, tumor site, pathological T stage, pathological N stage, MMR status, TP53 mutation status, KRAS mutation status and BRAF mutation status, to further testing the applicability of gene signatures. Univariable and multivariable cox regression analyses were adopted to calculate and validate the influence of variables, with $p \leq 0.05$. This research found that pathological N stage was independent prognostic factors that could be used in combination with signature to predict RFS and OS after ACT. Based on the multivariable cox regression analysis results, two nomograms integrating clinicopathological parameters with signature were formulated by applying the "rms" R package. The overall points for each patient in the training and validation cohorts were calculated using founded nomograms. Decision curve analysis (DCA) incorporates a risk prediction model into

clinical approach to evaluate a predictive model and visualizes the latent profit of therapy (20).

Statistical Analysis

All statistical analyses were performed with use of R (version 3.5.1, www.r-project.org). All statistical tests were two-sided, and p values < 0.05 were considered statistically significant.

RESULTS

Concentration on the HCL Signaling Pathway

The R package of FactoMineR was used to calculate m^{6}A score based on the expression of 21 m^{6}A regulators and to classify patients with qualitatively different m^{6}A modification patterns (**Supplementary Figure 1**). The demographical information and Three databases used in this research and the sample size are listed in the **Supplementary Table 3**. The m^{6}A score of patients in the GSE39582 and GSE14333 was calculated and displayed in **Supplementary Table 4**. This study carried out GSVA of KEGG gene sets in 2 independent GEO data sets: GSE39582 and GSE14333. The results displayed in heatmap (**Figures 2A,B**) and **Supplementary Table 5**, concentrated on the active HCL signaling pathway and significantly focused on the m^{6}A modification subtype groups. Meanwhile, we performed a GSEA of the KEGG gene sets and found that HCL was noticeably enriched in 2 data sets (**Figures 2C,D**). After fully considering the results of GSVA and GSEA, we selected the KEGG pathway with logFC >0.15, Enrichment Score >0.65 in GSE39582 and logFC >0.1, Enrichment Score >0.45 in GSE14333, respectively. Comprehensively, the results of the GSVA and GSEA showed that genes in HCL signaling pathway might be related to m^{6}A modification levels in stage III CRC patients.

Development of Efficacy Evaluation Signature From GSE39582 Set

LASSO cox regression analyses were used to screen 87 response-related HCL genes in stage III CRC patients with ACT. The analysis of discrepantly expressed HCL-related genes (DEHG) between early relapse and long-term survival groups was performed using LIMMA method. 42 HCL-related genes were found associated with stage III CRC patients' survival in LASSO analyses (**Supplementary Figure 2**). Besides, 4 genes (**Supplementary Table 6**) expressed differentially using LIMMA method and the heatmap of those genes was displayed in **Supplementary Figure 3**. Screening LASSO results by DEHG, it was found that 7 HCL-related genes were differentially expressed in patients with different ACT responses. The risk score formula of the gene marker predicting the ACT response was calculated by weighting the relative expression of each prognostic gene and its associated expression value through the LASSO cox regression coefficient of gene. Patients were divided into high-risk and low-risk groups according to this specific risk score formula. The formula was as follows: 0.64973 * *CD36* expression + 0.50566 * *ITGA3* expression – 1.06119 * *FLT3* expression + 0.43809 * *CR2* expression – 0.24174 * *IL7* expression — 0.43412 * *CD2* expression – 0.03472 * *CD55* expression. According to the signature, stage III CRC patients were divided into low-risk and high-risk group using the value with acceptable sensitivity and specificity as the cutoff point. Based on the Youden's index in the ROC curve, a simple cutoff point of this signature could be figured out, which is −1.193094. If the signature score exceeds the cutoff point, patents will be classified as the high risk and vice versa. The heatmap of the signature was displayed in **Figure 3A**. The distribution of relapse after ACT related to risk scores was shown in **Figure 3B**, suggesting that patients with lower risk scores tend to have better ACT response than others. Time-dependent ROC analysis at 1-, 3-, and 5-year RFS after resection were conducted to distinguish how accurate the signature was at predicting prognosis conditions. The AUC was 0.663, 0.708, and 0.708 at the survival time of 1, 3, and 5 years in GSE39582, respectively (**Figure 3C**). The results reflected our signature could predict the ACT effects among patients with stage III CRC.

Validation of the Signature in GEO and TCGA Datasets

We validated the HCL-related signature based on the cases from GSE14333 and TCGA. In order to explore the effect of signature on relapse and survival outcomes, this research subsequently validated the results in GSE39582 OS cohorts. Risk scores were calculated according to the HCL-related signature.

In GSE39582 OS cohorts, the clustered different expression patterns of the seven genes between low-, high-risk and survival, death group were analyzed and shown in **Figures 4A,D**. Compared to the patients in high risk group, the death rates after ACT for patients in the low-risk group were remarkably lower (**Figure 4B**). Distribution of the survival time and status among the 146 stage III CRC patients with ACT in GSE39582 was displayed in **Figure 4C**. Time-dependent ROC analyses at 1, 3, and 5 years were conducted to assess the predictive accuracy of the seven-HCL-based classifier and AUC of ROC proved that the classifier had excellent predictive preciseness (**Figure 4E**). In GSE14333 and TCGA cohorts, patients were also divided into low-risk and high-risk group in the same way as GSE39582. The K-M survival analysis (**Figures 4G,L**) and distribution of patients' survival time and status (**Figures 4I,N**) showed that this classifier's performance in predicting the RFS after ACT was consistent in external validation cohorts. The heatmap showed that the expression patterns of seven-HCL-related genes were the same regardless of whether they were grouped by risk or recurrence (**Figures 4F,K,H,M**). Besides, the AUC of the time-dependent ROC analysis proved that the classifier had good predictive specificity and sensitivity in 1-, 3-, and 5-year survival for GSE14333 and TCGA (**Figures 4J,O**).

Distinguishing Ability of Signature on Chemotherapy Response and Potential Biological Function

As shown in **Figure 5A**, there was a significant difference in OS between patients with stage III CRC receiving chemotherapy and those without chemotherapy. After that, this study used signature

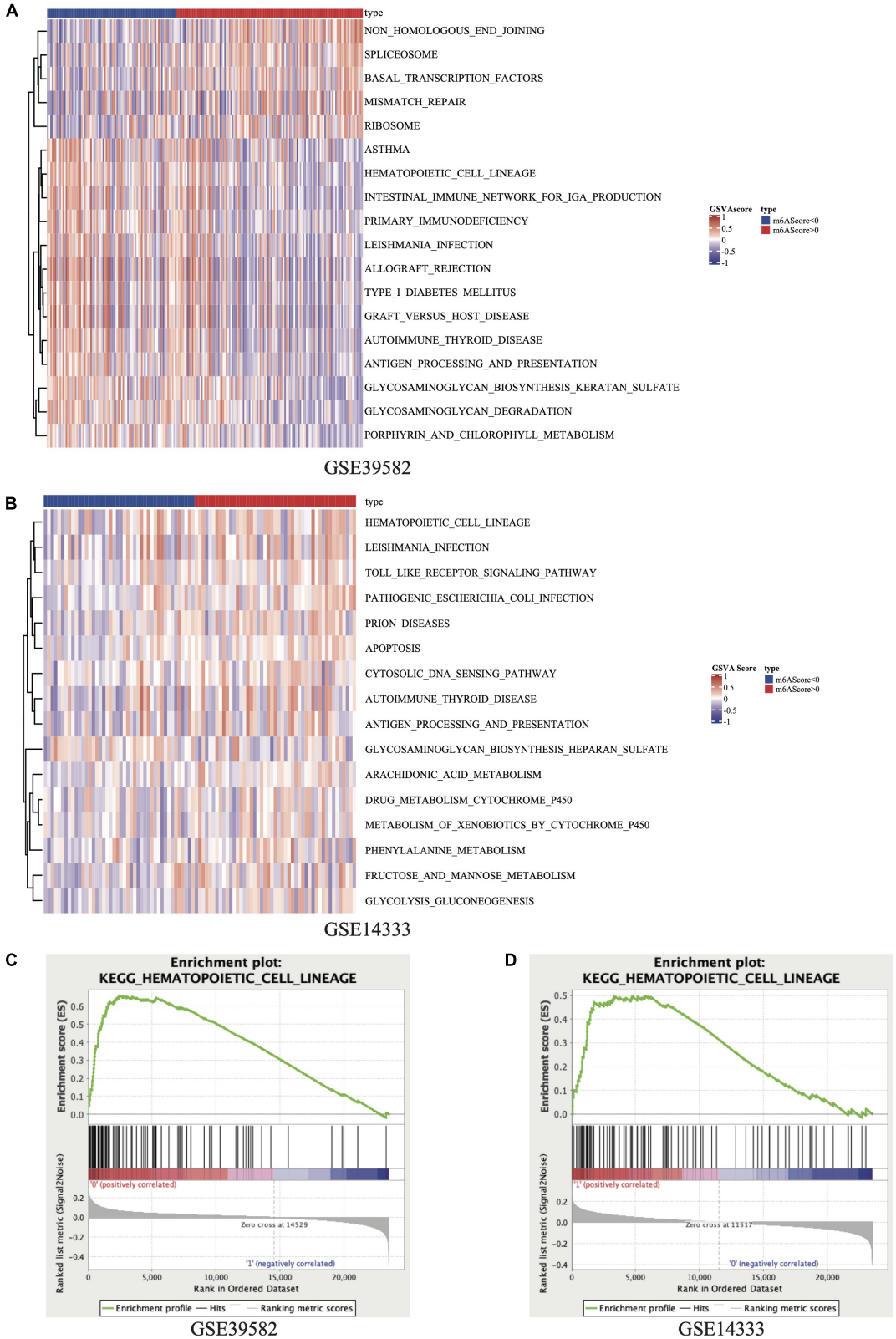

FIGURE 2 | Heatmap of GSVA results in GSE39582 **(A)** and GSE14333 **(B)**. Results of GSEA on KEGG_HEMATOPOIETIC_CELL_LINEAGE pathway in GSE39582 **(C)** and GSE14333 **(D)**.

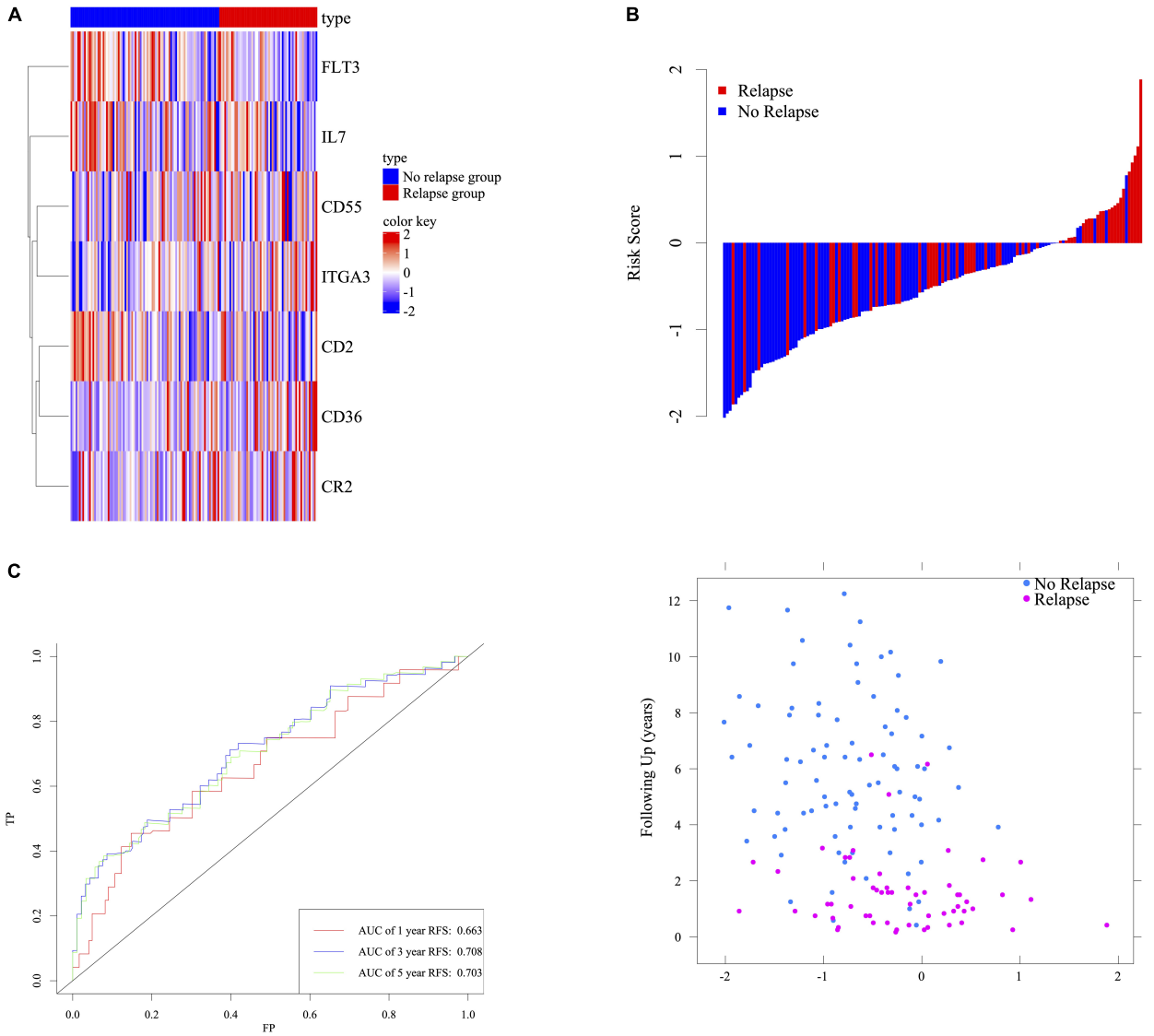

FIGURE 3 | Determination and analysis of the seven-HCL-related signature in GSE39582 cohort. The expression pattern of the seven-HCL-related signature **(A)**. The distribution of patients' risk score and relapse status **(B)**. Time dependent ROC curves at 1, 3, and 5 years **(C)**.

to stratify the risk of stage III CRC patients and performed K-M survival analysis and log-rank test for chemotherapy factors in high-risk and low-risk groups, respectively (**Figures 5B,C**). ACT for low-risk group could help improve the stage III CRC patients' OS, while ACT for high-risk groups might not have no significance for the survival. This result supported that stage III CRC patients with low-ACT-sensitivity were classified into high-risk groups and those with high-ACT-sensitivity were classified into low-risk groups. According to functional enrichment analysis of KEGG pathway (**Supplementary Figures 4B–D**), seven HCL-related biomarkers might play a role through PI3K-Akt signaling pathway and ECM-receptor interaction pathway. The protein-protein interaction network illustrated that these biomarkers also had strong and complex connections with each other (**Supplementary Figure 4A**).

Stratification Analysis

To determine whether the prognostic model can apply to other clinical factors, stratification analysis was performed according to age, sex, tumor site, pathological T stage, pathological N stage, MMR status, TP53 mutation status, KRAS mutation status, and BRAF mutation status. As the result of K-M analysis, seven-HCL-related-gene signature was quite meaningful in most clinically subgroups, although it did not reach the statistical difference in some factors due to the limitation of the number of cases (**Figure 6** and **Supplementary Figure 6**).

Setting Up a Clinical Prediction Model

Taking the univariable and multivariable cox regression model in GSE39582 cohort (**Supplementary Tables 7**, **8**),

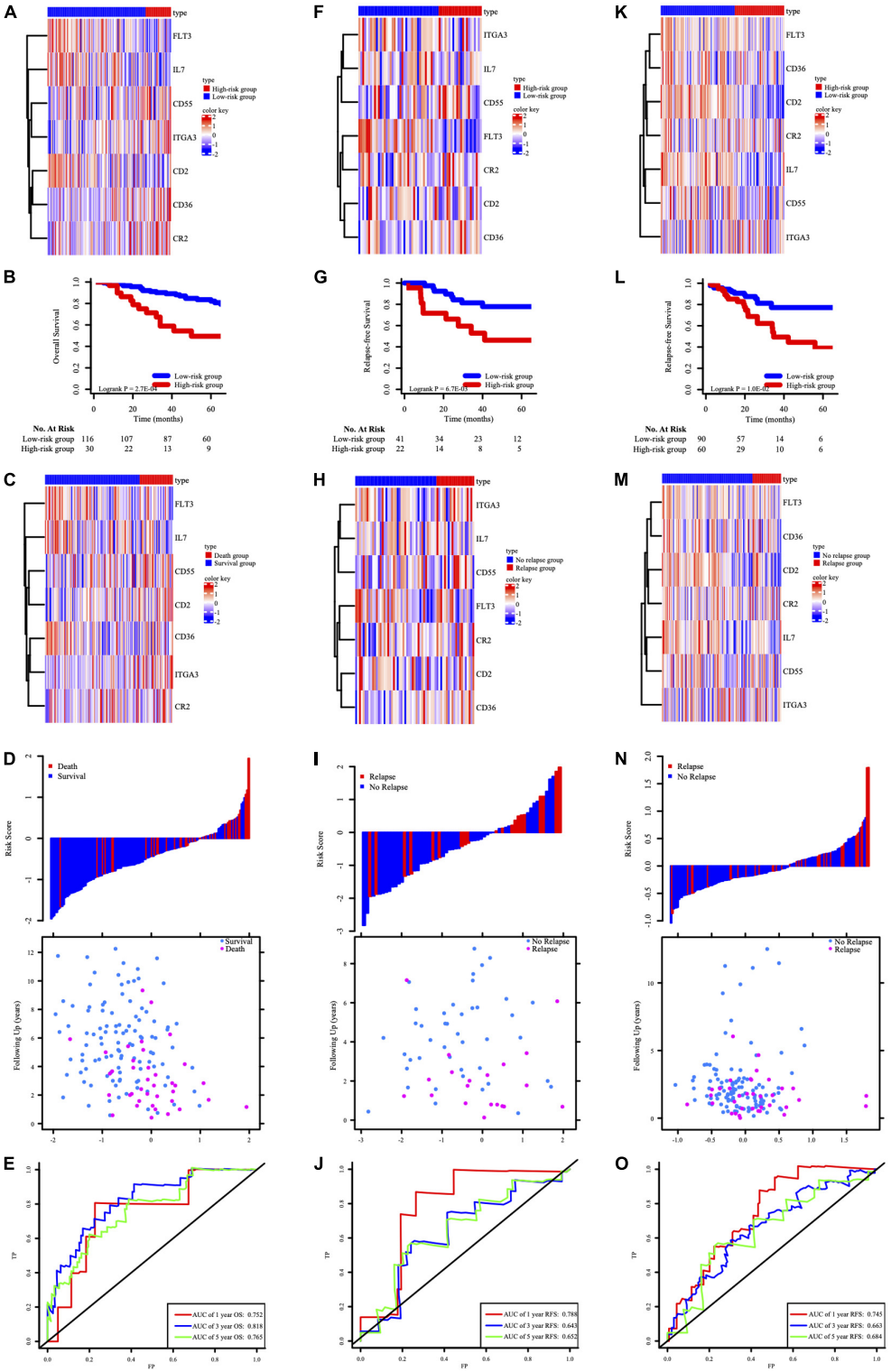

FIGURE 4 | The expression pattern of the seven-HCL-related signature based on risk groups in the GSE39582 OS cohort **(A)**, GSE14333 RFS cohorts **(F)**, and TCGA RFS cohorts **(K)**. The K-M survival curves in the GSE39582 OS cohort **(B)**, GSE14333 RFS cohorts **(G)**, and TCGA RFS cohorts **(L)**. The expression pattern of the seven-HCL-related signature based on survival or relapse status in the GSE39582 OS cohort **(C)**, GSE14333 RFS cohorts **(H)**, and TCGA RFS cohorts **(M)**. The distribution of patients' risk score and relapse status in GSE14333 **(I)**, and TCGA **(N)**. The distribution of patients' risk score and survival status in GSE39582 **(D)**. AUC values of ROC for predicting response of ACT in stage III CRC patients in the GSE39582 OS cohort **(E)**, GSE14333 RFS cohorts **(J)**, and TCGA RFS cohorts **(O)**.

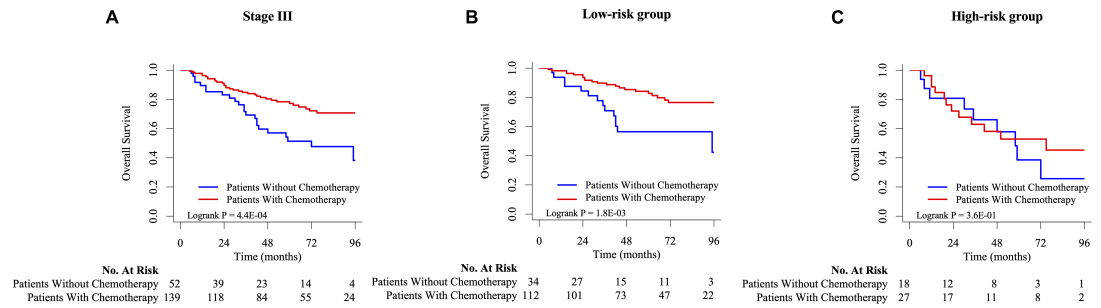

FIGURE 5 | The K-M survival analysis between chemotherapy and non-chemotherapy group on stage III **(A)**, low-risk **(B)**, and high-risk **(C)** CRC patients in GSE39582.

this study constructed two nomograms to satisfy the needs of clinicians to quantify the prognosis of stage III CRC patients (**Figure 7A** referred to RFS and **Figure 7F** referred to OS). To ensure its efficacy in predicting RFS and OS, time-dependent ROC was applied, which suggested that the nomogram had good prognostic accuracy (**Figures 7B,G**). The sensitivity of nomogram in predicating the relapse status in the GSE39582 is 0.5787923. Calibration curves of the nomogram revealed no deviations from the reference line (**Figures 7C,H** as 1-year, **Figures 7D,I** as 3-year, **Figures 7E,J** as 5-year). To verify this conclusion, the same protocol was duplicated in the TCGA RFS cohort, shown in **Supplementary Figure 6** and **Supplementary Table 9**. The sensitivity of nomogram in predicting the relapse status in TCGA cohort is 0.6179945. The DCA curves for the developed nomogram and signature in GSE39582 and TCGA cohorts were shown in **Figure 8**. Both DCA showed high net benefits, so it had excellent clinical outcome values, DCA of nomograms described that integration of clinical and gene expression pattern was more reliable than gene signature. Detailed standardized net benefits were listed in **Supplementary Table 10**.

DISCUSSION

Radical surgery combined with ACT is the prominent treatment to enhance the survival of patients with stage III CRC. However, for stage III CRC patients, there is a lack of molecular markers for predicting chemotherapy response and clinical prognosis. In this research, we put forward the idea that m6A modifications might be determinant in the ACT response of patients with stage III CRC (21). Then, a novel prognostic predictive signature in view of 7 HCL-related genes was formulated based on GSE39582 and GSE14333 cohorts. The divergence of ACT effects between low-risk and high-risk patient with stage III CRC was fully displayed in several methods. The prognostic signature has also been validated in GSE14333 and TCGA cohort. Furthermore, combing the pathological N stage and the signature, two nomograms have been set up to help clinician predict ACT response of stage III CRC patients.

The genes in the signature are closely related to the cancer and might be the potential treatment targets. Proteins in HCL pathway, like *CR2*, have already become biomarkers in the treatment and classification of hematologic tumor (22, 23). *CD2* was also reported to be highly associated with acute promyelocytic leukemia (APL). The expression of *CD2* was also considered as a prognostic factor in the APL (24). According to the pervious researches, the expression level of *CD2* and *CR2* demonstrated the status of our immune system and other immunological diseases. Our work indicated that *CD2* and *CR2* might account for the resistance and ineffectiveness of ACT. The relationship between those two genes and ACT effects need to be further confirmed in the molecular level. Recently, (25) also demonstrated those proteins like *IL7* may affect the formation and metastasis of breast cancer. Based on the *IL7* pathway, signaling cytokine receptor was established to improve the effects of the CAR-T therapy in preclinical tumor models (26). Our work also revealed the potential of improving ACT sensitivity via *IL7* pathway. Talking about *ITGA3*, this gene priorly was priorly found to predict the relapse of right-side colon cancer in stage II (27). Statistics disclosed the relationship between the *ITGA3* integrin and disease-free survival in patients with colorectal tumors (28). Researchers also established a link between miR-124 and anoikis susceptibility and proved that a miR-124/*ITGA3* axis could be a potential target for the treatment of metastatic CRC (29). As an important gene in AML, *FLT3* mutation happened in almost 30% AML cases and the mutation of *FLT3* kept changing in the processing of AML and also showed poor prognosis in AML patient (30). Patients with metastatic CRC and *FLT3* translocation might be sensitive to sorafenib treatment (31). Combing the pervious study and our outcome, the value of the *FLT3* in predicting the relapse and survival of tumor patients have been explored. Experiments for the molecular pathway of the *FLT3* and tumor progress should be set off. Researches into the expression level of *CD55* in CRC patients proved that patients with tumors expressing high levels of *CD55* had a significantly worse survival than patients with low *CD55* levels (32), which means the expression of *CD55* may serve as a marker for the CRC patients. *CD36* is a cell adhesion receptor and it was reported that it could modulate the vascularization of tumor tissues. *CD36* expression might decrease stromal vascularization which contributed to better prognosis of colon cancer (33). *CD36* is the upstream regulator of the PPAR signaling pathway, which can inhibit the procession of CRC. Generally speaking, the genes,

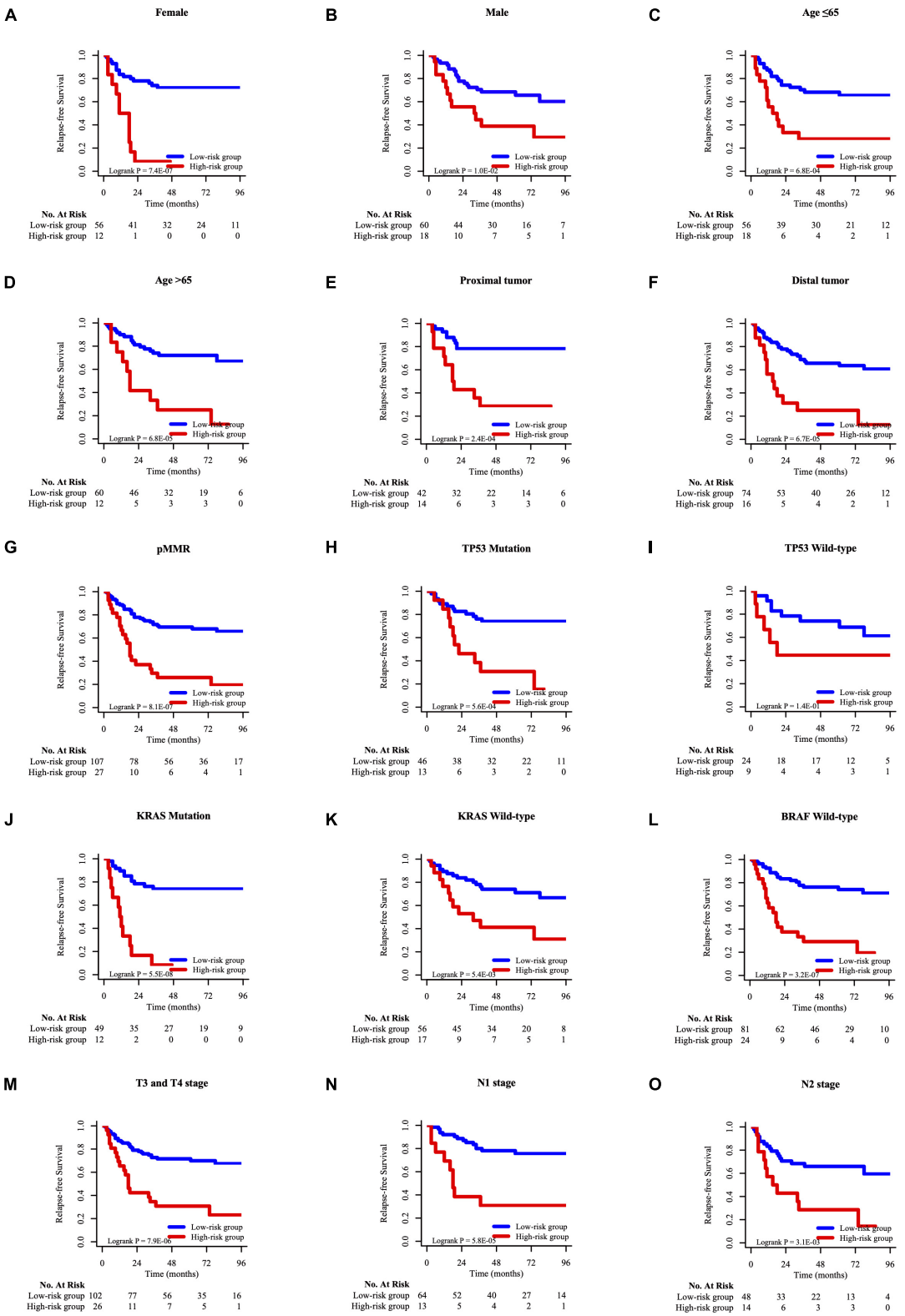

FIGURE 6 | The K–M survival curves of overall survival between high-risk and low-risk group of different clinicopathological features, including gender **(A,B)**, age **(C,D)**, tumor site **(E,F)**, MMR status **(G)**, TP53 mutation status **(H,I)**, KRAS mutation status **(J,K),** BRAF mutation status **(L)**, pathological T stage **(M)**, pathological N stage **(N,O)**.

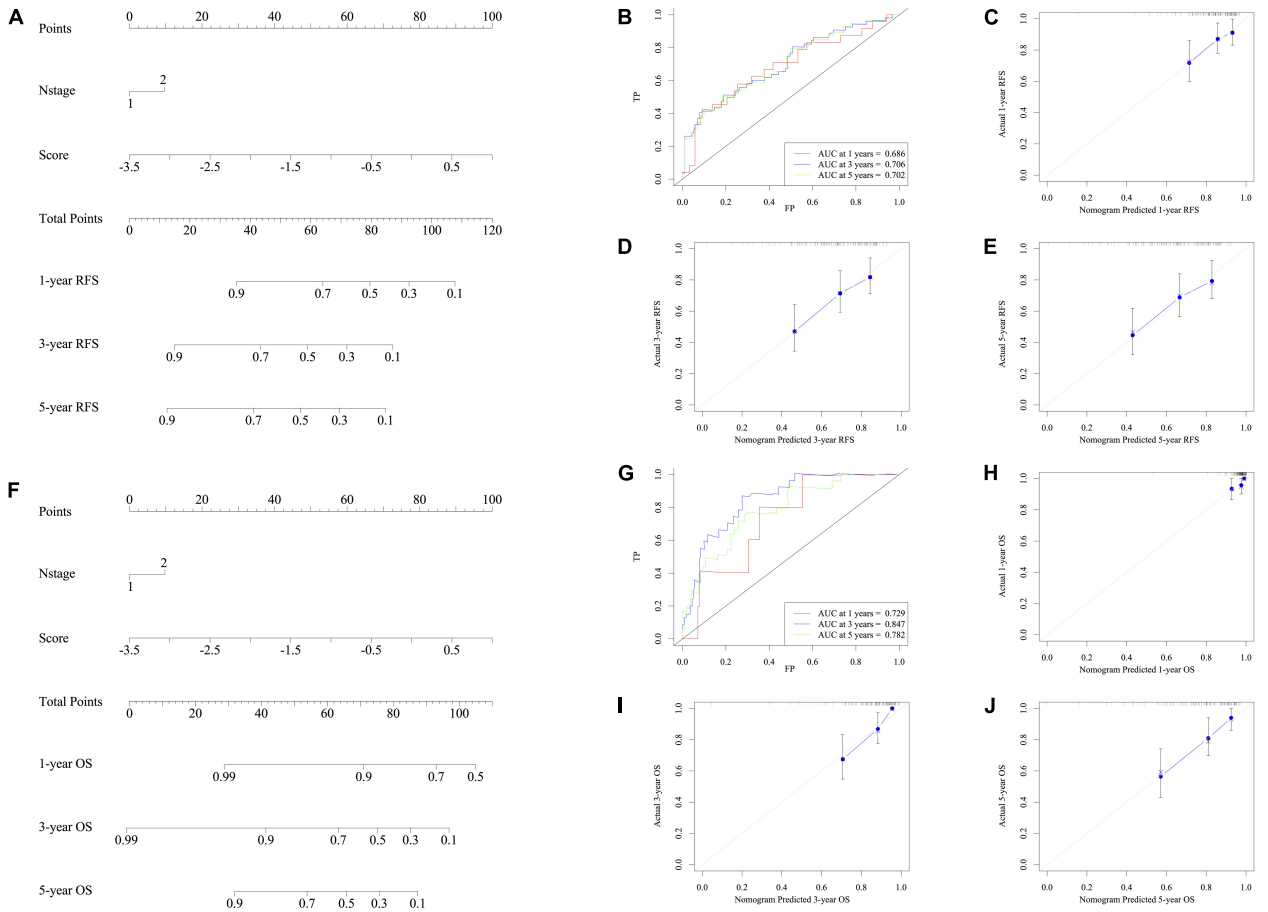

FIGURE 7 | Nomograms convey the results of prognostic models using the seven-HCL-related signature and pathology N stage to predict RFS of patients with CRC in TCGA cohort. The AUC at 1-year prediction was 0.686 **(A,B)**. The *x*-axis is nomogram-predicted probability of survival and *y*-axis is actual survival. The reference line is 45o and indicates perfect calibration (**C** as 1-year, **D** as 3-year, and **E** as 5-year). Nomograms convey the results of prognostic models using the seven-HCL-related signature and pathology N stage to predict OS of patients with CRC in TCGA cohort. The AUC at 1-year prediction was 0.729 **(F,G)**. The *x*-axis is nomogram-predicted probability of survival and *y*-axis is actual survival. The reference line is 45o and indicates perfect calibration (**H** as 1-year, **I** as 3-year, and **J** as 5-year).

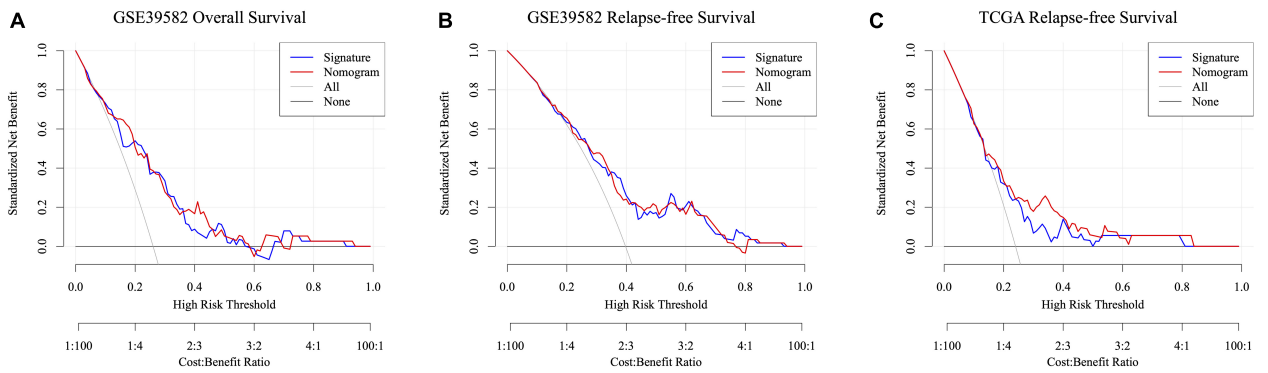

FIGURE 8 | Decision curve analysis of the nomogram and signature for predicting ACT-response of stage III CRC patients in the GSE39582 RFS cohort **(A)**, GSE39582 OS cohorts **(B)**, and TCGA RFS cohorts **(C)**. The gray line and black line represent the assumption regarding all patients with and without risk stratification, respectively. The red line represents the nomogram, and the blue line represents the signature.

figured out in this research, have been proved by others to be associated with the progress and prognosis of hematologic tumors and other solid tumors. There are few articles in CRC treatment and ACT sensitivity concerning genes like *CR2*, *CD2*, and *IL7*. Apart from the scientific values, genes like *IL7* can easily been tested in the current examine methods. Using our signature and biomarker doesn't need to develop new testing method and antibody. Low cost and high sensitivity are one of the advantages of our research.

There are indeed some limitations in this study. On the one hand, our study was based on the data from public datasets without testing *in vitro* and *in vivo*. Further study is needed to validate whether expression of HCL genes was associated with m6A methylation. On the other hand, the sample capacity of our research is relatively small. Besides, our external confirmation cohorts are mainly from the same race. Thus, more patients' data are needed for our further research and confirmation.

CONCLUSION

In conclusion, we developed a seven-HCL-related mRNA signature composed of various regulation mRNA that effectively classify CRC patients into low-risk group (with high ACT sensitivity) and high-risk groups (with low ACT sensitivity). Application of the signature in clinical treatments should also be further observed to verify the validity of our findings.

DATA AVAILABILITY STATEMENT

The datasets presented in this study can be found in online repositories. The names of the repository/repositories and accession number(s) can be found in the article/ **Supplementary Material**.

AUTHOR CONTRIBUTIONS

ZZ, SM, and RG had the idea for this study. XZ and LH supervised the acquisition of the data. SM, ZZ, and WD undertook the statistical analysis. RW and LZ provided statistical advice. All authors contributed to interpretation of the results, approved the final version of the manuscript, and including the authorship list. SM, ZZ, and RG wrote the manuscript. LZ, RW, and GC revised the manuscript and other authors contributed to the content.

FUNDING

This study was supported by the Grant of National Natural Science Foundation of China (No. 81871958), the National Key R&D Program of China (Nos. 2016YFC0905300 and 2016YFC0905301), and the Grant of Science and Technology Commission of Shanghai Municipality (No. 16401970502). The funders had no role in the study design, data collection and analysis, decision to publish, or preparation of the manuscript.

ACKNOWLEDGMENTS

We would like to thank Wenqiang Xiang, Qingguo Li, and Sanjun Cai. We also would like to express our sincere gratefulness to the GEO, TCGA, GSEA database for the support.

SUPPLEMENTARY MATERIAL

The Supplementary Material for this article can be found online at: https://www.frontiersin.org/articles/10.3389/fonc.2020.572708/full#supplementary-material

Supplementary Figure 1 | Results of PCA in view of patients from GSE39582 and 21 m^6A regulators **(A,B)**. Consensus index after regrouping cases by PCA **(C)**. Heatmap of 21 m^6A regulators expression in GSE39582 **(D)**.

Supplementary Figure 2 | Results of LASSO lambda filtering **(A)**. Relationship between LASSO regression coefficient and lambda **(B)**.

Supplementary Figure 3 | The heatmap of four genes found differentially expressed using LIMMA method.

Supplementary Figure 4 | The protein-protein interaction network **(A)**. Dot plot of the functional enrichment analysis of KEGG pathway **(B)**. Protein and pathway relationship network **(C)**. Pathway and pathway interaction network **(D)**.

Supplementary Figure 5 | The K–M survival curves of overall survival between high-risk and low-risk group of different clinicopathological features, including gender **(A,B)**, age **(C,D)**, tumor site **(E,F)**, MMR status **(G)**, TP53 mutation status **(H,I)**, KRAS mutation status **(J,K)**, BRAF mutation status **(L)**, pathological T stage **(M)**, pathological N stage **(N,O)**.

Supplementary Figure 6 | Nomograms convey the results of prognostic models using the seven-HCL-related signature and pathology N stage to predict RFS of patients with CRC in TCGA cohort. The AUC at 1-year prediction was 0.759 **(A,B)**. The *x*-axis is nomogram-predicted probability of survival and *y*-axis is actual survival. The reference line is 45◦ and indicates perfect calibration (**C** as 1-year, **D** as 3-year, **E** as 5-year).

Supplementary Table 1 | 21 genes of m^6A regulators list obtained from the GSEA database.

Supplementary Table 2 | 87 HCL genes list obtained from the GSEA database.

Supplementary Table 3 | Demographic information of patients with stage III CRC in GSE39582, GSE14333, and TCGA cohorts.

Supplementary Table 4 | Result scores of PCA in GSE39582 and GSE14333.

Supplementary Table 5 | Result scores of GSVA in GSE39582 and GSE14333.

Supplementary Table 6 | Gene list through LASSO analyses and LIMMA method.

Supplementary Table 7 | Univariable and multivariable Cox regression model analyses of relapse-free survival in GSE39582 cohort.

Supplementary Table 8 | Univariable and multivariable Cox regression model analyses of overall survival in GSE39582 cohort.

Supplementary Table 9 | Univariable and multivariable Cox regression model analyses of relapse-free survival in TCGA cohort.

Supplementary Table 10 | Standardized net benefit for specific optimal thresholds using DCA based on GSE39582 and TCGA.

REFERENCES

1. Siegel RL, Miller KD, Jemal A. Cancer statistics, 2020. *CA Cancer J Clin.* (2020) 70:7–30. doi: 10.3322/caac.21590
2. Chen W. Cancer statistics: updated cancer burden in China. *Chin J Cancer Res.* (2015) 27:1. doi: 10.3978/j.issn.1000-9604.2015.02.07
3. McQuade RM, Stojanovska V, Bornstein JC, Nurgali K. Colorectal cancer chemotherapy: the evolution of treatment and new approaches. *Curr Med Chem.* (2017) 24:1537–57. doi: 10.2174/0929867324666170111152436
4. Redston M, Compton CC, Miedema BW, Niedzwiecki D, Dowell JM, Jewell SD, et al. Analysis of micrometastatic disease in sentinel lymph nodes from resectable colon cancer: results of cancer and leukemia group B Trial 80001. *J Clin Oncol.* (2006) 24:878–83. doi: 10.1200/jco.2005.03.6038
5. Fujita S, Shimoda T, Yoshimura K, Yamamoto S, Akasu T, Moriya Y. Prospective evaluation of prognostic factors in patients with colorectal cancer undergoing curative resection. *J Surg Oncol.* (2003) 84:127–31. doi: 10.1002/jso.10308
6. Boland GM, Chang GJ, Haynes AB, Chiang YJ, Chagpar R, Xing Y, et al. Association between adherence to national comprehensive cancer network treatment guidelines and improved survival in patients with colon cancer. *Cancer.* (2013) 119:1593–601. doi: 10.1002/cncr.27935
7. Grothey A, Sobrero AF, Shields AF, Yoshino T, Paul J, Taieb J, et al. Duration of adjuvant chemotherapy for stage III colon cancer. *N Engl J Med.* (2018) 378:1177–88. doi: 10.1056/NEJMoa1713709
8. Fu Y, Dominissini D, Rechavi G, He C. Gene expression regulation mediated through reversible m6A RNA methylation. *Nat Rev Genet.* (2014) 15:293–306. doi: 10.1038/nrg3724
9. Kwok CT, Marshall AD, Rasko JE, Wong JJ. Genetic alterations of m(6)A regulators predict poorer survival in acute myeloid leukemia. *J Hematol Oncol.* (2017) 10:39. doi: 10.1186/s13045-017-0410-6
10. Zhang B, Wu Q, Li B, Wang D, Wang L, Zhou YL. m(6)A regulator-mediated methylation modification patterns and tumor microenvironment infiltration characterization in gastric cancer. *Mol Cancer.* (2020) 19:53. doi: 10.1186/s12943-020-01170-0
11. Meng Y, Li S, Gu D, Xu K, Du M, Zhu L, et al. Genetic variants in m6A modification genes are associated with colorectal cancer risk. *Carcinogenesis.* (2020) 41:8–17. doi: 10.1093/carcin/bgz165
12. Raghuwanshi S, Dahariya S, Kandi R, Gutti U, Undi RB, Sharma DS, et al. Epigenetic mechanisms: role in hematopoietic stem cell lineage commitment and differentiation. *Curr Drug Targets.* (2018) 19:1683–95. doi: 10.2174/1389450118666171122141821
13. Irizarry RA, Hobbs B, Collin F, Beazer-Barclay YD, Antonellis KJ, Scherf U, et al. Exploration, normalization, and summaries of high density oligonucleotide array probe level data. *Biostatistics.* (2003) 4:249–64. doi: 10.1093/biostatistics/4.2.249
14. Hanzelmann S, Castelo R, Guinney J. GSVA: gene set variation analysis for microarray and RNA-seq data. *BMC Bioinformatics.* (2013) 14:7. doi: 10.1186/1471-2105-14-7
15. Subramanian A, Tamayo P, Mootha VK, Mukherjee S, Ebert BL, Gillette MA, et al. Gene set enrichment analysis: a knowledge-based approach for interpreting genome-wide expression profiles. *Proc Natl Acad Sci USA.* (2005) 102:15545–50. doi: 10.1073/pnas.0506580102
16. Friedman J, Hastie T, Tibshirani R. Regularization paths for generalized linear models via coordinate descent. *J Stat Softw.* (2010) 33:1–22.
17. Lu CY, Uen YH, Tsai HL, Chuang SC, Hou MF, Wu DC, et al. Molecular detection of persistent postoperative circulating tumour cells in stages II and III colon cancer patients via multiple blood sampling: prognostic significance of detection for early relapse. *Br J Cancer.* (2011) 104:1178–84. doi: 10.1038/bjc.2011.40
18. Heagerty PJ, Zheng Y. Survival model predictive accuracy and ROC curves. *Biometrics.* (2005) 61:92–105. doi: 10.1111/j.0006-341X.2005.030814.x
19. Bindea G, Mlecnik B, Hackl H, Charoentong P, Tosolini M, Kirilovsky A, et al. ClueGO: a Cytoscape plug-in to decipher functionally grouped gene ontology and pathway annotation networks. *Bioinformatics.* (2009) 25:1091–3. doi: 10.1093/bioinformatics/btp101
20. Vickers AJ, Elkin EB. Decision curve analysis: a novel method for evaluating prediction models. *Medical Decision Making.* (2006) 26:565–74. doi: 10.1177/0272989x06295361
21. Liu X, Liu L, Dong Z, Li J, Yu Y, Chen X, et al. Expression patterns and prognostic value of m(6)A-related genes in colorectal cancer. *Am J Transl Res.* (2019) 11:3972–91.
22. Mori T, Ohue M, Takii Y, Hashizume T, Kato T, Kotake K, et al. Factors predicting the response to oral fluoropyrimidine drugs: a phase II trial on the individualization of postoperative adjuvant chemotherapy using oral fluorinated pyrimidines in stage III colorectal cancer treated by curative resection (ACT-01 Study). *Oncol Rep.* (2013) 29:437–44. doi: 10.3892/or.2012.2177
23. Kharfan-Dabaja MA, Labopin M, Bazarbachi A, Socie G, Kroeger N, Blaise D, et al. Higher busulfan dose intensity appears to improve leukemia-free and overall survival in AML allografted in CR2: an analysis from the acute leukemia working party of the European group for blood and marrow transplantation. *Leuk Res.* (2015) 39:933–7. doi: 10.1016/j.leukres.2015.04.009
24. Kaito K, Katayama T, Masuoka H, Nishiwaki K, Sano K, Sekiguchi N, et al. CD2+ acute promyelocytic leukemia is associated with leukocytosis, variant morphology and poorer prognosis. *Clin Lab Haematol.* (2005) 27:307–11. doi: 10.1111/j.1365-2257.2005.00715.x
25. Patin EC, Soulard D, Fleury S, Hassane M, Dombrowicz D, Faveeuw C, et al. Type I IFN receptor signaling controls IL7-dependent accumulation and activity of protumoral IL17A-producing γδT cells in breast cancer. *Cancer Res.* (2018) 78:195–204. doi: 10.1158/0008-5472.Can-17-1416
26. Shum T, Omer B, Tashiro H, Kruse RL, Wagner DL, Parikh K, et al. Constitutive signaling from an engineered IL7 receptor promotes durable tumor elimination by tumor-redirected T cells. *Cancer Discov.* (2017) 7:1238–47. doi: 10.1158/2159-8290.Cd-17-0538
27. Bauer KM, Watts TN, Buechler S, Hummon AB. Proteomic and functional investigation of the colon cancer relapse-associated genes NOX4 and ITGA3. *J Proteome Res.* (2014) 13:4910–8. doi: 10.1021/pr500557n
28. Linhares MM, Affonso RJ Jr., Viana Lde S, Silva SR, Denadai MV, de Toledo SR, et al. Genetic and immunohistochemical expression of integrins ITGAV, ITGA6, and ITGA3 as prognostic factor for colorectal cancer: models for global and disease-free survival. *PLoS One.* (2015) 10:e0144333. doi: 10.1371/journal.pone.0144333
29. Sa KD, Zhang X, Li XF, Gu ZP, Yang AG, Zhang R, et al. A miR-124/ITGA3 axis contributes to colorectal cancer metastasis by regulating anoikis susceptibility. *Biochem Biophys Res Commun.* (2018) 501:758–64. doi: 10.1016/j.bbrc.2018.05.062
30. Daver N, Schlenk RF, Russell NH, Levis MJ. Targeting FLT3 mutations in AML: review of current knowledge and evidence. *Leukemia.* (2019) 33:299–312. doi: 10.1038/s41375-018-0357-9
31. Moreira RB, Peixoto RD, de Sousa Cruz MR. Clinical response to sorafenib in a patient with metastatic colorectal cancer and FLT3 amplification. *Case Rep Oncol.* (2015) 8:83–7. doi: 10.1159/000375483
32. Durrant LG, Chapman MA, Buckley DJ, Spendlove I, Robins RA, Armitage NC. Enhanced expression of the complement regulatory protein CD55 predicts a poor prognosis in colorectal cancer patients. *Cancer Immunol Immunother.* (2003) 52:638–42. doi: 10.1007/s00262-003-0402-y
33. Tsuchida T, Kijima H, Tokunaga T, Oshika Y, Hatanaka H, Fukushima Y, et al. Expression of the thrombospondin 1 receptor CD36 is correlated with decreased stromal vascularisation in colon cancer. *Int J Oncol.* (1999) 14:47–51.

Conflict of Interest: The authors declare that the research was conducted in the absence of any commercial or financial relationships that could be construed as a potential conflict of interest.

frontiers in Oncology

ORIGINAL RESEARCH
published: 05 October 2020
doi: 10.3389/fonc.2020.541401

Prognosis Analysis and Validation of m^{6}A Signature and Tumor Immune Microenvironment in Glioma

Shaojian Lin[1,2], *Houshi Xu*[1†], *Anke Zhang*[1†], *Yunjia Ni*[1], *Yuanzhi Xu*[1], *Tong Meng*[3*], *Mingjie Wang*[4*] and *Meiqing Lou*[1*]

[1] Department of Neurosurgery, Shanghai General Hospital, Shanghai Jiao Tong University School of Medicine, Shanghai, China, [2] School of Medicine, Tongji University, Shanghai, China, [3] Department of Orthopedics, Shanghai General Hospital, Shanghai Jiao Tong University School of Medicine, Shanghai, China, [4] Department of Digestive Diseases, Ruijin Hospital North, Shanghai Jiao Tong University School of Medicine, Shanghai, China

OPEN ACCESS

Edited by:
Shicheng Guo,
University of Wisconsin-Madison,
United States

Reviewed by:
Chenkai Ma,
Commonwealth Scientific and Industrial Research Organisation (CSIRO), Australia
Pawel Buczkowicz,
PhenoTips, Canada

***Correspondence:**
Tong Meng
mengtong@medmail.com.cn
Mingjie Wang
huzai920621@126.com
Meiqing Lou
loumq68128@hotmail.com

[†] These authors have contributed equally to this work and share first authorship

Specialty section:
This article was submitted to Cancer Genetics, a section of the journal Frontiers in Oncology

Received: 09 March 2020
Accepted: 24 August 2020
Published: 05 October 2020

Citation:
Lin S, Xu H, Zhang A, Ni Y, Xu Y, Meng T, Wang M and Lou M (2020) Prognosis Analysis and Validation of m^{6}A Signature and Tumor Immune Microenvironment in Glioma. Front. Oncol. 10:541401. doi: 10.3389/fonc.2020.541401

Glioma is one of the most typical intracranial tumors, comprising about 80% of all brain malignancies. Several key molecular signatures have emerged as prognostic biomarkers, which indicate room for improvement in the current approach to glioma classification. In order to construct a more veracious prediction model and identify the potential prognosis-biomarker, we explore the differential expressed m^{6}A RNA methylation regulators in 665 gliomas from TCGA-GBM and TCGA-LGG. Consensus clustering was applied to the m6A RNA methylation regulators, and two glioma subgroups were identified with a poorer prognosis and a higher grade of WHO classification in cluster 1. The further chi-squared test indicated that the immune infiltration was significantly enriched in cluster 1, indicating a close relation between m^{6}A regulators and immune infiltration. In order to explore the potential biomarkers, the weighted gene co-expression network analysis (WGCNA), along with Least absolute shrinkage and selection operator (LASSO), between high/low immune infiltration and m^{6}A cluster 1/2 groups were utilized for the hub genes, and four genes (*TAGLN2, PDPN, TIMP1, EMP3)* were identified as prognostic biomarkers. Besides, a prognostic model was constructed based on the four genes with a good prediction and applicability for the overall survival (OS) of glioma patients (the area under the curve of ROC achieved 0.80 (0.76–0.83) and 0.72 (0.68–0.76) in TCGA and Chinese Glioma Genome Atlas (CGGA), respectively). Moreover, we also found *PDPN* and *TIMP1* were highly expressed in high-grade glioma from The Human Protein Atlas database and both of them were correlated with m6A and immune cell marker in glioma tissue samples. In conclusion, we construct a novel prognostic model which provides new insights into glioma prognosis. The *PDPN* and *TIMP1* may serve as potential biomarkers for prognosis of glioma.

Keywords: glioma, m^{6}A, immune infiltration, WGCNA, prognostic model

INTRODUCTION

Glioma is a common primary tumor in the central nervous system (CNS), accounting for about 80% of brain malignancies (1, 2). The lower-grade gliomas (LGGs) has a relatively favorable prognosis, consisting of the diffuse low-grade and intermediate-grade gliomas (World Health Organization [WHO] grades II and III), whereas glioblastoma (GBM) are generally high-grade gliomas (grade IV) (3, 4). Despite recent medical advances, patients with high-grade GBM are still associated with poor prognosis. Thus, identifying the difference in various gliomas may assist oncologists in finding the prognostic biomarkers and potential targets for glioma patients.

N6-Methyladenosine (m^{6}A) is the most popular internal mRNA modification in diverse cell types and consists of the m6A methyltransferases, reverted by the demethylases and identified by m^{6}A binding proteins (5–10). Generally, m^{6}A modification has various regulatory functions in tumorigenesis, progression and immunity modulation (11–15). Meanwhile, tumor immune microenvironment also participates in tumor initiation and progression and influences the clinical outcomes of patients (16–18). Immune classification of cancers is crucial in therapeutic strategy establishing and prognosis assessment of patients with tumors (19, 20).

Several studies have revealed the correlation between tumor microenvironment (TME) infiltrating immune cells and m^{6}A modification. In the gastric tumors, m6A modification patterns could predict the stages of tumor inflammation, TME stromal activity, genetic variation and patient prognosis. Lower m6A score indicated an inflamed TME phenotype and enhanced response to anti-PD-1/L1 immunotherapy (21). The high expression of WTAP, a m6A methyltransferase, was also associated with RNA methylation and its low expression was related to a high T cell-related immune response in gastric cancer (22). Additionally, m^{6}A was reduced in the high immunity subtype of lung adenocarcinoma, indicating that m^{6}A may mediate immune signatures and help to provide potential strategies (23). However, the potential roles of m6A modification in immune infiltration remain obscure, especially in glioma. Therefore, identification of immune infiltration characterizations mediated by multiple m6A regulators might be helpful for the survival prognosis of patients with glioma.

In this study, in order to investigate the novel prediction model and potential biomarkers for glioma, WGCNA and LASSO were applied to identify candidate genes that might take part in both m6A and immune infiltration in glioma based on TCGA database. Differentially expressed genes (DEGs) were identified, along with their prognostic values, and further validated by external datasets and tissue microarray. Besides, the constructed prediction model revealed a high efficacy for prognosis prediction. The potential predictive biomarkers were also identified to assist oncologists in clinic treatment.

METHODS AND MATERIALS

Datasets Acquisition From TCGA Datasets

The Cancer Genome Altas (TCGA) GBMLGG datasets (n = 665) were downloaded from the University of California Santa Cruz (UCSC) Xena browser (https://xenabrowser.net/datapages/). The gene expression data were presented as FPKM values derived from TCGA level 3 data. Batch effects were removed before analyzing (24). Clinical data of TCGA datasets were downloaded from the UCSC Xena browser, including clinical information (age, gender), tumor information (subtypes) and survival information (overall survival) for patients with gliomas (**Table 1**). The RNA-seq transcriptome data and corresponding clinicopathological information of 420 LGG patients and 237 GBM patients were obtained from CGGA (www.cgga.org.cn) as a validation set. The RNA-seq transcriptome data were transformed as FPKM values. GSE16011 (25) expression data was downloaded from GEO database. Robust multi-array average (RMA) normalized files were used in this study. The probe was converted into gene symbol by median gene expression. The microarray data were estimated as log2(x+1) normalized expression value.

Selection of m^{6}A RNA Methylation Regulators

We used 12 m^{6}A RNA methylation regulators from published literature. Then, the expression of these m6A RNA methylation regulators in gliomas were systematically compared with different clinical outcomes using Gliovis (http://gliovis.bioinfo.cnio.es/) (26).

Unsupervised Analysis With ConsensusClusterPlus

In order to investigate the function of m^{6}A RNA methylation regulators in glioma, we divided patients with glioma into different groups with "ConsensusClusterPlus" (50 iterations, resample rate of 80%). The principal component analysis was then performed with the R package "PCA" for R v3.5.1 to study the gene expression patterns in different glioma clusters. In order to determine the optimal K, Average Silhouette method and Gap Statistic method were applied, the results showed that the two groups were the best grouping number (**Supplementary Figure 1**). Wilcoxon signed rank test was used to compare the tumor mutation burden of cluster 1 and cluster 2.

Function Analysis of m^{6}A Cluster Subgroups and Immune Infiltration Analysis Based on Single-Sample Gene Set Enrichment Analysis (ssGSEA)

Gene Set Variation Analysis (GSVA) was performed with the R package "gsva" to evaluate pathway enrichment for different clusters. To investigate the immune infiltration landscape of

TABLE 1 | Summary table of the TCGA clinical information.

	Level	Cluster1	Cluster2	*p*
N		190	475	
Study (%)	GBM	87 (46.8)	63 (13.4)	<0.001
	LGG	99 (53.2)	407 (86.6)	
Grade (%)	II	42 (23.9)	182 (41.8)	<0.001
	III	48 (27.3)	191 (43.9)	
	IV	87 (49.1)	63 (14.4)	
Histology (%)	Astrocytoma	42 (22.6)	149 (31.7)	<0.001
	GBM	87 (46.8)	63 (13.4)	
	Oligoastrocytoma	28 (15.1)	100 (21.3)	
	Oligodendroglioma	29 (15.6)	158 (33.6)	
Recurrence (%)	Primary	176 (92.6)	432 (90.9)	NA
Subtype (%)	Classic-like	33 (20.0)	34 (7.5)	<0.001
	Codel	26 (15.8)	143 (31.6)	
	G-CIMP-high	54 (32.7)	178 (39.4)	
	G-CIMP-low	8 (4.8)	7 (1.5)	
	LGm6-GBM	4 (2.4)	6 (1.3)	
	Mesenchymal-like	36 (21.8)	62 (13.7)	
	PA-like	4 (2.4)	22 (4.9)	
survival [mean (*SD*)]		25.96 (31.55)	27.31 (28.24)	0.596
status [mean (*SD*)]		0.50 (0.50)	0.31 (0.46)	<0.001
Transcriptome.Subtype (%)	CL	36 (23.4)	48 (13.1)	<0.001
	ME	38 (24.7)	57 (15.5)	
	NE	13 (8.4)	96 (26.2)	
	PN	67 (43.5)	166 (45.2)	
Pan_Glioma.RNA.Expression.Cluster (%)	LGr1	36 (19.5)	102 (21.8)	<0.001
	LGr2	11 (5.9)	77 (16.5)	
	LGr3	59 (31.9)	174 (37.2)	
	LGr4	79 (42.7)	115 (24.6)	
IDH_specific.RNA.Expression.Cluster (%)	IDHmut-R1	15 (8.2)	89 (19.2)	<0.001
	IDHmut-R2	14 (7.7)	82 (17.7)	
	IDHmut-R3	59 (32.2)	157 (33.9)	
	IDHwt-R1	22 (12.0)	24 (5.2)	
	IDHwt-R2	34 (18.6)	44 (9.5)	
	IDHwt-R3	30 (16.4)	38 (8.2)	
	IDHwt-R4	9 (4.9)	29 (6.3)	
Pan_Glioma.DNA.Methylation.Cluster (%)	LGm1	19 (11.4)	30 (6.6)	<0.001
	LGm2	51 (30.5)	199 (43.4)	
	LGm3	19 (11.4)	102 (22.3)	
	LGm4	32 (19.2)	32 (7.0)	
	LGm5	37 (22.2)	67 (14.6)	
	LGm6	9 (5.4)	28 (6.1)	
IDH_specific.DNA.Methylation.Cluster (%)	IDHmut-K1	16 (9.7)	24 (5.3)	<0.001
	IDHmut-K2	46 (27.9)	162 (35.8)	
	IDHmut-K3	26 (15.8)	143 (31.6)	
	IDHwt-K1	33 (20.0)	34 (7.5)	
	IDHwt-K2	36 (21.8)	62 (13.7)	
	IDHwt-K3	8 (4.8)	28 (6.2)	
Subtype.original (%)	Classical	25 (13.5)	13 (2.8)	<0.001
	G-CIMP	6 (3.2)	2 (0.4)	

(Continued)

TABLE 1 | Continued

	Level	Cluster1	Cluster2	*p*
	IDHmut-codel	25 (13.5)	140 (30.0)	
	IDHmut-non-codel	57 (30.8)	186 (39.8)	
	IDHwt	16 (8.6)	79 (16.9)	
	Mesenchymal	26 (14.1)	22 (4.7)	
	Neural	11 (5.9)	15 (3.2)	
	Proneural	19 (10.3)	10 (2.1)	
Random.Forest.Sturm.Cluster (%)	G34	0 (0.0)	1 (0.2)	0.175
	IDH	81 (65.3)	318 (74.5)	
	K27	0 (0.0)	1 (0.2)	
	Mesenchymal	22 (17.7)	67 (15.7)	
	RTK I 'PDGFRA'	3 (2.4)	9 (2.1)	
	RTK II 'Classic'	18 (14.5)	31 (7.3)	
IDH.status (%)	Mutant	89 (48.4)	330 (71.0)	<0.001
	WT	95 (51.6)	135 (29.0)	
Chr.1p_19q.codeletion (%)	Codel	25 (13.7)	140 (29.9)	<0.001
	non-codel	158 (86.3)	328 (70.1)	
IDH_codel.subtype (%)	IDHmut-codel	25 (13.8)	140 (30.2)	<0.001
	IDHmut-non-codel	64 (35.4)	188 (40.6)	
	IDHwt	92 (50.8)	135 (29.2)	
MGMT.promoter.status (%)	Methylated	117 (70.1)	353 (77.1)	0.091
	Unmethylated	50 (29.9)	105 (22.9)	
Chr.7.gain_Chr.10.loss (%)	Gain chr 7 & loss chr 10	69 (37.9)	81 (17.4)	<0.001
	No combined can	113 (62.1)	385 (82.6)	
Chr.19_20.co_gain (%)	Gain chr 19/20	12 (6.6)	18 (3.9)	0.201
	No chr 19/20 gain	170 (93.4)	448 (96.1)	
TERT.promoter.status (%)	Mutant	39 (47.0)	113 (49.1)	0.836
	WT	44 (53.0)	117 (50.9)	
TERT.expression.status (%)	Expressed	118 (63.8)	227 (48.5)	0.001
	Not expressed	67 (36.2)	241 (51.5)	
ATRX.status (%)	Mutant	46 (25.1)	146 (31.5)	0.132
	WT	137 (74.9)	317 (68.5)	
DAXX.status (%)	Mutant	2 (1.1)	0 (0.0)	0.142
	WT	181 (98.9)	463 (100.0)	
Telomere.Maintenance (%)	-/-	15 (18.1)	35 (15.5)	0.86
	ATRX	29 (34.9)	82 (36.3)	
	TERT	39 (47.0)	109 (48.2)	
BRAF.V600E.status (%)	Mutant	1 (0.5)	2 (0.4)	1
	WT	182 (99.5)	461 (99.6)	
BRAF_KIAA1549.fusion (%)	Fusion	0 (0.0)	1 (0.2)	1
	WT	185 (100.0)	467 (99.8)	
RPPA.cluster (%)	K1	47 (49.5)	46 (20.5)	<0.001
	K2	48 (50.5)	178 (79.5)	

glioma, ssGSEA was performed to assess the level of immune infiltration (recorded as ssGSEA score) in a sample according to the expression levels of immune cell-specific marker genes with R package "gsva." Most immune cell types related marker genes were obtained from the article published by Bindea et al. (27).

Cox Regression Analysis

We assessed the impact of immune cell types on clinical survival data and survival time by Cox proportional hazards regression analysis based on the R package "survival" and "forestplot." Cell types with a high hazard ratio were considered to be risk factors to OS.

Hub Genes Correlated With m^{6}A RNA Methylation Clusters and Immune Infiltration Based on Weighted Correlation Network Analysis (WGCNA)

We extracted all the DEGs (according to adj. p-value < 0.01, $|\log FC| \geq 2$, total $= 729$) from limma analysis with expression data retrieved from TCGA GBM/LGG datasets to perform Weighted correlation network analysis (WGCNA) using R package "limma." We applied R package "WGCNA" to find clinical traits-related modules and hub genes among them (28). The adjacency matrix was then transformed into topological overlap matrix (TOM). Genes were divided into different gene modules according to the TOM-based dissimilarity measure. We set soft-thresholding power as 9 (scale free R2 = 0.85), cut height as 0.2, and minimal module size as 30 to identify key modules. Those with gene significance (GS) > 0.5 and module membership (MM) > 0.9 were defined as hub genes.

Validation of Prognostic Values of Hub Genes

To predict the clinical outcomes of glioma patients with the hub genes, we applied LASSO Cox regression algorithm to the 5 hub genes in the TCGA datasets. We selected four genes to build the risk signature based on the minimum criteria, and the coefficients obtained from the LASSO algorithm were used to calculate the risk score for each patient as follows:

$$Riskscore = \sum_{i=1}^{n} * \beta_i$$

where n was the number of prognostic genes, $\exp_i$ the expression value of gene i, and β_i the regression coefficient of gene i in the LASSO algorithm. Using the median risk score as a cutoff value, glioma patients were divided into high- and low-risk score groups. Moreover, the relation between the prognosis signature and OS was investigated based on the external cohort CGGA datasets.

The Kaplan-Meier method was used to assess the differences of overall survival (OS) between low- and high-risk score glioma patients with R package "survival".

The time-dependent receiver operating characteristic (ROC) curve was used to measure the prognostic performance by comparing the areas under the ROC curves (AUC) using R package "pROC." 10-fold cross method was applied for ROC validation and AUC value calculation.

All the scripts were uploaded at Github website (https://github.com/mvpsc30/FIO-m6A-immune).

Assessment of Immunohistochemistry Data

The *PDPN* and *TIMP1* immunohistochemistry results were acquired from the Human Protein Atlas (HPA, https://www.proteinatlas.org/) database (29). The *EMP3* and *TAGLN2* protein levels of selected genes were evaluated through commercially glioma tissue-microarrays and H-scores between Low-grade gliomas and High-grade gliomas.

Real-Time RT-PCR

Total RNA was extracted from tissue samples and cells using TRIzol reagent (Invitrogen) after washing with PBS. cDNA was synthesized from purified RNA using a SuperScript III First-Strand cDNA synthesis system (18080051, Life Technologies) according to the manufacturer's instruction. SYBR Green PCR Master Mix (Applied Biosystems, CA, USA) was used for PCR amplification and a real-time PCR machine (iQ5, Bio-Rad Laboratories) was used to quantify the expression of mRNAs. β-actin was used as endogenous control and the expression levels were quantified using the methods of $2-\Delta\Delta Ct$.

Primers:

	Forward	Reverse
CD68	GGAAATGCCACGGTTCATCCA	TGGGGTTCAGTACAGAGATGC
YTHDC1	AACTGGTTTCTAAGCCACTGAGC	GGAGGCACTACTTGATAGACGA
WTAP	CATTTTGTGGCAGCGAGACC	AATCCTCTCCAGGCAGAAGC
TIMP1	CTTCTGCAATTCGACCTCGT	ACGCTGGTATAAGGTGGTCTG
PDPN	GTGTAACAGGCATTCGCATCG	TGTGGCGCTTGGACTTTGT

Cell Culture and Transfection

Human glioma cell line U87 and A172 were acquired from the American Type Culture Collection (ATCC) and cultured in DMEM medium (Gibco, Life Technologies, Grand Island, NY) supplemented with 10% fetal bovine serum (Gibco) and 100 U/ml penicillin/streptomycin (Gibco). According to the manufacturer's instructions, the Lipo 2000 transfection reagent was applied for the transfection. The siRNAs against *TIMP1* (siRNA ID: s14143, ThermoFiher), *PDPN* (EHU119431, Sigma) and negative control (SIC001, Sigma) were purchased.

Western Blotting

Western blot (WB) assays was performed as previously described (30). Briefly, we prepared cell extracts for Western blotting in RIPA buffer. Then, lysates were separated by SDS-PAGE and were transferred to PVDF membranes (Millipore, Billerica, MA). Primary antibodies *PDPN* (Abcam, ab236529,1:1000), *TIMP1* (Abcam, ab109125,1:1000), *EMP3* (Santa cruz, sc-81797, 1:100), *TAGLN2* (Proteintech, 10234-2-AP, 1:200), and *GAPDH* (Abcam, ab181602, 1:10000) were used along with HRP-labeled secondary antibody (1:10000, Sigma) in Western blot. The immune complex was detected by chemiluminescence (GE Healthcare, Wauwatosa, WI).

Cell Viability and Cell Death Measurement

Cell viability was measured using the CellTiter-Glo® luminescent cell viability assay (Promega) based on the manufacturer's instructions. For phosphatidylserine exposure, cells were stained with annexin V-PE as instructed by the manufacturer (BD Biosciences, San Jose, CA), and assayed by flow cytometry (CyAn ADP, Beckman Coulter, Brea, CA, USA).

Statistical Analysis

Experimental results were analyzed with a Student's *t*-test and graphed using Graphpad Prism application (GraphPad Software, Inc., La Jolla, CA). Data are expressed as mean ± *SD*. A $p < 0.05$ was considered with statistical significance. The correlation between the expression profiles of TIMP1 and PDPN with immune and macrophage marker was analyzed using Spearman's rank test.

RESULTS

Consensus Clustering of m^{6}A RNA Methylation Regulators Identified Two Clusters of Gliomas With Distinct Immune Infiltration

A flowchart of this study is shown in **Supplementary Figure 1**. Based on biological functions of each m^{6}A RNA methylation regulator in clinical prognosis, we performed consensus clustering based on gene expression of 12 key m^{6}A RNA regulators in TCGA datasets. Due to the expression analogy of m^{6}A regulators, the clustering analysis would classify the samples into different clusters. After evaluating the relative change in the area under the cumulative distribution function (CDF) curve and consensus heatmap, we selected a three-cluster solution ($K = 2$), which has no obvious increase in the area under the CDF curve (**Supplementary Figures 2A–D**). To further determine the optimal *K*, two methods (Average Silhouette method and Gap Statistic method) were applied. Based on these methods, two subgroups clustered by $k = 2$, namely, cluster 1 and cluster 2 subgroups were found (**Supplementary Figures 2E,F**). Most parts of m6A RNA methylation regulators' expressions showed clear distinction and significant difference in two cluster subgroups (**Figures 1A,B**). In order to better understand the interaction among the 12 m^{6}A regulators, we assessed the interaction and correlation among these regulators (**Supplementary Figure 3**).

The Kaplan-Meier survival analysis revealed a significant shorter OS in cluster 1 subgroup than the cluster 2 subgroup (**Figure 1C**). Moreover, we analyzed the DEGs between cluster1

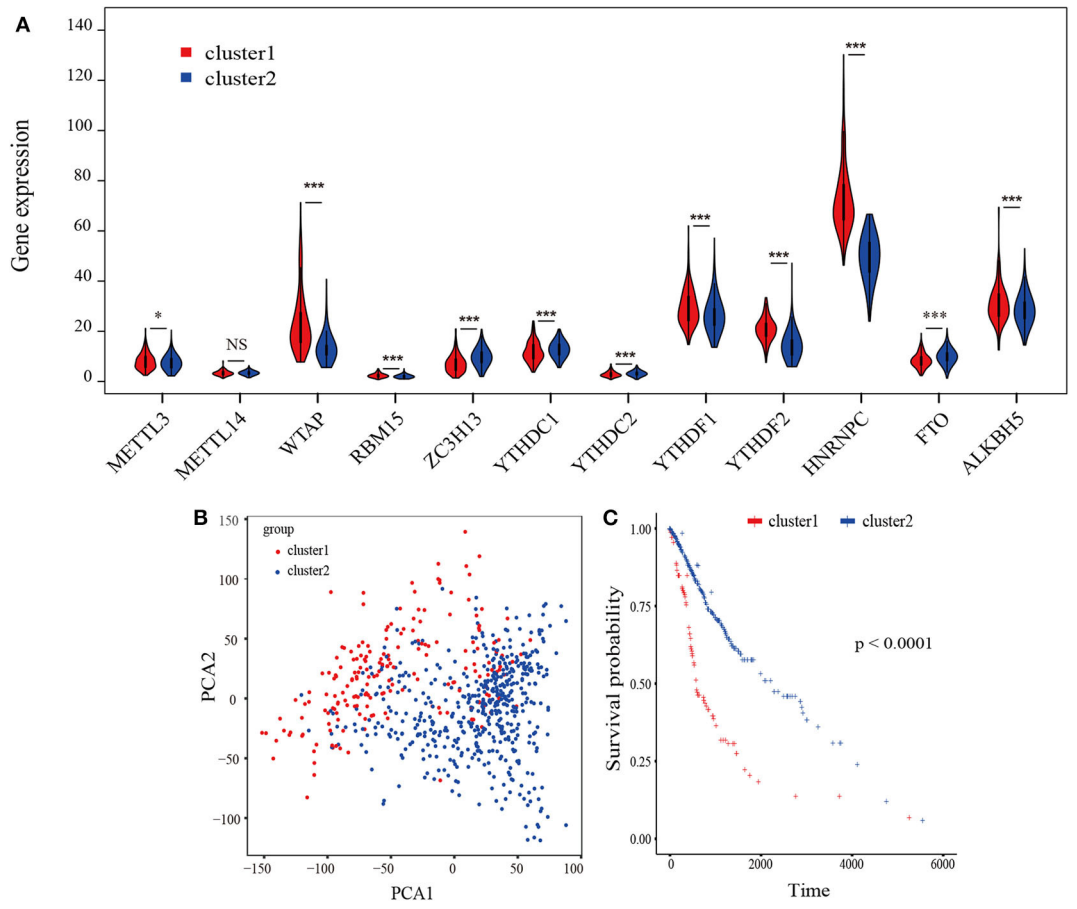

FIGURE 1 | Identification of consensus clusters by m^{6}A RNA methylation regulators overall survival of gliomas in the cluster 1/2 subgroups. **(A)** Violin plot of the two clusters (cluster1/2) defined by the m6A RNA methylation regulators consensus expression. **(B)** Principal component analysis of the total RNA expression profiles in the TCGA-GBM/LGG datasets. Gliomas in the cluster1 subgroup are marked with red. **(C)** Kaplan–Meier overall survival (OS) curves for 665 TCGA glioma patients of different cluster. *$P < 0.05$; **$P < 0.01$; ***$P < 0.001$; ****$P < 0.0001$.

TABLE 2 | Differences in pathway activities scored per sample by GSVA between cluster 1 and cluster 2, cluster 2 vs. cluster 1.

	logFC	adj.P.Val
HALLMARK_MYC_TARGETS_V1	−0.53	4.08E-69
HALLMARK_DNA_REPAIR	−0.35	8.65E-59
HALLMARK_E2F_TARGETS	−0.48	1.84E-49
HALLMARK_UNFOLDED_PROTEIN_RESPONSE	−0.29	1.01E-37
HALLMARK_MTORC1_SIGNALING	−0.28	1.84E-33
HALLMARK_GLYCOLYSIS	−0.19	4.81E-27
* HALLMARK_TNFA_SIGNALING_VIA_NFKB	−0.28	2.16E-24
HALLMARK_G2M_CHECKPOINT	−0.29	8.59E-23
HALLMARK_MYC_TARGETS_V2	−0.30	1.45E-21
HALLMARK_P53_PATHWAY	−0.15	1.18E-20
HALLMARK_ALLOGRAFT_REJECTION	−0.25	1.18E-16
HALLMARK_EPITHELIAL_MESENCHYMAL_TRANSITION	−0.18	1.17E-13
HALLMARK_OXIDATIVE_PHOSPHORYLATION	−0.21	3.01E-13
* HALLMARK_INTERFERON_ALPHA_RESPONSE	−0.29	2.45E-12
* HALLMARK_IL6_JAK_STAT3_SIGNALING	−0.20	1.26E-11
* HALLMARK_TGF_BETA_SIGNALING	−0.16	9.81E-11
HALLMARK_ANDROGEN_RESPONSE	−0.12	7.44E-10
HALLMARK_PEROXISOME	−0.11	2.67E-09
* HALLMARK_INTERFERON_GAMMA_RESPONSE	−0.19	3.11E-09
HALLMARK_IL2_STAT5_SIGNALING	−0.13	2.72E-08

Pathways related to immune response are marked with asterisk.

and cluster2, and annotated their function Gene Set Variation Analysis (GSVA) for biological processes. The results indicated that DEGs are enriched in immune-related biological processes, including IL2/STAT5, IL6/JAK/STAT3, and Interferon-γ response signaling (**Table 2**) and the two categories identified by consensus clustering are correlated with immune infiltration of glioma.

Immune Landscape Was Significantly Associated With m^{6}A RNA Methylation Regulators

To explore the roles of immune cells in the malignant progression of gliomas, the RNA-seq data of 665 patients with gliomas from TCGA-GBM/LGG datasets were analyzed to evaluate the immune landscape. The high and low immune infiltration were defined by Euclidean distance and the ssGSEA scores of immune cells. The results indicated that B cells, Tcm cells, and T helper cells were enriched in high immune infiltration glioma. Relatively, gliomas with low infiltration were characterized for macrophages, eosinophils, neutrophils, and aDC cells (**Figure 2A**).

In order to analyze the relationship between m^{6}A cluster group and immune infiltration, Chi-squared test was carried out ($p < 2.2 \times 10{-}16$, **Figure 2A**). Moreover, we compared the immune infiltration score between cluster 1 and cluster 2, indicating that the proportion of most immune cells types was significantly different between clusters 1 and 2 (**Supplementary Figure 4**). Then Kaplan-Meier survival curve analysis was performed to explore the roles of immune cell infiltration on the prognosis of patients with glioma. The results revealed that patients with low immune infiltration had worse OS compared with patients with high immune infiltration (**Figure 2B**). We also applied a univariate Cox regression analysis on the immune cells of TCGA datasets, and found that 23/24 cell types were significantly correlated with OS ($P < 0.05$). Among these 23 immune cells, aDC, DC, iDC, cytotoxic cells, Eosinophils, Macrophages, Neutrophils, NK.CD56dim cells, NK cells, T cells, Th17 cells, and Th2 cells are risky immune cells with HR > 1, while CD8 T cells, B cells, Mast cells, NK.CD56bright cells, pDC, Tem, Tcm, T helper cells, TFH, Tgd, and Th1 cells were protective immune cells with HR < 1 (**Figure 2C**).

To further determine the relationship between m^{6}A RNA methylation regulators and immune cell infiltration, we assessed the relationships between the expressions of m^{6}A RNA methylation regulators and immune cells infiltration subgroups. The results indicated that high immune infiltration was strongly related to higher expressions of FTO, MELLT14, METTL3, YTHDC1, YTHDC2, and ZC3H13. Correspondingly, low immune infiltration with higher expressions of ALKBH5, HNRNPC, WTAP, YTHDF1, and YTHDF2 (**Supplementary Figure 5**). Then we calculated the relationships between each m^{6}A RNA methylation regulators and immune cells, revealing that FTO, ZC3H13, and YTHDC1 had a significant positive correlation with Tcm cells. Meanwhile, macrophages had a negative relationship with FTO and ZC3H13 (**Figure 2D**). These data indicated that m^{6}A clusters were highly associated with immune infiltration.

WGCNA and Identification of the Key Module

In order to explore the key genes that were mostly associated with m6A and immune cell infiltration subtypes in glioma, we performed WGCNA on the TCGA-GBM/LGG datasets. Glioma sample information such as age, m6A cluster subgroups, immune infiltration subgroups, OS and OS status were retrieved from TCGA-GBM/LGG (**Supplementary Figure 6A**). Eventually identified 6 modules by setting soft-thresholding power as 9 (scale-free R2 = 0.85) and cut height as 0.2 (**Supplementary Figures 6B,C**). From the heatmap of module-trait correlations, we evaluated that the black module was the most highly related to clinical traits (**Supplementary Figure 6D**), especially the immune infiltration and outcomes (correlation coefficient = −0.86 and 0.5, P = 4E-206 and 1E-39; respectively, **Supplementary Figures 6E–G**). Lastly, we selected 5 hub genes (TAGLN2, PDPN, TIMP1, EMP3, CHI3L1) from the black module by setting module membership (MM) >0.9 and gene significance (GS) >0.5. These genes were closely related to each other **Supplementary Figure 6H**).

Association of Hub Genes With m^{6}A RNA Methylation Regulators and Immune Infiltration

We explored the relationship between the expression levels of five hub genes and m^{6}A RNA methylation regulators to elucidate the underlying mechanisms of abnormal up-regulation in glioma. The correlation analysis showed that the expression of many hub

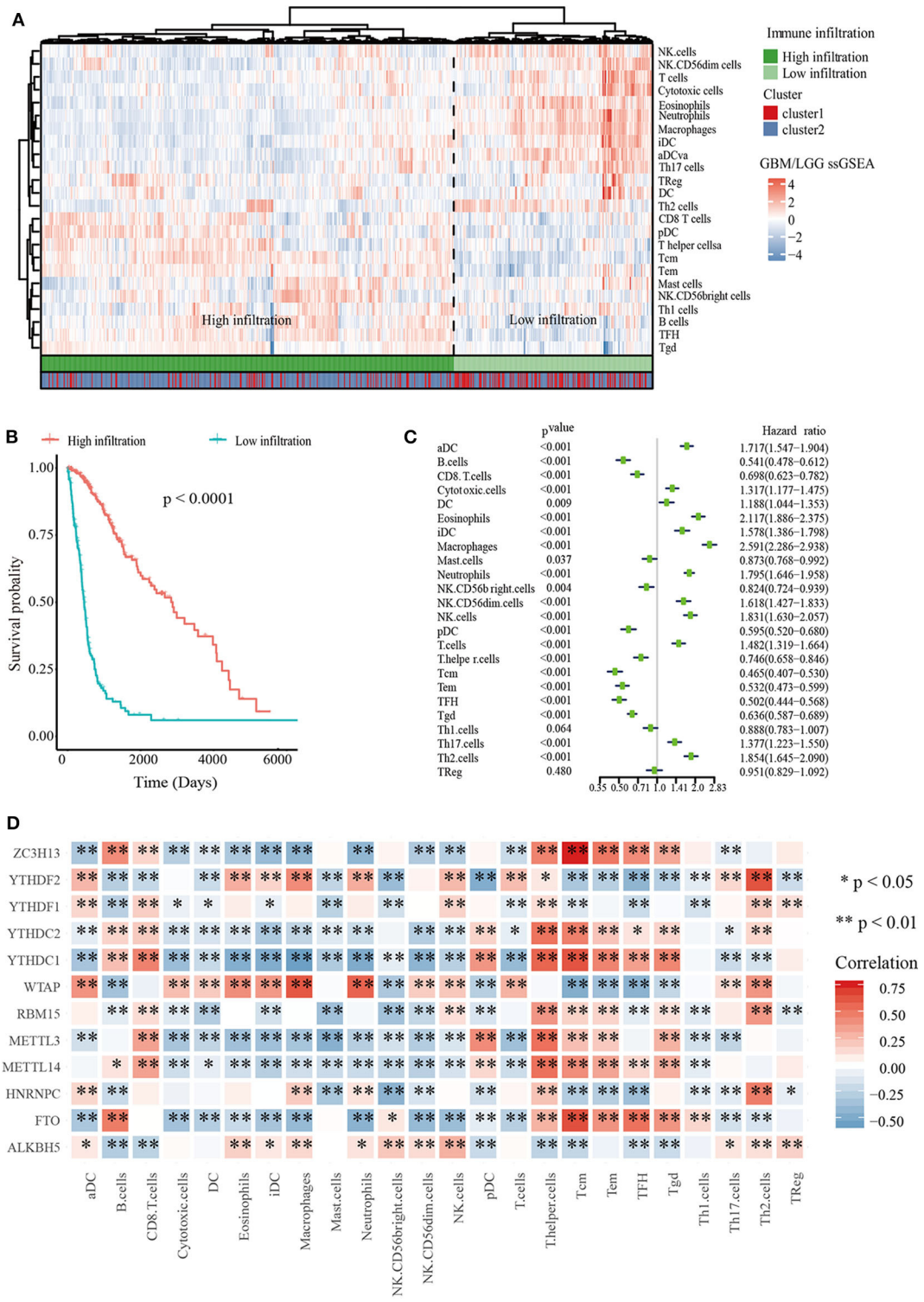

FIGURE 2 | Immune landscape of glioma. **(A)** Heatmap of ssGSEA scores of TCGA-GBM/LGG and Table of cluster and immune infiltration subgroups (Chi-square test: X-squared = 116.63, $p < 2.2e{-}16$). **(B)** Kaplan–Meier overall survival (OS) curves for 665 TCGA glioma patients of different immune infiltration subgroups. **(C)** Forest plot for immune cells. The hazard ratios (HR), 95% confidence intervals (CI) calculated by univariate Cox regression are shown. **(D)** Mine plot of relationships between 12 m^{6}A methylation regulators and 24 immune cells (*$P < 0.05$, **$P < 0.01$).

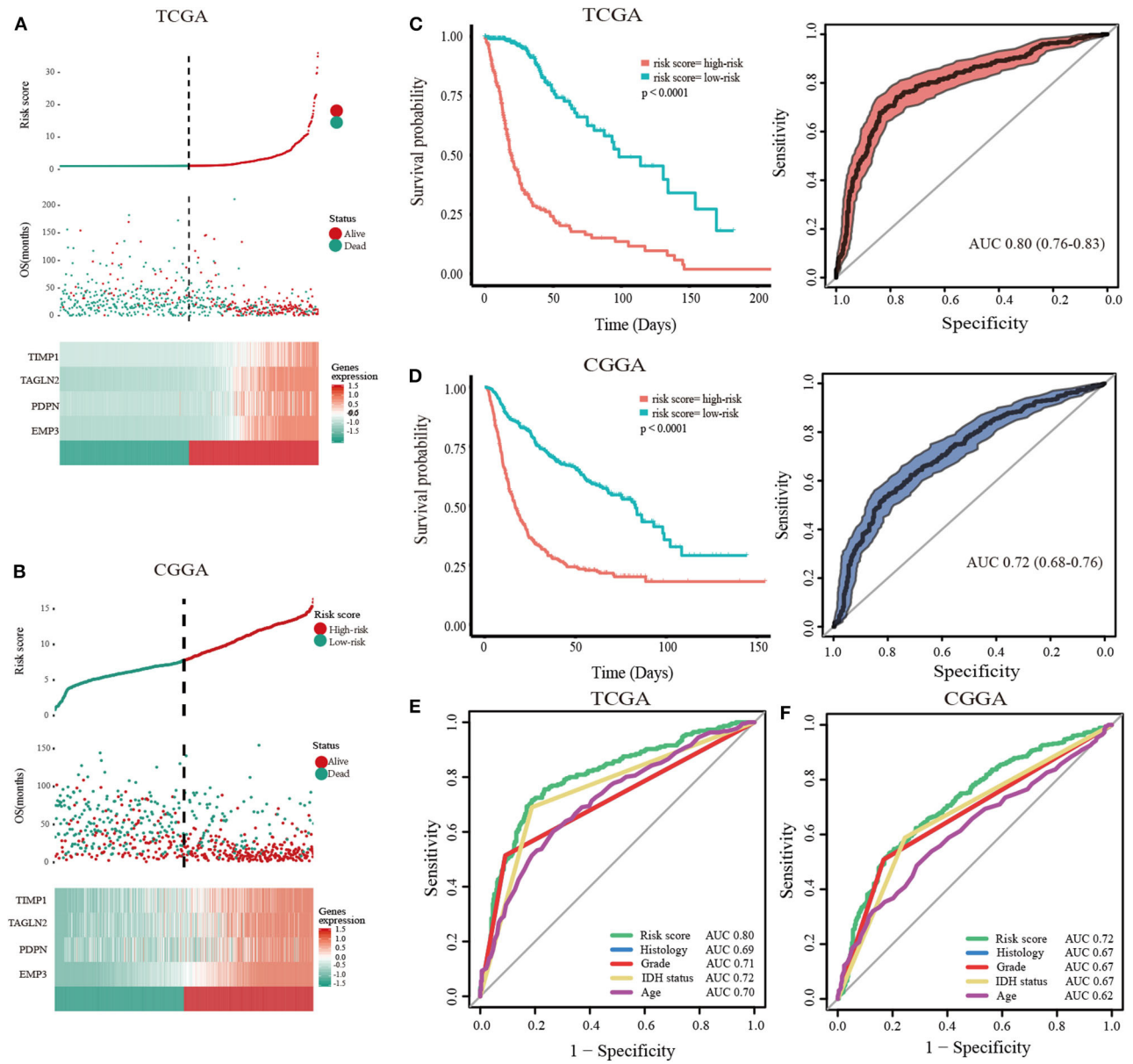

FIGURE 3 | Validation of hub genes highly correlated with clinical traits. In each dataset, the risk score distribution, gene expression profiles, and patients' survival status are displayed (**A**, TCGA; **B**, CGGA). The black-dotted line represents the median cut-off, dividing patients into high- and low-risk groups. Kaplan-Meier and ROC curves with 95% confidence interval for the 4-gene signature in the four datasets. Patients with high risk scores had poor outcome in terms of overall survival (**C**, TCGA; **D**, CGGA). ROC curves comparing prognostic accuracy of risk score with clinical histology, grade, IDH status, and age in internal validation, and external validation cohorts (**E**, TCGA; **F**, CGGA).

genes was significantly correlated with m^{6}A RNA methylation regulators (**Supplementary Figure 7**). Additionally, we found that TAGLN2, PDPN, EMP3, and CHI3L1 were positively associated with WTAP (**Supplementary Figure 7**), while TIMP1 was negatively correlated with YTHDC1.

Then we utilized the Spearman method to study the potential relationship between the expression of glioma hub genes and infiltration of immune cells. Interestingly, hub genes were all positively associated with Macrophages (**Supplementary Figure 8**). Conversely, negative relationship was observed between these five genes and the infiltration of B cells, Tcm cells and Tem cells (**Supplementary Figure 8**). These data indicated that the selected five hub genes were highly correlated with m^{6}A RNA regulators and immune infiltration.

Validation of Hub Genes in Datasets

To predict the clinical outcomes of glioma with the hub genes, we applied the LASSO Cox regression algorithm to the five hub

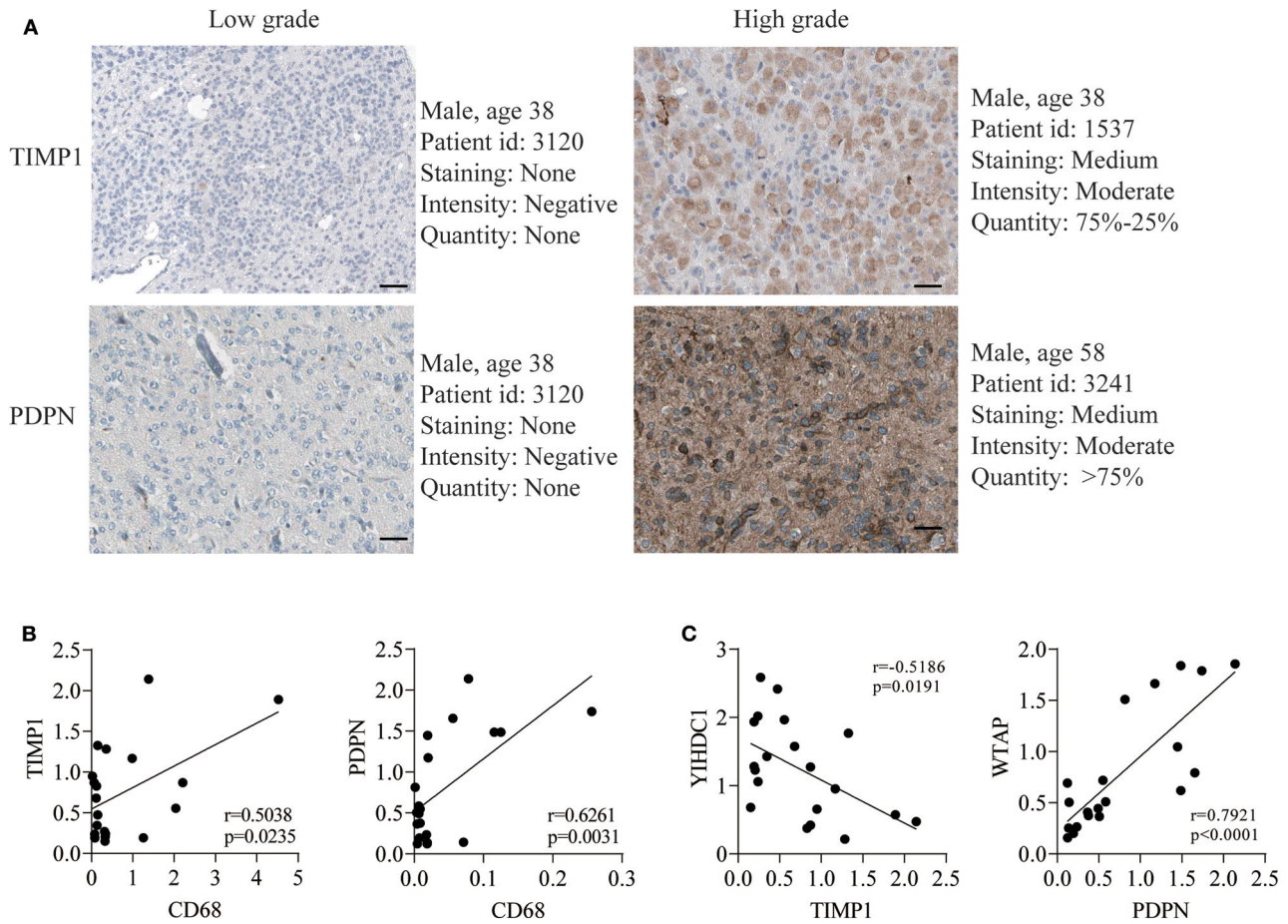

FIGURE 4 | TIMP1 and PDPN reveal its higher expression in GBM and malignant biological phenotype *in vitro*. **(A)** The translation expression level of the TIMP1 and PDPN were positively correlated with disease status as they were upregulated in gliomas samples. **(B)** The relationship of TIMP1 and PDPN with macrophage marker CD68. **(C)** The relationship of TIMP1 and PDPN with indicated m6A gene.

genes in the TCGA datasets (**Supplementary Figures 9A,B**). Four genes were highly associated with clinical features, such as grades, transcriptome subtype and IDH status (**Supplementary Figures 10A–C**). Moreover, these four genes were used to set up the risk signature based on the minimum criteria. Next, to assess the differences of survival time between low- and high-risk glioma patients, the Kaplan-Meier method was performed. Meanwhile, the log-rank test was also used to determine the statistical significance between groups. The time-dependent ROC curve was employed to measure the prognostic performance by comparing the AUC. Compared with those in the low-risk group, we illustrated that the glioma patients in the high-risk group had shorter OS, (**Figures 3A,B**, TCGA: HR = 1.07, 95% CI = 1.06–1.08, $P < 0.01$; CGGA: HR = 1.19, 95% CI = 1.16–2.23, $P < 0.01$). The time-dependent ROC curves revealed that the AUC for the 4-gene signature achieved 0.80 (0.76–0.83) and 0.72 (0.68–0.76) for the OS in TCGA and CGGA datasets, respectively (**Figures 3C,D**). Furthermore, the risk score exhibited a higher prognostic accuracy for OS than clinical histology, grade, IDH status and age (**Figures 3E,F**). These findings suggested an effective performance for predicting OS for glioma patients.

Validation the Expression and Function of TIMP1 and PDPN

To further validate the expression of four genes in gliomas, we next detected their expressions in The Human Protein Atlas database, and the results revealed the PDPN and TIMP1 were higher expression in high-grade gliomas (**Figure 4A**). In addition, TAGLN2 and EMP3 were performed in commercially glioma tissue-microarrays. The H-score of both proteins was not statistically significant between low and high-grade gliomas (**Supplementary Figure 11**). Moreover, in the correlation analysis, we uncovered that TIMP1 and PDPN were positively correlated with marker genes of macrophage (**Figure 4B**, **Table 3** and **Supplementary Figure 8**). TIMP1 was negatively related with YHDC1, while PDPN was positively related with WTAP (**Figure 4C** and **Supplementary Figure 7**). By knockdown the expression of PDPN or TIMP1, the cell proliferation was decreased, and the apoptosis and necrosis were increased in U87 and A172 (**Supplementary Figure 12**).

TABLE 3 | Clinical data of patients.

Case	Sex	Age	Tumor volume (cm^3)	Grade	Application
1	F	56	12.1	1	PCR
2	M	46	8.42	1	PCR
3	F	44	21.1	1	PCR
4	F	64	25.2	1	PCR
5	M	41	23.1	1	PCR
6	F	67	31.8	1	PCR
7	F	45	33.4	1	PCR
8	F	66	31.6	1	PCR
9	M	70	26.1	1	PCR
10	M	54	12.9	1	PCR
11	M	70	21.1	1	PCR
12	M	33	35.4	1	PCR
13	F	55	33.1	4	PCR
14	F	76	46.1	4	PCR
15	M	33	32.7	4	PCR
16	F	71	27.8	4	PCR
17	M	62	36.0	4	PCR
18	F	59	33.5	4	PCR
19	M	59	42.1	4	PCR
20	F	60	26.9	4	PCR

DISCUSSION

As the most aggressive primary brain tumor, glioma is considered as an enigma in neurosurgery (31, 32). Advanced knowledge of its genomic changes has promoted the discovery of prognostic signatures to facilitate the personalized treatment decisions (33–35). However, no previous studies have investigated the efficacy of the combination of m^{6}A and immune infiltration. Here, we developed and validated a novel 4-gene prognostic model based on the combination of m^{6}A RNA methylation and landscape of immune microenvironment. The developed 4-gene signature was able to identify the glioma patients with different risk levels for prognosis, which may compensate the already known prognostic indicators, such as age, tumor grade or histology. Additionally, we confirmed that *PDPN* and *TIMP1* were higher expressed in high-grade glioma, and the Pearson correlation validated that *PDPN* and *TIMP1* were correlated with marker gene of macrophage and indicated m6A gene.

m^{6}A, the most prevalent intra-mRNA modification, is required for post-transcriptional regulation of mRNA in various cell types (11, 12, 36). Previous studies have shown that m6A could be a signature for predicting the prognosis in different type of cancers, such as renal cell carcinoma, hepatocellular carcinoma, bladder cancer and head and neck squamous cell carcinoma (37–40). We found that WTAP and HNRNPC were significantly increased in cluster 1 than cluster 2 (**Figure 2**). In the GBM, WTAP was found to be overexpressed and regulate migration and invasion *in vitro* (41). Its high expression was associated with poor postoperative survival (42). In addition, HNRNPC could also control the aggressiveness of GBM cells and be regarded as the potential prognostic biomarker and therapeutic targets of GBM (43).

With the high-speed development of omics, high-throughput tumor databases have been established, including TCGA and CGGA, which provided a solid foundation for analyzing the RNA modification and microenvironments of glioma (3, 44–46). One of the emerging strategies of management is based on the roles of immune cells in the growth and maintenance of tumors (47). According to the recent studies, myeloid-derived suppressor cells (MDSC) and tumor-associated macrophages (TAMs) have been identified as promising targets for anti-cancer treatment (48, 49). Neoantigen-targeting vaccines have also increased tumor-infiltrating T cells and altered the immune milieu of glioblastoma (50). According to the TCGA database, Jia et al. has drawn a list of 44 tumor microenvironment related genes and proved them in an independent GBM cohort as potential biomarkers for GBM (51). However, the outcomes may lead to the discordance generally based on only one factor (51, 52). In our current study, we integrated m6A and immune infiltration in TCGA to build a model to improve the overall prediction of outcome for patients with glioma. Four survival-related genes (*TAGLN2, PDPN, TIMP1,* and *EMP3*) were identified and verified by four external datasets. These combination of these four genes provided a more reliable signature, relative to that extracted from a single dataset. Furthermore, *PDPN* and *TIMP1* were confirmed that they were higher expression in high-grade glioma and knockdown their expression decreased the glioma cell proliferation *in vitro.*

TAGLN2 is considered as a smooth muscle cytoskeletal protein (53). It has been proposed to be associated with growth and migration in bladder cancer (54, 55), esophageal squamous cell carcinoma (56), and gliomas (57). Moreover, it's up-regulation is associated with tumorigenesis and tumor progression (54, 58). Silence of *TAGLN2* in gliomas cell lines significantly inhibited invasion and tumor growth (57). Increased expression of *TAGLN2* was correlated with deteriorative tumor grade, and the function and regulation made it as a candidate prognostic biomarker (57). Jin et al. has also shown *TAGLN2* as a potential biomarker of tumor-derived lung-cancer endothelial cells (59). Another study demonstrated that *TAGLN2* could be a prospective tumor tissue marker for diagnosis and evaluating lymph node metastasis in bladder cancer patients (60).

EMP3 belongs to the PMP-22/EMP/MP20 family, which is thought to be involved in cell proliferation, cell-cell interactions and function as a tumor suppressor. Alaminos et al. have suggested that *EMP3* was associated with poor survival (61). *EMP3* overexpression in breast cancer was related to stronger HER-2 expression that may indicate a novel therapeutic target (62). Ma et al. have demonstrated that *EMP3*-mediated miR-663a inhibits the gallbladder cancer progression via the MAPK/ERK pathway (63). Recently, the bioinformatics analysis also found that *EMP3* was one of the validated gene panel independently and was correlated with the GBM survival (64, 65). Another bioinformatics analysis though significant analysis of microarray (SAM) identified that *EMP3* could be used to estimate glioma patient prognosis (66).

TIMP metallopeptidase inhibitor 1 (*TIMP1*) is a glycoprotein which antagonized mostly known MMPs. The encoded protein can promote cell proliferation in many cell types and may also

have an anti-apoptotic function. A high serum level was found as a poor prognostic indicator in GBMs (67). *TIMP1* has been suggested to interact with *P75NTR* in metastatic carcinoma and glioma cells (68), and silence of *TIMP1* or inhibition of NF-kappa B activity led to slower tumor growth *in vivo* (69). Several studies have shown that *TIMP1* was an important part of prognosis model and could be a biomarker for diagnosis (70–72). Furthermore, Jackson et al. have reviewed that *TIMP1* overexpression is consistently correlated with cancer progression or poor prognosis (73).

Podoplanin (*PDPN*) is a transmembrane receptor that participates in various physiological and pathological processes, such as cell motility, tumor metastasis and angiogenesis (74–76). It regulated mammary stem cell function that reduced mammary tumor formation in breast cancer and could be a new regulator of Wnt/β-catenin signaling (77). PDPN receptor are upregulated in cancer cells, immune cells, synoviocytes, and fibroblasts that increase tissue inflammation and invasion to promote both arthritis and cancer (78). *PDPN*-expressing macrophages (PoEMs) stimulated local matrix remodeling, and macrophage-specific *PDPN* knockout restrained lymphangiogenesis and reduced lymphatic cancer spread (79). *PDPN*-positive cancer-associated fibroblasts (CAFs) contributed to an essential role in primary resistance to epidermal growth factor receptor tyrosine kinase inhibitors (EGFR-TKI) (80). Moreover, *PDPN* has been considered as a novel biomarker, chemotherapeutic target and a target for CAR T-cell therapy that may be a potential adoptive immunotherapy to treat GBM (81, 82).

Our finding provides a novel insight into the relationship between m6A and immune infiltration, and we laid a solid foundation for four genes that could be a new prognosis indicator for gliomas patients. In addition, we also developed a user-friendly R shiny web app (http://www.houshixu.cn:3838/sample-apps/fio/) for easier usage. Remarkably, several limitations should be noted. In this study, prognostic factors were found by combining m6A and immune microenvironment. However, we do not have large quantities of samples to verify them and the clustering of glioma by m6A regulators is probably skewed by the grade of glioma. Whether *TAGLN2* and *EMP3* modulate cell proliferation were unclear. Moreover, the signature requires further validation in prospective studies and multicenter clinical trials.

CONCLUSIONS

We construct a novel prognostic model that provides new insights into glioma prognosis. The *PDPN* and *TIMP1* may serve as potential biomarkers for prognosis of glioma.

DATA AVAILABILITY STATEMENT

Publicly available datasets were analyzed in this study, these can be found in The Cancer Genome Atlas via the University of California Santa Cruz (UCSC) Xena browser (https://xenabrowser.net/datapages/).

ETHICS STATEMENT

The studies involving human participants were reviewed and approved by Shanghai General Hospital, Shanghai Jiao Tong University School of Medicine, Shanghai 200080, China. The patients/participants provided their written informed consent to participate in this study.

AUTHOR CONTRIBUTIONS

This work was carried out in collaboration with all authors. ML, MW, and TM contributed to the conception and design of the study. SL and HX carried out the experiments. SL, HX, and AZ contributed to all figures and tables. SL, TM, MW, and YN revised the manuscript. SL, HX, AZ, and YX contributed to data collection and analysis. All authors have read and approved the final manuscript. All authors contributed to the article and approved the submitted version.

FUNDING

This work was supported by National Natural Science Foundation of China (No. 81701359), Natural science foundation of Shanghai (18ZR1430400), and the Cross Research Fund of Medicine and Engineering of Shanghai Jiaotong University (Nos. YG2016QN32 and YG2019QNA67).

SUPPLEMENTARY MATERIAL

The Supplementary Material for this article can be found online at: https://www.frontiersin.org/articles/10.3389/fonc.2020.541401/full#supplementary-material

Supplementary Figure 1 | An overall flowchart of this work.

Supplementary Figure 2 | Identification of consensus clusters by m6A RNA methylation regulators. Consensus clustering matrix for $k = 2$ to $K = 5$ **(A–D)**. **(E)** Consensus clustering cumulative distribution function (CDF) for $k = 2$–9. **(F)** Relative change in area under CDF curve for $k = 2$–5. Silhouette analysis **(G)** and Gap analysis **(H)** showed that 2 clusters were appropriate classification for the data.

Supplementary Figure 3 | Spearman correlation analysis of the 12 m^{6}A modification regulators.

Supplementary Figure 4 | The immune infiltration score between cluster 1 and cluster 2.

Supplementary Figure 5 | Relationship between m^{6}A RNA methylation regulators and immune infiltration **(A–J)** violin plot for 12 m^{6}A regulators and immune infiltration subgroups.

Supplementary Figure 6 | Identification of key modules correlated with clinical traits in the TCGA-GBM/LGG datasets through WGCNA. **(A)** Clustering dendrograms of genes. Color intensity varies positively with age, m^{6}A cluster subgroups, immune infiltration subgroups, overall survival and overall survival status. Analysis of the scale-free fit index **(B)** and the mean connectivity **(C)** for various soft-thresholding powers. **(D)** Heatmap of the correlation between module eigengenes and clinical traits of diffuse gliomas. Each cell contains the correlation coefficient and *P*-value. **(E)** Dendrogram of all DEGs clustered based on a dissimilarity measure (1- TOM). **(F)** Clustering of module eigengenes. The red line indicates cut height (0.2). **(G)** Scatter plot of module eigengenes in the black module. **(H)** Hub genes show strong associations with each other. Red and blue colors indicate positive and negative coefficients and labels from−1 to 1 indicate correlation strength.

Supplementary Figure 7 | Association of hub genes' expression with 12 m6A RNA methylation regulators in gliomas. **(A)** TAGLN2 **(B)** PDPN **(C)** TIMP1 **(D)** EMP3 **(E)** CHI3L1.

Supplementary Figure 8 | Association of hub genes' expression with immune infiltration cells in gliomas. **(A)** TAGLN2 **(B)** PDPN **(C)** TIMP1 **(D)** EMP3 **(E)** CHI3L1.

Supplementary Figure 9 | (A,B) The process of building the risk scores containing 4 hub genes and the coefficients calculated by least absolute shrinkage and selection operator (LASSO) Cox regression algorithm are shown.

Supplementary Figure 10 | Expression of 4 hub genes in gliomas with different clinicopathological features, from right to left, TIMP1, TAGLN2, PDPN, and EMP3, respectively. **(A)** The expression levels of 4 hub genes in gliomas with different WHO grades. **(B)** The expression levels of 4 hub genes in gliomas with different transcriptome subtypes. **(C)** The expression levels of 4 hub genes in gliomas with different IDH status.

Supplementary Figure 11 | H-score of EMP3 **(A)** and TAGLN2 **(B)** of glioma tissue-microarrays.

Supplementary Figure 12 | (A,D) Western blot analysis validated the knockdown of TIPM1 or PDPN in U87 and A172 cells. **(B,E)** Cell proliferation was determined by ATP assay. **(C,F)** Flow cytometric analysis of Annexin V/PI staining in U87 and A172 cells after transfection with 50 nmol/L siTIMP1 or siPDPN and siCtrl for 72 h.

REFERENCES

1. Ostrom QT, Gittleman H, Truitt G, Boscia A, Kruchko C, Barnholtz-Sloan JS. CBTRUS statistical report: primary brain and other central nervous system tumors diagnosed in the United States in 2011–2015. *Neuro Oncol.* (2018) 20:iv1–86. doi: 10.1093/neuonc/noy131
2. Gittleman H, Sloan AE, Barnholtz-Sloan JS. An independently validated survival nomogram for lower grade glioma. *Neuro Oncol.* (2019) 22:665–74. doi: 10.1093/noajnl/vdz007
3. Brat DJ, Verhaak RG, Aldape KD, Yung WK, Salama SR, Cooper LA, et al. Comprehensive, integrative genomic analysis of diffuse lower-grade gliomas. *N Engl J Med.* (2015) 372:2481–98. doi: 10.1056/NEJMoa1402121
4. Perry JR, Laperriere N, O'callaghan CJ, Brandes AA, Menten J, Phillips C, et al. Short-course radiation plus temozolomide in elderly patients with glioblastoma. *N Engl J Med.* (2017) 376:1027–37. doi: 10.1056/NEJMoa1611977
5. Wojtas MN, Pandey RR, Mendel M, Homolka D, Sachidanandam R, Pillai RS. Regulation of m(6)A transcripts by the 3'−>5' RNA helicase YTHDC2 is essential for a successful meiotic program in the mammalian germline. *Mol Cell.* (2017) 68:374–87.e312. doi: 10.1016/j.molcel.2017.09.021
6. Deng X, Su R, Weng H, Huang H, Li Z, Chen J. RNA N(6)-methyladenosine modification in cancers: current status and perspectives. *Cell Res.* (2018) 28:507–17. doi: 10.1038/s41422-018-0034-6
7. Ding C, Zou Q, Ding J, Ling M, Wang W, Li H, et al. Increased N6-methyladenosine causes infertility is associated with FTO expression. *J Cell Physiol.* (2018) 233:7055–66. doi: 10.1002/jcp.26507
8. Tang C, Klukovich R, Peng H, Wang Z, Yu T, Zhang Y, et al. ALKBH5-dependent m6A demethylation controls splicing and stability of long 3'-UTR mRNAs in male germ cells. *Proc Natl Acad Sci USA.* (2018) 115:E325–e333. doi: 10.1073/pnas.1717794115
9. Yang Y, Hsu PJ, Chen YS, Yang YG. Dynamic transcriptomic m(6)A decoration: writers, erasers, readers and functions in RNA metabolism. *Cell Res.* (2018) 28:616–24. doi: 10.1038/s41422-018-0040-8
10. Yao QJ, Sang L, Lin M, Yin X, Dong W, Gong Y, et al. Mettl3-Mettl14 methyltransferase complex regulates the quiescence of adult hematopoietic stem cells. *Cell Res.* (2018) 28:952–4. doi: 10.1038/s41422-018-0062-2
11. Desrosiers R, Friderici K, Rottman F. Identification of methylated nucleosides in messenger RNA from Novikoff hepatoma cells. *Proc Natl Acad Sci USA.* (1974) 71:3971–5. doi: 10.1073/pnas.71.10.3971
12. Wang X, Lu Z, Gomez A, Hon GC, Yue Y, Han D, et al. N6-methyladenosine-dependent regulation of messenger RNA stability. *Nature.* (2014) 505:117–20. doi: 10.1038/nature12730
13. Cui Q, Shi H, Ye P, Li L, Qu Q, Sun G, et al. m A RNA methylation regulates the self-renewal and tumorigenesis of glioblastoma stem cells. *Cell Rep.* (2017) 18:2622–34. doi: 10.1016/j.celrep.2017.02.059
14. Zheng Q, Hou J, Zhou Y, Li Z, Cao X. The RNA helicase DDX46 inhibits innate immunity by entrapping mA-demethylated antiviral transcripts in the nucleus. *Nat Immunol.* (2017) 18:1094–103. doi: 10.1038/ni.3830
15. Visvanathan A, Patil V, Arora A, Hegde AS, Arivazhagan A, Santosh V, et al. Essential role of METTL3-mediated mA modification in glioma stem-like cells maintenance and radioresistance. *Oncogene.* (2018) 37:522–33. doi: 10.1038/onc.2017.351
16. Cooper LA, Gutman DA, Chisolm C, Appin C, Kong J, Rong Y, et al. The tumor microenvironment strongly impacts master transcriptional regulators and gene expression class of glioblastoma. *Am J Pathol.* (2012) 180:2108–19. doi: 10.1016/j.ajpath.2012.01.040
17. Galon J, Pages F, Marincola FM, Thurin M, Trinchieri G, Fox BA, et al. The immune score as a new possible approach for the classification of cancer. *J Transl Med.* (2012) 10:1. doi: 10.1186/1479-5876-10-1
18. Senbabaoglu Y, Gejman RS, Winer AG, Liu M, Van Allen EM, De Velasco G, et al. Tumor immune microenvironment characterization in clear cell renal cell carcinoma identifies prognostic and immunotherapeutically relevant messenger RNA signatures. *Genome Biol.* (2016) 17:231. doi: 10.1186/s13059-016-1092-z
19. Hanahan D, Weinberg RA. The hallmarks of cancer. *Cell.* (2000) 100:57–70. doi: 10.1016/S0092-8674(00)81683-9
20. Hanahan D, Coussens LM. Accessories to the crime: functions of cells recruited to the tumor microenvironment. *Cancer Cell.* (2012) 21:309–22. doi: 10.1016/j.ccr.2012.02.022
21. Zhang B, Wu Q, Li B, Wang D, Wang L, Zhou YL. m(6)A regulator-mediated methylation modification patterns and tumor microenvironment infiltration characterization in gastric cancer. *Mol Cancer.* (2020) 19:53–53. doi: 10.1186/s12943-020-01170-0
22. Li H, Su Q, Li B, Lan L, Wang C, Li W, et al. High expression of WTAP leads to poor prognosis of gastric cancer by influencing tumour-associated T lymphocyte infiltration. *J Cell Mol Med.* (2020) 24:4452–65. doi: 10.1111/jcmm.15104
23. Xu F, Chen J-X, Yang X-B, Hong X-B, Li Z-X, Lin L, et al. Analysis of lung adenocarcinoma subtypes based on immune signatures identifies clinical implications for cancer therapy. *Mol Therapy Oncolyt.* (2020) 17:241–9. doi: 10.1016/j.omto.2020.03.021
24. Leek JT, Johnson WE, Parker HS, Jaffe AE, Storey JD. The sva package for removing batch effects and other unwanted variation in high-throughput experiments. *Bioinformatics.* (2012) 28:882–3. doi: 10.1093/bioinformatics/bts034
25. Gravendeel LaM, Kouwenhoven MCM, Gevaert O, De Rooi JJ, Stubbs AP, Duijm JE, et al. Intrinsic gene expression profiles of gliomas are a better predictor of survival than histology. *Cancer Res.* (2009) 69:9065–72. doi: 10.1158/0008-5472.CAN-09-2307
26. Bowman RL, Wang Q, Carro A, Verhaak RGW, Squatrito M. GlioVis data portal for visualization and analysis of brain tumor expression datasets. *Neuro Oncol.* (2017) 19:139–41. doi: 10.1093/neuonc/now247
27. Bindea G, Mlecnik B, Tosolini M, Kirilovsky A, Waldner M, Obenauf AC, et al. Spatiotemporal dynamics of intratumoral immune cells reveal the immune landscape in human cancer. *Immunity.* (2013) 39:782–95. doi: 10.1016/j.immuni.2013.10.003
28. Langfelder P, Horvath S. WGCNA: an R package for weighted correlation network analysis. *BMC Bioinform.* (2008) 9:559. doi: 10.1186/1471-2105-9-559
29. Uhlen M, Fagerberg L, Hallstrom BM, Lindskog C, Oksvold P, Mardinoglu A, et al. Proteomics. *Tissue Based Map Human Proteome Sci.* (2015) 347:1260419. doi: 10.1126/science.1260419

30. Lin SJ, Wu ZR, Cao L, Zhang Y, Leng ZG, Guo YH, et al. Pituitary tumor suppression by combination of cabergoline and chloroquine. *J Clin Endocrinol Metab.* (2017) 102:3692–703. doi: 10.1210/jc.2017-00627
31. Shergalis A, Bankhead A 3rd, Luesakul U, Muangsin N, Neamati N. Current challenges and opportunities in treating glioblastoma. *Pharmacol Rev.* (2018) 70:412–45. doi: 10.1124/pr.117.014944
32. Van Tellingen O, Yetkin-Arik B, De Gooijer MC, Wesseling P, Wurdinger T, De Vries HE. Overcoming the blood-brain tumor barrier for effective glioblastoma treatment. *Drug Resist Updat.* (2015) 19:1–12. doi: 10.1016/j.drup.2015.02.002
33. Davis B, Shen Y, Poon CC, Luchman HA, Stechishin OD, Pontifex CS, et al. Comparative genomic and genetic analysis of glioblastoma-derived brain tumor-initiating cells and their parent tumors. *Neuro Oncol.* (2016) 18:350–60. doi: 10.1093/neuonc/nov143
34. Wang J, Cazzato E, Ladewig E, Frattini V, Rosenbloom DI, Zairis S, et al. Clonal evolution of glioblastoma under therapy. *Nat Genet.* (2016) 48:768–76. doi: 10.1038/ng.3590
35. Zhou D, Alver BM, Li S, Hlady RA, Thompson JJ, Schroeder MA, et al. Distinctive epigenomes characterize glioma stem cells and their response to differentiation cues. *Genome Biol.* (2018) 19:43. doi: 10.1186/s13059-018-1420-6
36. Dominissini D, Moshitch-Moshkovitz S, Schwartz S, Salmon-Divon M, Ungar L, Osenberg S, et al. Topology of the human and mouse m6A RNA methylomes revealed by m6A-seq. *Nature.* (2012) 485:201–6. doi: 10.1038/nature11112
37. Chen M, Nie ZY, Wen XH, Gao YH, Cao H, Zhang SF. m6A RNA methylation regulators can contribute to malignant progression and impact the prognosis of bladder cancer. *Biosci Rep.* (2019) 39:2892. doi: 10.1042/BSR20192892
38. Zhao X, Cui L. Development and validation of a m(6)A RNA methylation regulators-based signature for predicting the prognosis of head and neck squamous cell carcinoma. *Am J Cancer Res.* (2019) 9:2156–69.
39. Qu N, Qin S, Zhang X, Bo X, Liu Z, Tan C, et al. Multiple m(6)A RNA methylation modulators promote the malignant progression of hepatocellular carcinoma and affect its clinical prognosis. *BMC Cancer.* (2020) 20:165. doi: 10.1186/s12885-020-6638-5
40. Wang J, Zhang C, He W, Gou X. Effect of m(6)A RNA methylation regulators on malignant progression and prognosis in renal clear cell carcinoma. *Front Oncol.* (2020) 10:3. doi: 10.3389/fonc.2020.00003
41. Jin D-I, Lee SW, Han M-E, Kim H-J, Seo S-A, Hur G-Y, et al. Expression and roles of Wilms' tumor 1-associating protein in glioblastoma. *Cancer Sci.* (2012) 103:2102–9. doi: 10.1111/cas.12022
42. Xi Z, Xue Y, Zheng J, Liu X, Ma J, Liu Y. WTAP expression predicts poor prognosis in malignant glioma patients. *J Mol Neurosci.* (2016) 60:131–6. doi: 10.1007/s12031-016-0788-6
43. Park YM, Hwang SJ, Masuda K, Choi K-M, Jeong M-R, Nam D-H, et al. Heterogeneous nuclear ribonucleoprotein C1/C2 controls the metastatic potential of glioblastoma by regulating PDCD4. *Mol Cell Biol.* (2012) 32:4237–44. doi: 10.1128/MCB.00443-12
44. Li J, Lu Y, Akbani R, Ju Z, Roebuck PL, Liu W, et al. TCPA: a resource for cancer functional proteomics data. *Nat Methods.* (2013) 10:1046–7. doi: 10.1038/nmeth.2650
45. Ceccarelli M, Barthel FP, Malta TM, Sabedot TS, Salama SR, Murray BA, et al. Molecular profiling reveals biologically discrete subsets and pathways of progression in diffuse glioma. *Cell.* (2016) 164:550–63. doi: 10.1016/j.cell.2015.12.028
46. Wang Q, Hu B, Hu X, Kim H, Squatrito M, Scarpace L, et al. Tumor evolution of glioma-intrinsic gene expression subtypes associates with immunological changes in the microenvironment. *Cancer Cell.* (2017) 32:42–56.e46. doi: 10.1016/j.ccell.2017.06.003
47. Maximov V, Chen Z, Wei Y, Hope Robinson M, Herting CJ, Shanmugam NS, et al. Tumour-associated macrophages exhibit anti-tumoural properties in Sonic Hedgehog medulloblastoma. *Nat Commun.* (2019) 10:2410. doi: 10.1038/s41467-019-10458-9
48. Kohanbash G, McKaveney K, Sakaki M, Ueda R, Mintz AH, Amankulor N, et al. GM-CSF promotes the immunosuppressive activity of glioma-infiltrating myeloid cells through interleukin-4 receptor-α. *Cancer Res.* (2013) 73:6413–23. doi: 10.1158/0008-5472.CAN-12-4124
49. Pyonteck SM, Akkari L, Schuhmacher AJ, Bowman RL, Sevenich L, Quail DF, et al. CSF-1R inhibition alters macrophage polarization and blocks glioma progression. *Nat Med.* (2013) 19:1264–72. doi: 10.1038/nm.3337
50. Keskin DB, Anandappa AJ, Sun J, Tirosh I, Mathewson ND, Li S, et al. Neoantigen vaccine generates intratumoral T cell responses in phase Ib glioblastoma trial. *Nature.* (2019) 565:234–9. doi: 10.1038/s41586-018-0792-9
51. Jia D, Li S, Li D, Xue H, Yang D, Liu Y. Mining TCGA database for genes of prognostic value in glioblastoma microenvironment. *Aging.* (2018) 10:592–605. doi: 10.18632/aging.101415
52. Chai RC, Wu F, Wang QX, Zhang S, Zhang KN, Liu YQ, et al. m(6)A RNA methylation regulators contribute to malignant progression and have clinical prognostic impact in gliomas. *Aging.* (2019) 11:1204–25. doi: 10.18632/aging.101829
53. Jang SH, Jun CD, Park ZY. Label-free quantitative phosphorylation analysis of human transgelin2 in Jurkat T cells reveals distinct phosphorylation patterns under PKA and PKC activation conditions. *Proteome Sci.* (2015) 13:14. doi: 10.1186/s12953-015-0070-9
54. Zhang HJ, Jiang MJ, Liu QJ, Han ZX, Zhao YQ, Ji SQ. miR-145-5p inhibits the proliferation and migration of bladder cancer cells by targeting TAGLN2. *Oncol Lett.* (2018) 16:6355–60. doi: 10.3892/ol.2018.9436
55. Zhao F, Zhou LH, Ge YZ, Ping WW, Wu X, Xu ZL, et al. MicroRNA-133b suppresses bladder cancer malignancy by targeting TAGLN2-mediated cell cycle. *J Cell Physiol.* (2019) 234:4910–23. doi: 10.1002/jcp.27288
56. Du YY, Zhao LM, Chen L, Sang MX, Li J, Ma M, et al. The tumor-suppressive function of miR-1 by targeting LASP1 and TAGLN2 in esophageal squamous cell carcinoma. *J Gastroenterol Hepatol.* (2016) 31:384–93. doi: 10.1111/jgh.13180
57. Han MZ, Xu R, Xu YY, Zhang X, Ni SL, Huang B, et al. TAGLN2 is a candidate prognostic biomarker promoting tumorigenesis in human gliomas. *J Exp Clin Cancer Res.* (2017) 36:9. doi: 10.1186/s13046-017-0619-9
58. Pei J, Li P, Zhang ZY, Zhang HL, Gao YH, Wang DY, et al. Effect of TAGLN2 in the regulation of meningioma tumorigenesis and development. *Eur Rev Med Pharmacol Sci.* (2018) 22:307–13. doi: 10.26355/eurrev_201801_14173
59. Jin H, Cheng X, Pei Y, Fu Y, Lyu Z, Peng H, et al. Identification and verification of transgelin-2 as a potential biomarker of tumor-derived lung-cancer endothelial cells by comparative proteomics. *J Proteom.* (2016) 136:77–88. doi: 10.1016/j.jprot.2015.12.012
60. Chen C-L, Chung T, Wu C-C, Ng K-F, Yu J-S, Tsai C-H, et al. Comparative tissue proteomics of microdissected specimens reveals novel candidate biomarkers of bladder cancer. *Mol Cell Proteom.* (2015) 14:2466–78. doi: 10.1074/mcp.M115.051524
61. Alaminos M, Davalos V, Ropero S, Setien F, Paz MF, Herranz M, et al. EMP3, a myelin-related gene located in the critical 19q13.3 region, is epigenetically silenced and exhibits features of a candidate tumor suppressor in glioma and neuroblastoma. *Cancer Res.* (2005) 65:2565–71. doi: 10.1158/0008-5472.CAN-04-4283
62. Wang Y-W, Cheng H-L, Ding Y-R, Chou L-H, Chow N-H. EMP1, EMP2, and EMP3 as novel therapeutic targets in human cancer. *Biochim Biophys Acta Rev Cancer.* (2017) 1868:199–211. doi: 10.1016/j.bbcan.2017.04.004
63. Ma Q, Zhang YJ, Liang HB, Zhang F, Liu FT, Chen SL, et al. EMP3, which is regulated by miR-663a, suppresses gallbladder cancer progression via interference with the MAPK/ERK pathway. *Cancer Lett.* (2018) 430:97–108. doi: 10.1016/j.canlet.2018.05.022
64. Shu C, Wang Q, Yan XL, Wang JH. Whole-genome expression microarray combined with machine learning to identify prognostic biomarkers for high-grade glioma. *J Mol Neurosci.* (2018) 64:491–500. doi: 10.1007/s12031-018-1049-7
65. Guo XX, Su J, He XF. A 4-gene panel predicting the survival of patients with glioblastoma. *J Cell Biochem.* (2019) 120:16037–43. doi: 10.1002/jcb.28883
66. Gao Y-F, Zhu T, Mao C-X, Liu Z-X, Wang Z-B, Mao X-Y, et al. (2016). PPIC, EMP3, and CHI3L1 are novel prognostic markers for high grade glioma. *Int J Mol Sci.* 17:111808. doi: 10.3390/ijms17111808
67. Sreekanthreddy P, Srinivasan H, Kumar DM, Nijaguna MB, Sridevi S, Vrinda M, et al. Identification of potential serum biomarkers of glioblastoma: serum osteopontin levels correlate with poor prognosis. *Cancer Epidemiol Biomarkers Prev.* (2010) 19:1409–22. doi: 10.1158/1055-9965.EPI-09-1077

68. Rojiani M, Brem S, Murphy S, Obadia M, Rojiani A. TIMP1 interactions with P75(NTR) in metastatic carcinoma and glioma cells. *Cancer Res.* (2009) 69. Available online at: https://cancerres.aacrjournals.org/content/69/9_Supplement/1129
69. Friedmann-Morvinski D, Narasimamurthy R, Xia YF, Myskiw C, Soda Y, Verma IM. Targeting NF-kappa B in glioblastoma: a therapeutic approach. *Sci Adv.* (2016) 2:1501292. doi: 10.1126/sciadv.1501292
70. Resovi A, Bani MR, Porcu L, Anastasia A, Minoli L, Allavena P, et al. Soluble stroma-related biomarkers of pancreatic cancer. *EMBO Mol Med.* (2018) 10:e8741. doi: 10.15252/emmm.201708741
71. Zhong C, Wang G, Xu T, Zhu Z, Guo D, Zheng X, et al. Tissue inhibitor metalloproteinase-1 and clinical outcomes after acute ischemic stroke. *Neurology.* (2019) 93:e1675–85. doi: 10.1212/WNL.0000000000008564
72. Loon EV, Gazut S, Yazdani S, Lerut E, de Loor H, Coemans M, et al. Development and validation of a peripheral blood mRNA assay for the assessment of antibody-mediated kidney allograft rejection: a multicentre, prospective study. *EBioMed.* (2019) 46:463–72. doi: 10.1016/j.ebiom.2019.07.028
73. Jackson HW, Defamie V, Waterhouse P, Khokha R. TIMPs: versatile extracellular regulators in cancer. *Nat Rev Cancer.* (2017) 17:38–53. doi: 10.1038/nrc.2016.115
74. Hwang YS, Zhang X, Park KK, Chung WY. Functional invadopodia formation through stabilization of the PDPN transcript by IMP-3 and cancer-stromal crosstalk for PDPN expression. *Carcinogenesis.* (2012) 33:2135–46. doi: 10.1093/carcin/bgs258
75. Sikorska J, Gawel D, Domek H, Rudzinska M, Czarnocka B. Podoplanin (PDPN) affects the invasiveness of thyroid carcinoma cells by inducing ezrin, radixin and moesin (E/R/M) phosphorylation in association with matrix metalloproteinases. *BMC Cancer.* (2019) 19:5239. doi: 10.1186/s12885-018-5239-z
76. Suzuki-Inoue K, Inoue O, Ozaki Y. Novel platelet activation receptor CLEC-2: from discovery to prospects. *J Thrombosis Haemostasis.* (2011) 9:44–55. doi: 10.1111/j.1538-7836.2011.04335.x
77. Bresson L, Faraldo MM, Di-Cicco A, Quintanilla M, Glukhova MA, Deugnier M-A. Podoplanin regulates mammary stem cell function and tumorigenesis by potentiating Wnt/β-catenin signaling. *Development.* (2018) 145:160382. doi: 10.1242/dev.160382
78. Krishnan H, Miller WT, Blanco FJ, Goldberg GS. Src and podoplanin forge a path to destruction. *Drug Disc Today.* (2019) 24:241–9. doi: 10.1016/j.drudis.2018.07.009
79. Bieniasz-Krzywiec P, Martín-Pérez R, Ehling M, García-Caballero M, Pinioti S, Pretto S, et al. Podoplanin-expressing macrophages promote lymphangiogenesis and lymphoinvasion in breast cancer. *Cell Metabol.* (2019) 30:917–36.e910. doi: 10.1016/j.cmet.2019.07.015
80. Yoshida T, Ishii G, Goto K, Neri S, Hashimoto H, Yoh K, et al. Podoplanin-positive cancer-associated fibroblasts in the tumor microenvironment induce primary resistance to EGFR-TKIs in lung adenocarcinoma with EGFR mutation. *Clin Cancer Res.* (2015) 21:642–51. doi: 10.1158/1078-0432.CCR-14-0846
81. Krishnan H, Ochoa-Alvarez J, Shen Y, Nevei E, Kephart D, Nguyen A, et al. Podoplanin (PDPN): novel biomarker and chemotherapeutic target. *Cancer Res.* (2015) 75:4375. doi: 10.1158/1538-7445.AM2015-4375
82. Shiina S, Ohno M, Ohka F, Kuramitsu S, Yamamichi A, Kato A, et al. CAR T cells targeting podoplanin reduce orthotopic glioblastomas in mouse brains. *Cancer Immunol Res.* (2016) 4:259–68. doi: 10.1158/2326-6066.CIR-15-0060

Conflict of Interest: The authors declare that the research was conducted in the absence of any commercial or financial relationships that could be construed as a potential conflict of interest.

frontiers in Oncology

ORIGINAL RESEARCH
published: 02 November 2020
doi: 10.3389/fonc.2020.578816

IGF2BP2 Promotes Liver Cancer Growth Through an m6A-FEN1-Dependent Mechanism

Jian Pu[1†], Jianchu Wang[2†], Zebang Qin[3], Anmin Wang[3], Ya Zhang[3], Xianjian Wu[3], Yi Wu[3], Wenchuan Li[2], Zuoming Xu[2], Yuan Lu[3], Qianli Tang[2] and Huamei Wei[4*]*

[1] Department of General Surgery, Affiliated Hospital of Youjiang Medical University for Nationalities, Guangxi, China, [2] Department of Hepatobiliary Surgery, Affiliated Hospital of Youjiang Medical University for Nationalities, Guangxi, China, [3] Graduate College of Youjiang Medical University for Nationalities, Guangxi, China, [4] Department of Pathology, Affiliated Hospital of Youjiang Medical University for Nationalities, Guangxi, China

OPEN ACCESS

Edited by:
Xiangqian Zheng,
Tianjin Medical University Cancer Institute and Hospital, China

Reviewed by:
Jorge Melendez-Zajgla,
Instituto Nacional de Medicina Genómica (INMEGEN), Mexico
Bryan Raymond George Williams,
Hudson Institute of Medical Research, Australia

***Correspondence:**
Huamei Wei
huameiwei1983@163.com
Qianli Tang
htmgx@163.com

[†]These authors have contributed equally to this work

Specialty section:
This article was submitted to Cancer Genetics, a section of the journal Frontiers in Oncology

Received: 01 July 2020
Accepted: 07 October 2020
Published: 02 November 2020

Citation:
Pu J, Wang J, Qin Z, Wang A, Zhang Y, Wu X, Wu Y, Li W, Xu Z, Lu Y, Tang Q and Wei H (2020) IGF2BP2 Promotes Liver Cancer Growth Through an m6A-FEN1-Dependent Mechanism. Front. Oncol. 10:578816. doi: 10.3389/fonc.2020.578816

Hepatocellular carcinoma (HCC) is one of the most common malignant tumors in China. N6–methyladenosine (m6A) plays an important role in posttranscriptional gene regulation. METTL3 and IGF2BP2 are key genes in the m6A signal pathway and have recently been shown to play important roles in cancer development and progression. In our work, higher METTL3 and IGF2BP2 expression were found in HCC tissues and were associated with a poor prognosis. In addition, IGF2BP2 overexpression promoted HCC proliferation *in vitro* and *in vivo*. Mechanistically, IGF2BP2 directly recognized and bound to the m6A site on FEN1 mRNA and enhanced FEN1 mRNA stability. Overall, our study revealed that METTL3 and IGF2BP2, acting as an oncogene, maintained FEN1 expression through an m6A-IGF2BP2-dependent mechanism in HCC cells, and indicated a potential biomarker panel for prognostic prediction in liver cancer.

Keywords: liver cancer, N6-methyladenosine, METTL3, IGF2BP2, FEN1

INTRODUCTION

HCC is a highly lethal cancer (1). The estimated number of new patients that were diagnosed with HCC was about 900,000 and would result in approximately 800,000 deaths all over the world in 2018 (2). In China, the mortality and morbidity rates of HCC have demonstrated an increasing trend. Although medical treatment has been improved, the 5-year relative survival rate for HCC patients is still unsatisfactory. Therefore, identifying novel biomarkers and therapeutic targets for HCC diagnosis and treatment is an urgent need.

As one of the most prevalent modifications in eukaryotic messenger RNA (mRNA), N6-methyladenosine (m6A) affects almost every step of metabolism of messenger RNA (mRNA), such as mRNA processing, transport, translation, degradation and so on (3, 4). It is regulated by m6A modification enzymes (methyltransferases and demethylases) in a dynamically reversible manner (5, 6). In addition, there are also m6A-binding proteins, which can specifically bind to m6A and mediate their biological functions (7, 8). In recent years, m6A has been found to be associated with malignant tumors by more and more studies (9, 10). It has been reported to contribute to the self-renewal of tumor stem cells and promote the proliferation of malignant tumor cells. m6A is closely related to the phenotype and mechanism of malignant transformation, showing the possibility of m6A targeting

therapy for human malignant tumors (10). In other words, m6A may become a new target for the treatment of malignant tumors. However, the functions of m6A modification and the underlying connections between the m6A methyltransferases, demethylases, and m6A-binding proteins are still unexplored in HCC.

Here, we first demonstrated the function of insulin-like growth factor 2 mRNA binding protein 2 (IGF2BP2) in facilitating HCC progression, and identified FEN1 as the downstream target of IGF2BP2. Overall, our study reveals that the METTL3-IGF2BP2-FEN1 axis is a potential therapeutic target for HCC.

MATERIALS AND METHODS

Database and Bioinformatics

Level 3 gene expression profile (level 3 data) for HCC patients was obtained from the TCGA data portal (https://tcga-data.nci.nih.gov/tcga/). Differentially expressed genes (DEGs) were identified by Student's t-test (Unpaired t test, two-tailed, ****P < 0.0001). The processed TCGA data is in **supplementary material**.

Patient Samples

A total of 20 HCC tissues and 20 paired nontumorous liver samples were collected for qRT-CPR and IHC from the Affiliated Hospital of YouJiang Medical College for Nationalities from 2018 to 2019. The histological features of all specimens were evaluated by pathologists according to the standard criteria. The researchers were granted approval to conduct the research by Departmental Research Ethics Committee at the YouJiang Medical College for Nationalities. The study protocol was approved by the institutional review board of YouJiang Medical College for Nationalities. All the procedures were performed in accordance with the Declaration of Helsinki and relevant policies in China.

m6A RNA Methylation Assay

Total RNA was extracted from samples using the Invitrogen life technologies TRIZOL. The change in m6A level relative to total mRNA was measured using EZ RNA Methylation Kit (ZYMO) following the manufacturer's protocol. Each sample was analyzed using 200 ng of RNA isolated from different samples. Relative antification: To determine the relative m A RNA methylation status of two different RNA samples, a simple calculation for the percentage of m6A in total RNA was carried out using the following formula:

$$\text{m6A \%} = (\text{Sample OD} - \text{NCOD})/\text{S} \times 100\,\%\,(\text{PCOD} - \text{OD})/\text{PS}:$$

is the amount of input sample RNA in ngP : is the amount of input positive control(PC)in ng.

Immunohistochemistry

IHC was performed as described previously (11). The tissues were incubated with primary antibody against IGF2BP2 (ab128175, Abcam, 1:100) overnight in the refrigerator at 4°C. For negative controls, irrelevant primary antibodies were used. The corresponding secondary antibodies, conjugated to horseradish peroxidase (ab6721, Abcam, 1:1000), were incubated with the sections for 1 h at room temperature. After washing with PBS, the sections were incubated in horseradish enzyme-labeled chain avid in solution for 30 min at 37°C and washed again. The IHC score (0–9) was calculated by multiplying the intensity and the percentage scores (12).

Western Blot Analysis

Tissues and cells were lysed in RIPA buffer (Beyotime, China). The lysates were denatured at 95°C for 5 min and then cooled down on ice. Then lysates were loaded on sodium dodecyl sulfatepolyacrylamide gel (SDS-PAGE) (10%) and electrotransferred onto polyvinylidene difluoride (PVDF) membrane. After blocking with 5% BSA blocking solution (SW3015, solarbio) for 1 h at room temperature, PVDF membranes were blotted with primary antibody at 4°C for 12 h, then incubated with HRP-labeled secondary antibody (CST, USA) at room temperature for 2 h. The bands were visualized using Tanon 5200 (Tanon, China). Primary antibodies are as follows: mouse monoclonal antibody to IGF2BP2 (ab128175, Abcam), rabbit monoclonal antibody to FEN1 (ab109132), and mouse monoclonal antibody to β-actin (CST, USA).

Copy Number Variation (CNV) Detection Using the AccuCopy® Assay

The AccuCopy assay (Shanghai, China) was used to evaluate the CNV of IGF2BP2. The basic molecular principle of AccuCopy is competitive PCR amplification. The primers used in this assay were:

Chr2-84500611-84500685(Reference gene): F: 5'- TGAG CCAAAAATTCAGAATACAAGGA -3'

R: 5'- TTGCTTGGAAGGCAGGCAAAC -3'

Chr16-25258413-25258537(Reference gene): F: 5'- GGGACA GGCCTGAAGTGTTTC -3'

R: 5'- AGCAGCAGCAGTGGGGTTTAG -3'

Chr3-185362000-185364000: F: 5'- CCGCAGACTTCT CATTCCTC -3'

R: 5'- GCAGCAGGAGCAGAAATACC -3'

Chr3-185367000-185369000: F: 5'- ATGGGCATTCATGT TTTGGT -3'

R: 5'- ACCCTGTGGTGATGGGATAA -3'

Cell Culture and Transfection

HCC cell lines HepG2 and Huh-7 were gifts from obtained from Dr. C.M.W (HongKong University). MHCC97L and PLC were gifts from Dr. Z.Y. Tang (Fudan University). All cells were grown in a humidified incubator at 37°C with 5% CO_2. shRNA that targets human IGF2BP2 or FEN1 (psi-LVRU6MP- IGF2BP2) and the scrambled shRNA were purchased from GeneCopoeia (Rockville, MD, USA). The following sequences were targeted to human IGF2BP2 or FEN1:

IGF2BP2: 5'- GCATATACAACCCGGAAAGAA-3'.

FEN1: 5'- GATGCCTCTATGAGCATTTAT-3'

Cell Proliferation and Colony Formation Assay

For cell proliferation assays, CCK-8 kit (Dojindo, Kumamoto, Japan) and EdU Apollo® 567 In Vitro Imaging Kit (Ribobio, Guangzhou, China) were used according to the manufacturer's instruction. For the colony formation assay, 2×10^3 cells were plated into six-well plate, and cultured in complete culture medium. After 10 days, colonies were fixed with 4% paraformaldehyde and stained with 0.1% crystal violet (Beyotime, Beijing, China). Finally, visible colonies were photographed (Nikon, Tokyo, Japan) and counted. All experiments were performed in triplicate.

MeRIP-Seq and RNA-Seq

50 μg of total RNA was extracted and purified using PolyTtract mRNA Isolation System (Promega, Hong Kong). After fragmentation, RNA was incubated with an anti-m6A antibody for one hour at 4°C, and then mixed with prewashed Protein A/G Magnetic Beads (Merck Millipore, Germany) in immunoprecipitation buffer at 4°C overnight. Enrichment of m6A containing mRNA was purified for further MeRIP sequencing by RiboBio (Guangzhou, China). RNA-seq was conducted in accordance with a previously reported protocol (13). Fold change of >1.5 and false discovery rate $P < 0.05$ were set as the cutoffs to screen for differentially expressed genes (DEGs).

RIP-qPCR

RIP was conducted with the Magna RIP RNA-Binding Protein Immunoprecipitation Kit (Merck Millipore, Germany) according to the manufacturer's protocol. Mouse immunoglobulin G or IGF2BP2 (ab128175, Abcam) were coated with Magnetic beads. Then the coated beads were incubated with prepared cell lysates overnight at 4°C. Then, the RNA was finally extracted. The relative interaction between FEN1 and IGF2BP2 transcripts was determined by qPCR and normalized to the input.

Animals

The animal studies were approved by the Institutional Animal Care and Use Committee of Affiliated Hospital of YouJiang Medical College for Nationalities, and were carried out according to institutional guidelines. A total of 40 BALB/c nude mice were chosen and assigned to two groups: shCtrl group (injected with HepG2 cells) and shIGF2BP2 group (injected with HepG2 cells with IGF2BP2 knockdown). 200 μl of the above cell suspension containing 2×10^5 cells was injected into the left or right back of each mice. Tumor sizes and tumor volume were measured as described previously (14).

RESULTS

Elevated METTL3 and IGF2BP2 Expression Correlate With Poor Prognosis of Patients With HCC

To elucidate the functional roles of m^6A modification in HCC, we investigated the expression of 20 genes involved in m^6A RNA modification in the TCGA-LIHC databases (15). The results revealed that METTL3 and IGF2BP2 were significantly upregulated in tumor tissues compared with those in adjacent normal tissues (**Figure 1A**). Utilizing the online bioinformatics tool GEPIA (http://gepia.cancer-pku.cn/detail.php) (16), we also found that patients with HCC with increased METTL3 and IGF2BP2 mRNA levels had worse overall survival (OS) (**Figure 1B**) (the group cutoff was set as quartile [cutoff-high (%) was 75% and cutoff-low (%) was 25%)]. This result was consistent with previous reports that the METTL3 expression was up-regulated in the tumor tissue of liver cancer (17). To further validate the expression level of IGF2BP2 in the real world, we tested the expression of IGF2BP2 protein in 20 patients' HCC tissues and adjacent normal tissues by IHC. The results displayed that the high expression of IGF2BP2 was detected in 13/20 (65%) HCC (**Figure 1C**). Higher expression of IGF2BP2 was also found in HCC tissues than in the corresponding adjacent nontumor HCC tissues by western blot analysis (**Figure 1D**). Furthermore, statistical analysis of the 20 HCC patients' tumor tissues showed that expression of IGF2BP2 was associated with tumor size ($p = 0.031$) (**Table 1**). We then examined the m6A RNA levels in 20 HCC tissues and paired adjacent tissues by m6A RNA methylation assay. We found that the m6A RNA levels were significantly higher in HCC tissues than paired adjacent tissues (**Figure 1E**). Thus, the above results reveal that the m6A modification and the expression of IGF2BP2 are increased in HCC and that IGF2BP2 might be an independent prognostic factor for patients with HCC.

DNA Copy Number Aberrations Promote IGF2BP2 Overexpression in HCC

Since the copy number amplification (CNA) is closely related with gene expression. To detect whether DNA CNA contributes to IGF2BP2 overexpression or not, we extracted the CNA and expression data of IGF2BP2 from TCGA. After analyzing the data, we identified that IGF2BP2 copy number in HCC tissues was significantly higher than that in normal tissues (**Figure 2A**). Then, we evaluated the correlation of the CNA with the expression of IGF2BP2 by Pearson correlation coefficient [32]. The results showed that the expression of IGF2BP2 was significantly associated with the CNA in TCGA-LIHC samples (**Figure 2B**, $P < 0.01$). To further verify the association between the expression and CNA, the AccuCopy copy number assay (18) was applied to validate 20 pairs of primary HCC tissues compared with adjacent normal tissues. We discovered that the copy number of IGF2BP2 in tumor tissues was higher than that in adjacent normal tissues (**Figure 2C**). Additionally, the CAN was also correlated with mRNA expression of IGF2BP2 in the real world *via* qRT-PCR (**Figure 2D**, $P < 0.05$). Therefore, our results proved that CNA was one of the mechanisms that contributed to the overexpression of IGF2BP2 in HCC.

IGF2BP2 Promotes HCC Cells Tumorigenicity *In Vitro* and *In Vivo*

To select suitable cell lines for *in vitro* experiments, the IGF2BP2 expression was detected by qRT-PCR. Consistent with results in

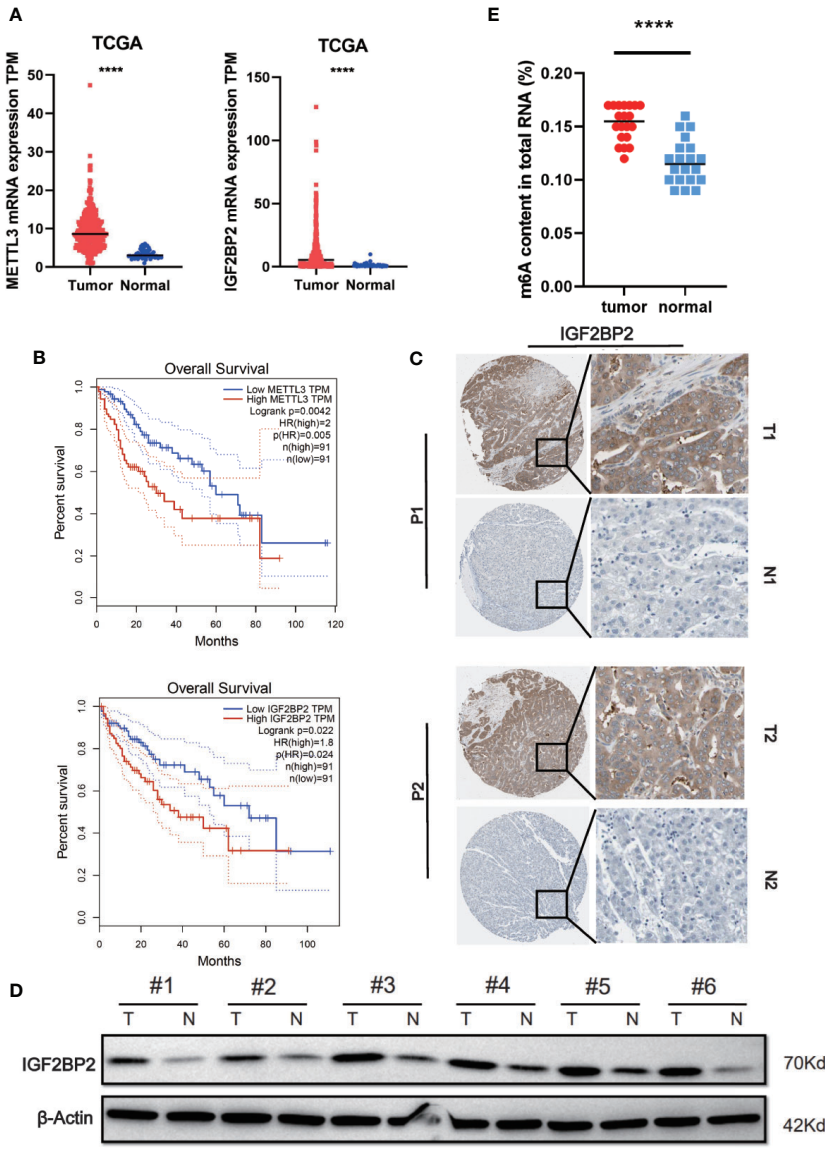

FIGURE 1 | Elevated IGF2BP2 expression correlates with poor prognosis of patients with HCC. **(A)** METTL3 (left) and IGF2BP2 (right) mRNA levels in the TCGA databases. **(B)** Kaplan-Meier survival curves of OS based on METTL3 and IGF2BP2 expression using the online bioinformatics tool GEPIA. **(C)** Representative IHC images of IGF2BP2 protein expression in HCC tissues (T) and adjacent normal tissue (N) of two patients (P1–P2). **(D)** IGF2BP2 protein levels were measured in HCC tissues and paired normal tissues by western blotting. **(E)** An m6A RNA methylation assay revealed the m6A content in HCC tissues and adjacent normal tissues. (****P < 0.0001, Student's t-test).

tumor tissue, the IGF2BP2 expression was significantly up-regulated in HCC cell lines (**Figure 3A**). Then, we selected HepG2 and Hun7 cell lines to investigate the the function of IGF2BP2 *in vitro*. To confirm the oncogenic function of IGF2BP2, shRNAs specifically targeting IGF2BP2 were transfected into HepG2 and Hun7 cells by lentivirus infection, respectively. The silencing effect was determined by western blot and qRT-PCR analysis, and the results showed that shRNA specifically downregulated the expression of IGF2BP2 (**Figures 3B, C**). The influence of IGF2BP2 knockdown on cell proliferation was examined by using the CCK-8 and EdU proliferation assays. CCK-8 and EdU analysis suggested that cell proliferation in HepG2 and Hun7 cell lines was impeded after IGF2BP2 knockdown (**Figures 3D–F**). Furthermore, knockdown the expression of IGF2BP2 reduced growth ability owing to fewer colonies formed after 10 days than the shCtrl group in both cell lines (**Figure 3G**). To determine if knockdown the IGF2BP2 expression could reduce tumor growth *in vivo*,

TABLE 1 | Relationship between IGF2BP2 expression in patients with HCC and clinicopathologic characteristics.

Feature	No.	YTHDF1 expression		P value
		High	Low	
Age (years)				
≥60	12	5	7	0.142
<60	8	6	2	
Tumor size(cm)				
≥2.0	13	9	4	0.019*
<2.0	7	1	6	
Lymph node metastasis				
Yes	12	6	6	0.582
No	8	5	3	
Clinical Stage				
I/II	6	2	4	0.202
III/IV	14	9	5	

(The P value was calculated by chi-squared analysis).
**P < 0.05.*

normal IGF2BP2 expression and knockdown HepG2 cells were transfected into the animals, respectively. The tumor growth was monitored. As shown in **Figures 4A, B**, knockdown the IGF2BP2 expression reduced tumor growth, as evidenced by the higher tumor volume and tumor weight; IGF2BP2 expression could not be detected in tumor tissues of IGF2BP2 knockdown mice (**Figure 4C**). Tumor tissues from knockdown IGF2BP2 mice showed lower levels of KI-67, as compared to control mice (**Figure 4D**). Together, the findings above suggested that the IGF2BP2 expression promoted HCC cell proliferation *in vitro* and *in vivo*.

FEN1 Is Regulated by METTL3-Mediated m6A Modification and Recognized by IGF2BP2 *via* an m6A-Dependent Manner

To map target transcripts by which IGF2BP2 promotes HCC progression, we first performed immunoprecipitation sequencing (MeRIP-seq) in HepG2 cells with stable METTL3 knockdown. We identified 1124 m6A modified genes in HepG2 cells (fold change of >1.2). We next conducted RNA sequencing (RNA-seq) in IGF2BP2 knockdown HepG2 cells. In addition, we analyzed RIP–seq data in HepG2 cells from the GEO database (19). We categorized transcripts into three groups: non-m6A marked transcripts, m6A-containing transcripts, and m6A-marked transcripts bound by IGF2BP2. Knockdown of IGF2BP2 globally and preferentially inhibited the expression of RIP targets (**Figure 5A**). Intriguingly, two genes were overlapped in the RNA-seq, MeRIP-seq, and RIP-seq data, and they were E2F1 and FEN1 (**Figure 5B**). Next, we validated the mRNA

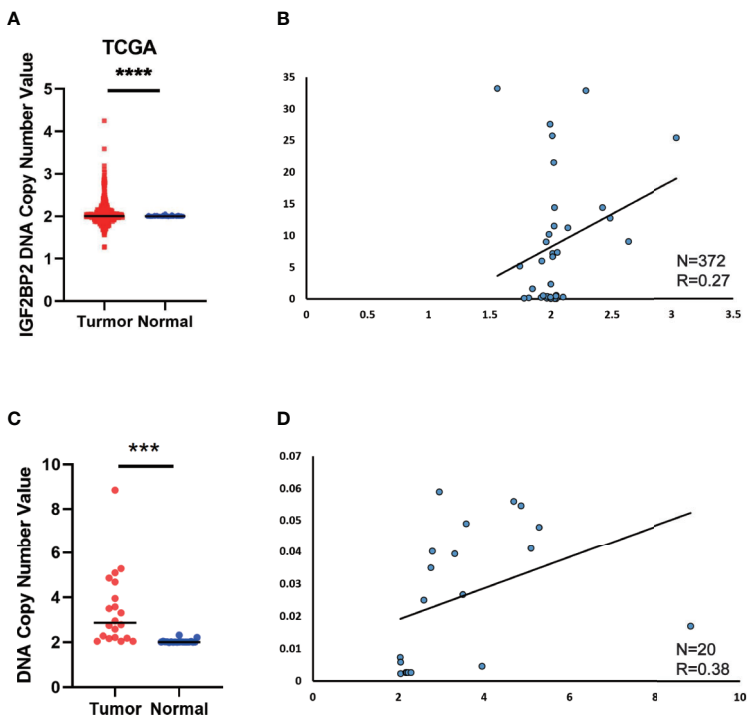

FIGURE 2 | DNA Copy Number Aberrations Promote IGF2BP2 Overexpression in HCC. **(A)** IGF2BP2 copy numbers in the TCGA databases. **(B)** Correlation between the DNA copy number and mRNA expression of IGF2BP2 in TCGA. **(C, D)** The comparison of the IGF2BP2 DNA copy number between HCC tissues (T) and adjacent normal tissues (N) in 20 patients and the correlation between the DNA copy number and mRNA expression of IGF2BP2 in 20 HCC tissue. (****P < 0.0001, ***P < 0.001, Student's t-test).

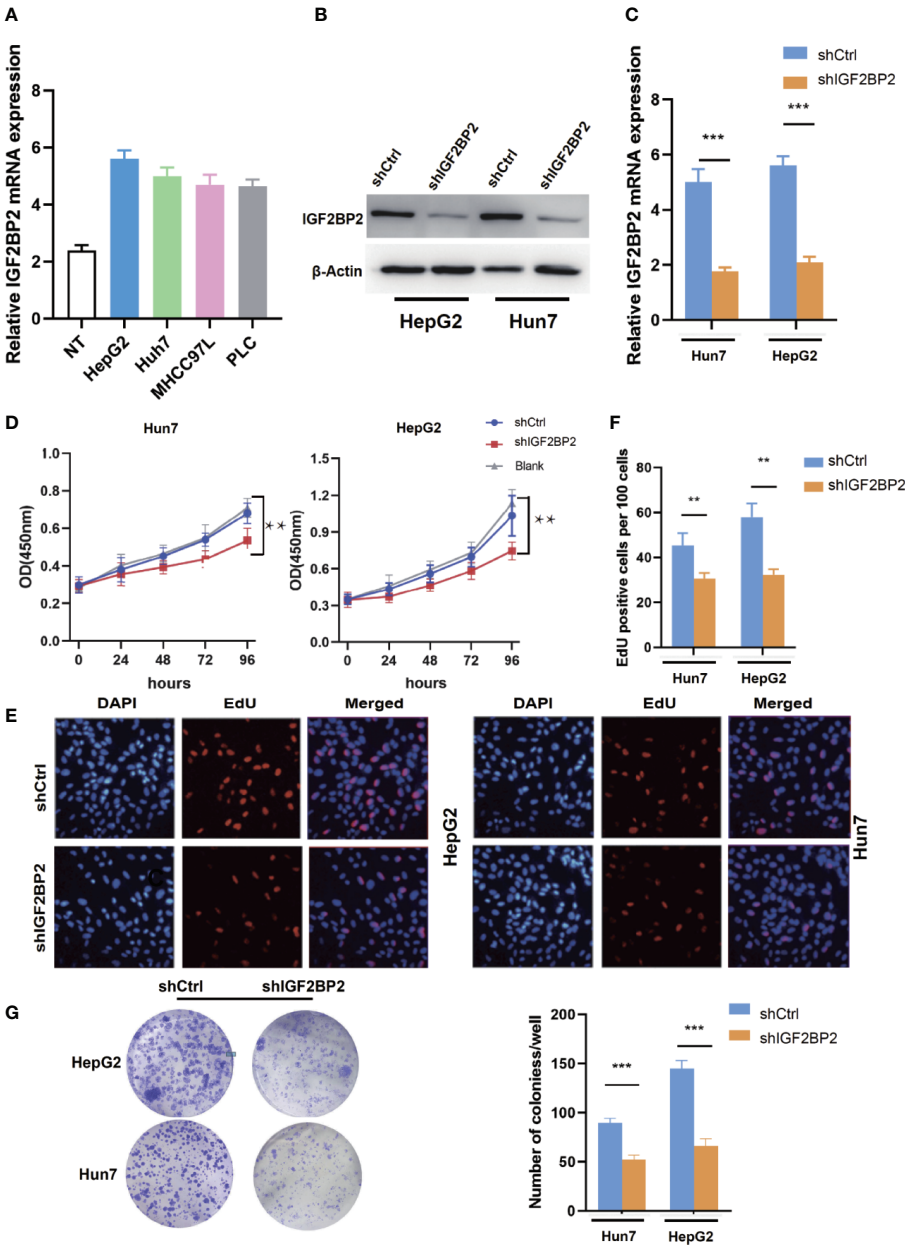

FIGURE 3 | IGF2BP2 Promotes HCC Cells Tumorigenicity *in vitro*. **(A)** The expression of IGF2BP2 mRNA in HCC cells was determined using qRT-PCR (The experiment was repeated three times). **(B, C)** Expression level of IGF2BP2 knockdown efficiency in HepG2 and Hun7 cell lines was detected by western blot and qRT-PCR. **(D)** The influences of IGF2BP2 knockdown on cell proliferation were confirmed using the CCK-8 assay (**P < 0.01, Student's t-test). **(E, F)** The influences of IGF2BP2 knockdown on cell proliferation were confirmed by EdU assay (**P < 0.01, Student's t-test). **(G)** The representative picture of colony formation assay, and the quantification of colonies per well (***P < 0.001, Student's t-test).

levels of these two candidate genes in other IGF2BP2 knockdown HCC cell lines *via* qRT-PCR (Huh7 and PLC). Only FEN1 but not E2F2 was consistently regulated by IGF2BP2 in all three HCC cell lines (**Figure 5C**). We also confirmed *via* a western blot assay that the FEN1 protein levels were positively regulated by IGF2BP2 in different HCC cell lines (**Figure 5D**). Next, RIP-qPCR demonstrated a strong binding of IGF2BP2 with FEN1 in all three HCC cell lines (**Figure 5E**). We also found that the expression of IGF2BP2 was significantly correlated with FEN1 expression in the TCGA-LIHC database (**Figure 5F**). Together, our experiments indicate that METTL3-mediated m6A modification

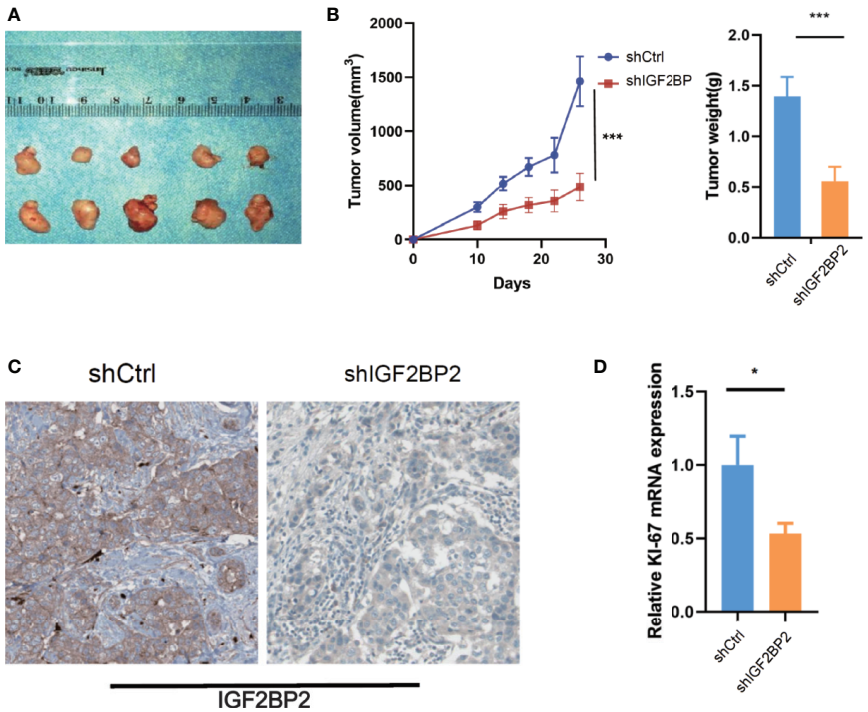

FIGURE 4 | IGF2BP2 Promotes HCC Cells Tumorigenicity *in vivo*. **(A, B)** Knockdown of IGF2BP2 effectively inhibited HepG2 cells subcutaneous tumor growth in nude mice (***P < 0.001, Student's t-test). **(C)** IHC analysis of IGF2BP2 in tumor tissue samples. **(D)** qRT-PCR analysis of KI-67 in tumor samples. (*P <0.05, Student's t-test).

maintains FEN1 expression *via* IGF2BP2-dependent FEN1 mRNA stability.

FEN1 Plays an Oncogenic Role in Ovarian Cancer Cells in HCC

To further examine the role of FEN1 in HCC, we analyzed the cellular phenotypes in HepG2 and Hun7 cells, including cell growth and colony formation ability upon FEN1 knockdown. shRNA specifically targeting FEN1 was transfected into HepG2 and Hun7 cells by lentivirus infection, respectively. The silencing effect was determined by western blot and qRT-PCR analysis, and the results showed that shRNA specifically downregulated the expression of FEN1 (**Figure 6A**). Notably, cell growth and colony formation capacities were markedly suppressed upon FEN1 knockdown in both HepG2 and Hun7 cells (**Figures 6B, C**). Based on the mechanism we identified above, we proceeded to explore the clinical relevance of FEN1. Utilizing the online bioinformatics tool oncomine (https://www.oncomine.org/), we found that FEN1 was significantly upregulated in tumor tissues compared with that in normal tissues (**Figure 6D**). Moreover, we also found that patients with HCC with increased FEN1 mRNA levels had worse overall survival (OS) (**Figure 6E**) (The group cutoff was set as Quartile [cutoff-High (%) was 75% and cutoff-Low (%) was 25%)].

DISCUSSION

HCC is one of the most common cancers and the leading cause of cancer-related mortality in developing countries (20). However, the molecular pathogenesis of HCC remains largely unknown (21, 22). Therefore, better prognostic indicators are needed to identify patients with poor prognosis and intervene as early as possible.

m6A, the most abundant post-transcriptional modification, is mainly regulated by m6A WERs ("writers", "erasers," and "readers") in diverse cell types (23, 24). m6A can affect the stability of mRNA *via* the m6A-binding protein IGF2BPs (IGF2BP1, IGF2BP2, and IGF2BP3) (19, 25). Dysregulation of m6A pathway components could affect oncogene expression, thereby linking m6A with tumorigenesis (26–28). In the present work, by utilizing the TCGA database, we identified that the expression of METTL3 and IGF2BP2 was upregulated in HCC tissues and that the high expression was correlated with poor prognosis. Our data with the clinical HCC samples were similar to the online data, in which IGF2BP2 was upregulated in HCC tissues at both the mRNA and protein levels, and the CNA might promote the high expression of IGF2BP2 in HCC. Moreover, the IGF2BP2 expression was found to be correlated with tumor size. But note that the clinical HCC specimens were just 20 pairs, further clinical trials in a multicenter are needed.

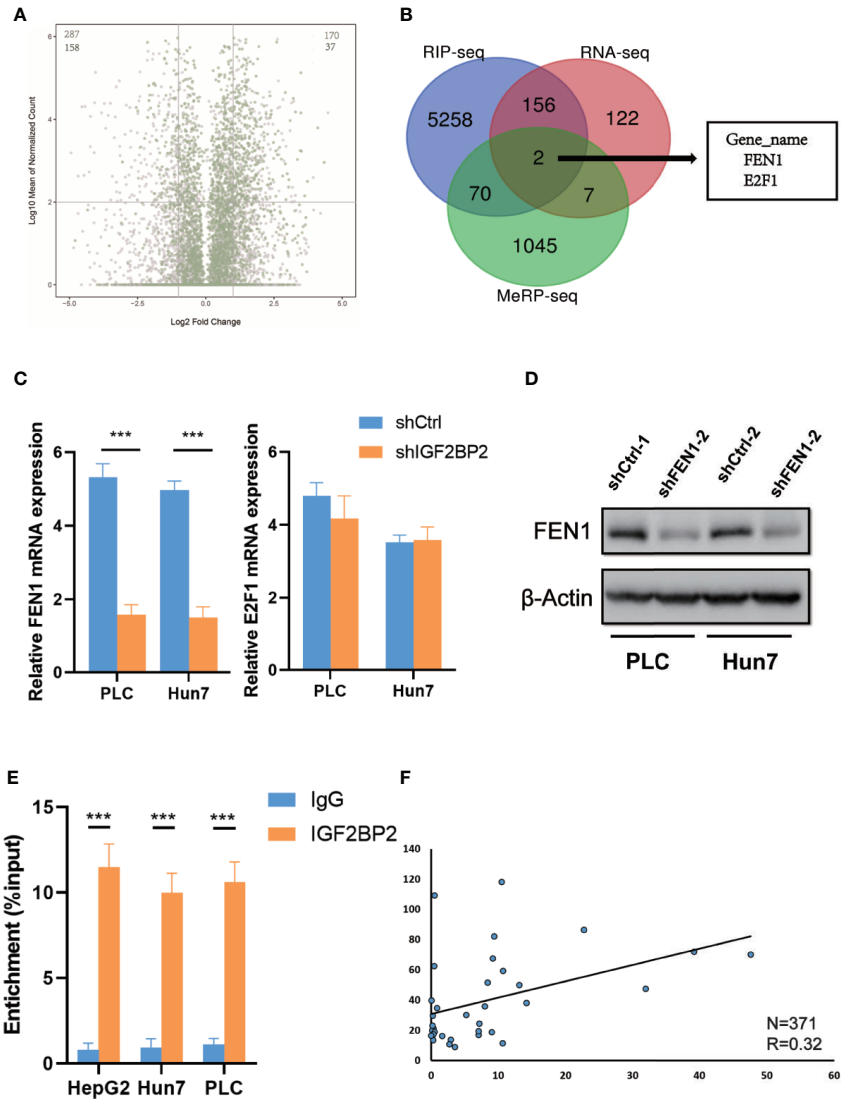

FIGURE 5 | FEN1 is regulated by METTL3-mediated m6A modification and recognized by IGF2BP2 *via* an m6Adependent manner. **(A)** Volcano plots displaying enrichment of dysregulated target genes in IGF2BP-knockdown (shIGF2BP) versus control (shNS) HepG2 cells. The numbers of significantly downregulated or upregulated genes (|log2 FC| > 1, P < 0.01, two-tailed Student's t-test) in the RIP-seq target group. **(B)** RNA-seq, MeRIP-seq and RIP-seq identified differentially expressed genes in HepG2 cells when compared with their corresponding controls. **(C)** Relative changes in FEN1 and E2F1 mRNA levels upon IGF2BP2 silencing in other HCC cell lines (***P < 0.001, Student's t-test). **(D)** The protein levels of FEN1 in other HCC cell lines were measured by western blotting. **(E)** RIP–qPCR showing the binding of IGF2BP2 to FEN1 (***P < 0.001, Student's t-test). **(F)** IGF2BP2 expression was positively correlated with FEN1 expression in HCC in TCGA database.

Flap endonuclease-1 (FEN1) is a multifunctional, structure-specific nuclease that has a critical role in maintaining human genome stability (28). Regulatory mechanisms of FEN1 in cells are crucial to maintaining normal cell growth (29). He et al. compared the expression of FEN1 in cancer tissues and normal tissues, and found that the expression of FEN1 in lung cancer tissues was significantly increased (30). In addition, high expression of FEN1 was also found in breast cancer and gastric cancer (31, 32). However, the mechanism of FEN1 up regulation is still unclear. In our study, m6A-seq and RNA-seq revealed that FEN1 was the downstream gene of IGF2BP2 and confirmed the oncogenic effect of FEN1 and revealed an m6A-dependent regulatory mechanism to partially explain the common upregulation of FEN1 in cancer.

In conclusion, our study identified that CAN was the major mechanism that promoted the high expression of IGF2BP2 in HCC. Additionally, the panoramic network of "writer" METTL3, "reader" IGF2BP2, and "target" FEN1 emphasized a novel m6A-dependent gene regulatory biological process. Our study suggests that targeting METTL3-IGF2BP2-FEN1 may be a novel and efficient strategy for a tumor-targeting therapy for HCC.

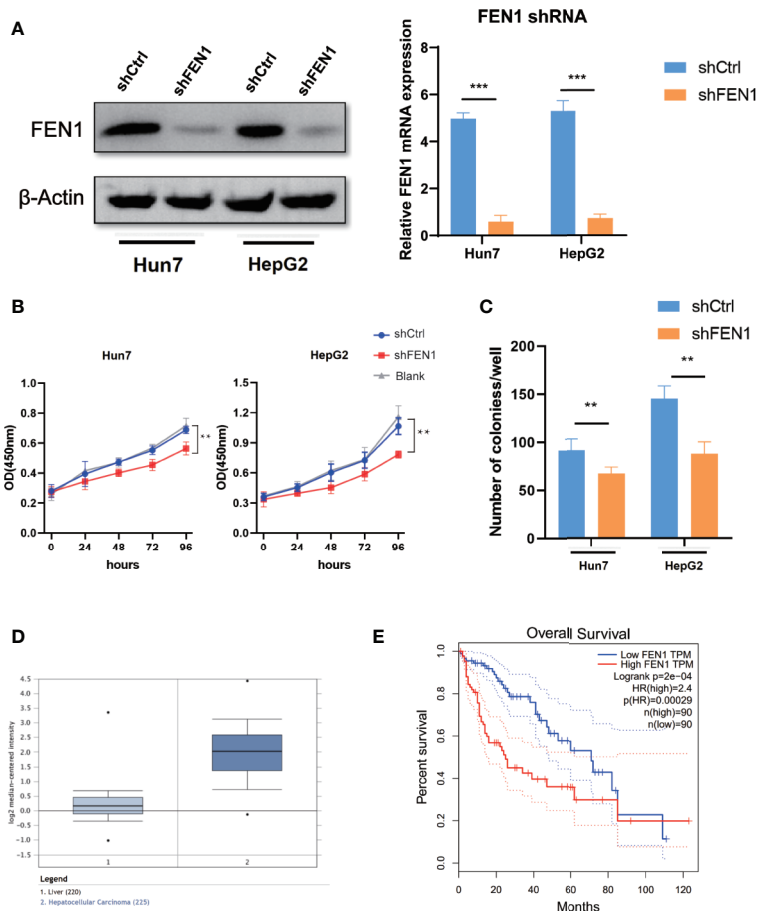

FIGURE 6 | FEN1 plays an oncogenic role in ovarian cancer cells in HCC. **(A)** Expression level of FEN1 knockdown efficiency in HepG2 and Hun7 cell lines was detected by western blot and qRT-PCR (***P < 0.001, **P < 0.01, Student's t-test). **(B)** The influences of FEN1 knockdown on cell proliferation were confirmed using the CCK-8 assay. **(C)** The influences of FEN1 knockdown on the quantification of colonies per well. **(D)** FEN1 mRNA levels in the oncomine databases. **(E)** Kaplan-Meier survival curves of OS based on FEN1 expression using the online bioinformatics tool GEPIA.

DATA AVAILABILITY STATEMENT

The raw data supporting the conclusions of this article will be made available by the authors, without undue reservation.

ETHICS STATEMENT

The study protocol was reviewed and approved by the institutional review board of YouJiang Medical College for Nationalities. All the procedures were performed in accordance with the Declaration of Helsinki and relevant policies in China. The patients/participants provided their written informed consent to participate in this study. The animal studies were reviewed and approved by the Institutional Animal Care and Use Committee of Affiliated Hospital of YouJiang Medical College for Nationalities.

AUTHOR CONTRIBUTIONS

Methodology: ZQ, AW, and YZ. Grammar Correction: YW and WL. Sample Collection: QT. All authors contributed to the article and approved the submitted version.

FUNDING

This work was supported by Science and Technology Project, Guangxi, AD17129025.

SUPPLEMENTARY MATERIAL

The Supplementary Material for this article can be found online at: https://www.frontiersin.org/articles/10.3389/fonc.2020.578816/full#supplementary-material

REFERENCES

1. International BM. Retracted: Hepatocellular Carcinoma: Novel Molecular Targets in Carcinogenesis for Future Therapies. *BioMed Res Int* (2018) 2018:1–. doi: 10.1155/2018/4560161
2. Syed YY. Ramucirumab: A Review in Hepatocellular Carcinoma. *Drugs* (2020) 80(3):315–22. doi: 10.1007/s40265-020-01263-6
3. Yang Y, Hsu PJ, Chen YS, Yang YG. Dynamic transcriptomic m6A decoration: writers, erasers, readers and functions in RNA metabolism. *Cell Res* (2018) 28:616–24. doi: 10.1038/s41422-018-0040-8
4. Zlotorynski E. RNA metabolism: m6A modulates RNA structure. *Nat Rev Mol Cell Biol* (2015) 16(4):204–. doi: 10.1038/nrm3974
5. Taketo K, Konno M, Asai A, Koseki J, Ogawa K. The epitranscriptome m6A writer METTL3 promotes chemo- and radioresistance in pancreatic cancer cells. *Int J Oncol* (2017) 52(2):621–9. doi: 10.3892/ijo.2017.4219
6. Balacco LD, Soller M. The m6A writer: Rise of a machine for growing tasks. *Biochemistry* (2018) 58(5):363–78. doi: 10.1021/acs.biochem.8b01166
7. Deng X, Jiang Q, Liu Z, Chen W. Clinical Significance of an m6A Reader Gene, IGF2BP2, in Head and Neck Squamous Cell Carcinoma. *Front Mol Bioences* (2020) 7:68. doi: 10.3389/fmolb.2020.00068
8. Li Z, Qian P, Shao W, Shi H, He XC, Madelaine G, et al. Author Correction: Suppression of m6A reader Ythdf2 promotes hematopoietic stem cell expansion. *Cell Res* (2018) 28(10):1042. doi: 10.1038/s41422-018-0083-x
9. Dai D, Wang H, Zhu L, Jin H, Wang X. N6-methyladenosine links RNA metabolism to cancer progression. *Cell Death Disease* (2018) 9(2):124. doi: 10.1038/s41419-017-0129-x
10. Wang S, Sun C, Li J, Zhang E, Ma Z, Xu W, et al. Roles of RNA methylation by means of N6-methyladenosine (m6A) in human cancers. *Cancer Lett* (2017). doi: 10.1016/j.canlet.2017.08.030
11. Chao X, Li L, Wu M, Ma S, Tan X, Zhong S, et al. Comparison of screening strategies for Lynch syndrome in patients with newly diagnosed endometrial cancer: a prospective cohort study in China. *Cancer Commun* (2019) 39(1):42. doi: 10.1186/s40880-019-0388-2
12. Hu J, Meng Y, Zhang Z, Yan Q, Jiang X, Lv Z, et al. MARCH5 RNA promotes autophagy, migration, and invasion of ovarian cancer cells. *Autophagy* (2017) 13(2):333–44. doi: 10.1080/15548627.2016.1256520
13. Tong M, Deng Z, Yang M, Xu C, Zhang X, Zhang Q, et al. Transcriptomic but not genomic variability confers phenotype of breast cancer stem cells. *Cancer Commun* (2018) 38(1):56. doi: 10.1186/s40880-018-0326-8
14. Cardenas M, Blank VC, Zotta E, Marder NM, Roguin LP. Induction of apoptosis in vitro and in vivo effects of a synthetic nitroflavone derivative on murine mammary adenocarcinoma cells. *Cancer Res* (2009) 69(2 Supplement):2145. doi: 10.1158/0008-5472.SABCS-2145
15. Tomczak K, Czerwińska P, Wiznerowicz M. The Cancer Genome Atlas (TCGA): an immeasurable source of knowledge. *Contemp Oncol* (2015) 19 (1A):A68. doi: 10.5114/wo.2014.47136
16. Tang Z, Li C, Kang B, Ge G, Cheng L, Zhang Z. GEPIA: a web server for cancer and normal gene expression profiling and interactive analyses. *Nucleic Acids Res* (2017) 45(W1):W98–102. doi: 10.1093/nar/gkx247
17. Chen M, Wei L, Law CT, Tsang FHC, Shen J, Cheng CLH, et al. RNA N6-methyladenosine methyltransferase-like 3 promotes liver cancer progression through YTHDF2-dependent posttranscriptional silencing of SOCS2. *Hepatol Off J Am Assoc Study Liver Dis* (2018) 67(6):2254–70. doi: 10.1002/hep.29683
18. Du R, Lu C, Jiang Z, Li S, Ma R, An H, et al. Efficient typing of copy number variations in a segmental duplication-mediated rearrangement hotspot using multiplex competitive amplification. *J Hum Genet* (2012) 57(8):545–51. doi: 10.1038/jhg.2012.66
19. Huang H, Weng H, Sun W, Qin X, Shi H, Wu H, et al. Recognition of RNA N6-methyladenosine by IGF2BP proteins enhances mRNA stability and translation. *Nat Cell Biol* (2018) 20(3):285. doi: 10.1038/s41556-018-0045-z
20. Xin WW, Hussain SP, Huo TI, Wu CG, Harris CC. Molecular pathogenesis of human hepatocellular carcinoma. *Toxicology* (2003) 181-182(1-3):43–7. doi: 10.1038/ng0802-339
21. Mortezaee K. Human hepatocellular carcinoma: Protection by melatonin. *J Cell Physiol* (2018) 233(10):6486–508. doi: 10.1002/jcp.26586
22. Qin LX, Tang ZY. Recent progress in predictive biomarkers for metastatic recurrence of human hepatocellular carcinoma: a review of the literature. *J Cancer Res Clin Oncol* (2004) 130(9):497–513. doi: 10.1007/s00432-004-0572-9
23. Zhang C, Fu J, Zhou Y. A Review in Research Progress Concerning m6A Methylation and Immunoregulation. *Front Immunol* (2019) 10:922. doi: 10.3389/fimmu.2019.00922
24. Years IR. Rethinking m6A Readers, Writers, and Erasers. *Annu Rev Cell Dev Biol* (2017) 33(1):319. doi: 10.1146/annurev-cellbio-100616-060758
25. Tong J, Flavell RA, Li HB. RNA m6A modification and its function in diseases. *Front Med* (2018) 12(4):481–9. doi: 10.1007/s11684-018-0654-8
26. Zhou J, Wang J, Hong B, Ma K, Xie H, Li L, et al. Gene signatures and prognostic values of m6A regulators in clear cell renal cell carcinoma - a retrospective study using TCGA database. *Aging* (2019). doi: 10.18632/aging.101856
27. Zhu S, Wang J-Z, Chen D, He Y-T, Yan G-R. An oncopeptide regulates m6A recognition by the m6A reader IGF2BP1 and tumorigenesis. *Nat Commun* (2020) 11(1):1685. doi: 10.1038/s41467-020-15403-9
28. Liu S, Li Q, Chen K, Zhang Q, Xie T. The emerging molecular mechanism of m6A modulators in tumorigenesis and cancer progression. *Biomed Pharmacother* (2020) 127:110098. doi: 10.1016/j.biopha.2020.110098
29. Zaher MS, Fahad R, Bo S, Joudeh LI, Sobhy MA, Muhammad T, et al. Missed cleavage opportunities by FEN1 lead to Okazaki fragment maturation via the long-flap pathway. *Nucleic Acids Res* (2018) 6:6. doi: 10.1093/nar/gky082
30. He L, Luo L, Zhu H, Yang H, Zhang Y, Wu H, et al. FEN1 promotes tumor progression and confers cisplatin resistance in non-small-cell lung cancer. *Mol Oncol* (2017). doi: 10.1002/1878-0261.12058
31. Chen B, Zhang Y, Wang Y, Rao J, Jiang X, Xu Z. Curcumin inhibits proliferation of breast cancer cells through Nrf2-mediated down-regulation of Fen1 expression. *J Steroid Biochem Mol Biol* (2014) 143:11–8. doi: 10.1016/j.jsbmb.2014.01.009
32. Li L, Zhou C, Zhou L, Li P, Li D, Zhang X, et al. Functional FEN1 genetic variants contribute to risk of hepatocellular carcinoma, esophageal cancer, gastric cancer and colorectal cancer. *Carcinogenesis* (2011) 1:1. doi: 10.1093/carcin/bgr250

Conflict of Interest: The authors declare that the research was conducted in the absence of any commercial or financial relationships that could be construed as a potential conflict of interest.

frontiers in Genetics

ORIGINAL RESEARCH
published: 04 November 2020
doi: 10.3389/fgene.2020.561566

The N6-Methyladenosine Features of mRNA and Aberrant Expression of m6A Modified Genes in Gastric Cancer and Their Potential Impact on the Risk and Prognosis

Liang Sang[1,2†], Liping Sun[1,3,4†], Ang Wang[1,3,4], Han Zhang[1,3,4] and Yuan Yuan[1,3,4]*

[1] Tumor Etiology and Screening Department of Cancer Institute and General Surgery, The First Hospital of China Medical University, Shenyang, China, [2] Department of Ultrasound, The First Hospital of China Medical University, Shenyang, China, [3] Key Laboratory of Cancer Etiology and Prevention in Liaoning Education Department, The First Hospital of China Medical University, Shenyang, China, [4] Key Laboratory of GI Cancer Etiology and Prevention in Liaoning Province, The First Hospital of China Medical University, Shenyang, China

OPEN ACCESS

Edited by:
Zhifu Sun,
Mayo Clinic, United States

Reviewed by:
Minghua Wang,
Soochow University Medical College, China
Yanqiang Li,
Houston Methodist Research Institute, United States

***Correspondence:**
Yuan Yuan,
yuanyuan@cmu.edu.cn

[†]These authors have contributed equally to this work

Specialty section:
This article was submitted to Cancer Genetics, a section of the journal Frontiers in Genetics

Received: 12 May 2020
Accepted: 07 October 2020
Published: 04 November 2020

Citation:
Sang L, Sun L, Wang A, Zhang H and Yuan Y (2020) The N6-Methyladenosine Features of mRNA and Aberrant Expression of m6A Modified Genes in Gastric Cancer and Their Potential Impact on the Risk and Prognosis. Front. Genet. 11:561566. doi: 10.3389/fgene.2020.561566

Although N6-methyladenosine (m6A) mRNA methylation is known to be closely related to tumor events, its role in carcinogenesis and the development of gastric cancer (GC) is not yet clear. The aim of this study was to identify common m6A features and novel aberrant expression of m6A modified genes in GC and to further explore their potential impact on risk and prognosis. Three paired GC and paracancerous (PCa) tissues were collected to perform an m6A sequencing by MeRIP-seq and microarray assays. The expression profile of m6A and mRNA were determined. Gene function note and enrichment analysis were performed, and protein–protein interaction networks of differentially m6A methylated genes (DMGs) were generated using the DAVID and STRING databases, respectively. Validation of the m6A related differentially expressed genes by matching TCGA and GTEx data and human tissues. Clinical and pathological correlation and survival analysis were performed by TCGA data. The m6A motif sequence GGACAR (*R* = U or A) C was the consensus in both GC and PCa tissues. m6A peaks were significantly related to different coordinates, however, for most samples, the end of the coding sequence (CDS) was more prominent than the start of CDS. The genes with higher levels of m6A in their mRNAs were mainly enriched in transcriptional misregulation in carcinogenesis pathways, whereas the genes with decreased methylation mainly regulated digestion and absorption of protein. There are genes with differential m6A modifications in GC and paired PCa tissues, and these genes are mainly enriched in transcriptional misregulation and digestion/absorption pathways. m6A-GC with the down- and up-regulated genes may play an important role in gastric carcinogenesis, which can affect the risk and prognosis in GC.

Keywords: M6A, methylation, gastric cancer, expression, risk, prognosis

INTRODUCTION

The identification of RNA modifications that regulate gene expression has resulted in the advance of the novel field of "RNA epigenetics" (He, 2010). To date, in multiple RNA species, more than 160 RNA modifications have been identified as post-transcriptional regulatory marks (Boccaletto et al., 2018; Yang et al., 2018). N6-methyladenosine (m6A) is the most prevalent form of mRNA modification in higher eukaryotes, and it plays a significant role in gene expression and metabolism (Wei et al., 1975; Dominissini et al., 2012; Meyer et al., 2012; Huang et al., 2020). m6A was discovered with a canonical RNA motif of RRACH (R = A or G; H = A, U, or C) and was found to be mainly enriched near stop codons and 3′ untranslated regions (3′ UTRs) (Linder et al., 2015). Because of the involvement of methyltransferases and demethylases, m6A methylation is regulated and reversible in nearly each step of mRNA metabolism, stem cell self-renewal, and cancer progression (Dai et al., 2018; Yang et al., 2018; Chen et al., 2019; Hu et al., 2019; Wang X. et al., 2020).

Recent studies have shown that the methylation of m6A mRNA plays a key role in the occurrence and development of cancers (Lan et al., 2019), such as glioblastoma (Cui et al., 2017; Du et al., 2020), hematologic malignancies (Bansal et al., 2014; Kwok et al., 2017), breast cancer (Zhang et al., 2016a,b), cervical cancer (Wang et al., 2017), hepatocellular carcinoma (HCC) (Ma et al., 2017), renal clear cell carcinoma (Wang J. et al., 2020), and pancreatic cancer (Geng et al., 2020). These studies show that phenotypes could be altered as a result of changes in the expression of key genes related to the function of the m6A modulator. However, for gastric cancer (GC), there are only a few studies on m6A methylation regulators (Xu et al., 2017; Li et al., 2019; Su et al., 2019; Yue et al., 2019). The gene expression effects, the target genes modified with m6A in GC, the extent of such modifications, and the functions and pathways of genes differentially modified with m6A, as well as the potential impacts of the modifications on mRNA expression, all remain elusive.

In this study, we collected three paired GC and paracancerous (PCa) tissues to obtain the first transcriptome-mRNA m6A profiles. Moreover, we investigated the genes with m6A modifications and performed functional annotations and pathway analyses of differentially m6A methylated genes using online tools. Subsequently, we performed a combined data analysis on the genes with differential m6A methylation and expression that were obtained from the sequence and array using GC and PCa tissues, and we explored whether m6A modification could affect mRNA expression, which could be related to the risk and prognosis in GC. Thus, we expected to find common features of m6A and novel aberrantly methylated pathways in GC and key m6A-related genes that might regulate gene expression to play a vital role in gastric carcinogenesis.

MATERIALS AND METHODS

Tissue Specimen Collection

Cancerous tissue and normal tissue (>3 cm adjacent to the cancer) were taken from three surgically removed GC specimens at the First Hospital of China Medical University. Fresh samples were immediately frozen in liquid nitrogen and maintained at −80°C. This study was conducted with the approval of the institutional ethics board of the First Hospital of China Medical University.

High-Throughput m6A Sequencing

MeRIP-Seq was executed by Cloudseq Biotech Inc. (Shanghai, China) in line with the printed procedure (Meyer et al., 2012) with minor adjustments. In brief, RNA was fragmented and incubated for 2 h with an anti-m6A polyclonal antibody (Synaptic Systems, 202003) in IPP buffer at 4°C. The mixture was then immunoprecipitated by incubation for an extra 2 h at 4°C with protein-A beads (Thermo Fisher). Next, the bound RNA was eluted from the beads with m6A (Berry and Associates, PR3732) in IPP buffer and was then collected with TRIzol reagent (Thermo Fisher) according to the manufacturer's instructions. The RNA sequence library was generated from purified RNA with a NEBNext® Ultra™ RNA Library Prep Kit (NEB). The m6A IP samples and input samples without immunoprecipitation were both subjected to 150-bp paired-end sequencing on an Illumina HiSeq sequencer.

mRNA Expression Assay by Microarray

The experiment used NanoDrop ND-2000 (Thermo Scientific) to quantify total RNA and Agilent Bioanalyzer 2100 (Agilent Technologies) to assess RNA integrity. Sample labeling, microarray hybridization, and washing were performed in accordance with the manufacturer's instructions. In short, total RNA was transcribed into double-stranded cDNA, and then cRNA was manufactured and tagged with cyanine-3-CTP. The tagged cRNAs were hybridized to the microarray. Finally, the array was scanned using an Agilent Scanner G2505C (Agilent Technologies) after washing.

Data Analysis

Analysis of N6-Methyladenosine Features of Differentially Methylated Genes Between GC and Paired PCa Issues

First, quality control was performed by Q30 after obtaining paired-end reads from Illumina HiSeq 4000 sequencer, and then low-quality and 3′ adaptor-trimming reads were deleted by cutadapt software (v1.9.3). Next, HISAT2 software (v2.0.4) was used to align all clean reads of libraries with the reference genome (UCSC HG19). MACS software was used to identify the methylated sites of RNAs (peaks). In addition, diffReps was used to discover differentially methylated sites. In this study, we used P < 1e-05 and $|$ fold change$|$ > 2 as the cutoff criteria for differentially methylated genes (DMGs). The conserved m6A motif in GC tissues was constructed by MEME software using 100-nt RNA fragments, including methylation sites.

DMGs Related Enrichment Analysis and Protein–Protein Interaction Network Construction

Gene Ontology and pathway enrichment analyses were performed for DMGs using the DAVID database. A protein–protein interaction (PPI) network of genes with increased or decreased m6A levels was built through the STRING (Search

Tool for the Retrieval of Interacting Genes/Proteins)[1] database. An interaction score (median confidence) of 0.4 was adopted as the cutoff standard.

Effect Analysis of Differential m6A Methylated Genes on the Related mRNA Expression Levels

Differentially expressed genes were recognized from microarray and TCGA and GTEx data by fold change and P value together analyzed with t test. Consequently, we performed a combined analysis of differently m6A methylated genes and differently expressed genes by the standard of $P < 0.05$ and $|$ fold change$| > 2$.

Validation of m6A Modified Gene Expression Levels From Microarray by Matching TCGA and GTEx Data

To confirm the results, we validated the levels of m6A modified gene expression in stomach adenocarcinoma (STAD) by using the TCGA and GTEx data. $|$ logFC$| > 1$ and $P < 0.05$ were considered to indicate statistically significant differences. A boxplot graph was produced for the visualization of the results.

Validation of m6A Modified Gene Expression Levels From Microarray in Human Tissues

We further verified the hub genes using 10 pairs of tumor and adjacent non-tumor tissues in GC that were matched according to age and sex (this validation was approved by the Human Ethics Review Committee of the First Hospital of China Medical University). Quantitative real-time polymerase chain reaction (PCR) was performed to profile the mRNA expression levels. Differences between the groups were compared by the use of a Mann–Whitney U test, and $P < 0.05$ was considered to be statistically significant. All of the primers that were used are shown in **Table 1**.

TABLE 1 | Real-time PCR primer sequence.

Name		Sequence
SCD	F	CTTTCTGATCATTGCCAACACA
	R	TGTTTCTGAAAACTTGTGGTGG
MTHFD1L	F	GAGGAAGTGAGTAAATTTGCCC
	R	GCCCGATGGTTATTTTTCGTAG
IGF2	F	CTGGAGACGTACTGTGCTAC
	R	CATATTGGAAGAACTTGCCCAC
ORM1	F	TAACACCACCTACCTGAATGTC
	R	AAAAGCAAGCATGTAGGTCTTG
FGA	F	GGATCGTCTGCCTGGTCCTA
	R	CCTTCAGCTAGAAAGTCACCTTCA
GC	F	AAATGATGAAATCTGTGAGGCG
	R	AGCTTGTCCGTAATTAGTGGAA
GIF	F	GCCCTCTACCTCCTGAGCCTTC
	R	GCTGATGAAGTCACCGAGTTCTCC
MT1E	F	CATTCTGCTTTCCAACTGCCTG
	R	GCAGCTCTTCTTGCAGGAGG
GALNT1	F	ATGGCCCAGTTACAATGCTC
	R	ATATTTCTGGCAGGGTGACG
beta-actin	F	ATGTGGCCGAGGACTTTGATT
	R	AGTGGGGTGGCTTTTAGGATG

Clinical and Pathological Correlation and Survival Analysis of m6A Modified Genes by TCGA Data

We considered the differentially m6A modified genes as hub genes, and we performed clinical and pathological correlation and survival analyses of the TCGA data that were based on gene expression. A boxplot graph was produced for the visualization of the relationships. Overall survival was assessed by using Kaplan–Meier survival curves, and the hazard ratio with 95% confidence interval information and log-rank P values were calculated and included in the survival plots. Values of $P < 0.05$ were considered to indicate significant differences.

RESULTS

Common Features of the m6A Modification of mRNA in GC and PCa Tissues

After removing low-quality data, approximately 9,700,000 to 21,200,000 high-quality reads were obtained from every PCa IP sample, as well as approximately 14,800,000 to 24,200,000 reads from every GC IP sample, and they were mapped to the reference genome with an efficiency of greater than 66%. Moreover, we found the consensus sequence GGACAR (R = U or A) C by analyzing the top 100 most significant peaks from every sample using MEME software (Machanick and Bailey, 2011); this sequence resembles the common m6A motif described in human diseases. Furthermore, the results showed that m6A peaks were significantly related to different gene locations in both GC and paired PCa tissues: near the middle of the 5' UTRs, start of the coding sequence (CDS), near the end of the CDS, and 3′ UTRs. Moreover, for most samples, the peaks at the end of CDS were more pronounced than those at the start, and to further confirm the preferential locations of m6A on transcripts, we investigated the metagene profiles of m6A peaks (**Figures 1A–C**).

DMGs Between GC and Paired PCa Tissues

We detected 1,487 genes with 2,103 m6A sites in GC tissues and 1,230 genes with 1,688 m6A sites in PCa tissues. On average, 1.41 and 1.37 m6A sites occurred per gene mutation in GC and PCa tissues, respectively. A total of 365 genes were comethylated in GC and PCa tissues, accounting for 15.52% of the total methylated genes. A total of 1,122 and 865 genes were only methylated in GC and PCa tissues, respectively. Statistics for m6A genes of each sample are shown in a Venn diagram (**Figure 2**), and the heatmap of intersecting m6A signals for the represent group is shown in **Figure 3**. We searched for differential m6A modifications in mRNAs by analyzing GC and PCa tissues, and we identified 81 up-regulated and 62 down-regulated methylated protein coding genes (**Supplementary Table S1**). The top 10 up- and down-regulated genes and their related information are shown in **Table 2**.

[1] http://string-db.org/

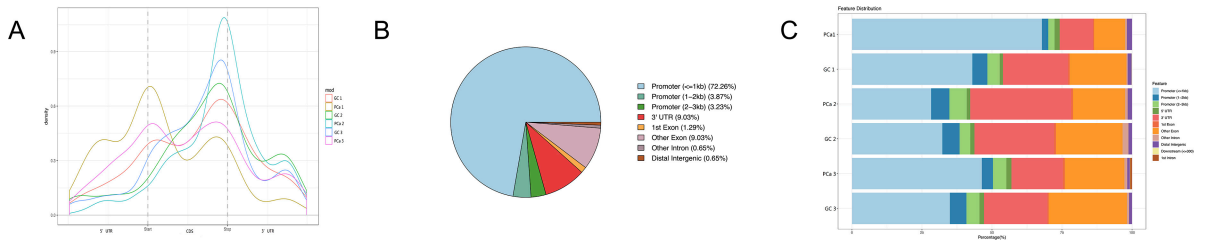

FIGURE 1 | Distribution of m6A peaks along transcripts. **(A)** Each transcript is divided into three parts: 5' untranslated regions (5' UTRs), coding sequence (CDS), and 3′ untranslated region (3′ UTRs). **(B)** The m6A peak distribution within different gene contexts. **(C)** The m6A peak distribution along a metagene.

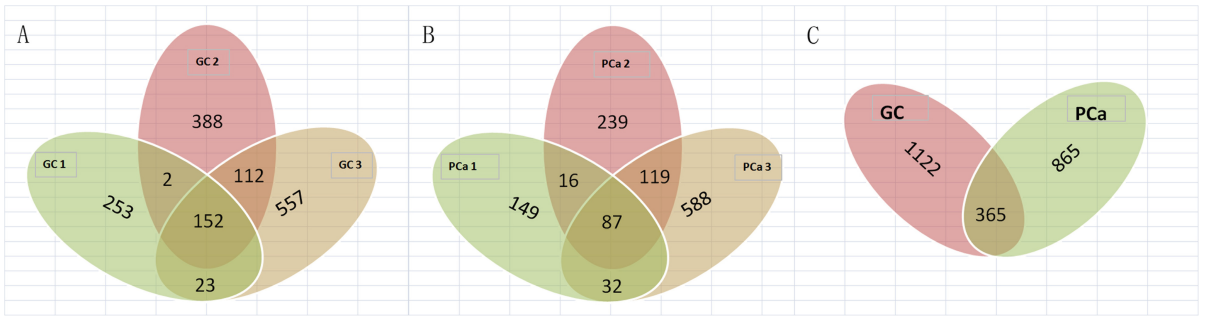

FIGURE 2 | Statistics for genes with m6A modifications in each sample. **(A)** Number of genes with m6A sites in three GC samples; **(B)** number of genes with m6A sites in three PCa samples; **(C)** number of genes in GC and PCa tissues. We detected 1,487 m6A genes in GC tissues and 1,230 genes in PCa tissues, respectively, 365 genes were comethylated in GC and PCa tissues, accounting for 15.52% of the total methylated genes; 1,122 and 865 genes were only methylated in GC and PCa tissues, respectively.

DMGs Related Pathway and PPI Network Between GC and PCa Tissues

GO analysis demonstrated that the up-methylated genes of m6A are chiefly enriched in the histone deacetylase complex, ionotropic glutamate receptor complex, and transcription factor complex. Further, these genes are engaged in various molecular functions, such as sequence-specific DNA binding, transcription factor–binding, and complement binding, and they are involved in biological progresses, such as forebrain regionalization and positive regulation of transcription from the RNA polymerase III promoter (**Figure 4**).

The down-methylated genes of m6A modifications are mainly enriched in the ribonucleoprotein complex, extracellular region part, and cytosolic ribosome; further, the gene products are engaged in various molecular functions, such as poly(A) RNA binding, RNA binding, aspartic-type endopeptidase, and peptidase activity, and they are involved in biological progresses, such as nuclear-transcribed mRNA catabolic process, translational elongation, and mRNA catabolic process (**Figure 5**).

Furthermore, we investigated the Kyoto Encyclopedia of Genes and Genomes (KEGG) pathways of m6A methylated mRNAs. From the results, we found that the up-methylated mRNAs were mostly enriched in pathways including complement and coagulation cascades, transcriptional misregulation in cancer, and viral carcinogenesis. However, the down-methylated mRNAs were mostly involved in pathways including ribosome, vitamin digestion and absorption, antigen processing and presentation, protein digestion, and absorption.

Differentially m6A methylated genes were investigated using STRING. In total, 81 nodes and 44 edges were discovered in the up-regulated genes, and the PPI networks displayed even more interactions with a PPI enrichment *P* value of 9.08e-07 (**Figure 6A**). In addition, 62 nodes and 74 edges were discovered in down-regulated methylated genes, and the PPI networks displayed even more interactions with a PPI enrichment *P* value of 3.32e-12 (**Figure 6B**).

The Effect Analysis of Differential m6A Modification of Genes on the Related mRNA Expression

We identified 472 up-regulated genes and 346 down-regulated genes among three paired GC and PCa tissues, respectively (**Supplementary Table S2**). In addition, we analyzed 415 tumors and 262 normal control tissues in TCGA + GTEX database. A total of 3,017 differentially expressed genes were obtained, including 1,226 up-regulated genes and 1,791 down-regulated genes (**Supplementary Table S3**). We performed a combination analysis of 1,487 m6A methylation genes with the above mRNAs that were differentially expressed in GC. We found 120 up-regulated genes and 92 down-regulated genes related to m6A methylation (**Figure 7**). Further, we analyzed the differentially expressed genes related to differential m6A methylation. We finally identified 18 genes with increased

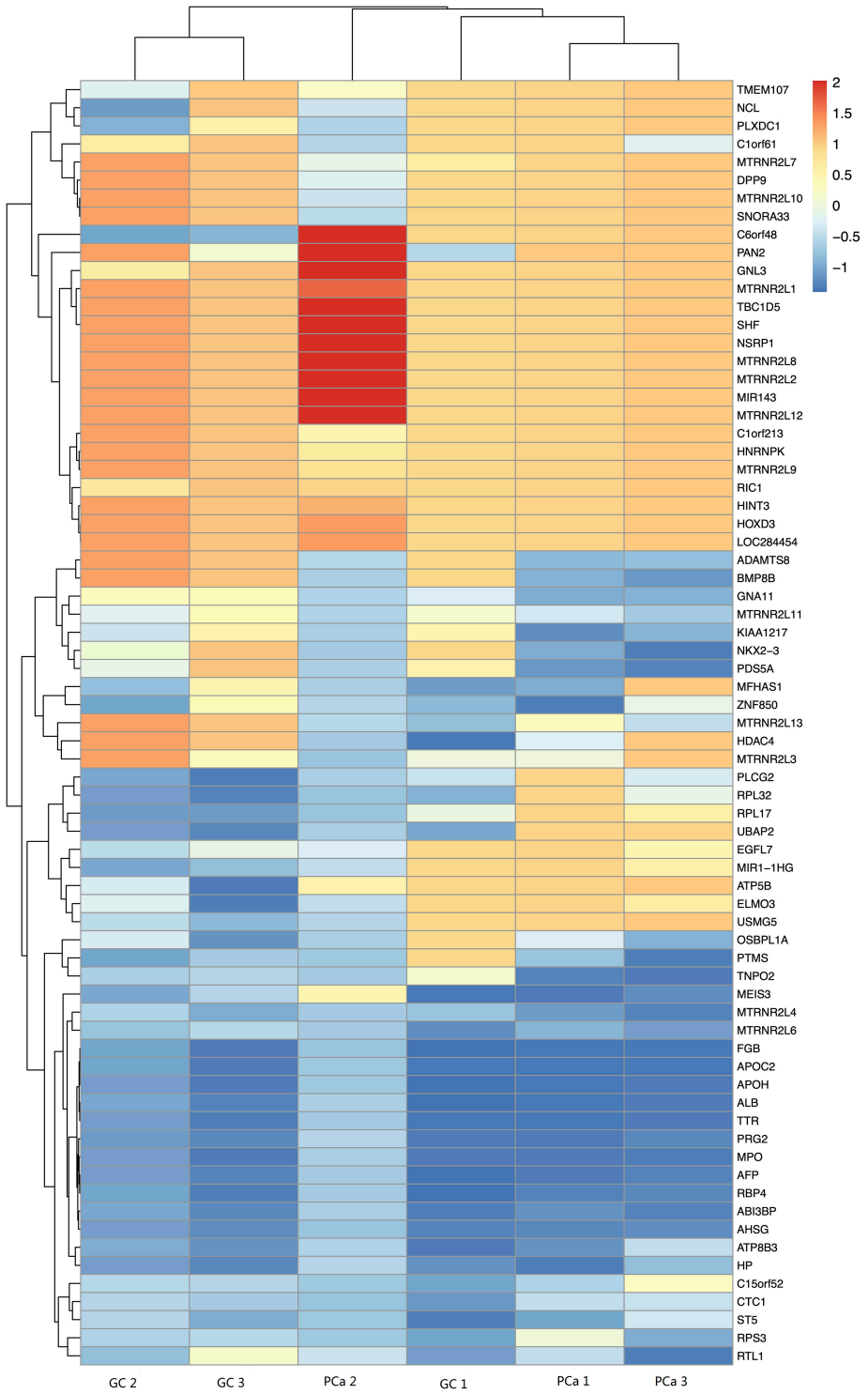

FIGURE 3 | The heatmap of intersecting m6A signals for the represent group.

m6A levels and 9 genes with decreased m6A levels that had differential m6A methylation between GC and PCa tissues. Among these genes, 15 genes revealed a positive correlation between m6A methylation and gene expression, whereas 12 genes had a negative correlation that may affect their expression in GC (**Table 3**).

TABLE 2 | Top 10 up- and down-regulated differential methylated genes in GC tissues.

Catalog	Gene name	Chrom	txStart	txEnd	Peak ID	Fold change	*P* value
Up	F13A1	chr6	6152045	6152182	diffreps_peak_958	167	1.11E-16
	GOLPH3L	chr1	150620621	150620880	diffreps_peak_87	136	6.73E-14
	BDKRB2	chr14	96709521	96709720	diffreps_peak_355	131	1.78E-13
	BTNL9	chr5	180480468	180480620	diffreps_peak_947	114	0
	ZFHX3	chr16	72991561	72991820	diffreps_peak_492	91	1.02E-09
	PGP	chr16	2264561	2264822	diffreps_peak_449	81	8.92E-09
	PROC	chr2	128180681	128180984	diffreps_peak_677	70	0
	TLCD1	chr17	27053221	27053230	diffreps_peak_531	65	2.35E-07
	TSPAN9	chr12	3186520	3186560	diffreps_peak_253	64	0
	PANX2	chr22	50616361	50616740	diffreps_peak_794	57	0
Down	IST1	chr16	71929395	71929492	diffreps_peak_490	125	7.59E-13
	GIF	chr11	59612733	59612972	diffreps_peak_214	80	0
	PGA4	chr11	60989817	60989928	diffreps_peak_215	62	0
	PGA5	chr11	61008647	61008754	diffreps_peak_218	57	0
	SCOC	chr4	141264681	141264862	diffreps_peak_884	56	1.6E-06
	HES1	chr3	193853930	193854080	diffreps_peak_854	52	3.94E-06
	ATP5B	chr12	57038601	57038739	diffreps_peak_273	36	0
	PGC	chr6	41704448	41704580	diffreps_peak_1009	35	0
	LSS	chr21	47648401	47648738	diffreps_peak_776	31	5.17E-09
	RPL3	chr22	39715032	39715116	diffreps_peak_788	26	0

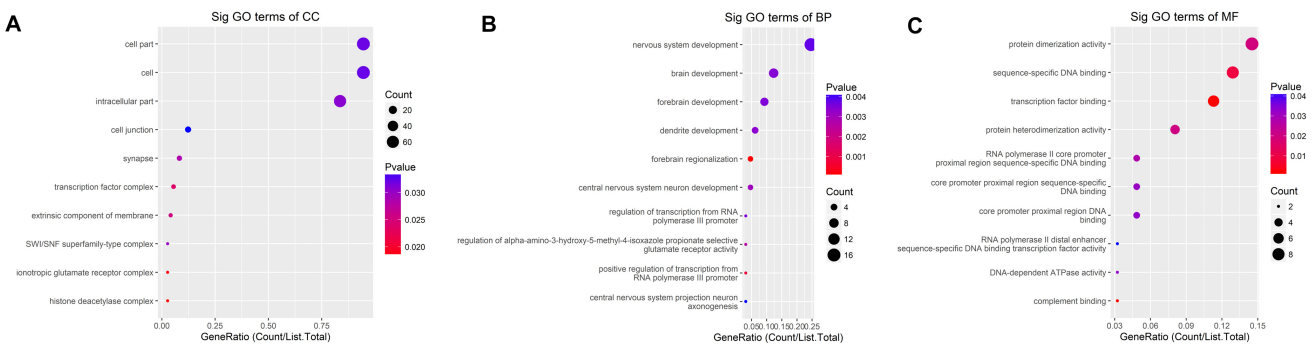

FIGURE 4 | GO terms for mRNAs with increased m6A levels. **(A)** Cellular component, **(B)** biological process, **(C)** molecular function. The genes are mainly enriched in the histone deacetylase complex, ionotropic glutamate receptor complex, and transcription factor complex and are involved in a variety of molecular functions including transcription factor binding, complement binding, sequence-specific DNA binding, and biological progresses referred to forebrain regionalization and positive regulation of transcription from RNA polymerase III promoter.

The Differential Expression of m6A Modified Genes From Microarray Validated by Matching TCGA and GTEx Data and in Human Tissues

We selected the hub m6A modified genes from microarray to validate the expression in STAD by matching 408 tumor tissues and 211 normal tissues. The results demonstrated that nine hub genes, (MTHFD1L, IGF2, SCD, GC, ORM1, FGA, GALNT1, MT1E, and GIF) exhibited significant differences between the cancer and normal tissues. A boxplot graph was produced for the visualization of these differences (**Figure 8**). Next, we sought to verify the nine identified hub genes in human tissues and demonstrated that MT1E, GC, FGA, GALNT1, ORM1, and GIF exhibited statistical difference ($P < 0.05$); additionally, IGF2, MTHFD1L, and SCD exhibited no significant differences ($P > 0.05$), which may be related to the small sample size that we verified.

Clinical and Pathological Correlation and Survival Analyses of Hub m6A Modified Genes by the Use of TCGA Data

Using TCGA data, we analyzed the correlation between the expression levels of hub m6A modified genes and clinicopathological parameters and prognoses. We observed that IGF2, SCD, GALNT1, TLCD1, SHISA9, NLGN1, and F13A1 expression levels were related to the T stage; IGF2, NLGN1, ADAMTS8, and F13A1 expression levels were related to the pathological stage; SCD, GALNT1, GIF, TLCD1, SHISA9,

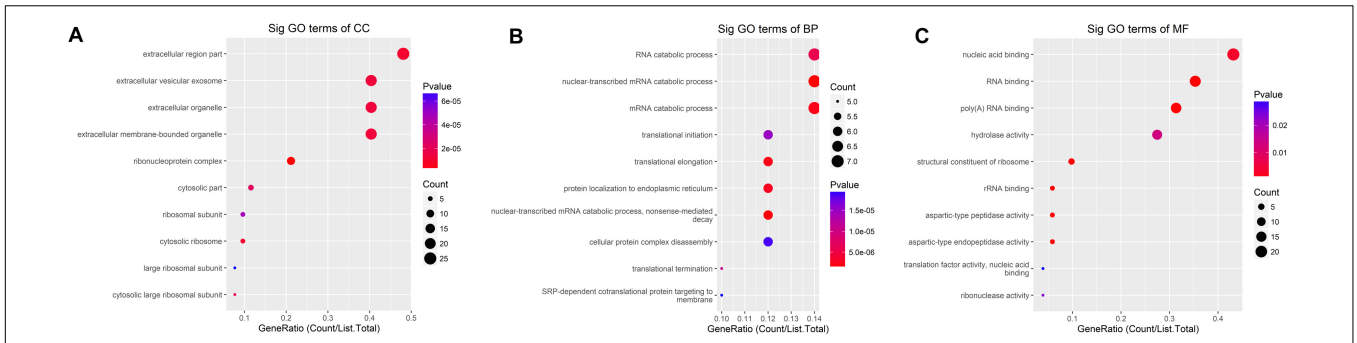

FIGURE 5 | GO terms of mRNAs with decreased m6A levels. **(A)** Cellular component, **(B)** biological process, **(C)** molecular function. The genes are mainly enriched in the ribonucleoprotein complex, extracellular region part, and cytosolic ribosome and are involved in a variety of molecular functions including poly(A) RNA binding, RNA binding, aspartic-type endopeptidase and peptidase activity, and biological progresses referred to nuclear-transcribed mRNA catabolic process, translational elongation, and mRNA catabolic process.

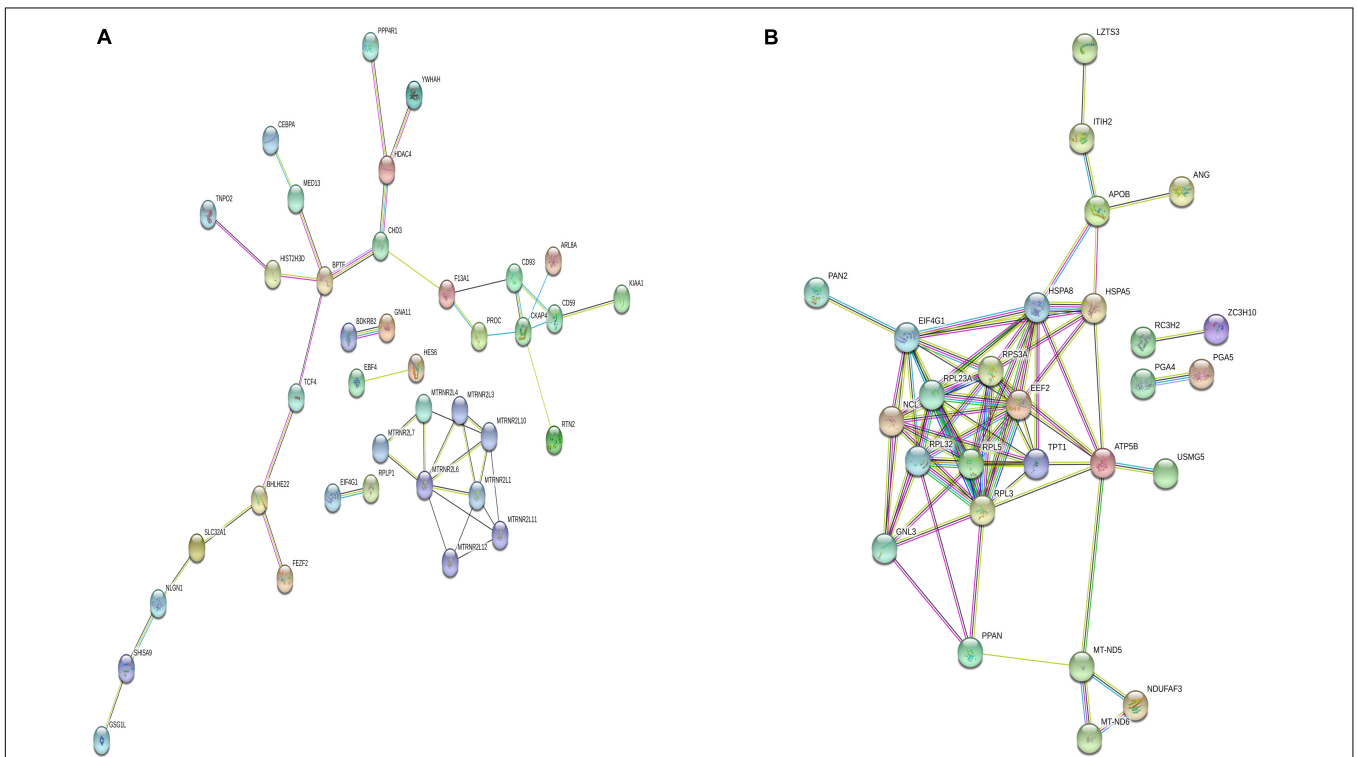

FIGURE 6 | Protein–protein interaction network of DMGs. Disconnected nodes are not shown in the network. **(A)** total of 81 nodes and 44 edges were established in genes with increased methylation, and **(B)** 62 nodes and 74 edges were established in genes with decreased methylation. PPI networks both revealed a significantly more interactions.

NLGN1, PLD5, ADAMTS8, F13A1, and SLC13A3 expression levels were related to the histological grade; ORM1, GIF, TLCD1, SHISA9, BTNL9, PGA5, PGA4, and RPL5 expression levels were related to anatomical subdivisions; ORM1 and F13A1 expression levels were consistently associated with metastasis; FGA expression levels were related to gender; NLGN1 expression levels were related to lymph node metastasis; PLD5 expression levels were related to reflux history; and EBF4 expression levels were related to Barrett esophagus (**Supplementary Table S4**). In addition, the survival analysis of the hub genes demonstrated that GNLAT1, EBF4, F13A1, and NLGN1 expression levels were related to the overall survival. The visualization of the survival analysis is displayed on the plots (**Figure 9**).

DISCUSSION

In this study, we first outlined the patterns and characteristics of m6A in GC, such as m6A modification of specific genes,

FIGURE 7 | m6A methylation genes with the related mRNA differentially expressed genes in GC. We performed a combination analysis of 1,487 m6A methylation genes with related mRNA differently expression genes in GC and found 120 up-regulation genes and 92 down-regulation genes were related m6A methylation.

TABLE 3 | Gene and relationship between differential m6A methylation and gene expression levels.

Category	Up-methylated	Down-methylated
Hyperexpression	MTHFD1L	GALNT1
	IGF2	
	SCD	
	BMP8B	
	TSPAN9	
	TLCD1	
	CEBPA	
Hypoexpression	GC	
	ORM1	
	FGA	
	HS3ST4	MT1E
	SHISA9	GIF
	NLGN1	CPEB2
	BTNL9	PGA5
	PLD5	PGA4
	ADAMTS8	SLC13A3
	EBF4	RPL5
	F13A1	PGC

distribution in transcripts, and the consensus m6A motif. In addition, we identified the DMGs between GC and PCa tissues and further analyzed their functions and enrichment pathways using bioinformatics tools. Finally, by combining analysis of differently m6A methylated and expression genes, we discovered some key genes that may exhibit dynamic expression because of m6A methylation and that are associated with GC risk and prognoses.

Previous studies have proven that the consensus motif sequence RRACH is the characterized in the m6A motif (Wei and Moss, 1977; Harper et al., 1990), and this has further been confirmed in many high-throughput m6A RNA sequencing databases (Dominissini et al., 2012; Luo et al., 2014). In our study, we found the consensus sequence GGACAR (R = U or A) C, which resembles the common m6A motif described in human diseases. The consistent sequence detected in the present study suggested that m6A methylation was conserved among various organs and tissues. Although, as mentioned before, m6A is mainly enriched in the vicinity of stop codons and 3′ UTRs in most mRNAs from different mammalian organs (Batista et al., 2014; Li et al., 2014), the distribution of m6A could be affected by the origin of tissue and genetic backgrounds of organisms, and the modified sites could remain unchanged, while the modified segments of each site may vary based on environmental factors (Luo et al., 2014). We found that m6A in both GC and PCa tissues was enriched around the CDS and at 3′ UTRs, as had been found in mammals. The m6A methylation peaks for most GC tissues were higher at the end of a CDS than they were at the start. According to our results, we speculate that when the stomach tissue evolves from a normal lesion to a cancerous lesion, changes in genetic and microenvironment factors are most focused on the end of the CDS. Moreover, the expansively abundant m6A modifications at the CDS or 3′ UTRs may be in charge of RNA stability, transport, and translocation signals or protein synthesis (Niu et al., 2013); these observations may also demonstrate a molecular mechanism, but further study is needed to verify these findings.

N6-methyladenosine RNA modifications show population-specific regulation at the cellular or species level in response to environmental changes (Luo et al., 2014; Tao et al., 2017). Some present studies have shown that m6A differs between cancers and adjacent tissues, such as HCC, cervical cancer, and breast cancer (Zhang et al., 2016b; Ma et al., 2017; Wang et al., 2017). Here, we detected an average of 1.41 and 1.37 m6A sites per gene mutation in GC and PCa tissues, respectively. In addition, we found that approximately 15.52% of genes were comethylated, but most of them were methylated separately in the GC and PCa tissues. In total, we identified 81 up-regulated and 62 down-regulated differentially methylated protein coding genes in GC, such as MTHFD1L, IGF2, SCD, BMP8B, TSPAN9, GC, ORM1, FGA, HS3ST4, GALNT1, MT1E, GIF, and CPEB2, suggesting that the epigenetic mechanism of mRNA may lead to the development of GC through m6A modifications.

Regarding the function and pathway of DMGs, we performed GO, KEGG enrichment analysis, and PPI construction for DMGs. The genes with increased m6A levels in their mRNAs are mainly enriched in transcriptional misregulation in the carcinogenesis pathway and are engaged in various transcription factor–binding functions. In accordance with previous observations, hypermethylation of transcription factors may give signal recognition and change the stability of the target transcripts related to carcinogenesis (Dominissini et al., 2012; Niu et al., 2013; Wang et al., 2014). The genes with fewer m6A modifications in their mRNAs mainly regulate ribosome, digestion and absorption of vitamin and protein, antigen processing, and presentation signal pathways; further, they are engaged in various molecular functions, such as RNA binding, aspartic-type endopeptidase, and peptidase activity. According to the PPI network produced by the identified DMGs, more interactions that were expected to be found were observed. These

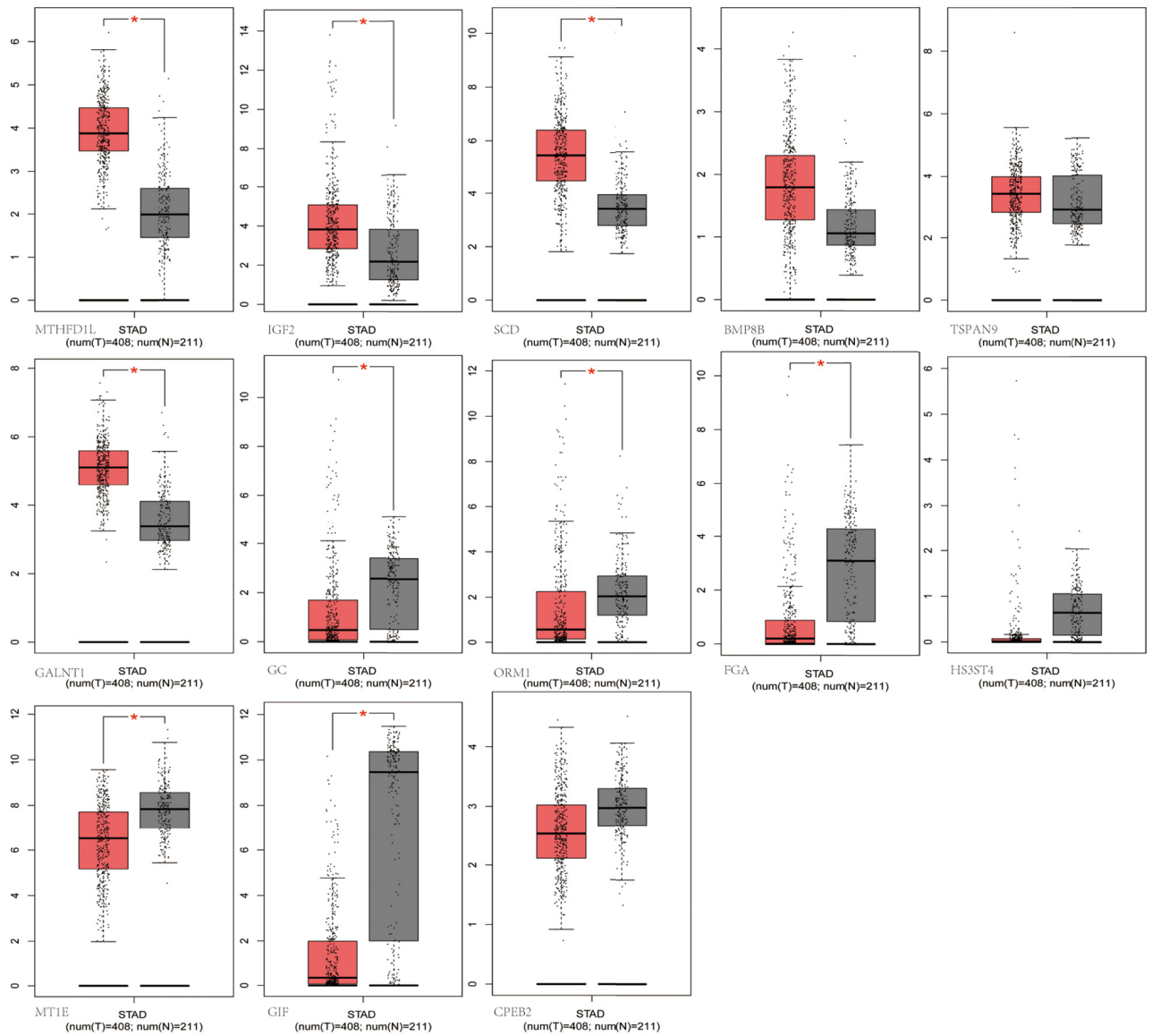

FIGURE 8 | Validation of the differentially m6A related expressed genes. MTHFD1L, IGF2, SCD, GC, ORM1, FGA, GALNT1, MT1E, and GIF had significant differences ($P < 0.05$).

findings indicated that m6A methylation affected metabolic processes that reflected the specific functions and activities of the cancerous progression in GC.

The significance of m6A in many biological processes has mainly been studied in relation to the regulation of expression of m6A-related genes (Liu and Pan, 2016; Zhao et al., 2020). For the first time, we performed a combination analysis among the m6A methylated genes and their expression. Further validation of the differential expressed genes by matching TCGA normal and GTEx data, we identified six genes with increased methylation (MTHFD1L, IGF2, SCD, GC, ORM1, and FGA) and three genes with decreased methylation (GALNT1, MT1E, and GIF), which may be key m6A-related genes that play a role in gastric carcinogenesis as indicated by their regulated expression levels. We further performed quantitative real-time PCR to profile mRNA expression levels. The results showed that MT1E, GC, FGA, GALNT1, ORM1, and GIF had statistical difference ($P < 0.05$), and IGF2, MTHFD1L, and SCD had no statistical difference ($P > 0.05$). Previous studies discovered that one of the main functions of m6A is to mediate mRNA degradation (Liu et al., 2014; Wang et al., 2014), suggesting that there may be a negative correlation between the degree of m6A methylation and the level of transcription. However, in our results, four genes revealed a negative relationship between m6A methylation and gene expression, whereas five genes showed a positive correlation. According to our pathway analysis, increased m6A levels are mainly enriched during transcriptional misregulation in carcinogenesis, while decreased m6A mainly functions with

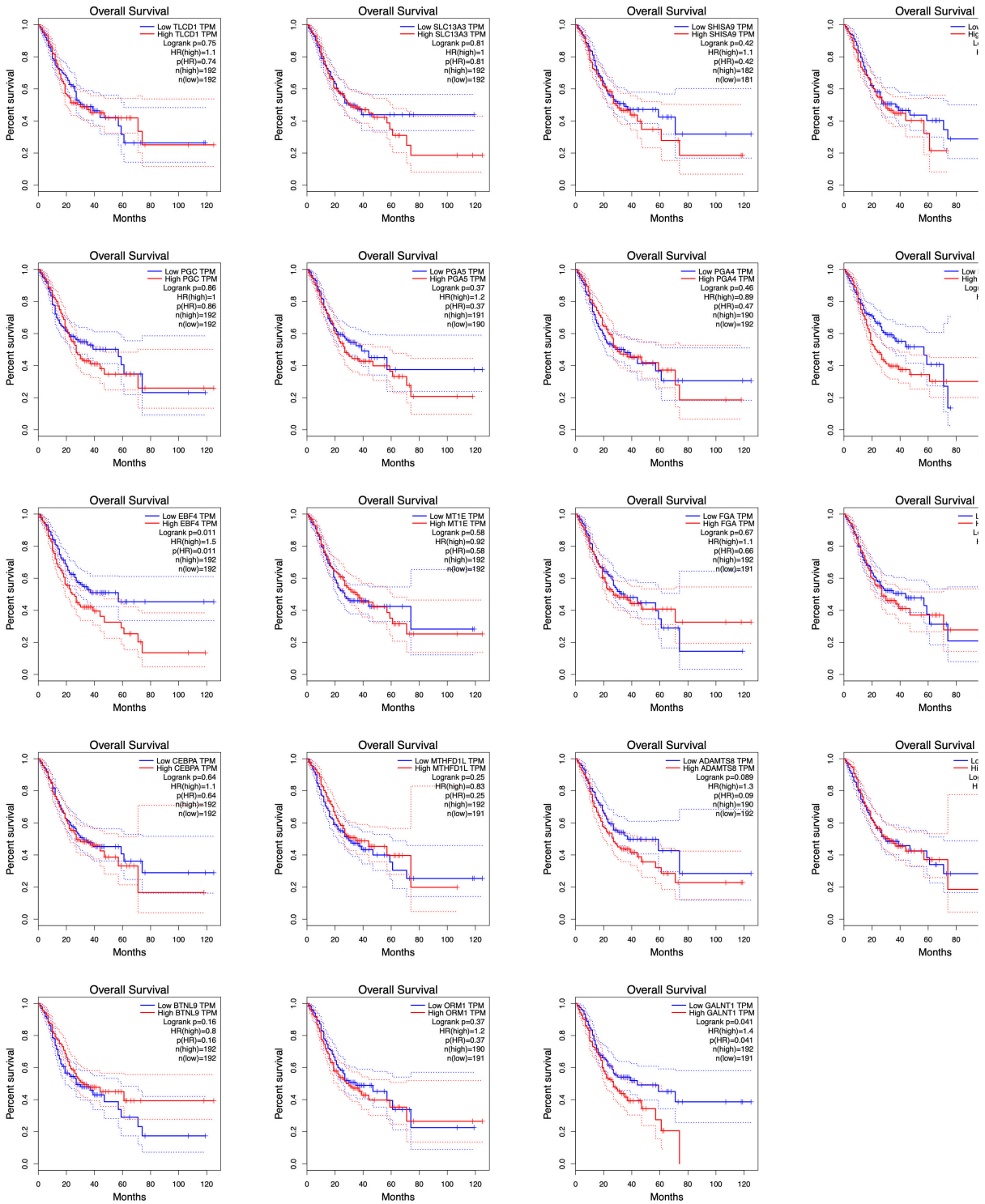

FIGURE 9 | Survival analyses of hub genes by TCGA data. GNLAT1, EBF4, F13A1, and NLGN1 expression levels were related to the overall survival ($P < 0.05$).

digestion and absorption of protein. We speculate that m6A is related to the degradation of some genes in GC patients and is more likely to promote their protein translation and transcription factor–binding functions. Although these findings may play a significant guiding role in the progression of GC caused by m6A modification-related special genes, it needs to be confirmed by further studies on the mechanism and functional regions of these key genes.

In this study, we analyzed the correlation between the expression of m6A modified genes and clinicopathological parameters and prognoses. We demonstrated the hub genes (IGF2, SCD, GALNT1, TLCD1, SHISA9, NLGN1, F13A1, ADAMTS8, GIF, PLD5, SLC13A3, ORM1, BTNL9, PGA5, and PGA4, and RPL5, FGA, and EBF4) were related to clinical and pathological indices, including gender, anatomical subdivisions, reflux history and Barrett esophagus, histological grade, pathological stages, and TNM stages. In addition, GNLAT1, EBF4, F13A1, and NLGN1 expression levels were related to the overall survival. High expression levels were consistently associated with worse overall survival for 5-year survival rate, and the relative risk of death in patients with high expression levels was 1.4 or 1.5 times higher than that in patients with low expression levels. Briefly, the m6A related differently expressed genes may have potential predictive and prognostic values and can be used as m6A methylation-based biomarkers for precise GC diagnoses and treatments. However, a long-term follow-up of a large sample of clinical data is needed for further verification.

In conclusion, we first comprehensively analyzed the different m6A features of mRNA methylation between GC and paired PCa tissues and their potential impact on the related mRNA expression. We confirmed that the consensus m6A motif sequence was GGACAR (R = U or A) C and that the m6A peaks at the end of the CDS were more pronounced than they were at the start. Through the analysis of differential m6A methylated and expressed genes, we confirmed that m6A may play a role mainly through transcriptional misregulation in carcinogenesis or digestion and absorption of protein pathway, which then affects the expression of specific genes related to GC progression. The key genes IGF2, SCD, GALNT1, TLCD1, SHISA9, NLGN1, F13A1, ADAMTS8, GIF, PLD5, SLC13A3, ORM1, BTNL9, PGA5, and PGA4 and RPL5, FGA, and EBF4 were related to clinicopathological parameters and prognoses, which may be used as novel m6A methylation-based molecular markers that can provide accurate targets for the diagnosis and treatment of GC.

DATA AVAILABILITY STATEMENT

MeRIP-seq data has been uploaded to SRA repository (PRJNA665272). Microarray data has been uploaded to GEO repository (GSE158662).

ETHICS STATEMENT

The studies involving human participants were reviewed and approved by the institutional ethics board of the First Hospital of China Medical University. The patients/participants provided their written informed consent to participate in this study.

AUTHOR CONTRIBUTIONS

YY contributed to study design and revising the manuscript. LS contributed to data interpretation and drafting manuscript. LPS and AW contributed to sample collection and data interpretation. HZ contributed to qPCR validation. All authors contributed to the article and approved the submitted version.

FUNDING

This study was supported by the National Key R&D Program of China (Grant #2018YFC1311600).

SUPPLEMENTARY MATERIAL

The Supplementary Material for this article can be found online at: https://www.frontiersin.org/articles/10.3389/fgene.2020.561566/full#supplementary-material

REFERENCES

Bansal, H., Yihua, Q., Iyer, S. P., Ganapathy, S., Proia, D. A., Penalva, L. O., et al. (2014). WTAP is a novel oncogenic protein in acute myeloid leukemia. *Leukemia* 28, 1171–1174. doi: 10.1038/leu.2014.16

Batista, P. J., Molinie, B., Wang, J., Qu, K., Zhang, J., Li, L., et al. (2014). m(6)A RNA modification controls cell fate transition in mammalian embryonic stem cells. *Cell Stem Cell* 15, 707–719. doi: 10.1016/j.stem.2014.09.019

Boccaletto, P., Machnicka, M. A., Purta, E., Piatkowski, P., Baginski, B., Wirecki, T. K., et al. (2018). MODOMICS: a database of RNA modification pathways. 2017 update. *Nucleic Acids Res.* 46, D303–D307. doi: 10.1093/nar/gkx1030

Chen, X. Y., Zhang, J., and Zhu, J. S. (2019). The role of m(6)A RNA methylation in human cancer. *Mol. Cancer* 18:103. doi: 10.1186/s12943-019-1033-z

Cui, Q., Shi, H., Ye, P., Li, L., Qu, Q., Sun, G., et al. (2017). m(6)A RNA methylation regulates the self-renewal and tumorigenesis of glioblastoma stem cells. *Cell Rep.* 18, 2622–2634. doi: 10.1016/j.celrep.2017.02.059

Dai, D., Wang, H., Zhu, L., Jin, H., and Wang, X. (2018). N6-methyladenosine links RNA metabolism to cancer progression. *Cell Death Dis.* 9:124. doi: 10.1038/s41419-017-0129-x

Dominissini, D., Moshitch-Moshkovitz, S., Schwartz, S., Salmon-Divon, M., Ungar, L., Osenberg, S., et al. (2012). Topology of the human and mouse m6A RNA methylomes revealed by m6A-seq. *Nature.* 485, 201–206. doi: 10.1038/nature11112

Du, J., Hou, K., Mi, S., Ji, H., Ma, S., Ba, Y., et al. (2020). Malignant evaluation and clinical prognostic values of m6A RNA methylation regulators in glioblastoma. *Front. Oncol.* 10:208. doi: 10.3389/fonc.2020.00208

Geng, Y., Guan, R., Hong, W., Huang, B., Liu, P., Guo, X., et al. (2020). Identification of m6A-related genes and m6A RNA methylation regulators in pancreatic cancer and their association with survival. *Ann. Transl. Med.* 8:387. doi: 10.21037/atm.2020.03.98

Harper, J. E., Miceli, S. M., Roberts, R. J., and Manley, J. L. (1990). Sequence specificity of the human mRNA N6-adenosine methylase in vitro. *Nucleic Acids Res.* 18, 5735–5741.

He, C. (2010). Grand challenge commentary: RNA epigenetics? *Nat. Chem. Biol.* 6, 863–865. doi: 10.1038/nchembio.482

Hu, B. B., Wang, X. Y., Gu, X. Y., Zou, C., Gao, Z. J., Zhang, H., et al. (2019). N(6)-methyladenosine (m(6)A) RNA modification in gastrointestinal tract cancers: roles, mechanisms, and applications. *Mol. Cancer* 18:178. doi: 10.1186/s12943-019-1099-7

Huang, H., Weng, H., and Chen, J. (2020). The biogenesis and precise control of RNA m(6)A methylation. *Trends Genet.* 36, 44–52. doi: 10.1016/j.tig.2019.10.011

Kwok, C. T., Marshall, A. D., Rasko, J. E., and Wong, J. J. (2017). Genetic alterations of m(6)A regulators predict poorer survival in acute myeloid leukemia. *J. Hematol. Oncol.* 10:39. doi: 10.1186/s13045-017-0410-6

Lan, Q., Liu, P. Y., Haase, J., Bell, J. L., Huttelmaier, S., and Liu, T. (2019). The critical role of RNA m(6)A methylation in cancer. *Cancer Res.* 79, 1285–1292. doi: 10.1158/0008-5472.CAN-18-2965

Li, Y., Wang, X., Li, C., Hu, S., Yu, J., and Song, S. (2014). Transcriptome-wide N(6)-methyladenosine profiling of rice callus and leaf reveals the presence of tissue-specific competitors involved in selective mRNA modification. *RNA Biol.* 11, 1180–1188. doi: 10.4161/rna.36281

Li, Y., Zheng, D., Wang, F., Xu, Y., Yu, H., and Zhang, H. (2019). Expression of demethylase genes, FTO and ALKBH1, is associated with prognosis of gastric cancer. *Dig. Dis. Sci.* 64, 1503–1513. doi: 10.1007/s10620-018-5452-2

Linder, B., Grozhik, A. V., Olarerin-George, A. O., Meydan, C., Mason, C. E., and Jaffrey, S. R. (2015). Single-nucleotide-resolution mapping of m6A and m6Am throughout the transcriptome. *Nat. Methods.* 12, 767–772. doi: 10.1038/nmeth.3453

Liu, J., Yue, Y., Han, D., Wang, X., Fu, Y., Zhang, L., et al. (2014). A METTL3-METTL14 complex mediates mammalian nuclear RNA N6-adenosine methylation. *Nat. Chem. Biol.* 10, 93–95. doi: 10.1038/nchembio.1432

Liu, N., and Pan, T. (2016). N6-methyladenosine-encoded epitranscriptomics. *Nat. Struct. Mol. Biol.* 23, 98–102. doi: 10.1038/nsmb.3162

Luo, G. Z., MacQueen, A., Zheng, G., Duan, H., Dore, L. C., Lu, Z., et al. (2014). Unique features of the m6A methylome in *Arabidopsis thaliana*. *Nat. Commun.* 5:5630. doi: 10.1038/ncomms6630

Ma, J. Z., Yang, F., Zhou, C. C., Liu, F., Yuan, J. H., Wang, F., et al. (2017). METTL14 suppresses the metastatic potential of hepatocellular carcinoma by modulating N(6) -methyladenosine-dependent primary MicroRNA processing. *Hepatology* 65, 529–543. doi: 10.1002/hep.28885

Machanick, P., and Bailey, T. L. (2011). MEME-ChIP: motif analysis of large DNA datasets. *Bioinformatics* 27, 1696–1697. doi: 10.1093/bioinformatics/btr189

Meyer, K. D., Saletore, Y., Zumbo, P., Elemento, O., Mason, C. E., and Jaffrey, S. R. (2012). Comprehensive analysis of mRNA methylation reveals enrichment in 3′. UTRs and near stop codons. *Cell* 149, 1635–1646. doi: 10.1016/j.cell.2012.05.003

Niu, Y., Zhao, X., Wu, Y. S., Li, M. M., Wang, X. J., and Yang, Y. G. (2013). N6-methyl-adenosine (m6A) in RNA: an old modification with a novel epigenetic function. *Genomics Proteomics Bioinformatics* 11, 8–17. doi: 10.1016/j.gpb.2012.12.002

Su, Y., Huang, J., and Hu, J. (2019). m(6)A RNA methylation regulators contribute to malignant progression and have clinical prognostic impact in gastric cancer. *Front. Oncol.* 9:1038. doi: 10.3389/fonc.2019.01038

Tao, X., Chen, J., Jiang, Y., Wei, Y., Chen, Y., Xu, H., et al. (2017). Transcriptome-wide N (6) -methyladenosine methylome profiling of porcine muscle and adipose tissues reveals a potential mechanism for transcriptional regulation and differential methylation pattern. *BMC Genomics* 18:336. doi: 10.1186/s12864-017-3719-1

Wang, J., Zhang, C., He, W., and Gou, X. (2020). Effect of m(6)A RNA methylation regulators on malignant progression and prognosis in renal clear cell carcinoma. *Front. Oncol.* 10:3. doi: 10.3389/fonc.2020.00003

Wang, X., Wu, R., Liu, Y., Zhao, Y., Bi, Z., Yao, Y., et al. (2020). m(6)A mRNA methylation controls autophagy and adipogenesis by targeting Atg5 and Atg7. *Autophagy* 16, 1221–1235. doi: 10.1080/15548627.2019.1659617

Wang, X., Li, Z., Kong, B., Song, C., Cong, J., Hou, J., et al. (2017). Reduced m(6)A mRNA methylation is correlated with the progression of human cervical cancer. *Oncotarget* 8, 98918–98930. doi: 10.18632/oncotarget.22041

Wang, X., Lu, Z., Gomez, A., Hon, G. C., Yue, Y., Han, D., et al. (2014). N6-methyladenosine-dependent regulation of messenger RNA stability. *Nature* 505, 117–120. doi: 10.1038/nature12730

Wei, C. M., Gershowitz, A., and Moss, B. (1975). Methylated nucleotides block 5' terminus of HeLa cell messenger RNA. *Cell* 4, 379–386.

Wei, C. M., and Moss, B. (1977). Nucleotide sequences at the N6-methyladenosine sites of HeLa cell messenger ribonucleic acid. *Biochemistry.* 16, 1672–1676.

Xu, D., Shao, W., Jiang, Y., Wang, X., Liu, Y., and Liu, X. (2017). FTO expression is associated with the occurrence of gastric cancer and prognosis. *Oncol. Rep.* 38, 2285–2292. doi: 10.3892/or.2017.5904

Yang, Y., Hsu, P. J., Chen, Y. S., and Yang, Y. G. (2018). Dynamic transcriptomic m(6)A decorationriters, erasers, readers and functions in RNA metabolism. *Cell Res.* 28, 616–624. doi: 10.1038/s41422-018-0040-8

Yue, B., Song, C., Yang, L., Cui, R., Cheng, X., Zhang, Z., et al. (2019). METTL3-mediated N6-methyladenosine modification is critical for epithelial-mesenchymal transition and metastasis of gastric cancer. *Mol. Cancer* 18:142. doi: 10.1186/s12943-019-1065-4

Zhang, C., Samanta, D., Lu, H., Bullen, J. W., Zhang, H., Chen, I., et al. (2016a). Hypoxia induces the breast cancer stem cell phenotype by HIF-dependent and ALKBH5-mediated m(6)A-demethylation of NANOG mRNA. *Proc. Natl. Acad. Sci. U.S.A.* 113, E2047–E2056. doi: 10.1073/pnas.1602883113

Zhang, C., Zhi, W. I., Lu, H., Samanta, D., Chen, I., Gabrielson, E., et al. (2016b). Hypoxia-inducible factors regulate pluripotency factor expression by ZNF217- and ALKBH5-mediated modulation of RNA methylation in breast cancer cells. *Oncotarget* 7, 64527–64542. doi: 10.18632/oncotarget.11743

Zhao, K., Yang, C. X., Li, P., Sun, W., and Kong, X. Q. (2020). Epigenetic role of N6-methyladenosine (m6A) RNA methylation in the cardiovascular system. *J. Zhejiang Univ. Sci. B* 21, 509–523. doi: 10.1631/jzus.B1900680

Conflict of Interest: The authors declare that the research was conducted in the absence of any commercial or financial relationships that could be construed as a potential conflict of interest.

frontiers in Oncology

REVIEW
published: 13 November 2020
doi: 10.3389/fonc.2020.580018

The Roles of Base Modifications in Kidney Cancer

Chunyue Feng[1,2], *Xiaoli Huang*[1,2], *Xuekun Li*[1,2,3]* *and Jianhua Mao*[1,2]*

[1] The Children's Hospital, Zhejiang University School of Medicine, Hangzhou, China, [2] National Clinical Research Center for Child Health, Hangzhou, China, [3] Institute of Translational Medicine of Zhejiang University School of Medicine, Hangzhou, China

Epigenetic modifications including histone modifications and DNA and RNA modifications are involved in multiple biological processes and human diseases. One disease, kidney cancer, includes a common type of tumor, accounts for about 2% of all cancers, and usually has poor prognosis. The molecular mechanisms and therapeutic strategy of kidney cancer are still under intensive study. Understanding the roles of epigenetic modifications and underlying mechanisms in kidney cancer is critical to its diagnosis and clinical therapy. Recently, the function of DNA and RNA modifications has been uncovered in kidney tumor. In the present review, we summarize recent findings about the roles of epigenetic modifications (particularly DNA and RNA modifications) in the incidence, progression, and metastasis of kidney cancer, especially the renal cell carcinomas.

Keywords: DNA methylation, DNA hydroxymethylation, RNA methylation, ten-eleven translocases, tumor

OPEN ACCESS

Edited by:
Xiang Shu,
Vanderbilt University Medical Center, United States

Reviewed by:
Alessandra Montecucco,
Italian National Research Council, Italy
Tanja Kunej,
University of Ljubljana, Slovenia

***Correspondence:**
Xuekun Li
xuekun_li@zju.edu.cn
Jianhua Mao
maojh88@zju.edu.cn

Specialty section:
This article was submitted to Cancer Genetics, a section of the journal Frontiers in Oncology

Received: *04 July 2020*
Accepted: *19 October 2020*
Published: *13 November 2020*

Citation:
Feng C, Huang X, Li X and Mao J (2020) The Roles of Base Modifications in Kidney Cancer. Front. Oncol. 10:580018. doi: 10.3389/fonc.2020.580018

INTRODUCTION

Kidney cancer presents about 2% of all cancers and is the seventh most common cancer worldwide with 295,000 new cases being diagnosed annually (1). The most prevalent solid tumor of the kidney in adults is renal cell carcinoma (RCC), which accounts for about 90% of adult kidney cancer (2–4). RCC is a heterogeneous malignant tumor with more than ten histological subtypes, although it mainly stems from renal tubular epithelial cells. In addition to the high prevalence of kidney cancer in adults, this disease can also be diagnosed in children, where the main form is Wilms tumor (5). Because of the high malignancy rate and the unclear mechanisms of kidney cancer, current treatments, which include surgery, chemotherapy and radiation, cannot significantly inhibit tumor progression. In the past few years, targeted therapy has been shown to prolong survival of patients, but the overall survival rate still remains very low (4).

Epigenetic modifications including histone modifications, DNA and RNA modifications, and non-coding RNAs regulate gene expression at transcriptional, translational and posttranslational levels and therefore are involved in human diseases (6). DNA methylation at the 5' position of cytosine (5-methylcytosine, 5mC) is an intensively studied type of epigenetic modification, and it plays a critical role in development and diseases (7). In addition, more than one hundred types of RNA modifications have been identified on mRNA, tRNA, etc. Among all RNA modifications, N^6-methyladenosine (m^6A) is the most common modification in eukaryotic mRNAs (8). RNA modification has been shown to play important roles in multiple biological processes and in diseases, as well as in DNA methylation (9). The dysfunction of epigenetic modifications leads to

global changes in genomic structure and thus affects the expression of genes involved in cancer progression (10, 11).

During the past decade the important roles of epigenetic modifications have been revealed in kidney cancer (especially in RCC). Epigenetic alterations have been suggested as promising biomarkers for RCC diagnosis and potential therapeutic targets (3, 4, 11–14). In this review we summarize the landscape of main epigenetic modifications with a focus on DNA methylation and RNA methylation. We then discuss the function and underlying mechanisms of aberrant DNA and RNA modifications in kidney cancer.

DNA Modifications and Kidney Cancer

Diverse Modifications of DNA

DNA methylation mainly occurs at the fifth carbon atom of cytosine (5mC) in mammalian DNA and is catalyzed by DNA methyltransferases (DNMTs), which use S-adenosyl methionine (SAM) as a methyl group donor. Currently, there are five members of the DNMT family, which includes DNMT1, DNMT3a, and DNMT3b. DNMT1 displays a preference for hemi-methylated DNA at the CpG islands during DNA replication, whereas DNMT3a and DNMT3b are *de novo* methyltransferases. DNA methylation exhibits dynamic features of expression during embryonic and postnatal development, and the dysregulation of DNA methylation has been shown to result in changes in gene expression (15). In general, hypomethylation activates or increases gene expression, whereas hypermethylation leads to gene silencing or decreased gene expression (**Figure 1**).

For quite some time, 5mC has been considered as a stable epigenetic marker of DNA that cannot be further modified. However, in 2009 researchers found that 5mC can be oxidized to 5-hydroxymethylcytosine (5hmC) under the catalysis of ten-eleven-translocation (TET) family proteins (16–18). The TET family proteins consist of three members, TET1, TET2, and TET3, which share common typical characteristics of 2-oxoglutarate (2OG)- and FeII(II)-dependent dioxygenases (2OGFeDO) (19–21). TET enzymes can further oxidize 5-hmC to 5-carboxylcytosine (5caC) and 5-formylcytosine (5fC) (22, 23). Thymine-DNA glycosylase (TDG) is in charge of recognition and excision of 5caC and 5fC in mammals (22, 23). Under the catalysis of activation-induced cytidine deaminase (AID), 5mC can be transformed to 5-hydroxymethyluracil (5hmU) with a deamination reaction. In addition, previous studies have demonstrated that IDH1/2 can catalyze isocitrate to α-KG and can participate in the regulation of TETs and 5hmC (24). However, mutant IDH1/2 has been found to catalyze isocitrate to 2-hydroxyglutarate (2-HG), which is a competitive inhibitor of α-KG. IDH1/2 also can inhibit the transformation of 5mC to 5hmC by TETs; therefore, it plays a pivotal role in the regulation of 5hmC (24).

Current findings indicate that 5-hmC modification not only serves as an intermediate product, but also plays a pivotal role in development, aging, and diseases. Tissue/cell-specific distribution features and the content of 5hmC have been observed among varied tissues and organs. 5hmC is the most abundant in neuronal cells compared to other types of cells. In addition, 5hmC is mainly enriched at gene bodies, promoters, and distal regulatory regions

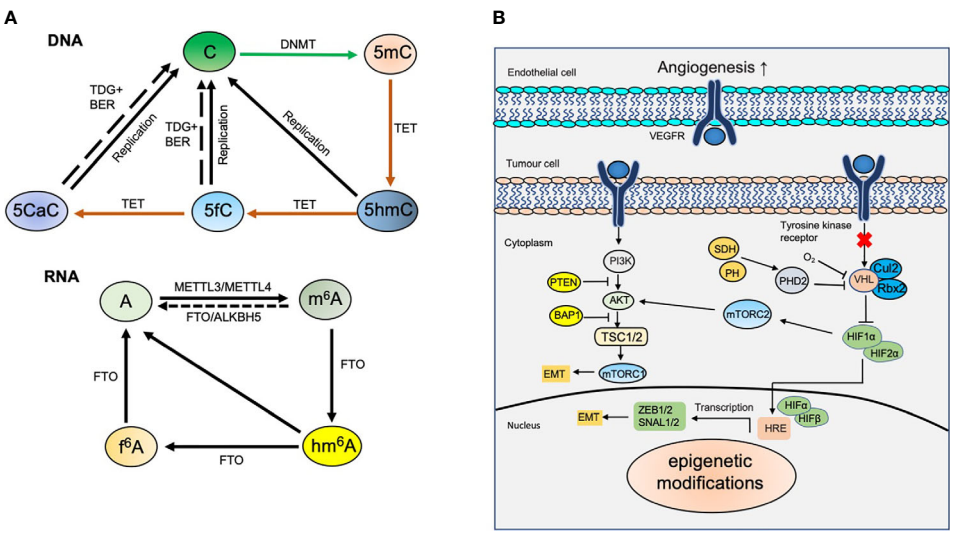

FIGURE 1 | Dynamic modifications in kidney cancer. **(A)** Dynamic DNA and RNA modifications. DNA methyltransferases (DNMTs) including *de novo* methyltransferases DNMT3A, DNMT3B and maintenance methyltransferase DNMT1 convert unmodified cytosine (C) to 5-methylcytosine (5mC). 5mC can be converted to 5-hydroxymethylcytosine (5hmC) by ten-eleven translocation (TET) proteins-mediated oxidation. TET proteins also catalyze the oxidation of 5hmC to 5-formylcytosine (5fC) and 5-carboxylcytosine (5caC). 5fC and 5caC can be further excised by thymine DNA glycosylase (TDG) coupled with base excision repair (BER) to generate unmodified cytosine. N^6-methyladenosine (m^6A) in mRNA is installed by methyltransferase-like protein 3 (METTL3) and METTL14, and erased by fat mass and obesity-associated protein (FTO) and α-ketoglutarate-dependent dioxygenase alkB homologue 5 (ALKBH5). m^6A can be further oxidized to N^6-hydroxymethyladenosine (hm^6A) and N^6-formyladenosine (f^6A) sequentially by FTO. **(B)** Epigenetic modifications involve in kidney cancer. Epigenetic modifications regulate diverse signaling pathways including HIF and PI3K-AKT and involve in kidney cancer.

of the genome. The enrichment of 5hmC at distinct genomic regions is correlated with gene expression, which can also be regulated by histone modifications (25). Abnormal distribution and/or level of 5hmC modification can induce disease. All of these findings suggest several important functions for dynamic DNA modifications.

The Function of DNA Methylation in Kidney Cancer

The aberrant level and distribution of DNA methylation have been revealed in various types of cancer including liver, colon, lung, and prostate cancer. These cancers are associated with the severity and metastatic potential of diseases (26). For example, DNA hypermethylation in cancer cells may be an alternative complementary mechanism, which triggers the silence of tumor-inhibiting genes and consequently results in tumorigenesis and metastasis (10, 27). In general, the global level of DNA methylation is decreased, while the acquisition of DNA methylation is observed at the promoter regions of some specific genes.

In studies of kidney cancer, Chen et al. applied the bisulfite sequencing method to map 5mC and found that the global level of 5mC is not changed (28). However, Mendoza-Pérez J et al. performed the analysis of 899 RCC cases and found that a low level of genomic DNA methylation (measured as 5mC%) in peripheral blood could significantly increase the risk of RCC (29). One possibility for these inconsistent results could be the ability of the methods used to distinguish DNA methylation and demethylation.

The Function of DNA Demethylation in Kidney Cancer

Mounting evidence has demonstrated that 5hmC plays an important function in a variety of tumors, such as acute myeloid leukemia, liver cancer, and melanoma (30, 31). Although the level of global 5mC is not altered, Chen et al. observed the decreased level of global 5hmC as well as the hypermethylation at gene body regions in kidney tumors (28). Their results also suggested that decreased 5hmC is correlated with the prognosis and survival. It has also been found that 5hmC is closely related with capsule invasion, vein invasion and clinical progress of RCC (32). RCC patients with high level of 5hmC show increased survival; therefore, 5hmC may serve as an independent prognostic and progression marker for RCC (32). Consistently, 5hmC hydroxymethylase TET1 can promote cell apoptosis and can inhibit cell proliferation and invasion, therefore inhibiting tumor growth in RCC (33). The inhibited expression of TET1 reduces 5hmC level at the promoter region of CCNY/CDK16 and consequently results in cell cycle arrest and inhibits self-renewal of renal cancer stem cells (34) (**Figure 1**).

The oxidation reaction of 5mC to 5hmC requires 2-ketoglutarate (2-KG) as co-substrates, which is generated by isocitrate dehydrogenase 1 (IDHs) during the tricarboxylic acid cycle (TCA). The down-regulated expression of IDH1 in kidney cancer contributes to the global loss of 5hmC in RCC (28). Consistently, ectopic expression of IDH1 and pharmacologically increasing intracellular 2-KG can restore the global levels of 5hmC, and consequently, can inhibit tumor growth (28, 35). IDH1 mutation leads to the increase of 2-hydroxyglutarate (2-HG), and the loss of 5hmC is partly mediated by the decrease 2-HG dehydrogenase (L2-HGDH), which has tumor inhibitory effects (36). The loss of L2HGDH is correlated with a worse prognosis, whereas the restoration of L2HGDH can increase 2-HG and can promote the accumulation of 5hmC in RCC cells (37). Ascorbic acid (AA), a cofactor for TET, can enhance the activities of TET enzymes and can restore the level of genomic 5hmC, thus reversing epigenetic aberrancy (38, 39). These findings suggest an interplay between DNA demethylation and metabolites that has an important role in kidney cancer (39, 40).

RNA METHYLATION AND KIDNEY CANCER

Diverse Modifications of RNA and Molecular Mechanism of m^6A Modification

To date, more than 110 types of RNA modifications have been identified, such as N^1-methyladenosine (m^1A), N^6-methyladenosine (m^6A), N^6-methyl-2′-O-methyladenosine (m^6A_m), 5-methylcytosine (m^5C), 5-hydroxymethylcytosine (hm^5C) in messenger RNA (mRNA), transfer RNA (tRNA), ribosomal RNA (rRNA), long non-coding RNAs (lncRNAs), etc (41). Among these modifications, m^6A is the most abundant internal chemical modification in eukaryotic mRNA. In mammals, 0.1%–0.4% of adenosines (~3–5 m^6A sites per mRNA) are modified by m^6A, accounting for nearly half of total methylated ribonucleotides (42). m^6A mainly enriches at the 3′ untranslated regions (3′UTRs), around the termination codons and the internal long exons (43).

m^6A modification is mediated by three key elements called "writers", "erasers", and "readers" (44, 45). m^6A modification is mainly catalyzed by the RNA methyltransferase complex (writers), including methyltransferase-like 3 and 4 (METTL3 and METTL14) and Wilms' tumor 1-associated protein (WTAP) (46). METTL3 is in charge of m^6A installation, while METTL14 participates in the interacting with target mRNA, and WTAP is responsible for the localization in the nuclear speckle (47). m^6A modifications can be removed by RNA demethylases (erasers), including alkB homolog 5 (ALKBH5) and fat mass and obesity-associated protein (FTO, alpha-ketoglutarate dependent dioxygenase) (48). Both ALKBH5 and FTO belong to the alpha-ketoglutarate dependent dioxygenase family, which catalyze m^6A demethylation in a Fe(II)-and alpha-ketoglutarate dependent manner. Similar to ALKBH5, alkB homolog 3 (ALKBH3) has been shown the demethylase activity for 1-methyladenine and 5-methylcytosine (49). m^6A readers include the YTH domain family (YTHDF), insulin-like growth factor 2 mRNA binding protein 2 (IGF2BP), and HNRNPA2B1 (50). YTHDF proteins act as m^6A readers, which can maintain the stability of m^6A transcripts (51, 52) (**Figure 1**).

The dynamic and reversible m^6A modification regulates various aspects of RNAs fate, such as nuclear exit, splicing, stability, efficiency of translation (41, 53); therefore, this modification has crucial roles in embryonic development, sex determination, neurogenesis, stress responses, and tumorigenesis in mammals (54, 55). Previous studies have shown that the

dysregulation of m^{6}A was induced, but was not limited to, the aberrant expression of its writers, erasers and readers. These result in profound outcomes in multiple biological processes, such as cell proliferation and fate determination, DNA damage response, embryogenesis, and heat shock responses, and therefore are involved in diseases (56–59). In addition, emerging evidence indicates that m^{6}A modification plays a significant role in tumorigenesis and progression of a variety of cancers including breast cancer, gastric cancer, and pancreatic cancer (49, 55, 60–62).

The Function of m^{6}A in Renal Cell Carcinoma

Although the function of m^{6}A has been shown in several types of tumors, the important roles of m^{6}A in RCC are still not completely known. Recent findings show that the level of global m^{6}A decreases in RCC compared with adjacent non-tumor tissues (63), suggesting that the expression of m^{6}A regulatory genes may be a biomarker for RCC. The protein level of m^{6}A eraser FTO displays a significant decrease in RCC compared with normal tissues (64). Lower levels of m^{6}A modification eraser FTO are usually associated with malignant prognosis whereas higher levels of FTO are associated with benign prognosis, suggesting that FTO may serve as a protective factor in RCC (65). Published findings about the role of ALKBH5 in RCC are controversial. Both increased and decreased expression of ALKBH5 in RCC have been reported (64, 66). In a retrospective study using TCGA database, Zhou et al. examined the alteration of m^{6}A regulatory genes in clear cell renal cell carcinoma (ccRCC) and found that these m^{6}A regulatory genes are significantly correlated with von Hippel-Lindau (*VHL*) and *TP53*, two key suppressors for RCC. This result suggests a relationship between m^{6}A regulatory genes and the pathologic stage (63); however, it still lacks solid evidence about the roles of m^{6}A writers METTL3 and METTL14 in RCC (**Figure 1**).

In human RCC tissues, mitochondrial enzyme methylenetetrahydrofolate dehydrogenase 2 (MTHFD2) is highly expressed, and the knockdown of *MTHFD2* inhibits cell migration and invasion (67). High level of *MTHFD2* is positively correlated with RCC grade, clinical stage, progression, and poor prognosis (68). Interestingly, *MTHFD2* knockdown leads to a decrease of global m^{6}A, and a hypomethylation of HIF-2α mRNA increases the translation of HIF-2α (67, 69), which in turn promotes the aerobic glycolysis (67). These findings establish a connection between m^{6}A modification and MTHFD2-mediated one-carbon metabolism in RCC.

CONCLUSIONS

During the past several decades, significant progress has been made in understanding the function of epigenetic modifications in kidney cancer. However, the detailed molecular mechanisms underlying the kidney cancer carcinogenesis are still not completely known, and it has been challenging to explore the accurate diagnosis and effective treatment of kidney cancer. First, the interactions between DNA modifications, RNA modifications, and histone modifications in regulating gene expression in kidney cancer need to be determined. How these interactions cooperate to regulate diverse signaling pathways involved in kidney cancer requires further clarification. Second, the precise map of DNA and RNA modifications should be established in kidney cancer with high-throughput sequencing technologies. The identification of therapeutic targets relies on the analysis of high-throughput sequencing data. The therapeutic implications of epigenetic hallmarks are to be expected in kidney cancer considering the successful application of these hallmarks in other types of cancers.

AUTHOR CONTRIBUTIONS

CF, XH, JM, and XL wrote the manuscript. All authors contributed to the article and approved the submitted version,

FUNDING

This work was supported in part by the Medicine & Health Technology Project of Zhejiang Province (2018RC007 to CF), Zhejiang Provincial Research Center for Cancer Intelligent Diagnosis and Molecular Technology (JBZX-202003 to JM) and the National Natural Science Foundation of China (grants 31571518, 31771395 to XL).

REFERENCES

1. Ferlay J, Soerjomataram I, Dikshit R, Eser S, Mathers C, Rebelo M, et al. Cancer incidence and mortality worldwide: sources, methods and major patterns in GLOBOCAN 2012. *Int J Cancer* (2015) 136:E359–86. doi: 10.1002/ijc.29210
2. Moch H. An overview of renal cell cancer: pathology and genetics. *Semin Cancer Biol* (2013) 23:3–9. doi: 10.1016/j.semcancer.2012.06.006
3. Joosten SC, Smits KM, Aarts MJ, Melotte V, Koch A, Tjan-Heijnen VC, et al. Epigenetics in renal cell cancer: mechanisms and clinical applications. *Nat Rev Urol* (2018) 15:430–51. doi: 10.1038/s41585-018-0023-z
4. Hsieh JJ, Purdue MP, Signoretti S, Swanton C, Albiges L, Schmidinger M, et al. Renal cell carcinoma. *Nat Rev Dis Primers* (2017) 3:17009. doi: 10.1038/nrdp.2017.9
5. Davidoff AM. Wilms' tumor. *Curr Opin Pediatr* (2009) 21:357–64. doi: 10.1097/MOP.0b013e32832b323a
6. Wanner N, Bechtel-Walz W. Epigenetics of kidney disease. *Cell Tissue Res* (2017) 369:75–92. doi: 10.1007/s00441-017-2588-x
7. Jones PA. Functions of DNA methylation: islands, start sites, gene bodies and beyond. *Nat Rev Genet* (2012) 13:484–92. doi: 10.1038/nrg3230
8. Shi H, Wei J, He C. Where, When, and How: Context-Dependent Functions of RNA Methylation Writers, Readers, and Erasers. *Mol Cell* (2019) 74:640–50. doi: 10.1016/j.molcel.2019.04.025
9. Deng X, Su R, Feng X, Wei M, Chen J. Role of N 6 -methyladenosine modification in cancer. *Curr Opin Genet Dev* (2018) 48:1–7. doi: 10.1016/j.gde.2017.10.005
10. Chi H-C, Tsai C-Y, Tsai M-M, Lin K-H. Impact of DNA and RNA Methylation on Radiobiology and Cancer Progression. *Int J Mol Sci* (2018) 19:555. doi: 10.3390/ijms19020555

11. de Cubas AA, Rathmell WK. Epigenetic modifiers: activities in renal cell carcinoma. *Nat Rev Urol* (2018) 15:599–614. doi: 10.1038/s41585-018-0052-7
12. Morris MR, Latif F. The epigenetic landscape of renal cancer. *Nat Rev Nephrol* (2017) 13:47–60. doi: 10.1038/nrneph.2016.168
13. Linehan WM, Ricketts CJ. The Cancer Genome Atlas of renal cell carcinoma: findings and clinical implications. *Nat Rev Urol* (2019) 16:539–52. doi: 10.1038/s41585-019-0211-5
14. Larkin J, Goh XY, Vetter M, Pickering L, Swanton C. Epigenetic regulation in RCC: opportunities for therapeutic intervention? *Nat Rev Urol* (2012) 9:147–55. doi: 10.1038/nrurol.2011.236
15. Dahl C, Gronbaek K, Guldberg P. Advances in DNA methylation: 5-hydroxymethylcytosine revisited. *Clin Chim Acta* (2011) 412:831–6. doi: 10.1016/j.cca.2011.02.013
16. Tahiliani M, Koh KP, Shen Y, Pastor WA, Bandukwala H, Brudno Y, et al. Conversion of 5-methylcytosine to 5-hydroxymethylcytosine in mammalian DNA by MLL partner TET1. *Science* (2009) 324:930–5. doi: 10.1126/science.1170116
17. Koh KP, Yabuuchi A, Rao S, Huang Y, Cunniff K, Nardone J, et al. Tet1 and Tet2 regulate 5-hydroxymethylcytosine production and cell lineage specification in mouse embryonic stem cells. *Cell Stem Cell* (2011) 8:200–13. doi: 10.1016/j.stem.2011.01.008
18. Ko M, An J, Rao A. DNA methylation and hydroxymethylation in hematologic differentiation and transformation. *Curr Opin Cell Biol* (2015) 37:91–101. doi: 10.1016/j.ceb.2015.10.009
19. Mohr F, Dohner K, Buske C, Rawat VP. TET genes: new players in DNA demethylation and important determinants for stemness. *Exp Hematol* (2011) 39:272–81. doi: 10.1016/j.exphem.2010.12.004
20. Aravind L, Koonin EV. The DNA-repair protein AlkB, EGL-9, and leprecan define new families of 2-oxoglutarate- and iron-dependent dioxygenases. *Genome Biol* (2001) 2:research0007.1. doi: 10.1186/gb-2001-2-3-research0007
21. Loenarz C, Schofield CJ. Oxygenase catalyzed 5-methylcytosine hydroxylation. *Chem Biol* (2009) 16:580–3. doi: 10.1016/j.chembiol.2009.06.002
22. He YF, Li BZ, Li Z, Liu P, Wang Y, Tang Q, et al. Tet-mediated formation of 5-carboxylcytosine and its excision by TDG in mammalian DNA. *Science* (2011) 333:1303–7. doi: 10.1126/science.1210944
23. Ito S, Shen L, Dai Q, Wu SC, Collins LB, Swenberg JA, et al. Tet Proteins Can Convert 5-Methylcytosine to 5-Formylcytosine and 5-Carboxylcytosine. *Science* (2011) 333:1300–3. doi: 10.1126/science.1210597
24. Wang J, Tang J, Lai M, Zhang H. 5-Hydroxymethylcytosine and disease. *Mutat Res Rev Mutat Res* (2014) 762:167–75. doi: 10.1016/j.mrrev.2014.09.003
25. Sun W, Zang L, Shu Q, Li X. From development to diseases: The role of 5hmC in brain. *Genomics* (2014) 104:347–51. doi: 10.1016/j.ygeno.2014.08.021
26. Robertson KD, Wolffe AP. DNA methylation in health and disease. *Nat Rev Genet* (2000) 1:11–9. doi: 10.1038/35049533
27. Jones PA, Baylin SB. The fundamental role of epigenetic events in cancer. *Nat Rev Genet* (2002) 3:415–28. doi: 10.1038/nrg816
28. Chen K, Zhang J, Guo Z, Ma Q, Xu Z, Zhou Y, et al. Loss of 5-hydroxymethylcytosine is linked to gene body hypermethylation in kidney cancer. *Cell Res* (2016) 26:103–18. doi: 10.1038/cr.2015.150
29. Mendoza-Perez J, Gu J, Herrera LA, Tannir NM, Matin SF, Karam JA, et al. Genomic DNA Hypomethylation and Risk of Renal Cell Carcinoma: A Case-Control Study. *Clin Cancer Res* (2016) 22:2074–82. doi: 10.1158/1078-0432.CCR-15-0977
30. Ficz G, Gribben JG. Loss of 5-hydroxymethylcytosine in cancer: cause or consequence? *Genomics* (2014) 104:352–7. doi: 10.1016/j.ygeno.2014.08.017
31. Thomson JP, Ottaviano R, Unterberger EB, Lempiainen H, Muller A, Terranova R, et al. Loss of Tet1-Associated 5-Hydroxymethylcytosine Is Concomitant with Aberrant Promoter Hypermethylation in Liver Cancer. *Cancer Res* (2016) 76:3097–108. doi: 10.1158/0008-5472.CAN-15-1910
32. Chen S, Zhou Q, Liu T, Zhang W, Zeng X-T, Guo Z. Prognostic value of downregulated 5-hydroxymethylcytosine expression in renal cell carcinoma: a 10 year follow-up retrospective study. *J Cancer* (2020) 11:1212–22. doi: 10.7150/jca.38283
33. Fan M, He X, Xu X. Restored expression levels of TET1 decrease the proliferation and migration of renal carcinoma cells. *Mol Med Rep* (2015) 12:4837–42. doi: 10.3892/mmr.2015.4058
34. Si Y, Liu J, Shen H, Zhang C, Wu Y, Huang Y, et al. Fisetin decreases TET1 activity and CCNY/CDK16 promoter 5hmC levels to inhibit the proliferation and invasion of renal cancer stem cell. *J Cell Mol Med* (2019) 23:1095–105. doi: 10.1111/jcmm.14010
35. Ge G, Peng D, Xu Z, Guan B, Xin Z, He Q, et al. Restoration of 5-hydroxymethylcytosine by ascorbate blocks kidney tumour growth. *EMBO Rep* (2018) 19:e45401. doi: 10.15252/embr.201745401
36. Xu W, Yang H, Liu Y, Yang Y, Wang P, Kim SH, et al. Oncometabolite 2-hydroxyglutarate is a competitive inhibitor of alpha-ketoglutarate-dependent dioxygenases. *Cancer Cell* (2011) 19:17–30. doi: 10.1016/j.ccr.2010.12.014
37. Shelar S, Shim EH, Brinkley GJ, Kundu A, Carobbio F, Poston T, et al. Biochemical and Epigenetic Insights into L-2-Hydroxyglutarate, a Potential Therapeutic Target in Renal Cancer. *Clin Cancer Res* (2018) 24:6433–46. doi: 10.1158/1078-0432.CCR-18-1727
38. Shenoy N, Bhagat TD, Cheville J, Lohse C, Bhattacharyya S, Tischer A, et al. Ascorbic acid-induced TET activation mitigates adverse hydroxymethylcytosine loss in renal cell carcinoma. *J Clin Invest* (2019) 130:1612–25. doi: 10.1172/JCI98747
39. Shenoy N. Epigenetic dysregulation by aberrant metabolism in renal cell carcinoma can be reversed with Ascorbic acid. *Mol Cell Oncol* (2019) 6:1595309. doi: 10.1080/23723556.2019.1595309
40. Shim EH, Livi CB, Rakheja D, Tan J, Benson D, Parekh V, et al. L-2-Hydroxyglutarate: An Epigenetic Modifier and Putative Oncometabolite in Renal Cancer. *Cancer Discov* (2014) 4:1290–8. doi: 10.1158/2159-8290.CD-13-0696
41. Li S, Mason CE. The pivotal regulatory landscape of RNA modifications. *Annu Rev Genomics Hum Genet* (2014) 15:127–50. doi: 10.1146/annurev-genom-090413-025405
42. Desrosiers R, Friderici K, Rottman F. Identification of methylated nucleosides in messenger RNA from Novikoff hepatoma cells. *Proc Natl Acad Sci U S A* (1974) 71:3971–5. doi: 10.1073/pnas.71.10.3971
43. Ke S, Alemu EA, Mertens C, Gantman EC, Fak JJ, Mele A, et al. A majority of m6A residues are in the last exons, allowing the potential for 3′ UTR regulation. *Genes Dev* (2015) 29:2037–53. doi: 10.1101/gad.269415.115
44. Heck AM, Wilusz CJ. Small changes, big implications: The impact of m(6)A RNA methylation on gene expression in pluripotency and development. *Biochim Biophys Acta Gene Regul Mech* (2019) 1862:194402. doi: 10.1016/j.bbagrm.2019.07.003
45. Zhao W, Qi X, Liu L, Ma S, Liu J, Wu J. Epigenetic Regulation of m(6)A Modifications in Human Cancer. *Mol Ther Nucleic Acids* (2020) 19:405–12. doi: 10.1016/j.omtn.2019.11.022
46. Lan Q, Liu PY, Haase J, Bell JL, Hüttelmaier S, Liu T. The Critical Role of RNA m6A Methylation in Cancer. *Cancer Res* (2019) 79:1285–92. doi: 10.1158/0008-5472.CAN-18-2965
47. Selberg S, Blokhina D, Aatonen M, Koivisto P, Siltanen A, Mervaala E, et al. Discovery of Small Molecules that Activate RNA Methylation through Cooperative Binding to the METTL3-14-WTAP Complex Active Site. *Cell Rep* (2019) 26:3762–71.e5. doi: 10.1016/j.celrep.2019.02.100
48. Song H, Feng X, Zhang H, Luo Y, Huang J, Lin M, et al. METTL3 and ALKBH5 oppositely regulate m(6)A modification of TFEB mRNA, which dictates the fate of hypoxia/reoxygenation-treated cardiomyocytes. *Autophagy* (2019) 15:1419–37. doi: 10.1080/15548627.2019.1586246
49. He L, Li J, Wang X, Ying Y, Xie H, Yan H, et al. The dual role of N6-methyladenosine modification of RNAs is involved in human cancers. *J Cell Mol Med* (2018) 22:4630–9. doi: 10.1111/jcmm.13804
50. Zhao W, Cui Y, Liu L, Ma X, Qi X, Wang Y, et al. METTL3 Facilitates Oral Squamous Cell Carcinoma Tumorigenesis by Enhancing c-Myc Stability via YTHDF1-Mediated m6A Modification. *Mol Ther - Nucleic Acids* (2020) 20:1–12. doi: 10.1016/j.omtn.2020.01.033
51. Hesser CR, Karijolich J, Dominissini D, He C, Glaunsinger BA. N6-methyladenosine modification and the YTHDF2 reader protein play cell type specific roles in lytic viral gene expression during Kaposi's sarcoma-associated herpesvirus infection. *PLoS Pathog* (2018) 14:e1006995. doi: 10.1371/journal.ppat.1006995
52. Berlivet S, Scutenaire J, Deragon JM, Bousquet-Antonelli C. Readers of the m(6)A epitranscriptomic code. *Biochim Biophys Acta Gene Regul Mech* (2019) 1862:329–42. doi: 10.1016/j.bbagrm.2018.12.008
53. Fu Y, Dominissini D, Rechavi G, He C. Gene expression regulation mediated through reversible m(6)A RNA methylation. *Nat Rev Genet* (2014) 15:293–306. doi: 10.1038/nrg3724

54. Niu Y, Zhao X, Wu Y-S, Li M-M, Wang X-J, Yang Y-G. N6-methyl-adenosine (m6A) in RNA: An Old Modification with A Novel Epigenetic Function. *Genomics Proteomics Bioinf* (2013) 11:8–17. doi: 10.1016/j.gpb.2012.12.002
55. Pan Y, Ma P, Liu Y, Li W, Shu Y. Multiple functions of m6A RNA methylation in cancer. *J Hematol Oncol* (2018) 11(1):48. doi: 10.1186/s13045-018-0590-8
56. Wang Y, Li Y, Toth JI, Petroski MD, Zhang Z, Zhao JC. N6-methyladenosine modification destabilizes developmental regulators in embryonic stem cells. *Nat Cell Biol* (2014) 16:191–8. doi: 10.1038/ncb2902
57. Chen T, Hao Y-J, Zhang Y, Li M-M, Wang M, Han W, et al. m6A RNA Methylation Is Regulated by MicroRNAs and Promotes Reprogramming to Pluripotency. *Cell Stem Cell* (2015) 16:289–301. doi: 10.1016/j.stem.2015.01.016
58. Zhou J, Wan J, Gao X, Zhang X, Jaffrey SR, Qian SB. Dynamic m(6)A mRNA methylation directs translational control of heat shock response. *Nature* (2015) 526:591–4. doi: 10.1038/nature15377
59. Xiang Y, Laurent B, Hsu CH, Nachtergaele S, Lu Z, Sheng W, et al. RNA m(6) A methylation regulates the ultraviolet-induced DNA damage response. *Nature* (2017) 543:573–6. doi: 10.1038/nature21671
60. Vu LP, Pickering BF, Cheng Y, Zaccara S, Nguyen D, Minuesa G, et al. The N6-methyladenosine (m6A)-forming enzyme METTL3 controls myeloid differentiation of normal hematopoietic and leukemia cells. *Nat Med* (2017) 23:1369–76. doi: 10.1038/nm.4416
61. Sun T, Wu R, Ming L. The role of m6A RNA methylation in cancer. *Biomed Pharmacother* (2019) 112:108613. doi: 10.1016/j.biopha.2019.108613
62. Wang S, Chai P, Jia R, Jia R. Novel insights on m(6)A RNA methylation in tumorigenesis: a double-edged sword. *Mol Cancer* (2018) 17:101. doi: 10.1186/s12943-018-0847-4
63. Zhou J, Wang J, Hong B, Ma K, Xie H, Li L, et al. Gene signatures and prognostic values of m6A regulators in clear cell renal cell carcinoma - a retrospective study using TCGA database. *Aging* (2019) 11:1633–47. doi: 10.18632/aging.101856
64. Strick A, von Hagen F, Gundert L, Klumper N, Tolkach Y, Schmidt D, et al. The N(6) -methyladenosine (m(6) A) erasers alkylation repair homologue 5 (ALKBH5) and fat mass and obesity-associated protein (FTO) are prognostic biomarkers in patients with clear cell renal carcinoma. *BJU Int* (2020) 125:617–24. doi: 10.1111/bju.15019
65. Wen L, Yu Y, Lv H, He Y, Yang B. FTO mRNA expression in the lower quartile is associated with bad prognosis in clear cell renal cell carcinoma based on TCGA data mining. *Ann Diagn Pathol* (2019) 38:1–5. doi: 10.1016/j.anndiagpath.2018.10.009
66. Zheng Z, Mao S, Guo Y, Zhang W, Liu J, Li C, et al. N6methyladenosine RNA methylation regulators participate in malignant progression and have prognostic value in clear cell renal cell carcinoma. *Oncol Rep* (2020) 43:1591–605. doi: 10.3892/or.2020.7524
67. Green NH, Galvan DL, Badal SS, Chang BH, LeBleu VS, Long J, et al. MTHFD2 links RNA methylation to metabolic reprogramming in renal cell carcinoma. *Oncogene* (2019) 38:6211–25. doi: 10.1038/s41388-019-0869-4
68. Lin H, Huang B, Wang H, Liu X, Hong Y, Qiu S, et al. MTHFD2 Overexpression Predicts Poor Prognosis in Renal Cell Carcinoma and is Associated with Cell Proliferation and Vimentin-Modulated Migration and Invasion. *Cell Physiol Biochem* (2018) 51:991–1000. doi: 10.1159/000495402
69. Martinez-Saez O, Gajate Borau P, Alonso-Gordoa T, Molina-Cerrillo J, Grande E. Targeting HIF-2 alpha in clear cell renal cell carcinoma: A promising therapeutic strategy. *Crit Rev Oncol Hematol* (2017) 111:117–23. doi: 10.1016/j.critrevonc.2017.01.013

Conflict of Interest: The authors declare that the research was conducted in the absence of any commercial or financial relationships that could be construed as a potential conflict of interest.

frontiers in Genetics

REVIEW
published: 16 November 2020
doi: 10.3389/fgene.2020.559138

FTO – A Common Genetic Basis for Obesity and Cancer

*Ning Lan[1,2,3], Ying Lu[1,2,3], Yigan Zhang[1,2,3], Shuangshuang Pu[1], Huaze Xi[4], Xin Nie[1], Jing Liu[5] and Wenzhen Yuan[1,2,3]**

[1] The First School of Clinical Medicine, Lanzhou University, Lanzhou, China, [2] The First Hospital of Lanzhou University, Lanzhou, China, [3] Key Laboratory for Resources Utilization Technology of Unconventional Water of Gansu Province, Gansu Membrane Science and Technology Research Institute Co., Ltd., Lanzhou, China, [4] The Second Hospital of Lanzhou University, Lanzhou, China, [5] Changjiang Scholar's Laboratory/Guangdong Provincial Key Laboratory for Diagnosis and Treatment of Breast Cancer, Shantou University Medical College, Shantou, China

In recent years, the prevalence of obesity and cancer have been rising. Since this poses a serious threat to human health, the relationship between the two has attracted much attention. This study examined whether fat mass and obesity-associated (*FTO*) genes are linked, taking into account a Genome-wide Association Study (GWAS) that revealed multiple single nucleotide polymorphism sites (SNPs) of the *FTO* gene, indicating an association between obesity and cancer in different populations. FTO proteins have been proved to participate in adipogenesis and tumorigenesis with post-transcriptional regulation of downstream molecular expression or through the target of the mammalian target protein rapamycin (mTOR). FTO inhibitors have also been found to share anti-obesity and anti-cancer effects *in vivo*. In this review, we comprehensively discuss the correlation between obesity and cancer by measuring *FTO* gene polymorphism, as well as the molecular mechanism involved in these diseases, emphasizing FTO as the common genetic basis of obesity and cancer.

Keywords: obesity, cancer, FTO, SNP, M^{6}A modification, mTOR, FTO inhibitors

OPEN ACCESS

Edited by:
Xiang Shu,
Vanderbilt University Medical Center, United States

Reviewed by:
Jie Tan,
Huazhong University of Science and Technology, China
Minghua Wang,
Soochow University Medical College, China

***Correspondence:**
Wenzhen Yuan
yuanwzh@lzu.edu.cn

Specialty section:
This article was submitted to Cancer Genetics, a section of the journal Frontiers in Genetics

Received: *05 May 2020*
Accepted: *02 September 2020*
Published: *16 November 2020*

Citation:
Lan N, Lu Y, Zhang Y, Pu S, Xi H, Nie X, Liu J and Yuan W (2020) FTO – A Common Genetic Basis for Obesity and Cancer. Front. Genet. 11:559138. doi: 10.3389/fgene.2020.559138

INTRODUCTION

The morbidity of obesity and cancer is increasing year by year in most countries around the world and represents a threat to human health (Ng et al., 2014; Siegel et al., 2018). Obesity causes changes in the body's physiological and hormonal environments that promote many diseases, including diabetes and cardiovascular diseases. Obesity has been proven to increase the risks of at least 13 different types of cancers, such as esophageal adenocarcinoma, colon cancer, endometrial cancer, postmenopausal breast cancer, kidney cancer, and hematopoietic cancers (Calle and Kaaks, 2004; Goodwin and Stambolic, 2015). Of all Americans diagnosed with cancer in 2014, the overweight and obese population account for 40% (Steele et al., 2017). Furthermore, another prospective study of large samples of Americans confirmed that 14% of cancer deaths in males and 20% of females are due to them being overweight or having obesity (Calle et al., 2003). The biological mechanism of obesity and cancer are complex, including obesity-related hormones, growth factors, multiple signaling pathways, and chronic inflammation (Chen, 2011; Vucenik and Stains, 2012). In recent years, *FTO* SNPs have been firmly associated with increased body mass index (BMI) and higher risks of various types of cancers in people of multiple races, and the role of *FTO* SNPs in the development of obesity and cancer has been gradually revealed (Loos and Yeo, 2014; Hernández-Caballero and Sierra-Ramírez, 2015; Deng et al., 2018a; Chen and Du, 2019). This review details this role and the molecular mechanisms of *FTO* in obesity and cancer, as well as its potential clinical applications as a therapeutic target.

FTO GENE AND FUNCTIONS

In 1999, *FTO* was first cloned by exon trapping analysis in Fused toes (Ft) mutation mice (Peters et al., 1999). Initially, *FTO* was expected to be associated with programmed cell death because scientists observed that heterozygous mice with Ft mutation developed syndactyly in the forelimb part and thymus hyperplasia (Van Der Hoeven et al., 1994). In 2007, the GWAS study identified *FTO* as an obesity sensitivity gene, and multiple SNPs in the intron 1 region were strongly associated with BMI, body fat rate, waist circumference, hip circumference, and energy intake (Dina et al., 2007; Frayling et al., 2007; Scuteri et al., 2007). As a result, the gene was named as the fat mass and obesity-associated (*FTO*) gene and has received extensive attention.

According to current genomics research, the *FTO* gene only exists in vertebrates and a few kinds of marine algae with highly conserved nucleotide and amino acid sequences (Robbens et al., 2008). The human *FTO* gene is located on chromosome 16q12.2, encoding a 2-oxoglutarate (2-OG) Fe(II)-dependent AlkB family dioxygenase, with a total length of 410.50 kb including 9 exons and 8 introns. About 3.4 kb upstream of *FTO* gene was Merkel's diverticulum syndrome-associated gene (*RPGRIP1L*), and its downstream was close to Iroquois gene family (including *IRX3*, *IRX5*, *IRX6*) (**Supplementary Figure**). *FTO* is extensively expressed in adipose tissues and the skeletal muscles of human tissues, with the highest expression in the hypothalamus in the region that controls energy balance, namely the arcuate nucleus, which indicates that it may play a critical role in regulating appetite and energy metabolism (Frayling et al., 2007).

In 2007, Thomas et al. revealed that the *FTO* gene encodes Fe(II)/2-OG dependent demethylase, which is the ninth AlkB family protein found in mammals (also called ALKBH9) (Gerken et al., 2007). They also used purified FTO protein from recombinant mice or humans that can catalyze the demethylation of 3-methylthymine(3-meT) and 3-methyluracil (3-meU) with the help of Fe(II)/2-OG (Gerken et al., 2007; Jia et al., 2008). Later, He et al. found that N^6-methyladenosine (m^6A) in nuclear RNA was a main substrate of the FTO (Jia et al., 2011). Therefore, the FTO was identified as the first RNA demethylase, thus initiating a wave of research on epigenetic modifications of RNA. Since then, the complex and diverse functions of FTO proteins have been gradually revealed. FTO can bind to multiple types of RNAs, including mRNA, snRNA, and tRNA, and can demethylate m^6A and N^6,2′-O-dimethyladenosine (m^6Am) in mRNA, m^6A in U6RNA, m^6Am in snRNAs, and N^1-methyladenosine (m^1A) in tRNA (Wei J. et al., 2018; **Figure 1A**). However, m^6A is the most favorable nucleobase substrate of FTO (Zhang X. et al., 2019).

M^6A, methylation modification on the sixth nitrogen atom of adenine (Wei et al., 1975) is the most common mRNA methylation enriched in the 3′-untranslated region (3′-UTRs), between the stop codon and the start codon (Roundtree et al., 2017). M^6A modifications were subjected to reversible and dynamic regulations including writers (METTL3, METTL14, and WTAP), erasers (FTO and ALKBH5), and readers (YTH domain family and IGF2BPs) (Aik et al., 2014; Liu et al., 2014; Ping et al., 2014; Schwartz et al., 2014; Wang et al., 2014, 2015, 2016; Huang et al., 2018; Liao et al., 2018; **Figure 1B**). Based on this extensive existence and dynamic regulation, m^6A plays an important role in post-transcriptional regulatory processes such as RNA splicing, nuclear production, degradation, and translation (Fustin et al., 2013; Wang et al., 2014, 2015; Bartosovic et al., 2017; Huang et al., 2018).

ASSOCIATION OF *FTO* SNPS WITH OBESITY OR CANCER

Since *FTO* has been identified as the first obesity-related gene. By conducting GWAS analysis, researchers have found that *FTO* SNPs are associated with obesity and higher risks of various cancers in multiracial populations (**Supplementary Figure**).

Association of *FTO* SNPs With Obesity

The connection between *FTO* SNPs and BMI was first found in European people with diabetes. The classic BMI-related *FTO* SNPs were rs9939609 (T/A), and compared with those who did not carry the risk allele, 16% of adults who carried the homozygous risk allele gained nearly 3 kg in weight, and the risk of obesity increased by 1.67 times (Frayling et al., 2007). Serial GWAS studies on obesity-related traits in people of European descent have confirmed the important role of the *FTO* locus, and many other *FTO* SNPs in the intron 1 region have been reported, such as rs9930506, rs1421085, rs8050136, rs1121980, and so forth (Dina et al., 2007; Scuteri et al., 2007; Haupt et al., 2008; Cauchi et al., 2009). The obesity-associated *FTO* SNPs in East Asian populations are comparable to that of people of European descent. The risk allele A of *FTO* SNP rs9939609 was closely related to obesity and BMI in Chinese, ethnic Chinese, Malaysian, Singaporean, East, and South Asian people (Chang et al., 2008; Tan et al., 2008; Li et al., 2012). A large-scale meta-analysis targeting GWAS analysis of East Asian populations found that *FTO* SNPs rs17817449 have the most significant correlation with BMI in people of Chinese descent (Wen et al., 2012). In recent years, global studies have associated the rs9939609 variant with higher obesity risks in other populations (including Brazilian people, early adolescence in China, and adults in Shiraz, Iran) (Fonseca et al., 2019; Jiang et al., 2019; Mehrdad et al., 2020b). It is also associated with increased BMI and waist circumference (in Brazilian youths) (Reuter et al., 2016), adipose tissue distribution (in Italian people), and increased metabolic syndrome susceptibility (in Chinese populations) (Merra et al., 2020; Wang et al., 2020). In terms of the potential mechanisms between mutations in *FTO* and increased risks of obesity, studies have proven the role of *FTO* in the influence of food intake. People carrying *FTO* risk alleles and are inclined to higher energy intake foods like fat or proteins, reduced satiety, resulting in overeating, and many even lose control when eating (Cecil et al., 2008; Sonestedt et al., 2009; Tanofsky-Kraff et al., 2009; Ahmad et al., 2011). Another large-scale meta-analysis showed that the homozygous *FTO* risk allele was associated with a 27% lower risk of obesity in physically active adults (Kilpeläinen et al., 2011).

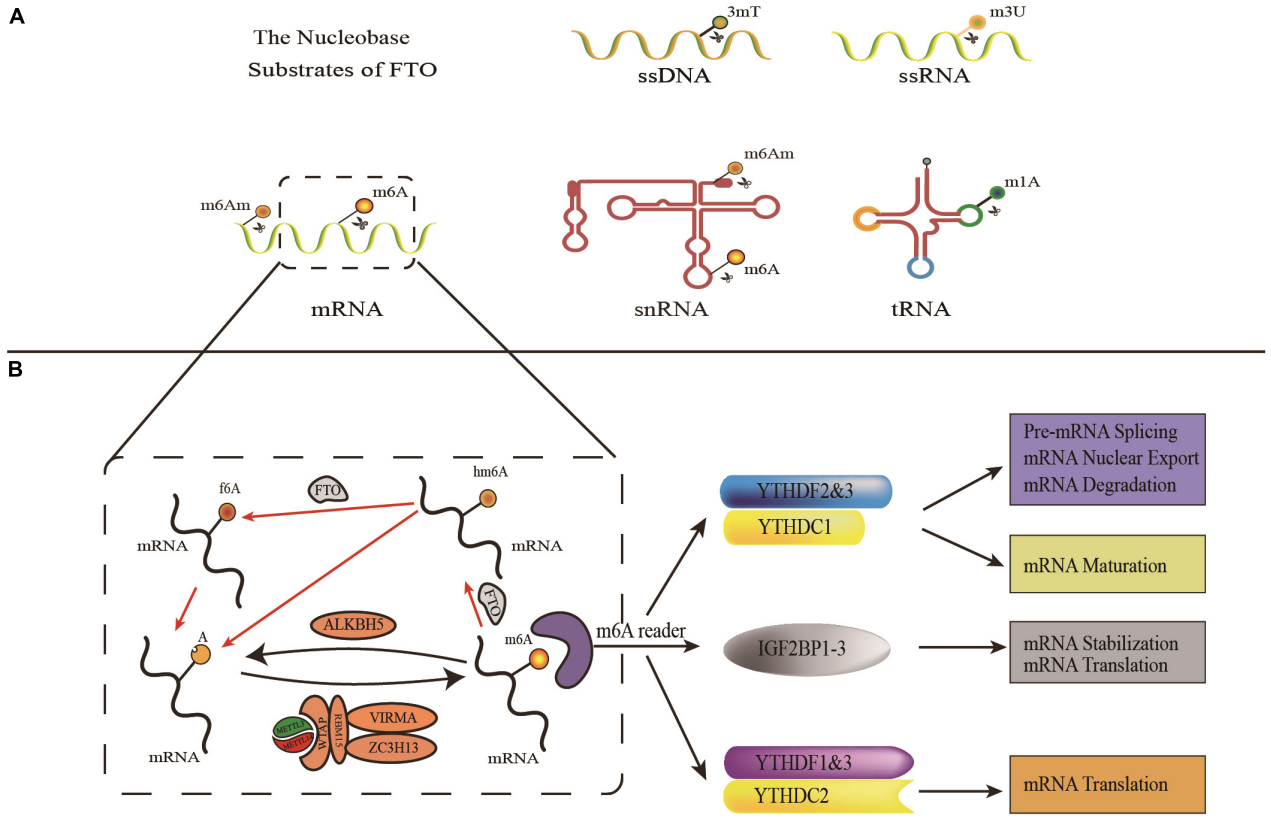

FIGURE 1 | The demethylases activity of FTO. **(A)** The nucleobase substrates of FTO. **(B)** m^6A modification is induced by METTL3, METTL14, and their cofactors(writers), reversed by FTO and ALKBH5 (erasers), and functionally facilitated by m^6A binding proteins including YTHDF1-3, YTHDC1-2, and IGF2BP1-3(readers).

Association of *FTO* SNPs With Cancer

To date, it has been studied that variants of *FTO* rs9939609, rs8050136, rs1477196, rs6499640, rs1121980, rs17817449, rs11075995, rs8047395, and rs7206790 have an association with a higher risk of cancers (Hernández-Caballero and Sierra-Ramírez, 2015). The most typical *FTO* SNP rs9939609 was associated with lung cancer, renal cancer, breast cancer, prostate cancer, pancreatic cancer, endometrial cancer (Delahanty et al., 2011; Kaklamani et al., 2011; Lin et al., 2013; Huang et al., 2017). Multiple SNPs in the intron 1 region of the *FTO* (including rs9939609, rs1477196, rs7206790, rs8047395) have been correlated with the risk of breast cancer, with rs1477196 strongly associated (Kaklamani et al., 2011). Interestingly, Da et al. observed that the interaction of *FTO* and *MC4R* polymorphisms showed a strong association with breast cancer: there was a 4.59-fold increased risks for women who have the allele combination C/T/C (*FTO* rs1121980/*FTO* rs9939609/*MC4R* rs17782313) (Da Cunha et al., 2013). In addition, in 2013, Iles et al. found an association between *FTO* rs16953002 and rs12596638 and melanoma susceptibility. However, these two SNPs are located in intron 8 of the *FTO* gene rather than intron 1 (the BMI-related region). This suggests that the association between the *FTO* variant and a wide range of diseases may play a role beyond BMI (Iles et al., 2013).

FTO IS INVOLVED IN THE PATHOGENESIS OF OBESITY AND CANCER

FTO, as the RNA m^6A Demethylase, Is Involved in the Development of Obesity and Cancer

FTO proteins are widely involved in both adipogenesis and tumorigenesis by m^6A-dependent demethylase activity which influences several mRNA processing events (**Table 1**).

FTO, as the RNA m^6A Demethylase, Is Involved in the Development of Obesity

FTO proteins are involved in the development of obesity by affecting the m^6A level of hormones related to eating or molecules related to adipogenesis (**Figure 2A**). In 2013, Efthimia et al. found that FTO over-expression limited the m^6A modification of ghrelin mRNA in cell models and increased ghrelin mRNA and peptide levels concomitantly. This article provided insights into how FTO predisposes to stimulated energy intake and obesity in humans (Karra et al., 2013). Simultaneously, substantial evidence has proved that FTO participates in the process of adipogenesis (Ben-Haim et al., 2015). Zhao et al.

TABLE 1 | FTO proteins are widely involved in both adipogenesis and tumorigenesis by m^6A-dependent demethylase activity.

Disease	FTO biological function	Target RNA	References
Obesity	FTO overexpression increased energy intake through reduce ghrelin mRNA m^6A.	Ghrelin	Karra et al., 2013
Obesity	FTO regulates pre-adipocyte differentiation by regulating m^6A levels around splice sites to control the splicing of the exon of adipogenic regulatory factor RUNX1T1.	SRSF2	Zhao et al., 2014
Obesity	FTO regulated adipogenesis by regulating cell cycle protein by m^6A-YTHDF2 dependent pathway.	CCNA2, CDK2	Wu et al., 2018a,b
Acute myeloid leukemia (AML)	FTO enhanced leukemic cell transformation and leukemogenesis and limited all-*trans*-retinoic acid (ATRA)-induced AML cell differentiation.	ASB2, RARA	Li et al., 2017
Glioblastoma	FTO induced Glioblastoma Stem Cells (GSC)growth, self-renewal, tumor progression, and prolonged mouse lifespan by regulating m^6A of cancer-associated genes.	ADAM19, EPHA3, KLF4, CDKN2A, BRCA2, TP53I11	Cui et al., 2017
Breast cancer	FTO promoted breast cancer cells malignant phenotypes such as proliferation, colony formation, and metastasis.	BNIP3	Niu et al., 2019
Gastric cancer (GC)	FTO knockdown increased m^6A level promoting GC cell proliferation and invasion by activating Wnt and PI3K-Akt signaling.	Wnt/PI3K-Akt pathway	Zhang C. et al., 2019
Lung squamous cell carcinoma (LUSC)	FTO effectively promoted cell proliferation and invasiveness and inhibited cell apoptosis of lung squamous cells.	MZF1	Liu et al., 2018
Non-small cell lung cancer (NSCLC)	FTO promoted the proliferation, colony formation ability of lung cancer cells *in vitro*, and promoted lung cancer cell growth *in vivo*.	USP7	Li et al., 2019a
Hepatocellular carcinoma (HCC)	Knockdown of FTO suppressed the proliferation and *in vivo* tumor growth, and induced the G0/G1 phase arrest.	PKM2	Li et al., 2019b
Cervical squamous cell carcinoma (CSCC)	FTO increased β-catenin mRNA expression, increased DNA repair activity, and induced resistance to chemoradiotherapy.	β-catenin	Zhou et al., 2018
Leukemia	The demethylation mediated by FTO promoted the stability of proliferation-related genes.	MERTK, BCL-2	Yan et al., 2018
Melanoma	FTO accelerated melanoma tumorigenesis and anti-PD-1 resistance by regulating the expression of critical cell-intrinsic genes in an m^6A-YTHDF2 dependent manner.	PD-1 (PDCD1), CXCR4, SOX10	Yang et al., 2019

found that FTO regulates the exonic splicing of the adipogenic regulator RUNX1T1 by influencing the level of m^6A around the splice site, thereby modulating cell differentiation (Zhao et al., 2014). Moreover, FTO affects adipogenesis by regulating the process of mitotic clonal expansion (MCE), which is a prerequisite for adipocyte differentiation that occurs within 48 h of adipogenic stimulation (Merkestein et al., 2015). The overexpression of FTO can induce MCE and regulate the differentiation of preadipocytes by influencing the expression of m^6A-dependent transcription factors (Tang et al., 2003; Merkestein et al., 2015; Zhang et al., 2015). Furthermore, Wu et al. found that FTO regulated adipogenesis by dominating cell cycle proteins such as CCNA2 and CDK2 by m^6A-YTHDF2 dependent pathway, revealing a new mechanism about anti-obesity and anti-adipogenesis activity of Epigallocatechin gallate (EGCG) (Wu et al., 2018a,b).

FTO, as the RNA m^6A Demethylase, Regulates the Malignant Phenotype and Therapeutic Response of Cancer Cells

FTO is highly expressed in many cancer tissues, which plays the role of an oncogene in an m^6A-dependent way and participates in the regulation of the malignant phenotype of cancer cells (**Figure 2A**). In 2017, Li et al. found that FTO enhanced leukemia oncogene-mediated cell transformation and leukemogenesis and inhibited all-*trans*-retinoic acid (ATRA)-induced AML cell differentiation by affecting the expression of targets mRNAs such as ASB2 and RARA, through reducing the level of m^6A (Li et al., 2017). Moreover, the elevated level of m^6A was found to promote the growth, self-renewal, and tumorigenesis of Glioblastoma Stem Cells (GSC) as well as prolong the lifespan of GSC-grafted mice (Cui et al., 2017). In 2018, Niu et al. showed that FTO can promote breast cancer cell malignant phenotype through epigenetically demethylated m^6A in BNIP3 mRNA 3′UTR (Niu et al., 2019). Similarly, the overexpression level of FTO was also found in gastric cancer, advanced non-small cell lung cancer, and hepatocellular carcinoma, which can regulate cell proliferation and/or migration/invasion through targeting demethylation for the m^6A of Wnt/PI3K-Akt, USP7, MZF1, or PKM2, respectively (Liu et al., 2018; Li et al., 2019a,b; Zhang C. et al., 2019).

FTO may also have an impact on the therapeutic response of cancer (**Figure 2A**). In 2018, Zhou et al. found that FTO enhanced the chemo-radiotherapy resistance of cervical squamous cell carcinoma both *in vitro* and *in vivo* through influencing the expression of ß-catenin by reducing m^6A levels (Zhou et al., 2018). The overexpression of FTO in leukemia cells can promote its expression by catalyzing the demethylation of cell proliferation-related genes such as m^6A of MERTL and BCL-2 mRNA and affecting the generation of resistance phenotypes in the treatment with tyrosine kinase inhibitors (TKI) (Yan et al., 2018). Recently, He et al. found that the down-regulation of FTO

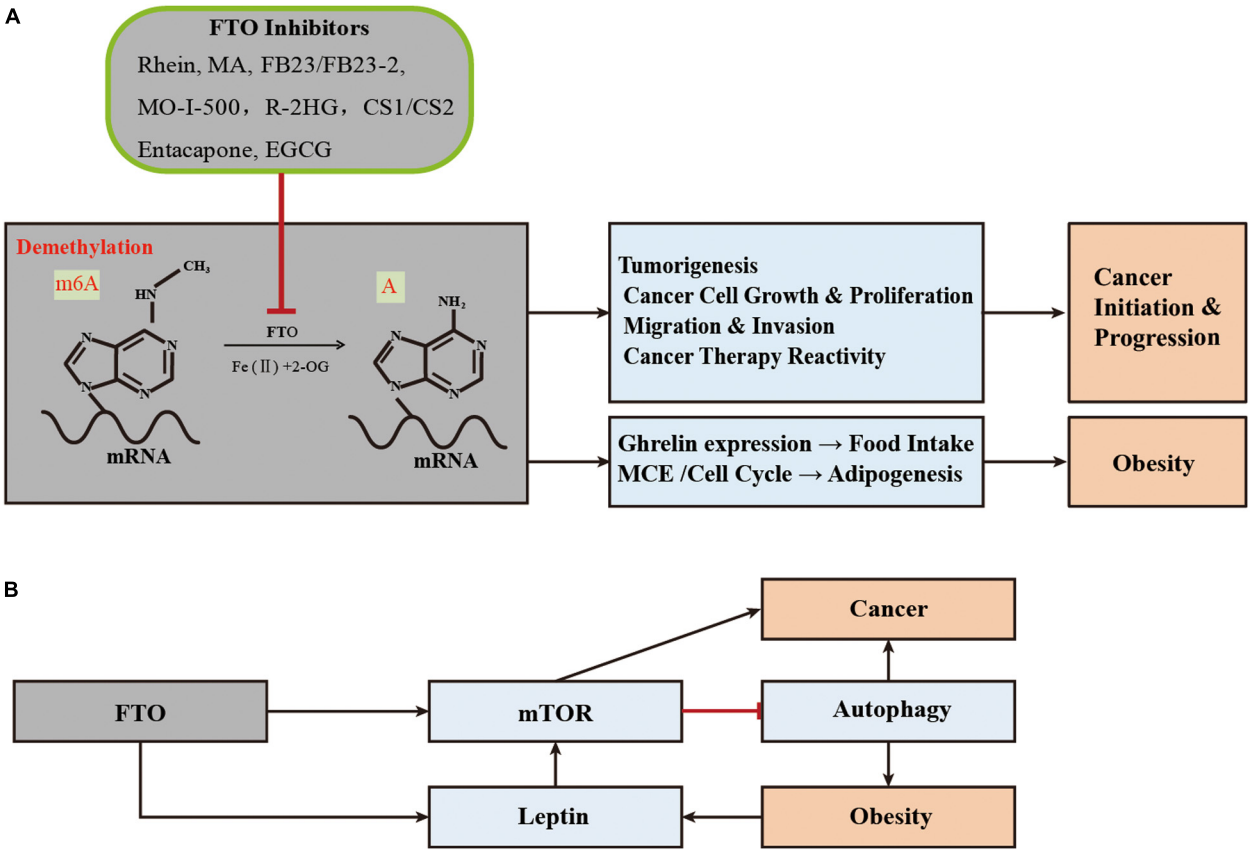

FIGURE 2 | Schematic illustration of the roles of FTO in obesity and tumorigenesis/drug response. **(A)** As the m^{6}A demethylase, FTO post-transcriptionally regulates expression of its critical target genes and thereby contributes to obesity (through affecting adipogenesis and food intake) and cancers (including tumorigenesis, cancer cell growth, migration, and drug response). MA, meclofenamic acid; R-2HG, 2-hydroxyglutarate; EGCG, Epigallocatechin gallate; **(B)** FTO regulates the development and progression of obesity and cancer through the mTOR or adipofactor-mTOR pathway.

made melanoma cells sensitive to interferon-gamma (IFN-γ) and anti-PD-1. FTO played a crucial role by promoting melanoma tumorigenesis and anti-PD-1 resistance (Yang et al., 2019).

FTO-mTOR Axis Affects Obesity and Cancer

The mammalian target protein rapamycin (mTOR) is an atypical serine/threonine kinase, which is the core component of regulating mRNA translation and can promote cell growth according to environmental signals (Laplante and David, 2012). mTOR binds to a variety of chaperone proteins to form two different kinase complexes, i.e., mTOR complex 1 (mTORC1) and mTORC2.

In 2013, *in vivo* experiments demonstrated that FTO played a role in the coupling of amino acid level and mTORC1 signaling pathway. FTO deficient cells showed reduced activation of the mTORC1 pathway, decreased mRNA translation rate, and increased autophagy (Cheung et al., 2013; Gulati et al., 2013). mTORC1 is a negative regulator of autophagy, which is a major cellular digestion process. In response to nutrition and environmental stress, autophagy plays a critical role in the occurrence and progression of obesity and cancer (White and Dipaola, 2009; Kim and Guan, 2015; Zhang Y. et al., 2018). Furthermore, mTOR activates the Warburg effect by inducing PKM2 and other glycolytic enzymes under normoxic conditions (Sun et al., 2011). In summary, mTORC1 can regulate the development of obesity and cancer through autophagy or direct activation of downstream signaling pathways (Laplante and David, 2012).

Mutations in the *FTO* gene raise blood levels of leptin, a known mediator or growth factor between obesity and colon cancer, which activates a variety of pathways associated with colon cancer (Drew, 2012; Mehrdad et al., 2020a). In addition, leptin has been suggested as an intermediate link between obesity and breast or prostate cancer (Stattin et al., 2001; Barone et al., 2020). Intriguingly, mTOR is also one of the signal mediators of obesity related factors, such as leptin, adiponectin, and inflammatory cytokines, through the Akt/PI3K or AMPK pathways (Maya-Monteiro and Bozza, 2008; Wang et al., 2012; Mauro et al., 2018). This seems to coincide with the FTO-mTOR pathway, discussed in the previous paragraph. In summary, FTO can directly or indirectly target mTOR, thus regulating the occurrence and progress of obesity and cancer in a broad manner (**Figure 2B**).

EFFECTS OF FTO INHIBITORS IN OBESITY AND CANCER

With the gradual disclosure of the important functions of FTO as mRNA demethylase in many diseases, the crystal structure of FTO has been resolved since 2010, and the development and applications of its specific inhibitors have attracted extensive attention (Han et al., 2010). FTO inhibitors that have been shown to have anti-obesity or anti-cancer effects *in vitro* or *in vivo* are summarized in **Table 2**.

Effects of FTO Inhibitors in Obesity

In 2012, Yang et al. reported natural product Rhein as an inhibitor of human FTO demethylase, which can competitively bind to the FTO catalytic site (Chen et al., 2012). Before this study, Rhein was thought to prevent or even reverse weight gain and obesity caused by high-fat diets (Liu et al., 2011; Zhang et al.,

TABLE 2 | Summary of the effects and application of FTO inhibitors in obesity and cancer.

Inhibitor	Mechanisms for inhibiting FTO	Specific inhibition?	The mechanisms of anti-cancer effect	Anti-obesity?	References
Rhein	Rhein reversibly binds to the FTO enzyme, competitively preventing the recognition of the m^6A substrate.	No	Rhein can be used in combination with nilotinib to inhibit the progression of leukemia in mice; Rhein inhibited subcutaneous breast tumor growth in mice.	Rhein has anti-obesity effect, but it needs to be further clarified whether by inhibiting FTO.	Liu et al., 2011; Chen et al., 2012; Zhang et al., 2012; Yan et al., 2018; Niu et al., 2019
MA/MA2	MA/MA2 competed with FTO to bind with m^6A.	Yes	MA2 inhibited the progression of glioblastoma and extended the life span of GSC transplanted animals.	Unknown	Huang et al., 2015; Cui et al., 2017
FB23/FB23-2	FB23/FB23-2 binds to FTO and selectively inhibits the m^6A demethylase activity of FTO.	Yes	FB23 and FB23-2 significantly increased the abundance of ASB2 and RARA and inhibited MYC and CEBPA expression in AML cells.	Unknown	Huang et al., 2019
R-2HG	R-2HG is structurally close to 2-OG so that it can competitively inhibit FTO.	No	R-2HG can inhibit leukemia and glioma through the regulation of R-2HG-FTO-m^6A axis to MYC/CEBPA expression and downstream pathways.	Unknown	Su et al., 2018
CS1/CS2	Direct interaction between CS1/CS2 and intracellular FTO protein inhibits its demethylase activity.	Unknown	CS1 and CS2 play an anti-leukemic role by manipulating FTO-related signaling pathways, such as the MYC pathway.	Unknown	Su et al., 2019
MO-I-500	MO-I-500 is a mimic of 2-OG, which can inhibit the RNA demethylase activity of FTO and increase the content of m^6A in the total RNA of cells.	Yes	As a pharmacological inhibitor of FTO, MO-I-500 plays an important role in the cell survival of refractory triple-negative inflammatory breast cancer.	Unknown	Zheng et al., 2014; Singh et al., 2016
Epigallocatechin gallate (EGCG)	EGCG will reduce the protein stability of FTO and affect its protein expression.	No	EGCG has an anti-cancer effect, but it needs to be further clarified if it through inhibiting FTO.	EGCG prevents mitotic cloning amplification (MCE) at the early stage of adipocyte differentiation by inhibiting FTO expression.	Stuart et al., 2006; Forester and Lambert, 2014; Negri et al., 2018; Wei R. et al., 2018; Wu et al., 2018b; La et al., 2019; Wei et al., 2019; Zhang L. et al., 2019
Entacapone	Entacapone can directly combine with FTO and inhibit the activity of FTO.	Yes	Entacapone has an anti-cancer effect, but it needs to be further clarified if it through inhibiting FTO.	Entacapone has an effect on gluconeogenesis and adipose tissue heat production in mouse liver by acting on the FTO-FOXO1 axis.	Forester and Lambert, 2014; Peng et al., 2019

2012). The catechin EGCG, another natural compound rich in green tea, was found to play anti-obesity and anti-adipogenesis roles through the FTO-m^{6}A-YTHDF2 axis (Wu et al., 2018b). Recently, Peng et al. identified Entacapone as a potential FTO inhibitor, which has the effect of reducing weight and lowering blood glucose (Peng et al., 2019). It was initially approved as an adjunctive therapy combined with levodopa and carbidopa for the treatment of Parkinson's disease. Entacapone had an effect on gluconeogenesis and adipogenesis in the liver of mice by acting on an FTO-FOXO1 regulatory axis (Peng et al., 2019).

Effects of FTO Inhibitors in Cancer

As for cancers, there are more studies on the application of FTO inhibitors, especially in the treatment of leukemia, glioblastoma, and breast cancer. Compared with single drug therapy, Rhein combined with nilotinib is a more effective treatment for leukemia in mice (Yan et al., 2018). Recently, Yang et al. identified meclofenamic acid (MA) as a highly selective inhibitor of FTO, which can compete with FTO binding for the m^{6}A-containing nucleic acids (Huang et al., 2015). The inhibitor FB23 was designed and synthesized from the chemical scaffold of MA, which exhibited a more potent inhibition for FTO demethylation *in vitro* (Huang et al., 2019). Its bioisostere FB23-2 can inhibit the leukemogenesis in cells and in the patient-derived xenografted (PDX) mouse model (Huang et al., 2019). Su et al. found that R-2HG (oncometabolite produced by mutant isocitrate dehydrogenase 1/2 (IDH1/2) enzymes), compounds CS1 and CS2 were also targeted inhibitors of FTO. By inhibiting its demethylation function, they affected related signaling pathways (such as the MYC pathway) and played an active role in inhibiting the proliferation of AML cells *in vivo* and *in vitro* (Su et al., 2018, 2019). Compounds CS1 and CS2 extended the overall survival of transplanted mice with primary MLL-AF16 cells and made AML cells sensitive to other curative drugs, such as decitabine, a tyrosine kinase inhibitor, and IDH2^{mut} inhibitor (Su et al., 2019). Comparing the anti-leukemic activities of the four FTO inhibitors, CS1 and CS2 showed higher activity in inhibiting cell viability, and their IC50 values were 10–30 times lower than FB23-2 or MO-I-500 (Su et al., 2019). MO-I-500 is another FTO inhibitor, which selectively inhibits the demethylation of FTO and increases the m^{6}A levels in cells (Zheng et al., 2014). In addition, among the above-mentioned FTO inhibitors, Rhein and MO-I-500 have been reported to significantly inhibit the growth ability of breast cancer cells *in vivo* and *in vitro* (Singh et al., 2016; Niu et al., 2019). MA2 (the ethyl ester form of MA) and R-2HG had inhibitory effects on glioma (Cui et al., 2017; Su et al., 2018; Deng et al., 2018b). Compared with MA, MA2 has a better cell penetration, significantly increased m^{6}A methylation in cells, suppresses glioblastoma progression, and prolongs the lifespan of GSC-grafted animals (Huang et al., 2015; Cui et al., 2017). Interestingly, the previous anti-obesity EGCG, Entacapone, also had an inhibitory effect on cancer. For example, EGCG had an inhibitory effect on lung cancer, breast cancer, colon cancer, metastatic pancreatic cancer, and prostate cancer or had a sensitivity to chemotherapy. It was noted that it can be used as an adjuvant drug in cancer treatments (Negri et al., 2018; Wei R. et al., 2018; La et al., 2019; Wei et al., 2019). The combination of Entacapone and EGCG can synergistically enhance the growth inhibitor of lung cancer cell lines (Forester and Lambert, 2014).

In summary, more FTO inhibitors are displaying positive therapeutic effects in animal disease models, and represent promising therapeutic targets for obesity and cancer (**Figure 2A**).

CONTROVERSY ON THE MECHANISM OF ASSOCIATION BETWEEN *FTO* RISK ALLELES AND DISEASES

Single nucleotide polymorphism sites are the main form of human genome DNA sequence variation and can regulate gene expression. From *FTO* polymorphisms which have a risk for obesity and cancer to the specific mechanisms regulating these diseases through nucleic acid demethylation of FTO proteins, *FTO* SNPs seem to regulate the expression level of FTO and affect its enzymatic function, playing an important role in obesity and cancer. Some studies support this hypothesis. For example, In 2008, a study of a Mexican population revealed that in obese patients, the *FTO* risk allele was significantly correlated with high FTO expression (Villalobos-Comparán et al., 2008). Subsequently, Tea et al. and Efthimia et al. revealed that *FTO* mRNA caused by the risk allele was more abundant than non-risk alleles at least in blood cells (Berulava and Horsthemke, 2010; Karra et al., 2013). Unfortunately, the mechanism for the correlation between *FTO* SNPs and obesity or cancer has been elusive. So far, there are no studies that provide indisputable evidence for these associations.

Moreover, some studies have suggested that *FTO* SNPs may be associated with obesity by regulating the expression of adjacent genes (Tung et al., 2014; **Figure 3A**). The Leibel group found that the rs8050136 of the intron 1 region of *FTO* overlapped with the binding site of transcription factor Cut Like Homeobox 1 (CUX1). This SNP nucleotide type can affect the transcriptional activation of *FTO* and retinitis pigmentosa GTPase regulator interacting protein 1 like (*RPGRIP1L*) by CUX1 P110 (Stratigopoulos et al., 2008, 2011). For individuals with the obesity risk allele at rs8050136, the expression of *RPGRIP1L* and *FTO* in the hypothalamus were decreased due to the low binding affinity of CUX1 P110 to DNA, RPGRIP1L can affect the location of leptin receptors and leptin signaling in neurons and lead to increased food intake and obesity (Stratigopoulos et al., 2011). In addition, Jowett et al. found that in combination with gene variation and expression data from the human cohort, the A allele of rs8050136 was positively associated with the expression level of *RBL2*, and an increase in RBL2 level might help to restrict the clonal expansion of A population of precursor adipose cells during development (Jowett et al., 2010). Moreover, Smemo et al. found that these sites also contained an enhancer sequence that can bind to the promoter of *IRX3*. Using expression quantitative trait loci (eQTL), they found that obesity-related SNPs such as rs9930506 were correlated with the expression of *IRX3* in human brain samples. Mice lacking *IRX3* lost 25–30% of their body weight through increasing basal metabolic rate and browning of white adipose tissues

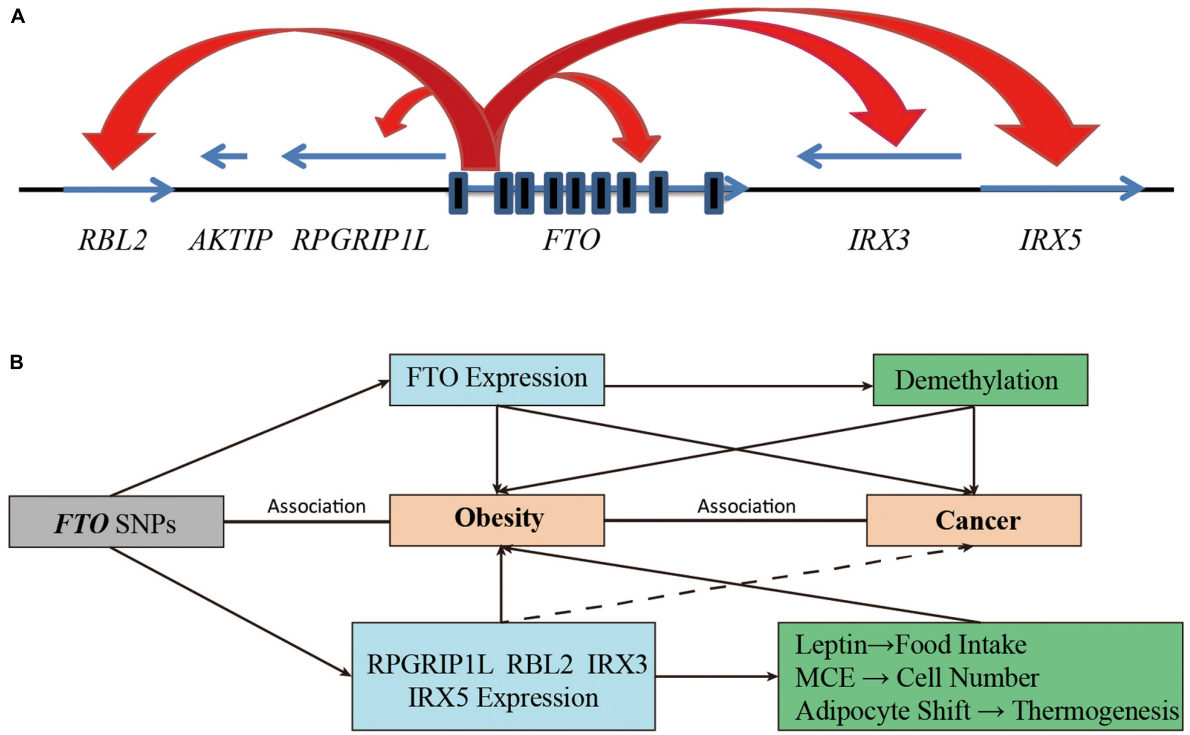

FIGURE 3 | Increasing functional complexity around the FTO Locus. **(A)** SNPs in the intron 1 of *FTO* can regulate the expression of FTO itself and adjacent genes (including *RBL2, RPGRIP1L, IRX3,* and *IRX5*). **(B)** The *FTO* SNPs are involved in the development of obesity and cancer by affecting the demethylation function of FTO or by regulating the expression of adjacent genes.

(Smemo et al., 2014). The study of Claussnitzer et al. also supported the regulatory relationships between *FTO* SNPs and *IRX3* expression. They suggested that changes in the rs1421085 risk allele led to a double expression of *IRX3* and *IRX5* through disruption of the conservative motif of the ARID5B repressor in the early stage of adipocyte differentiation. In this case, brown fat cells transform automatically into white fat cells and lower down the mitochondrial thermogenesis by five times (Claussnitzer et al., 2015). This study explained the correlation between *FTO* SNPs and obesity by using the effect of the autonomous transformation of fat cells on thermogenesis. These studies provided a plausible mechanism for the correlation between SNP variation of *FTO* intron 1 and obesity (**Figure 3B**).

Adjacent genes (*RPGRIP1L, RBL2, IRX3, IRX5*) regulated by *FTO* SNPs are also involved in the occurrence and progression of cancer in various ways (**Figure 3B**). For example, studies have shown that RPGRIP1L was one of the tumor suppressor genes of human hepatocellular carcinoma (Lin et al., 2009). RBL2, a member of the retinoblastoma (Rb) family, was inactivated by cell cycle kinases and was the basis of various cancer types (Pentimalli et al., 2015). The emerging role of RBL2 in aging and apoptosis also appeared to play an active part in tumor inhibition (Pentimalli et al., 2015). IRX3 was highly expressed in approximately 30% of patients with AML, and high expression of IRX3 alone can perpetuate hematopoietic stem cells and progenitor cells (HSPC) in bone marrow cultures and induce lymphoid leukemia *in vivo* (Somerville et al., 2018). In addition, IRX3 and IRX5 have been reported to participate in the transition from intestinal adenoma to colorectal cancer by negatively regulating the Dpp/TGF-ß pathway (Martorell et al., 2014). IRX5 alone has also been reported to be an oncogenic gene in hepatocellular carcinoma, colorectal cancer, prostate cancer, and non-small cell lung cancer by regulating cancer cell cycle and apoptosis (Myrthue et al., 2008; Zhang D.L. et al., 2018; Zhu et al., 2019, 2020). Although there is no direct evidence that *FTO* SNPs are associated with cancer by affecting the expression of adjacent genes, we cannot rule it out as a possibility.

Based on these findings, the correlation between *FTO* SNPs and obesity and cancer may be due to the regulation of FTO enzyme activity or expression of adjacent genes. However, more convincing and systematic research studies are needed to decipher the causal mechanism between *FTO* non-coding variants and obesity or cancer. A healthy lifestyle such as proper diet and moderate exercise is recommended to minimize the negative effects of obesity susceptibility genes before we can fully understand the underlying mechanisms.

CONCLUSION

Although the specific mechanisms for *FTO* polymorphism and high risk of obesity and cancer are elusive, the correlation is

definite. As for FTO, it can participate in the disease progression of obesity and cancer in m^6A-dependent post-transcriptional regulation, or by targeting mTOR. More importantly, some drugs have been shown to inhibit obesity, and some cancers such as leukemia, glioblastoma, and breast cancer by targeting FTO. In particular, FB23, R-2HG, and CS1/CS2 have shown anti-leukemia effects through *in vivo* experiments, and MA2 can also inhibit the activities of glioblastoma cells *in vivo*. This evidence suggests *FTO* as the common genetic basis of obesity and cancer and a potential target for obesity and some cancers.

AUTHOR CONTRIBUTIONS

WY oversaw and guided the process of writing this manuscript. NL wrote and edited the manuscript. YL, YZ, SP, XN, HX, and JL put forward suggestions for the manuscript. All authors read and approved the final manuscript.

FUNDING

This study was supported by the Gansu Natural Science Foundation (18JR3RA343) and the Science and Technology Bureau 2018 Fund of the Chengguan District (2018KJGG0037).

ACKNOWLEDGMENTS

Thanks to the First School of Clinical Medicine of Lanzhou University and the Key Laboratory for Resources Utilization Technology of Unconventional Water of Gansu Province.

SUPPLEMENTARY MATERIAL

The Supplementary Material for this article can be found online at: https://www.frontiersin.org/articles/10.3389/fgene.2020.559138/full#supplementary-material

REFERENCES

Ahmad, T., Lee, I., Paré, G., Chasman, D., Rose, L., Ridker, P. M., et al. (2011). Lifestyle interaction with fat mass and obesity-associated (fto) genotype and risk of obesity in apparently healthy U.S. Women. *Diabetes Care* 34, 675–680. doi: 10.2337/dc10-0948

Aik, W., Scotti, J. S., Choi, H., Gong, L., Demetriades, M., Schofield, C. J., et al. (2014). Structure of human rna n 6-methyladenine demethylase alkbh5 provides insights into its mechanisms of nucleic acid recognition and demethylation. *Nucleic Acids Res.* 42, 4741–4754. doi: 10.1093/nar/gku085

Barone, I., Giordano, C., Bonofiglio, D., Andò, S., and Catalano, S. (2020). The weight of obesity in breast cancer progression and metastasis: clinical and molecular perspectives. *Semin. Cancer Biol.* 60, 274–284. doi: 10.1016/j.semcancer.2019.09.001

Bartosovic, M., Molares, H. C., Gregorova, P., Hrossova, D., Kudla, G., and Vanacova, S. (2017). N6-methyladenosine demethylase fto targets pre-mrnas and regulates alternative splicing and 3′-end processing. *Nucleic Acids Res.* 45, 11356–11370. doi: 10.1093/nar/gkx778

Ben-Haim, M. S., Moshitch-Moshkovitz, S., and Rechavi, G. (2015). Fto: linking m 6 a demethylation to adipogenesis. *Cell Res.* 25, 3–4. doi: 10.1038/cr.2014.162

Berulava, T., and Horsthemke, B. (2010). The obesity-associated snps in intron 1 of the fto gene affect primary transcript levels. *Eur. J. Hum. Genet.* 18, 1054–1056.

Calle, E. E., and Kaaks, R. (2004). Overweight, obesity and cancer: epidemiological evidence and proposed mechanisms. *Nature Rev. Cancer* 4, 579–591. doi: 10.1038/nrc1408

Calle, E. E., Rodriguez, C., Walker-Thurmond, K., and Thun, M. J. (2003). Overweight, obesity, and mortality from cancer in a prospectively studied cohort of us adults. *N. Engl. J. Med.* 348, 1625–1638.

Cauchi, S., Stutzmann, F., Cavalcanti-Proença, C., Durand, E., Pouta, A., Hartikainen, A. L., et al. (2009). Combined effects of mc4r and fto common genetic variants on obesity in european general populations. *J. Mol. Med.* 87, 537–546. doi: 10.1007/s00109-009-0451-6

Cecil, J. E., Tavendale, R., Watt, P., Hetherington, M. M., and Palmer, C. N. (2008). An obesity-associated fto gene variant and increased energy intake in children. *N. Engl. J. Med.* 359, 2558–2566.

Chang, Y., Liu, P., Lee, W., Chang, T., Jiang, Y., Li, H., et al. (2008). Common variation in the fat mass and obesity-associated (fto) gene confers risk of obesity and modulates bmi in the chinese population. *Diabetes* 57, 2245–2252. doi: 10.2337/db08-0377

Chen, B., Ye, F., Yu, L., Jia, G., Huang, X., Zhang, X., et al. (2012). Development of cell-active n 6-methyladenosine rna demethylase fto inhibitor. *J. Am. Chem. Soc.* 134, 17963–17971.

Chen, J. (2011). Multiple signal pathways in obesity-associated cancer. *Obes. Rev.* 12, 1063–1070. doi: 10.1111/j.1467-789X.2011.00917.x

Chen, J., and Du, B. (2019). Novel positioning from obesity to cancer: fto, an m6a rna demethylase, regulates tumour progression. *J. Cancer Res. Clin. Oncol.* 145, 19–29. doi: 10.1007/s00432-018-2796-0

Cheung, M. K., Gulati, P., O'rahilly, S., and Yeo, G. S. (2013). Fto expression is regulated by availability of essential amino acids. *Int. J. Obes.* 37, 744–747. doi: 10.1038/ijo.2012.77

Claussnitzer, M., Dankel, S., Kim, K., Quon, G., Meuleman, W., Haugen, C., et al. (2015). Fto obesity variant circuitry and adipocyte browning in humans. *N. Engl. J. Med.* 373, 895–907. doi: 10.1056/NEJMoa1502214

Cui, Q., Shi, H., Ye, P., Li, L., Qu, Q., Sun, G., et al. (2017). M6a rna methylation regulates the self-renewal and tumorigenesis of glioblastoma stem cells. *Cell Rep.* 18, 2622–2634. doi: 10.1016/j.celrep.2017.02.059

Da Cunha, P. A., De Carlos, B. L. K., Sereia, A. F., Kubelka, C., Ribeiro, M. C., Fernandes, B. L., et al. (2013). Interaction between obesity-related genes, fto and mc4r, associated to an increase of breast cancer risk. *Mol. Biol. Rep.* 40, 6657–6664. doi: 10.1007/s11033-013-2780-3

Delahanty, R. J., Beeghly-Fadiel, A., Xiang, Y.-B., Long, J., Cai, Q., Wen, W., et al. (2011). Association of obesity-related genetic variants with endometrial cancer risk: a report from the shanghai endometrial cancer genetics study. *Am. J. Epidemiol.* 174, 1115–1126.

Deng, X., Su, R., Stanford, S., and Chen, J. (2018a). Critical enzymatic functions of fto in obesity and cancer. *Front. Endocrinol.* 9:396. doi: 10.3389/fendo.2018.00396

Deng, X., Su, R., Weng, H., Huang, H., Li, Z., and Chen, J. (2018b). Rna n-methyladenosine modification in cancers: current status and perspectives. *Cell Res.* 28, 507–517. doi: 10.1038/s41422-018-0034-6

Dina, C., Meyre, D., Gallina, S., Durand, E., Körner, A., Jacobson, P., et al. (2007). Variation in fto contributes to childhood obesity and severe adult obesity. *Nat. Genet.* 39, 724–726. doi: 10.1038/ng2048

Drew, J. (2012). Molecular mechanisms linking adipokines to obesity-related colon cancer: focus on leptin. *Proc. Nutr. Soc.* 71, 175–180. doi: 10.1017/s0029665111003259

Fonseca, A. C. P. D., Abreu, G. D. M., Zembrzuski, V. M., Junior, M. C., Carneiro, J. R. I., Neto, J. F. N., et al. (2019). The association of the fat mass and obesity-associated gene (fto) rs9939609 polymorphism and the severe obesity in a brazilian population. *Diabetes Metab. Syndr. Obes. Targets Ther.* 12, 667–684. doi: 10.2147/DMSO.S199542

Forester, S. C., and Lambert, J. D. (2014). Synergistic inhibition of lung cancer cell lines by (-)-epigallocatechin-3-gallate in combination with clinically used nitrocatechol inhibitors of catechol-o-methyltransferase. *Carcinogenesis* 35, 365–372. doi: 10.1093/carcin/bgt347

Frayling, T. M., Timpson, N. J., Weedon, M. N., Zeggini, E., Freathy, R. M., Lindgren, C. M., et al. (2007). A common variant in the fto gene is associated with body mass index and predisposes to childhood and adult obesity. *Science* 316, 889–894.

Fustin, J. M., Doi, M., Yamaguchi, Y., Hida, H., Nishimura, S., Yoshida, M., et al. (2013). Rna-methylation-dependent rna processing controls the speed of the circadian clock. *Cell* 155, 793–806. doi: 10.1016/j.cell.2013.10.026

Gerken, T., Girard, C. A., Tung, Y. C., Webby, C. J., Saudek, V., Hewitson, K. S., et al. (2007). The obesity-associated fto gene encodes a 2-oxoglutarate-dependent nucleic acid demethylase. *Science* 318, 1469–1472. doi: 10.1126/science.1151710

Goodwin, P. J., and Stambolic, V. (2015). Impact of the obesity epidemic on cancer. *Annu. Rev. Med.* 66, 281–296. doi: 10.1146/annurev-med-051613-012328

Gulati, P., Cheung, M. K., Antrobus, R., Church, C. D., Harding, H. P., Tung, Y. C., et al. (2013). Role for the obesity-related fto gene in the cellular sensing of amino acids. *Proc. Natl. Acad. Sci. U.S.A.* 110, 2557–2562. doi: 10.1073/pnas.1222796110

Han, Z., Niu, T., Chang, J., Lei, X., Zhao, M., Wang, Q., et al. (2010). Crystal structure of the fto protein reveals basis for its substrate specificity. *Nature* 464, 1205–1209. doi: 10.1038/nature08921

Haupt, A., Thamer, C., Machann, J., Kirchhoff, K., Stefan, N., Tschritter, O., et al. (2008). Impact of variation in the fto gene on whole body fat distribution, ectopic fat, and weight loss. *Obesity* 16, 1969–1972. doi: 10.1038/oby.2008.283

Hernández-Caballero, M. E., and Sierra-Ramírez, J. A. (2015). Single nucleotide polymorphisms of the fto gene and cancer risk: an overview. *Mol. Biol. Rep.* 42, 699–704. doi: 10.1007/s11033-014-3817-y

Huang, H., Weng, H., Sun, W., Qin, X., Shi, H., Wu, H., et al. (2018). Recognition of rna n-methyladenosine by igf2bp proteins enhances mrna stability and translation. *Nat. Cell Biol.* 20, 285–295. doi: 10.1038/s41556-018-0045-z

Huang, X., Zhao, J., Yang, M., Li, M., and Zheng, J. (2017). Association between fto gene polymorphism (rs9939609 t/a) and cancer risk: a meta-analysis. *Eur. J Cancer Care* 26:e12464. doi: 10.1111/ecc.12464

Huang, Y., Su, R., Sheng, Y., Dong, L., Dong, Z., Xu, H., et al. (2019). Small-molecule targeting of oncogenic fto demethylase in acute myeloid leukemia. *Cancer Cell* 35, 677.e10–691.e10. doi: 10.1016/j.ccell.2019.03.006

Huang, Y., Yan, J., Li, Q., Li, J., Gong, S., Zhou, H., et al. (2015). Meclofenamic acid selectively inhibits fto demethylation of m6a over alkbh5. *Nucleic Acids Res.* 43, 373–384. doi: 10.1093/nar/gku1276

Iles, M. M., Law, M. H., Stacey, S. N., Han, J., Fang, S., Pfeiffer, R., et al. (2013). A variant in fto shows association with melanoma risk not due to bmi. *Nat. Genet.* 45:428.

Jia, G., Fu, Y., Zhao, X., Dai, Q., Zheng, G., Yang, Y., et al. (2011). N6-methyladenosine in nuclear rna is a major substrate of the obesity-associated fto. *Nat. Chem. Biol.* 7, 885–887. doi: 10.1038/nchembio.687

Jia, G., Yang, C.-G., Yang, S., Jian, X., Yi, C., Zhou, Z., et al. (2008). Oxidative demethylation of 3-methylthymine and 3-methyluracil in single-stranded DNA and rna by mouse and human fto. *FEBS Lett.* 582, 3313–3319. doi: 10.1016/j.febslet.2008.08.019

Jiang, Y., Mei, H., Lin, Q., Wang, J., Liu, S., Wang, G., et al. (2019). Interaction effects of fto rs9939609 polymorphism and lifestyle factors on obesity indices in early adolescence. *Obes. Res. Clin. Pract.* 13, 352–357. doi: 10.1016/j.orcp.2019.06.004

Jowett, J. B., Curran, J. E., Johnson, M. P., Carless, M. A., Göring, H. H., Dyer, T. D., et al. (2010). Genetic variation at the fto locus influences rbl2 gene expression. *Diabetes* 59, 726–732. doi: 10.2337/db09-1277

Kaklamani, V., Yi, N., Sadim, M., Siziopikou, K., Zhang, K., Xu, Y., et al. (2011). The role of the fat mass and obesity associated gene (fto) in breast cancer risk. *BMC Med. Genet.* 12:52. doi: 10.1186/1471-2350-12-52

Karra, E., O'daly, O. G., Choudhury, A. I., Yousseif, A., Millership, S., Neary, M. T., et al. (2013). A link between fto, ghrelin, and impaired brain food-cue responsivity. *J. Clin. Investig.* 123, 3539–3551.

Kilpeläinen, T. O., Qi, L., Brage, S., Sharp, S. J., Sonestedt, E., Demerath, E., et al. (2011). Physical activity attenuates the influence of fto variants on obesity risk: a meta-analysis of 218,166 adults and 19,268 children. *PLoS Med.* 8:e1001116. doi: 10.1371/journal.pmed.1001116

Kim, Y. C., and Guan, K. L. (2015). Mtor: a pharmacologic target for autophagy regulation. *J. Clin. Investig.* 125, 25–32. doi: 10.1172/jci73939

La, X., Zhang, L., Li, Z., Li, H., and Yang, Y. (2019). (-)-epigallocatechin gallate (egcg) enhances the sensitivity of colorectal cancer cells to 5-fu by inhibiting grp78/nf-κb/mir-155-5p/mdr1 pathway. *J. Agric. Food Chem.* 67, 2510–2518. doi: 10.1021/acs.jafc.8b06665

Laplante, M., and David, M. S. (2012). Mtor signaling in growth control and disease. *Cell* 149, 285–293.

Li, H., Kilpeläinen, T., Liu, C., Zhu, J., Liu, Y., Hu, C., et al. (2012). Association of genetic variation in fto with risk of obesity and type 2 diabetes with data from 96,551 east and south asians. *Diabetologia* 55, 981–995. doi: 10.1007/s00125-011-2370-7

Li, J., Han, Y., Zhang, H., Qian, Z., Jia, W., Gao, Y., et al. (2019a). The m6a demethylase fto promotes the growth of lung cancer cells by regulating the m6a level of usp7 mrna. *Biochem. Biophys. Res. Commun.* 512, 479–485. doi: 10.1016/j.bbrc.2019.03.093

Li, J., Zhu, L., Shi, Y., Liu, J., Lin, L., and Chen, X. (2019b). M6a demethylase fto promotes hepatocellular carcinoma tumorigenesis via mediating pkm2 demethylation. *Am. J. Transl. Res.* 11:6084.

Li, Z., Weng, H., Su, R., Weng, X., Zuo, Z., Li, C., et al. (2017). Fto plays an oncogenic role in acute myeloid leukemia as a n6-methyladenosine rna demethylase. *Cancer Cell* 31, 127–141. doi: 10.1016/j.ccell.2016.11.017

Liao, S., Sun, H., and Xu, C. (2018). Yth domain: a family of n-methyladenosine (ma) readers. *Genomics Proteomics Bioinformatics* 16, 99–107. doi: 10.1016/j.gpb.2018.04.002

Lin, Y., Ueda, J., Yagyu, K., Ishii, H., Ueno, M., Egawa, N., et al. (2013). Association between variations in the fat mass and obesity-associated gene and pancreatic cancer risk: a case–control study in japan. *BMC Cancer* 13:337. doi: 10.1186/1471-2407-13-337

Lin, Y. W., Yan, M. D., Shih, Y. L., and Hsieh, C. B. (2009). The basal body gene, rpgrip1l, is a candidate tumour suppressor gene in human hepatocellular carcinoma. *Eur. J. Cancer* 45, 2041–2049. doi: 10.1016/j.ejca.2009.04.012

Liu, J., Ren, D., Du, Z., Wang, H., Zhang, H., and Jin, Y. (2018). M6a demethylase fto facilitates tumor progression in lung squamous cell carcinoma by regulating mzf1 expression. *Biochem. Biophys. Res. Commun.* 502, 456–464. doi: 10.1016/j.bbrc.2018.05.175

Liu, J., Yue, Y., Han, D., Wang, X., Fu, Y., Zhang, L., et al. (2014). A mettl3-mettl14 complex mediates mammalian nuclear rna n6-adenosine methylation. *Nat. Chem. Biol.* 10, 93–95. doi: 10.1038/nchembio.1432

Liu, Q., Zhang, X.-L., Tao, R.-Y., Niu, Y.-J., Chen, X.-G., Tian, J.-Y., et al. (2011). Rhein, an inhibitor of adipocyte differentiation and adipogenesis. *J. Asian Nat. Prod. Res.* 13, 714–723.

Loos, R. J. F., and Yeo, G. S. H. (2014). The bigger picture of fto—the first gwas-identified obesity gene. *Nat. Rev. Endocrinol.* 10, 51–61. doi: 10.1038/nrendo.2013.227

Martorell, Ò, Barriga, F. M., Merlos-Suárez, A., Stephan-Otto Attolini, C., Casanova, J., Batlle, E., et al. (2014). Iro/irx transcription factors negatively regulate dpp/tgf-β pathway activity during intestinal tumorigenesis. *EMBO Rep.* 15, 1210–1218. doi: 10.15252/embr.201438622

Mauro, L., Naimo, G. D., Gelsomino, L., Malivindi, R., Bruno, L., Pellegrino, M., et al. (2018). Uncoupling effects of estrogen receptor α on lkb1/ampk interaction upon adiponectin exposure in breast cancer. *FASEB J.* 32, 4343–4355. doi: 10.1096/fj.201701315R

Maya-Monteiro, C., and Bozza, P. (2008). Leptin and mtor: partners in metabolism and inflammation. *Cell Cycle* 7, 1713–1717.

Mehrdad, M., Doaei, S., Gholamalizadeh, M., Fardaei, M., Fararouei, M., and Eftekhari, M. H. (2020a). Ftoassociation of rs9939609 polymorphism with serum leptin, insulin, adiponectin, and lipid profile in overweight adults. *Adipocyte* 9, 51–56. doi: 10.1080/21623945.2020.1722550

Mehrdad, M., Fardaei, M., Fararouei, M., and Eftekhari, M. H. (2020b). The association between fto rs9939609 gene polymorphism and anthropometric indices in adults. *J. Physiol. Anthropol.* 39:14. doi: 10.1186/s40101-020-00224-y

Merkestein, M., Laber, S., Mcmurray, F., Andrew, D., Sachse, G., Sanderson, J., et al. (2015). Fto influences adipogenesis by regulating mitotic clonal expansion. *Nat. Commun.* 6, 1–9. doi: 10.1038/ncomms7792

Merra, G., Gualtieri, P., Cioccoloni, G., Falco, S., Bigioni, G., Tarsitano, M., et al. (2020). Fto rs9939609 influence on adipose tissue localization in the italian population. *Eur. Rev. Med. Pharmacol. Sci.* 24, 3223–3235. doi: 10.26355/eurrev_202003_20689

Myrthue, A., Rademacher, B. L., Pittsenbarger, J., Kutyba-Brooks, B., Gantner, M., Qian, D., et al. (2008). The iroquois homeobox gene 5 is regulated by 1,25-dihydroxyvitamin d3 in human prostate cancer and regulates apoptosis and the cell cycle in lncap prostate cancer cells. *Clin. Cancer Res.* 14, 3562–3570. doi: 10.1158/1078-0432.Ccr-07-4649

Negri, A., Naponelli, V., Rizzi, F., and Bettuzzi, S. (2018). Molecular targets of epigallocatechin-gallate (egcg): a special focus on signal transduction and cancer. *Nutrients* 10:1936. doi: 10.3390/nu10121936

Ng, M., Fleming, T., Robinson, M., Thomson, B., Graetz, N., Margono, C., et al. (2014). Global, regional, and national prevalence of overweight and obesity in children and adults during 1980-2013: a systematic analysis for the global burden of disease study 2013. *Lancet* 384, 766–781. doi: 10.1016/s0140-6736(14)60460-8

Niu, Y., Lin, Z., Wan, A., Chen, H., Liang, H., Sun, L., et al. (2019). Rna n6-methyladenosine demethylase fto promotes breast tumor progression through inhibiting bnip3. *Mol. Cancer* 18, 46. doi: 10.1186/s12943-019-1004-4

Peng, S., Xiao, W., Ju, D., Sun, B., Hou, N., Liu, Q., et al. (2019). Identification of entacapone as a chemical inhibitor of fto mediating metabolic regulation through foxo1. *Sci. Transl. Med.* 11:eaau7116. doi: 10.1126/scitranslmed.aau7116

Pentimalli, F., Esposito, L., Forte, I. M., Iannuzzi, C. A., and Giordano, A. (2015). Abstract lb-080: reactivating rbl2/p130 oncosuppressive function as a new, possible antitumoral strategy. *Cancer Res.* 75, 18–22.

Peters, T., Ausmeier, K., and Rüther, U. (1999). Cloning of fatso (fto), a novel gene deleted by the fused toes (ft) mouse mutation. *Mamm. Genome* 10, 983–986. doi: 10.1007/s003359901144

Ping, X. L., Sun, B. F., Wang, L., Xiao, W., Yang, X., Wang, W. J., et al. (2014). Mammalian wtap is a regulatory subunit of the rna n6-methyladenosine methyltransferase. *Cell Res.* 24, 177–189. doi: 10.1038/cr.2014.3

Reuter, C. P., Rosane De Moura Valim, A., Gaya, A. R., Borges, T. S., Klinger, E. I., Possuelo, L. G., et al. (2016). Fto polymorphism, cardiorespiratory fitness, and obesity in brazilian youth. *Am. J. Hum. Biol.* 28, 381–386. doi: 10.1002/ajhb.22798

Robbens, S., Rouzé, P., Cock, J., Spring, J., Worden, A., and Van De Peer, Y. (2008). The fto gene, implicated in human obesity, is found only in vertebrates and marine algae. *J. Mol. Evol.* 66, 80–84. doi: 10.1007/s00239-007-9059-z

Roundtree, I. A., Evans, M. E., Pan, T., and He, C. (2017). Dynamic rna modifications in gene expression regulation. *Cell* 169, 1187–1200. doi: 10.1016/j.cell.2017.05.045

Schwartz, S., Mumbach, M. R., Jovanovic, M., Wang, T., Maciag, K., Bushkin, G. G., et al. (2014). Perturbation of m6a writers reveals two distinct classes of mrna methylation at internal and 5′ sites. *Cell Rep.* 8, 284–296. doi: 10.1016/j.celrep.2014.05.048

Scuteri, A., Sanna, S., Chen, W. M., Uda, M., Albai, G., Strait, J., et al. (2007). Genome-wide association scan shows genetic variants in the fto gene are associated with obesity-related traits. *PLoS Genet.* 3:e115. doi: 10.1371/journal.pgen.0030115

Siegel, R. L., Jemal, A., Wender, R. C., Gansler, T., Ma, J., and Brawley, O. W. (2018). An assessment of progress in cancer control. *CA Cancer J. Clin.* 68, 329–339. doi: 10.3322/caac.21460

Singh, B., Kinne, H. E., Milligan, R. D., Washburn, L. J., Olsen, M., and Lucci, A. (2016). Important role of fto in the survival of rare panresistant triple-negative inflammatory breast cancer cells facing a severe metabolic challenge. *PLoS One* 11:e0159072. doi: 10.1371/journal.pone.0159072

Smemo, S., Tena, J. J., Kim, K.-H., Gamazon, E. R., Sakabe, N. J., Gómez-Marín, C., et al. (2014). Obesity-associated variants within fto form long-range functional connections with irx3. *Nature* 507, 371–375. doi: 10.1038/nature13138

Somerville, T. D. D., Simeoni, F., Chadwick, J. A., Williams, E. L., Spencer, G. J., Boros, K., et al. (2018). Derepression of the iroquois homeodomain transcription factor gene irx3 confers differentiation block in acute leukemia. *Cell Rep.* 22, 638–652. doi: 10.1016/j.celrep.2017.12.063

Sonestedt, E., Roos, C., Gullberg, B., Ericson, U., Wirfält, E., and Orho-Melander, M. (2009). Fat and carbohydrate intake modify the association between genetic variation in the fto genotype and obesity. *Am. J. Clin. Nutr.* 90, 1418–1425. doi: 10.3945/ajcn.2009.27958

Stattin, P., Söderberg, S., Hallmans, G., Bylund, A., Kaaks, R., Stenman, U. H., et al. (2001). Leptin is associated with increased prostate cancer risk: a nested case-referent study. *J. Clin. Endocrinol. Metab.* 86, 1341–1345. doi: 10.1210/jcem.86.3.7328

Steele, C. B., Thomas, C. C., Henley, S. J., Massetti, G. M., Galuska, D. A., Agurs-Collins, T., et al. (2017). Vital signs: trends in incidence of cancers associated with overweight and obesity – United States, 2005–2014. *MMWR* 66, 1052–1058. doi: 10.15585/mmwr.mm6639e1

Stratigopoulos, G., Leduc, C. A., Cremona, M. L., Chung, W. K., and Leibel, R. L. (2011). Cut-like homeobox 1 (cux1) regulates expression of the fat mass and obesity-associated and retinitis pigmentosa gtpase regulator-interacting protein-1-like (rpgrip1l) genes and coordinates leptin receptor signaling. *J. Biol. Chem.* 286, 2155–2170.

Stratigopoulos, G., Padilla, S. L., Leduc, C. A., Watson, E., Hattersley, A. T., Mccarthy, M. I., et al. (2008). Regulation of fto/ftm gene expression in mice and humans. *Am. J. Physiol. Regul. Integr. Comp. Physiol.* 294, R1185–R1196.

Stuart, E. C., Scandlyn, M. J., and Rosengren, R. J. (2006). Role of epigallocatechin gallate (egcg) in the treatment of breast and prostate cancer. *Life Sci.* 79, 2329–2336. doi: 10.1016/j.lfs.2006.07.036

Su, R., Dong, L., Li, C., Nachtergaele, S., Wunderlich, M., Qing, Y., et al. (2018). R-2hg exhibits anti-tumor activity by targeting fto/ma/myc/cebpa signaling. *Cell* 172, 90.e23–105.e23. doi: 10.1016/j.cell.2017.11.031

Su, R., Dong, L., Li, Y., Han, L., Gao, M., Wunderlich, M., et al. (2019). Effective novel fto inhibitors show potent anti-cancer efficacy and suppress drug resistance. *Blood* 134, 233–233. doi: 10.1182/blood-2019-124535

Sun, Q., Chen, X., Ma, J., Peng, H., Wang, F., Zha, X., et al. (2011). Mammalian target of rapamycin up-regulation of pyruvate kinase isoenzyme type m2 is critical for aerobic glycolysis and tumor growth. *Proc. Natl. Acad. Sci. U.S.A.* 108, 4129–4134. doi: 10.1073/pnas.1014769108

Tan, J., Dorajoo, R., Seielstad, M., Sim, X., Ong, R. T., Chia, K., et al. (2008). Fto variants are associated with obesity in the chinese and malay populations in singapore. *Diabetes* 57, 2851–2857. doi: 10.2337/db08-0214

Tang, Q.-Q., Otto, T. C., and Lane, M. D. (2003). Mitotic clonal expansion: a synchronous process required for adipogenesis. *Proc. Natl. Acad. Sci. U.S.A.* 100, 44–49.

Tanofsky-Kraff, M., Han, J. C., Anandalingam, K., Shomaker, L. B., Columbo, K. M., Wolkoff, L. E., et al. (2009). The fto gene rs9939609 obesity-risk allele and loss of control over eating. *Am. J. Clin. Nutr.* 90, 1483–1488.

Tung, Y. C. L., Yeo, G. S. H., O'rahilly, S., and Coll, A. P. (2014). Obesity and fto: changing focus at a complex locus. *Cell Metab.* 20, 710–718.

Van Der Hoeven, F., Schimmang, T., Volkmann, A., Mattei, M., Kyewski, B., and Rüther, U. (1994). Programmed cell death is affected in the novel mouse mutant fused toes (ft). *Development* 120, 2601–2607.

Villalobos-Comparán, M., Flores-Dorantes, M. T., Villarreal-Molina, M. T., Rodríguez-Cruz, M., García-Ulloa, A. C., Robles, L., et al. (2008). The fto gene is associated with adulthood obesity in the mexican population. *Obesity* 16, 2296–2301.

Vucenik, I., and Stains, J. (2012). Obesity and cancer risk: evidence, mechanisms, and recommendations. *Ann. N.Y. Acad. Sci.* 1271, 37–43. doi: 10.1111/j.1749-6632.2012.06750.x

Wang, D., Chen, J., Chen, H., Duan, Z., Xu, Q., Wei, M., et al. (2012). Leptin regulates proliferation and apoptosis of colorectal carcinoma through pi3k/akt/mtor signalling pathway. *J. Biosci.* 37, 91–101. doi: 10.1007/s12038-011-9172-4

Wang, D., Wu, Z., Zhou, J., and Zhang, X. (2020). Rs9939609 polymorphism of the fat mass and obesity-associated (fto) gene and metabolic syndrome susceptibility in the chinese population: a meta-analysis. *Endocrine* 69, 278–285. doi: 10.1007/s12020-020-02280-x

Wang, P., Doxtader, K. A., and Nam, Y. (2016). Structural basis for cooperative function of mettl3 and mettl14 methyltransferases. *Mol. Cell* 63, 306–317. doi: 10.1016/j.molcel.2016.05.041

Wang, X., Lu, Z., Gomez, A., Hon, G. C., Yue, Y., Han, D., et al. (2014). N6-methyladenosine-dependent regulation of messenger rna stability. *Nature* 505, 117–120. doi: 10.1038/nature12730

Wang, X., Zhao, B. S., Roundtree, I. A., Lu, Z., Han, D., Ma, H., et al. (2015). N(6)-methyladenosine modulates messenger rna translation efficiency. *Cell* 161, 1388–1399. doi: 10.1016/j.cell.2015.05.014

Wei, C. M., Gershowitz, A., and Moss, B. (1975). Methylated nucleotides block 5′ terminus of hela cell messenger rna. *Cell* 4, 379–386. doi: 10.1016/0092-8674(75)90158-0

Wei, J., Liu, F., Lu, Z., Fei, Q., Ai, Y., He, P., et al. (2018). Differential ma, ma, and ma demethylation mediated by fto in the cell nucleus and cytoplasm. *Mol. Cell* 71, 973.e5–985.e5. doi: 10.1016/j.molcel.2018.08.011

Wei, R., Mao, L., Xu, P., Zheng, X., Hackman, R., Mackenzie, G., et al. (2018). Suppressing glucose metabolism with epigallocatechin-3-gallate (egcg) reduces breast cancer cell growth in preclinical models. *Food Funct.* 9, 5682–5696. doi: 10.1039/c8fo01397g

Wei, R., Penso, N. E. C., Hackman, R. M., Wang, Y., and Mackenzie, G. G. (2019). Epigallocatechin-3-gallate (egcg) suppresses pancreatic cancer cell growth, invasion, and migration partly through the inhibition of akt pathway and epithelial-mesenchymal transition: enhanced efficacy when combined with gemcitabine. *Nutrients* 11:1856. doi: 10.3390/nu11081856

Wen, W., Cho, Y. S., Zheng, W., Dorajoo, R., Kato, N., Qi, L., et al. (2012). Meta-analysis identifies common variants associated with body mass index in east asians. *Nat. Genet.* 44, 307–311. doi: 10.1038/ng.1087

White, E., and Dipaola, R. S. (2009). The double-edged sword of autophagy modulation in cancer. *Clin. Cancer Res.* 15, 5308–5316. doi: 10.1158/1078-0432.Ccr-07-5023

Wu, R., Liu, Y., Yao, Y., Zhao, Y., Bi, Z., Jiang, Q., et al. (2018a). Fto regulates adipogenesis by controlling cell cycle progression via m6a-ythdf2 dependent mechanism. *Biochim. Biophys. Acta Mol. Cell Biol. Lipids* 1863, 1323–1330. doi: 10.1016/j.bbalip.2018.08.008

Wu, R., Yao, Y., Jiang, Q., Cai, M., Liu, Q., Wang, Y., et al. (2018b). Epigallocatechin gallate targets fto and inhibits adipogenesis in an mrna m 6 a-ythdf2-dependent manner. *Int. J. Obes.* 42, 1378–1388. doi: 10.1038/s41366-018-0082-5

Yan, F., Al-Kali, A., Zhang, Z., Liu, J., Pang, J., Zhao, N., et al. (2018). A dynamic n 6-methyladenosine methylome regulates intrinsic and acquired resistance to tyrosine kinase inhibitors. *Cell Res.* 28, 1062–1076. doi: 10.1038/s41422-018-0097-4

Yang, S., Wei, J., Cui, Y.-H., Park, G., Shah, P., Deng, Y., et al. (2019). M 6 a mrna demethylase fto regulates melanoma tumorigenicity and response to anti-pd-1 blockade. *Nat. Commun.* 10, 1–14. doi: 10.1038/s41467-019-10669-0

Zhang, C., Zhang, M., Ge, S., Huang, W., Lin, X., Gao, J., et al. (2019). Reduced m6a modification predicts malignant phenotypes and augmented wnt/pi3k-akt signaling in gastric cancer. *Cancer Med.* 8, 4766–4781.

Zhang, D. L., Qu, L. W., Ma, L., Zhou, Y. C., Wang, G. Z., Zhao, X. C., et al. (2018). Genome-wide identification of transcription factors that are critical to non-small cell lung cancer. *Cancer Lett.* 434, 132–143. doi: 10.1016/j.canlet.2018.07.020

Zhang, L., Xie, J., Gan, R., Wu, Z., Luo, H., Chen, X., et al. (2019). Synergistic inhibition of lung cancer cells by egcg and nf-κb inhibitor bay11-7082. *J. Cancer* 10, 6543–6556. doi: 10.7150/jca.34285

Zhang, M., Zhang, Y., Ma, J., Guo, F., Cao, Q., Zhang, Y., et al. (2015). The demethylase activity of fto (fat mass and obesity associated protein) is required for preadipocyte differentiation. *PLoS One* 10:e0133788. doi: 10.1371/journal.pone.0133788

Zhang, X., Wei, L.-H., Wang, Y., Xiao, Y., Liu, J., Zhang, W., et al. (2019). Structural insights into fto's catalytic mechanism for the demethylation of multiple rna substrates. *Proc. Natl. Acad. Sci. U.S.A.* 116, 2919–2924. doi: 10.1073/pnas.1820574116

Zhang, Y., Fan, S., Hu, N., Gu, M., Chu, C., Li, Y., et al. (2012). Rhein reduces fat weight in db/db mouse and prevents diet-induced obesity in c57bl/6 mouse through the inhibition of pparγ signaling. *PPAR Res.* 2012: 374936.

Zhang, Y., Sowers, J. R., and Ren, J. (2018). Targeting autophagy in obesity: from pathophysiology to management. *Nat. Rev. Endocrinol.* 14, 356–376. doi: 10.1038/s41574-018-0009-1

Zhao, X., Yang, Y., Sun, B.-F., Shi, Y., Yang, X., Xiao, W., et al. (2014). Fto-dependent demethylation of n6-methyladenosine regulates mrna splicing and is required for adipogenesis. *Cell Res.* 24, 1403–1419. doi: 10.1038/cr.2014.151

Zheng, G., Cox, T., Tribbey, L., Wang, G. Z., Iacoban, P., Booher, M. E., et al. (2014). Synthesis of a fto inhibitor with anticonvulsant activity. *ACS Chem. Neurosci.* 5, 658–665. doi: 10.1021/cn500042t

Zhou, S., Bai, Z. L., Xia, D., Zhao, Z. J., Zhao, R., Wang, Y. Y., et al. (2018). Fto regulates the chemo-radiotherapy resistance of cervical squamous cell carcinoma (cscc) by targeting β-catenin through mrna demethylation. *Mol. Carcinogenesis* 57, 590–597.

Zhu, L., Dai, L., Yang, N., Liu, M., Ma, S., Li, C., et al. (2020). Transcription factorirx5 promotes hepatocellular carcinoma proliferation and inhibits apoptosis by regulating the p53 signalling pathway. *Cell Biochem. Funct.* 38, 621-629. doi: 10.1002/cbf.3517

Zhu, Q., Wu, Y., Yang, M., Wang, Z., Zhang, H., Jiang, X., et al. (2019). Irx5 promotes colorectal cancer metastasis by negatively regulating the core components of the rhoa pathway. *Mol. Carcinogenesis* 58, 2065–2076. doi: 10.1002/mc.23098

Conflict of Interest: The authors declare that the research was conducted in the absence of any commercial or financial relationships that could be construed as a potential conflict of interest.

frontiers in Oncology

ORIGINAL RESEARCH
published: 08 January 2021
doi: 10.3389/fonc.2020.526866

IL-37 Confers Anti-Tumor Activity by Regulation of m6A Methylation

Xiaofeng Mu[1,2†], Qi Zhao[2†], Wen Chen[3], Yuxiang Zhao[4,5], Qing Yan[2], Rui Peng[2], Jie Zhu[2], Chunrui Yang[6], Ketao Lan[2], Xiaosong Gu[1] and Ye Wang[2*]*

[1] Academy of Medical Engineering and Translational Medicine, Tianjin University, Tianjin, China, [2] Clinical Laboratory, Qingdao Central Hospital, The Second Affiliated Hospital of Medical College of Qingdao University, Qingdao, China, [3] Department of Hyperbaric Oxygen, Qingdao Central Hospital, The Second Affiliated Hospital of Medical College of Qingdao University, Qingdao, China, [4] Institute of Bioengineering, Biotrans Technology Co., LTD., Shanghai, China, [5] United New Drug Research and Development Center, Biotrans Technology Co., LTD., Ningbo, China, [6] Department of Pathology, Second Hospital of Tianjin Medical University, Tianjin, China

OPEN ACCESS

Edited by:
Zhifu Sun,
Mayo Clinic, United States

Reviewed by:
Yanqiang Li,
Boston Children's Hospital and Harvard Medical School, United States
Yanan Yang,
Mayo Clinic, United States

***Correspondence:**
Xiaosong Gu
xiaosonggu@tju.edu.cn
Ye Wang
yewang@qdu.edu.cn

[†]These authors have contributed equally to this work

Specialty section:
This article was submitted to Cancer Genetics, a section of the journal Frontiers in Oncology

Received: *08 August 2020*
Accepted: *26 November 2020*
Published: *08 January 2021*

Citation:
Mu X, Zhao Q, Chen W, Zhao Y, Yan Q, Peng R, Zhu J, Yang C, Lan K, Gu X and Wang Y (2021) IL-37 Confers Anti-Tumor Activity by Regulation of m6A Methylation. Front. Oncol. 10:526866. doi: 10.3389/fonc.2020.526866

N6-methyladenosine (m6A) is a common transcriptomic modification in cancer. Recently, it has been found to be involved in the regulation of non-small cell lung cancer (NSCLC) formation and metastasis. Interleukin 37 (IL-37) plays a crucial protective role in lung cancer. In our previous studies, we found that IL-37 is a potential novel tumor suppressor by inhibiting IL-6 expression to suppress STAT3 activation and decreasing epithelial-to-mesenchymal transition. Moreover, we found that treatment of IL-37 in lung cancer cells induced widespread and dynamic RNA m6A methylation. The effects of RNA m6A methylation of IL-37 treatment require further study. However, the functions of RNA m6A methylation of IL-37 treatment still await elucidation. Using MeRIP-seq and RNA-seq, we uncovered a unique m6A methylation profile in the treatment of IL-37 on the A549 cell line. We also showed the expression of m6A writers METTL3, METTL14, and WTAP and erasers ALKBH5 and FTO in A549 cells and lung cancer tissues after the treatment of IL-37. This study showed that IL-37 could lead to changes in m6A methylation level and related molecule expression level in A546 cells and may downregulate the proliferation by inhibiting Wnt5a/5b pathway in A549 cells. We conclude that IL-37 suppresses tumor growth through regulation of RNA m6A methylation in lung cancer cells.

Keywords: N6-methyladenosine, RNA methylation, interleukin 37, lung cancer, A549 cells

INTRODUCTION

N6-methyladenosine (m6A) is a common RNA modification and has been shown to be critically important in the regulation of tumorigenesis of alternative splicing, stability, and translation (1). m6A profiling experiments in various species revealed that its enrichment not only in ribosome-associated mRNA but also near stop codons or long internal exons (2–4). Regulation by m6A is determined by m6A methyltransferases (writers, including METTL3/4/14) (5), m6A-binding proteins [readers, including fat

mass and obesity-associated protein (FTO), and AlkB homolog 5 (ALKBH5)] (6, 7) and m6A demethylases (erasers, including YTHDC1 and YTHDF1) (8, 9). The role of m6A methylation is essential in various important biological processes, such as cellular differentiation, pluripotency, and stress response (10–12), particularly in cancer stem cell self-renewal and differentiation. Therefore, m6A may serve as an important pathway regulating initiation and progression in cancers (13, 14).

Interleukin (IL)-37 has been reported to have antitumor effects in hepatocellular carcinoma (HCC) (15), fibrosarcoma (16), breast cancer (17), and so on. IL-37 isolated *in silico* in 2000 (18), belongs to the IL-1 family and is also named IL-1F7. The IL-37 gene was mapped to chromosome 2, and the six exons of the IL-37 gene encode five isoforms (IL-37a–e). IL-37b is the largest isoform and has been best characterized so far (19). The N-terminus of IL-37 encloses a caspase-1 cleavage site (20) and must be cleaved by caspase-1 to be activated (21). IL-37 acts as an anti-inflammatory cytokine by inhibiting innate responses (22) and plays a pivotal role in acute and chronic inflammation inflammation by balancing the cytokine expression (23). Therefore, IL-37 may serve as a potential key factor in restoring inflammatory balance in cancer development and treatment. In our previous study, we found IL-37 can inhibit cell invasion and metastasis through the IL-6/STAT3 signaling in non-small cell lung cancer (NSCLC) (24). However, how IL-37 affects cell growth and its underlying mechanisms have not been fully elucidated.

How IL-37 suppresses human lung adenocarcinoma growth is not completely understood. Given broad regulatory roles of IL-37 in cell growth, we hypothesized that IL-37 confers anti-tumor activity through regulation of m6A methylation. We studied the m6A status of IL-37–treated human lung adenocarcinoma A549 cells and investigated the differences between the m6A modification patterns of untreated controls and the IL-37 treated model. To explore the protective role of IL-37 in lung cancer, we performed an m6A-specific RNA immunoprecipitation assay coupled with high throughput sequencing (MeRIP-seq). We also tested the expression of m6A writers METTL3, METTL14, and WTAP and of erasers ALKBH5 and FTO after the treatment of IL-37 in A549 cells and lung cancer tissues. This study showed that IL-37 could lead to changes in m6A methylation level and related molecule expression level in A546 cells, and may downregulate the proliferation by inhibiting Wnt5a/5b pathway in A549 cells.

MATERIAL AND METHODS

Cell Culture and Treatment

The human NSCLC A549 cell line was obtained from the Shanghai Institute of Cell Biology of the Chinese Academy of Sciences (Shanghai, China) and preserved in the biotechnology therapeutic center at our hospital. Cells were cultured at 37°C in 90% Dulbecco's modified Eagle medium (DMEM) (Thermo Fisher Scientific, Inc., Waltham, MA, USA) plus 10% fetal bovine serum (FBS) (Life Technologies, Gaithersburg, MD, USA) supplemented with 1% penicillin/streptomycin. Cells were treated with lentivirus (Lv)-expressing IL-37 (HanBio, Shanghai, China) for at least 72 h. Lv-expressing green fluorescent protein (GFP) served as a control.

Global m6A/m Measurements

The global m6A/m in total RNA was detected with the EpiQuik m6A/m RNA Methylation Quantification Kit (Epigentek Group, Farmingdale, NY, USA) following manufacturers' specifications with 100–300 ng input RNA (in triplicate).

RNA Preparation, RNA MeRIP-Seq Library Construction and Sequencing

For Lv-IL-37 or Lv-GFP treated cells, three biological replicates were selected. Total RNA was extracted from A549 cells using an RNeasy® Mini Kit (QIAGEN, Valencia, CA, USA) according to the manufacturer's directions. To eliminate the ribosomal RNA from total RNAs, we used the Ribo-Zero rRNA Removal Kit (Illumina, Inc., CA, USA), and the RNA was then fragmented into pieces of about 100 nt nucleotides using the M220 Focused-ultrasonicator (Covaris. Woburn, MA, USA). Fragmented RNA was incubated with anti-m6A antibody 202,003 (Synaptic Systems, Göttingen, Germany) for 2 h in IP buffer (50 mM Tris-HCl, 750 mM NaCl and 0.5% Igepal CA-630) in accordance with a previously referenced study (25). The mixture was then purified with Protein A beads and precipitated by 75% ethanol. Purified RNA was used for NEBNext® Ultra™ Directional RNA Library Prep Kit (New England Biolabs, MA, USA) according to a published protocol (26). Sequencing was performed on an Illumina HiSeq 4000 sequencer (Illumina, Inc.) with 2 × 100 100 cycles Solexa paired-end sequencing.

Data Analysis

Sequence analyses were performed using the procedure described by Luo, Zhang et al. (27). The Q30 was used as quality control of the paired-end reads, the 3′ adaptors were trimmed, and cutadapt software (v1.9.3) was used to remove the low-quality reads. HISAT2 software (v2.0.4) was used to align the clean reads of all libraries to the reference genome (hg18) (28). MACS software was used to detect the peaks with a score (−10*log10, *p*-value) of >3 (29). Differentially methylated sites with a fold change cutoff of ≥2 and a false discovery rate cutoff of ≤0.0001 were identified using the diffReps differential analysis package (30). Gene expression was calculated with Cufflinks (31) using the input-sequencing reads, and Cuffdiff software was used to find the different expression genes of IL-37 treated and untreated cells. DAVID tool and Kyoto Encyclopedia of Genes and Genomes (KEGG) were used for gene function analysis (GO enrichment) pathway enrichment analysis. The *p*-value denotes significant pathway correlated to the conditions.

Western Blotting

Lv-IL-37 treated and untreated A549 cells were collected and ruptured with RIPA lysis buffer (Sigma-Aldrich, St. Louis, MO, USA) containing 5 mM of EDTA, PMSF, cocktail inhibitor,

and phosphatase inhibitor cocktail. Cell extracts were resolved by SDS-polyacrylamide gel electrophoresis and transferred onto polyvinylidene difluoride (PVDF) membranes. Membranes were blocked with 5% BSA in tris-buffered saline containing 0.1% Tween 20 (TBST buffer) and incubated with anti-Wnt5a antibody (ab179824) and anti-Wnt5b antibody (ab124818, Cambridge, UK). The membranes were then incubated with secondary antibodies and appropriate chemiluminescent substrates.

Proliferation Assay

Lv-IL-37 treated and untreated A549 cells (5 × 103) were seeded into 96 well plates, and proliferation assay was performed with the MTT (3-(4, 5-dimethyl thiazol-2-yl) 2, 5-diphenyltetrazolium bromide) method. Four, 24, 48, 72, and 96 h later, 10 µl MTT (final concentration, 5 mg/ml) was added, and the purple formazan crystals were then dissolved by adding 100 µl acid-isopropanol (0.04 N HCl in isopropanol) into each well. The absorbance was determined at 550 nm against a reference wavelength of 630 nm and stimulation index (SI).

Transwell Cell Migration and Invasion Assay

Transwell cell migration and invasion assay were analyzed according to the procedure described by Justus CR (32).

Statistical Analysis

Two-tailed *t*-test was used to identify significantly different expression level between two groups ($p < =0.05$) in western blotting. Data are presented as the mean ± SEM.

RESULTS

Expression of m6A Methylation Related Proteins in IL-37 Treated A549 Cells

Firstly, we tested the expression of methylation related proteins by western blot. As shown in **Figure 1A**, the protein level of METTL3 and YTHDF3 were much higher in IL-37 treated A549 cells than in non-treated control. The protein expression of METTL14, WTAP, and ALKBH5 decreased in IL-37 treated A549 cells, compared with that in non-treated control. However, there were no significant differences of FTO and YTHDF2 between IL-37 treated A549 cells and control. From these results, the downregulation of ALKBH5 maybe one of the potential reasons for the significant decrease in the overall methylation of RNA after IL-37 treatment of A549 cells. As shown in **Figure 1B**, survival analysis of functional genes related to m6A modification shows that YTHDF2 significantly affects the survival of lung cancer patients, and the low expression of YTHDF2 is a visible risk factor, which indicates that the expression level of m6A reader is related to the prognosis of lung cancer patients.

The Expression of IL-37 Is Downregulated in Human Lung Adenocarcinoma

Data on mRNA expression from lung adenocarcinoma and matched adjacent, non-cancerous tissues were downloaded from the Cancer Genome Atlas (TCGA) data portal (https://tcga-data.nci.nih.gov/tcga/) that represent a total of 48 lung adenocarcinoma samples without metastases. The differential expression analysis of IL-37 between the lung adenocarcinoma and matched tumor normal tissues showed that the expression of IL-37 was lower in lung adenocarcinoma tissues than in adjacent, non-cancerous tissues (**Figure 2A**). Compared with normal human lung epithelial cell line BEAS-2b, a similar downregulation of IL-37 was also observed in human LAD A549, SPC-A-1, Calu-3, NCI-H1395, NCI-H1975 cell lines (**Figure 2B**). In primary tumors, the degree of IL-37 downregulation was greater in stages I and II than in stages 0 (**Figure 2C**). Based on the data of 445 cases from cbioportal (https://www.cbioportal.org/), and the analysis of Kaplan–Meier (http://kmplot.com/analysis/), IL-37 might have an effect on overall patient survival, which suggesting IL-37 can be potentially used as an independent prognostic marker (**Figure 2D**).

General Features of m6A Methylation in IL-37 Treated and Untreated A549 Cells

To identify the role of IL-37 on the alteration of m6A modification in A549 cells, we compared the m6A distribution in control and IL-37 treated cells using the colorimetric m6A quantification assay. We found higher global m6A modification sites in IL-37 treated cells than in IL-37 untreated cells (**Figure 3A**).

To explore the mechanism underlying IL-37's inhibition of cell invasion and metastasis through alteration of m6A modification, we mapped the m6A methylome in IL-37 treated and untreated A549 cells by methylated RNA immunoprecipitation coupled with next generation sequencing (MeRIP-seq or m6A-seq). The results revealed significantly different m6A methylome profiles. There were 2005 non-overlapping m6A peaks in IL-37 untreated cells within 1647 coding gene transcripts (mRNAs) and 231 non-overlapping m6A peaks within 220 long non-coding RNAs (lncRNAs) in two biological replicates. In IL-37 treated cells, there were 1,498 non-overlapping m6A peaks within 1,300 mRNAs and 180 non-overlapping m6A peaks within 175 lncRNAs in two biological replicates. Of these, 35 peaks within mRNAs were overlapped between the IL-37 treated and untreated cells (**Figure 3B**) and only one peak within lncRNAs was overlapped (**Figure S1**).

The results of the motif analysis of 1,000 peaks within mRNAs with the highest scores (−10*log10, p-value) showed that IL-37 binding sites have abundant conserved m6A motif (**Figure 3C**).

We also found that, for mRNA assay, 81.2% of the m6A-methylated coding genes in the control group (85.5% in the IL-37 treated cells) contained only one m6A peak, and 14.9% of the m6A-methylated coding genes in the control group (12.2% in the IL-37 treated cells) contained two m6A peaks (**Figure 2D**). For lncRNA assay, 96.0% of the m6A-methylated coding genes in the control group (96.6% in the IL-37 treated cells) contained only one m6A peak, and 3.19% of the m6A-methylated coding

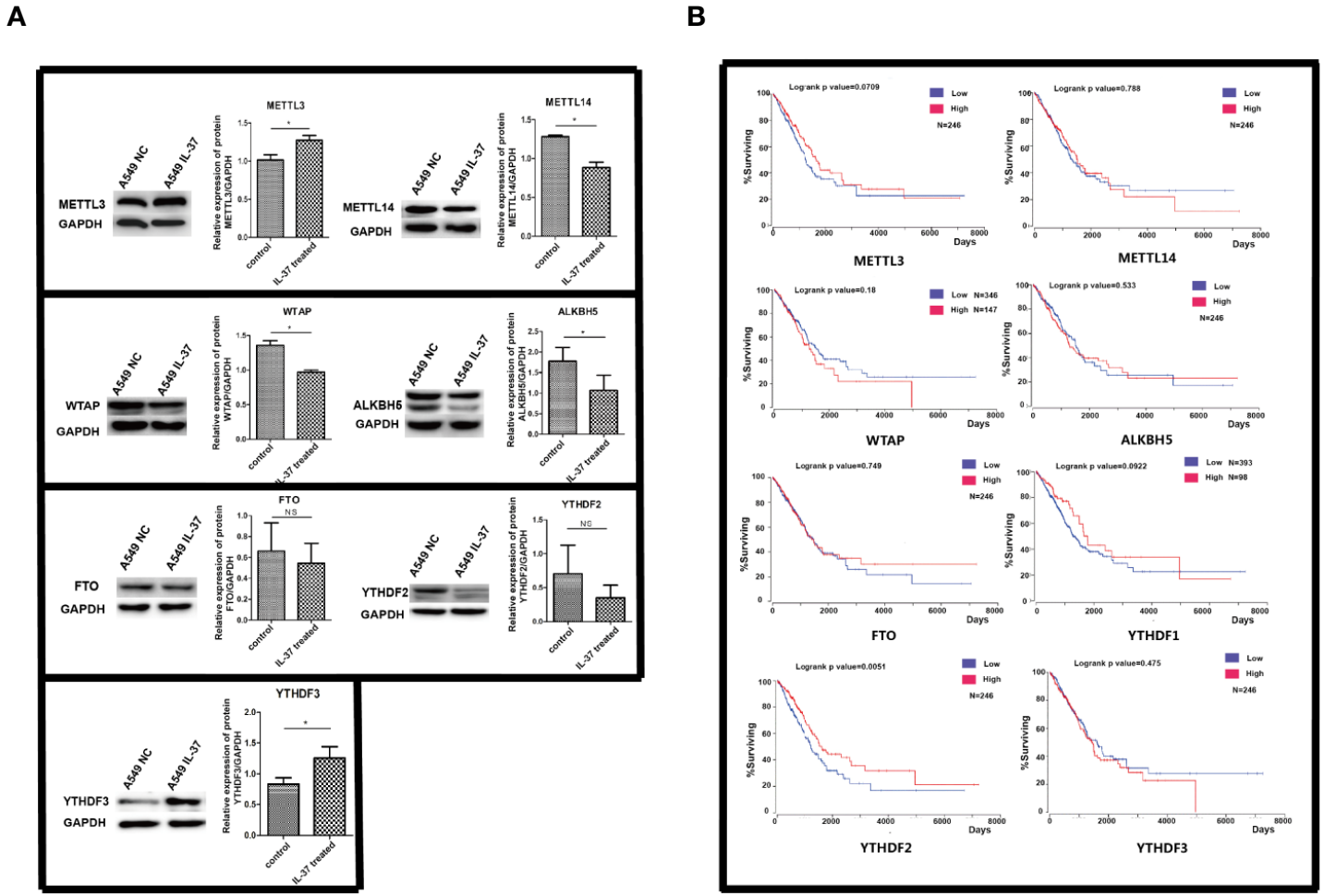

FIGURE 1 | **(A)** Expression of m6A methylation related proteins in IL-37 treated A549 cells. Data are mean ± SEM. *$P < 0.05$. **(B)** The results of survival analysis of proteins with m6A changes using public lung cancer data from TCGA database.

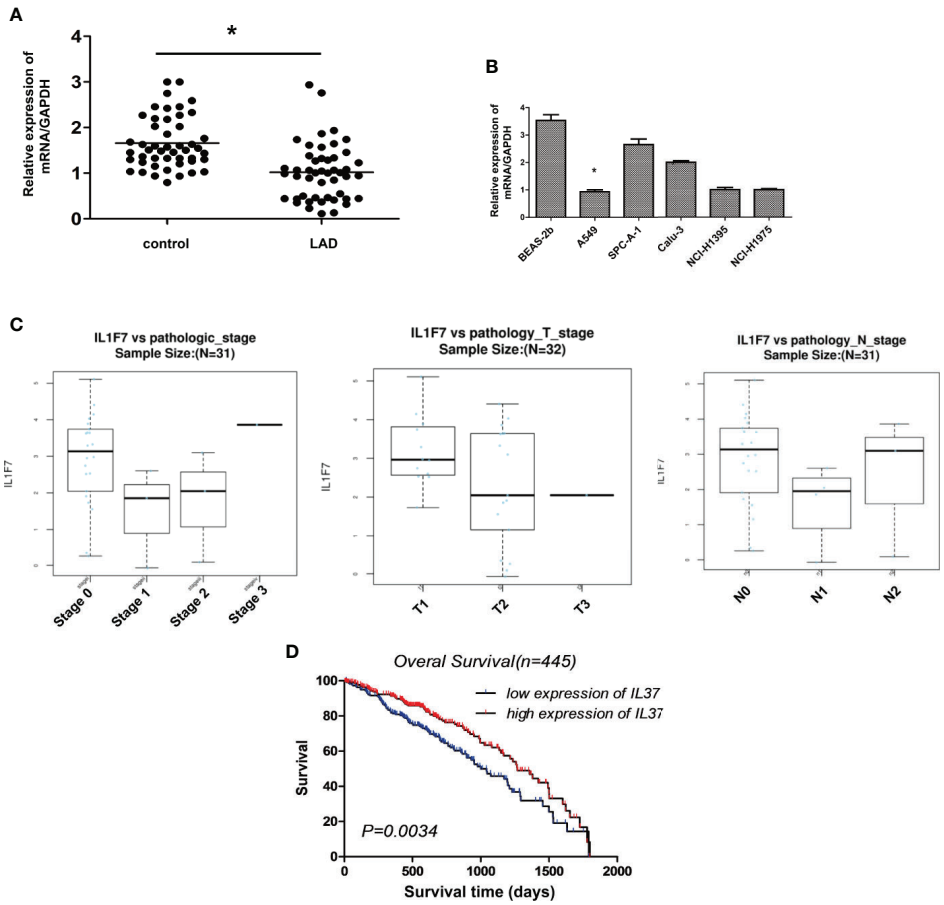

FIGURE 2 | The expression of IL-37 is downregulated in human lung adenocarcinoma (LAD). **(A)** The results of differential expression analysis of IL-37 between the lung adenocarcinoma and matched tumor normal tissues. Data are mean ± SEM (n = 48 per group); **(B)** The expression of IL-37 in different LAD cell lines. Data are mean ± SEM (n = 6 per group); **(C)** The degree of IL-37 downregulation was greater in stages I and II than in stages 0 in primary LAC tumors. Data are mean ± SEM (n = 10 per group); **(D)** Results of analysis from starBase. Data are mean ± SEM. *$P < 0.05$.

genes in the control group (3.43% in the IL-37 treated cells) contained two m6A peaks (**Figure 3D**).

We further investigated the m6A distribution patterns of total peaks within mRNAs. Peaks were categorized into seven transcript segments: the 5′ untranslated region (UTR), the start codon segment (400 nucleotides centered on the start codon), the stop codon segment (400 nucleotides centered on the stop codon), the 3′ UTR, the intron region, the exon region, and the unknown region (other). The results show a similar pattern of total m6A distribution in the control and in IL-37 treated cells. In the control group, the total m6A peaks included 1,021 peaks from exon (50.05%), 480 peaks from 3′ UTR (23.53%), 218 peaks from intron (10.69%), and 158 peaks from 5′ UTR (7.75%). In IL-37 treated cells, the total m6A peaks included 758 peaks from exon (49.45%), 352 peaks from 3 UTR (22.96%), 182 peaks from intron (11.87%), and 102 peaks from 5– UTR (6.65%) (**Figure 3E**). We also found that m6A peaks had a higher fold enrichment in stop codon segments both in the control group and IL-37 treated cells (**Figure 3F**). The profiling of the m6A peaks or signals compared between the IL-37 and control samples is shown in **Tables S1** and **S2**.

M6A Distribution of Differentially Methylated m6A Sites

We next analyzed the distribution of m6A for both IL-37 treated and untreated cells. In total, we identified 604 differentially hypermethylated sites within 567 coding genes and 451 differentially hypomethylated sites within 430 coding genes (IL-37 treated cells *vs* untreated cells) (**Table 1**). Also, 198 DMMSs within 192 lncRNA genes were hypermethylated sites, and 165 DMMSs within 160 lncRNA genes were hypomethylated sites (IL-37 treated cells *vs* untreated cells) (**Table 1**). **Tables 2** and **3** show the top ten hypomethylated m6A sites within mRNAs with the highest fold change values.

To access the distribution profile, we mapped all DMMSs within mRNAs and lncRNAs to chromosomes, as shown in – When the number of DMMSs harbored by chromosomes was

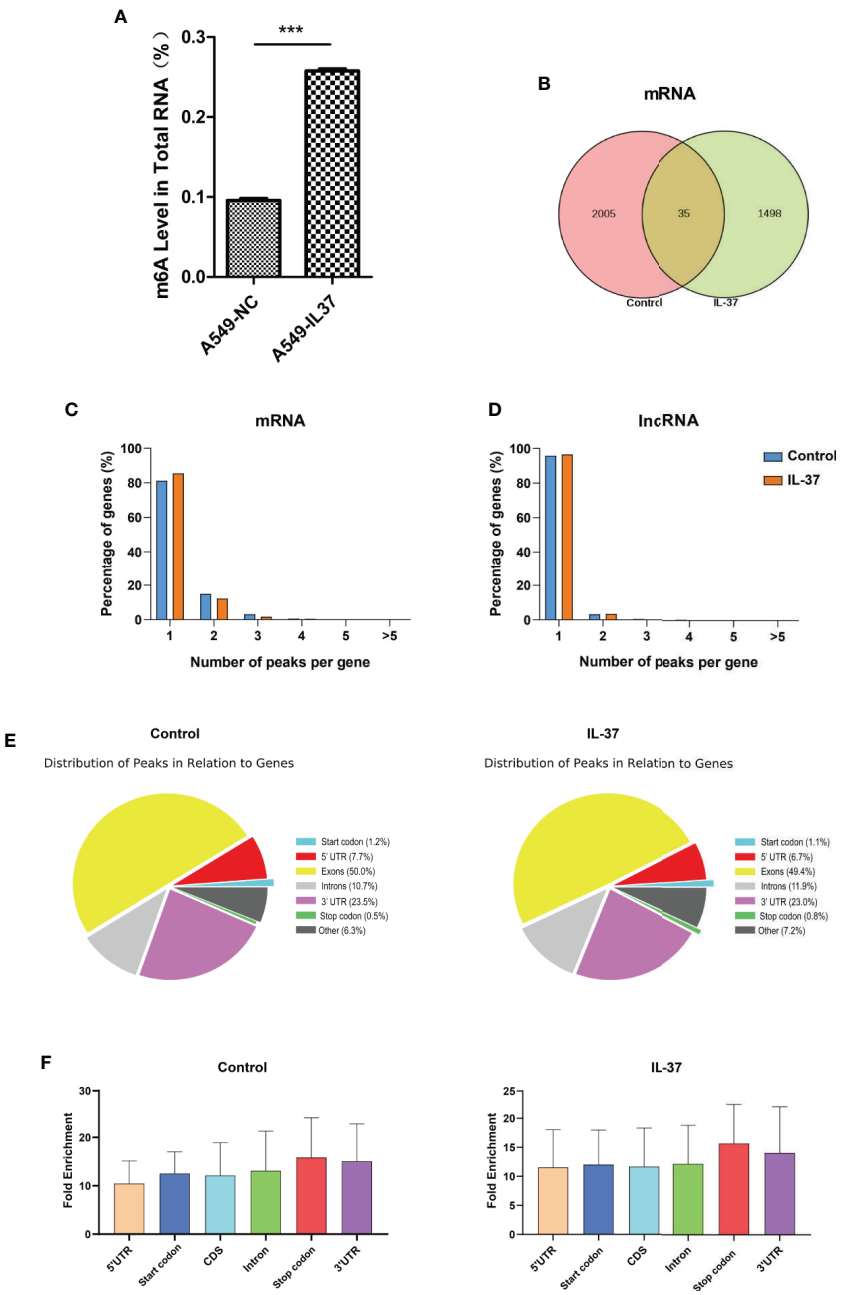

FIGURE 3 | General features of m6A methylation in IL-37 treated and untreated A549 cells. **(A)** Higher global m6A modification sites in IL-37 treated cells than in IL-37 untreated cells. Data are mean ± SEM (n = 6 per group) (*** means $P < 0.001$); **(B)** Venn diagram showing the overlap of m6A peaks within mRNAs in two groups; **(C)** Proportion of mRNAs harboring different numbers of m6A peaks in two groups. The majority of genes harboring only one m6A peak; **(D)** Proportion of lncRNAs harboring different numbers of m6A peaks in two groups. The majority of genes harboring also only one m6A peak; **(E)** Pie charts showing the percentage of m6A peaks in nonoverlapping segments of transcripts; **(F)** Distributions of fold enrichment of m6A peaks. Data are mean ± SEM.

TABLE 1 | General numbers of differentially methylated peaks and associated genes.

Item	Upmethylated peak	Upmethylated gene	Downmethylated peak	Downmethylated gene
mRNA	604	567	451	430
lncRNA	198	192	165	160

TABLE 2 | Top 10 upmethylated peaks.

Chromosome	txStart	txEnd	Gene name	Fold change
chr2	131414301	131414500	POTEJ	117.5
chr21	39671701	39671920	KCNJ15	93.1
chr19	54720201	54720500	LILRB3	74.7
chr1	53074221	53074420	GPX7	73.7
chr4	73148821	73149120	ADAMTS3	70.9
chr6	117710661	117710860	ROS1	66.5
chr11	64513981	64514180	PYGM	53.9
chr18	65177321	65177540	DSEL	50.3
chr19	46916541	46916780	CCDC8	49.1
chr1	31887221	31887420	SERINC2	49.1

txStart/txEnd, Start/end position of the differentially methylated RNA peaks.

TABLE 3 | Top 10 downmethylated peaks.

Chromosome	txStart	txEnd	Gene name	Fold change
chr2	231281470	231281596	SP100	103.2
chr3	156763561	156763780	LEKR1	84.1
chr2	207041181	207041460	GPR1	81.6
chr9	684421	684574	KANK1	75.3
chr3	52715761	52715836	PBRM1	48.3
chr16	3293321	3293540	MEFV	48.3
chr11	129733530	129733640	NFRKB	47.1
chr21	30925961	30926025	GRIK1	45.8
chr2	61404552	61404560	AHSA2	45.8
chr9	113312128	113312340	SVEP1	44.5

txStart/txEnd, Start/end position of the differentially methylated RNA peaks.

normalized by the length of the respective chromosomes, the altered m6A peaks were transcribed from chromosomes 19, 17, 16, and 12 (**Figure S2B**). Further analysis showed that most identified DMMSs within mRNAs were mainly enriched in coding sequence (CDS) (**Figure S2C**). Of both the hypermethylated and hypomethylated sites, those within the 3′ UTR had the highest fold change (**Figure S2D**).

GO and KEGG Pathway Analysis

To reveal the functions of m6A methylation in IL-37 treated A549 cells, protein coding genes containing DMMSs were tested by GO and KEGG pathway analysis. For the biological process (BP) category, genes with up-methylated m6A sites were significantly ($p < 0.05$) enriched in regulation of RNA exported from the nucleus, nucleobase-containing compound transports, protein–DNA complex subunit organization, and positive regulation of nucleobase-containing compound metabolic process (**Figure 4A1**), while genes with down-methylated m6A sites were highly enriched in regulation of protein imported into the nucleus, regulation of protein imports, regulation of nucleobase-containing compound metabolic process, and regulation of cellular macromolecule biosynthetic process (**Figure 4A2**). The results of the cellular component (CC) and molecular function (MF) are shown in **Figure S3**. The results of the KEGG pathway analysis of DMMS- containing lncRNA-associated genes demonstrated that hypermethylated genes were significantly associated with regulation of the NOD-like receptor signaling pathway and arginine and proline metabolism (**Figure 5A**). Hypomethylated genes were significantly associated with regulation of the actin cytoskeleton pathway, oxytocin signaling pathway, and cell adhesion molecules (CAMs) pathway (**Figures 4B1, 4B2**). These results suggest that differentially methylated RNAs are involved in important biological pathways of IL-37 treated A549 cells, such as Wnt-5a, within which m6A was hypermethylated (IL-37 treated A549 cells *vs* untreated control) near the start codon (**Figure 5A**), and Wnt-5b, within which m6A was hypomethylated upstream of the 5′ UTR (**Figure 5B**). Next, the protein expression of Wnt5a and Wnt5b was also down-regulated after IL-37 treatment (**Figure 5C**). Whereas, the correlation between down-regulation of ALKBH5 and Wnt5a or Wnt5b should be investigated further.

Analysis of RBPs of Differentially Methylated mRNAs

To investigate how the above DMMSs act on the genes, we analyzed the RBPs of differentially methylated mRNAs through the RMBase v2.0 database (33). From this database, we obtained the modification sites and related RBP-binding regions. A total of 22 proteins were predicted to be RBPs (**Figure 6A**). The RBPs were highly distributed with a fold change (log2) = approximately −2. Then, GO enrichment analysis was performed to determine the function of the RBP genes. For the BP category, RBP genes were mainly enriched in processes associated with regulation of the mRNA metabolic process and cytokine-mediated signaling pathway (**Figure 6B**). For the CC category, RBP genes were enriched in the cytoplasmic ribonucleoprotein granule (**Figure 6C**). For the MF category, those genes were mainly related to N6-methyladenosine-containing RNA binding, mRNA 3′ UTR binding, and ribonucleoprotein complex binding (**Figure 6D**).

DISCUSSION

In the tumor microenvironment, production and secretion of multiple cytokines are disordered, and the immune function of the body is dysfunctional, which reduces the body's anti-tumor ability (34, 35). In recent years, changes in the expression levels of various cytokines have become a hot topic in tumor immunology research.

IL-37 is not only an inflammatory inhibitor but also an inhibitor of inherent inflammatory and immune responses (36), and it may play a role in inhibiting tumor growth in the tumor microenvironment (37). It was reported the elevated serum levels of interleukin-37 was correlated with poor prognosis in gastric cancer (38). The level of IL-37 in the serum of renal cell carcinoma patients was significantly lower than that in a healthy control group and was negatively correlated with the TNM Classification of Malignant Tumors

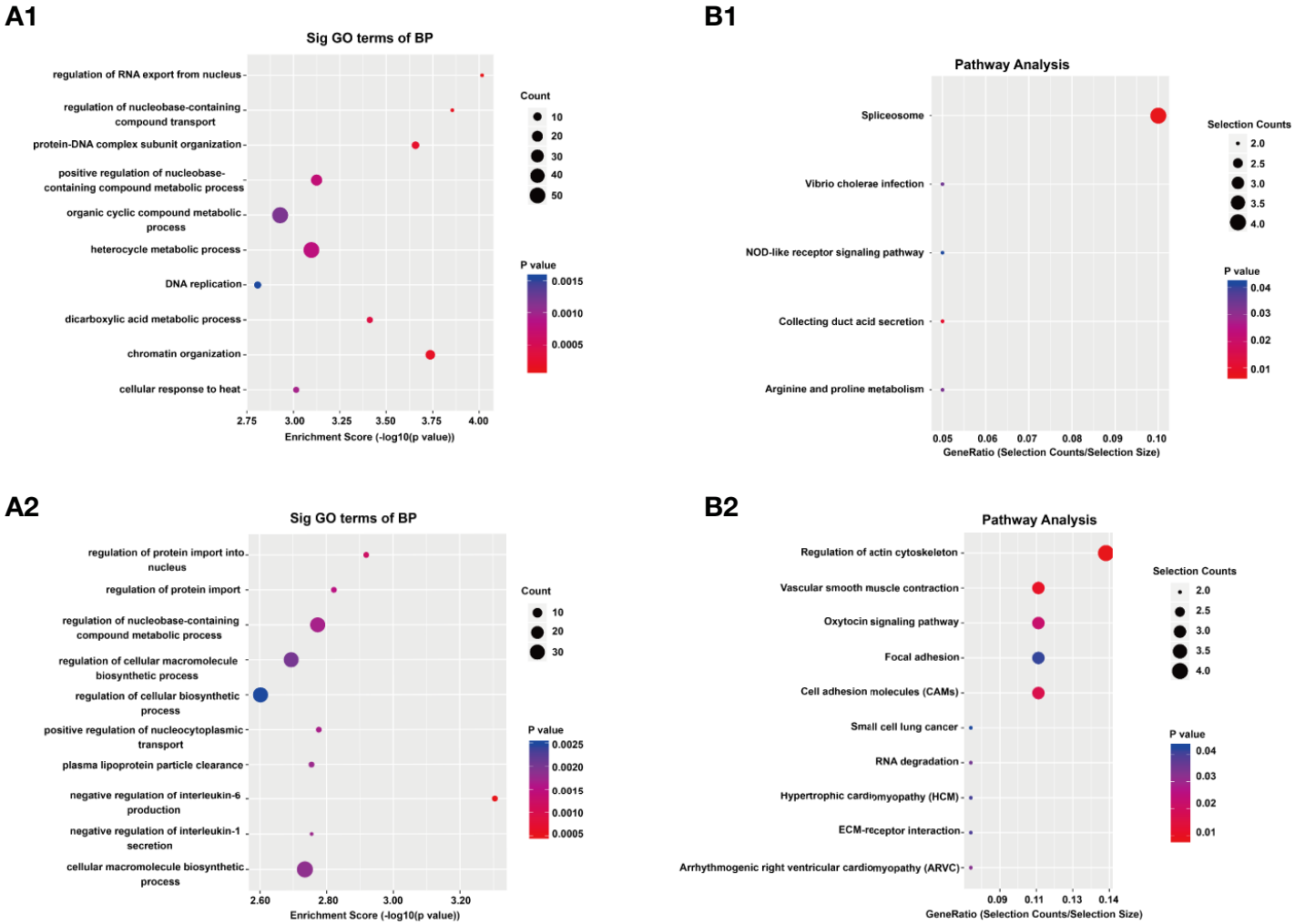

FIGURE 4 | Results of Gene ontology (GO) and Kyoto Encyclopedia of Genes and Genomes analyses. **(A)** Gene ontology (GO) analyses of coding genes harboring differentially methylated N6-methyladenosine sites. The GO classifications biological process (BP) in the most significantly hypermethylated genes (A1); BP in the most significantly hypomethylated genes (A2). **(B)** Kyoto Encyclopedia of Genes and Genomes analyses of coding genes harboring differentially methylated N6-methyladenosine sites. Pathway analysis of the most significantly hypermethylated genes (B1); Pathway analysis of the most significantly hypomethylated genes (B2).

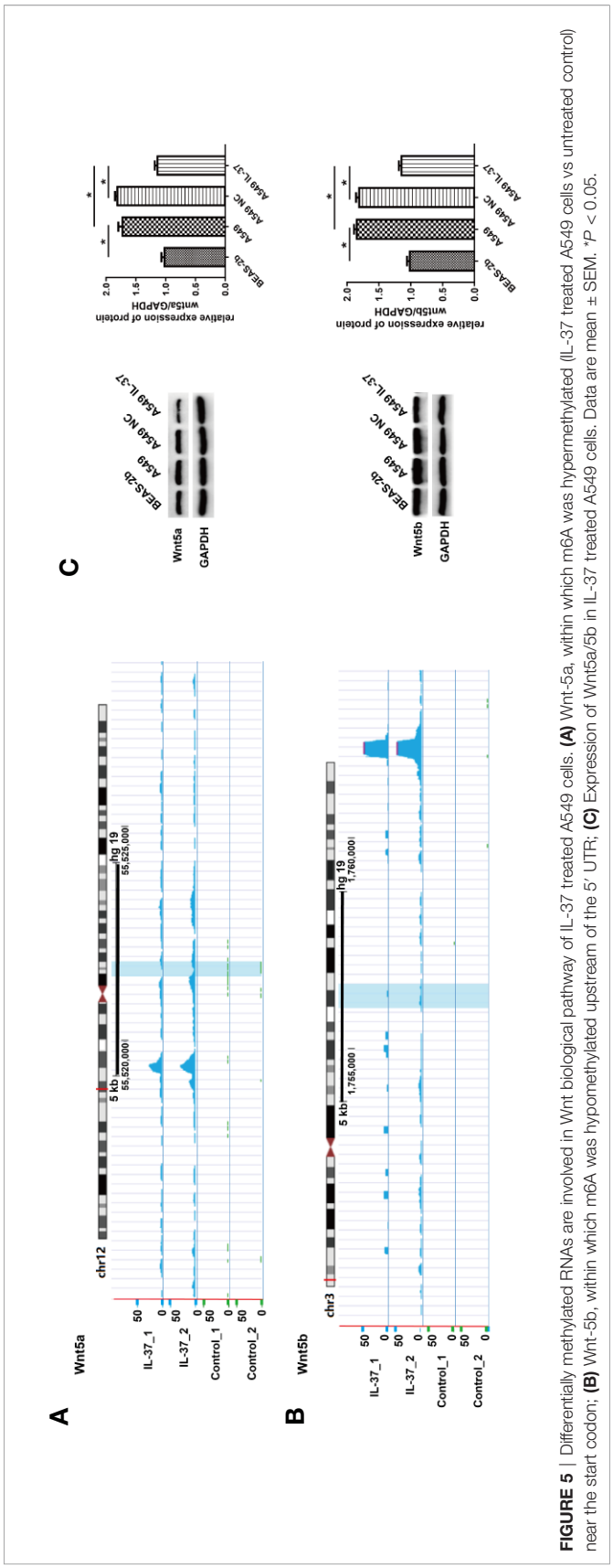

FIGURE 5 | Differentially methylated RNAs are involved in Wnt biological pathway of IL-37 treated A549 cells. **(A)** Wnt-5a, within which m6A was hypermethylated (IL-37 treated A549 cells vs untreated control) near the start codon; **(B)** Wnt-5b, within which m6A was hypomethylated upstream of the 5′ UTR; **(C)** Expression of Wnt5a/5b in IL-37 treated A549 cells. Data are mean ± SEM. *$P < 0.05$.

(TNM) stage of the tumor (39). When IL-37 levels are normal, non-hepatocellular carcinoma tissues are minimal and negatively correlated with the tumor size, microvascular metastasis, and BCLC staging of hepatocellular carcinoma (40). Our previous research showed the plasma IL-37 level in an NSCLC group was significantly lower than that in a healthy control group and that a more advanced TNM stage was associated with a more precipitous drop in IL-37 (24). We found that a decrease in IL-37 expression level is closely related to the occurrence and development of NSCLC and that increased tumor malignancy is associated with a more significant decrease in IL-37 expression. In this study, we found that the expression of IL-37 in lung adenocarcinoma tissue was significantly reduced compared to adjacent controls. After IL-37 was overexpressed in lung cancer cell line A549 cells, the overall methylation level of RNA increased significantly, suggesting that the inhibitory effect of IL-37 on the proliferation of lung adenocarcinoma cells may be caused by RNA methylation.

The most common RNA methylation modifications are m6A (N6-methyladenosine, 6-methyl adenine) and uridylation (U-tail) (25). m6A modification occurs in the methylation modification of the adenine (A) of RNA, such as mRNA and lncRNA, and U-tail occurs in the uracil modification of RNA, which is usually related to the RNA degradation. RNA modification can regulate the stability, localization, transport, splicing, and translation of RNA at the post-transcriptional level, such as the translation and alternative splicing of mRNA and the maturation of microRNA (41). Reversible RNA methylation regulates gene expression mainly at the post-transcriptional level.

Before its identification as an RNA demethylase, ALKBH5 is a dioxygenase that uses α-ketoglutarate and O2 as substrates in the m6A demethylation reaction (7). It was reported that hypoxia induces the breast cancer stem cell phenotype by HIF-dependent and ALKBH5-mediated m6A-demethylation of NANOG mRNA (42). ALKBH5 also maintains tumorigenicity of glioblastoma stem-like cells by sustaining FOXM1 expression and cell proliferation program (14). In the present study, we found the expression of ALKDH5 decreased significantly after IL-37 overexpression, which is potentially a reason for the significant decrease in the overall methylation of RNA.

The Wnt signaling pathways are a group of signal transduction pathways which begin with proteins that pass signals into a cell through cell surface receptors (43). It directly controls the expression levels of a large number of genes related to growth and metabolism and is involved in the regulation of a variety of biological processes, including embryonic growth and morphological development, tissue stability, the balance of energy metabolism, and stem cell maintenance. The excessive activation of the Wnt pathway is closely related to the occurrence of a variety of cancers (including colon cancer, gastric cancer, and breast cancer) (44). In this study, we found the expression of Wnt5a/5b decreased significantly, which prompted us to speculate that Wnt5a/5b may be affected by IL-37 methylation. However, the mechanisms of how IL-37 affected Wnt5a/5b pathway need to be further studied.

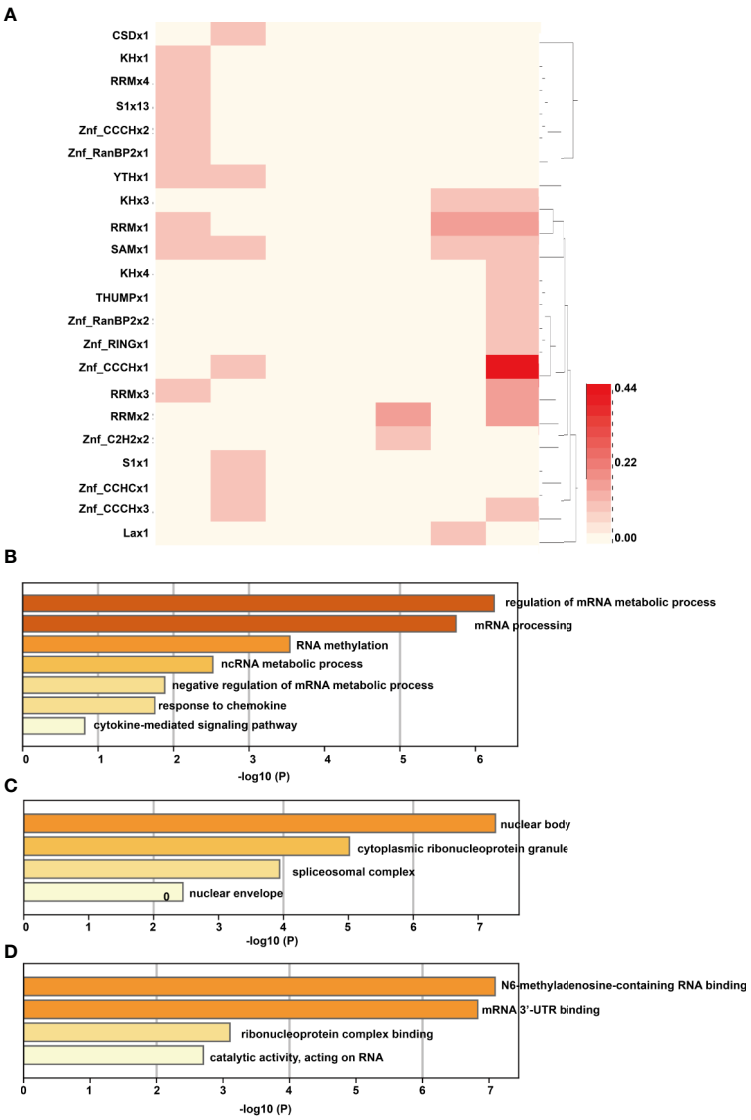

FIGURE 6 | Analysis of RBPs of differentially methylated mRNAs. **(A)** The RNA binding proteins of differentially methylated mRNAs; the column of the heatmap represents the expression level of RNA (log2FC), with the first column on the left being –3 and the last column on the right as 3. **(B)** For the BP category, RBP genes were mainly enriched in processes associated with regulation of the mRNA metabolic process and cytokine-mediated signaling pathway; **(C)** For the CC category, RBP genes were enriched in the cytoplasmic ribonucleoprotein granule; **(D)** For the MF category, those genes were mainly related to N6-methyladenosine-containing RNA binding, mRNA 3′ UTR binding, and ribonucleoprotein complex binding.

DATA AVAILABILITY STATEMENT

The original contributions presented in the study are publicly available. This data can be found here: https://www.ncbi.nlm.nih.gov/sra/PRJNA603214.

ETHICS STATEMENT

This study was approved by the Institutional Ethics Committee for Clinical Research and Animal Trials of the Qingdao Central Hospital, The Second Affiliated Hospital of Medical College of Qingdao University. Informed consents were obtained from all patients before analysis. All the experimental methods involved in this study comply with the Helsinki Declaration.

AUTHOR CONTRIBUTIONS

XM, QZ, WC, and RP conceived and performed experiments. YZ and QY analyzed data and performed the bioinformatics analysis. LX, JL, JZ, and CY performed experiments. KL and XG provided

supervision. YW conceived the project, analyzed data, wrote the manuscript, and provided supervision. All authors contributed to the article and approved the submitted version.

FUNDING

This study was supported by the National Natural Science Foundation of China (No. 81670822, 81370990, and 81800805), and Qingdao Key Research Project (No. 17-3-3-10-nsh and 19-6-1-3-nsh).

ACKNOWLEDGMENTS

We would like to thank Ms. Meifang Dai (CloudSeq Biotech Inc., Shanghai 201612, PR China) for their excellent technical support.

SUPPLEMENTARY MATERIAL

The Supplementary Material for this article can be found online at: https://www.frontiersin.org/articles/10.3389/fonc.2020.526866/full#supplementary-material

SUPPLEMENTARY FIGURE 1 | In IL-37 treated cells, there were 1,498 non-overlapping m6A peaks within 1,300 mRNAs and 180 non-overlapping m6A peaks within 175 lncRNAs in two biological replicates. Of these, 35 peaks within mRNAs were overlapped between the IL-37 treated and untreated cells (**Figure 3B**) and only one peak within lncRNAs was overlapped.

SUPPLEMENTARY FIGURE 2 | m6A distribution of differentially methylated m6A sites for both IL-37 treated and untreated cells. **(A)** Chromosomal distribution of all differentially methylated m6A sites within mRNAs and lncRNAs; **(B)** Relative occupancy of differentially methylated m6A sites in chromosome; **(C)** The percentage of differentially methylated m6A sites; **(D)** Fold change of differentially methylated m6A sites.

SUPPLEMENTARY FIGURE 3 | Results of the cellular component (CC) and molecular function (MF) analysis.

REFERENCES

1. Roignant JY, Soller M. m(6)A in mRNA: An Ancient Mechanism for Fine-Tuning Gene Expression. *Trends Genet* (2017) 33(6):380–90. doi: 10.1016/j.tig.2017.04.003
2. Bodi Z, Bottley A, Archer N, May ST, Fray RG. Yeast m6A Methylated mRNAs Are Enriched on Translating Ribosomes during Meiosis, and under Rapamycin Treatment. *PLoS One* (2015) 10(7):e0132090. doi: 10.1371/journal.pone.0132090
3. Wang X, Zhao BS, Roundtree IA, Lu Z, Han D, Ma H, et al. N(6)-methyladenosine Modulates Messenger RNA Translation Efficiency. *Cell* (2015) 161(6):1388–99. doi: 10.1016/j.cell.2015.05.014
4. Haussmann IU, Bodi Z, Sanchez-Moran E, Mongan NP, Archer N, Fray RG, et al. m(6)A potentiates Sxl alternative pre-mRNA splicing for robust Drosophila sex determination. *Nature* (2016) 540(7632):301–4. doi: 10.1038/nature20577
5. Liu J, Yue Y, Han D, Wang X, Fu Y, Zhang L, et al. A METTL3-METTL14 complex mediates mammalian nuclear RNA N6-adenosine methylation. *Nat Chem Biol* (2014) 10(2):93–5. doi: 10.1038/nchembio.1432
6. Jia G, Fu Y, Zhao X, Dai Q, Zheng G, Yang Y, et al. N6-methyladenosine in nuclear RNA is a major substrate of the obesity-associated FTO. *Nat Chem Biol* (2011) 7(12):885–7. doi: 10.1038/nchembio.687
7. Zheng G, Dahl JA, Niu Y, Fedorcsak P, Huang CM, Li CJ, et al. ALKBH5 is a mammalian RNA demethylase that impacts RNA metabolism and mouse fertility. *Mol Cell* (2013) 49(1):18–29. doi: 10.1016/j.molcel.2012.10.015
8. Xiao W, Adhikari S, Dahal U, Chen YS, Hao YJ, Sun BF, et al. Nuclear m(6)A Reader YTHDC1 Regulates mRNA Splicing. *Mol Cell* (2016) 61(4):507–19. doi: 10.1016/j.molcel.2016.01.012
9. Wang X, Lu Z, Gomez A, Hon GC, Yue Y, Han D, et al. N6-methyladenosine-dependent regulation of messenger RNA stability. *Nature* (2014) 505 (7481):117–20. doi: 10.1038/nature12730
10. Wang Y, Li Y, Toth JII, Petroski MD, Zhang Z, Zhao JC. N6-methyladenosine modification destabilizes developmental regulators in embryonic stem cells. *Nat Cell Biol* (2014) 16(2):191–8. doi: 10.1038/ncb2902
11. Zhang C, Chen Y, Sun B, Wang L, Yang Y, Ma D, et al. m(6)A modulates haematopoietic stem and progenitor cell specification. *Nature* (2017) 549 (7671):273–6. doi: 10.1038/nature23883
12. Chen T, Hao YJ, Zhang Y, Li MM, Wang M, Han W, et al. m(6)A RNA methylation is regulated by microRNAs and promotes reprogramming to pluripotency. *Cell Stem Cell* (2015) 16(3):289–301. doi: 10.1016/j.stem.2015.01.016
13. Li Z, Weng H, Su R, Weng X, Zuo Z, Li C, et al. FTO Plays an Oncogenic Role in Acute Myeloid Leukemia as a N(6)-Methyladenosine RNA Demethylase. *Cancer Cell* (2017) 31(1):127–41. doi: 10.1016/j.ccell.2016.11.017
14. Zhang S, Zhao BS, Zhou A, Lin K, Zheng S, Lu Z, et al. m(6)A Demethylase ALKBH5 Maintains Tumorigenicity of Glioblastoma Stem-like Cells by Sustaining FOXM1 Expression and Cell Proliferation Program. *Cancer Cell* (2017) 31(4):591–606.e6. doi: 10.1016/j.ccell.2017.02.013
15. Zhang Z, Zhang J, He P, Han J, Sun C. Interleukin-37 suppresses hepatocellular carcinoma growth through inhibiting M2 polarization of tumor-associated macrophages. *Mol Immunol* (2020) 122:13–20. doi: 10.1016/j.molimm.2020.03.012
16. Hasegawa K, Saga R, Takahashi R, Fukui R, Chiba M, Okumura K, et al. 4-methylumbelliferone inhibits clonogenic potency by suppressing high molecular weight-hyaluronan in fibrosarcoma cells. *Oncol Lett* (2020) 19 (4):2801–8. doi: 10.3892/ol.2020.11370
17. Fasoulakis Z, Kolios G, Papamanolis V, Kontomanolis EN. Interleukins Associated with Breast Cancer. *Cureus* (2018) 10(11):e3549. doi: 10.7759/cureus.3549
18. Kumar S, McDonnell PC, Lehr R, Tierney L, Tzimas MN, Griswold DE, et al. Identification and initial characterization of four novel members of the interleukin-1 family. *J Biol Chem* (2000) 275(14):10308–14. doi: 10.1074/jbc.275.14.10308
19. Dunn E, Sims JE, Nicklin MJ, O'Neill LA. Annotating genes with potential roles in the immune system: six new members of the IL-1 family. *Trends Immunol* (2001) 22(10):533–6. doi: 10.1016/s1471-4906(01)02034-8
20. Bulau AM, Nold MF, Li S, Nold-Petry CA, Fink M, Mansell A, et al. Role of caspase-1 in nuclear translocation of IL-37, release of the cytokine, and IL-37 inhibition of innate immune responses. *Proc Natl Acad Sci U S A* (2014) 111 (7):2650–5. doi: 10.1073/pnas.1324140111
21. Kumar S, Hanning CR, Brigham-Burke MR, Rieman DJ, Lehr R, Khandekar S, et al. Interleukin-1F7B (IL-1H4/IL-1F7) is processed by caspase-1 and mature IL-1F7B binds to the IL-18 receptor but does not induce IFN-gamma production. *Cytokine* (2002) 18(2):61–71. doi: 10.1006/cyto.2002.0873
22. Nold MF, Nold-Petry CA, Zepp JA, Palmer BE, Bufler P, Dinarello CA. IL-37 is a fundamental inhibitor of innate immunity. *Nat Immunol* (2010) 11 (11):1014–22. doi: 10.1038/ni.1944
23. Dinarello CA, Bufler P. Interleukin-37. *Semin Immunol* (2013) 25(6):466–8. doi: 10.1016/j.smim.2013.10.004
24. Jiang M, Wang Y, Zhang H, Ji Y, Zhao P, Sun R, et al. IL-37 inhibits invasion and metastasis in non-small cell lung cancer by suppressing the IL-6/STAT3 signaling pathway. *Thorac Cancer* (2018) 9(5):621–9. doi: 10.1111/1759-7714.12628
25. Meyer KD, Saletore Y, Zumbo P, Elemento O, Mason CE, Jaffrey SR. Comprehensive analysis of mRNA methylation reveals enrichment in 3' UTRs and near stop codons. *Cell* (2012) 149(7):1635–46. doi: 10.1016/j.cell.2012.05.003
26. Song Y, Milon B, Ott S, Zhao X, Sadzewicz L, Shetty A, et al. A comparative analysis of library prep approaches for sequencing low input translatome samples. *BMC Genomics* (2018) 19(1):696. doi: 10.1186/s12864-018-5066-2
27. Luo Z, Zhang Z, Tai L, Zhang L, Sun Z, Zhou L. Comprehensive analysis of differences of N(6)-methyladenosine RNA methylomes between high-fat-fed

and normal mouse livers. *Epigenomics* (2019) 11(11):1267–82. doi: 10.2217/epi-2019-0009
28. Kim D, Langmead B, Salzberg SL. HISAT: a fast spliced aligner with low memory requirements. *Nat Methods* (2015) 12(4):357–60. doi: 10.1038/nmeth.3317
29. Zhang Y, Liu T, Meyer CA, Eeckhoute J, Johnson DS, Bernstein BE, et al. Model-based analysis of ChIP-Seq (MACS). *Genome Biol* (2008) 9(9):R137. doi: 10.1186/gb-2008-9-9-r137
30. Shen L, Shao NY, Liu X, Maze I, Feng J, Nestler EJ. diffReps: detecting differential chromatin modification sites from ChIP-seq data with biological replicates. *PLoS One* (2013) 8(6):e65598. doi: 10.1371/journal.pone.0065598
31. Trapnell C, Roberts A, Goff L, Pertea G, Kim D, Kelley DR, et al. Differential gene and transcript expression analysis of RNA-seq experiments with TopHat and Cufflinks. *Nat Protoc* (2012) 7(3):562–78. doi: 10.1038/nprot.2012.016
32. Justus CR, Leffler N, Ruiz-Echevarria M, Yang LV. In vitro cell migration and invasion assays. *J Vis Exp* (2014) 1(88):51046–53. doi: 10.3791/51046
33. Xuan JJ, Sun WJ, Lin PH, Zhou KR, Liu S, Zheng LL, et al. RMBase v2.0: deciphering the map of RNA modifications from epitranscriptome sequencing data. *Nucleic Acids Res* (2018) 46(D1):D327–34. doi: 10.1093/nar/gkx934
34. Landskron G, De la Fuente M, Thuwajit P, Thuwajit C, Hermoso MA. Chronic inflammation and cytokines in the tumor microenvironment. *J Immunol Res* (2014) 2014:149185. doi: 10.1155/2014/149185
35. Morizawa Y, Miyake M, Shimada K, Hori S, Tatsumi Y, Nakai Y, et al. Correlation of Immune Cells and Cytokines in the Tumor Microenvironment with Elevated Neutrophil-To-Lymphocyte Ratio in Blood: An Analysis of Muscle-Invasive Bladder Cancer. *Cancer Invest* (2018) 36(7):395–405. doi: 10.1080/07357907.2018.1506800
36. Allam G, Gaber AM, Othman SII, Abdel-Moneim A. The potential role of interleukin-37 in infectious diseases. *Int Rev Immunol* (2020) 39(1):3–10. doi: 10.1080/08830185.2019.1677644
37. Mantovani A, Barajon I, Garlanda C. IL-1 and IL-1 regulatory pathways in cancer progression and therapy. *Immunol Rev* (2018) 281(1):57–61. doi: 10.1111/imr.12614
38. Zhang Y, Tang M, Wang XG, Gu JH, Zhou LN, Jin J, et al. Elevated serum levels of interleukin-37 correlate with poor prognosis in gastric cancer. *Rev Esp Enferm Dig* (2019) 111(12):941–5. doi: 10.17235/reed.2019.6460/2019
39. Tawfik MG, Nasef SII, Omar HH, Ghaly MS. Serum Interleukin-37: a new player in Lupus Nephritis? *Int J Rheum Dis* (2017) 20(8):996–1001. doi: 10.1111/1756-185X.13122
40. Liu Y, Zhao JJ, Zhou ZQ, Pan QZ, Zhu Q, Tang Y, et al. IL-37 induces anti-tumor immunity by indirectly promoting dendritic cell recruitment and activation in hepatocellular carcinoma. *Cancer Manag Res* (2019) 11:6691–702. doi: 10.2147/CMAR.S200627
41. Alarcon CR, Lee H, Goodarzi H, Halberg N, Tavazoie SF. N6-methyladenosine marks primary microRNAs for processing. *Nature* (2015) 519(7544):482–5. doi: 10.1038/nature14281
42. Zhang C, Samanta D, Lu H, Bullen JW, Zhang H, Chen I, et al. Hypoxia induces the breast cancer stem cell phenotype by HIF-dependent and ALKBH5-mediated m(6)A-demethylation of NANOG mRNA. *Proc Natl Acad Sci U S A* (2016) 113(14):E2047–56. doi: 10.1073/pnas.1602883113
43. Nusse R. Wnt signaling in disease and in development. *Cell Res* (2005) 15 (1):28–32. doi: 10.1038/sj.cr.7290260
44. Klaus A, Birchmeier W. Wnt signalling and its impact on development and cancer. *Nat Rev Cancer* (2008) 8(5):387–98. doi: 10.1038/nrc2389

Conflict of Interest: Author YZ was employed by Biotrans Technology Co., LTD.

The remaining authors declare that the research was conducted in the absence of any commercial or financial relationships that could be construed as a potential conflict of interest.

frontiers in Oncology

ORIGINAL RESEARCH
published: 08 January 2021
doi: 10.3389/fonc.2020.607047

Genome-Wide Identification and Analysis of the Methylation of lncRNAs and Prognostic Implications in the Glioma

Yijie He[1], *Lidan Wang*[1,2], *Jing Tang*[1,2*] *and Zhijie Han*[1*]

[1] *Department of Bioinformatics, School of Basic Medicine, Chongqing Medical University, Chongqing, China,* [2] *Joint International Research Laboratory of Reproduction & Development, Chongqing Medical University, Chongqing, China*

OPEN ACCESS

Edited by:
Shicheng Guo,
University of Wisconsin—Madison,
United States

Reviewed by:
Nan Lin,
Regeneron Genetic Center,
United States
Peng Song,
Nanjing Drum Tower Hospital, China
Yi-Qing Qu,
Shandong University, China

***Correspondence:**
Zhijie Han
zhijiehan@cqmu.edu.cn
Jing Tang
tang_jing@cqmu.edu.cn

Specialty section:
This article was submitted to Cancer Genetics, a section of the journal Frontiers in Oncology

Received: *16 September 2020*
Accepted: *24 November 2020*
Published: *08 January 2021*

Citation:
He Y, Wang L, Tang J and Han Z (2021) Genome-Wide Identification and Analysis of the Methylation of lncRNAs and Prognostic Implications in the Glioma. Front. Oncol. 10:607047. doi: 10.3389/fonc.2020.607047

Glioma is characterized by rapid cell proliferation and extensive infiltration among brain tissues, but the molecular pathology has been still poorly understood. Previous studies found that DNA methylation modifications play a key role in contributing to the pathogenesis of glioma. On the other hand, long noncoding RNAs (lncRNAs) has been discovered to be associated with some key tumorigenic processes of glioma. Moreover, genomic methylation can influence expression and functions of lncRNAs, which contributes to the pathogenesis of many complex diseases. However, to date, no systematic study has been performed to detect the methylation of lncRNAs and its influences in glioma on a genome-wide scale. Here, we selected the methylation data, clinical information, expression of lncRNAs, and DNA methylation regulatory proteins of 537 glioma patients from TCGA and TANRIC databases. Then, we performed a differential analysis of lncRNA expression and methylated regions between low-grade glioma (LGG) and glioblastoma multiform (GBM) subjects, respectively. Next, we further identified and verified potential key lncRNAs contributing the pathogenesis of glioma involved in methylation modifications by an annotation and correlation analysis, respectively. In total, 18 such lncRNAs were identified, and 7 of them have been demonstrated to be functionally linked to the pathogenesis of glioma by previous studies. Finally, by the univariate Cox regression, LASSO regression, clinical correlation, and survival analysis, we found that all these 18 lncRNAs are high-risk factors for clinical prognosis of glioma. In summary, this study provided a strategy to explore the influence of lncRNA methylation on glioma, and our findings will be benefit to improve understanding of its pathogenesis.

Keywords: glioma, methylation modification, long non-coding RNAs, clinical prognosis, the cancer genome atlas (TCGA)

INTRODUCTION

Glioma is the most common and highly malignant tumor in the intraparenchymal central nervous system (CNS) tumors (1). It is characterized by the rapid and extensive proliferation among brain tissues (2, 3). The high grade glioma subtype, glioblastoma multiform (GBM), could cause the significant mortality that are disproportionate to their relatively rare incidence (4). Even under the best treatment, the median survival time is just over a year, and the few GBM patients survive more than 3 years (1). The etiology and pathogenesis of GBM have been extensively investigated, but the epigenetic mechanisms contributing to its pathogenesis were much less understood (2, 3, 5).

To date, DNA methylation is the most widely studied epigenetic mechanisms (6). Tremendous evidences shows that the DNA methylation is involved in tumorigenesis and development of the GBM (1, 7). For example, the promoter DNA methylation pattern of genes involved in RB1 and TP53 signaling pathways were identified in GBM patients (7). The promoter methylation of the DNA repair enzyme (O6-methylguanine-DNA methyltransferase) was discovered as a significant prognostic factor for temozolomide resistance in GBM patients (8).

The long non-coding RNAs (lncRNAs), a kind of non-protein coding transcripts of >200 nucleotides (9–11), has been reported to be a key regulator in a broad range of biological and cellular processes of GBM, including cell proliferation, motility, hypoxia response, and apoptosis (12–14). The expression levels and functions of lncRNAs could be significantly affected by the genomic methylation in many complex diseases (15–18). Moreover, there is increasing evidences that the methyltransferase, demethylase, and binding protein dynamically regulate the methylation level of the lncRNAs, which influences their expression in specific biological processes (18, 19). However, to date, no systematic study has been conducted to discovery the methylation of lncRNAs and its influences in the glioma on a genome-wide scale.

Herein, to address this lack of knowledge, we used a cohort of low-grade glioma (LGG) and GBM from The Cancer Genome Atlas (TCGA) database to investigate the contribution of lncRNA methylation to tumorigenesis and development in glioma. Specifically, we first downloaded the expression data of lncRNAs from The Atlas of Noncoding RNAs in Cancer (TANRIC) database, and then implemented a differential expression analysis between the LGG and GBM subjects. Second, we obtained the glioma-related methylation array data and the protein-coding gene expression data of the same samples from TCGA database, and then identified the differentially methylated regions of the differentially expressed lncRNAs according the GENCODE reference annotation for human genomes. Third, we conducted a correlation analysis between methylation level and expression of the lncRNAs and the genes involving in the three kinds of methylation regulatory proteins, and identified the potential key lncRNAs contributing the pathogenesis of glioma. Finally, we conducted the univariate Cox regression, least absolute shrinkage and selection operator (LASSO) regression, clinical correlation, and survival analysis based on the clinical data of these samples to explore the influence of these methylated and potentially disease-related lncRNAs on clinical prognosis of glioma. The flow chart was shown in **Figure 1**.

MATERIALS AND METHODS

Data Collection and Preprocessing

The clinical information and the methylation information of patients with glioma were downloaded from the TCGA database (http://cancergenome.nih.gov), a comprehensive resource for investigating the molecular basis in various cancers. According to TCGA annotation, glioma is classified as the LGG and the GBM. The Genomic Data Commons (GDC) Data Portal (https://portal.gdc.cancer.gov/) was used to access these TCGA data. Particularly, we selected "DNA methylation" in the Data Category, "Illumina human methylation 450" in the Platform, "brain" in the Primary Site, and "gliomas" in the Disease Type to screen out the methylation information of patients. Then, we selected "clinical" in the Data Category, "brain" in the Primary Site, and "gliomas" in the Disease Type to screen out the clinical information of patients. Next, we removed the samples which lack the methylation or clinical information. Finally, the lncRNA expression data of the same patients was downloaded from the TANRIC database, which quantified the expression profiles of lncRNAs in Ensembl using the TCGA data (20).

Moreover, we further searched all the possible studies in PubMed database (http://www.ncbi.nlm.nih.gov/pubmed) using the keywords to "methylase gene," "methyltransferase gene," "binding protein gene," "demethylase gene" to identify the DNA methylation regulatory proteins. The search was performed before the last update of this database on May 13, 2020. The gene expression of the methylation regulatory proteins was obtained from TCGA database. The expression data of lncRNAs and methylation regulatory proteins have been normalized as reads per kilobase of exon model per million mapped reads (RPKM) and RNA-Seq by Expectation-Maximization (RSEM), respectively. The DNA methylation values were normalized using the "betaqn" function of the R package "wateRmelon" (http://bioconductor.org/packages/release/bioc/html/wateRmelon.html) (21).

Differential Expression Analysis of lncRNAs Between Low-Grade Glioma and Glioblastoma Multiform

To identify the key lncRNAs which are potentially associated with the gliomas progression, we performed a differential expression analysis of all the lncRNAs obtained from TANRIC database between LGG and GBM subjects using the R package "lncDIFF" with its default parameter settings (i.e. link.function = "log," simulated.pvalue = FALSE, permutation = 100) (https://

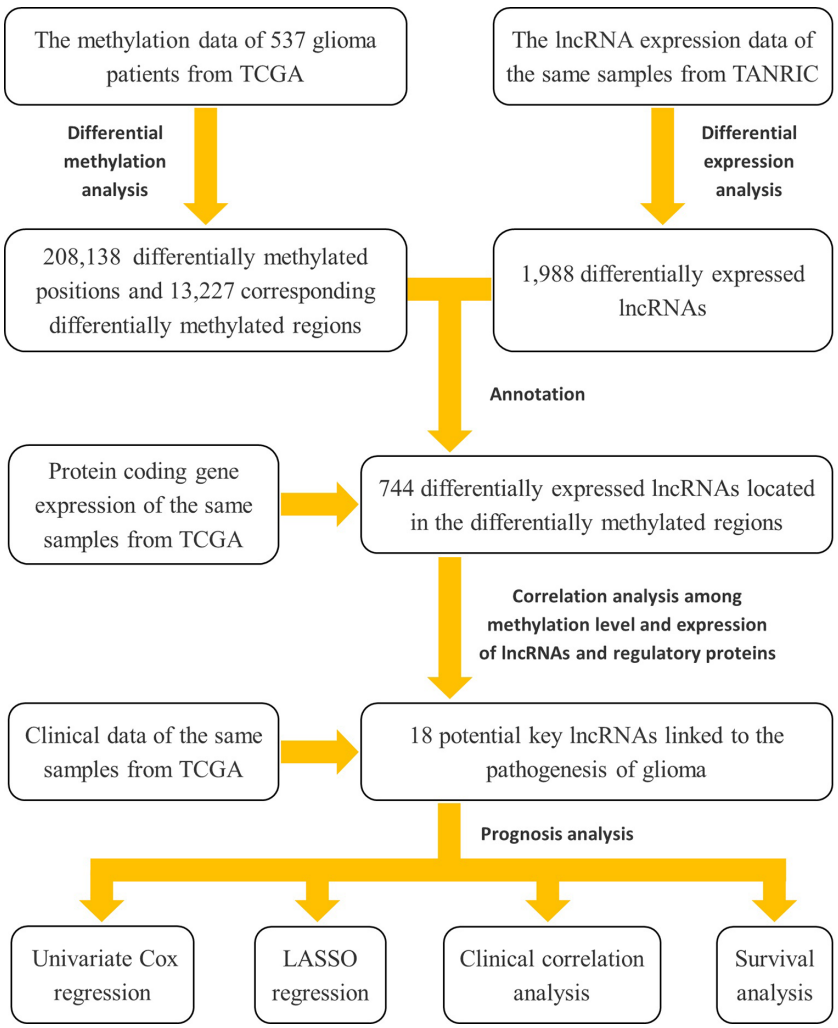

FIGURE 1 | The flow chart of the study design for exploring the potential key lncRNAs contributing the pathogenesis of glioma involved in methylation modifications and their impact on disease prognosis.

CRAN.R-project.org/package=lncDIFF). It is a powerful differential analysis tool by the normalized expression data (e.g. RPKM values) as the input, and has high sensitivity to identify the low abundant differentially expressed genes, as commonly observed in lncRNAs. This package adopts the generalized linear model with zero-inflated exponential quasi-likelihood to estimate group effect on normalized counts, and employs the likelihood ratio test to detect differential expressed genes. The proposed method and tool are applicable to data processed with standard RNA-seq preprocessing and normalization pipelines (22). We first removed 21 lncRNAs whose expression is zero in all the LGG or GBM subjects. Then, we set significance level according to the common threshold of the absolute value of fold change (*FC*) ≥ 2 and false discovery rate (FDR) $p < 0.05$. The p values are corrected for multiple testing by Benjamini–Hochberg method. Finally, we used a volcano plot to describe the profile of whole lncRNA expression by the R package "ggplot2" (https://CRAN.R-project.org/package=ggplot2), and used a heatmap to visualize the cluster pattern of the differentially expressed lncRNAs based on Manhattan distance by the R package "gplots" (https://CRAN.R-project.org/package=gplots).

Differential Methylation Analysis and lncRNA Annotation

To identify the glioma-related methylation positions and regions, and the differentially expressed lncRNAs located in these regions, we performed a differential methylation analysis and lncRNA annotation. The differential methylation analysis was conducted by the R package "minfi" which is a specialized tool designed to process the Illumina methylation 450 array data (http://bioconductor.org/packages/release/bioc/html/minfi.html). It used the Subset-quantile Within Array Normalization method to preprocess data and the bump-hunting algorithm to discover the differential methylation information (23). Firstly, we used the

"densityBeanPlot" function of this package to conduct the quality control for each array. The qualified samples should have the characteristic that the methylation levels (beta values) of CpG positions are distributed around 0 and 1, respectively. Then, we used the "dmpFinder" function (type = "categorical") of this package to identify the differentially methylated positions between LGG and GBM subjects based on the methylation array. The significance level was set according to a common threshold of the absolute intercept ≥ 0.2 (i.e. 20% difference on the beta values) and $p < 1\times10^{-3}$ (24). Next, based on these differentially methylated positions, we further used the "bumphunter" function (B = 10, type = "Beta") of this package to look for the differentially methylated regions between LGG and GBM subjects with the common threshold of average methylation level difference ≥ 0.2 (25, 26). The differentially methylated regions are the consecutive genomic locations containing a battery of differentially methylated positions in the same direction. Finally, we download the ensGene annotation file (hg19) from the Ensembl (release 75) which stores the location information of lncRNA transcripts and exons in human genome. Based on this file, the ANNOVAR software was used to perform an lncRNA annotation and identify the differentially expressed lncRNAs located in the differentially methylated regions. ANNOVAR is a Perl command-line tool for rapidly and efficiently annotating the genomic variants, including gene-based, region-based and filter-based annotations on a variant call format (VCF) file generated from human genomes (27).

Correlation Analysis Between Methylation and Expression of lncRNAs

To explore the influence of methylation on the corresponding lncRNAs, and identify the potential key lncRNAs contributing the pathogenesis of glioma, we performed a correlation analysis between methylation and expression of lncRNAs. Particularly, we first selected the differentially methylated positions to be included in each of the identified lncRNAs in the previous step, and calculated the average values of these methylation positions for each lncRNAs, respectively. Then, we calculated the Pearson's correlation coefficient between the expression of these lncRNAs and their average methylation level using the R function "cor.test." The threshold of significance was set at the absolute value of r > 0.6 and FDR p < 0.05. The p values are corrected for multiple testing by Benjamini–Hochberg method. Finally, it is reported that the methylation regulatory proteins (including methyltransferase, demethylase, and binding protein) dynamically regulate the methylation level of lncRNAs, which influences their expression in specific biological processes (18, 19). Therefore, to explore which methylation regulatory proteins are involved in the methylation modification of the potential key lncRNAs and further increase the reliability of our findings, we selected the known methylation regulatory proteins and calculated the Pearson's correlation coefficient between their expression and the average methylation level of these lncRNAs using the same significance threshold.

Influence of the Methylated lncRNAs on Clinical Prognosis of Glioma

We further analyzed the Influence of these identified methylated lncRNAs potentially contributing the pathogenesis of glioma on the clinical prognosis of glioma. First, we calculated the average expression of the key lncRNAs obtained above in each patient and get the median of these average expressions. According to the median, the patients were separated into the lncRNAs low and high expression groups. We compared prognosis between the high expression and low expression subjects using a Kaplan-Meier overall survival curves. Then, we performed a univariate Cox regression analysis to assess the association between these methylated lncRNAs and the prognosis of glioma. The threshold of significance was set at 95% confidence interval (CI) of hazard ratio (HR) $\not\supseteq 1$ and $p < 0.05$. The R package "survival" (https://CRAN.R-project.org/package=survival) was used for these analyses. Next, based on the results of univariate Cox regression analysis, we further used the LASSO regression algorithm to identify the key lncRNAs whose methylation and expression impact on the prognosis of glioma by R package "glmnet." It is a pathwise algorithm for the Cox proportional hazards model, regularized by convex combinations of $\ell1$ and $\ell2$ penalties (elastic net). The algorithm fits *via* cyclical coordinate descent, and employs warm starts to find a solution along a regularization path (28). The parameter familiy, maxit, and alpha were set to Cox, 1000 and 1, respectively (others were set by their default values). And then we calculated the risk score of each subject using them through the "survival" package. Finally, we used a receiver operator characteristic (ROC) curve to verify the reliability of the risk score by the R package "survivalROC" (https://CRAN.R-project.org/package=survivalROC). In addition, we also assessed the association between these lncRNA expressions and other clinical features of the patients (including age at initial pathologic diagnosis, vital status, and gender) using the chi-square test. The threshold of significance was set at $p < 0.05$.

RESULTS AND DISCUSSION

Methylation, Expression, and Clinical Information of 537 Glioma Samples

After the data collection, we found a total of 537 glioma samples (including 486 LGG and 51 GBM patients from TCGA) with the DNA methylation values, expression levels of protein-coding genes, and clinical information. Particularly, according to the annotation of Illumina human methylation 450 array, a total of 369,531 CpGs methylation positions were quantified after removing the missing values. We normalized the CpGs methylation values for the subsequent analyses. The results were shown in **Supplementary Figure S1**. The lncRNA expression data of the 537 glioma samples were obtained from TANRIC database. A total of 12,727 lncRNAs of these samples were quantified as RPKM values. Through the keyword search and the title/abstract screening, 23 articles containing genes for methylation-related enzymes were obtained from PubMed.

In total, we identified 32 DNA methylation regulatory proteins (including methyltransferase, demethylase, and binding protein) from the 23 articles (**Table 1**). We extracted the expression data of these 32 methylation regulatory proteins for each sample (quantified as RSEM values) from the TCGA database. The clinical information of these samples contains age, gender, survival time, and vital status. The summary of these glioma samples was listed in **Table 2**.

Differential Expression Analysis of lncRNAs Between Low-Grade Glioma and Glioblastoma Multiforme

We used the R package "lncDIFF" to perform the differential expression analysis of lncRNAs between LGG and GBM subjects according to the significance threshold of $|FC| \geq 2$ and FDR $p < 0.05$. In total, we identified 1,988 significantly differentially expressed lncRNAs, which include 1,284 highly expressed (i.e. $FC \geq 2$) and 704 lowly expressed lncRNAs ($FC \leq -2$) in the GBM subjects. The details are described in **Supplementary Table S1**. We used a volcano plot to describe the profile of whole lncRNA expression (**Figure 2A**). Then, to verify these findings, we contrasted these identified differentially expressed lncRNAs with another independent study. This study used 19 glioblastoma and 9 control brain samples to perform the differential expression analysis of 30,586 lncRNA transcripts (Arraystar Human lncRNA Microarray V3.0, nearly 30% of them overlap with our study). According to its results, about 71.5% differentially expressed lncRNAs overlapped with our findings (52). Further, we selected the top most 100 differentially expressed lncRNAs to visualize the cluster pattern of their expression by a heatmap. As **Figure 2B** shows, the GBM and LGG subjects are mainly grouped under a cluster according to high

TABLE 1 | The information of the 32 DNA methylation regulatory proteins.

Gene	ID	Description	Type	Reference
DNMT3A	1788	DNA methyltransferase 3 alpha	Methyltransferase	(29, 30, 31)
DNMT3B	1789	DNA methyltransferase 3 beta	Methyltransferase	(29, 30, 31)
DNMT3L	29947	DNA methyltransferase 3 like	Methyltransferase	(30)
DNMT1	1786	DNA methyltransferase 1	Methyltransferase	(31–33)
DMAP1	55929	DNA methyltransferase 1 associated protein 1	Binding protein	(33)
SUV39H1	6839	Suppressor of variegation 3-9 homolog 1	Methyltransferase	(34)
MECP2	4204	Methyl-CpG binding protein 2	Binding protein	(35)
MBD1	4152	Methyl-CpG binding domain protein 1	Binding protein	(35)
MBD2	8932	Methyl-CpG binding domain protein 2	Binding protein	(35)
MBD3	53615	Methyl-CpG binding domain protein 3	Binding protein	(35)
MBD4	8930	Methyl-CpG binding domain 4, DNA glycosylase	Binding protein	(35)
SETDB1	9869	SET domain bifurcated histone lysine methyltransferase 1	Methyltransferase	(31, 35)
MGMT	4255	O-6-methylguanine-DNA methyltransferase	Methyltransferase	(36)
TET1	80312	tet methylcytosine dioxygenase 1	Demethylase	(37)
TET2	54790	Tet methylcytosine dioxygenase 2	Demethylase	(37)
TET3	200424	Tet methylcytosine dioxygenase 3	Demethylase	(37)
JMJD6	23210	Jumonji domain containing 6, arginine demethylase and lysine hydroxylase	Demethylase	(38)
KDM3A	55818	Lysine demethylase 3a	Demethylase	(39)
KDM5C	8242	Lysine demethylase 5c	Demethylase	(39)
KDM1A	23028	Lysine demethylase 1a	Demethylase	(40)
KDM5B	10765	Lysine demethylase 5b	Demethylase	(41)
KDM5A	5927	Lysine demethylase 5a	Demethylase	(42)
KDM5D	8284	Lysine demethylase 5d	Demethylase	(42)
KDM3B	51780	Lysine demethylase 3b	Demethylase	(43)
KDM4A	9682	Lysine demethylase 4a	Demethylase	(44, 45)
KDM4B	23030	Lysine demethylase 4b	Demethylase	(46)
KDM4C	23081	Lysine demethylase 4c	Demethylase	(47)
KDM4D	55693	Lysine demethylase 4d	Demethylase	(48)
KDM6A	7403	Lysine demethylase 6a	Demethylase	(42, 49)
KDM6B	23135	Lysine demethylase 6b	Demethylase	(42, 49)
KDM2A	22992	Lysine demethylase 2a	Demethylase	(48)
KDM2B	84678	Lysine demethylase 2b	Demethylase	(50, 51)

TABLE 2 | Summary of the 537 individuals studied in this work.

Individuals	Sample Type	Sample Size	Mean Age (SD)	Male/Female (%)	Death Rates (%)
GBM subjects	Primary Tumor	51	61.54 (13.41)	56.00/44.00	66.00
LGG subjects	Primary Tumor	486	42.91 (13.42)	54.64/45.36	25.15
Total		537	44.66 (14.48)	54.77/45.23	28.97

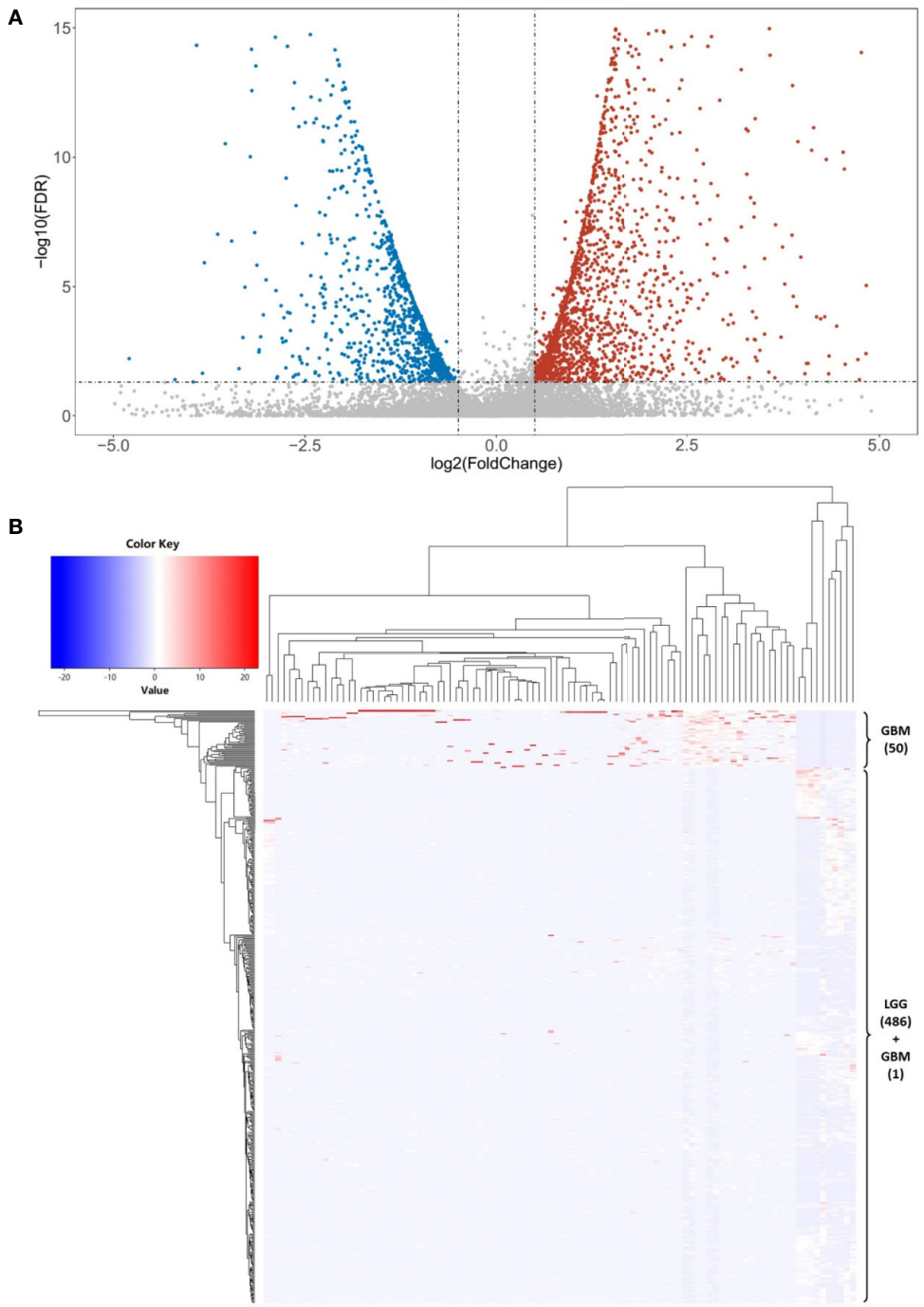

FIGURE 2 | The differential expression analysis of lncRNAs. **(A)** The volcano plot shows a profile of the expression of all these lncRNAs in this study. There are 1,284 highly expressed (i.e. and FDR $p < 0.05$) and 704 lowly expressed lncRNAs (and FDR $p < 0.05$) in the GBM subjects. **(B)** The clustered heatmap of the top 100 most differentially expressed lncRNAs between LGG and GBM subjects. Most of these lncRNAs (83%) are significantly highly expressed in the GBM than LGG subjects. There are 50 GBM subjects (about 98.04%) grouped into a cluster base on the lncRNA expression.

and low expression of the lncRNAs, respectively, and most of these lncRNAs (83%) are significantly highly expressed in the GBM than LGG subjects. These differentially expressed lncRNAs may contribute to the progress of glioma. Thus, we used these significantly differentially expressed lncRNAs to conduct the subsequent analysis.

Differential Methylation Analysis and lncRNA Annotation

We performed a differential methylation analysis and lncRNA annotation to identify the glioma-related DNA methylation and the differentially expressed lncRNAs located in the regions. The results of array quality control showed that the beta values of DNA methylation positions are mainly distributed around 0 and 1, respectively, for each sample (**Supplementary Figure S2**). Then, we used these arrays to identify the differentially methylated positions and regions, respectively. The results showed that there are a total of 208,138 positions and 13,227 corresponding regions with a significantly differential methylation level between LGG and GBM subjects (**Supplementary Tables S2**, **S3**). The methylation array GSE90496 (contains 347 GBM and 301 LGG subjusts) was used to verify these findings. The results showed that about 71.1% differential methylation positions are consistent with our findings (53). Finally, based on these differentially methylated regions, we performed the location annotation of the differentially expressed lncRNAs. In total, we identified 744 lncRNAs which are located in the differentially methylated regions. According to the results of annotation, these differentially methylated regions are at five categories of different genomic locations, i.e. intergenic, ncRNA_exonic, ncRNA_intronic, upstream and downstream, and the proportion of intergenic areas is significantly increased compared with other types (**Supplementary Table S4**). We further calculated the proportion of them in the different genomic locations. We found that these lncRNAs are mainly distributed in chromosome 1, 2, 7, and 12 (11.42, 10.48, 8.06, and 8.06%, respectively) (**Supplementary Table S5**). Moreover, as the **Supplementary Table S1** shown, these identified lncRNAs include 1,284 highly and 704 lowly expressed ones in the GBM subjects. But not all of these highly and lowly expressed lncRNAs have significantly reduced and increased methylation levels in the GBM subjects, respectively, which imply that not all of DNA methylation changes can affect the expression of lncRNAs in the corresponding genomic regions.

Correlation Analysis Between Methylation and Expression of lncRNAs

We first conducted a Shapiro-Wilk normality test for each vector by the R function "shapiro.test." According to the threshold $P > 0.05$, 11 lncRNAs that do not obey the normal distribution were removed. Then, to identify the differentially expressed lncRNAs affected by the glioma-related DNA methylation, we performed a Pearson's correlation analysis between methylation and expression of lncRNAs. The results revealed that there are a total of 18 lncRNAs (including 16 highly and 2 lowly expressed ones) whose expression is significantly associated with their DNA methylation level, and all of them show a significant negative correlation ($r < -0.6$ and FDR $p < 0.05$) (**Table 3**). It is consistent with the common understanding that DNA methylation inhibits the corresponding gene expression in a variety of tissues and cell lines (54, 55). Next, we further measured the association between the expression of the 32 methylation regulatory proteins and methylation level of these lncRNAs. The results showed that there is a significantly negative correlation between *TET1* expression and most of the 18 lncRNAs' methylation level. *TET1* is a demethylase which can catalyze the conversion of 5-methylcytosine to 5-hydroxymethylcytosine and maintains hypomethylation status of the corresponding regions (37). Besides this gene, the expression of *KDM4B* and *MBD2* also show a significantly negative and positive correlation ($r > 0.6$ and FDR $p < 0.05$) with a part of the 18 lncRNAs' methylation level, respectively. *KDM4B* is also a demethylase of histone lysine by a hypoxia-induced pathway, and an important epigenetic modifier in cancer (46). *MBD2* is a methyl-CpG binding protein which binds and maintains methylated gene promoter to repress its transcriptional activity (35). However, this significant correlation is not observed in the other 29 genes, which imply that the DNA methylation of lncRNAs in glioma may be influenced predominantly by some specific methylation regulatory proteins (**Table 3** and **Supplementary Table S5**). Moreover, the mean differential methylation of the 18 lncRNAs was calculated. We found that all of the lowly expressed lncRNAs have significantly reduced methylation levels and most of them have significantly reduced methylation levels in the GBM subjects. It is also consistent with the understanding that DNA methylation inhibits gene expression (56, 57). Therefore, we considered them as the potential key lncRNAs contributing the pathogenesis of glioma involved in methylation modifications. Finally, we further queried PubMed for the functions of the 18 potential key lncRNAs contributing the pathogenesis of glioma. We found that seven of them have been demonstrated to be functionally linked to the pathogenesis of glioma by the previous studies. For example, the overexpression of the ENSG00000222041 (CYTOR) partially reversed the inhibitory effects of UPF1 on proliferation and invasion abilities in glioma (58, 59). The more details were described in the **Supplementary Table S6**.

Influence of the Methylated lncRNAs on Clinical Prognosis of Glioma

We further analyzed the influence of the 18 identified lncRNAs, which potentially contribute the glioma pathogenesis by methylation modifications, on the clinical prognosis of glioma. For the 16 lncRNAs highly expressed in GBM patients, we found that the overall survival curve of the subjects with high lncRNA expression is significantly longer than the subjects with low lncRNA expression ($p = 1.38 \times 10^{-10}$) (**Figure 3A**). On the contrary, the overall survival curve of the subjects with low lncRNA expression is significantly longer than the subjects with high lncRNA expression for the two lowly expressed lncRNAs ($p = 3.11 \times 10^{-10}$) (**Figure 3B**). It reflects an association between the dysregulation of lncRNA expression and a bad prognosis of glioma patients. To avoid dependence on the tumor grade, we performed the univariate Cox regression analysis of the 18 lncRNAs in GBM and LGG subjects, respectively. We did not find a significant association between lncRNA expression and poor patient outcomes in GBM subjects. However, the results showed that all of the 18 identified methylated lncRNAs are high-risk factors for the prognosis of glioma in LGG subjects (i.e. 95% CI HR $\not\geq 1$ and $p < 0.001$) (**Figure 3C**). This suggests that both over-expression of those 16 lncRNAs and under-expression of other 2 ones can

TABLE 3 | The information of the 16 potential key lncRNAs contributing the pathogenesis of glioma involved in methylation modifications.

LncRNAs	Symbol	Differentially Methylated Regions			Fold Change (FDR)	Correlation LL (FDR)	Correlation LP (FDR)			MeanDM
		Chr	Start	End			TET1	KDM4B	MBD2	
ENSG00000177738	AC025171.1	chr5	43312201	43312201	2.09 (5.1E-07)	−0.63 (4.8E-60)	−0.71 (6.5E-82)	−0.61 (1.4E-54)	0.52 (2.4E-37)	−1.985
ENSG00000222041	CYTOR	chr2	88751786	88752553	7.32 (7.3E-65)	−0.62 (4.4E-57)	−0.72 (2.8E-85)	−0.63 (1.6E-60)	0.61 (1.7E-54)	−0.800
ENSG00000224081	SLC44A3-AS1	chr1	95286125	95286125	2.85 (1.5E-14)	−0.65 (1.0E-64)	−0.66 (1.1E-66)	−0.60 (7.4E-53)	0.51 (1.2E-35)	0.801
ENSG00000226445	BX322234.1	chr6	169613210	169613372	2.15 (8.4E-08)	−0.64 (4.2E-62)	−0.67 (6.7E-70)	−0.61 (5.3E-54)	0.57 (2.5E-47)	2.763
ENSG00000227372	TP73-AS1	chr1	3807168	3807312	2.81 (2.6E-14)	−0.90 (2.2E-189)	−0.72 (3.2E-84)	−0.62 (4.8E-58)	0.50 (6.7E-34)	−2.153
ENSG00000230074	AL162231.2	chr9	34666173	34666173	3.89 (1.6E-25)	−0.79 (4.3E-112)	−0.72 (3.2E-84)	−0.63 (3.2E-59)	0.50 (2.9E-34)	−2.442
ENSG00000231609	AC007098.1	chr2	63850056	63850056	2.94 (6.2E-11)	−0.65 (3.5E-64)	−0.66 (1.2E-65)	−0.53 (8.2E-39)	0.50 (3.5E-35)	−0.246
ENSG00000232533	AC093673.1	chr7	143081287	143081287	3.73 (1.5E-24)	−0.78 (1.3E-108)	−0.63 (3.0E-58)	−0.48 (2.2E-31)	0.57 (3.7E-46)	−1.423
ENSG00000234883	MIR155HG	chr21	26934424	26934885	6.02 (1.2E-50)	−0.61 (1.9E-54)	−0.74 (2.9E-90)	−0.62 (1.2E-56)	0.54 (2.9E-40)	−0.780
ENSG00000246100	LINC00900	chr11	115631116	115631389	2.96 (7.0E-16)	−0.71 (3.1E-80)	−0.68 (1.7E-73)	−0.57 (1.7E-46)	0.49 (5.4E-33)	−2.839
ENSG00000249249	AC010226.1	chr5	114937919	114938439	3.75 (8.7E-25)	−0.74 (5.8E-92)	−0.75 (2.0E-96)	−0.65 (6.4E-65)	0.58 (6.4E-48)	−2.047
ENSG00000249859	PVT1	chr8	129284837	129284837	4.31 (3.6E-31)	−0.72 (2.1E-84)	−0.68 (1.1E-73)	−0.56 (1.1E-44)	0.60 (1.8E-53)	1.356
ENSG00000250786	SNHG18	chr5	9546404	9546404	3.55 (1.6E-22)	−0.66 (1.0E-65)	−0.74 (4.5E-90)	−0.63 (1.6E-60)	0.53 (8.7E-39)	−2.027
ENSG00000251131	AC025171.3	chr5	43019660	43020716	2.59 (7.6E-12)	−0.65 (1.9E-64)	−0.72 (1.8E-86)	−0.64 (2.4E-61)	0.51 (1.6E-36)	−2.032
ENSG00000254675	AP003032.1	chr11	77734334	77734334	3.85 (1.4E-02)	−0.61 (2.4E-55)	−0.71 (4.3E-83)	−0.60 (2.9E-53)	0.55 (1.9E-42)	−0.167
ENSG00000255571	MIR9-3HG	chr15	89921845	89922989	-2.99 (2.3E-09)	−0.65 (8.0E-64)	−0.13 (3.9E-02)	−0.13 (3.9E-02)	−0.14 (3.9E-02)	0.215
ENSG00000256802	AC022613.1	chr15	29969096	29969096	3.71 (2.6E-24)	−0.62 (1.0E-56)	−0.68 (8.6E-72)	−0.59 (1.8E-51)	0.54 (1.4E-41)	−1.557
ENSG00000263874	LINC00672	chr17	37081875	37081875	-2.72 (4.6E-08)	−0.75 (1.1E-95)	0.004 (9.9E-01)	0.02 (9.3E-01)	0.03 (9.3E-01)	0.138

Correlation LL, correlation between the average methylation level of lncRNAs and their expression; Correlation LP, correlation between the methylation level of lncRNAs and the expression of methylation regulatory proteins; MeanDM, mean differential methylation level.

lead to a poor prognosis in LGG patients, which is also consistent with common sense, given that GBM patients are in advanced stages of the disease and their survival may be affected by other complications or factors. In addition, the univariate Cox regression analysis was further performed for all the 1,988 significantly differentially expressed lncRNAs in LGG patients. We found that only about 39% of the lncRNAs unlikely affected by methylation modifications are associated with poor patient outcomes (**Supplementary Table S7**). We further applied LASSO regression algorithm to the 18 lncRNAs to identify the key ones for glioma prognosis and calculate the risk score of each subject. As **Figures 3D, 3E** show, there are four key lncRNAs (i.e. ENSG00000256802, ENSG00000232533, ENSG00000227372, ENSG00000222041) selected when the cross-validated partial likelihood deviance reaches its minimum value, and the coefficients of all these lncRNAs are positive (i.e. increase risk of disease). The area under the curve (AUC) of the ROC is 0.903, which shows the reliability of the risk score (**Figure 3F**). According to the median of risk scores, the patients were separated into the low and high-risk groups. We found that the GBM subjects are mainly distributed in high-risk group, while the LGG subjects are mainly distributed in low-risk group. This demonstrates the consistency between the sample risk score by the key lncRNAs and the severity of glioma. Moreover, as **Figure 4A** shows, the risk classification by the key lncRNAs is significantly associated with the age at initial pathologic diagnosis ($p = 1.32 \times 10^{-2}$) and vital status ($p = 1.72 \times 10^{-8}$). But we observed no association with the gender of the patients ($p = 1.97 \times 10^{-1}$). The similar results were also observed for all the 18 identified methylated lncRNAs (p value of age, vital status and gender is 2.87×10^{-14}, 2.01×10^{-9}, and 1.45×10^{-1}, respectively) (**Figure 4B**).

CONCLUSIONS

In this study, we used the TCGA data to identify potential key lncRNAs contributing the pathogenesis of glioma involved in methylation modifications and further explore influence of them on the clinical prognosis of glioma. In total, we identified 18 such lncRNAs which has the following four characteristics: 1) they are significantly differentially expressed between the LGG and GBM subjects; 2) at least one of the differentially methylated regions, which cover the contiguous differentially methylated positions, is located in these lncRNA sequences; 3) there is a strong correlation between the methylation level of these lncRNAs and the expression of methylation regulatory proteins; 4) the expression of these lncRNAs is significantly associated with their methylation level. Further, the results of clinical data analysis show that all these 18 lncRNAs are high-risk factors for the clinical prognosis of glioma, and four of them (i.e. ENSG00000256802, ENSG00000232533, ENSG00000227372 and ENSG00000222041) are most important for the severity of glioma. All in all, we performed a strategy to explore the influence of the lncRNA methylation on the pathogenesis of glioma, and these findings will be benefit to further glioma research in the future.

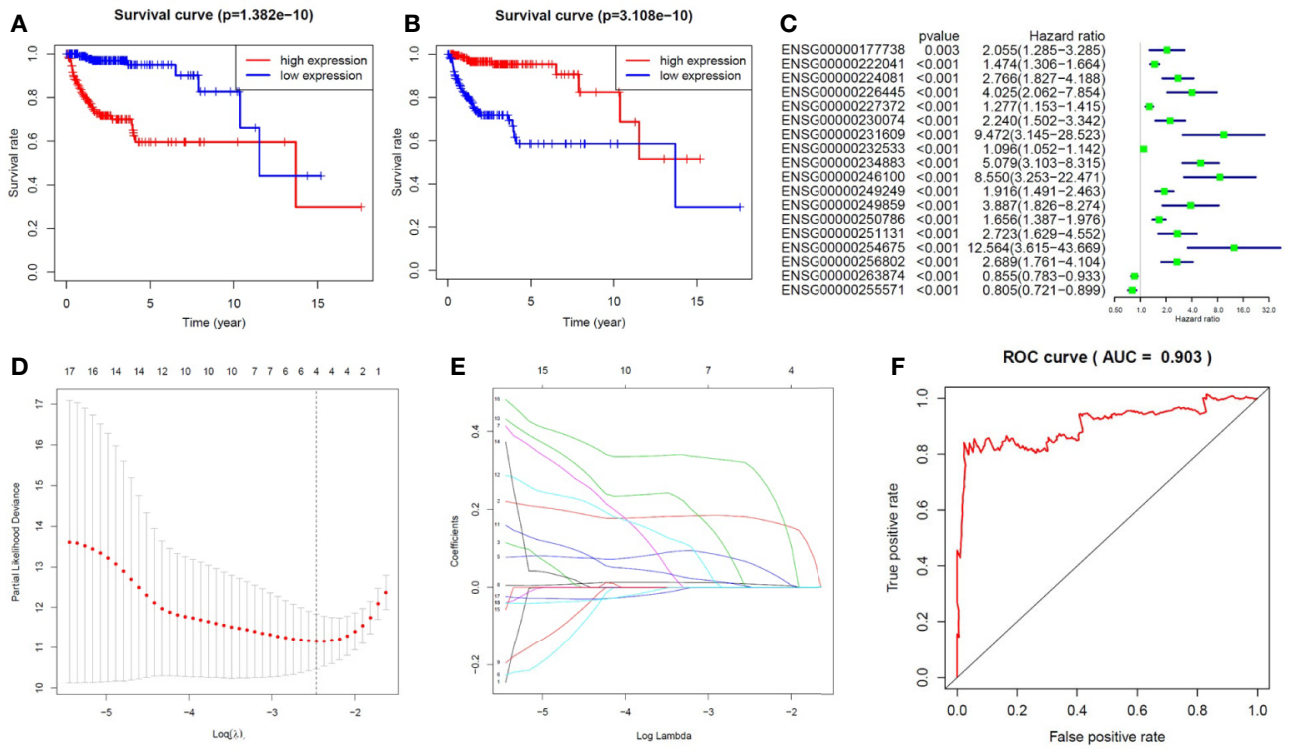

FIGURE 3 | The influence of the methylated lncRNAs on the prognosis of glioma. **(A)** For the 16 lncRNAs highly expressed in GBM patients, the Kaplan-Meier overall survival curve of the subjects with high lncRNA expression is significantly longer than the subjects with low lncRNA expression. **(B)** For the two lncRNAs lowly expressed in GBM patients, the Kaplan-Meier overall survival curve of the subjects with low lncRNA expression is significantly longer than the subjects with high lncRNA expression. **(C)** The forest plot for the results of univariate Cox regression analysis in LGG. **(D)** The relationship between the partial likelihood deviance and the penalty coefficient λ value. The log (λ) is equal to about 2.5 when the partial likelihood deviance reaches its minimum value. **(E)** The LASSO regression for calculating the coefficient of each lncRNA. There are four lncRNAs with non-zero coefficients when the log (λ) is equal to 2.5. **(F)** The ROC curve shows the reliability of the risk score.

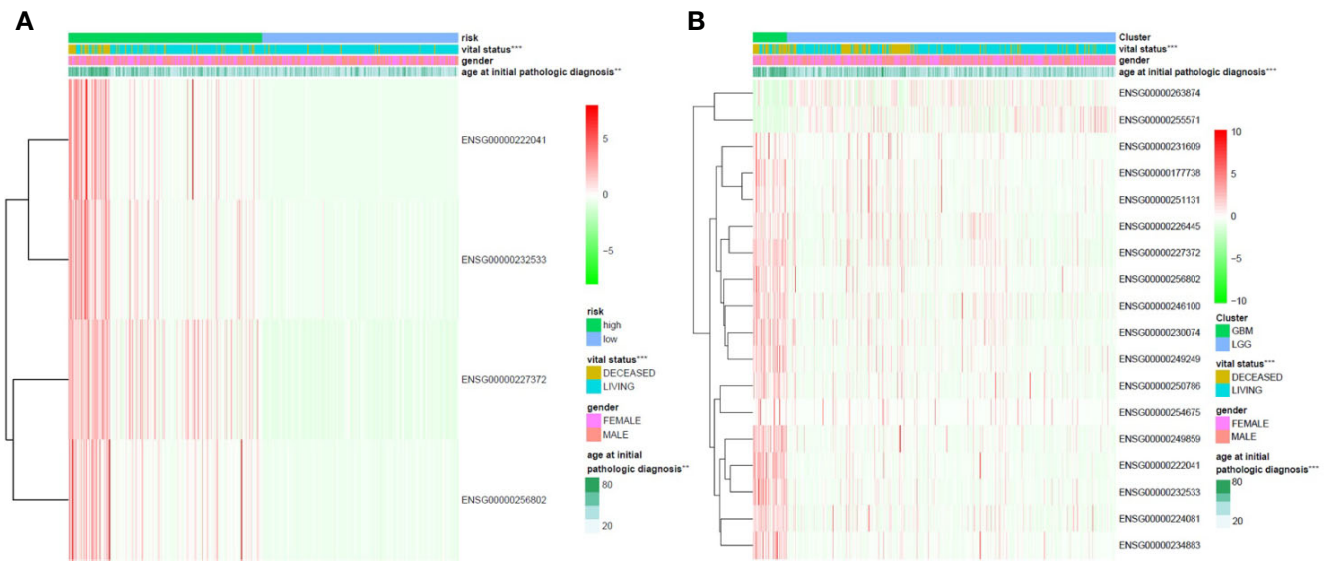

FIGURE 4 | The association between the methylated lncRNAs and the clinical features of glioma patients. **(A)** The risk classification by the four key methylated lncRNAs is significantly associated with the age at initial pathologic diagnosis and vital status, but not with the gender of the patients. **(B)** The 18 glioma-related lncRNAs are significantly differentially expressed between GBM and LGG groups, which are also significantly associated with the age and vital status, but not with the gender.

DATA AVAILABILITY STATEMENT

Publicly available datasets were analyzed in this study. This data can be found here: TCGA (http://cancergenome.nih.gov), GDC Data Portal (https://portal.gdc.cancer.gov/), and PubMed (http://www.ncbi.nlm.nih.gov/pubmed).

AUTHOR CONTRIBUTIONS

ZH designed the research. ZH, YH, JT, and LW collected the data. ZH and YH performed the research and analyzed data. ZH, JT, and YH wrote the paper. ZH and JT reviewed and modified the manuscript. All authors discussed the results and contributed to the final manuscript. All authors contributed to the article and approved the submitted version.

FUNDING

This research is financially supported by the Start-up fund of Chongqing Medical University (R1017).

SUPPLEMENTARY MATERIAL

The Supplementary Material for this article can be found online at: https://www.frontiersin.org/articles/10.3389/fonc.2020.607047/full#supplementary-material

REFERENCES

1. Klughammer J, Kiesel B, Roetzer T, Fortelny N, Nemc A, Nenning KH, et al. The DNA methylation landscape of glioblastoma disease progression shows extensive heterogeneity in time and space. *Nat Med* (2018) 24:1611–24. doi: 10.1038/s41591-018-0156-x
2. Schwartzbaum JA, Fisher JL, Aldape KD, Wrensch M. Epidemiology and molecular pathology of glioma. *Nat Clin Pract Neurol* (2006) 2:494–503. doi: 10.1038/ncpneuro0289
3. Weller M, Wick W, Aldape K, Brada M, Berger M, Pfister SM, et al. Glioma. *Nat Rev Dis Primers* (2015) 1:1–18. doi: 10.1038/nrdp.2015.17
4. Ostrom QT, Gittleman H, Stetson L, Virk SM, Barnholtz-Sloan JS. Epidemiology of gliomas. *Cancer Treat Res* (2015) 163:1–14. doi: 10.1007/978-3-319-12048-5_1
5. Tang J, He D, Yang P, He J, Zhang Y. Genome-wide expression profiling of glioblastoma using a large combined cohort. *Sci Rep* (2018) 8:15104. doi: 10.1038/s41598-018-33323-z
6. Hwang JY, Aromolaran KA, Zukin RS. The emerging field of epigenetics in neurodegeneration and neuroprotection. *Nat Rev Neurosci* (2017) 18:347–61. doi: 10.1038/nrn.2017.46
7. Etcheverry A, Aubry M, de Tayrac M, Vauleon E, Boniface R, Guenot F, et al. DNA methylation in glioblastoma: impact on gene expression and clinical outcome. *BMC Genomics* (2010) 11:701. doi: 10.1186/1471-2164-11-701
8. Chen WJ, Zhang X, Han H, Lv JN, Kang EM, Zhang YL, et al. The different role of YKL-40 in glioblastoma is a function of MGMT promoter methylation status. *Cell Death Dis* (2020) 11:668. doi: 10.1038/s41419-020-02909-9
9. Rion N, Ruegg MA. LncRNA-encoded peptides: More than translational noise? *Cell Res* (2017) 27:604–05. doi: 10.1038/cr.2017.35
10. Tang J, Wu X, Mou M, Wang C, Wang L, Li F, et al. GIMICA: host genetic and immune factors shaping human microbiota. *Nucleic Acids Res* (2020). doi: 10.1093/nar/gkaa851
11. Han Z, Xue W, Tao L, Lou Y, Qiu Y, Zhu F. Genome-wide identification and analysis of the eQTL lncRNAs in multiple sclerosis based on RNA-seq data. *Briefings Bioinf* (2020) 21:1023–37. doi: 10.1093/bib/bbz036
12. Li Q, Jia H, Li H, Dong C, Wang Y, Zou Z. LncRNA and mRNA expression profiles of glioblastoma multiforme (GBM) reveal the potential roles of lncRNAs in GBM pathogenesis. *Tumour Biol* (2016) 37:14537–52. doi: 10.1007/s13277-016-5299-0
13. Zhang X-Q, Leung GK-K. Long non-coding RNAs in glioma: functional roles and clinical perspectives. *Neurochem Int* (2014) 77:78–85. doi: 10.1016/j.neuint.2014.05.008
14. Kopp F, Mendell JT. Functional classification and experimental dissection of long noncoding RNAs. *Cell* (2018) 172:393–407. doi: 10.1016/j.cell.2018.01.011
15. Wu Z, Liu X, Liu L, Deng H, Zhang J, Xu Q, et al. Regulation of lncRNA expression. *Cell Mol Biol Lett* (2014) 19:561. doi: 10.2478/s11658-014-0212-6
16. Heilmann K, Toth R, Bossmann C, Klimo K, Plass C, Gerhauser C. Genome-wide screen for differentially methylated long noncoding RNAs identifies Esrp2 and lncRNA Esrp2-as regulated by enhancer DNA methylation with prognostic relevance for human breast cancer. *Oncogene* (2017) 36:6446–61. doi: 10.1038/onc.2017.246
17. Dong Z, Zhang A, Liu S, Lu F, Guo Y, Zhang G, et al. Aberrant methylation-mediated silencing of lncRNA MEG3 functions as a ceRNA in esophageal cancer. *Mol Cancer Res* (2017) 15:800–10. doi: 10.1158/1541-7786.MCR-16-0385
18. Wu SC, Kallin EM, Zhang Y. Role of H3K27 methylation in the regulation of lncRNA expression. *Cell Res* (2010) 20:1109–16. doi: 10.1038/cr.2010.114
19. Lai F, Shiekhattar R. Where long noncoding RNAs meet DNA methylation. *Cell Res* (2014) 24:263–4. doi: 10.1038/cr.2014.13
20. Li J, Han L, Roebuck P, Diao L, Liu L, Yuan Y, et al. TANRIC: An Interactive Open Platform to Explore the Function of lncRNAs in Cancer. *Cancer Res* (2015) 75:3728–37. doi: 10.1158/0008-5472.CAN-15-0273
21. Fortin JP, Labbe A, Lemire M, Zanke BW, Hudson TJ, Fertig EJ, et al. Functional normalization of 450k methylation array data improves replication in large cancer studies. *Genome Biol* (2014) 15:503. doi: 10.1186/s13059-014-0503-2
22. Li Q, Yu X, Chaudhary R, Slebos RJC, Chung CH, Wang X. lncDIFF: a novel quasi-likelihood method for differential expression analysis of non-coding RNA. *BMC Genomics* (2019) 20:539. doi: 10.1186/s12864-019-5926-4
23. Aryee MJ, Jaffe AE, Corrada-Bravo H, Ladd-Acosta C, Feinberg AP, Hansen KD, et al. Minfi: a flexible and comprehensive Bioconductor package for the analysis of Infinium DNA methylation microarrays. *Bioinformatics* (2014) 30:1363–9. doi: 10.1093/bioinformatics/btu049
24. Guo X, Xu Y, Zhao Z. In-depth genomic data analyses revealed complex transcriptional and epigenetic dysregulations of BRAFV600E in melanoma. *Mol Cancer* (2015) 14:60. doi: 10.1186/s12943-015-0328-y
25. Lu T, Klein KO, Colmegna I, Lora M, Greenwood CMT, Hudson M. Whole-genome bisulfite sequencing in systemic sclerosis provides novel targets to understand disease pathogenesis. *BMC Med Genomics* (2019) 12:144. doi: 10.1186/s12920-019-0602-8
26. Torabi Moghadam B, Etemadikhah M, Rajkowska G, Stockmeier C, Grabherr M, Komorowski J, et al. Analyzing DNA methylation patterns in subjects diagnosed with schizophrenia using machine learning methods. *J Psychiatr Res* (2019) 114:41–7. doi: 10.1016/j.jpsychires.2019.04.001
27. Yang H, Wang K. Genomic variant annotation and prioritization with ANNOVAR and wANNOVAR. *Nat Protoc* (2015) 10:1556–66. doi: 10.1038/nprot.2015.105
28. Simon N, Friedman J, Hastie T, Tibshirani R. Regularization Paths for Cox's Proportional Hazards Model via Coordinate Descent. *J Stat Software* (2011) 39:1–13. doi: 10.18637/jss.v039.i05
29. Okano M, Bell DW, Haber DA, Li E. DNA methyltransferases Dnmt3a and Dnmt3b are essential for de novo methylation and mammalian development. *Cell* (1999) 99:247–57. doi: 10.1016/s0092-8674(00)81656-6
30. Aapola U, Kawasaki K, Scott HS, Ollila J, Vihinen M, Heino M, et al. Isolation and initial characterization of a novel zinc finger gene, DNMT3L, on 21q22.3, related to the cytosine-5-methyltransferase 3 gene family. *Genomics* (2000) 65:293–8. doi: 10.1006/geno.2000.6168
31. Matsui T, Leung D, Miyashita H, Maksakova IA, Miyachi H, Kimura H, et al. Proviral silencing in embryonic stem cells requires the histone methyltransferase ESET. *Nature* (2010) 464:927–31. doi: 10.1038/nature08858

32. Bewick AJ, Schmitz RJ. Gene body DNA methylation in plants. *Curr Opin Plant Biol* (2017) 36:103–10. doi: 10.1016/j.pbi.2016.12.007
33. Gegner J, Gegner T, Vogel H, Vilcinskas A. Silencing of the DNA methyltransferase 1 associated protein 1 (DMAP1) gene in the invasive ladybird Harmonia axyridis implies a role of the DNA methyltransferase 1-DMAP1 complex in female fecundity. *Insect Mol Biol* (2020) 29:148–59. doi: 10.1111/imb.12616
34. Vandel L, Nicolas E, Vaute O, Ferreira R, Ait-Si-Ali S, Trouche D. Transcriptional repression by the retinoblastoma protein through the recruitment of a histone methyltransferase. *Mol Cell Biol* (2001) 21:6484–94. doi: 10.1128/mcb.21.19.6484-6494.2001
35. Chakraborty A, Viswanathan P. Methylation-Demethylation Dynamics: Implications of Changes in Acute Kidney Injury. *Anal Cell Pathol* (2018) 2018:8764384. doi: 10.1155/2018/8764384
36. Verbeek B, Southgate TD, Gilham DE, Margison GP. O6-Methylguanine-DNA methyltransferase inactivation and chemotherapy. *Br Med Bull* (2008) 85:17–33. doi: 10.1093/bmb/ldm036
37. Ross SE, Bogdanovic O. TET enzymes, DNA demethylation and pluripotency. *Biochem Soc Trans* (2019) 47:875–85. doi: 10.1042/BST20180606
38. Chang B, Chen Y, Zhao Y, Bruick RK. JMJD6 is a histone arginine demethylase. *Science* (2007) 318:444–7. doi: 10.1126/science.1145801
39. Blanc RS, Richard S. Arginine Methylation: The Coming of Age. *Mol Cell* (2017) 65:8–24. doi: 10.1016/j.molcel.2016.11.003
40. Hosseini A, Minucci S. A comprehensive review of lysine-specific demethylase 1 and its roles in cancer. *Epigenomics* (2017) 9:1123–42. doi: 10.2217/epi-2017-0022
41. Han M, Xu W, Cheng P, Jin H, Wang X. Histone demethylase lysine demethylase 5B in development and cancer. *Oncotarget* (2017) 8:8980–91. doi: 10.18632/oncotarget.13858
42. Hojfeldt JW, Agger K, Helin K. Histone lysine demethylases as targets for anticancer therapy. *Nat Rev Drug Discov* (2013) 12:917–30. doi: 10.1038/nrd4154
43. Kim JY, Kim KB, Eom GH, Choe N, Kee HJ, Son HJ, et al. KDM3B is the H3K9 demethylase involved in transcriptional activation of lmo2 in leukemia. *Mol Cell Biol* (2012) 32:2917–33. doi: 10.1128/MCB.00133-12
44. Patani N, Jiang WG, Newbold RF, Mokbel K. Histone-modifier gene expression profiles are associated with pathological and clinical outcomes in human breast cancer. *Anticancer Res* (2011) 31:4115–25. doi: 10.1016/j.canrad.2011.03.008
45. Kauffman EC, Robinson BD, Downes MJ, Powell LG, Lee MM, Scherr DS, et al. Role of androgen receptor and associated lysine-demethylase coregulators, LSD1 and JMJD2A, in localized and advanced human bladder cancer. *Mol Carcinog* (2011) 50:931–44. doi: 10.1002/mc.20758
46. Yang J, Harris AL, Davidoff AM. Hypoxia and Hormone-Mediated Pathways Converge at the Histone Demethylase KDM4B in Cancer. *Int J Mol Sci* (2018) 19:240. doi: 10.3390/ijms19010240
47. Liu G, Bollig-Fischer A, Kreike B, van de Vijver MJ, Abrams J, Ethier SP, et al. Genomic amplification and oncogenic properties of the GASC1 histone demethylase gene in breast cancer. *Oncogene* (2009) 28:4491–500. doi: 10.1038/onc.2009.297
48. Hyun K, Jeon J, Park K, Kim J. Writing, erasing and reading histone lysine methylations. *Exp Mol Med* (2017) 49:e324. doi: 10.1038/emm.2017.11
49. Jiang W, Wang J, Zhang Y. Histone H3K27me3 demethylases KDM6A and KDM6B modulate definitive endoderm differentiation from human ESCs by regulating WNT signaling pathway. *Cell Res* (2013) 23:122–30. doi: 10.1038/cr.2012.119
50. Kottakis F, Polytarchou C, Foltopoulou P, Sanidas I, Kampranis SC, Tsichlis PN. FGF-2 regulates cell proliferation, migration, and angiogenesis through an NDY1/KDM2B-miR-101-EZH2 pathway. *Mol Cell* (2011) 43:285–98. doi: 10.1016/j.molcel.2011.06.020
51. He J, Nguyen AT, Zhang Y. KDM2b/JHDM1b, an H3K36me2-specific demethylase, is required for initiation and maintenance of acute myeloid leukemia. *Blood* (2011) 117:3869–80. doi: 10.1182/blood-2010-10-312736
52. Paul Y, Thomas S, Patil V, Kumar N, Mondal B, Hegde AS, et al. Genetic landscape of long noncoding RNA (lncRNAs) in glioblastoma: identification of complex lncRNA regulatory networks and clinically relevant lncRNAs in glioblastoma. *Oncotarget* (2018) 9:29548. doi: 10.18632/oncotarget.25434
53. Capper D, Jones DTW, Sill M, Hovestadt V, Schrimpf D, Sturm D, et al. DNA methylation-based classification of central nervous system tumours. *Nature* (2018) 555:469–74. doi: 10.1038/nature26000
54. Siegfried Z, Eden S, Mendelsohn M, Feng X, Tsuberi BZ, Cedar H. DNA methylation represses transcription in vivo. *Nat Genet* (1999) 22:203–6. doi: 10.1038/9727
55. Razin A, Cedar H. DNA methylation and gene expression. *Microbiol Rev* (1991) 55:451–8. doi: 10.1128/MMBR.55.3.451-458.1991
56. Hashimshony T, Zhang J, Keshet I, Bustin M, Cedar H. The role of DNA methylation in setting up chromatin structure during development. *Nat Genet* (2003) 34:187–92. doi: 10.1038/ng1158
57. Kayser M, de Knijff P. Improving human forensics through advances in genetics, genomics and molecular biology. *Nat Rev Genet* (2011) 12:179–92. doi: 10.1038/nrg2952
58. Liang J, Wei X, Liu Z, Cao D, Tang Y, Zou Z, et al. Long noncoding RNA CYTOR in cancer: A TCGA data review. *Clin Chim Acta* (2018) 483:227–33. doi: 10.1016/j.cca.2018.05.010
59. Zou SF, Yang XY, Li JB, Ding H, Bao YY, Xu J. UPF1 alleviates the progression of glioma via targeting lncRNA CYTOR. *Eur Rev Med Pharmacol Sci* (2019) 23:10005–12. doi: 10.26355/eurrev_201911_19567

Conflict of Interest: The authors declare that the research was conducted in the absence of any commercial or financial relationships that could be construed as a potential conflict of interest.

frontiers in Oncology

REVIEW
published: 21 January 2021
doi: 10.3389/fonc.2020.623634

Regulation of Gene Expression Associated With the N6-Methyladenosine (m6A) Enzyme System and Its Significance in Cancer

Shuoran Tian[1†], *Junzhong Lai*[2†], *Tingting Yu*[1], *Qiumei Li*[1] *and Qi Chen*[1*]

[1] *Fujian Key Laboratory of Innate Immune Biology, Biomedical Research Center of South China, College of Life Science, Fujian Normal University, Fuzhou, China,* [2] *The Cancer Center, Union Hospital, Fujian Medical University, Fuzhou, China*

OPEN ACCESS

Edited by:
Xiangqian Zheng, Tianjin Medical University Cancer Institute and Hospital, China

Reviewed by:
Chunjie Jiang, University of Pennsylvania, United States
Tzu Pin Lu, National Taiwan University, Taiwan

****Correspondence:***
Qi Chen
chenqi@fjnu.edu.cn

[†]These authors have contributed equally to this work

Specialty section:
This article was submitted to Cancer Genetics, a section of the journal Frontiers in Oncology

Received: *30 October 2020*
Accepted: *04 December 2020*
Published: *21 January 2021*

Citation:
Tian S, Lai J, Yu T, Li Q and Chen Q (2021) Regulation of Gene Expression Associated With the N6-Methyladenosine (m6A) Enzyme System and Its Significance in Cancer. Front. Oncol. 10:623634. doi: 10.3389/fonc.2020.623634

N6-methyladenosine (m6A), an important RNA modification, is a reversible behavior catalyzed by methyltransferase complexes (m6A "writers"), demethylated transferases (m6A "erasers"), and binding proteins (m6A "readers"). It plays a vital regulatory role in biological functions, involving in a variety of physiological and pathological processes. The level of m6A will affect the RNA metabolism including the degradation of mRNA, and processing or translation of the modified RNA. Its abnormal changes will lead to disrupting the regulation of gene expression and promoting the occurrence of aberrant cell behavior. The abnormal expression of m6A enzyme system can be a crucial impact disturbing the abundance of m6A, thus affecting the expression of oncogenes or tumor suppressor genes in various types of cancer. In this review, we elucidate the special role of m6A "writers", "erasers", and "readers" in normal physiology, and how their altered expression affects the cell metabolism and promotes the occurrence of tumors. We also discuss the potential to target these enzymes for cancer diagnosis, prognosis, and the development of new therapies.

Keywords: N6-methyladenosine, m6A, m6A enzyme system, oncogene and tumor suppressor gene, cancer

INTRODUCTION

RNA methylation is one of the most important epigenetic modifications in RNA post-transcriptional modification. RNA methylation includes several types such as m6A, N1-methyladenosine (m1A), Eukaryotic 5-methylcytosine (m5C), 7-methylguanosine (m7G), RNA 2′-O-Methylation (Nm), etc. (1). m6A mainly occurs in the CDS region and the 3′-UTR region, especially in the region near the stop codon of mRNA. m1A and m5C modifications are initially found on tRNA and rRNA, but later, also on the mRNA. The m1A modification on mRNA mainly occurs near the initiation codon AUG, on the upstream of the first splicing site. It is found that m1A is often rich in GC bases but without strong sequence specificity (2). And m5C is mainly enriched in the untranslated region (5′-UTR and 3′-UTR), GC-rich region, and the vicinity of the AGO protein

binding site, and it has the conserved sequence of AU(m5C)GANGU (3). In tRNA, m5C is mainly distributed in the variable arm and anti-cipher ring. In rRNA, m5C often appears in the region where associated with the translation activity (4). RNA methylation modification is a dynamic and reversible process regulated by RNA methylase and demethylase, and it needs the participation of RNA methylation binding protein. In the case of RNA m5C methylation, as a methyl donor, S-adenosine methionine (SAM) forms 5-methylcytosine (m5C) through the NSUN protein family (including NOL1, NOP2, and Sun) (5). The m5C methylated RNA exerts its biological function by binding to the reading protein ALYREF (6). TET3 may be the demethyltransferase of RNA m5C, and the specific mechanism of action needs to be further explored (7). Recent studies also found a synergistic effect between m5C and m6A in terms of the regulatory function of RNA. Nsun2-mediated m5C methylation and METTL3/METTL14-mediated m6A methylation can synergistically enhance the translation of P21 (8). Due to the space limitation, this review will focus on the recent progress on the m6A modification.

In 1974, m6A was first discovered in poly(A) RNA (9, 10), however, due to the scarcity of methodologies, research interest in m6A largely faded in the late 1970s (11). Since 2012, with the development of the antibody-based immunoprecipitation and high-throughput sequencing techniques for transcriptome-wide analysis of m6A, over 10,000 m6A peaks have been identified and validated in approximately 25% of human transcripts (12, 13). Modification of m6A has been found occurring in mRNA, non-coding RNA, 18S rRNA, 28S rRNA, U2-, U4-, and U6-spliceosomal RNA (14–17). In addition, following the development of a variety of antibody-independent detection methods and the sequencing depth reaching to a single base level, m6A modifications can be tested with high resolution in a variety of cellular environments (18, 19).

m6A is a methylation modification for the N6 position of adenylate, which is mainly found in the stop codon, 3′-UTR and long exon region (CDS). The modification site is often on the conserved sequence of RRACH (R = A or G; H = A, C, or U) (20–22). They are also found in many internal exon sequences and in 5′-UTR, which has been proven to participate in translation regulation. Typically, translation begins with the recruitment of the 43S ribosomal complex to the 5′ cap of mRNAs, however it seems that mRNAs containing m6A in their 5′-UTR can directly binds eukaryotic initiation factor 3 (eIF3) to initiate translation in the absence of the cap-binding factor eIF4e (23). Recent studies have shown that m6A modification of the first nucleotide near the cap of 7-methylguanine protects the mRNA from deacetylation and is involved in maintaining mRNA stability (24).

The m6A modification process is dynamically reversible and regulated by the methylase complex, demethylase, and related binding proteins. The methyltransferase complex is mainly composed of methyltransferase like protein 3 (METTL3) (25), methyltransferase like protein 14 (METTL14) (26), Wilm's tumor-associated protein 1 (WTAP) (27), the human homologous gene of Drosophila VIR protein (KIAA1429) (28), RNA binding motif protein 15 (RBM15) (29), and zinc finger CCCH domain protein 13 (ZC3H13) (30), as well as ZFP217 (31) and HAKAI (32). Most of them are able to catalyze m6A methylation modification *in vivo* and *in vitro*. METTL3 and METTL14 form the center of the complex. METTL14 has no catalytic domain but provides a backbone for RNA binding and assist METTL3 in increasing its catalytic efficiency. The important function of WTAP is to recruit METTL3 and METTL14 (33, 34). Therefore, these enzymes are collectively referred to as m6A "writers". On the other hand, the obesity-related gene FTO and the demethylase ALKBH5 have been described as m6A "erasers" which are able to remove m6A modifications from RNAs (35, 36). In addition, the m6A "reader" proteins recognize methyl groups and promote downstream mRNA effects. The related proteins belong to YTH protein family, which include YTHDC1 found in the nucleus or YTHDC2 and YTHDF1/2/3 in the cytoplasm (37–41). Regulation and mechanism of the N6-methyladenosine (m6A) enzyme system can be seen in **Figure 1**. This review summarizes the latest progress in epigenetics research related to m6A methylation modification and its regulation involved in the occurrence and progression of multitudinous cancers.

STRUCTURE AND FUNCTION OF M6A ENZYME SYSTEM

RNA Methyltransferase

m6A Methyltransferase Complex

METTL3 was first m6A modification enzyme identified, but METTL3 alone cannot perform catalytic enzyme activity (25). Later, WTAP and METTL14 were discovered by using tandem affinity precipitation combined with mass spectrometry (26, 27). Both METTL3 and METTL14 belong to a conserved family of methyltransferases which contain a MT-A70 domain (also known as MTD) that catalyzes the transfer of methyl group to adenosine (26). In the methyltransferase complex, METTL3 binds to methyl donor S-adenosine methionine (SAM) and catalyzes methyl transfer. Although not involved in catalytic reactions, METTL14 helps stabilize the structure of the catalytic center and acts as a scaffold for RNA binding (43). WTAP is functionally related to alternative splicing (44) and transports METTL3-METTL14 to the nucleus (27). In addition, KIAA1429 was also found to be a protein that participates in alternative splicing, interact with WTAP, and significantly affect the m6A methylation levels (28, 45). Besides, RBM15 has been found to interact with RNA substrates near the m6A site and introduces METTL3-METTL14 into RNA for the modification (29).

Other Components

More recently, Methyltransferase like protein 5 (METTL5) and Methyltransferase like protein 16 (METTL16) have also been shown to be m6A RNA methyltransferases. They both can catalyze m6A on certain structured RNAs (46, 47). METTL16 encodes SAM synthetase and can catalyze the modification of N6-methyladenosine at the 43rd position of U6 snRNA (47, 48).

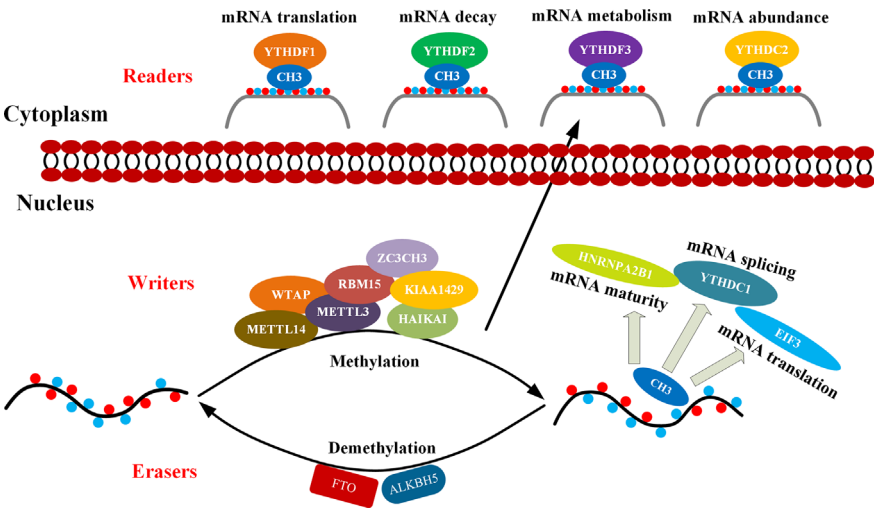

FIGURE 1 | Mechanism of m6A. m6A methylation occurs through methyltransferase complexes: mainly by METTL3, METTL14 and WTAP complex (cofactors: KIAA1429, RBM15, ZC3CH3, and HAIKAI). The m6A modification is removed by demethylase FTO or ALKBH5. Reader proteins recognize m6A and determine target RNA fate (42).

METTL16 can directly bind the hairpin structure in the 3′-UTR, and adjust the residence time and methylation efficiency immediately according to the changes in the intracellular SAM concentration, thereby completing the splicing of MAT2A mRNA and maintaining its stability (47, 49). Unlike METTL3-METTL14 heterodimers, METTL16-dependent m6A markers do not generally appear in the RRACH sequence motif but often exist at intron or intron-exon boundaries. Thus, METTL16 can take advantage of the sequence and structure specificity to bind corresponding RNA subunits (47, 48). Interestingly, one study suggests that METTL16 may play a multiplicity role in mRNA pre-splicing, acting as both m6A "writer" and m6A "reader". As the "writer" of m6A, METTL16 rapidly methylated MAT2A mRNA in the presence of SAM, leading to intron retention and subsequent nuclear degradation. When SAM levels were low, METTL16 could remain on MAT2A mRNA for a long time, thus function as "reader" to enhance the preservation of intron splicing (48).

Recent studies have revealed that METTL5 is the m6A methyltransferase for 18S rRNA (46). Particularly, METTL5 forms a heterodimer with TRMT112 and provides the catalytic subunit to specifically methylate the 6th position of adenine in position 1832 of 18S rRNA (46). METTL5 may be essential for efficient translation, with profound implications for cellular function and pluripotency. Biallele variation of METTL5 may lead to lack of m6A modification on 18S rRNA, which has been shown to be associated with autosomal recessive intelligence and microcephaly in humans (50). These studies highlight the important role of METTL5 and ribosomal RNA modifications in gene expression, brain development and neurological function (51). ZCCHC4 is located at the nucleolus, where the ribosomes are assembled. ZCCHC4 has a potential m6A methyltransferase domain, with conserved catalytic motif "DPPF" and CCHC-ZNF domain, and can induce m6A methylation at 4220 in human 28srRNA (52, 53). When deleted, the accumulated level of m6A is significantly reduced in total rRNA, leading to unsteadiness in ribosome activity, which is associated with codon specific translation defects (54).

RNA Demethylase

FTO and ALKBH5 are two currently known m6A demethylases and belong to the AlkB family of Fe (II)/α-ketoglutarate (α-KG) dependent dioxygenases. The AlkB demethylase family, which depends on a-KG, mainly catalyzes the oxidative demethylation of nucleic acid bases, and contains 9 members in mammals, including ALKBH1-8 and FTO (ALKBH9). Although these members have similar catalytic cores, they exhibit different substrate preferences (55). Both FTO and ALKBH5 specifically demethylate m6A on single-stranded RNA, but FTO demethylates m6A through three rounds of oxidation to produce two intermediate products hm6A and fm6A, while ALKBH5 directly converts m6A to adenosine with no intermediate products observed (56).

m6A Demethylase: FTO

In the early research, it was found that the m6A level in the mRNA of the FTO gene knockdown cells increased, and the opposite result occurs when FTO is overexpressed, suggesting the demethylation function of FTO (36). Later on, the existence of other substrates for FTO, such as N6, 2′-O-dimethyladenosine (m6Am), has been demonstrated (24). Therefore, FTO can mediate the demethylation of m6A and m6Am on RNA with polyA tail. The preference of FTO to m6A or m6Am is affected by its position in the cell. FTO has different positions in different cells. FTO in the nucleus can mediate the demethylation of m6A, while FTO in the cytoplasm can mediate the demethylation of

both m6Am and m6A. In addition, FTO can also bind tRNA, function as a m1A demethylase of tRNA, and further affect the rate of protein translation (57).

m6A Demethylase: ALKBH5

ALKBH5, as a homologous protein of FTO in the ALKB family, is the second m6A demethylase identified. ALKBH5 knockdown results in a significant increase in the m6A level of mRNA, while ALKBH5 overexpression has an opposite effect (35). Different than FTO, ALKBH5 has no activity toward m6Am and appears specific to m6A (24).

RNA Methylation-Modified Binding Protein

m6A-Binding Proteins: YTHDF1, YTHDF2, and YTHDF3

Members of the YTH family are highly conserved and contain an aromatic pocket of the YTH domain used to identify m6A-modified adenosine. These proteins are widely found in mammals, fruit flies, yeasts, and arabidopsis include YTHDF1/2/3 and YTHDC1/2 (38, 40, 41).

YTHDF1 was initially found to bind to the termination codon of m6A-modified transcripts, and its overall distribution is highly similar to that of m6A-modified transcripts (38). In addition, YTHDF1 can interact directly with the translation initiation complex, thus promoting the translation efficiency of m6A-modified RNA substrates. YTHDF1 is normally localized in the cytoplasm, but may also play a role in facilitating translation initiation and protein synthesis similar to that of eIF3 in the nucleus (58).

In 2014, YTHDF2 was first reported to act as a m6A binding protein to mediate m6A-modified mRNA degradation. Normally, YTHDF2 can co-localize with the adenylate enzyme complex and recruit CCR4-NOT, and the transcript of its target gene can be brought to the mRNA decay site (such as P body) through m6A modification, which then triggers the transcript adenylylation and degradation. YTHDF2 can alter its own cellular localization during heat shock stress (59).

Through tandem affinity precipitation combined with mass spectrometry and GST-pull down experiments, YTHDF3 and YTHDF1 were identified to interact with ribosomal 40S small subunit and 60S large subunit proteins (37). YTHDF3 and YTHDF1 have similar binding motif, mainly located at 3′-UTR. YTHDF3 together with YTHDF1, are cable to enhance the translation efficiency of target genes, showing a synergistic effect. In addition, YTHDF3 can mediate mRNA degradation through direct interaction with YTHDF2 (60).

m6A binding Proteins: YTHDC1 and YTHDC2

To investigate how m6A modification in the nucleus regulates selective splicing of mRNA, the researchers identified the m6A-binding protein YTHDC1, which is localized in the nucleus. YTHDC1 is responsible for splicing and output of mRNAs with m6A modification (61). YTHDC1 regulates selective splicing of RNA by interacting with SRSF3 (serine and arginine rich splicing factor 3) and SRSF10 (serine and arginine rich splicing factor 10). Either SRSF3 or SRSF10 can interact directly and competitively with YTHDC1. After YTHDC1 knockdown, the binding ability of SRSF3 to RNA and the nuclear localization signal of the protein were significantly weakened, while SRSF10 showed an opposite trend (62). YTHDC1 also plays an important role in the pre-mRNA processing of oocyte nuclei by interacting with the pre-mRNA 3′-end processing factors CPSF6, SRSF3 and SRSF7 (40). As the largest member of the YTH protein family, YTHDC2 preferred to bind a specific motif (GGACU) with m6A modification, thus accelerating the mRNA degradation and enhancing the translation efficiency (41).

Other m6A Binding Proteins

Other m6A binding proteins, including IGF2BPs (the family of insulin-like growth factor mRNA binding proteins), were identified by RNA pull-down method. In contrast to the function of YTHDF2/3, IGF2BP1/2/3 protects m6A-modified mRNAs in P-body and stress particles from degradation, and can facilitate mRNA translation by interacting with embryonic lethal abnormal vision (ELAV) such as RNA-binding protein 1 (HuR), matrix protein 3 (MATR3) and poly(A) binding protein cytoplasm 1 (PABPC1) (63, 64).

In the recent studies, HNRNPA2B1 of the HNRNP (splicing factors heterogeneous ribonucleoprotein) protein family is also considered to be an m6A binding protein. But it is different from YTHDC1 in that it cannot directly bind to the m6A. It usually activates the downstream pathway of pri-miRNA or participates in the processing of pre-miRNA. HNRNPA2B1 can recognize the binding of m6A-modified RGAC (R = A or G) motif in the miRNA transcript subset, and further exert alternative splicing effects by recruiting microprocessor complexes to promote miRNA processing. The m6A modification on pre-mRNA can recruit HNRNPA2B1, or increases the accessibility of the lateral RNA sequence with HNRNPC and HNRNPG by changing the local structure, thus becoming a "m6A switch" (65).

In addition, METTL3 may also have a function independent of its methyltransferase activity and act as a reader in the cytoplasm. METTL3, located near the termination codon of the mRNA, can interact with the 5′ cap by binding to elF3h, which promotes the ring formation of the mRNA, thereby promoting mRNA translation (66).

ROLES OF THE M6A ENZYME SYSTEM IN HUMAN CANCERS

Although m6A modification does not alter the normal pairing and coding functions of nucleotide sequence, it can affect gene expression extensively by interacting with various m6A modulating proteins. These proteins are involved in almost all processes of m6A-induced RNA metabolism, including mRNA translation, degradation, splicing and play important roles in cell function, development, and cancer progression (67). In addition, m6A modification can also affect the cleavage, transport, stability, and degradation process of miRNA, LncRNA and circRNA. Recent studies have revealed that the overall level of modification of m6A and its associated expression levels of regulatory proteins as well as the expression of affected non-coding RNA are often dysregulated in many types of cancer and can play an important role in the

occurrence, progression, metastasis, drug resistance, and recurrence of cancer (68).

Interaction Between m6A Enzyme System and mRNA in cancer

METTL3

METTL3 can affect cancer progression both positively and negatively (**Table 1**). In lung adenosarcoma, METTL3 promotes tumor cell growth, survival, and proliferation by promoting the translation of EGFR, TAZ, MK2, DNMT3A, and BRD4 (69–71). In hepatocellular carcinoma, METTL3 affects the occurrence of cancer by targeting SOCS2, a tumor suppressor gene, and m6A degradation mediated by YTHDF2 (72). In acute myelogenous leukemia (AML), METTL3 controls myeloid differentiation of normal hematopoietic and leukemia cells by promoting m6A-mediated translation of apoptotic genes such as C-MYC, BCL-2, and PTEN (73).

In other types of cancer, such as endometrial cancer, METTL3 expression was found to be reduced, promoting proliferation by altering AKT signaling (74). In malignant gliomas. the deletion of METTL3 can lead to upregulation of oncogenes such as ADAM19, EPHA3 and KLF4, and downregulation of tumor suppressor genes such as CDKN2A, BRCA2 and TP53, thereby promoting the growth and self-renewal of gastric stump cancer. Deficiency of the METTL3 in renal carcinoma cell lines significantly promotes cell proliferation, migration and invasion, and induced cell cycle G0/G1 phase arrest (75). Therefore, METTL3 was identified as a suppressor or promoter in certain cancers and further studies have indicated that the m6A level was changing following the development of cancer, which may partly explain the contradiction (76).

When involved in the regulation of tumor behavior, m6A modification can not only affect cell proliferation and migration, but also, equally important, regulate intracellular energy metabolism, such as glycolysis (77). Some data show that METTL3 is related to abnormal glucose metabolism and mTOR signaling pathway thereby is directly involved in the

TABLE 1 | Functions of m6A writers in cancer.

m6A Enzyme system	Cancer type	Overexpressed or Underexpressed	Target(s)	Changes in the behavior of tumor cells	Reference
Wrirers					
METTL3	lung adenocarcinoma.	Overexpressed	EGFR, TAZ, MK2, DNMT3A and BRD4	Promote the growth, survival, and proliferation	(69–71)
	breast carcinoma	Overexpressed	The positive feedback loop HBXIP/LET7G/HBX2P	Promote cell proliferation	(71)
	hepatocellular carcinoma	Overexpressed	SOCS2	Affect the occurrence of cancer through YTHDF2-mediated degradation of m6A	(72)
	acute myelogenous leukemia	Overexpressed	C-MYC, BCL-2 and PTEN	Promote the survival and proliferation	(73)
	endometrial carcinoma	Underexpressed	AKT signaling	Promotes cell proliferation	(74)
	endometrial carcinoma	Underexpressed	ADAM19, EPHA3 and KLF4/CDKN2A, BRCA2 and TP53	Promote the growth and self-renewal	(75)
	renal carcinoma	Underexpressed	Cell cycle	Promote cell proliferation, migration, and invasion	(76)
	gastric carcinoma	Overexpressed	H3K27-METTL3-HDGF-GLUT4/ENO2	Glycolysis	(77)
	hepatocellular carcinoma	Underexpressed	mTOR	Glycolysis	(78)
	colorectal cancer	Overexpressed	HK2/SLC2A1	Glycolysis	(77)
METTL14	pancreatic carcinoma	Overexpressed	AMPK α, ERK1/2 and mTOR signaling pathways	Promote cell apoptosis	(79)
	acute myelogenous leukemia	Overexpressed	MYC and MYB	Promote cell proliferation	(80)
	breast carcinoma	Underexpressed		Promote tumor growth, angiogenesis, and tumor development	(81)
	endometrial carcinoma	Underexpressed	AKT signaling	Promote cell proliferation	(82)
	bladder carcinoma	Underexpressed	Notch1	Negative regulation in proliferation, metastasis, and tumor initiation	(83)
WTAP	malignant glioma	Overexpressed	EGF	Oncogene	(84, 85)
	acute myelogenous leukemia	Overexpressed	HSP90	Regulation in abnormal proliferation and arrested differentiation	(86)
	renal carcinoma	Overexpressed	CDK2	Promote cell proliferation	(87)
	hepatocellular carcinoma	Overexpressed	HUR-ETS1	Promote proliferation of hepatocellular carcinoma cells *in vitro* and *in vivo*	(88)
	High-grade serous ovarian cancer	Overexpressed	MAPK and AKT signaling pathways	Associated with proliferation of cancer cells and lymph node metastasis	(89)

regulation of glycolytic activity in hepatocellular carcinoma. The down-regulation of METTL3 can weaken the glycolysis ability and cooperate with the glycolysis inhibitor 2-deoxyglucose (2-DG) to inhibit tumor growth *in vitro* (78). In addition, METTL3 is also shown to induce colorectal cancer relying on glycolysis. METTL3 can directly interact with the 5′ or 3′-UTR region of HK2 and the 3′-UTR region of SLC2A1 (GLUT1), relying on IGF2BP2 or IGF2BP3 to further stabilize these two genes and activate the glycolysis pathway (77). In gastric cancer, it can be found that m6A level is at a high level for the reason that METTL3 is activated by p300-mediated H3K27, which then leads to the enhancement of the stability of hepatocellular growth factor (HDGF) mRNA by m6A modification identified by "reader" IGF2BP3. HDGF can promote tumor angiogenesis, and nuclear HDGF activates the expression of GLUT4 and ENO2 which are associated with proliferation and liver metastasis of gastric cancer cells (90). In addition, studies have found that the enhancement of the "Warburg effect" (including glycolytic and lactic acid fermentation activity) can become a new sign of malignant cancer cells. The latest research shows that it is expected to become a new type of cancer treatment that reverses the Warburg effect and targets lactic acid, the end product of glycolysis, to reactivate oxidative phosphorylation (91). Therefore, the research on the relationship between m6A and glycolysis is becoming progressively significant. The studies elucidated above suggest that METTL3 and its related pathways may become a reasonable therapeutic target for cancer patients with high glucose metabolism.

METTL14

METTL14 also shows both promoting and anti-cancer effects (**Table 1**). Down-regulation of METTL14 expression interferes with AMPKα, ERK1/2 and mTOR signaling pathways, promotes apoptosis and can increase the sensitivity of pancreatic cancer cells to cisplatin (79). METTL14 promotes proliferation of cancer cells by promoting the translation of oncogenes MYC and MYB through m6A modification in AML, and its absence promotes the myeloid differentiation (80).

On the other hand, METTL14 expression is downregulated in glioblastoma, breast carcinoma, endometrial cancer, and bladder cancer cells and tissues. METTL14 expression level is down-regulated in breast cancer, in turn to promote tumor growth, angiogenesis and tumor occurrence and development (81). In endometrial cancer, METTL14 is deviancy due to mutation, which promotes cell proliferation by altering AKT signaling (92). METTL14 gene knockout promotes the proliferation, metastasis, and tumor initiation capacity of bladder cancer cell lines (TICs), this phenomenon disappears once METTL14 is overexpressed. Specifically, the m6A modification regulated by METTL14 is involved in the stability of Notch1 mRNA, which is a key factor in maintaining proliferation and invasion (83).

WTAP

WTAP has shown anti-cancer effect and been suggested as a novel therapeutic target (**Table 1**). In malignant gliomas, WTAP can regulate migration and invasion through EGF signaling, and closely related to glioma severity and postoperative survival rate of glioma patients (84, 85). WTAP is a novel client protein of HSP90 and promotes proliferation and clonal inhibition of differentiation in AML (86). In renal carcinoma, WTAP promotes cell proliferation, cell migration *in vitro*, and tumorigenesis *in vivo* by enhancing CDK2 expression (87). It was also found that WTAP is highly expressed in liver cancer tissue, and the progress of hepatocellular carcinoma (HCC) is related to the phenotype caused by WTAP deficiency. WTAP through m6A methylation modification leads to the post-transcriptional inhibition of HuR-ETS1, inhibits the E21-mediated P21/P27-dependent regulation of G2/M phase progression of hepatoma cell cycle, and promotes the proliferation and tumor growth of hepatoma cells (88). High expression of WTAP is associated with the overall survival of high-grade serous ovarian cancer (HGSOC). In ovarian cancer cell lines, after WTAP is down-regulated, cell proliferation and migration are significantly reduced, while the apoptosis rate is increased, which may be related to MAPK and AKT signaling pathways (89).

FTO

FTO also presents both pro- and anti-cancer effects (**Table 2**). It interacts with MYC and bHLH transcription factors to promote the proliferation of pancreatic cancer cells (93). FTO promotes proliferation and colony formation of lung cancer cells by increasing the expression of USP7 (ubiquitin-specific protease 7) (94).

In lung squamous cell carcinoma, FTO enhances the expression of M2F1 by reducing the level of m6A in the M2F1 transcript and maintaining the stability of mRNA, thus inducing carcinogenic function (107). FTO reduces the level of β-catenin mRNA through m6A modification, thus increasing the activity of resecting and repairing cross complementary group 1 (ERCC1) and enhances the resistance of the body to chemotherapy in cervical squamous cell carcinoma (95). FTO can interact with E2F1 and MYC transcripts, thus significantly reducing the translation efficiency of E2F1 and MYC, and promoting the proliferation and migration of cervical cancer tumor cells (96). FTO-mediated demethylation of m6A in the 3′-UTR of BNIP3 mRNA, a pro-apoptotic factor, and induced its degradation through YTHDF2 independent mechanism to promote breast cancer cell proliferation, colony formation and metastasis (97). FTO can induce demethylation and translation of the PKM2 gene and promote the occurrence of hepatocellular carcinoma (98). In AML, FTO affects the stability of ASB2 and RARA by lowering m6A levels to prevent bone marrow differentiation and promote survival, proliferation, and cloning (99).

In contrast, the deletion of FTO significantly promotes the proliferation and migration of bladder cancer including 5637 and T24 cells. It was found that the cells can be protected from the cytotoxicity induced by cisplatin when FTO expression was inhibited (108).

ALKBH5

ALKBH5 promotes the self-renewal of cells and regulates the occurrence of brain tumors by regulating FOXM1 in

TABLE 2 | Functions of m6A erasers in cancer.

m6A Enzyme system	Cancer type	Overexpressed or Underexpressed	Target(s)	Changes in the behavior of tumor cells	Reference
Erasers					
FTO	pancreatic carcinoma	Overexpressed	MYC and bHLH	Promote cell proliferation	(93)
	Non-Small Cell Lung Cancer	Overexpressed	USP7	Promote cell proliferation	(94)
	Cervical squamous carcinoma	Overexpressed	β-catenin and ERCC1	Regulate the chemo-radiotherapy resistance of cervical squamous cell carcinoma	(95)
	Cervical squamous carcinoma	Overexpressed	E2F1 and MYC	Promote proliferation and migration	(96)
	Cervical squamous carcinoma	Overexpressed	BNIP3	In collaboration with YTHDF2 and promote cell proliferation, colony formation and metastasis	(97)
	hepatoma	Overexpressed	PMK2	Regulate the cell cycle and ectopic expression is associated with poor prognosis	(98)
	acute myelogenous leukemia	Overexpressed	ASB2 and RARA	Promote survival, proliferation, and cloning	(99)
ALKBH5	glioblastoma	Overexpressed	FOXM1	Promote cell self-renewal and its occurrence in brain tumor	(100)
	breast carcinoma	Overexpressed	NANOG	Maintain the tumor microenvironment	(101)
	Epithelial ovarian carcinoma	Overexpressed	EGFR-PIK3CA-AKT-mTOR signaling pathway and BCL-2	Enhance the autophagy in SKOV3 cells	(102)
	gastric carcinoma	Overexpressed	NEA-T1 and E2H2	Promote the invasion and metastasis	(103)
	lung adenocarcinoma	Overexpressed	FOXM1	Promote tumor progression	(104)
	pancreatic cancer	Underexpressed	WIF-1	Inhibit tumorigenesis and make tumor cells more sensitive to chemotherapy	(105)
	pancreatic cancer	Underexpressed	ATM-CHk2-p53/CDC25C	Inhibit the growth of tumor cells	(106)

glioblastoma stem cells (100). In ovarian cancer, ALKBH5 activates the EGFR-PIK3CA-AKT-mTOR signaling pathway, enhances the stability of BCL-2 mRNA, and promotes the interaction between BCL-2 and Beclin 1. Silencing ALKBH5 enhanced autophagy in ovarian cancer SKOV3 cells (102). ALKBH5, through m6A and NEA-T1, affects the expression of the polyclonal inhibitor complex subunit E2H2, thereby promoting the invasion and metastasis of gastric cancer cells (103). ALKBH5 regulates the mRNA level of FOXM1 by reducing m6A modification, participates in the generation of intermittent hypoxia (IH) tumor microenvironment, and promotes proliferation and invasion of lung adenocarcinoma cells (104).

On the other hand, the loss of ALKBH5 often indicates a poor prognosis for colon and pancreatic cancers. ALKBH5 can inhibit the invasion and metastasis of colorectal cancer cells (102). In pancreatic cancer, ALKBH5 relies on the demethylation of Wnt inhibitory factor 1 (WIF-1) and the activation of Wnt signal to inhibit tumorigenesis and make tumor cells more sensitive to chemotherapy (105). In another study of pancreatic cancer, ALKBH5 is shown to activate PER1 in an m6A-YTHDF2-dependent manner, and induce the activation of the ATM-CHk2-p53/CDC25C signaling pathway to inhibit the growth of tumor cells (106) (**Table 2**).

YTHDF1/2/3

The deletion of YTHDF1 can greatly reduce the translation efficiency of CDK2, CDK4 and cyclin D1, which are closely related to cell cycle regulation, and can effectively inhibit the proliferation of NSCLC cells and the formation of xenograft tumors. However, in clinical treatments, researchers have found that the absence of YTHDF1 often makes cancer cells resistant to cisplatin (DDP) (109). In another study, researchers also found that silencing YTHDF1 expression can significantly inhibit the Wnt/β-catenin pathway, thereby inhibiting the tumorigenicity of colorectal cancer cells (110). YTHDF1 binds with m6A-modified EIF3C (a subunit of protein translation initiation factor EIF3) mRNA to enhance EIF3C translation, and at the same time promotes the overall translation output, thereby promoting the ovarian cancer occurrence and transfer (58).

In prostate cancer, YTHDF2 can promote cancer cell migration. In pancreatic cancer, the expression level of YTHDF2 increases with the extension of the cancer stage, which can inhibit epithelial-mesenchymal transition by inhibiting YAP signaling (111). In lung cancer, YTHDF2 directly binds to the m6A modification site (3′-UTR) of glucose 6-phosphate dehydrogenase (6PGD) to promote the translation of 6-PGD and the proliferation of lung cancer cells (112). YTHDF2 is highly expressed in AML, down-regulates TNFR2 and protects AML cell apoptosis, which is crucial for the development of leukemia. Hematopoietic stem cells (HSC) have the ability to differentiate and self-renew, which involves the regeneration and degradation of a large amount of mRNA. In the cytoplasm, YTHDF2 can promote m6A-dependent mRNA decay under normal and stress conditions, and play an important role in HSC homeostasis and hematological stress (113). In testicular germ cell tumors, YTHDF3 maintains cancer cell phenotypes through m6A modification (114).

In hepatocellular carcinoma, YTHDF2 not only exhibits a cancer-promoting effect, but also can exert a cancer-suppressing effect. YTHDF2 promotes CSC liver phenotype and tumor metastasis by regulating the 5′-UTR m6A level of OCT4

mRNA (115). YTHDF2 directly binds to the m6A modification site of EGFR 3′-UTR, promotes the degradation of EGFR mRNA, and inhibits the proliferation of cancer cells and tumor growth (116). YTHDF2 silencing in human hepatoma cells or ablating in mouse hepatocytes can cause inflammation, vascular reconstruction, or cancer metastasis (117).

YTHDC2 and IGF2BPs

Other studies of YTH family expression disorders have emerged in recent years (**Table 3**). The expression level of YTHDC2 is positively correlated with the stage or metastasis of colon tumor by promoting translation of HIF-1α (118). In hepatocellular carcinoma, IGF2BP1 can bind and stabilize c-MYC and MKI67 mRNAs, increase the expression of c-MYC and MKI-67 proteins, which are effective regulators of cell proliferation and apoptosis, and thus participate in regulation of tumor progression (119).

Interaction Between the m6A Enzyme System and Noncoding RNAs in Cancer

In addition to mRNAs, m6A has also been found in a variety of non-coding RNAs (ncRNAs), such as miRNAs, long non-coding RNAs (LncRNAs), circular RNAs (circRNAs), ribosomal RNAs (rRNAs), small nuclear RNAs (snRNAs)), and small nucleolar RNAs (snoRNAs), can have an important impact on their metabolism and function (120–123), suggesting the potential association between tumor and m6A-ncRNA modification (124). Here, we discuss the interaction between m6A modification and non-coding RNA by focusing on the functional relevance of m6A in cancer progression, metastasis, and drug resistance (**Table 4**).

m6A methylation regulates miRNA processing

miRNAs are a type of non-coding single-stranded RNA composed of 21 to 25 nucleotides. They regulate the expression of related genes after transcription by forming RNA-induced silencing complex (RISC). RISC binds to the target mRNA 3′-UTR, inhibits post-transcriptional modification and translation or induces mRNA degradation (125).

In recent years, m6A has been observed in miRNAs targeting oncogenes or tumor suppressor genes and is involved in tumor progression by affecting the biogenesis or stability of miRNAs. Changes in METTL3 can affect the steady state level of various miRNAs such as miR-25, miR-93, miR126, miR-221/222, and miR-4485. METTL3 may have a carcinogenic effect in bladder cancer by interacting with the microprocessor protein DGCR8 and actively regulating the pri-miR221/222 process in an m6A-dependent manner (126). The upregulation of METTL3 is related to the abnormal changes of m6A and positively correlated with colorectal tumor metastasis. In this context, the METTL3/miR-1246/SPRED2 axis plays an important role and provides a new m6A modification mode for the development of colorectal cancer (127). In another study, the cleavage of pre-miR-143-3p is m6A-dependent, and METTL3 can positively regulate the miR-143-3p/VASH1 axis, increase lung cancer angiogenesis, and thereby regulate the VEGFA degradation and depolymerization of tubulin, playing an important role in the progress of non-small cell lung cancer (NSCLC) (128).

Overexpression of miR-29a inhibits WTAP expression by down-regulating QKI6, inhibits PI3K/AKT and extracellular signal-related kinase pathways, thereby inhibiting cell proliferation, migration and invasion, but promotes apoptosis in glioblastoma (129). As a conservative oncogenic driver network, IGF2BP1 promotes SRF expression in a conservative, m6A-dependent manner by inhibiting miRNA-induced SRF mRNA decay, leading to enhanced transcriptional activity of SRF, promoting tumor cell growth and invasion. At the post-transcriptional level, IGF2BP1 regulates the expression of various SRF target genes (including PDLIM7 and FOXK1) (130). IGF2BP1 is considered to be the direct target of miR-491-5p, and its expression is significantly up-regulated in non-small cell lung cancer tissues and inversely correlated with miR-491-5p expression (131).

TABLE 3 | Functions of m6A readers in cancer.

m6A Enzyme system	Cancer type	Overexpressed or Underexpressed	Target(s)	Changes in the behavior of tumor cells	Reference
Readers					
YTHDF1	Non-Small Cell Lung Cancer	Overexpressed	CDK2, CDK4 and Cyclin D1	Inhibit cell proliferation and the formation of a xenograft tumor	(109)
	colorectal cancer	Overexpressed	Wnt/β-catenin	Inhibiting the tumorigenicity	(110)
	ovarian carcinoma	Overexpressed	EIF3C	Promote the occurrence and metastasis	(58)
YTHDF2	pancreatic carcinoma	Overexpressed	YAP signal transduction	Inhibition of epithelial mesenchymal transformation	(111)
	lung cancer	Overexpressed	Glucose-6-phosphate dehydrogenase	Promote cell proliferation	(112)
	hepatocellular carcinoma	Underexpressed	EGFR 3′-UTR	Inhibit the proliferation and growth	(116)
	hepatocellular carcinoma	Overexpressed	OCT4 5′-UTR	Promote CSC liver phenotype and tumor metastasis	(115)
YTHDF3	germinal cell tumor of testis	Overexpressed		Oncogene	(117)
YTHDC2	Colorectal carcinoma	Overexpressed	HIF-1α	Promote the metastasis	(118)
IGF2BP1	Hepatocellular Carcinoma	Overexpressed	C-MYC and MKI67	Regulate cell proliferation and apoptosis	(119)

TABLE 4 | Functions of m6A regulators in ncRNA metabolism.

ncRNA	Molecule	Cancer type	Biological function	Effect	Reference
miR221/222	METTL3	Bladder Cancer	Promote pri-miRNA processing	Positive	(126)
miR-1246	METTL3	Colorectal Carcinoma	Promote pri-miRNA processing	Positive	(127)
miR-143-3p	METTL3	Non-Small Cell Lung Cancer	Promote pre-miRNA processing	Positive	(128)
miR-29a	WTAP	Glioblastoma	Regulatory gene expression	Negative	(129)
miR-34-5p/miR-181-5p	IGF2BP1	Ovarian, Liver and Lung cancer	Maintain SRF target genes expression	Negative	(130)
miR-491-5p	IGF2BP1	Non-Small Cell Lung Cancer	Regulatory gene expression	Negative	(131)
miR-29A-3P, miR-29B-3P, miR-222, miR-1266-5P, miR-1268a, and miR-671-3p	HNRNPA2B1	Breast Carcinoma	Alter miRNAs transcriptome	Bidirectional	(132)
Linc00958 and miR3619-5p	METTL3	Hepatic Carcinoma	Stabilize lncRNA and enable the ceRNA model	Positive	(134)
lncRNA-NEAT1	ALKBH5	Gastric Carcinoma	Promote interaction	Positive	(103)
LINC01234	HNRNPA2B1	Non-Small Cell Lung Cancer	Promote interaction	Positive	(135)
lncRNA-DANCR	IGF2BP2	Pancreatic Carcinoma	Stabilize lncRNA	Positive	(136)
XIST	WTAP/RBM15/ RBM15B	Gene silencing on the X chromosome	Promote XIST -mediated gene repression	Positive	(29, 138)
XIST	METTL14/ YTHDF2	Colorectal Carcinoma	Mediate XIST degradation	Positive	(139)
circNSun2	YTHDC1	Colorectal Carcinoma	Promote cytoplasmic export of circRNAs	Positive	(140)
circRNAs	YTHDF2	Innate Immunity	Mediate circRNA degradation	Negative	(141)

Interestingly, it has been found that the overexpression of HNRNPA2/B1 in breast cancer cells can have an impact on the miRNA transcription group. HNRNPA2B1 can promote the endocrine resistance of breast cancer cells by down-regulating mir-29a-3p, mir-29b-3p, and mir-222, up-regulating mir-1266-5p, mir-1268a, and mir-671-3p, to reducing the sensitivity to 4-hydroxytamoxiphenylamine and fulva statin (132).

m6A methylation regulates in long Noncoding RNA

In recent years, more and more evidence has shown that LncRNA can control gene expression and cell functions at the transcriptional and post-transcriptional levels (133).

In terms of regulating the structure and function of LncRNA, METTL3-mediated m6A modification can stabilize the transcription process and lead to upregulation of lnc00958 which can promote the expression of miR3619-5p and further upregulate the expression of HDGF, thereby promoting liver cancer fat generation and progress (134). ALKBH5 combines with lncRNA-NEAT1 to remove the m6A modification that occurs on it and then affects the expression of the polyclonal inhibition complex subunit, EZH2, which in turn affects the invasion and metastasis of gastric cancer cells (103). Compared with normal lung tissue, the expression of LINC01234 in NSCLC was significantly increased, and it was positively correlated with poor prognosis. Further studies have found that LINC01234 can interact with HNRNPA2B1, which in turn leads to the recruitment of DiGeorge syndrome critical region gene 8 (DGCR8), promoting cell proliferation *in vitro* and tumor growth *in vivo* (135). IGF2BP2 is highly expressed in pancreatic cancer patients with poor prognosis, and inhibition of IGF2BP2 can inhibit cancer cell proliferation. The experiments further demonstrate that IGF2BP2 can stabilize lncRNA-DANCR by enhancing m6A modification to stabilize DANCR RNA, thus promoting cancer cell proliferation (136).

LncRNA-XIST can mediate transcriptional silencing of genes on the X chromosome. XIST is highly methylated, and m6A modification is necessary for XIST-mediated gene silencing (137). The formation of m6A on XIST is mediated by RBM15 and RBM15B. These m6A methylation complexes are often recruited to the specific sites within XIST, resulting in the formation of m6A on the adjacent sites. In addition, the m6A reader YTHDC1 is also recruited to XIST to promote XIST-mediated gene suppression (29, 138). As mentioned above, the loss of METTL14 is related to the poor prognosis of colorectal cancer patients. XIST mRNA is recognized by the m6A reading protein YTHDF2 which are further brought to be methylated by METTL14 through m6A, leading to XIST degradation, and thereby inhibits the tumorigenesis and metastasis of colorectal cancer cells (139).

m6A Methylation Regulates in CircRNAs

CircRNAs are post-splicing products of the precursor mRNA and have extensive cell-type-specific m6A methylation characteristics (142).

The presence of m6A circRNA is corroborated by interaction between circRNA and YTHDF1/YTHDF2, the proteins that read m6A sites in mRNAs, and by reduced m6A levels upon depletion of METTL3. Despite sharing m6A readers and writers, m6A circRNAs are frequently derived from the exons that are not methylated in mRNAs, whereas mRNAs that are methylated on the same exons that compose m6A circRNA exhibit less stability in a process regulated by YTHDF2 (140). In terms of regulating cancer, YTHDC1 can participate in m6A modification of circNSun2 to increase its output to the cytoplasm. By forming the RNA-protein ternary complex of circNSun2/IGF2BP2/

HMGA2 in the cytoplasm, circNSun2 enhances the stability of HMGA2 mRNA and promotes colorectal cancer cell infiltration and liver metastasis (141).

CONCLUSIONS AND PERSPECTIVES

m6A is key to regulating multiple biological processes by determining the fate of RNA. The m6A modification is precisely regulated by "writer", "eraser" and "reader" as well as non-coding RNAs, and involves almost any step of mRNA metabolism, as well as ncRNAs processing and circRNAs translation. Although research on m6A is still in its infancy, more and more studies on m6A in cancer have shown that m6A modification and its related regulatory proteins play an important role in a variety of cancers (**Table 1**). Although there are some inconsistencies in the current literature, many of the proteins involved in m6A regulation have only recently been identified (including ZC3H13 and CBLL1) and have not been investigated in the context of cancer and require further detailed study. Interestingly, we might think that the methyltransferase and dimethyl transferase involved in m6A play opposite roles in a cancer. However, this is not always the case. The methylation enzyme complex composed of METTL3-METTL14-WTAP and the demethylase of FTO can often show the same effect in cancer (73, 76). Consistent with this, the DNA demethylase and DNA methyltransferase (such as TET2 and DNMT3A) are known to acting as antineoplastic factors in myeloid malignancies (143). In addition, they work synergistically to suppress the lineage differentiation of hematopoietic stem cells (144). Therefore, in the similar tumor microenvironment, methylases and demethylases may work coordinately by regulating different target genes to exhibit cancer-promoting or anti-tumor effects. When targeting the same gene, it may also trigger similar biological results through different regulatory pathways. In addition, the fate of RNA transcripts modified by m6A is usually determined by the reader protein. Different readers may target different transcriptomes. However, in some cases, they may preferentially bind to different regions of the same transcriptome, or even competitively bind to the same regions of the same transcriptome. Therefore, to better understand how m6A modification is involved in regulating mRNA, it is important to understand which regions of mRNA transcription products are modified by m6A and the type of readers that binds to the modified regions.

The important role of m6A regulatory proteins observed in a variety of cancers suggests that they may be potential therapeutic targets for cancer therapy. In fact, many studies have been focused on developing inhibitors of FTO due to it demethylates N6 -adenosine modified (m6A) sites and N6,2 -O-dimethyladenosine modified (m6Am) sites of mRNA, thereby influencing multiple mRNA related processes including transcript stability, alternative splicing, mRNA translocation, and protein translation (145–147). For the other m6A modulators, the situation can be more complicated. For instance, METTL3 may have diametrically opposite regulatory effects by affecting m6A modification in different cancers. METTL3 may also have other independent activities independent of its catalytic activity (70). Therefore, the development of inhibitors targeting the catalytic activity of METTL3 may not be sufficient to inhibit its overall function, and further research is required to carry out to unravel its precise function and regulation.

Clinically, maladjustment of m6A and its regulatory proteins is related to the diagnosis and prognosis of cancer. Abnormal expression of one or more m6A modified proteins may serve as a biomarker for diagnosis and prognosis. It is worth noting that m6A is involved in the regulation of immune responses (either innate immunity or adaptive immunity) (148), The combination of immune checkpoint inhibitors and m6A enzyme system inhibitors may provide new and more effective treatment strategies for cancer.

In summary, there are still many difficulties that need to be overcome in order to target the proteins involved in the m6A enzyme system and establish an effective treatment. Small-molecule inhibitors targeting multiple enzymes for cancer therapy, like other drugs, will require more *in vivo* trials to rule out harmful off-target effects in the hope of reducing toxicity and increasing therapeutic specificity. However, the emerging research on RNA modification has provided new insights into the development of cancer, as well as opportunities to develop new treatments.

AUTHOR CONTRIBUTIONS

ST drafted the manuscript. JL, QL, and TY collected and sorted out literatures. ST and QC revised the manuscript. All authors contributed to the article and approved the submitted version.

ACKNOWLEDGMENTS

We would like to thank colleagues in the Qi Chen lab for discussion and comments. Work in the Qi Chen lab is funded by the Innovative Research Teams Program II of Fujian Normal University in China (IRTL1703), Youth Program of National Natural Science Foundation of China (grant 31900128), and Fujian Key Laboratory of Innate Immune Biology (grant 2015J1001).

REFERENCES

1. Motorin Y, Helm M. RNA nucleotide methylation. *Wiley Interdiscip Rev RNA* (2011) 2:611–31. doi: 10.1002/wrna.79
2. Oerum S, Dégut C, Barraud P, Tisné C. m^{1}A Post-Transcriptional Modification in tRNAs. *Biomolecules* (2017) 7:20–34. doi: 10.3390/biom7010020
3. de Crécy-Lagard V, Edelheit S, Schwartz S, Mumbach MR, Wurtzel O, Sorek R. Transcriptome-Wide Mapping of 5-methylcytidine RNA Modifications

in Bacteria, Archaea, and Yeast Reveals m5C within Archaeal mRNAs. *PLoS Genet* (2013) 9:e1003602. doi: 10.1371/journal.pgen.1003602
4. Chow CS, Lamichhane TN, Mahto SK. Expanding the Nucleotide Repertoire of the Ribosome with Post-Transcriptional Modifications. *ACS Chem Biol* (2007) 2:610–9. doi: 10.1021/cb7001494
5. Bohnsack K, Höbartner C, Bohnsack M. Eukaryotic 5-methylcytosine (m^5C) RNA Methyltransferases: Mechanisms, Cellular Functions, and Links to Disease. *Genes* (2019) 10:102–18. doi: 10.3390/genes10020102
6. Yang X, Yang Y, Sun B-F, Chen Y-S, Xu J-W, Lai W-Y, et al. 5-methylcytosine promotes mRNA export — NSUN2 as the methyltransferase and ALYREF as an m^5C reader. *Cell Res* (2017) 27:606–25. doi: 10.1038/cr.2017.55
7. Fu L, Guerrero CR, Zhong N, Amato NJ, Liu Y, Liu S, et al. Tet-Mediated Formation of 5-Hydroxymethylcytosine in RNA. *J Am Chem Soc* (2014) 136:11582–5. doi: 10.1021/ja505305z
8. Li Q, Li X, Tang H, Jiang B, Dou Y, Gorospe M, et al. NSUN2-Mediated m^5C Methylation and METTL3/METTL14-Mediated m^6A Methylation Cooperatively Enhance p21 Translation. *J Cell Biochem* (2017) 118:2587–98. doi: 10.1002/jcb.25957
9. Desrosiers R, Friderici K, Rottman F. Identification of Methylated Nucleosides in Messenger RNA from Novikoff Hepatoma Cells. *Proc Natl Acad Sci* (1974) 71(10):3971–5. doi: 10.1073/pnas.71.10.3971
10. Perry RP, Kelley DE, Friderici K, Rottman F. The Methylated Constituents of L Cell Messenger RNA: Evidence for an Unusual Cluster at the 5' Terminus. *Cell* (1975) 4:387–94. doi: 10.1016/0092-8674(75)90159-2
11. Meyer KD, Jaffrey SR. Rethinking m^6A Readers, Writers, and Erasers. *Annu Rev Cell Dev Biol* (2017) 33:319–42. doi: 10.1146/annurev-cellbio-100616-060758
12. Meyer KD, Saletore Y, Zumbo P, Elemento O, Mason CE, Jaffrey SR. Comprehensive analysis of mRNA methylation reveals enrichment in 3' UTRs and near stop codons. *Cell* (2012) 149:1635–46. doi: 10.1016/j.cell.2012.05.003
13. Dominissini D, Moshitch-Moshkovitz S, Schwartz S, Salmon-Divon M, Ungar L, Osenberg S, et al. Topology of the human and mouse m^6A RNA methylomes revealed by m^6A-seq. *Nature* (2012) 485:201–6. doi: 10.1038/nature11112
14. Roundtree IA, Evans ME, Pan T, He C. Dynamic RNA Modifications in Gene Expression Regulation. *Cell* (2017) 169:1187–200. doi: 10.1016/j.cell.2017.05.045
15. Batista PJ, Molinie B, Wang J, Qu K, Zhang J, Li L, et al. m^6A RNA modification controls cell fate transition in mammalian embryonic stem cells. *Cell Stem Cell* (2014) 15:707–19. doi: 10.1016/j.stem.2014.09.019
16. Gilbert WV, Bell TA, Schaening C. Messenger RNA modifications: Form, distribution, and function. *Science* (2016) 352:1408–12. doi: 10.1126/science.aad8711
17. Zhao BS, Roundtree IA, He C. Post-transcriptional gene regulation by mRNA modifications. *Nat Rev Mol Cell Biol* (2017) 18:31–42. doi: 10.1038/nrm.2016.132
18. Meyer KD. DART-seq: an antibody-free method for global m^6A detection. *Nat Methods* (2019) 16:1275–80. doi: 10.1038/s41592-019-0570-0
19. Garcia-Campos MA, Edelheit S, Toth U, Safra M, Shachar R, Viukov S, et al. Deciphering the "m^6A Code" via Antibody-Independent Quantitative Profiling. *Cell* (2019) 178:731–47. doi: 10.1016/j.cell.2019.06.013
20. Saletore Y, Meyer K, Korlach J, Vilfan ID, Jaffrey S, Mason CE. The birth of the Epitranscriptome: deciphering the function of RNA modifications. *Genome Biol* (2012) 13:175–85. doi: 10.1186/gb-2012-13-10-175
21. Fu XD, Ares MJr. Context-dependent control of alternative splicing by RNA-binding proteins. *Nat Rev Genet* (2014) 15:689–701. doi: 10.1038/nrg3778
22. Maity A, Das B. N6-methyladenosine modification in mRNA: machinery, function and implications for health and diseases. *FEBS J* (2016) 283:1607–30. doi: 10.1111/febs.13614
23. Meyer KD, Patil DP, Zhou J, Zinoviev A, Skabkin MA, Elemento O, et al. 5' UTR m^6A Promotes Cap-Independent Translation. *Cell* (2015) 163:999–1010. doi: 10.1016/j.cell.2015.10.012
24. Mauer J, Luo X, Blanjoie A, Jiao X, Grozhik AV, Patil DP, et al. Reversible methylation of m^6A_m in the 5' cap controls mRNA stability. *Nature* (2017) 541:371–5. doi: 10.1038/nature21022
25. Tuck MT. Partial purification of a 6-methyladenine mRNA methyltransferase which modifies internal adenine residues. *Biochem J* (1992) 288:233–40. doi: 10.1042/bj2880233
26. Bujnicki JM, Feder M, Radlinska M, Blumenthal RM. Structure prediction and phylogenetic analysis of a functionally diverse family of proteins homologous to the MT-A70 subunit of the human mRNA:m(6)A methyltransferase. *J Mol Evol* (2002) 55:431–44. doi: 10.1007/s00239-002-2339-8
27. Ping XL, Sun BF, Wang L, Xiao W, Yang X, Wang WJ, et al. Mammalian WTAP is a regulatory subunit of the RNA N6-methyladenosine methyltransferase. *Cell Res* (2014) 24:177–89. doi: 10.1038/cr.2014.3
28. Schwartz S, Mumbach MR, Jovanovic M, Wang T, Maciag K, Bushkin GG, et al. Perturbation of m6A writers reveals two distinct classes of mRNA methylation at internal and 5' sites. *Cell Rep* (2014) 8:284–96. doi: 10.1016/j.celrep.2014.05.048
29. Patil DP, Chen CK, Pickering BF, Chow A, Jackson C, Guttman M, et al. m^6A RNA methylation promotes XIST-mediated transcriptional repression. *Nature* (2016) 537:369–73. doi: 10.1038/nature19342
30. Wen J, Lv R, Ma H, Shen H, He C, Wang J, et al. Zc3h13 Regulates Nuclear RNA m^6A Methylation and Mouse Embryonic Stem Cell Self-Renewal. *Mol Cell* (2018) 69:1028–38 e6. doi: 10.1016/j.molcel.2018.02.015
31. Aguilo F, Zhang F, Sancho A, Fidalgo M, Di Cecilia S, Vashisht A, et al. Coordination of m(6)A mRNA Methylation and Gene Transcription by ZFP217 Regulates Pluripotency and Reprogramming. *Cell Stem Cell* (2015) 17:689–704. doi: 10.1016/j.stem.2015.09.005
32. Lesbirel S, Wilson SA. The m^6Amethylase complex and mRNA export. *Biochim Biophys Acta Gene Regul Mech* (2019) 1862:319–28. doi: 10.1016/j.bbagrm.2018.09.008
33. Liu J, Yue Y, Han D, Wang X, Fu Y, Zhang L, et al. A METTL3-METTL14 complex mediates mammalian nuclear RNA N6-adenosine methylation. *Nat Chem Biol* (2014) 10:93–5. doi: 10.1038/nchembio.1432
34. Edupuganti RR, Geiger S, Lindeboom RGH, Shi H, Hsu PJ, Lu Z, et al. N^6-methyladenosine (m^6A) recruits and repels proteins to regulate mRNA homeostasis. *Nat Struct Mol Biol* (2017) 24:870–8. doi: 10.1038/nsmb.3462
35. Zheng G, Dahl JA, Niu Y, Fedorcsak P, Huang CM, Li CJ, et al. ALKBH5 is a mammalian RNA demethylase that impacts RNA metabolism and mouse fertility. *Mol Cell* (2013) 49:18–29. doi: 10.1016/j.molcel.2012.10.015
36. Jia G, Fu Y, Zhao X, Dai Q, Zheng G, Yang Y, et al. N6-methyladenosine in nuclear RNA is a major substrate of the obesity-associated FTO. *Nat Chem Biol* (2011) 7:885–7. doi: 10.1038/nchembio.687
37. Li A, Chen YS, Ping XL, Yang X, Xiao W, Yang Y, et al. Cytoplasmic m^6A reader YTHDF3 promotes mRNA translation. *Cell Res* (2017) 27:444–7. doi: 10.1038/cr.2017.10
38. Wang X, Zhao BS, Roundtree IA, Lu Z, Han D, Ma H, et al. N^6-methyladenosine Modulates Messenger RNA Translation Efficiency. *Cell* (2015) 161:1388–99. doi: 10.1016/j.cell.2015.05.014
39. Wang X, Lu Z, Gomez A, Hon GC, Yue Y, Han D, et al. N6-methyladenosine-dependent regulation of messenger RNA stability. *Nature* (2014) 505:117–20. doi: 10.1038/nature12730
40. Kasowitz SD, Ma J, Anderson SJ, Leu NA, Xu Y, Gregory BD, et al. Nuclear m^6A reader YTHDC1 regulates alternative polyadenylation and splicing during mouse oocyte development. *PloS Genet* (2018) 14:e1007412. doi: 10.1371/journal.pgen.1007412
41. Hsu PJ, Zhu Y, Ma H, Guo Y, Shi X, Liu Y, et al. Ythdc2 is an N^6-methyladenosine binding protein that regulates mammalian spermatogenesis. *Cell Res* (2017) 27:1115–27. doi: 10.1038/cr.2017.99
42. Long WL, Guo H, Sheng J, Song RH, Xu Y. Role of m6A RNA methylation in tumorigenesis and progression. *Biotechnol Bull* (2019) 35(6):178–86. doi: 10.13560/j.cnki.biotech.bull.1985.2018-1082
43. Wang P, Doxtader KA, Nam Y. Structural Basis for Cooperative Function of Mettl3 and Mettl14 Methyltransferases. *Mol Cell* (2016) 63:306–17. doi: 10.1016/j.molcel.2016.05.041
44. Horiuchi K, Kawamura T, Iwanari H, Ohashi R, Naito M, Kodama T, et al. Identification of Wilms' tumor 1-associating protein complex and its role in alternative splicing and the cell cycle. *J Biol Chem* (2013) 288:33292–302. doi: 10.1074/jbc.M113.500397
45. Ortega A, Niksic M, Bachi A, Wilm M, Sanchez L, Hastie N, et al. Biochemical function of female-lethal (2)D/Wilms' tumor suppressor-1-

associated proteins in alternative pre-mRNA splicing. *J Biol Chem* (2003) 278:3040–7. doi: 10.1074/jbc.M210737200
46. van Tran N, Ernst FGM, Hawley BR, Zorbas C, Ulryck N, Hackert P, et al. The human 18S rRNA m6A methyltransferase METTL5 is stabilized by TRMT112. *Nucleic Acids Res* (2019) 47:7719–33. doi: 10.1093/nar/gkz619
47. Pendleton KE, Chen B, Liu K, Hunter OV, Xie Y, Tu BP, et al. The U6 snRNA m^6A Methyltransferase METTL16 Regulates SAM Synthetase Intron Retention. *Cell* (2017) 169:824–35 e14. doi: 10.1016/j.cell.2017.05.003
48. Warda AS, Kretschmer J, Hackert P, Lenz C, Urlaub H, Hobartner C, et al. Human METTL16 is a N^6-methyladenosine (m^6A) methyltransferase that targets pre-mRNAs and various non-coding RNAs. *EMBO Rep* (2017) 18:2004–14. doi: 10.15252/embr.201744940
49. Shima H, Matsumoto M, Ishigami Y, Ebina M, Muto A, Sato Y, et al. S-Adenosylmethionine Synthesis Is Regulated by Selective N^6-Adenosine Methylation and mRNA Degradation Involving METTL16 and YTHDC1. *Cell Rep* (2017) 21:3354–63. doi: 10.1016/j.celrep.2017.11.092
50. Leismann J, Spagnuolo M, Pradhan M, Wacheul L, Vu MA, Musheev M, et al. The 18S ribosomal RNA m^6A methyltransferase Mettl5 is required for normal walking behavior in Drosophila. *EMBO Rep* (2020) 21:e49443. doi: 10.15252/embr.201949443
51. Richard EM, Polla DL, Assir MZ, Contreras M, Shahzad M, Khan AA, et al. Bi-allelic Variants in METTL5 Cause Autosomal-Recessive Intellectual Disability and Microcephaly. *Am J Hum Genet* (2019) 105:869–78. doi: 10.1016/j.ajhg.2019.09.007
52. Ma H, Wang X, Cai J, Dai Q, Natchiar SK, Lv R, et al. N^6-Methyladenosine methyltransferase ZCCHC4 mediates ribosomal RNA methylation. *Nat Chem Biol* (2019) 15:88–94. doi: 10.1038/s41589-018-0184-3
53. Ren W, Lu J, Huang M, Gao L, Li D, Wang GG, et al. Structure and regulation of ZCCHC4 in m^6A-methylation of 28S rRNA. *Nat Commun* (2019) 10:5042. doi: 10.1038/s41467-019-12923-x
54. Pinto R, Vagbo CB, Jakobsson ME, Kim Y, Baltissen MP, O'Donohue MF, et al. The human methyltransferase ZCCHC4 catalyses N6-methyladenosine modification of 28S ribosomal RNA. *Nucleic Acids Res* (2020) 48:830–46. doi: 10.1093/nar/gkz1147
55. Alemu EA, He C, Klungland A. ALKBHs-facilitated RNA modifications and de-modifications. *DNA Repair (Amst)* (2016) 44:87–91. doi: 10.1016/j.dnarep.2016.05.026
56. Toh JDW, Crossley SWM, Bruemmer KJ, Ge EJ, He D, Iovan DA, et al. Distinct RNA N-demethylation pathways catalyzed by nonheme iron ALKBH5 and FTO enzymes enable regulation of formaldehyde release rates. *Proc Natl Acad Sci U S A* (2020) 117:25284–92. doi: 10.1073/pnas.2007349117
57. Wei J, Liu F, Lu Z, Fei Q, Ai Y, He PC, et al. Differential m^6A, m^6A_m, and m^1A Demethylation Mediated by FTO in the Cell Nucleus and Cytoplasm. *Mol Cell* (2018) 71:973–85. doi: 10.1016/j.molcel.2018.08.011
58. Liu T, Wei Q, Jin J, Luo Q, Liu Y, Yang Y, et al. The m6A reader YTHDF1 promotes ovarian cancer progression via augmenting EIF3C translation. *Nucleic Acids Res* (2020) 48:3816–31. doi: 10.1093/nar/gkaa048
59. Zhou J, Wan J, Gao X, Zhang X, Jaffrey SR, Qian SB. Dynamic m^6A mRNA methylation directs translational control of heat shock response. *Nature* (2015) 526:591–4. doi: 10.1038/nature15377
60. Shi H, Wang X, Lu Z, Zhao BS, Ma H, Hsu PJ, et al. YTHDF3 facilitates translation and decay of N^6-methyladenosine-modified RNA. *Cell Res* (2017) 27:315–28. doi: 10.1038/cr.2017.15
61. Roundtree IA, Luo GZ, Zhang Z, Wang X, Zhou T, Cui Y, et al. YTHDC1 mediates nuclear export of N^6-methyladenosine methylated mRNAs. *Elife* (2017) 6:e31311. doi: 10.7554/eLife.31311
62. Xiao W, Adhikari S, Dahal U, Chen YS, Hao YJ, Sun BF, et al. Nuclear m^6A Reader YTHDC1 Regulates mRNA Splicing. *Mol Cell* (2016) 61:507–19. doi: 10.1016/j.molcel.2016.01.012
63. Weidensdorfer D, Stohr N, Baude A, Lederer M, Kohn M, Schierhorn A, et al. Control of c-myc mRNA stability by IGF2BP1-associated cytoplasmic RNPs. *RNA* (2009) 15:104–15. doi: 10.1261/rna.1175909
64. Hafner M, Landthaler M, Burger L, Khorshid M, Hausser J, Berninger P, et al. Transcriptome-wide identification of RNA-binding protein and microRNA target sites by PAR-CLIP. *Cell* (2010) 141:129–41. doi: 10.1016/j.cell.2010.03.009
65. Alarcon CR, Goodarzi H, Lee H, Liu X, Tavazoie S, Tavazoie SF. HNRNPA2B1 Is a Mediator of m^6A-Dependent Nuclear RNA Processing Events. *Cell* (2015) 162:1299–308. doi: 10.1016/j.cell.2015.08.011
66. Choe J, Lin S, Zhang W, Liu Q, Wang L, Ramirez-Moya J, et al. mRNA circularization by METTL3-eIF3h enhances translation and promotes oncogenesis. *Nature* (2018) 561:556–60. doi: 10.1038/s41586-018-0538-8
67. Yang Y, Hsu PJ, Chen YS, Yang YG. Dynamic transcriptomic m^6A decoration: writers, erasers, readers and functions in RNA metabolism. *Cell Res* (2018) 28:616–24. doi: 10.1038/s41422-018-0040-8
68. Pinello N, Sun S, Wong JJ. Aberrant expression of enzymes regulating m^6A mRNA methylation: implication in cancer. *Cancer Biol Med* (2018) 15:323–34. doi: 10.20892/j.issn.2095-3941.2018.0365
69. He L, Li H, Wu A, Peng Y, Shu G, Yin G. Functions of N6-methyladenosine and its role in cancer. *Mol Cancer* (2019) 18:176–90. doi: 10.1186/s12943-019-1109-9
70. Lin S, Choe J, Du P, Triboulet R, Gregory RI. The m^6A Methyltransferase METTL3 Promotes Translation in Human Cancer Cells. *Mol Cell* (2016) 62:335–45. doi: 10.1016/j.molcel.2016.03.021
71. Zhou Z, Lv J, Yu H, Han J, Yang X, Feng D, et al. Mechanism of RNA modification N6-methyladenosine in human cancer. *Mol Cancer* (2020) 19:104. doi: 10.1186/s12943-020-01216-3
72. Chen M, Wei L, Law CT, Tsang FH, Shen J, Cheng CL, et al. RNA N6-methyladenosine methyltransferase-like 3 promotes liver cancer progression through YTHDF2-dependent posttranscriptional silencing of SOCS2. *Hepatology* (2018) 67:2254–70. doi: 10.1002/hep.29683
73. Vu LP, Pickering BF, Cheng Y, Zaccara S, Nguyen D, Minuesa G, et al. The N^6-methyladenosine (m^6A)-forming enzyme METTL3 controls myeloid differentiation of normal hematopoietic and leukemia cells. *Nat Med* (2017) 23:1369–76. doi: 10.1038/nm.4416
74. Liang S, Guan H, Lin X, Li N, Geng F, Li J. METTL3 serves an oncogenic role in human ovarian cancer cells partially via the AKT signaling pathway. *Oncol Lett* (2020) 19:3197–204. doi: 10.3892/ol.2020.11425
75. Li1 X, Tang J, Qin Z, Zou Q, Wei J, Huang W, et al. The M6A methyltransferase METTL3: acting as a tumor suppressor in renal cell carcinoma. *Oncotarget* (2017) 8:96103–16. doi: 10.18632/oncotarget.21726
76. Barbieri I, Tzelepis K, Pandolfini L, Shi J, Millan-Zambrano G, Robson SC, et al. Promoter-bound METTL3 maintains myeloid leukaemia by m^6A-dependent translation control. *Nature* (2017) 552:126–31. doi: 10.1038/nature24678
77. Shen C, Xuan B, Yan T, Ma Y, Xu P, Tian X, et al. m^6A-dependent glycolysis enhances colorectal cancer progression. *Mol Cancer* (2020) 19:72. doi: 10.1186/s12943-020-01190-w
78. Lin Y, Wei X, Jian Z, Zhang X. METTL3 expression is associated with glycolysis metabolism and sensitivity to glycolytic stress in hepatocellular carcinoma. *Cancer Med* (2020) 9:2859–67. doi: 10.1002/cam4.2918
79. Kong F, Liu X, Zhou Y, Hou X, He J, Li Q, et al. Downregulation of METTL14 increases apoptosis and autophagy induced by cisplatin in pancreatic cancer cells. *Int J Biochem Cell Biol* (2020) 122:105731. doi: 10.1016/j.biocel.2020.105731
80. Weng H, Huang H, Wu H, Qin X, Zhao BS, Dong L, et al. METTL14 Inhibits Hematopoietic Stem/Progenitor Differentiation and Promotes Leukemogenesis via mRNA m(6)A Modification. *Cell Stem Cell* (2018) 22:191–205 e9. doi: 10.1016/j.stem.2017.11.016
81. Panneerdoss S, Eedunuri VK, Yadav P, Timilsina S, Rajamanickam S, Viswanadhapalli S, et al. Cross-talk among writers, readers, and erasers of m6A regulates cancer growth and progression. *Sci Adv* (2018) 4:eaar8263. doi: 10.1126/sciadv.aar8263
82. Liu J, Eckert MA, Harada BT, Liu SM, Lu Z, Yu K, et al. m^6A mRNA methylation regulates AKT activity to promote the proliferation and tumorigenicity of endometrial cancer. *Nat Cell Biol* (2018) 20:1074–83. doi: 10.1038/s41556-018-0174-4
83. Gu C, Wang Z, Zhou N, Li G, Kou Y, Luo Y, et al. Mettl14 inhibits bladder TIC self-renewal and bladder tumorigenesis through N^6-methyladenosine of Notch1. *Mol Cancer* (2019) 18:168. doi: 10.1186/s12943-019-1084-1
84. Jin DI, Lee SW, Han ME, Kim HJ, Seo SA, Hur GY, et al. Expression and roles of Wilms' tumor 1-associating protein in glioblastoma. *Cancer Sci* (2012) 103:2102–9. doi: 10.1111/cas.12022

85. Xi Z, Xue Y, Zheng J, Liu X, Ma J, Liu Y. WTAP Expression Predicts Poor Prognosis in Malignant Glioma Patients. *J Mol Neurosci* (2016) 60:131–6. doi: 10.1007/s12031-016-0788-6
86. Bansal H, Yihua Q, Iyer SP, Ganapathy S, Proia DA, Penalva LO, et al. WTAP is a novel oncogenic protein in acute myeloid leukemia. *Leukemia* (2014) 28:1171–4. doi: 10.1038/leu.2014.16
87. Tang J, Wang F, Cheng G, Si S, Sun X, Han J, et al. Wilms' tumor 1-associating protein promotes renal cell carcinoma proliferation by regulating CDK2 mRNA stability. *J Exp Clin Cancer Res* (2018) 37:40. doi: 10.1186/s13046-018-0706-6
88. Chen Y, Peng C, Chen J, Chen D, Yang B, He B, et al. WTAP facilitates progression of hepatocellular carcinoma via m6A-HuR-dependent epigenetic silencing of ETS1. *Mol Cancer* (2019) 18:127. doi: 10.1186/s12943-019-1053-8
89. Yu HL, Ma XD, Tong JF, Li JQ, Guan XJ, Yang JH. WTAP is a prognostic marker of high-grade serous ovarian cancer and regulates the progression of ovarian cancer cells. *Onco Targets Ther* (2019) 12:6191–201. doi: 10.2147/OTT.S205730
90. Wang Q, Chen C, Ding Q, Zhao Y, Wang Z, Chen J, et al. METTL3-mediated m^6A modification of HDGF mRNA promotes gastric cancer progression and has prognostic significance. *Gut* (2020) 69:1193–205. doi: 10.1136/gutjnl-2019-319639
91. De Rosa V, Iommelli F, Monti M, Fonti R, Votta G, Stoppelli MP, et al. Reversal of Warburg Effect and Reactivation of Oxidative Phosphorylation by Differential Inhibition of EGFR Signaling Pathways in Non-Small Cell Lung Cancer. *Clin Cancer Res* (2015) 21:5110–20. doi: 10.1158/1078-0432.CCR-15-0375
92. Liu J, Eckert MA, Harada BT, Liu SM, Lu Z, Yu K, et al. m^6A mRNA methylation regulates AKT activity to promote the proliferation and tumorigenicity of endometrial cancer. *Nat Cell Biol* (2018) 20:1074–83. doi: 10.1038/s41556-018-0174-4
93. Tang X, Liu S, Chen D, Zhao Z, Zhou J. The role of the fat mass and obesity-associated protein in the proliferation of pancreatic cancer cells. *Oncol Lett* (2019) 17:2473–8. doi: 10.3892/ol.2018.9873
94. Li J, Han Y, Zhang H, Qian Z, Jia W, Gao Y, et al. The m6A demethylase FTO promotes the growth of lung cancer cells by regulating the m6A level of USP7 mRNA. *Biochem Biophys Res Commun* (2019) 512:479–85. doi: 10.1016/j.bbrc.2019.03.093
95. Zhou S, Bai ZL, Xia D, Zhao ZJ, Zhao R, Wang YY, et al. FTO regulates the chemo-radiotherapy resistance of cervical squamous cell carcinoma (CSCC) by targeting beta-catenin through mRNA demethylation. *Mol Carcinog* (2018) 57:590–7. doi: 10.1002/mc.22782
96. Zou D, Dong L, Li C, Yin Z, Rao S, Zhou Q. The m^6A eraser FTO facilitates proliferation and migration of human cervical cancer cells. *Cancer Cell Int* (2019) 19:321. doi: 10.1186/s12935-019-1045-1
97. Niu Y, Lin Z, Wan A, Chen H, Liang H, Sun L, et al. RNA N6-methyladenosine demethylase FTO promotes breast tumor progression through inhibiting BNIP3. *Mol Cancer* (2019) 18:46. doi: 10.1186/s12943-019-1004-4
98. Li J, Zhu L, Shi Y, Liu J, Lin L, Chen X. m6A demethylase FTO promotes hepatocellular carcinoma tumorigenesis via mediating PKM2 demethylation. *Am J Trans Res* (2019) 11:6084–92.
99. Li Z, Weng H, Su R, Weng X, Zuo Z, Li C, et al. FTO Plays an Oncogenic Role in Acute Myeloid Leukemia as a N^6-Methyladenosine RNA Demethylase. *Cancer Cell* (2017) 31:127–41. doi: 10.1016/j.ccell.2016.11.017
100. Zhang S, Zhao BS, Zhou A, Lin K, Zheng S, Lu Z, et al. m^6A Demethylase ALKBH5 Maintains Tumorigenicity of Glioblastoma Stem-like Cells by Sustaining FOXM1 Expression and Cell Proliferation Program. *Cancer Cell* (2017) 31:591–606 e6. doi: 10.1016/j.ccell.2017.02.013
101. Zhang C, Samanta D, Lu H, Bullen JW, Zhang H, Chen I, et al. Hypoxia induces the breast cancer stem cell phenotype by HIF-dependent and ALKBH5-mediated m(6)A-demethylation of NANOG mRNA. *Proc Natl Acad Sci U S A* (2016) 113:E2047–56. doi: 10.1073/pnas.1602883113
102. Yang P, Wang Q, Liu A, Zhu J, Feng J. ALKBH5 Holds Prognostic Values and Inhibits the Metastasis of Colon Cancer. *Pathol Oncol Res* (2020) 26:1615–23. doi: 10.1007/s12253-019-00737-7
103. Zhang J, Guo S, Piao HY, Wang Y, Wu Y, Meng XY, et al. ALKBH5 promotes invasion and metastasis of gastric cancer by decreasing methylation of the lncRNA NEAT1. *J Physiol Biochem* (2019) 75:379–89. doi: 10.1007/s13105-019-00690-8
104. Chao Y, Shang J, Ji W. ALKBH5-m^6A-FOXM1 signaling axis promotes proliferation and invasion of lung adenocarcinoma cells under intermittent hypoxia. *Biochem Biophys Res Commun* (2020) 521:499–506. doi: 10.1016/j.bbrc.2019.10.145
105. Tang B, Yang Y, Kang M, Wang Y, Wang Y, Bi Y, et al. m^6A demethylase ALKBH5 inhibits pancreatic cancer tumorigenesis by decreasing WIF-1 RNA methylation and mediating Wnt signaling. *Mol Cancer* (2020) 19:3. doi: 10.1186/s12943-019-1128-6
106. Guo X, Li K, Jiang W, Hu Y, Xiao W, Huang Y, et al. RNA demethylase ALKBH5 prevents pancreatic cancer progression by posttranscriptional activation of PER1 in an m6A-YTHDF2-dependent manner. *Mol Cancer* (2020) 19:91. doi: 10.1186/s12943-020-01158-w
107. Liu J, Ren D, Du Z, Wang H, Zhang H, Jin Y. m^6A demethylase FTO facilitates tumor progression in lung squamous cell carcinoma by regulating MZF1 expression. *Biochem Biophys Res Commun* (2018) 502:456–64. doi: 10.1016/j.bbrc.2018.05.175
108. Wen L, Pan X, Yu Y, Yang B. Down-regulation of FTO promotes proliferation and migration, and protects bladder cancer cells from cisplatin-induced cytotoxicity. *BMC Urol* (2020) 20:39–46. doi: 10.1186/s12894-020-00612-7
109. Shi Y, Fan S, Wu M, Zuo Z, Li X, Jiang L, et al. YTHDF1 links hypoxia adaptation and non-small cell lung cancer progression. *Nat Commun* (2019) 10:4892. doi: 10.1038/s41467-019-12801-6
110. Bai Y, Yang C, Wu R, Huang L, Song S, Li W, et al. YTHDF1 Regulates Tumorigenicity and Cancer Stem Cell-Like Activity in Human Colorectal Carcinoma. *Front Oncol* (2019) 9:332. doi: 10.3389/fonc.2019.00332
111. Chen J, Sun Y, Xu X, Wang D, He J, Zhou H, et al. YTH domain family 2 orchestrates epithelial-mesenchymal transition/proliferation dichotomy in pancreatic cancer cells. *Cell Cycle* (2017) 16:2259–71. doi: 10.1080/15384101.2017.1380125
112. Sheng H, Li Z, Su S, Sun W, Zhang X, Li L, et al. YTH domain family 2 promotes lung cancer cell growth by facilitating 6-phosphogluconate dehydrogenase mRNA translation. *Carcinogenesis* (2020) 41:541–50. doi: 10.1093/carcin/bgz152
113. Paris J, Morgan M, Campos J, Spencer GJ, Shmakova A, Ivanova I, et al. Targeting the RNA m^6A Reader YTHDF2 Selectively Compromises Cancer Stem Cells in Acute Myeloid Leukemia. *Cell Stem Cell* (2019) 25:137–48 e6. doi: 10.1016/j.stem.2019.03.021
114. Lobo J, Costa AL, Cantante M, Guimaraes R, Lopes P, Antunes L, et al. m^6A RNA modification and its writer/reader VIRMA/YTHDF3 in testicular germ cell tumors: a role in seminoma phenotype maintenance. *J Transl Med* (2019) 17:79. doi: 10.1186/s12967-019-1837-z
115. Zhang C, Huang S, Zhuang H, Ruan S, Zhou Z, Huang K, et al. YTHDF2 promotes the liver cancer stem cell phenotype and cancer metastasis by regulating OCT4 expression via m6A RNA methylation. *Oncogene* (2020) 39:4507–18. doi: 10.1038/s41388-020-1303-7
116. Zhong L, Liao D, Zhang M, Zeng C, Li X, Zhang R, et al. YTHDF2 suppresses cell proliferation and growth via destabilizing the EGFR mRNA in hepatocellular carcinoma. *Cancer Lett* (2019) 442:252–61. doi: 10.1016/j.canlet.2018.11.006
117. Hou J, Zhang H, Liu J, Zhao Z, Wang J, Lu Z, et al. YTHDF2 reduction fuels inflammation and vascular abnormalization in hepatocellular carcinoma. *Mol Cancer* (2019) 18:163. doi: 10.1186/s12943-019-1082-3
118. Tanabe A, Tanikawa K, Tsunetomi M, Takai K, Ikeda H, Konno J, et al. RNA helicase YTHDC2 promotes cancer metastasis via the enhancement of the efficiency by which HIF-1a mRNA is translated. *Cancer Lett* (2016) 376:34–42. doi: 10.1016/j.canlet.2016.02.022
119. Gutschner T, Hammerle M, Pazaitis N, Bley N, Fiskin E, Uckelmann H, et al. Insulin-like growth factor 2 mRNA-binding protein 1 (IGF2BP1) is an important protumorigenic factor in hepatocellular carcinoma. *Hepatology* (2014) 59:1900–11. doi: 10.1002/hep.26997
120. Yang Y, Fan X, Mao M, Song X, Wu P, Zhang Y, et al. Extensive translation of circular RNAs driven by N^6-methyladenosine. *Cell Res* (2017) 27:626–41. doi: 10.1038/cr.2017.31

121. Alarcon CR, Lee H, Goodarzi H, Halberg N, Tavazoie SF. N6-methyladenosine marks primary microRNAs for processing. *Nature* (2015) 519:482–5. doi: 10.1038/nature14281
122. Liu N, Dai Q, Zheng G, He C, Parisien M, Pan T. N^6-methyladenosine-dependent RNA structural switches regulate RNA-protein interactions. *Nature* (2015) 518:560–4. doi: 10.1038/nature14234
123. Linder B, Grozhik AV, Olarerin-George AO, Meydan C, Mason CE, Jaffrey SR. Single-nucleotide-resolution mapping of m6A and m6Am throughout the transcriptome. *Nat Methods* (2015) 12:767–72. doi: 10.1038/nmeth.3453
124. Li Y, Xiao J, Bai J, Tian Y, Qu Y, Chen X, et al. Molecular characterization and clinical relevance of m^6A regulators across 33 cancer types. *Mol Cancer* (2019) 18:137. doi: 10.1186/s12943-019-1066-3
125. Iwakawa HO, Tomari Y. The Functions of MicroRNAs: mRNA Decay and Translational Repression. *Trends Cell Biol* (2015) 25:651–65. doi: 10.1016/j.tcb.2015.07.011
126. Han J, Wang JZ, Yang X, Yu H, Zhou R, Lu HC, et al. METTL3 promote tumor proliferation of bladder cancer by accelerating pri-miR221/222 maturation in m6A-dependent manner. *Mol Cancer* (2019) 18:110. doi: 10.1186/s12943-019-1036-9
127. Peng W, Li J, Chen R, Gu Q, Yang P, Qian W, et al. Upregulated METTL3 promotes metastasis of colorectal Cancer via miR-1246/SPRED2/MAPK signaling pathway. *J Exp Clin Cancer Res* (2019) 38:393. doi: 10.1186/s13046-019-1408-4
128. Wang H, Deng Q, Lv Z, Ling Y, Hou X, Chen Z, et al. N6-methyladenosine induced miR-143-3p promotes the brain metastasis of lung cancer via regulation of VASH1. *Mol Cancer* (2019) 18:181. doi: 10.1186/s12943-019-1108-x
129. Xi Z, Wang P, Li Z, Bao M, Xue Y, Shang C, et al. Overexpression of miR-29a reduces the oncogenic properties of glioblastoma stem cells by downregulating Quaking gene isoform 6. *Oncotarget* (2017) 8:24949–63. doi: 10.18632/oncotarget.15327
130. Muller S, Glass M, Singh AK, Haase J, Bley N, Fuchs T, et al. IGF2BP1 promotes SRF-dependent transcription in cancer in a m6A- and miRNA-dependent manner. *Nucleic Acids Res* (2019) 47:375–90. doi: 10.1093/nar/gky1012
131. Gong F, Ren P, Zhang Y, Jiang J, Zhang H. MicroRNAs-491-5p suppresses cell proliferation and invasion by inhibiting IGF2BP1 in non-small cell lung cancer. *Am J Trans Res* (2016) 8:485–95.
132. Klinge CM, Piell KM, Tooley CS, Rouchka EC. HNRNPA2/B1 is upregulated in endocrine-resistant LCC9 breast cancer cells and alters the miRNA transcriptome when overexpressed in MCF-7 cells. *Sci Rep* (2019) 9:9430. doi: 10.1038/s41598-019-45636-8
133. Kopp F, Mendell JT. Functional Classification and Experimental Dissection of Long Noncoding RNAs. *Cell* (2018) 172:393–407. doi: 10.1016/j.cell.2018.01.011
134. Zuo X, Chen Z, Gao W, Zhang Y, Wang J, Wang J, et al. M6A-mediated upregulation of LINC00958 increases lipogenesis and acts as a nanotherapeutic target in hepatocellular carcinoma. *J Hematol Oncol* (2020) 13:5. doi: 10.1186/s13045-019-0839-x
135. Chen Z, Chen X, Lei T, Gu Y, Gu J, Huang J, et al. Integrative Analysis of NSCLC Identifies LINC01234 as an Oncogenic lncRNA that Interacts with HNRNPA2B1 and Regulates miR-106b Biogenesis. *Mol Ther* (2020) 28:1479–93. doi: 10.1016/j.ymthe.2020.03.010
136. Hu X, Peng WX, Zhou H, Jiang J, Zhou X, Huang D, et al. IGF2BP2 regulates DANCR by serving as an N6-methyladenosine reader. *Cell Death Differ* (2020) 27:1782–94. doi: 10.1038/s41418-019-0461-z
137. Chen CK, Blanco M, Jackson C, Aznauryan E, Ollikainen N, Surka C, et al. Xist recruits the X chromosome to the nuclear lamina to enable chromosome-wide silencing. *Science* (2016) 354:468–72. doi: 10.1126/science.aae0047
138. Chu C, Zhang QC, da Rocha ST, Flynn RA, Bharadwaj M, Calabrese JM, et al. Systematic discovery of Xist RNA binding proteins. *Cell* (2015) 161:404–16. doi: 10.1016/j.cell.2015.03.025
139. Yang X, Zhang S, He C, Xue P, Zhang L, He Z, et al. METTL14 suppresses proliferation and metastasis of colorectal cancer by down-regulating oncogenic long non-coding RNA XIST. *Mol Cancer* (2020) 19:46. doi: 10.1186/s12943-020-1146-4
140. Zhou C, Molinie B, Daneshvar K, Pondick JV, Wang J, Van Wittenberghe N, et al. Genome-Wide Maps of m6A circRNAs Identify Widespread and Cell-Type-Specific Methylation Patterns that Are Distinct from mRNAs. *Cell Rep* (2017) 20:2262–76. doi: 10.1016/j.celrep.2017.08.027
141. Chen RX, Chen X, Xia LP, Zhang JX, Pan ZZ, Ma XD, et al. N^6-methyladenosine modification of circNSUN2 facilitates cytoplasmic export and stabilizes HMGA2 to promote colorectal liver metastasis. *Nat Commun* (2019) 10:4695. doi: 10.1038/s41467-019-12651-2
142. Xiao MS, Ai Y, Wilusz JE. Biogenesis and Functions of Circular RNAs Come into Focus. *Trends Cell Biol* (2020) 30:226–40. doi: 10.1016/j.tcb.2019.12.004
143. Ley TJ, Ding L, Walter MJ, McLellan MD, Lamprecht T, Larson DE, et al. DNMT3A mutations in acute myeloid leukemia. *N Engl J Med* (2010) 363:2424–33. doi: 10.1056/NEJMoa1005143
144. Zhang X, Su J, Jeong M, Ko M, Huang Y, Park HJ, et al. DNMT3A and TET2 compete and cooperate to repress lineage-specific transcription factors in hematopoietic stem cells. *Nat Genet* (2016) 48:1014–23. doi: 10.1038/ng.3610
145. Elkashef SM, Lin AP, Myers J, Sill H, Jiang D, Dahia PLM, et al. IDH Mutation, Competitive Inhibition of FTO, and RNA Methylation. *Cancer Cell* (2017) 31:619–20. doi: 10.1016/j.ccell.2017.04.001
146. Su R, Dong L, Li C, Nachtergaele S, Wunderlich M, Qing Y, et al. R-2HG Exhibits Anti-tumor Activity by Targeting FTO/m^6A/MYC/CEBPA Signaling. *Cell* (2018) 172:90–105 e23. doi: 10.1016/j.cell.2017.11.031
147. Huang Y, Su R, Sheng Y, Dong L, Dong Z, Xu H, et al. Small-Molecule Targeting of Oncogenic FTO Demethylase in Acute Myeloid Leukemia. *Cancer Cell* (2019) 35:677–91 e10. doi: 10.1016/j.ccell.2019.03.006
148. Han D, Liu J, Chen C, Dong L, Liu Y, Chang R, et al. Anti-tumour immunity controlled through mRNA $m^{-6}A$ methylation and YTHDF1 in dendritic cells. *Nature* (2019) 566:270–4. doi: 10.1038/s41586-019-0916-x

Conflict of Interest: The authors declare that the research was conducted in the absence of any commercial or financial relationships that could be construed as a potential conflict of interest.

frontiers in Oncology

ORIGINAL RESEARCH
published: 29 January 2021
doi: 10.3389/fonc.2020.611191

RNA m^{6}A Methylation Regulators Subclassify Luminal Subtype in Breast Cancer

Lin Yang[1,2,3], *Shuangling Wu*[4], *Chunhui Ma*[1,2,3], *Shuhui Song*[5,6], *Feng Jin*[4], *Yamei Niu*[1,2,3]* *and Wei-Min Tong*[1,2,3]*

[1] Department of Pathology, Institute of Basic Medical Sciences, Chinese Academy of Medical Sciences, Beijing, China, [2] School of Basic Medicine, Peking Union Medical College, Beijing, China, [3] Molecular Pathology Research Center, Chinese Academy of Medical Sciences, Beijing, China, [4] Department of Breast Surgery, The First Affiliated Hospital of China Medical University, Shenyang, China, [5] China National Center for Bioinformation, Beijing, China, [6] National Genomics Data Center & CAS Key Laboratory of Genome Sciences and Information, Beijing Institute of Genomics, Chinese Academy of Sciences, Beijing, China

OPEN ACCESS

Edited by:
Shicheng Guo,
University of Wisconsin-Madison,
United States

Reviewed by:
Jun Wan,
Wuhan Textile University, China
Jianfeng Huang,
Sanford Burnham Prebys Medical Discovery Institute, United States

***Correspondence:**
Yamei Niu
niuym@ibms.pumc.edu.cn
Wei-Min Tong
wmtong@ibms.pumc.edu.cn

Specialty section:
This article was submitted to Cancer Genetics, a section of the journal Frontiers in Oncology

Received: 28 September 2020
Accepted: 07 December 2020
Published: 29 January 2021

Citation:
Yang L, Wu S, Ma C, Song S, Jin F, Niu Y and Tong W-M (2021) RNA m^{6}A Methylation Regulators Subclassify Luminal Subtype in Breast Cancer. Front. Oncol. 10:611191. doi: 10.3389/fonc.2020.611191

RNA N^6-methyladenosine (m^{6}A) methylation is the most prevalent epitranscriptomic modification in mammals, with a complex and fine-tuning regulatory system. Recent studies have illuminated the potential of m^{6}A regulators in clinical applications including diagnosis, therapeutics, and prognosis. Based on six datasets of breast cancer in The Cancer Genome Atlas (TCGA) database and two additional proteomic datasets, we provide a comprehensive view of all the known m^{6}A regulators in their gene expression, copy number variations (CNVs), DNA methylation status, and protein levels in breast tumors and their association with prognosis. Among four breast cancer subtypes, basal-like subtype exhibits distinct expression and genomic alteration in m^{6}A regulators from other subtypes. Accordingly, four representative regulators (IGF2BP2, IGF2BP3, YTHDC2, and RBM15) are identified as basal-like subtype-featured genes. Notably, luminal A/B samples are subclassified into two clusters based on the methylation status of those four genes. In line with its similarity to basal-like subtype, cluster1 shows upregulation in immune-related genes and cell adhesion molecules, as well as an increased number of tumor-infiltrating lymphocytes. Besides, cluster1 has worse disease-free and progression-free survival, especially among patients diagnosed with stage II and luminal B subtype. Together, this study highlights the potential functions of m^{6}A regulators in the occurrence and malignancy progression of breast cancer. Given the heterogeneity within luminal subtype and high risk of recurrence and metastasis in a portion of patients, the prognostic stratification of luminal A/B subtypes utilizing basal-featured m^{6}A regulators may help to improve the accuracy of diagnosis and therapeutics of breast cancer.

Keywords: RNA methylation, m^{6}A regulators, genomic regulation, breast cancer subtypes, subclassification, survival

INTRODUCTION

Breast cancer is the most ubiquitous cancer in women worldwide. It is a heterogeneous disease and has been classified into different subtypes according to the gene expression profile. These subtypes are termed as human epidermal growth factor 2 (HER2)-enriched, basal-like, and luminal subtypes (1, 2). Standardization of breast cancer classification and optimal treatment regimens for each subtype have acquired great progress since the concept of subtype was first proposed. Patients of HER2-enriched subtype benefit from HER2-targeted therapy, such as trastuzumab and pertuzumab (3). In contrast, patients of basal-like subtype have poor prognosis, high risk of recurrence, and lack efficient therapeutic strategy (1, 4, 5). Luminal subtype, accounting for 70% of breast cancers, has positive response to endocrine therapies and the best prognosis (6). However, substantial heterogeneity still exists within this subtype (7–9). By utilizing immunohistochemical analysis of progesterone receptor (PR) and Ki-67, luminal subtype could be further classified into less-aggressive luminal A and more-aggressive luminal B subtypes (10). Despite that, the standards of PR status and Ki-67 index remain controversial across the world or even among hospitals. Additionally, there also exists undeniable intragroup heterogeneity bringing about indeterminacy in clinical management (7, 11). Thus, continuous efforts have been made to subclassify the intrinsic subtypes into more precise subgroups. For instance, basal-like cancers were further classified into 6 (12) or 4 (13) subgroups based on their genomic and transcriptomic profiling. By taking advantage of DNA copy number, DNA methylation, and gene expression data, luminal subtype was successfully segregated into subgroups with distinct molecular and clinical characteristics (8, 9, 11, 14). Nevertheless, despite the extensive investigations on breast cancer, genetic variance still brings about different responses to standard treatment protocol within the same subtype. Therefore, it is important to comprehensively understand the regulatory mechanism of gene alterations in pathological status.

Other than extensively studied genomic, transcriptomic, and epigenetic modulations, RNA m^{6}A modification (m^{6}A) represents a vital layer of epitranscriptomic regulation of gene expression and has drawn much attention in recent years. m^{6}A is the most prevalent epitranscriptomic modification in mammals. Its formation is catalyzed by methyltransferase complex (also called "writers"), which is composed of core components METTL3, METTL14 (15–17), WTAP (18), and other subunits. Conversely, RNA m^{6}A methylation can be removed by demethylases, better known as "erasers," specifically FTO (19) and ALKBH5 (20). The effects of m^{6}A on gene expression are mediated by m^{6}A binding proteins which are usually called "readers." So far, m^{6}A regulators have been unveiled to function in regulating RNA alternative splicing, nuclear export, degradation, and translation (21). Given their crucial roles in many different physiological contexts, aberrant expression of m^{6}A regulators could incur the occurrence or progression of multiple cancers through disturbing the m^{6}A-dependent RNA metabolism (22).

Aberrant expression of m^{6}A regulators, including METTL3, METTL14, WTAP, ALKBH5, and FTO, has been identified in breast cancer, as well as their potential prognostic values (23, 24). Mechanistically, upregulation of METTL3, METTL14, and FTO expression exhibits oncogenic roles by promoting cells proliferation, migration, or invasion in m^{6}A-dependent manner (25–28). On the other side, hypoxia-dependent expression of ALKBH5 and ZNF217 is associated with the maintenance and specification of breast cancer stem cells *via* their inhibitory role on m^{6}A methylation of mRNAs encoding pluripotency factors NANOG or KLF4 (29, 30). Despite the progress in the above regulators, there is still a lack of comprehensive analysis to excavate the roles and clinical applications of all the known m^{6}A regulators in breast cancer.

Recently, bioinformatics analyses provide convenient tools in identifying the m^{6}A regulators applicable in tumor classification and prognosis prediction in multiple cancers (12, 31–35). In this study, we analyzed the molecular alterations of m^{6}A regulators and found their distinctive features in breast cancer. Besides, survival analysis revealed the prognostic values of several m^{6}A regulators in breast cancer. Our results suggest their critical roles in the initiation and progression of breast cancer and diverse regulatory mechanisms of them. Furthermore, according to the DNA methylation status of 11 probes located on basal-like subtype-featured m^{6}A regulators, luminal A and luminal B subtypes were further segregated into two clusters respectively, which differed in the enrichment of tumor infiltrating lymphocytes (TILs) and patients' prognosis. Subclassification of luminal subtype will provide additional prognostic information in an attempt to improve personalized treatment of breast cancer.

MATERIALS AND METHODS

Data Collection

Six types of breast cancer datasets (**Table S1**) originated from the Cancer Genome Atlas (TCGA) database (36) were downloaded from UCSC xena platform (37): the gene expression profiles obtained were originally generated from the Illunima HiSeq 2000 platform and transformed into $\log_2$(RSEM+1) format; somatic mutation data was compiled in Mutation Annotation Format (MAF); gene-level copy number variations (CNVs) were measured experimentally using the Affymetrix Genome-Wide Human SNP Array 6.0 platform and preprocessed with GISTIC2 method (38); DNA methylation levels estimated by beta values

Abbreviations: m^{6}A, N^6-methyladenosine; TCGA, The Cancer Genome Atlas; CNV, copy number variation; HER2, human epidermal growth factor 2; PR, progesterone receptor; MAF, Mutation Annotation Format; t-SNE, t-distributed Stochastic Neighbor Embedding; SD, standard deviation; CDF, cumulative distribution function; KEGG, Kyoto Encyclopedia of Genes and Genomes; TILs, tumor infiltrating lymphocytes; ssGSEA, single sample gene set enrichment analysis; TSS, Transcription Start Site; NS, not significant; OS, overall survival; DFS, disease-free survival; PFS, progression-free survival; UTR, untranslated region; HR, hazard ratio; GEO, Gene Expression Omnibus; ICGC, International Cancer Genome Consortium; CFEA, Cell-Free Epigenome Atlas.

were measured based on the GPL13534 platform (Illumina Infinium HumanMehytlation450 Bead-Chip array). The beta values of DNA methylation are continuous variables between 0 and 1, representing the percentage of methylated alleles; miRNA expression data was generated from IlluminaHiseq platform, while the miRNA-target interactions were downloaded from miRTarBase database (39); phenotype data contained the survival and subtype information of each sample.

Proteomic datasets were obtained from another two independent studies. The first proteomic study applied a quantitative liquid chromatography/mass spectrometry-based proteome analysis to 65 breast tumors and 53 adjacent non-cancerous tissues (40). This dataset was used for comparing expression between tumor and normal samples. The other study utilized high-resolution accurate-mass tandem mass spectrometry method and contained 105 breast tumors with explicit information of subtyping and prognosis, which was applied for comparison among subtypes and for survival analysis (41).

Correlation Analysis

The Pearson correlation coefficients between gene expression and DNA methylation, copy number, or miRNA expression were computed in R with *cor.test* function, respectively. Only the DNA methylation probes that had missing values in less than 50% of samples were included for the analysis. Different versions of miRNA IDs were converted through *miRBaseVersions.db* R package (42).

Determination of Basal-Featured m^{6}A Regulators

The importance of m^{6}A regulators in distinguishing basal-like samples from other subtypes was ranked by performing random forest algorithm based on their gene expression levels. This procedure was processed in R with *RandomForest* package (43). Furthermore, the variable selection was determined by using *varSelRF* R package (44).

Samples Clustering Analysis

Based on phenotype data, only normal samples and breast tumor samples allocated to explicit subtypes were included in sample clustering analysis. t-Distributed Stochastic Neighbor Embedding (t-SNE) analysis was performed with the expression values of all 28 m^{6}A regulators using the *tsne* R package (45). Unsupervised hierarchical clustering analysis was performed with filtered DNA methylation probes, whose beta values should meet the below criteria (1): absolute value of Pearson correlation coefficient with gene expression was greater than 0.3; (2) standard deviation (SD) among all samples was higher than 0.2. Consensus clustering that determined the number of clusters for luminal and basal-like samples was implemented with *ConsensusClusterPlus* package in R by resampling iteration (50 iterations, resampling rate of 80%). The cluster number was determined according to the relative change in area under the cumulative distribution function (CDF) curve (46). The heatmap corresponding to the consensus clustering was generated with *pheatmap* R package.

Differential Expression Analysis

Differentially expressed genes between cluster1 and cluster2 samples were defined with *DESeq2* R package (47). Briefly, the original $\log_2$(RSEM+1) values were transformed into RSEM values and grounded to integers, then the expression matrix was imported using the *DESeqDataSetFromMatrix* function. Genes that met the criteria of adjusted $P < 0.05$ and FoldChange > 1.5 or < 0.66 were regarded as differentially expressed genes between cluster1 and cluster2 samples.

Functional Enrichment Analysis

Kyoto Encyclopedia of Genes and Genomes (KEGG) pathway enrichment analysis of the differentially expressed genes between cluster1 and cluster2 samples was implemented with *clusterProfiler* R package (48). Marker genes for each immune cell population were curated from published research (49), the relative abundance of different types of TILs in each sample was assessed by single sample gene set enrichment analysis (ssGSEA) method (50) in *GSVA* R package.

Statistical Analysis

All analyses were implemented with R computing framework (v3.6.1). Wilcoxon rank-sum test was employed to compare the difference in expression of m^{6}A regulators between control and breast tumor samples. The comparison of gene expression among the four subtypes was implemented by Kruskal-Wallis analysis. Univariate cox proportional hazard regression analysis was performed to evaluate the correlation between gene expression level, CNV, DNA methylation level and survival time using the *coxph* function with *survival* R package. Kaplan-Meier survival analyses and log-rank test were performed for comparison of survival time between the two clusters which was processed with *survival* R package (51).

RESULTS

Alterations of m^{6}A Regulators Exhibited Prognostic Values in Breast Cancer

Accumulating evidence has confirmed that aberrant expression of m^{6}A regulators is associated with tumorigenesis and progression in multiple cancers. Thereby, we asked whether this phenomenon could be observed in breast cancer. At present, 28 genes have been identified as m^{6}A regulators due to their direct or indirect functions in m^{6}A deposition, removal, or recognition (**Figure S1A**). First, we examined the expression of those m^{6}A regulators in breast cancer and normal samples. Among them, 17 out of 28 genes exhibited significantly differential expression ($P < 0.001$), including KIAA1429, FMR1, HNRNPA2B21, HNRNPC, IGF2BP1, PRRC2A, YTHDF1, ZNF217 being upregulated and METTL14, WTAP, ZC3H13, METTL16, ZCCHC4, FTO, EIF3A, IGF2BP2, YTHDC1 being downregulated in breast cancer samples (**Figure 1A** and **Figure S1B**), suggesting their potential involvement in tumorigenesis of breast cancer.

To our knowledge, gene expression could be manipulated by multi-layered genomic features, such as DNA mutation, CNV, DNA methylation, and miRNA expression. To find out the abnormal regulatory elements for each m^{6}A regulator in breast cancer, comparisons were implemented sequentially in breast cancer *versus* normal samples. The frequencies of gene mutation in all 28 m^{6}A gene regulators were relatively low (**Table S2**). In contrast, their CNVs were prevalent for most m^{6}A regulators. Particularly, in contrast to their low CNV frequencies (< 5%) in normal samples, CBLL1, METTL14, RBM15, IGF2BP1, YTHDC1, and YTHDF2 exhibited more than 20% difference in their frequencies of CNVs between tumor and normal samples (**Figure 1B** and **Table S2**). Next, we performed correlation analysis between copy numbers and gene expression levels to evaluate the possible effect of CNVs on gene expression. Eight regulators, including KIAA1429, METTL16, WTAP, ZCCHC4, ALKBH5, YTHDF1, YTHDF2, and YTHDF3 exhibited significant correlations (R > 0.6) between gene expression levels and copy numbers in breast tumors (**Figure 1C** and **Table S3**). It indicated that CNVs of these eight genes might be one of the causal factors to perturb their gene expression in the tumors.

In parallel, we also compared the DNA methylation levels of m^{6}A regulators between tumor and normal samples. Among the 593 probes located in these 28 genes, 23 probes located on 6 genes, including CBLL1, FTO, IGF2BP1, IGF2BP2, IGF2BP3, and ZNF217, showed significant differences in their methylation patterns between tumor and normal samples ($|\Delta$beta-value$| > 0.2$ and $P < 0.05$) (**Figure 1D**). Correlation analysis between the levels of DNA methylation and gene expression was further performed with all the breast cancer samples. Significant correlation ($|R| > 0.3$ and $P < 0.05$) was observed in WTAP, ZC3H13, ZCCHC4, FTO, ALKBH5, YTHDC2, IGF2BP2, and IGF2BP3, implying a possible role of DNA methylation in shaping their gene expression in breast cancer (**Table S4**). Markedly, negative correlation with gene expression levels was solely observed in the probes located on potential promoter regions, while positive correlation existed in gene body and 3'UTR regions only (**Figure 1E** and **Table S4**). This phenomenon implied that the DNA methylation in different genomic regions might have opposite effects on the gene expression (52, 53). In terms of miRNA regulation, despite the positive and negative relation observed between miRNA and m^{6}A regulator expression, their correlation seemed to be weaker than that with copy number and DNA methylation (**Table S5**).

Given the roles of m^{6}A regulators in predicting prognosis observed in various cancers, we further sought to explore their potential prognostic values in breast cancer. Univariate cox regression analysis was performed with gene expression, copy number, and DNA methylation. In terms of gene expression, METTL3, RBM15B, HNRNPC, YTHDC1, and ZNF217 appeared to be protective factors with HR < 1, while IGF2BP1 and YTHDF3 were risky genes with HR > 1. Notably, higher expression of IGF2BP1 was a risky factor for overall survival (OS), disease-free survival (DFS) and progression-free survival (PFS) (**Figure 2A**). Additionally, it turned out that CNVs of m^{6}A regulators also had prognostic values. Thereinto, copy number loss of FTO was a protective factor, while copy number gain of another 9 m^{6}A regulators marked a worse prognosis (**Figure 2B**). Particularly, copy number loss of ZNF217 was associated with shorter OS, DFS and PFS of breast cancer patients. Regarding DNA methylation, we identified a total of 74 CpG sites located on 19 genes whose DNA methylation levels were associated with the OS, DFS or PFS of breast cancer patients (**Figure 2C**). Most of the methylation sites exhibited protective roles in prognosis. Conversely, higher methylation levels of 16 CpG sites located on WTAP, RBM15B, EIF3A, FMR1, HNRNPA2B1, IGF2BP1, IGF2BP2, IGF2BP3, and YTHDF3 were associated with poor prognosis. Intriguingly, although located on the same genes, methylation levels of distinct sites had opposite roles in predicting prognosis. Inconsistently, all significantly predictive methylation sites on FTO and YTHDC1 exhibited protective values in prognosis.

In addition to the genetic and transcriptional alterations of m^{6}A regulators, we further explored whether we could detect any changes at protein level. By comparing tumor and normal samples, we found that six proteins were differentially expressed in breast cancer significantly ($P < 0.001$), including EIF3A, HNRNPA2B1, HNRNPC, RBMX, YTHDF1, YTHDF2 (**Figure 3A**). Among them, three genes (HNRNPA2B1, HNRNPC, YTHDF1) exhibited consistently aberrant expression in both RNA and protein levels while EIF3A had reverse change direction in RNA and protein levels. Besides, we performed cox regression analysis to evaluate the prognostic values of m^{6}A regulators at protein level (**Figure 3B**). As a result, IGF2BP2 and IGF2BP3 showed significant prognostic values of being risk factors (HR > 1) for OS of breast cancer patients.

Together, we offered a comprehensive view of genetic, transcriptional, and post-transcriptional alterations of 28 known m^{6}A regulators in breast cancer, indicative of their possible roles in tumorigenesis and diverse regulatory mechanisms. Moreover, a few genes were identified to be potential predictors for patient survival based on their changes in gene expression, copy numbers, DNA methylation, or protein levels.

Diverse Expression Patterns and Regulations of m^{6}A Regulators Among the Four Subtypes Revealed the Unique Characters of Basal-Like Subtype

Given the undeniable diversity in molecular mechanisms and clinical characteristics among the four subtypes of breast cancer, we next explored whether those m^{6}A regulators exhibited any differences among them. First, by comparing the protein expression of all regulators, only IGF2BP2 exhibited differential expression among the four subtypes (**Figure S2**).

To further investigate the variance among different subtypes, we turned to compare them at the transcriptional level. Ultimately, we found that 23 out of 28 m^{6}A regulators exhibited significantly distinct expression levels among the four subtypes (**Figure 4A**). Next, to further explore and visualize the dispersion of m^{6}A regulators in all subtypes, we adopted t-SNE

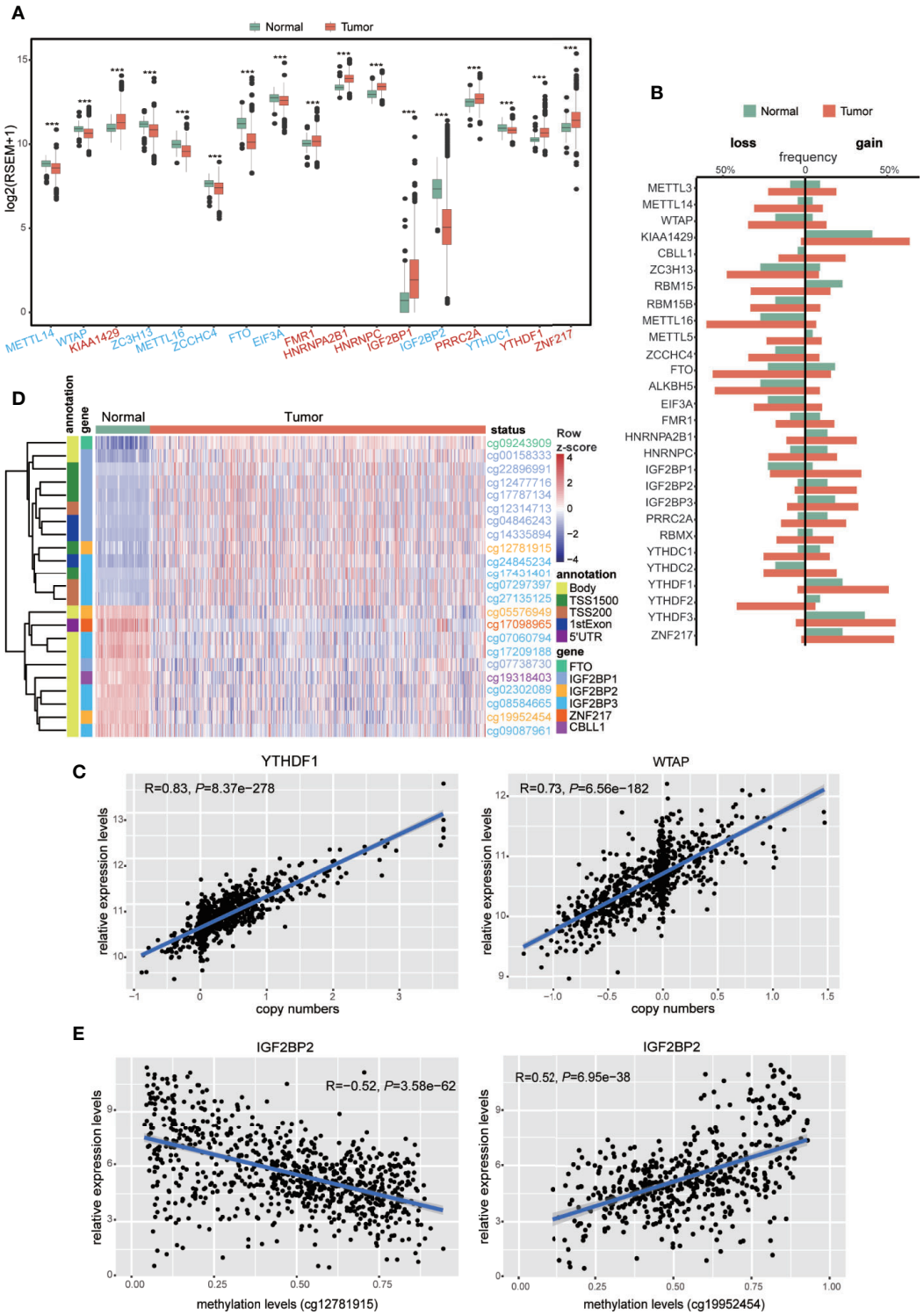

FIGURE 1 | Expressions and genetic variations of m^{6}A regulators in breast cancer. **(A)** Boxplot showing the m^{6}A regulators with highly significant difference in their RNA expression between normal and tumor samples (***$P < 0.001$). Different colors of axis labels stand for the changing direction of gene expression in tumor, with red labels representing upregulation and blue labels representing downregulation. **(B)** Frequencies of the copy number gain/loss of each m^{6}A regulator in normal and tumor samples. **(C)** Correlation analysis between the gene expression levels and copy numbers of two representative genes (YTHDF1 and WTAP) with the highest correlation coefficients. **(D)** Unsupervised hierarchical clustering heatmap showing the beta-values of 23 differentially methylated DNA probes between normal and tumor samples. **(E)** Correlation analysis between IGF2BP2 expression level and its DNA methylation levels at two sites (cg12781915 and cg19952454).

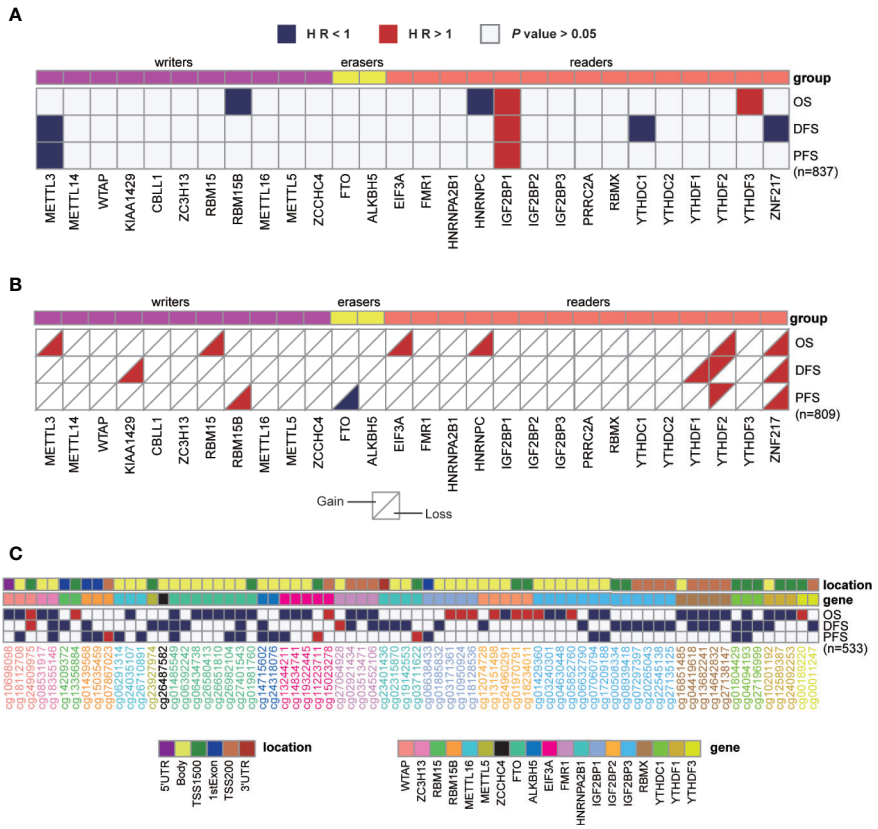

FIGURE 2 | Univariate cox regression analysis of m^{6}A regulators. **(A–C)** Univariate cox regression analysis of the association between overall survival (OS), disease-free survival (DFS), or progression-free survival (PFS) and gene expressions **(A)**, copy number variations **(B),** or DNA methylation levels **(C)**. Blue box, protective factors (HR < 1 and $P < 0.05$); Red box, risky factors (HR > 1 and $P < 0.05$); white box, $P > 0.05$. The sample size used in each cox regression analysis was marked in brackets.

method to reduce the high dimensional expression data into a lower-dimensional subspace. This result showed that breast cancer samples could be segregated from normal samples judged by the expression of m^{6}A regulators. Strikingly, basal-like subtype displayed evident segregation from another three subtypes as well (**Figure 4B**). These results implied that the function of those m^{6}A regulators in the four subtypes varied from each other. Particularly, basal-like subtype might exploit unique regulatory mechanisms in malignant progression driven by RNA m^{6}A modification.

Next, we examined the frequencies of copy number gain/loss in each subtype, respectively (**Table S6**). Although most genes showed high frequencies of CNV without apparent discrepancy among the four subtypes, we noticed that several genes involving CBLL1, RBM15, PRRC2A exhibited particularly high frequencies of copy number gain event in basal-like subtype. Of note, 51.1% of basal-like samples contained copy number gain of CBLL1, and other subtypes showed much lower proportion (23.9% of HER2, 18.3% of luminal A, and 19.8% of luminal B). Additionally, the frequency of copy number loss in METTL3 was higher (60.0%) in basal-like subtype than that in another three subtypes (HER2: 20.9%; luminal A: 11.6%; luminal B: 20.3%); copy number loss of YTHDC2 occurred in 75.6% of basal-like tumors while significantly less in other samples (HER2: 40.3%; luminal A: 7.2%; luminal B: 24.0%) (**Figure 4C**). In short, CNVs of m^{6}A regulators were prevalent in breast tumors, and the basal-like subtype exhibited the highest frequencies compared to other subtypes.

Next, DNA methylation status of the m^{6}A regulators was compared among the four subtypes. Among all the probes detected in the 28 regulators, we observed that most of the CpG loci exhibited similar methylation levels among all samples (**Figure S3**). Therefore, only the highly variable methylation loci that met the criteria of standard deviation greater than 0.2 (SD > 0.2) across all tumor samples were included for subsequent analysis. Unsupervised hierarchical clustering was performed on both samples and probes to reveal the diverse methylation patterns among tumor samples. As shown in **Figure 4D**, DNA methylation patterns of a cluster of CpG sites on IGF2BP1, IGF2BP2, and IGF2BP3 exhibited prominent variance among all clustered groups. As for the clustering results, the sharpest distinction was drawn between basal-like and other subtypes. Nevertheless, parts of luminal samples were clustered together with most basal-like samples and they shared similarities in

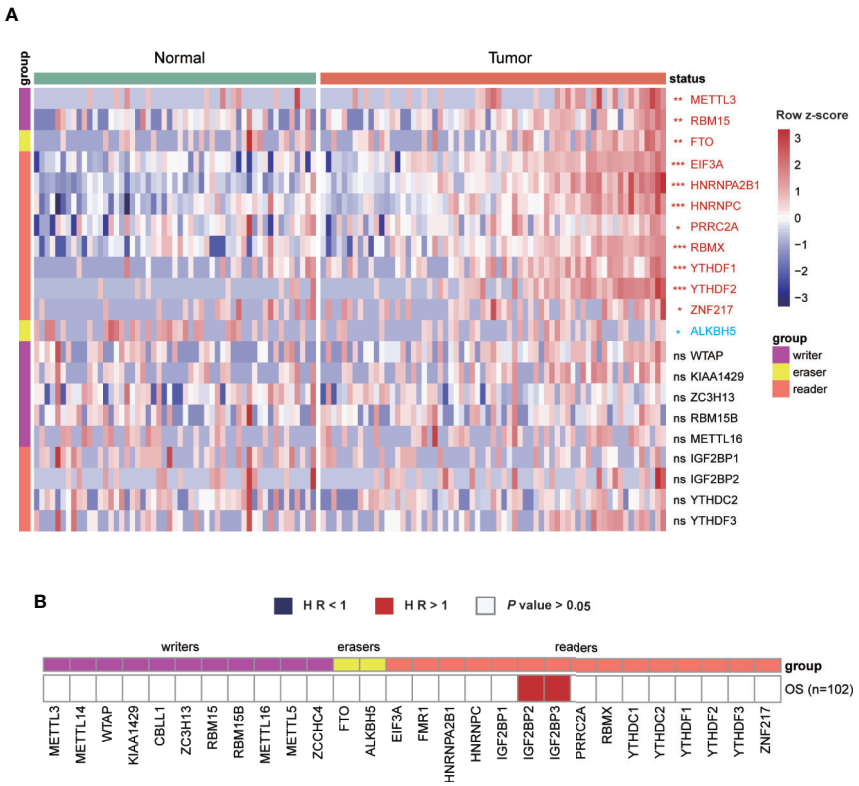

FIGURE 3 | Expressions and survival analyses of m^{6}A regulators at protein level. **(A)** Comparison of m^{6}A regulators between tumor and normal samples at protein level. The change direction was exhibited by label colors, with red representing for upregulation and blue representing for downregulation. ns, $P > 0.05$; $^*P < 0.05$; $^{**}P < 0.01$; $^{***}P < 0.001$. **(B)** Univariate cox regression analysis of the association between protein expression levels and OS of patients. Blue box, protective factors (HR < 1 and $P < 0.05$); Red box, risky factors (HR > 1 and $P < 0.05$); white box, $P > 0.05$.

methylation levels. The discrete distribution of luminal samples reflected the noticeable intragroup heterogeneity within luminal A/B subtype revealed by the DNA methylation levels of m^{6}A regulators.

In general, the above results indicated that most m^{6}A regulators examined in this study possessed distinct molecular characteristics among the four subtypes. Particularly, the basal-like subtype displayed a unique feature in the aspect of gene expression, CNV and DNA methylation. Of note, DNA methylation analysis distinguished a cluster of samples consisting of basal-like subtype and a part of luminal samples due to their similar DNA methylation patterns.

Subclassification of Luminal Subtype Breast Cancers Based on DNA Methylation of m^{6}A Regulators

Although it is widely accepted that basal-like breast cancers have the highest tendency of recurrence and metastasis, some patients allocated to luminal subtype also suffer from early recurrence and metastasis which poses a big challenge in clinical practice. Given the unique profile of m^{6}A regulators in basal-like subtype and high intragroup heterogeneity within luminal subtype, we asked if the m^{6}A features of basal-like subtype could be applied to subclassify the luminal subtype and to distinguish the luminal samples which resembled basal-like subtype in the recurrent and metastatic property. To address this question, we firstly made efforts to obtain the basal-like subtype-featured m^{6}A regulators. Based on the gene expression of 28 regulators, random forest machine learning was used to rank the gene importance and varSelRF method for variable selection. We consequently identified four genes (IGF2BP2, IGF2BP3, YTHDC2, and RBM15) as important predictors in distinguishing basal-like subtype from other subtypes (**Figures 5A, B**). Then, the expression values of those four genes were imported to consensus clustering analysis for both basal-like and luminal breast cancers. Unexpectedly, we failed to subclassify luminal samples in this way (**Figures S4A, B**).

Our previous clustering analysis of DNA methylation sites revealed that a certain number of luminal samples exhibited similar patterns to basal-like subtype in their DNA methylation patterns of highly variable CpG loci (**Figure 4D**). Therefore, we examined the possibility of using the DNA methylation status on those four genes for patients' subclassification. Following the criteria of large standard deviation (SD > 0.2) and high correlation with gene expression ($|R| > 0.3$), 11 probes located on IGF2BP2 and IGF2BP3 were screened out. Consensus clustering was subsequently implemented in R with the beta values of 11 probes, and k = 2 was the optimal result, with

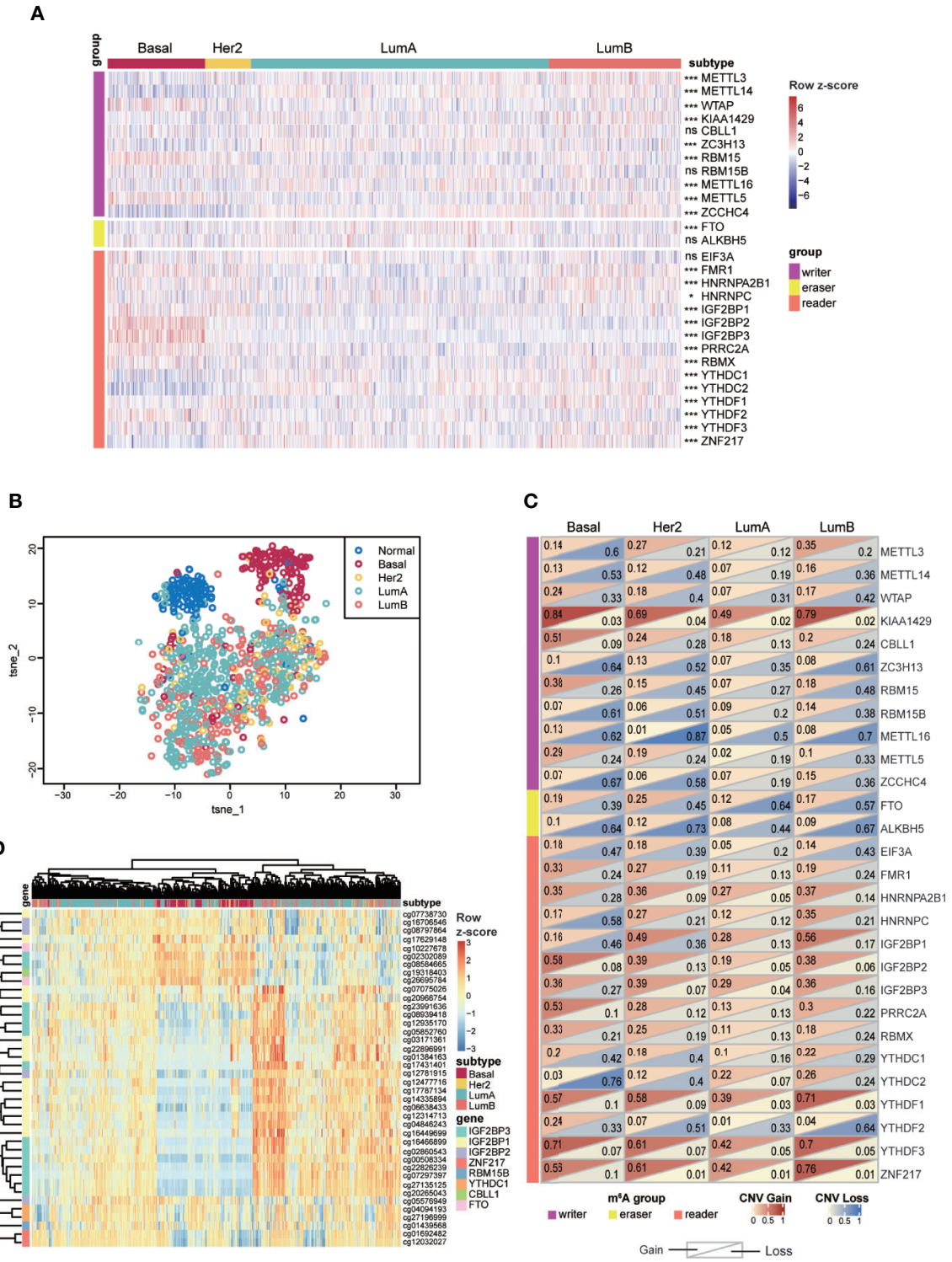

FIGURE 4 | Expressions and genetic variations of m^{6}A regulators among the four subtypes in breast cancer. **(A)** Heatmap showing the expression of m^{6}A regulators and their differences among the four subtypes. ns, $P > 0.05$; $^*P < 0.05$; $^{**}P < 0.01$; $^{***}P < 0.001$. **(B)** t-SNE plot of normal and breast tumor samples showing the separation of normal and Basal-like samples from other groups. The colors were assigned according to sample type. **(C)** Frequencies of copy number gain/loss of m^{6}A regulators in each subtype. The upper triangle of a single rectangle displays the frequency of copy number gain of each gene in each subtype, and the lower triangle displays the frequency of copy number loss. **(D)** Unsupervised hierarchical clustering analysis for four subtypes of tumors based on 40 highly variable DNA methylation probes (SD > 0.2). LumA, luminal A; LumB, luminal B; Her2, HER2-enriched; Basal, Basal-like.

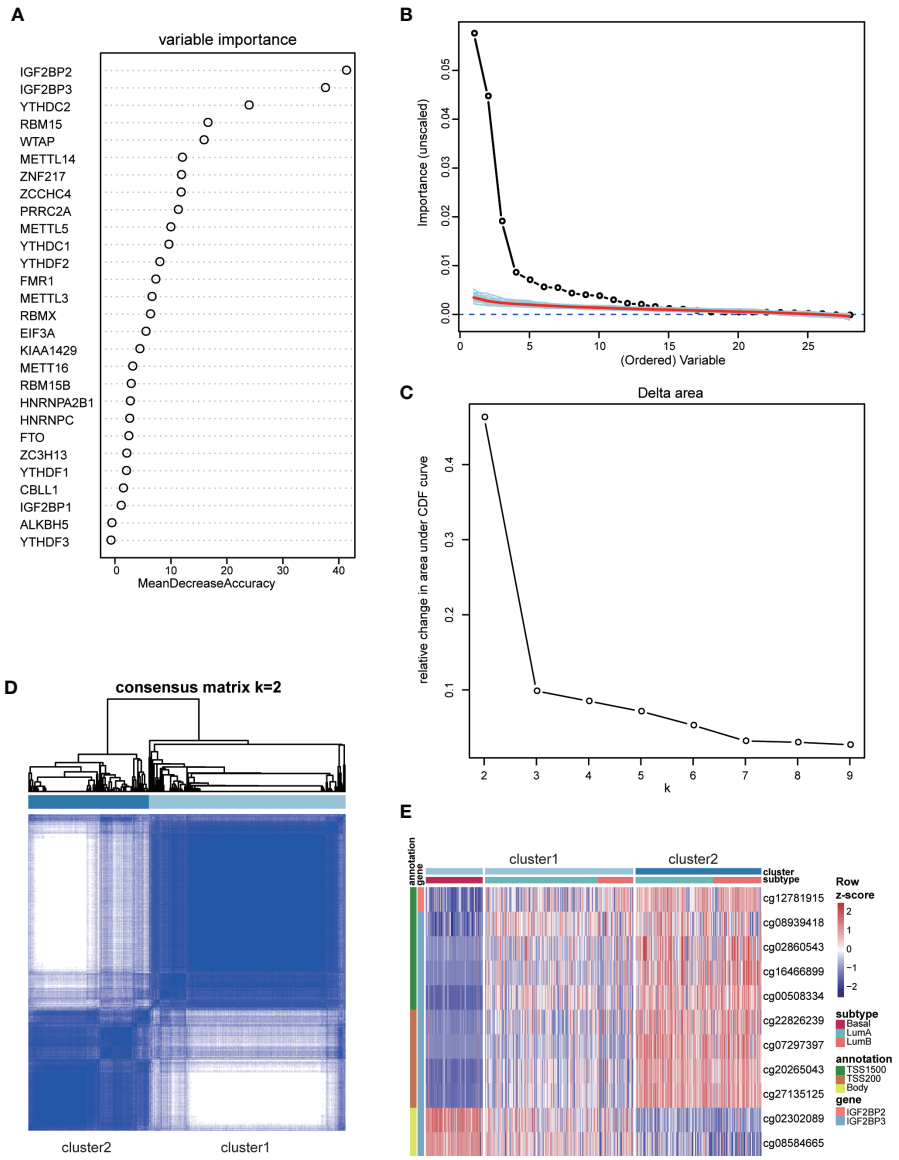

FIGURE 5 | Identification and consensus clustering analysis of basal-featured m^{6}A regulators. **(A)** Random forest analysis ranking the importance of m^{6}A regulators in basal subtype segregation based on their gene expression levels. **(B)** Importance spectrum plots for optimizing the number of relevant variables according to random forest analysis. **(C)** Relative change in area under cumulative distribution function (CDF) curve based on results of consensus clustering for k = 2 to 9. **(D)** Consensus clustering matrix for k = 2. **(E)** Heatmap showing the methylation levels of 11 probes utilized for samples classification in the two clusters.

clustering stability increasing from k = 2 to 9 (**Figures 5C, D**). Strikingly, according to the clustering results, luminal subtypes were successfully divided into two clusters, in which cluster1 was composed of all basal-like samples and parts of luminal samples, while cluster2 was composed of luminal samples only (**Figure 5E**). As for these two clusters, the methylation patterns of 11 probes in luminal-cluster1 samples were similar to basal-like samples rather than luminal-cluster2 samples. Interestingly, both luminal A and luminal B subtypes were divided into two groups and distributed in the two clusters.

To better understand the differences between the two clusters, we performed differential expression analysis and identified 2,071 upregulated and 655 downregulated genes (adjusted $P <$ 0.05 and FoldChange > 1.5 or < 0.66) (**Table S7**). Next, KEGG functional enrichment analysis revealed that the upregulated genes in cluster1 of both luminal A and luminal B subtypes were mostly enriched in immune-related and cell adhesion-related pathways (**Figure 6A** and **Table S8**). To further decipher the distinct immune traits between the two clusters, we took advantage of GSVA method to evaluate the relative quantity of immune cell populations infiltrated in each sample. The results showed that samples in cluster1, similar to that in basal-like subtype, had higher enrichment in most kinds of immune cells than those in cluster2 (**Figure 6B**).

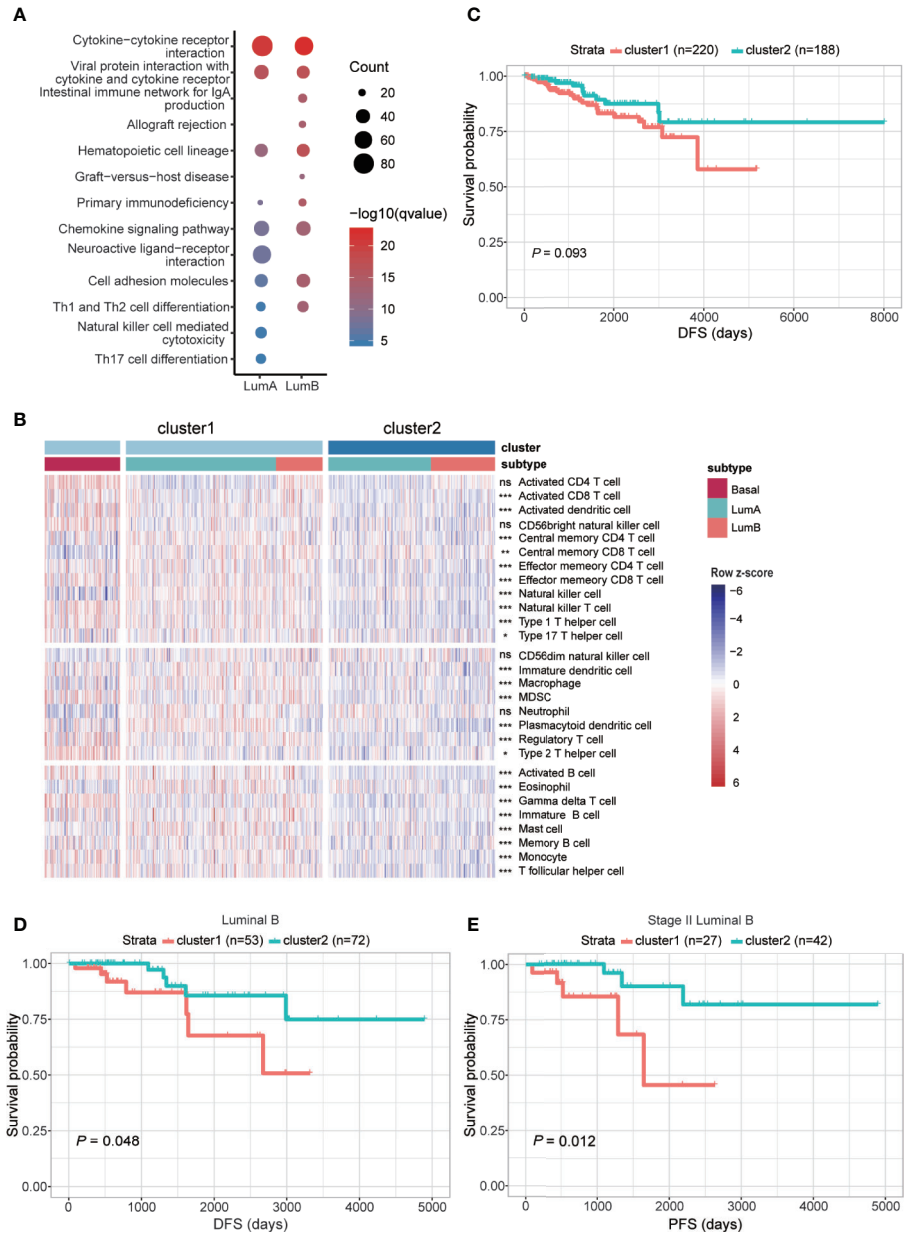

FIGURE 6 | Comparison of functional and clinical relevance between the two clusters in luminal samples. **(A)** KEGG enrichment analysis of genes upregulated in cluster1 within luminal A and luminal B subtypes, respectively. **(B)** Heatmap showing relative quantities of infiltrated lymphocytes in the two clusters. **(C)** Comparison of DFS between the two clusters. **(D)** Comparison of DFS between cluster1 and cluster2 samples in luminal B subtype. **(E)** Comparison of PFS between the two clusters among patients diagnosed as stage II in luminal B subtype. The sample size of each group was marked in brackets.

Given that cluster1 possessed similar m^{6}A features with basal-like subtype and higher expression of immune-related genes, we further examined their clinical relevance in the two clusters. Comparison of survival status revealed that patients fitting in cluster1 had worse DFS than those in cluster2 (**Figure 6C**), but the difference of OS and PFS between the two clusters was indistinct (**Figures S5A, B**). To rule out the impact of different subtypes on prognosis, we next compared the two clusters within each subtype separately. It turned out that within luminal B subtype, patients in cluster1 had worse DFS than cluster 2 (**Figure 6D**), although no significant difference was observed in luminal A subtype (**Figures S5C–E**). Furthermore, in further consideration of the impact of disease stage to patient prognosis, comparisons were processed within each stage of luminal B subtype. Consequently, the most significant difference in both DFS and PFS was observed within the patients diagnosed with stage II of luminal B subtype (**Figures 6E**, **S5F–G**).

Overall, we identified basal-like subtype-featured m^{6}A regulators, and further utilized their methylation patterns to successfully subclassify the luminal A/B tumors into two clusters, respectively. In line with the enrichment of immune-related genes, cell adhesion molecules and higher enrichment of tumor infiltrating lymphocytes, cluster1 samples, especially those allocated to luminal B subtype, had higher risk of disease recurrence.

DISCUSSION

With our increasing knowledge of m^{6}A methylation in modulating RNA metabolism, how dysregulated m^{6}A is involved in cancer has attracted much more attention than ever. Here, we examined the distinctive expression of m^{6}A regulators and the multilayered regulation on them in breast cancer. Comparison among the four subtypes revealed a unique m^{6}A feature of basal-like subtype from others. Furthermore, according to the DNA methylation status of 11 probes located on basal-featured m^{6}A regulators, luminal subtypes were subclassified into two clusters with significantly different prognosis.

Till now, a few of studies have shown aberrant expression of five m^{6}A regulators in breast cancer and clarified the molecular mechanism of ALKBH5- and ZNF217-mediated tumor occurrence (23, 25, 26, 28–30). Here we found a total of 17 m^{6}A regulators exhibiting aberrant gene expression in breast cancer. Despite that some of them have been confirmed an oncogenic or tumor-suppressive role in hepatocellular carcinoma, leukemia, glioblastoma, and others (21), how these regulators are involved in the onset and progression of breast cancer remains elusive yet. Besides, we reported for the first time that CNV and DNA methylation change of m^{6}A regulators might participate in tumorigenesis of breast cancer by shaping the gene expression. For instance, the highest correlation between copy numbers and gene expression levels was observed in YTHDF1, while IGF2BP2 has the strongest negative correlation between its DNA methylation and gene expression levels. Therefore, characterization of their functions and associated regulatory mechanism will shed new light into the mechanistic study of breast cancer from the viewpoint of RNA m^{6}A methylation. In addition, we found that gene expression, copy numbers, DNA methylation levels and protein expression of several m^{6}A regulators had significant correlation with either poor or improved disease outcomes, which could provide additional prognostic information and assist with precise medicine of breast cancer. It's worth noting that, since gene expression and copy numbers or DNA methylation levels are not always correlated, they may have different or even opposite prognostic values. This inconsistency may arise from the complicated regulatory network of gene expression. For instance, multiple copies of a gene could be regulated differentially due to their corresponding chromatin environments (54). Furthermore, gene duplications that do not include distal regulatory elements important for the gene expression will not contribute to higher expression (55). On the other side, the effects of DNA methylation on gene expression are dependent to a large extent on the genomic locations of DNA methylation sites. Concretely, methylation in promoter region usually negatively correlates with gene expression, while methylation in the gene body does not block and might even stimulate transcription elongation (56). For example, among the 15 DNA methylation probes of IGF2BP3 identified in our study, the levels of 10 methylation occurring in the promoter region showed a strong negative correlation with gene expression, while the opposite trend was observed with the four methylation sites in the gene body. Hence, although luminal subtype could be subclassified into two clusters based on the methylation levels at specified CpG loci of IGF2P2 and IGF2BP3, we did not observe apparent difference in their gene expression levels between the two clusters.

Among the 28 regulators, IGF2BP2, IGF2BP3, YTHDC2, and RBM15 were identified as basal-like subtype-featured m^{6}A regulators. Among them, IGF2BP2, IGF2BP3 and RBM15 were highly expressed in basal-like tumors while YTHDC2 was lowly expressed in them (**Figure 4A**). Consistent with our findings, Barghash et al. reported that increased expression of IGF2BP2 was regarded as a feature of basal-like subtype and correlated with short survival (57). In addition, suppressed IGF2BP2 could hinder cell proliferation and invasion in breast cancer (58). As to IGF2BP3, despite the comparable expression between breast cancer and normal samples in our data, its expression in basal-like subtype was significantly higher than that in other subtypes (**Figure 4A**). In agreement with that, tumors with higher IGF2BP3 expression were characterized by increased tumor size, advanced tumor stage, and lymph node metastasis (59). Similarly, higher protein levels of IGF2BP2 and IGF2BP3 were also proved to be associated with high-risk prognosis in our results (**Figure 3B**). Different from IGF2BP2 and IGF2BP3, although the oncogenic roles of YTHDC2 and RBM15 have been identified in colon cancer (60) and acute megakaryoblastic leukemia (61–63), their functions in breast cancer await to be identified.

Breast cancer is a complex disease with large degree of intertumoral and intratumoral heterogeneity. In recent years, molecular subtyping distinguished by gene expression profiling in breast cancer has contributed a lot to prolong patients' survival due to the improvement in precise diagnosis and targeting therapy (6). Nevertheless, within each subtype, there still exists substantial heterogeneity and therefore requires more extensive and thorough investigation of breast cancer. In this study, in addition to the significant difference between normal and cancer samples, the performances of these m^{6}A regulators in the four subtypes were distinct from each other as well. Particularly, basal-like subtype is unique in its gene expression, copy number, and DNA methylation. Given the fact that basal-like subtype is more aggressive and has a worse prognosis than other subtypes (1, 4, 5), the unique features of m^{6}A regulators in basal-like subtype suggest their possible involvement in tumor invasion and metastasis. In line with that, higher expression of cell adhesion molecules was detected in samples assigned to cluster1, further indicating the correlation between m^{6}A regulators and breast cancer malignancy.

Luminal breast tumors are the most common subtypes (64); meanwhile, they are also highly heterogeneous in the aspect of histology, gene expression profiles, genetic alterations, and clinical outcomes (65). Despite endocrine therapy and chemotherapy available for them, some patients of this subtype still suffer from

relapse and poor prognosis (7, 66), thereby highlighting the emergent need for early prediction for those latent patients. Effective biomarkers can accurately instruct patients to access suitable therapies, thus helping advanced patients to achieve positive clinical response to treatment in a short time. As DNA is more stable than RNAs or proteins and easily quantified, DNA methylation is considered as a robust biomarker and promising biomarker for early detection and diagnosis (67). In this study, based on DNA methylation of m^{6}A regulators, luminal samples were subclassified into two clusters with distinct expression levels of immune-related genes. According to previous studies, immune environment of breast tumors has profound effects on patients' prognosis and varies among the four subtypes. Accordingly, basal-like subtype has the highest rate of TILs than other subtypes (68). In the luminal-HER2$^-$ patients, a higher TIL number was associated with shorter overall survival as well (69). This is consistent with our results that cluster1 in luminal samples had higher number of TILs and worse prognosis. Since the presence of TILs indicates better sensitivity to neoadjuvant chemotherapy (69), our subclassification strategy may provide a clue to recognize those luminal tumors more suitable for neoadjuvant therapy. The unveiled immune variance within luminal subtype in our study was also illustrated in two published research. One of them performed segregation analysis of luminal group based on immune-related genes and identified three immune subtypes which owned distinct clinical characteristics (11). The other study highlighted that even within luminal A subtype, immune heterogeneity could not be ignored either, as revealed by a large-scale transcriptome analysis. Both gene expression and DNA methylation profiles were successfully applied to segregate luminal A samples into two biologically distinct subgroups with different expression patterns of immune-related genes (14). However, this method exploited a large number of partitioning genes for subclassification, which made it difficult to be translated into clinical application. By contrast, our study put forward a small gene set that could be applied to luminal subtype partition and thereby is of more practical use. Mechanistically, as sample clustering was implemented with DNA methylation of m^{6}A regulators, the different enrichment of TILs in luminal tumors between the two clusters may be associated with the m^{6}A RNA methylation. RNA m^{6}A methylation has already been reported to be correlated with immune responses, such as T cell homeostasis (70, 71), inflammatory response (72), antiviral immunity (73–77), and anti-tumor immune response (78). Thereby, intensive mechanistic studies are necessary to uncover the mechanism of how m^{6}A impacts tumor relapse or metastasis *via* its modulatory roles on immune response.

Although our strategy could be successfully applied to subclassify the luminal subtype and has predictive value in clinical, some limitations should be noted here. First, given the existing inconsistency between RNA and protein levels observed in other types of cancers (79–81), it is important to depict the performance of m^{6}A regulators in breast cancers at protein level. Although the additionally obtained two proteomic datasets provided certain information about the function of m^{6}A regulators in breast cancer at protein levels, the sample size was not sufficient. So the conclusions needed to be assured by well-designed experiments later on. Second, there was a lack of validation cohorts in our study. We searched out for Gene Expression Omnibus (GEO), International Cancer Genome Consortium (ICGC) and Cell-Free Epigenome Atlas (CFEA) databases to filter the datasets that provided detailed clinical information including intrinsic subtypes, survival status and supported by platform Illumina HumanMethylation450 BeadChip. While in consideration of all kinds of criteria, no proper data was available. Third, due to the limited information of miRNA-mRNA interactions available from database, miRNA-mRNA regulatory network specifically existing in breast cancer may not be completely included in our datasets. So extended interaction information, particularly breast tissue-specific data is necessary for more thorough studies. Last, the heterogeneity of breast tumors represents a formidable challenge of successful cancer treatment. Although our research has made efforts to explain the intertumoral heterogeneity in luminal subtype, the intratumoral heterogeneity remains elusive yet since the data analyzed here was obtained based on mixed cell population rather than single cells.

In summary, our study explored the alteration of m^{6}A regulators at multiple levels in breast cancer and revealed their potential prognostic values. Furthermore, by taking advantage of DNA methylation of basal-featured m^{6}A regulators, luminal A and luminal B subtypes were both segregated into two clusters, which are associated with different abundance of immune infiltrating lymphocytes and prognosis of patients. Together, our study expands the realm of mechanistic study in breast cancer and discovers novel strategy in subclassifying luminal subtype for the sake of personalized treatment.

DATA AVAILABILITY STATEMENT

Publicly available datasets were analyzed in this study. This data can be found here: https://xenabrowser.net/.

AUTHOR CONTRIBUTIONS

YN and W-MT conceived and designed the project. LY performed the bioinformatics analyses with the help of SS and CM. LY, YN, SW, FJ, and W-MT wrote the manuscript. All authors contributed to the article and approved the submitted version.

FUNDING

This study was supported by the Medical Epigenetics Research Center, Chinese Academy of Medical Sciences (2019PT310017, to YN).

SUPPLEMENTARY MATERIAL

The Supplementary Material for this article can be found online at: https://www.frontiersin.org/articles/10.3389/fonc.2020.611191/full#supplementary-material

REFERENCES

1. Sørlie T, Perou CM, Tibshirani R, Aas T, Geisler S, Johnsen H, et al. Gene expression patterns of breast carcinomas distinguish tumor subclasses with clinical implications. *Proc Natl Acad Sci* (2001) 98(19):10869–74. doi: 10.1073/pnas.191367098
2. Perou CM, Sørlie T, Eisen MB, van de Rijn M, Jeffrey SS, Rees CA, et al. Molecular portraits of human breast tumours. *Nature* (2000) 406(6797):747–52. doi: 10.1038/35021093
3. Dean-Colomb W, Esteva FJ. Her2-positive breast cancer: Herceptin and beyond. *Eur J Cancer* (2008) 44(18):2806–12. doi: 10.1016/j.ejca.2008.09.013
4. Sorlie T, Tibshirani R, Parker J, Hastie T, Marron JS, Nobel A, et al. Repeated observation of breast tumor subtypes in independent gene expression data sets. *Proc Natl Acad Sci USA* (2003) 100(14):8418–23. doi: 10.1073/pnas.0932692100
5. Fan C, Oh DS, Wessels L, Weigelt B, Nuyten DSA, Nobel AB, et al. Concordance among gene-expression-based predictors for breast cancer. *N Engl J Med* (2006) 355(6):560–9. doi: 10.1056/NEJMoa052933
6. Waks AG, Winer EP. Breast Cancer Treatment: A Review. *JAMA* (2019) 321 (3):288–300. doi: 10.1001/jama.2018.19323
7. Ciriello G, Sinha R, Hoadley KA, Jacobsen AS, Reva B, Perou CM, et al. The molecular diversity of Luminal A breast tumors. *Breast Cancer Res Treat* (2013) 141(3):409–20. doi: 10.1007/s10549-013-2699-3
8. Fleischer T, Klajic J, Aure MR, Louhimo R, Pladsen AV, Ottestad L, et al. DNA methylation signature (SAM40) identifies subgroups of the Luminal A breast cancer samples with distinct survival. *Oncotarget* (2017) 8(1):1074–82. doi: 10.18632/oncotarget.13718
9. Aure MR, Vitelli V, Jernström S, Kumar S, Krohn M, Due EU, et al. Integrative clustering reveals a novel split in the luminal A subtype of breast cancer with impact on outcome. *Breast Cancer Res* (2017) 19(1):44. doi: 10.1186/s13058-017-0812-y
10. Feeley LP, Mulligan AM, Pinnaduwage D, Bull SB, Andrulis IL. Distinguishing luminal breast cancer subtypes by Ki67, progesterone receptor or TP53 status provides prognostic information. *Mod Pathol* (2014) 27(4):554–61. doi: 10.1038/modpathol.2013.153
11. Zhu B, Tse LA, Wang D, Koka H, Zhang T, Abubakar M, et al. Immune gene expression profiling reveals heterogeneity in luminal breast tumors. *Breast Cancer Res* (2019) 21(1):147. doi: 10.1186/s13058-019-1218-9
12. Lehmann BD, Bauer JA, Chen X, Sanders ME, Chakravarthy AB, Shyr Y, et al. Identification of human triple-negative breast cancer subtypes and preclinical models for selection of targeted therapies. *J Clin Invest* (2011) 121(7):2750–67. doi: 10.1172/JCI45014
13. Burstein MD, Tsimelzon A, Poage GM, Covington KR, Contreras A, Fuqua SAW, et al. Comprehensive genomic analysis identifies novel subtypes and targets of triple-negative breast cancer. *Clin Cancer Res* (2015) 21(7):1688–98. doi: 10.1158/1078-0432.CCR-14-0432
14. Netanely D, Avraham A, Ben-Baruch A, Evron E, Shamir R. Expression and methylation patterns partition luminal-A breast tumors into distinct prognostic subgroups. *Breast Cancer Res* (2016) 18(1):74. doi: 10.1186/s13058-016-0724-2
15. Wang P, Doxtader Katelyn A, Nam Y. Structural Basis for Cooperative Function of Mettl3 and Mettl14 Methyltransferases. *Mol Cell* (2016) 63 (2):306–17. doi: 10.1016/j.molcel.2016.05.041
16. Wang X, Feng J, Xue Y, Guan Z, Zhang D, Liu Z, et al. Structural basis of N^6-adenosine methylation by the METTL3–METTL14 complex. *Nature* (2016) 534(7608):575–8. doi: 10.1038/nature18298
17. Śledź P, Jinek M. Structural insights into the molecular mechanism of the m^{6}A writer complex. *Elife* (2016) 5:e18434. doi: 10.7554/eLife.18434
18. Ping X-L, Sun B-F, Wang L, Xiao W, Yang X, Wang W-J, et al. Mammalian WTAP is a regulatory subunit of the RNA N^6-methyladenosine methyltransferase. *Cell Res* (2014) 24(2):177–89. doi: 10.1038/cr.2014.3
19. Jia G, Fu Y, Zhao X, Dai Q, Zheng G, Yang Y, et al. N^6-Methyladenosine in nuclear RNA is a major substrate of the obesity-associated FTO. *Nat Chem Biol* (2011) 7(12):885–7. doi: 10.1038/nchembio.687
20. Zheng G, Dahl John A, Niu Y, Fedorcsak P, Huang C-M, Li Charles J, et al. ALKBH5 Is a Mammalian RNA Demethylase that Impacts RNA Metabolism and Mouse Fertility. *Mol Cell* (2013) 49(1):18–29. doi: 10.1016/j.molcel.2012.10.015
21. Huang H, Weng H, Chen J. m^{6}A Modification in Coding and Non-coding RNAs: Roles and Therapeutic Implications in Cancer. *Cancer Cell* (2020) 37 (3):270–88. doi: 10.1016/j.ccell.2020.02.004
22. Liu L, Wang Y, Wu J, Liu J, Qin Z, Fan H. N^6-Methyladenosine: A Potential Breakthrough for Human Cancer. *Mol Ther Nucleic Acids* (2020) 19:804–13. doi: 10.1016/j.omtn.2019.12.013
23. Wu L, Wu D, Ning J, Liu W, Zhang D. Changes of N^6-methyladenosine modulators promote breast cancer progression. *BMC Cancer* (2019) 19 (1):326–. doi: 10.1186/s12885-019-5538-z
24. Liu L, Liu X, Dong Z, Li J, Yu Y, Chen X, et al. N^6-methyladenosine-related Genomic Targets are Altered in Breast Cancer Tissue and Associated with Poor Survival. *J Cancer* (2019) 10(22):5447–59. doi: 10.7150/jca.35053
25. Cai X, Wang X, Cao C, Gao Y, Zhang S, Yang Z, et al. HBXIP-elevated methyltransferase METTL3 promotes the progression of breast cancer via inhibiting tumor suppressor let-7g. *Cancer Lett* (2018) 415:11–9. doi: 10.1016/j.canlet.2017.11.018
26. Niu Y, Lin Z, Wan A, Chen H, Liang H, Sun L, et al. RNA N^6-methyladenosine demethylase FTO promotes breast tumor progression through inhibiting BNIP3. *Mol Cancer* (2019) 18(1):46–. doi: 10.1186/s12943-019-1004-4
27. Sun T, Wu Z, Wang X, Wang Y, Hu X, Qin W, et al. LNC942 promoting METTL14-mediated m^{6}A methylation in breast cancer cell proliferation and progression. *Oncogene* (2020) 39(31):5358–72. doi: 10.1038/s41388-020-1338-9
28. Yi D, Wang R, Shi X, Xu L, Yilihamu YE, Sang J. METTL14 promotes the migration and invasion of breast cancer cells by modulating N^6 −methyladenosine and hsa−miR−146a−5p expression. *Oncol Rep* (2020) 43 (5):1375–86. doi: 10.3892/or.2020.7515
29. Zhang C, Samanta D, Lu H, Bullen JW, Zhang H, Chen I, et al. Hypoxia induces the breast cancer stem cell phenotype by HIF-dependent and ALKBH5-mediated m^{6}A-demethylation of NANOG mRNA. *Proc Natl Acad Sci USA* (2016) 113(14):E2047–E56. doi: 10.1073/pnas.1602883113
30. Zhang C, Zhi WI, Lu H, Samanta D, Chen I, Gabrielson E, et al. Hypoxia-inducible factors regulate pluripotency factor expression by ZNF217- and ALKBH5-mediated modulation of RNA methylation in breast cancer cells. *Oncotarget* (2016) 7(40):64527–42. doi: 10.18632/oncotarget.11743
31. Zhou J, Wang J, Hong B, Ma K, Xie H, Li L, et al. Gene signatures and prognostic values of m^{6}A regulators in clear cell renal cell carcinoma - a retrospective study using TCGA database. *Aging (Albany NY)* (2019) 11 (6):1633–47. doi: 10.18632/aging.101856
32. Liu G-M, Zeng H-D, Zhang C-Y, Xu J-W. Identification of METTL3 as an Adverse Prognostic Biomarker in Hepatocellular Carcinoma. *Dig Dis Sci* (2020). doi: 10.1007/s10620-020-06260-z
33. Huang G-Z, Wu Q-Q, Zheng Z-N, Shao T-R, Chen Y-C, Zeng W-S, et al. m^{6}A-related bioinformatics analysis reveals that HNRNPC facilitates progression of OSCC via EMT. *Aging (Albany NY)* (2020) 12(12):11667–84. doi: 10.18632/aging.103333
34. Geng Y, Guan R, Hong W, Huang B, Liu P, Guo X, et al. Identification of m^{6}A-related genes and m^{6}A RNA methylation regulators in pancreatic cancer and their association with survival. *Ann Trans Med* (2020) 8(6):387. doi: 10.21037/atm.2020.03.98
35. Chai R-C, Wu F, Wang Q-X, Zhang S, Zhang K-N, Liu Y-Q, et al. m^{6}A RNA methylation regulators contribute to malignant progression and have clinical prognostic impact in gliomas. *Aging (Albany NY)* (2019) 11(4):1204–25. doi: 10.18632/aging.101829
36. Daniel CK, Robert SF, Michael DM, Heather S, Joelle KV, Joshua FM, et al. Comprehensive molecular portraits of human breast tumours. *Nature* (2012) 490(7418):61–70. doi: 10.1038/nature11412
37. Goldman MJ, Craft B, Hastie M, Repečka K, McDade F, Kamath A, et al. Visualizing and interpreting cancer genomics data via the Xena platform. *Nat Biotechnol* (2020) 38(6):675–8. doi: 10.1038/s41587-020-0546-8
38. Mermel CH, Schumacher SE, Hill B, Meyerson ML, Beroukhim R, Getz G. GISTIC2.0 facilitates sensitive and confident localization of the targets of focal somatic copy-number alteration in human cancers. *Genome Biol* (2011) 12(4): R41. doi: 10.1186/gb-2011-12-4-r41
39. Chou C-H, Shrestha S, Yang C-D, Chang N-W, Lin Y-L, Liao K-W, et al. miRTarBase update 2018: a resource for experimentally validated microRNA-target interactions. *Nucleic Acids Res* (2017) 46(D1):D296–302. doi: 10.1093/nar/gkx1067
40. Tang W, Zhou M, Dorsey TH, Prieto DA, Wang XW, Ruppin E, et al. Integrated proteotranscriptomics of breast cancer reveals globally increased protein-mRNA concordance associated with subtypes and survival. *Genome Med* (2018) 10(1):94. doi: 10.1186/s13073-018-0602-x

41. Mertins P, Mani DR, Ruggles KV, Gillette MA, Clauser KR, Wang P, et al. Proteogenomics connects somatic mutations to signalling in breast cancer. *Nature* (2016) 534(7605):55–62. doi: 10.1038/nature18003
42. Haunsberger S. miRBaseVersions.db: Collection of mature miRNA names of 22 different miRBase release versions. *R Package version 110* (2018).
43. Liaw A, Wiener M. Classification and Regression by randomForest. *R News* (2002) 2(3):18–22.
44. Diaz-Uriarte R. GeneSrF and varSelRF: a web-based tool and R package for gene selection and classification using random forest. *BMC Bioinform* (2007) 8:328–34. doi: 10.1186/1471-2105-8-328
45. Krijthe JH. Rtsne: T-Distributed Stochastic Neighbor Embedding using a Barnes-Hut Implementation. (2015).
46. Wilkerson MD, Hayes DN. ConsensusClusterPlus: a class discovery tool with confidence assessments and item tracking. *Bioinformatics* (2010) 26 (12):1572–3. doi: 10.1093/bioinformatics/btq170
47. Love MI, Huber W, Anders S. Moderated estimation of fold change and dispersion for RNA-seq data with DESeq2. *Genome Biol* (2014) 15(12):550–. doi: 10.1186/s13059-014-0550-8
48. Yu G, Wang L-G, Han Y, He Q-Y. clusterProfiler: an R package for comparing biological themes among gene clusters. *OMICS* (2012) 16(5):284–7. doi: 10.1089/omi.2011.0118
49. Charoentong P, Finotello F, Angelova M, Mayer C, Efremova M, Rieder D, et al. Pan-cancer Immunogenomic Analyses Reveal Genotype-Immunophenotype Relationships and Predictors of Response to Checkpoint Blockade. *Cell Rep* (2017) 18(1):248–62. doi: 10.1016/j.celrep.2016.12.019
50. Barbie DA, Tamayo P, Boehm JS, Kim SY, Moody SE, Dunn IF, et al. Systematic RNA interference reveals that oncogenic KRAS-driven cancers require TBK1. *Nature* (2009) 462(7269):108–12. doi: 10.1038/nature08460
51. Therneau TM, Grambsch PM. Modeling Survival Data: Extending the Cox Model. New York: Springer (2000).
52. Brenet F, Moh M, Funk P, Feierstein E, Viale AJ, Socci ND, et al. DNA Methylation of the First Exon Is Tightly Linked to Transcriptional Silencing. *PloS One* (2011) 6(1):e14524. doi: 10.1371/journal.pone.0014524
53. Ball MP, Li JB, Gao Y, Lee J-H, LeProust EM, Park I-H, et al. Targeted and genome-scale strategies reveal gene-body methylation signatures in human cells. *Nat Biotechnol* (2009) 27(4):361–8. doi: 10.1038/nbt.1533
54. Henrichsen CN, Chaignat E, Reymond A. Copy number variants, diseases and gene expression. *Hum Mol Genet* (2009) 18(R1):R1–8. doi: 10.1093/hmg/ddp011
55. Handsaker RE, Van Doren V, Berman JR, Genovese G, Kashin S, Boettger LM, et al. Large multiallelic copy number variations in humans. *Nat Genet* (2015) 47(3):296–303. doi: 10.1038/ng.3200
56. Jones PA. Functions of DNA methylation: islands, start sites, gene bodies and beyond. *Nat Rev Genet* (2012) 13(7):484–92. doi: 10.1038/nrg3230
57. Barghash A, Helms V, Kessler SM. Overexpression of IGF2 mRNA-Binding Protein 2 (IMP2/p62) as a Feature of Basal-like Breast Cancer Correlates with Short Survival. *Scand J Immunol* (2015) 82(2):142–3. doi: 10.1111/sji.12307
58. Li X, Li Y, Lu H. miR-1193 Suppresses Proliferation and Invasion of Human Breast Cancer Cells Through Directly Targeting IGF2BP2. *Oncol Res* (2017) 25(4):579–85. doi: 10.3727/97818823455816X14760504645779
59. Mancarella C, Scotlandi K. IGF2BP3 From Physiology to Cancer: Novel Discoveries, Unsolved Issues, and Future Perspectives. *Front Cell Dev Biol* (2019) 7:363:363. doi: 10.3389/fcell.2019.00363
60. Tanabe A, Tanikawa K, Tsunetomi M, Takai K, Ikeda H, Konno J, et al. RNA helicase YTHDC2 promotes cancer metastasis via the enhancement of the efficiency by which HIF-1α mRNA is translated. *Cancer Lett* (2016) 376 (1):34–42. doi: 10.1016/j.canlet.2016.02.022
61. Ma Z, Morris SW, Valentine V, Li M, Herbrick JA, Cui X, et al. Fusion of two novel genes, RBM15 and MKL1, in the t(1;22)(p13;q13) of acute megakaryoblastic leukemia. *Nat Genet* (2001) 28(3):220–1. doi: 10.1038/90054
62. Lee J-H, Skalnik DG. Rbm15-Mkl1 Interacts with the Setd1b Histone H3-Lys4 Methyltransferase via a SPOC Domain That Is Required for Cytokine-Independent Proliferation. *PloS One* (2012) 7(8):e42965. doi: 10.1371/journal.pone.0042965
63. Takeda A, Shimada A, Hamamoto K, Yoshino S, Nagai T, Fujii Y, et al. Detection of RBM15-MKL1 fusion was useful for diagnosis and monitoring of minimal residual disease in infant acute megakaryoblastic leukemia. *Acta Med Okayama* (2014) 68(2):119–23. doi: 10.18926/AMO/52408
64. Yersal O, Barutca S. Biological subtypes of breast cancer: Prognostic and therapeutic implications. *World J Clin Oncol* (2014) 5(3):412–24. doi: 10.5306/wjco.v5.i3.412
65. Ignatiadis M, Sotiriou C. Luminal breast cancer: from biology to treatment. *Nat Rev Clin Oncol* (2013) 10(9):494–506. doi: 10.1038/nrclinonc.2013.124
66. Haque R, Ahmed SA, Inzhakova G, Shi J, Avila C, Polikoff J, et al. Impact of breast cancer subtypes and treatment on survival: an analysis spanning two decades. *Cancer Epidemiol Biomarkers Prev* (2012) 21(10):1848–55. doi: 10.1158/1055-9965.EPI-12-0474
67. Szyf M. DNA methylation signatures for breast cancer classification and prognosis. *Genome Med* (2012) 4(3):26–. doi: 10.1186/gm325
68. Stanton SE, Disis ML. Clinical significance of tumor-infiltrating lymphocytes in breast cancer. *J Immunother Cancer* (2016) 4:59. doi: 10.1186/s40425-016-0165-6
69. Denkert C, von Minckwitz G, Darb-Esfahani S, Lederer B, Heppner BI, Weber KE, et al. Tumour-infiltrating lymphocytes and prognosis in different subtypes of breast cancer: a pooled analysis of 3771 patients treated with neoadjuvant therapy. *Lancet Oncol* (2018) 19(1):40–50. doi: 10.1016/S1470-2045(17)30904-X
70. Li H-B, Tong J, Zhu S, Batista PJ, Duffy EE, Zhao J, et al. m^{6}A mRNA methylation controls T cell homeostasis by targeting the IL-7/STAT5/SOCS pathways. *Nature* (2017) 548(7667):338–42. doi: 10.1038/nature23450
71. Tong J, Cao G, Zhang T, Sefik E, Amezcua Vesely MC, Broughton JP, et al. m^{6}A mRNA methylation sustains Treg suppressive functions. *Cell Res* (2018) 28(2):253–6. doi: 10.1038/cr.2018.7
72. Feng Z, Li Q, Meng R, Yi B, Xu Q. METTL3 regulates alternative splicing of MyD88 upon the lipopolysaccharide-induced inflammatory response in human dental pulp cells. *J Cell Mol Med* (2018) 22(5):2558–68. doi: 10.1111/jcmm.13491
73. Zheng Q, Hou J, Zhou Y, Li Z, Cao X. The RNA helicase DDX46 inhibits innate immunity by entrapping mA-demethylated antiviral transcripts in the nucleus. *Nat Immunol* (2017) 18(10):1094–103. doi: 10.1038/ni.3830
74. Shah A, Rashid F, Awan HM, Hu S, Wang X, Chen L, et al. The DEAD-Box RNA Helicase DDX3 Interacts with m^{6}A RNA Demethylase ALKBH5. *Stem Cells Int* (2017) 2017:8596135. doi: 10.1155/2017/8596135
75. Winkler R, Gillis E, Lasman L, Safra M, Geula S, Soyris C, et al. m^{6}A modification controls the innate immune response to infection by targeting type I interferons. *Nat Immunol* (2019) 20(2):173–82. doi: 10.1038/s41590-018-0275-z
76. Lichinchi G, Gao S, Saletore Y, Gonzalez GM, Bansal V, Wang Y, et al. Dynamics of the human and viral m^{6}A RNA methylomes during HIV-1 infection of T cells. *Nat Microbiol* (2016) 1:16011. doi: 10.1038/nmicrobiol.2016.11
77. Hesser CR, Karijolich J, Dominissini D, He C, Glaunsinger BA. N^6-methyladenosine modification and the YTHDF2 reader protein play cell type specific roles in lytic viral gene expression during Kaposi's sarcoma-associated herpesvirus infection. *PloS Pathog* (2018) 14(4):e1006995. doi: 10.1371/journal.ppat.1006995
78. Han D, Liu J, Chen C, Dong L, Liu Y, Chang R, et al. Anti-tumour immunity controlled through mRNA m^{6}A methylation and YTHDF1 in dendritic cells. *Nature* (2019) 566(7743):270–4. doi: 10.1038/s41586-019-0916-x
79. Zhang B, Wang J, Wang X, Zhu J, Liu Q, Shi Z, et al. Proteogenomic characterization of human colon and rectal cancer. *Nature* (2014) 513 (7518):382–7. doi: 10.1038/nature13438
80. Archer TC, Ehrenberger T, Mundt F, Gold MP, Krug K, Mah CK, et al. Proteomics, Post-translational Modifications, and Integrative Analyses Reveal Molecular Heterogeneity within Medulloblastoma Subgroups. *Cancer Cell* (2018) 34(3):396–410.e8. doi: 10.1016/j.ccell.2018.08.004
81. Rivero-Hinojosa S, Lau LS, Stampar M, Staal J, Zhang H, Gordish-Dressman H, et al. Proteomic analysis of Medulloblastoma reveals functional biology with translational potential. *Acta Neuropathol Commun* (2018) 6(1):48. doi: 10.1186/s40478-018-0548-7

Conflict of Interest: The authors declare that the research was conducted in the absence of any commercial or financial relationships that could be construed as a potential conflict of interest.

frontiers in Oncology

REVIEW
published: 01 February 2021
doi: 10.3389/fonc.2020.586789

Methyladenosine Modification in RNAs: Classification and Roles in Gastrointestinal Cancers

Qinghai Li[1,2], *Weiling He*[1,2*] *and Guohui Wan*[3*]

[1] Department of Gastrointestinal Surgery, the First Affiliated Hospital of Sun Yat-Sen University, Guangzhou, China, [2] Center for Precision Medicine, Sun Yat-Sen University, Guangzhou, China, [3] School of Pharmaceutical Sciences, Sun Yat-Sen University, Guangzhou, China

Cellular ribonucleic acids (RNAs), including messenger RNAs (mRNAs) and non-coding RNAs (ncRNAs), harbor more than 150 forms of chemical modifications, among which methylation modifications are dynamically regulated and play significant roles in RNA metabolism. Recently, dysregulation of RNA methylation modifications is found to be linked to various physiological bioprocesses and many human diseases. Gastric cancer (GC) and colorectal cancer (CRC) are two main gastrointestinal-related cancers (GIC) and the most leading causes of cancer-related death worldwide. In-depth understanding of molecular mechanisms on GIC can provide important insights in developing novel treatment strategies for GICs. In this review, we focus on the multitude of epigenetic changes of RNA methlyadenosine modifications in gene expression, and their roles in GIC tumorigenesis, progression, and drug resistance, and aim to provide the potential therapeutic regimens for GICs.

Keywords: RNA, methylation modification, m^{6}A, m^{6}Am, m^{1}A, gastrointestinal cancers

OPEN ACCESS

Edited by:
Shicheng Guo,
University of Wisconsin-Madison, United States

Reviewed by:
Huabing Li,
Shanghai Jiao Tong University School of Medicine, China
Ye Wang,
Peking University, China

***Correspondence:**
Guohui Wan
wanguoh@mail.sysu.edu.cn
Weiling He
hewling@mail.sysu.edu.cn

Specialty section:
This article was submitted to Cancer Genetics, a section of the journal Frontiers in Oncology

Received: *24 July 2020*
Accepted: *14 December 2020*
Published: *01 February 2021*

Citation:
Li Q, He W and Wan G (2021) Methyladenosine Modification in RNAs: Classification and Roles in Gastrointestinal Cancers. Front. Oncol. 10:586789. doi: 10.3389/fonc.2020.586789

INTRODUCTION

With the deepening of genetics research and the emergence of epigenetics, many reversible chemical modifications have been identified. In RNAs, human cells undergo various forms of modification with different levels (1–3). The constitutive non-coding RNAs (ncRNAs) are known to contain larger number of pseudouridine (Ψ) and 2'-O-methylations (2'-OMe or Nm) modifications (1). In addition, various modifications are identified in the regulatory ncRNAs including small ncRNAs (sncRNAs), long ncRNAs (lncRNAs), and circular RNAs (circRNAs) and play important roles in metabolism and functions (4–7). However, owing to the spatiotemporal specificity of regulatory ncRNAs in various tissues, the detailed and conserved biological characteristics of most RNA modifications are unclear. As for mRNAs, internal methylation modifications have been recently revealed with help of the advanced detection and analysis technologies as well as the common modification of N^7-methylguanosine (m^{7}G) cap in the 5' terminal region of mRNA (8–12). The most prevalent and crucial internal methylation form in mRNAs is N^6-methyladenosine (m^{6}A) modification that firstly identified in 1974 in eukaryotic cells (12–16), while the other major forms include N^6,2'-O-dimethyladenosine (m^{6}Am), N^1-methyladenosine (m^{1}A), 2'-OMe, and 5-methylcytosine (m^{5}C).

Gastric cancer (GC) and colorectal cancer (CRC) are the most common gastrointestinal-related cancers (GICs). CRC is the fourth most commonly diagnosed cancer (6.1%) and the second leading cause of cancer death (9.2%) worldwide, while GC is the sixth diagnosed caner and the third cause of cancer death (8.2%) (17). In-depth research on molecular mechanisms in GICs can provide important insights in developing novel treatment strategies for GICs.

Recently, RNA methylation has been found to play critical roles in various bioprocesses including embryonic development, RNAs metabolism, gene expression regulation, and its aberrant regulation has been linked to many human diseases including cancer (18). Herein, we mainly focus on the multitude of epigenetic changes of RNA methlyadenosine modifications in gene expression, and their roles in GIC tumorigenesis, progression, and drug resistance, and aim to provide the potential therapeutic regimens for GICs.

M^6A MODIFICATION

Biological Characteristics of m^6A Modification

Although m^6A is an "old" modification form that was firstly discovered in 1974 (13, 14), it had not gained enough attention until two breakthrough methods developed in 2011. The first breakthrough is the discovery of FTO (fat mass and obesity-associated protein), the first mammalian m^6A demethylase in 2011 (19) and AlkB homolog 5 (ALKBH5), another demethylase in mouse fertility and spermatogenesis in 2013 (20), which proves and highlights that the m^6A modification is a dynamic process and regulated by both methyltransferase and demethylase. The second breakthrough is that the transcriptome-wide distribution of m^6A modification has been well revealed at ~100–200-nucleotide resolution in 2012 owing to the development of methylated RNA immunoprecipitation sequencing (MeRIP-seq or m^6A-seq) technology (21, 22). Since then, other detection methods such as single-nucleotide resolution, antibody-independent, or isoform characterization analysis, have emerged as powerful tools for the m^6A analysis. These tools mainly include site-specific cleavage and radioactive labeling followed by ligation-assisted extraction and thin layer chromatography (SCARLET) (23), m^6A individual-nucleotide-resolution crosslinking and immunoprecipitation (miCLIP) (4), m^6A level and isoform characterization sequencing (m^6A-LAIC-seq) (24), deamination adjacent to RNA modification targets sequencing (DART-seq) (25), MAZTER-seq (26), m^6A-sensitive RNA-endoribonuclease-facilitated sequencing (m^6A-REF-seq) (27), m^6A-lable-seq (28), m^6A-SEAL (29), and the third-generation sequencing technologies (30). However, these methods have shortcomings such as inconvenient procedures (radioisotope p^{32}), high cost, unavailability to distinguish m^6A and m^6Am, and detection limits of a certain motif.

As reported, m^6A modification occurs in almost all transcripts with the ratio of m^6A/A in mRNAs ranges from 0.2 to 0.5% (15, 24, 31, 32). The distribution of m^6A modifications are not random but strictly restricted, where they are commonly confined in the consensus sequence RRACH that refers to [G/A/U][G>A]m^6AC[U>A>C] motif (7, 21, 33) and enriched in the long internal exons and regions next to the 3' untranslated region (3' UTR) within mRNAs (21, 22, 27). The deposition of m^6A is in the introns of the precursor mRNAs (pre-mRNAs) and in primary microRNAs (pri-miRNAs), which means that the m^6A modification can be regulated either before or simultaneously with RNAs splicing and processing (34) (**Table 1**, **Figure 1**).

Components of the m^6A Modification System

Writers

In 1994, Bokar and colleagues characterized a multicomponent complex of mRNA m^6A methyltransferases (MTases, "writers") that extracted from the nucleus, which is composed of three components with ~30 KDa, ~200 KDa, and ~875 kDa, respectively. The ~200 kDa component contains the S-adenosyl-L-methionine (SAM)-binding site on a 70 kDa subunit and the ~875kDa component may has affinity for mRNA strands (35, 36). Subsequently the SAM-binding ability of the 70 kDa subunit and was named as MT-A70 (now known as methyltransferase-like 3 (METTL3) (37). Hereafter,

TABLE 1 | The biological characteristics of methyladenosine modification in mRNA.

MT	Peaks/sites	Ratio	Distribution	Motif	Detection methods
m^6A	~10,000–20,000	~0.2–0.5% (m^6A/A)	Introns, long internal exons, near stop codon and 3' UTR	RRACH motif ([G/A/U][G>A] m^6AC[U>A>C])	MeRIP-seq, SCARLET, miCLIP, SELECT, m^6A-LAIC-seq, DART-seq, MAZTER-seq, m^6A-REF-seq, m^6A-lable-seq, m^6A-SEAL, and so on
m^6Am	~500–1,000	~0.01–0.02% (m^6Am/A)	Cap+1/2, 5'UTR	BCm^6Am motif (B represents C, G or U)	CITS miCLIP, refined RIP-seq, m^6A-SEAL
m^1A	~500–5,000 (but need more evidence)	~0.01–0.16% (m^1A/A)	5′ UTR, near start codons or TSS	GCA codon and GUUCRA tRNA-like motif (both not obviously)	m^1A-seq combined method, m^1A-ID-seq, m^1A-MAP

MT, modification types; m^6A, N^6-methyladenosine; m^6Am, N^6,2'-O-dimethyladenosine; m^1A, N^1-methyladenosine; A, adenosine; U, uridine; C, cytidine; G, Guanosine; 5'UTR, 5' untranslated region; 3'UTR, 3' untranslated region; TSS, transcription start site; MeRIP-seq, m^6A RNA immunoprecipitation followed by high-throughput sequencing; SCARLET, site-specific cleavage and radioactive labeling followed by ligation-assisted extraction and thin layer chromatography; miCLIP, m^6A individual-nucleotide-resolution crosslinking and immunoprecipitation; SELECT, single-base elongation and ligation-based qPCR amplification method; m6A-LAIC-seq, m^6A level and isoform characterization sequencing; DART-seq, deamination adjacent to RNA modification targets sequencing; m^6A-REF-seq, m^6A-sensitive RNA-endoribonuclease-facilitated sequencing; CITS miCLIP, the crosslinking-induced truncation sites-based miCLIP.

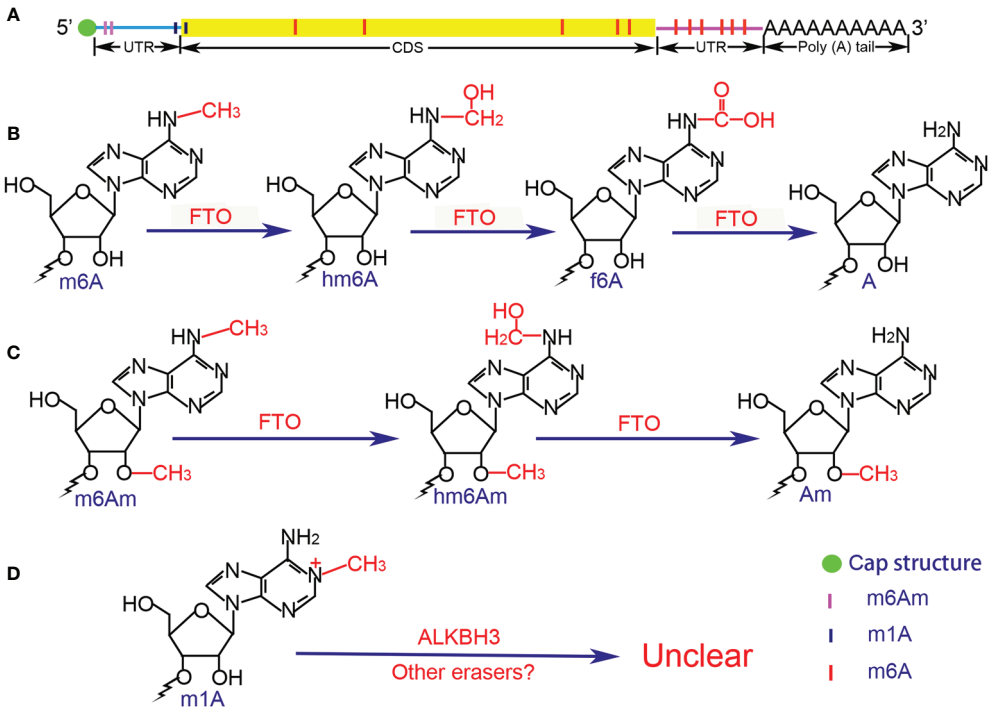

FIGURE 1 | Distribution and chemical structure of methylation modifications. **(A)** m^6Am and m^1A are mainly enriched in the 5'UTR, whereas m^6A is concentrated in the 3'UTR. **(B)** Demethylation of m^6A is in a stepwise manner, the intermediate of hm^6A is the direct oxidation product of m^6A, while f^6A is the further oxidized product of hm^6A, and the final product is A. **(C)** The demethylation process of m^6Am is similar to that of m^6A, but the potential intermediate f^6Am has not been reported. **(D)** The demethylation process of m^1A remains unclear due to the special chemical bond. UTR, untranslated region; CDS, coding sequence; FTO, fat mass and obesity-associated protein; ALKBH3, AlkB homolog 3; A, adenosine; Am, 2'-O-methyladenosine; m^6A, N^6-methyladenosine; hm^6A, N^6-hydroxymethyladenosine; f^6A, N^6-formyladenosine; m^6Am, 2'-O-dimethyladenosine; hm6Am, N^6-hydroxymethyl, 2'-O-methyladenosine; m^1A, N^1-methyladenosine.

methyltransferase-like 14 (METTL14) has been identified as the homologue of METTL3 and functions as another core component of the complex (38–41). Both METTL3 and METTL14 are highly conserved within the (D/E)PP(W/L) active site and the SAM–binding motif in mammals with ~35 and ~43% sequence homology of the MTase domain in mouse and human respectively (39, 40, 42). Despite METTL3 and METTL14 exhibit relatively weak MTase activity when acting alone, the METTL3-METTL14 complex with a stoichiometric ratio of 1:1 shows a much higher catalytic activity. The primary functions of METTL3 in the complex is to catalyze methyl-group transfer, whereas METTL14 is the aide that helps MTase complex positioning by identifying the histone H3 trimethylation at Lys36 (H3K36me3) (in co-transcriptional manner), and offers a structural scaffold that enhancing the catalytic activity of METTL3, even though METTL14 can affect the m^6A levels more significantly than METTL3 (40, 41, 43–46).

In addition, the Wilms tumor 1-associated protein (WTAP) that previously found to interact with the Wilms' tumor suppressor-1 (WT1) and participates alternative pre-mRNA splicing was identified as an additional component of the m^6A MTases complex (39, 47–49). Without the MTase domain, WTAP assists METTL3/14 to localize in the nuclear speckles where enriched with pre-mRNA processing factors and synergize to methylate the adenosines in mRNAs (39, 41).

Recent studies have identified other associated proteins in MTase complex. Schwartz et al. (50) found that KIAA1429 (VIRMA) is required for the m^6A methylation in human cells, and Yue et al. further demonstrated that KIAA1429 can play a role as region-selective factors by recruiting the catalytic core components METTL3/METTL14/WTAP to 3'UTR and near the stop codon (51). They also highlighted the importance of Cbl proto oncogene like 1 (HAKAI or CBLL1) and zinc finger CCCH-type containing 13 (ZC3H13) in the full methylation program, and ZC3H13 is required for the nuclear localization of MTase complex (51, 52). The RNA-binding motif protein 15 (RBM15) and its paralogue RBM15B are also identified as the regulators of m^6A modification in the lncRNA X-inactive specific transcript (XIST), as well as in mRNAs (53). In addition, the transcription factors zinc finger protein 217 (ZFP217), SMAD2/3, and CAAT-box binding protein (CEBPZ) are found to mediate the m^6A deposition in mRNAs (54–56). Some other m^6A methyltransferases such as METTL5, METTL16, and zinc finger CCHC-type-containing 4 (ZCCHC4) are also indispensable for m^6A formation, especially in ncRNAs and rRNAs (57–59).

Erasers

FTO was recognized as the first m6A eraser (19), which was originally discovered in 1999 and was officially named in 2007 (60, 61). Bioinformatics analysis revealed that FTO is one of the non-heme Fe^{II}/α-ketoglutarate(α-KG)-dependent dioxygenases (also known as non-heme Fe^{II}/2-oxoglutarate (2-OG)-dependent dioxygenases) (62). FTO was shown to mediate the demethylation of N^3-methylthymidine in single-stranded DNA and N^3-methyluridine in single-stranded RNA *in vitro* (63, 64). In 2011, Jia et al. (19) proved that FTO could participate in the demethylation process of nuclear RNAs in nuclear speckles, and Fu et al. (65) further revealed the role of FTO in the detailed process of RNA m^6A demethylation in 2013. They found that FTO oxidizes m^6A in a stepwise manner, and the intermediate of N^6-hydroxymethyladenosine (hm^6A) is the direct oxidation product of m^6A and turns into the form of N^6-formyladenosine (f^6A). The final products of m^6A demethylation are unmethylated adenosine and formaldehyde (from hm^6A) or formic acid (from f^6A). Interestingly, the half-lives of hm^6A and f^6A are suggested to be ~3 h under physiological conditions, meaning that the decomposing of hm^6A and f^6A do not occur simultaneously with the oxidation of m^6A.

As for ALKBH5, the second m^6A demethylase identified so far in mammals, belongs to the AlkB family, a class of the non-heme Fe^{II}/α-ketoglutarate (α-KG)-dependent dioxygenases superfamily which was originally shown to revert DNA base damage by catalyzed oxidative demethylation of N-alkylated nucleic acid bases (20, 66–68). Structure analysis indicates that ALKBH5 has comparable catalytic activity with FTO, whereas AlkB has low level (~17%) of the amino acid sequence identity to FTO (62, 69). While FTO can demethylate on both single-stranded RNA/DNA and double-stranded RNA/DNA (albeit low) (19, 70), ALKBH5 only demethylate the single-stranded RNA/DNA with the sequence preference (the activity in the consensus sequence is twice that in other sequences), which may be due to the fact that ALKBH5 mainly localizes in nuclear speckles and acts in regulating the nuclear export and metabolism of RNAs (20).

Readers

There are four main readers selectively bind the m^6A-containing mRNAs in the nucleus. In 1998 Imai et al. (71) isolated a novel RNA splicing-related protein YT521 by using yeast two-hybrid screens system with rat transformer-2-beta1 (RA301) as bait, and Hartmann et al. identified a homologous protein YT521-B by using htra2-beta1 as bait (72). Subsequently, the YT521-B homology (YTH) domain was defined as a new protein family, the YTH (YT521-B homology) domain containing protein family, and now YT521-B is known as the YTH domain-containing protein 1 (YTHDC1) (73). YTHDC1 localizes in a subnuclear structure named YT bodies that contain transcriptionally active sites and are close to other subnuclear compartments such as speckles and coiled bodies (74). Structure analysis demonstrated that the GG(m^6A)C sequence is the preferred binding site for YTH domain in YTHDC1 (75, 76). Since its localization is adjacent to the nuclear speckles, YTHDC1 is found to participate in pre-mRNAs splicing containing m^6A sites, and mediate its nuclear export. YTHDC1 facilitates the splicing pattern of exon inclusion in targeted mRNAs by recruiting pre-mRNA splicing factor SRSF3 (SRp20) and inhibiting SRSF10 (SRp38), by which it changes alternative splicing patterns *via* modulating splice sites selection in a concentration-dependent manner (72, 77). In addition, YTHDC1 is found to interact with the nuclear RNA export factor 1 (NXF1) to promote the nuclear export of the m^6A-containing mRNAs (78).

The other three readers in the nucleus belong to the heterogeneous nuclear ribonucleoprotein (hnRNP) family that is composed of more than 20 members. HnRNP protein contains at least one RNA-binding domain with RNA recognition motif (RRM), K-Homology (KH) domain, or an arginine/glycine-rich box (79). Recently, their role as the "reader" of m^6A remains controversial. Previously, Alarcon et al. showed that hnRNPA2/B1 can directly bind with m^6A by matching the m^6A consensus motif and regulate the alternative splicing of its mRNA targets (80), whereas Wu et al. (81) suggested that hnRNPA2/B1 may interact with m^6A *via* the "m^6A switch" mechanism instead of directly recognizing the m^6A-containing bases, by which the m^6A controls the RNA-structure-dependent accessibility of the RNA-binding domains to affect the RNA-protein interactions for biological regulation. In addition, heterogeneous nuclear ribonucleoprotein C (hnRNPC), an abundant nuclear RNA-binding protein, and heterogeneous nuclear ribonucleoprotein G (hnRNPG), a low-complexity protein, interact with the m^6A-containing mRNAs *via* the similar "m^6A switch" mechanism (6, 82, 83).

Besides readers in the nucleus, four members of the YTH domain-containing proteins are identified in the cytoplasm that are involved in mRNAs metabolism *via* interacting the m^6A with their hydrophobic pocket, an aromatic cage formed by tryptophan residues, within the YTH domain (76, 84, 85). YTHDF1, YTHDF2, and YTHDF3 are highly homologous, and all contain a ~40 kDa low-complexity domain and a prion-like domain (86). The most abundant YTHDF paralog, YTHDF2, is the first member to be fully studied, where it was originally implicated in regulating the instability and the decay of the m^6A-containing mRNAs by localizing the complex of YTHDF2-m^6A-mRNA from the translatable pool to the processing bodies (P-bodies) (87). However, another group demonstrated that the P-bodies only act an indirect role in the decay of m^6A-containing RNAs since no direct interaction between YTHDF2 and GW182, the core component of the P-bodies was found (88). Subsequent study revealed that YTHDF2-m^6A-mRNA complex was located in the stress granules or neuronal RNA granules through the phase separation mechanism upon stress stimulation and was subject to compartment-specific regulations (89).

Although all YTHDF proteins can recruit CCR4-NOT and promote mRNA deadenylation (88), YTHDF1 is the only member which is reported to facilitate translation by binding at the RRACH motifs instead of the flanking sequence that cluster around the stop codon and subsequently recruiting translation initiation factor (eIF) and ribosome. The association of YTHDF1 with translational initiation machinery

may be depend on the loop structure mediated by eIF4G and the interaction of YTHDF1 with eIF3 (90). Besides, YTHDF1 is found to bind to the nascent methylated mRNAs earlier than YTHDF2, which suggests that the translation of mRNAs occurs before their decay under various physiological conditions (90). As for YTHDF3, it plays dual functions in m^{6}A-containing mRNAs metabolism by either promoting the translation of the targeted mRNAs *via* interaction with YTHDF1 (91), or accelerating the decay of the targeted mRNAs *via* interaction with YTHDF2 (92). Controversially, Jaffrey et al. (93) proposed another brand new but opposite model for the role of YTHDF proteins in regulating m^{6}A-containing mRNAs. They demonstrated that YTHDF proteins binded with the same mRNA rather than different mRNAs and act redundantly to co-mediate mRNA degradation, and the stability of mRNA fails to restore until all YTHDF1,2,3 are depleted simultaneously (**Figure 2**).

The fifth member of the YTH protein family is YTHDC2, which is different from the other cytoplasmic "readers". YTHDC2 has a large molecular mass of ~160 kDa and contains the helicase domain (94). YTHDC2 is previously reported to enhance the translation efficiency of its targets and decrease their mRNA abundance by binding to the m^{6}A site at its consensus motif and influencing the mRNA secondary structures (94, 95). However, a latest report indicated that YTHDC2 could also reduce the m^{6}A-containing mRNAs stability and inhibit gene expression in certain situations (96).

The insulin-like growth factor 2 mRNA-binding proteins (IGF2BPs, originally called IMPs) family, including IGF2BP1/2/3, which is initially recognized as an IGF2 translation inhibitor (97), belongs to a new family of m^{6}A readers that mainly prevent the m^{6}A-containing mRNAs from degradation in cytoplasm (98). IGF2BPs are composed of two RRM domains and four KH domains, and preferentially bind the m^{6}A-modified mRNAs through recognizing the consensus GG(m^{6}A)C sequence and facilitate the stability and translation of thousands of its mRNA targets by co-localizing in the P-bodies or stress granules, thus upregulating the gene expression in globally (98). Recently, ELAV like RNA binding protein 1 (ELAVL1, also known as HuR), matrin 3 (MATR3), and poly (A) binding protein cytoplasmic 1 (PABPC1) have been identified as the cofactors of IGF2BPs that promote the stability of m^{6}A-containing mRNAs simultaneously.

In addition, fragile X mental retardation protein (FMRP) and proline rich coiled-coil 2 A (PRRC2A) are reported to play a role as the reader/stabilizer of the m^{6}A-containing mRNAs (99, 100). METTL3 is found to associate with ribosomes and promote translation in some cancers when it localizes in the cytoplasm

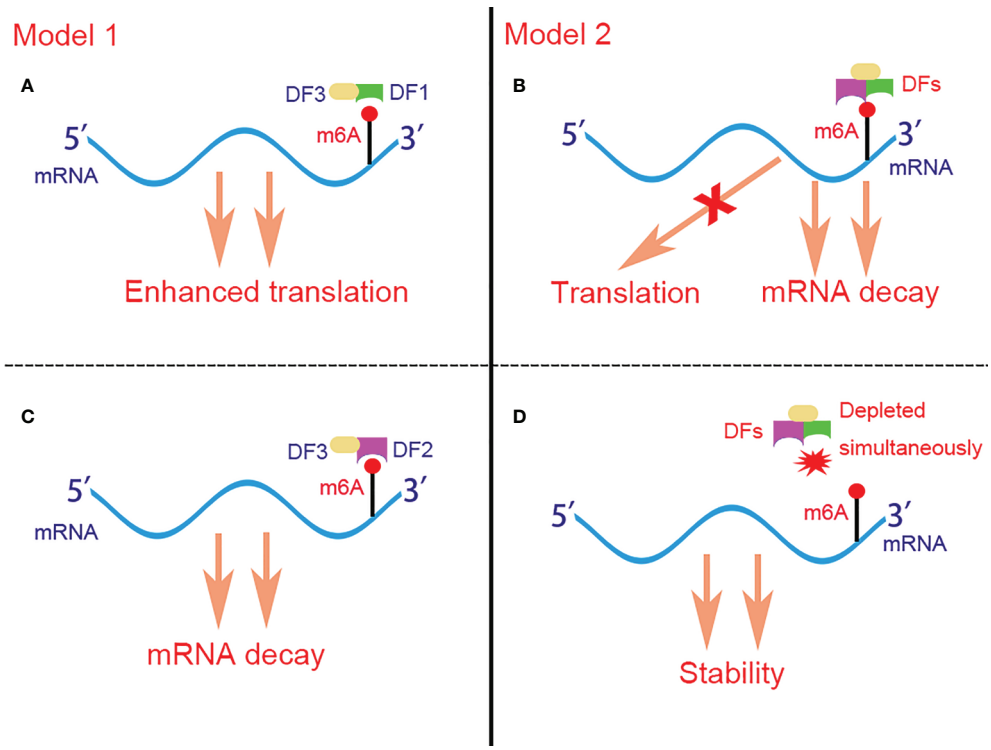

FIGURE 2 | Two controversial models for the function of DFs in regulating m^{6}A-containing mRNAs. In model 1 **(A, C)**, DF1 and DF2 bind to different mRNAs and promote their translation and degradation respectively. In model 2 **(B, D)**, DFs bind to the same mRNA rather than different mRNAs simultaneously and act redundantly to co-mediate mRNA degradation but not translation. The stability of mRNA can be restored only when DF1-3 are depleted simultaneously. DFs, YTHDF proteins; DF1, YTHDF1; DF2, YTHDF2; DF3, YTHDF3; m^{6}A, N^6-methyladenosine.

TABLE 2 | The main components of methyladenosine modification systems*.

MT	Writers	Erasers	Readers and its functions		
m^6A	METTL3/14, WTAP, KIAA1429 (VIRMA), RBM15/15B, ZC3H13, CBLL1, ZFP217, SMAD2/3, CEBPZ, METTL5, METTL16, ZCCHC4	FTO, ALKBH5	In nucleus	YTHDC1	Mediating splicing and nuclear export
				hnRNPA2/B1, hnRNPC and hnRNPG	Mediating splicing
			In cytoplasm	YTHDC2	Diversify
				YTHDF1 and METTL3	Facilitating translation
				YTHDF2	Facilitating decay
				YTHDF3	Work with YTHDF1 or YTHDF2
				IGF2BP1/2/3, FMRP, PRRC2A	Facilitating stability
m^6Am	PCIF1 (CAPAM), METTL4	FTO	There is no m^6Am reader that has been identified; and the functions of it still controversial (facilitating or preventing decay and translation)?		
m^1A	TRMT10C, TRMT6/61A, TRMT61B, BMT2, NML	FTO, ALKBH1, ALKBH3	YTHDF1	Facilitating translation	
			YTHDF2/3	Promoting decay	
			YTHDC1	Unclear	

*MT, modification types; writers, methyltransferases; erasers, demethylases; readers, the proteins that bind to methylation modifications; m^6A, N^6-methyladenosine; m^6Am, N^6,2'-O-dimethyladenosine; m^1A, N^1-methyladenosine; METTL3/5/14/16, methyltransferase-like3/5/14/15; WTAP, Wilms tumor 1-associated protein; RBM15/15B, RNA-binding motif protein 15/15B; ZC3H13, zinc finger CCCH-type containing 13; CBLL1, Cbl photo oncogene like 1; ZFP217, zinc finger protein 217; CEBPZ, CAATT-box binding protein; ZCCHC4, CCHC-type-containing 4; FTO, fat mass and obesity-associated protein; ALKBH1/3/5, AlkB homolog 1/3/5; YTHDC1/2, YT521-B homology (YTH) domain-containing protein 1/2; hnRNPA2/B1, heterogeneous nuclear ribonucleoprotein A2/B1; hnRNPC, heterogeneous nuclear ribonucleoprotein C; hnRNPG, heterogeneous nuclear ribonucleoprotein G; FMRP, fragile X mental retardation protein; PRRC2A, proline rich coiled-coil 2 A; PCIF1, phosphorylated CTD-interacting factor 1; TRMT10C/6/61A/61B, tRNA methyltransferase 10C/6/61A/61B; BMT2, base methyltransferase of 25S RNA; NML, nucleomethylin. *Has been identified at present.*

(101, 102). Moreover, accumulated readers of the m^6A in ncRNAs is summarized in **Table 2**.

THE M^6Am MODIFICATION

Biological Characteristics of m^6Am Modification

The m^6Am is the second most prevalent modification in cellular mRNAs and in some small nuclear RNAs (snRNAs). The structure of mRNAs after the m^7G cap can be divided into three main types, the $m^7G5'ppp5'NmpNp$ (p denotes phosphate group, Nm and N denote 2'-O-methylated nucleotide and nucleotide respectively), the $m^7G5'ppp5'NpNp$ and the $m^7G5'ppp5'NmpNmpNp$ (15, 103, 104). Recently, the 2'-O-methyladenosine (Am) was showed to be the first nucleotide adjacent to the m^7G cap and it can be further modified at the N^6 position by methylation to generate m^6Am (92% chance of being modified), where the structure of $m^7G5'ppp5'm^6AmpNp$ comprises 20–30% of all the structures (105, 106) (**Figure 1**). The second nucleotide can harbor a similar modification but with a lower frequency, whereas m^6Am rarely located in the third nucleotide and m^6A or A has not been found at the first nucleotide position (107). In addition, there are ~6% of the m^6Am occurs outside the 5'UTR, and motif analysis reveals that the m^6Am mainly deposit in a novel motif BCm^6Am (B represents C, G, or U) that enriched in the transcription start site (TSS), rather than the canonical m^6A motif RRACH (4, 108, 109). Molinie et al. used liquid chromatography-mass spectrometry (LC-MS) to quantify of the m^6Am in mRNAs and found that mRNAs contain ~3 m^6Am nucleotides per 10^5 nucleotides, revealing a 33-fold level of the m^6A modification than the m^6Am in mRNAs (24). Consistently, Liu et al. (108) confirmed the m^6Am/A ratio of total RNAs and mRNAs ranges from 0.0036 to 0.0169% and from ~0.01 to 0.02% respectively. Currently, the m^6Am transcriptome-wide expression can only be detected by the methods of the crosslinking-induced truncation sites-based miCLIP (CITS miCLIP) and the refined RIP-seq, and an antibody-free enzyme-assisted chemical approach termed m^6A-SEAL (29) (**Table 1**).

Components of m^6Am Modification System

Writer

The formation of m^6Am occurs on the basis of Am that formed by the MTases HENMT1 and FTSJ3 (110, 111), and its modification system rarely known yet. The m^6Am MTase was previously purified with a molecular weight of ~65 KD in 1978, and phosphorylated CTD-interacting factor 1 (PCIF1) was recognized as the first m^6Am MTase in 2019. It was named by its ability to directly bind to the phosphorylated carboxyl-terminal domain (CTD) of RNA polymerase II (RNAP II) by its WW domain, also called cap-specific adenosine methyltransferase (CAPAM) (106, 112, 113). Unlike the m^6A core readers that work in the form of a methyltransferase complex, PCIF1 is a "stand-alone" RNA MTase and functions in an m^7G cap-dependent manner. Recently, METTL4 was reported to catalyze m^6Am methylation in the U2 snRNA (114).

Eraser

FTO, the first m^6A demethylase, was found to mediate the demethylation of m^6Am in the similar manner to that of m^6A (115, 116). The intermediate of N^6-hydroxymethyl, 2'-O-methyladenosine (hm^6Am) was detected as well as the end product Am. Intriguingly, although both m^6A and m^6Am can be catalyzed by FTO, the priority between them is still controversial. Zhang et al. (116) showed that FTO displays the similar demethylation activity toward internal m^6A and cap m^6Am modifications *in vivo* and *in vitro*. But He et al. revealed that FTO shows different affinity to the m^6A and the

m^6Am among cells where the m^6A is most affected despite it prefers the m^6Am *in vitro* by the cellular cap-binding proteins (117). Controversially, Mauer et al. (115) found that FTO does not efficiently demethylate m^6A but preferentially demethylates m^6Am. They further showed that ALKBH5 did not affect the m^6Am in mRNAs and stated that FTO may targets the m^6Am whereas ALKBH5 targets the m^6A *in vivo*.

Functions of the m^6Am

Currently, there is no m^6Am reader that has been identified, and its function remains controversial. The first work showed that the m^6Am stabilizes mRNA by preventing the mRNA-decapping enzyme DCP2-mediated decapping and microRNA-mediated mRNA degradation (115), and it was confirmed by Mauer's work (109). However, Sendinc et al. (118) revealed that m^6Am fails to alter mRNA transcription and stability, and negatively impacts cap-dependent translation. Akichika et al. (106) further showed that the m^6Am facilitates the translation of capped mRNAs. The direct readers of the m^6Am are under investigated (**Table 2**).

THE M^1A MODIFICATION

Biological Characteristics of the m^1A Modification

The m^1A modification was firstly discovered in the total mixed RNA samples in 1961 (119) and was found that it can rearrange into the m^6A under alkaline conditions (Dimroth rearrangement) in 1968 (120). Subsequently, accumulating evidence has shown that the m^1A occurs in rRNAs and tRNAs where the m^1A is typically found at position 9 and 58 in the tRNA TΨC-loop and plays key roles in the structure formation and function execution *via* its methyl adduct and positive charge (121, 122). By using of the liquid chromatography-tandem mass spectrometry (LC-MS/MS), the ratio of m^1A/A in the mammalian cell lines and tissues can be easily detected, which ranging from approximately 0.015 to 0.054% and up to 0.16% (123, 124). Hereafter, He et al. (123) used the combined method of an antibody-based approach called m^1A-seq and an orthogonal chemical method based on Dimroth rearrangement to obtain a more detailed distribution of m^1A. They found that the distribution pattern and the peaks of the m^1A are highly conserved in the samples from multiple sources, and the m^1A enrich in the 5′ UTR, near the start codons or TSS, which is similar to that of m^6Am. Yi et al. further supported the finding by original technology m^1A-ID-seq (124). In addition, single-nucleotide resolution analysis (m^1A-MAP) showed that the m^1A lacks of obvious preference to certain motif, but the GCA codon and GUUCRA tRNA-like motif are frequently modified, and no m^1A is detected in the AUG start codon (123, 125). Finally, Safra et al. reported 15 m^1A sites in mRNAs and lncRNAs (126) (**Table 1**) (**Figure 1**).

Components of m^1A Modification System

Writers

Although a variety of the m^1A MTases, including tRNA methyltransferase 10C (TRMT10C), TRMT6/61A, TRMT61B, base MTase of 25S RNA (BMT2), MTR1, and nucleomethylin (NML), have been discovered, most of them catalyze the sites on tRNAs or rRNAs (122, 127–130). Li et al. unveiled that TRMT6/61A is able to methylate the m^1A sites that are confined in GUUCRA tRNA-like motifs in mRNAs, and some of the mitochondrial (mt)-mRNAs are the target of TRMT61B (125). In addition, Safra et al. (126) have identified that a single m^1A site in the mt-ND5 mRNA which is catalyzed by TRMT10C. Nonetheless, there is no direct specific m^1A writer has been identified for mRNA yet.

Erasers

The m^1A demethylases are found to only catalyze tRNAs so far. He et al. (131) showed that the human homolog of *E. coli* AlkB ALKBH1 is an important eraser that catalyzes the demethylation of the m^1A in tRNAs in 2016, and FTO, was proven to mediate the m^1A demethylation in tRNAs (117). However, neither ALKBH1 nor FTO mediates the removal of the methyl group from m^1A in mRNAs. Recently, another demethylase ALKBH3 was shown to have a strong preference for single stranded DNA/RNA and the ability of repairing methylation damage to RNA *in vitro* in both tRNAs and mRNAs (123, 124, 132, 133). Yi et al. (124) further showed that ALKBH3 has minimal sequence preference and acts globally in the transcriptome.

Functions of m^1A

The process of eukaryotic protein translation, especially the initiation step of translation, is strictly regulated in cells. Structure analysis showed that the secondary structure in the 5'UTR which is the target of the initiation factors such as eIF4A/B/H complex can affect the efficiency of the initiation of translation and the early elongation by impeding the binding and movement of the 40S ribosome (134, 135). He et al. (123) suggested that the m^1A plays a positive role for the translation initiation in mammalian mRNAs, which is further supported by Li et al. (125). Mechanically, the m^1A may inhibit Watson-Crick base pairing or introduce charge-charge interactions, leading to the alteration of the secondary/tertiary structure of 5'UTR in mRNAs. Potential readers specifically bound to the m^1A in mRNAs are supposed to promote the initiation of translation, which is analogous to the role of YTHDF1 in translation enhancement. However, there are controversial reports showed that the m^1A can repress the translation of mRNAs, especially mt-mRNAs while the underlying mechanism remains to be explored (126). In addition, the m^1A is found to promote mRNA degradation by interacting with its potential readers YTHDF2/3 (136, 137) (**Table 2**).

LINKS WITH GASTROINTESTINAL CANCERS AND POTENTIAL THERAPEUTIC STRATEGIES

Under normal physiological condition, methylation modification is precisely modulated by the methyltransferases and demethylases, and involved in regulating alternative splicing, nuclear export,

stability, translation, or degradation of the methylated RNAs, thereby affecting cell self-renew, cell proliferation, and cell differentiation. Recently, accumulating studies have revealed that abnormality in RNA methylation leaded by mutations or dysregulation that cause the gain or the loss of methylation sites are closely related to the initiation, progression metastasis, and suppression of various tumors including GICs (138).

Aberrant Writers in Gastrointestinal-Related Cancers

The writer, METTL3, is found to be upregulated in GC patients with poor prognosis, which is caused by the P300-mediated H3K27 acetylation activation in the promoter of METTL3 and mediation by the transcription factor GFI1 (139–143). Yue et al. (139) have identified the zinc finger MYM-type containing 1 (ZMYM1) mRNA as the direct target of METTL3. Mechanistically, the reader ELAVL1 binds to the m^{6}A sites within ZMYM1 mRNA and enhances the stability of ZMYM1. The induced ZMYM1 further inhibits the expression of E-cadherin by forming a complex of CtBP/LSD1/CoREST/ZMYM1 in the promoter region of E-cadherin, thus stimulating the epithelial-mesenchymal transition (EMT) and promoting metastasis of GC. In another report, the m^{6}A modification of hepatoma derived growth factor (HDGF) mRNA can be induced by high level of METTL3, and recognized by the reader IGF2BP3 to promote its stability. The upregulated HDGF could further facilitate tumor angiogenesis and increase glycolysis in GC, which in turn enhance the tumor growth and liver metastasis (140). Additionally, the mRNAs of pre-protein translocation factor (SEC62), ARHGAP5, and MCM5 and MCM6 (the component molecules in the MYC pathway) are highly modified by the aberrant METTL3, and led to the acceleration of GC progression (141, 143, 144).

Upregulated METTL3 in CRC primary or metastatic tissues is highly associated with unfavorable outcomes (145–150). One potential mechanism mediated by upregulated METTL3 is ceramide glycosylation that generates glycosphingolipids (particularly globotriaosylceramide) and activates cSrc and β-catenin signaling (151). Li et al. (145) unveiled that higher METTL3 expression in CRC facilitates the methylation of SRY (sex determining region Y)-box 2 (SOX2) mRNA, and the reader IGF2BP2 further recognized the m^{6}A-containing SOX2 mRNA and induced the expression level of SOX2 protein. SOX2 was previously reported to control the properties of the stem cells and enhance cell proliferation and invasion in squamous cell carcinoma (152). While in CRC, highly expressed SOX2 regulated its downstream targets, including *cyclin D1* (*CCND1*), *MYC (*mainly referred to as *c-Myc)*, and *POU class 5 homeobox 1* (*POU5F1*), and promoted their expression levels, thus upregulating CD133, CD44, and epithelial cell adhesion molecule (EpCAM). Shen et al. (148) found that METTL3 can directly interacts with the 5'/3'UTR regions of Hexokinase 2 (HK2) mRNA and the 3'UTR region of Glucose transporter type 1 (GLUT1, also SLC2A1) mRNA, and subsequently stabilized their mRNAs and activated the glycolysis pathway in CRC cells in a IGF2BP2- or IGF2BP2/3-dependent manner. In addition, upregulated METTL3 could facilitate CRC cell proliferation, progression, and metastasis by various signaling pathways including miR-1246/SPRED2/MAPK signaling pathway, p38/ERK pathway, and cyclin E1 (CCNE1) cell proliferation pathway (147, 149, 150).

Analogously, the high level of other writers WTAP and RBM15 also predicts poor prognosis for GC (153–155) Li et al. found that WTAP could be served as an independent predictor of GC and its high expression is closely related to the low T lymphocyte infiltration and T cell-related immune response (154).

Intriguingly, the writer METTL14 is reported to be downregulated in GC and CRC patients (139, 156). Zhang et al. (156) unveiled that METTL14 suppression may cause activation of the Wnt and PI3K-Akt signaling and thus promote GC progression. While Yang et al. (157) have revealed that the downregulated METTL14 is associated with the poor outcomes of CRC patients through up-regulating oncogenic lncRNA XIST. Specifically, the m^{6}A level within lncRNA XIST is reduced as METTL14 suppression, which could lead to the RNA degradation and decay mediated by the m^{6}A reader YTHDF2. The abundant lncRNA XIST due to downregulation of METTL14 acts as a carcinogen and promote cell proliferation and metastasis in CRC (158). Additionally, the downregulated METTL14 affects the m^{6}A level in pri-miR-375, by which it decreased the binding of DGCR8 to pri-miR-375 and results in the reduction of mature miR-375. The reduction of miR-375 causes induced level of Yes-associated protein 1 (YAP1) and SP1, and ultimately leads to cell growth in CRC *via* miR-375/YAP1 pathway and cell invasion *via* miR-375/SP1 pathway (159).

Aberrant Erasers in Gastrointestinal-Related Cancers

FTO, the first mammalian m^{6}A demethylase and the only m^{6}Am demethylase currently discovered, is found to mediate the progression in GICs. FTO was reported to serve as an independent prognostic marker due to its frequently higher expression in high-risk scores subtype of GC (153, 155, 160). Other erasers ALKBH3 and ALKBH5 are also upregulated in GC, and ALKBH5 is found to promote the invasion and metastasis of GC by interacting with the lncRNA NEAT1 (nuclear paraspeckle assembly transcript 1) (155, 161, 162).

However, the expression levels of ALKBH5 and FTO in CRC are still controversial (146). From The Cancer Genome Atlas (TCGA), the Gene Expression Omnibus (GEO) database, and the Human Protein Atlas, ALKBH5 shows weak expression in CRC tissues compared to the normal tissues, and FTO shows no significant difference between CRC tissues and normal tissues. Whereas Wu et al. revealed a potential CRC-promoting mechanism *via* the ALKBH5/m^{6}A/RP11/hnRNPA2B1/E-ligases/Zeb1 axis (163). They found that lncRNA RP11 in CRC is highly expressed and associated with the CRC stage in patients, by which lncRNA RP11 is regulated in an m^{6}A-dependent manner and negatively correlated with ALKBH5 although METTL3 is elevated in CRC patients. Mechanistically, m^{6}A-containing RP11 can interact with the reader hnRNPA2B1 and

bind to its downstream targets, two E3-ligase mRNAs Siah1 and Fbxo45 to accelerate their decay. The reduced Siah1 and Fbxo45 further downregulates the EMT-transcription factors Zeb1, and ultimately leads to the development of CRC. In addition, Relier et al. (164) showed that low expression of FTO in CRC cells causes increase of the m^6Am levels in mRNAs and results in the enhanced malignancy and chemo resistance in CRC cells, which can be partially reversed by inhibition of PCIF1.

Aberrant Readers in Gastrointestinal-Related Cancers

Emerging studies have reported the upstream regulatory mechanisms that lead to generation of the aberrant readers in CRC. Wang et al. (165) have identified a novel lncRNA LINRIS to stabilize IGF2BP2 *via* LINRIS/IGF2BP2/MYC axis and promote cell proliferation in CRC. Mechanistically, the elevated level of LINRIS in the CRC patients with unfavorable prognostic could act on IGF2BP2 and protect it from K139 ubiquitination and autophagy degradation, and maintain its stability. The upregulated IGF2BP2 subsequently promotes the expression of its downstream target MYC mRNA, and enhances the MYC-mediated glycolysis in CRC, which eventually leads to progression of CRC. Inhibition of this axis by GATA3 may provide a potential therapeutic strategy for CRC.

Recently, Ni et al. showed another lncRNA involved in the YAP signaling pathway during CRC progression *via* the GAS5/YAP/YTHDF3 axis (166). They found GAS5 is downregulated in most of CRC tissues and is negatively correlated with the protein levels of YAP and YTHDF3, while the increased YTHDF3 is a significant prognostic factor for poor overall survival in CRC patients (146). Mechanistically, downregulation of GAS5 inhibits phosphorylation of YAP and attenuates its ubiquitination and degradation. The increased YAP further promotes expression level of YTHDF3, however, the downstream regulatory pathway of YTHDF3 that facilitates CRC progression is unclear.

Additionally, YTHDF1 is reported to be overexpressed in CRC and plays a vital oncogenic role in CRC (146, 167). Silencing YTHDF1 not only reduces the number of colon spheres but also causes significant downregulation of cancer stem cell markers, including CD44, CD133, OCT4, ALDH1, and Lgr5 in CRC cells. These findings indicate that YTHDF1 plays a key role in maintaining CRC stemness, which is analogous to the role of METTL3 in CRC (145). YTHDF1 is found to regulate the Wnt/β-Catenin pathway in CRC as well (167). Silencing YTHDF1 leads to reduction of the expressions of the nonphospho (active)-β-catenin and the Wnt/β-catenin downstream targets, including c-JUN, CCND1, and CD44, and thus downregulates the β-catenin nuclear signals activity.

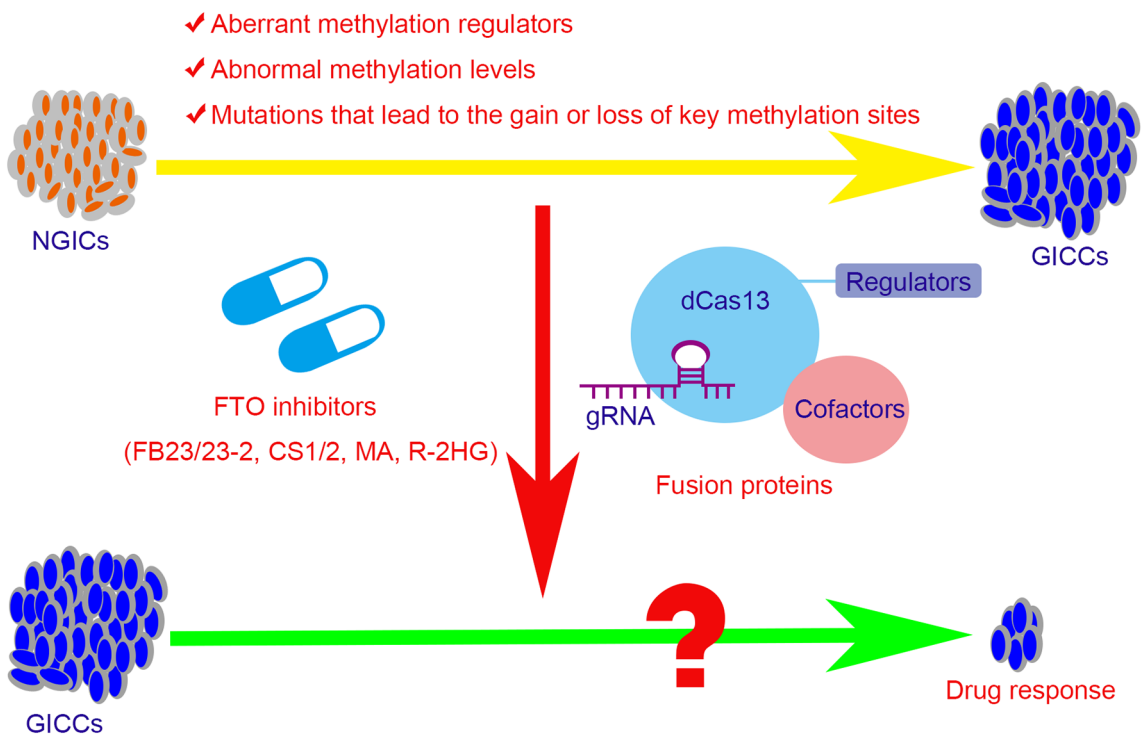

FIGURE 3 | The potential therapeutic strategies for the GICs with abnormal methylation regulators or levels. The aberrant methylation regulators, abnormal methylation levels, and the mutations that lead to the gain or loss of key methylation sites contribute partly in tumorigenesis, progression, and drug resistance in GICs. The potential therapeutic strategies include the small molecule inhibitors of the regulators and the targeted fusion proteins that based on CRISPR/Cas 13 system. FTO, fat mass and obesity-associated protein; NGICs, normal gastrointestinal cells; GICCs, gastrointestinal cancer cells; gRNA, guide RNA; dCas13, inactive Cas13 enzyme; MA, meclofenamic acid; R-2HG, R-2-hydroxyglutarate.

Other Gastric Cancer/Colorectal Cancer-Promoting Mechanisms Related to Methylation

Recent study has revealed that the m^{6}A modification in a circular RNA (circRNA), circNSUN2 that maps to the chromosome 5p15 amplicon in CRC, has an important role for promoting CRC liver metastasis (168). Mechanically, circNSUN2 contains an m^{6}A motif within its exon 5-exon 4 junction sequence where it can be modified by METTL3, and then YTHDC1 facilitates the nuclear export of m^{6}A-containing circNSUN2. In cytoplasm, circNSUN2 stabilizes its downstream target HMGA2 mRNA by forming the complex with an m^{6}A reader IGF2BP2, and promoting the EMT process and liver metastasis in CRC. Interestingly, upregulation of circNSUN2 in CRC is in an METTL3-independent manner, and silencing METTL3 does not change total expression of circNSUN2 nor increases the nuclear content or reduces the cytoplasmic content.

Mutations that cause the gain or loss of methylation sites are found to involve in generation, progression and drug resistance of GICs. Uddin et al. (151) have shown that the point-mutated codon 273 (G > A) of p53 pre-mRNA promotes expression of mutant protein in a METTL3- and m^{6}A-dependent manner, while the upregulated METTL3 is partly caused by a serial ceramide glycosylation mechanism. The mutant protein is found to lose its original role of cancer suppressing and obtain many oncogenic functions to generate the acquired multidrug resistance in CRC. Further, they showed that either silencing METTL3 by small interfering RNA (siRNA), or inhibiting RNA methylation with neplanocin A, or suppressing ceramide glycosylation is able to re-sensitize the resistant CRC cells to anticancer drugs. Recently, Tian et al. (169) revealed another type of mutations that are related to the m^{6}A modification, the missense variant rs8100241 (G > A) located in ANKLE1. Overexpression of the rs8100241[A] allele significantly increased the ANKLE1 m^{6}A level that was catalyzed by writers METTL3/14 and WTAP and recognized by reader of YTHDF1, thus the dysregulated ANKLE1 protein is facilitated compared to that of rs8100241[G] allele, which is significantly related to susceptibility of CRC.

POTENTIAL THERAPEUTIC STRATEGIES

In view of the relationship between methylation modifications and tumors, new tumor treatment strategies have been explored. Meclofenamic acid (MA), the non-steroidal anti-inflammatory drug, was found to compete with FTO binding for the m^{6}A-containing nucleic acid and functions as FTO inhibitor (170). R-2-hydroxyglutarate (R-2HG), generated from mutant isocitrate dehydrogenase 1/2 (IDH1/2) enzymes, was also found to inhibit FTO activity and increase the m^{6}A level in cells, which in turn

TABLE 3 | Relationship between aberrant regulators and GICs*.

Cancer types	Regulator	Role in RNA modification	Abnormal change	Results	Mechanisms/targets	Ref
GC	METTL3	Writer	Upregulated	Poor prognosis	METTL3/m^{6}A/ZMYM1/ELAVL1/E-cadherin/EMT axis	(139)
					METTL3/m^{6}A/HDFG/IGF2BP3 axis	(140)
					METTL3/m^{6}A/SEC62/IGF2BP1 axis	(141)
					METTL3/m^{6}A/MYC axis	(143)
					METTL3/m^{6}A/ARHGAP5 axis	(144)
	WTAP and RBM15	Writer	Upregulated	Poor prognosis; immune response	Unknown	(153–155)
	METTL14	Writer	Downregulated	Poor prognosis	METTL14/m^{6}A/Wnt and PI3K-AKT axis	(156)
	FTO	Eraser	Upregulated	Poor prognosis	Unknown	(153, 155) (160),
	ALKBH3	Eraser	Upregulated	Poor prognosis	ALKBH3/m^{1}A/ErbB2 and AKT1S1 axis	(161)
	ALKBH5	Eraser	Upregulated	Poor prognosis	ALKBH5/m^{6}A/lncRNA NEAT1/EZH2 axis	(155, 162)
CRC	METTL3	Writer	Upregulated	Poor prognosis	METTL3/m^{6}A/SOX2/IGF2BP2/tumor stemness axis	(145)
					METTL3/m^{6}A/HK2 and GLUT1/IGF2BP2/3 axis	(148)
					METTL3/m^{6}A/miR-1246/SPRED2/MAPK axis	(147)
					METTL3/m^{6}A/p38-ERK or CCNE1 axis	(149, 150)
	METTL14	Writer	Downregulated	Poor prognosis	METTL14/m^{6}A/lncRNA XIST/YTHDF2 axis	(158)
					METTL14/m^{6}A/miR-375/YAP1 and SP1 axis	(159)
	FTO	Eraser	Downregulated	Poor prognosis	FTO/m^{6}Am/tumor stemness axis	(146, 164)
	ALKBH5	Eraser	Downregulated	Poor prognosis	ALKBH5/m^{6}A/lncRNA RP11/hnRNPA2B1/E-ligases/Zeb1 axis	(163)
	IGF2BP2	Reader	Upregulated	Poor prognosis	lncRNA LINRIS/IGF2BP2/MYC/glycolysis axis	(165)
	YTHDF3	Reader	Upregulated	Poor prognosis	lncRNA GAS5/YAP/YTHDF3 axis	(166)
	YTHDF1	Reader	Upregulated	Poor prognosis	YTHDF1/Wnt/β-Catenin and tumor stemness axis	(167)

*GC, gastric cancer; CRC, colorectal cancer; writers, methyltransferases; erasers, demethylases; readers, the proteins that bind to methylation modifications; m^{6}A, N^6-methyladenosine; m^{1}A, N^1-methyladenosine; METTL3/14, methyltransferase-like3/14; WTAP, Wilms tumor 1-associated protein; RBM15, RNA-binding motif protein 15; FTO, fat mass and obesity-associated protein; ALKBH3/5, AlkB homolog 3/5; hnRNPA2/B1, heterogeneous nuclear ribonucleoprotein A2/B1; lncRNA, long non-coding RNA; miRNA, micro RNA; ZMYM1, zinc finger MYM-type containing 1; EMT, epithelial-mesenchymal transition; HDGF, hepatoma derived growth factor; SOX2, SRY (sex determining region Y)-box 2; HK2, Hexokinase 2; GLUT1, glucose transporter type 1; CCNE1, cyclin E1; XIST, X-inactive specific transcript; YAP1, Yes-associated protein 1; NEAT1, nuclear paraspeckle assembly transcript 1; EZH2,a subunit of the polycomb repressive complex; LINRIS, Long Intergenic Noncoding RNA for IGF2BP2 Stability; *has been identified at present.*

decreases the stability of MYC/CEBPA and thus block the MYC pathways (171). Recently, two synthetic high-efficient FTO inhibitors are identified. Chen et al. (172) have developed two potent FTO inhibitors FB23 and FB23-2 and showed that they could directly bind to FTO and selectively block the m^6A demethylase activity of FTO. Subsequently, they further developed two others promising FTO inhibitors, namely CS1 and CS2, which exhibit strong anti-tumor effects in multiple types of cancers. For leukemia cells, FTO inhibitors can not only block the signal axis of FTO/m^6A/MYC/CEBPA and inhibit the self-renewal of cancer stem cells, but also suppress the expression of immune checkpoint LILRB4 and immune evasion thus enhancing the cytotoxicity of T cells (173). However, the inhibitors of other m^6A regulators such as METTL3, METTL14, or WTAP have not been systematically developed. Moreover, targeted RNA demethylation or methylation by the engineered dCas13-containing fusion proteins may hold the potential to develop a treatment regimen for GICs (174–176) (**Figure 3**).

CONCLUSIONS AND FUTURE PERSPECTIVE

Since 2011, extensive studies have worked on the methylation modifications in RNAs, providing an extensive and accumulating database including m^6A, m^6Am, and m^1A. The formation of m^1A, m^6A, and m^6Am is no substantial correlated, and the roles of m^6Am and m^1A are partly similar to that of m^6A, by which the m^6Am and m^6A modifications are demethylated by FTO. It would be interesting to measure the interference produced by m^6Am and m^1A during the m^6A exploration process.

The dysregulation of RNA methylation has been linked to the abnormalities in the MYC pathway, the Wnt/β-Catenin pathway, the ErbB2 pathway, the PI3K-AKT pathway and EMT in many human cancers. For GICs, the upregulated METTL3 and erasers are mainly involved in the MAPK/ERK pathway, the CCNE1 pathway, the SOX2/tumor stemness pathway, glycolipid metabolism, and EMT and to facilitate CRC formation and progression, whereas the low expression of METTL14 mediates the lncRNA XIST axis and the miR-375/YAP1 and SP1 axis to promote CRC progression. Moreover, the upregulated readers, IGF2BP2, YTHDF3, and YTHDF1, represent as poor prognosis factors in CRC by regulating the lncRNA LINRIS/IGF2BP2/MYC/glycolysis axis, the lncRNA GAS5/YAP/YTHDF3 axis and the YTHDF1/Wnt/β-Catenin and tumor stemness pathway respectively (**Table 3**). Mutations that cause the gain of methylation sites, including the point-mutated codon 273 (G > A) of p53 pre-mRNA and the missense variant rs8100241 (G > A) located in ANKLE1, are also linked to tumorigenesis, progression and drug resistance in CRC.

However, there are some controversies and confusions in the RNA methylation: **i)** Binding mode of YTHDF proteins on different mRNAs or a single mRNA. **ii)** Affinity towards the m^6A and m^6Am sites by FTO. **iii)** mRNA stability affected by the m^6Am modification. **iv)** The role of the m^1A modification in RNA translation. **v)** Specificity of the targets regulated by the methylation regulators. **vi)** The distinguish expression signatures of both the writers and the erasers in certain type of GICs, and their downstream targets. **viii)** Inhibitors for METTL3 and readers.

AUTHOR CONTRIBUTIONS

GW and WH proposed these ideas and valuable comments, and QL drafted the manuscript. All authors contributed to the article and approved the submitted version.

FUNDING

This work was supported in part by grants from the National Natural Science Foundation of China (82073869, 81701834, 81871994); Guangdong Basic and Applied Basic Research Foundation (2019A050510019, 2019B151502063); Guangdong Provincial Key Laboratory of Construction Foundation (2017B030314030, 2020B1212060034); Guangzhou Science and Technology Planning Program (202002020051, 201902020018); National Engineering Research Centre for New Drug and Drug ability Evaluation, Seed Program of Guangdong Province (2017B090903004).

REFERENCES

1. Roundtree IA, Evans ME, Pan T, He C. Dynamic RNA modifications in gene expression regulation. *Cell* (2017) 169(7):1187–200. doi: 10.1016/j.cell.2017.05.045
2. Pan T. Modifications and functional genomics of human transfer RNA. *Cell Res* (2018) 28(4):395–404. doi: 10.1038/s41422-018-0013-y
3. Taoka M, Nobe Y, Yamaki Y, Sato K, Ishikawa H, Izumikawa K, et al. Landscape of the complete RNA chemical modifications in the human 80S ribosome. *Nucleic Acids Res* (2018) 46(18):9289–98. doi: 10.1093/nar/gky811
4. Linder B, Grozhik AV, Olarerin-George AO, Meydan C, Mason CE, Jaffrey SR. Single-nucleotide-resolution mapping of m6A and m6Am throughout the transcriptome. *Nat Methods* (2015) 12(8):767–72. doi: 10.1038/nmeth.3453
5. Yang Y, Fan X, Mao M, Song X, Wu P, Zhang Y, et al. Extensive translation of circular RNAs driven by N-methyladenosine. *Cell Res* (2017) 27(5):626–41. doi: 10.1038/cr.2017.31
6. Liu N, Dai Q, Zheng G, He C, Parisien M, Pan T. N(6)-methyladenosine-dependent RNA structural switches regulate RNA-protein interactions. *Nature* (2015) 518(7540):560–4. doi: 10.1038/nature14234
7. Alarcón CR, Lee H, Goodarzi H, Halberg N, Tavazoie SF. N6-methyladenosine marks primary microRNAs for processing. *Nature* (2015) 519(7544):482–5. doi: 10.1038/nature14281
8. Helm M, Motorin Y. Detecting RNA modifications in the epitranscriptome: predict and validate. *Nat Rev Genet* (2017) 18(5):275–91. doi: 10.1038/nrg.2016.169
9. Boccaletto P, Machnicka MA, Purta E, Piatkowski P, Baginski B, Wirecki TK, et al. MODOMICS: a database of RNA modification pathways. 2017 update. *Nucleic Acids Res* (2018) 46(D1):D303–7. doi: 10.1093/nar/gkx1030

10. Arango D, Sturgill D, Alhusaini N, Dillman AA, Sweet TJ, Hanson G, et al. Acetylation of cytidine in mRNA promotes translation efficiency. *Cell* (2018) 175(7):1872–86. doi: 10.1016/j.cell.2018.10.030
11. Grozhik AV, Jaffrey SR. Distinguishing RNA modifications from noise in epitranscriptome maps. *Nat Chem Biol* (2018) 14(3):215–25. doi: 10.1038/nchembio.2546
12. Gilbert WV, Bell TA, Schaening C. Messenger RNA modifications: form, distribution, and function. *Science (New York NY)* (2016) 352(6292):1408–12. doi: 10.1126/science.aad8711
13. Desrosiers R, Friderici K, Rottman F. Identification of methylated nucleosides in messenger RNA from Novikoff hepatoma cells. *Proc Natl Acad Sci U S A* (1974) 71(10):3971–5. doi: 10.1073/pnas.71.10.3971
14. Perry RP, Kelley DE. Existence of methylated messenger RNA in mouse L cells. *Cell* (1974) 1:37–42. doi: 10.1016/0092-8674(74)90153-6
15. Wei CM, Gershowitz A, Moss B. Methylated nucleotides block 5' terminus of HeLa cell messenger RNA. *Cell* (1975) 4(4):379–86. doi: 10.1016/0092-8674(75)90158-0
16. Niu Y, Wan A, Lin Z, Lu X, Wan GN. N (6)-methyladenosine modification: a novel pharmacological target for anti-cancer drug development. *Acta Pharm Sin B* (2018) 8(6):833–43. doi: 10.1016/j.apsb.2018.06.001
17. Bray F, Ferlay J, Soerjomataram I, Siegel RL, Torre LA, Jemal A. Global cancer statistics 2018: GLOBOCAN estimates of incidence and mortality worldwide for 36 cancers in 185 countries. *CA Cancer J Clin* (2018) 68 (6):394–424. doi: 10.3322/caac.21492
18. Jaffrey SR, Kharas MG. Emerging links between mA and misregulated mRNA methylation in cancer. *Genome Med* (2017) 9(1):2. doi: 10.1186/s13073-016-0395-8
19. Jia G, Fu Y, Zhao X, Dai Q, Zheng G, Yang Y, et al. N6-methyladenosine in nuclear RNA is a major substrate of the obesity-associated FTO. *Nat Chem Biol* (2011) 7(12):885–7. doi: 10.1038/nchembio.687
20. Zheng G, Dahl JA, Niu Y, Fedorcsak P, Huang C-M, Li CJ, et al. ALKBH5 is a mammalian RNA demethylase that impacts RNA metabolism and mouse fertility. *Mol Cell* (2013) 49(1):18–29. doi: 10.1016/j.molcel.2012.10.015
21. Meyer KD, Saletore Y, Zumbo P, Elemento O, Mason CE, Jaffrey SR. Comprehensive analysis of mRNA methylation reveals enrichment in 3' UTRs and near stop codons. *Cell* (2012) 149(7):1635–46. doi: 10.1016/j.cell.2012.05.003
22. Dominissini D, Moshitch-Moshkovitz S, Schwartz S, Salmon-Divon M, Ungar L, Osenberg S, et al. Topology of the human and mouse m6A RNA methylomes revealed by m6A-seq. *Nature* (2012) 485(7397):201–6. doi: 10.1038/nature11112
23. Liu N, Parisien M, Dai Q, Zheng G, He C, Pan T. Probing N6-methyladenosine RNA modification status at single nucleotide resolution in mRNA and long noncoding RNA. *RNA (New York NY)* (2013) 19 (12):1848–56. doi: 10.1261/rna.041178.113
24. Molinie B, Wang J, Lim KS, Hillebrand R, Lu Z-X, Van Wittenberghe N, et al. m (6)A-LAIC-seq reveals the census and complexity of the m(6)A epitranscriptome. *Nat Methods* (2016) 13(8):692–8. doi: 10.1038/nmeth.3898
25. Meyer KD. DART-seq: an antibody-free method for global mA detection. *Nat Methods* (2019) 16(12):1275–80. doi: 10.1038/s41592-019-0570-0
26. Garcia-Campos MA, Edelheit S, Toth U, Safra M, Shachar R, Viukov S, et al. Deciphering the "mA Code" via antibody-independent quantitative profiling. *Cell* (2019) 178(3):731–47.e16. doi: 10.1016/j.cell.2019.06.013
27. Zhang Z, Chen LQ, Zhao YL, Yang CG, Roundtree IA, Zhang Z, et al. Single-base mapping of mA by an antibody-independent method. *Sci Adv* (2019) 5 (7):eaax0250. doi: 10.1126/sciadv.aax0250
28. Shu X, Cao J, Cheng M, Xiang S, Gao M, Li T, et al. A metabolic labeling method detects mA transcriptome-wide at single base resolution. *Nat Chem Biol* (2020) 16(8):887–895. doi: 10.1038/s41589-020-0526-9
29. Wang Y, Xiao Y, Dong S, Yu Q, Jia G. Antibody-free enzyme-assisted chemical approach for detection of N-methyladenosine. *Nat Chem Biol* (2020) 16(8):896–903. doi: 10.1038/s41589-020-0525-x
30. Liu H, Begik O, Lucas MC, Ramirez JM, Mason CE, Wiener D, et al. Accurate detection of mA RNA modifications in native RNA sequences. *Nat Commun* (2019) 10(1):4079. doi: 10.1038/s41467-019-11713-9
31. Rottman F, Shatkin AJ, Perry RP. Sequences containing methylated nucleotides at the 5' termini of messenger RNAs: possible implications for processing. *Cell* (1974) 3(3):197–9. doi: 10.1016/0092-8674(74)90131-7
32. Perry RP, Kelley DE, Friderici K, Rottman F. The methylated constituents of L cell messenger RNA: evidence for an unusual cluster at the 5' terminus. *Cell* (1975) 4(4):387–94. doi: 10.1016/0092-8674(75)90159-2
33. Harper JE, Miceli SM, Roberts RJ, Manley JL. Sequence specificity of the human mRNA N6-adenosine methylase in vitro. *Nucleic Acids Res* (1990) 18 (19):5735–41. doi: 10.1093/nar/18.19.5735
34. Ke S, Pandya-Jones A, Saito Y, Fak JJ, Vågbø CB, Geula S, et al. mA mRNA modifications are deposited in nascent pre-mRNA and are not required for splicing but do specify cytoplasmic turnover. *Genes Dev* (2017) 31(10):990–1006. doi: 10.1101/gad.301036.117
35. Bokar JA, Rath-Shambaugh ME, Ludwiczak R, Narayan P, Rottman F. Characterization and partial purification of mRNA N6-adenosine methyltransferase from HeLa cell nuclei. Internal mRNA methylation requires a multisubunit complex. *J Biol Chem* (1994) 269(26):17697–704.
36. Rottman FM, Bokar JA, Narayan P, Shambaugh ME, Ludwiczak R. N6-adenosine methylation in mRNA: substrate specificity and enzyme complexity. *Biochimie* (1994) 76(12):1109–14. doi: 10.1016/0300-9084(94)90038-8
37. Bokar JA, Shambaugh ME, Polayes D, Matera AG, Rottman FM. Purification and cDNA cloning of the AdoMet-binding subunit of the human mRNA (N6-adenosine)-methyltransferase. *RNA (New York NY)* (1997) 3(11):1233–47.
38. Bujnicki JM, Feder M, Radlinska M, Blumenthal RM. Structure prediction and phylogenetic analysis of a functionally diverse family of proteins homologous to the MT-A70 subunit of the human mRNA:m(6)A methyltransferase. *J Mol Evol* (2002) 55(4):431–44. doi: 10.1007/s00239-002-2339-8
39. Ping X-L, Sun BF, Wang L, Xiao W, Yang X, Wang WJ, et al. Mammalian WTAP is a regulatory subunit of the RNA N6-methyladenosine methyltransferase. *Cell Res* (2014) 24(2):177–89. doi: 10.1038/cr.2014.3
40. Wang Y, Li Y, Toth JI, Petroski MD, Zhang Z, Zhao JC. N6-methyladenosine modification destabilizes developmental regulators in embryonic stem cells. *Nat Cell Biol* (2014) 16(2):191–8. doi: 10.1038/ncb2902
41. Liu J, Yue Y, Han D, Wang X, Fu Y, Zhang L, et al. A METTL3-METTL14 complex mediates mammalian nuclear RNA N6-adenosine methylation. *Nat Chem Biol* (2014) 10(2):93–5. doi: 10.1038/nchembio.1432
42. Fu Y, Dominissini D, Rechavi G, He C. Gene expression regulation mediated through reversible m^6A RNA methylation. *Nat Rev Genet* (2014) 15(5):293–306. doi: 10.1038/nrg3724
43. Śledź P, Jinek M. Structural insights into the molecular mechanism of the m (6)A writer complex. *eLife* (2016) 5. doi: 10.7554/eLife.18434
44. Wang X, Feng J, Xue Y, Guan Z, Zhang D, Liu Z, et al. Structural basis of N (6)-adenosine methylation by the METTL3-METTL14 complex. *Nature* (2016) 534(7608):575–8. doi: 10.1038/nature18298
45. Wang P, Doxtader KA, Nam Y. Structural basis for cooperative function of Mettl3 and Mettl14 methyltransferases. *Mol Cell* (2016) 63(2):306–17. doi: 10.1016/j.molcel.2016.05.041
46. Huang H, Weng H, Zhou K, Wu T, Zhao BS, Sun M, et al. Histone H3 trimethylation at lysine 36 guides mA RNA modification co-transcriptionally. *Nature* (2019) 567(7748):414–9. doi: 10.1038/s41586-019-1016-7
47. Ortega A, Niksic M, Bachi A, Wilm M, Sánchez L, Hastie N, et al. Biochemical function of female-lethal (2)D/Wilms' tumor suppressor-1-associated proteins in alternative pre-mRNA splicing. *J Biol Chem* (2003) 278(5):3040–7. doi: 10.1074/jbc.M210737200
48. Zhong S, Li H, Bodi Z, Button J, Vespa L, Herzog M, et al. MTA is an Arabidopsis messenger RNA adenosine methylase and interacts with a homolog of a sex-specific splicing factor. *Plant Cell* (2008) 20(5):1278–88. doi: 10.1105/tpc.108.058883
49. Small TW, Penalva LO, Pickering JG. Vascular biology and the sex of flies: regulation of vascular smooth muscle cell proliferation by wilms' tumor 1-associating protein. *Trends Cardiovasc Med* (2007) 17(7):230–4. doi: 10.1016/j.tcm.2007.08.002
50. Schwartz S, Mumbach MR, Jovanovic M, Wang T, Maciag K, Bushkin GG, et al. Perturbation of m6A writers reveals two distinct classes of mRNA methylation at internal and 5' sites. *Cell Rep* (2014) 8(1):284–96. doi: 10.1016/j.celrep.2014.05.048
51. Yue Y, Liu J, Cui X, Cao J, Luo G, Zhang Z, et al. VIRMA mediates preferential mA mRNA methylation in 3'UTR and near stop codon and associates with alternative polyadenylation. *Cell Discov* (2018) 4:10. doi: 10.1038/s41421-018-0019-0
52. Wen J, Lv R, Ma H, Shen H, He C, Wang J, et al. Zc3h13 Regulates nuclear RNA mA methylation and mouse embryonic stem cell self-renewal. *Mol Cell* (2018) 69(6):1028–38.e6. doi: 10.1016/j.molcel.2018.02.015

53. Patil DP, Chen CK, Pickering BF, Chow A, Jackson C, Guttman M, et al. m(6)A RNA methylation promotes XIST-mediated transcriptional repression. *Nature* (2016) 537(7620):369–73. doi: 10.1038/nature19342
54. Aguilo F, Zhang F, Sancho A, Fidalgo M, Di Cecilia S, Vashisht A, et al. Coordination of m(6)A mRNA methylation and gene transcription by ZFP217 regulates pluripotency and reprogramming. *Cell Stem Cell* (2015) 17(6):689–704. doi: 10.1016/j.stem.2015.09.005
55. Bertero A, Brown S, Madrigal P, Osnato A, Ortmann D, Yiangou L, et al. The SMAD2/3 interactome reveals that TGFβ controls mA mRNA methylation in pluripotency. *Nature* (2018) 555(7695):256–9. doi: 10.1038/nature25784
56. Barbieri I, Tzelepis K, Pandolfini L, Shi J, Millán-Zambrano G, Robson SC, et al. Promoter-bound METTL3 maintains myeloid leukaemia by mA-dependent translation control. *Nature* (2017) 552(7683):126–31. doi: 10.1038/nature24678
57. Brown JA, Kinzig CG, DeGregorio SJ, Steitz JA. Methyltransferase-like protein 16 binds the 3'-terminal triple helix of MALAT1 long noncoding RNA. *Proc Natl Acad Sci USA* (2016) 113(49):14013–8. doi: 10.1073/pnas.1614759113
58. Ma H, Wang X, Cai J, Dai Q, Natchiar SK, Lv R, et al. Publisher Correction: N-Methyladenosine methyltransferase ZCCHC4 mediates ribosomal RNA methylation. *Nat Chem Biol* (2019) 15(5):549. doi: 10.1038/s41589-019-0233-6
59. van Tran N, Ernst FGM, Hawley BR, Zorbas C, Ulryck N, Hackert P, et al. The human 18S rRNA m6A methyltransferase METTL5 is stabilized by TRMT112. *Nucleic Acids Res* (2019) 47(15):7719–33. doi: 10.1093/nar/gkz619
60. Frayling TM, Timpson NJ, Weedon MN, Zeggini E, Freathy RM, Lindgren CM, et al. A common variant in the FTO gene is associated with body mass index and predisposes to childhood and adult obesity. *Science (New York NY)* (2007) 316(5826):889–94. doi: 10.1126/science.1141634
61. Peters T, Ausmeier K, Rüther U. Cloning of Fatso (Fto), a novel gene deleted by the Fused toes (Ft) mouse mutation. *Mamm Genome* (1999) 10(10):983–6. doi: 10.1007/s003359901144
62. Sanchez-Pulido L, Andrade-Navarro MA. The FTO (fat mass and obesity associated) gene codes for a novel member of the non-heme dioxygenase superfamily. *BMC Biochem* (2007) 8:23. doi: 10.1186/1471-2091-8-23
63. Gerken T, Girard CA, Tung Y-CL, Webby CJ, Saudek V, Hewitson KS, et al. The obesity-associated FTO gene encodes a 2-oxoglutarate-dependent nucleic acid demethylase. *Science (New York NY)* (2007) 318(5855):1469–72. doi: 10.1126/science.1151710
64. Jia G, Yang C-G, Yang S, Jian X, Yi C, Zhou Z, et al. Oxidative demethylation of 3-methylthymine and 3-methyluracil in single-stranded DNA and RNA by mouse and human FTO. *FEBS Lett* (2008) 582(23-24):3313–9. doi: 10.1016/j.febslet.2008.08.019
65. Fu Y, Jia G, Pang X, Wang RN, Wang X, Li CJ, et al. FTO-mediated formation of N6-hydroxymethyladenosine and N6-formyladenosine in mammalian RNA. *Nat Commun* (2013) 4:1798. doi: 10.1038/ncomms2822
66. Aravind L, Koonin EV. The DNA-repair protein AlkB, EGL-9, and leprecan define new families of 2-oxoglutarate- and iron-dependent dioxygenases. *Genome Biol* (2001) 2(3):RESEARCH0007. doi: 10.1186/gb-2001-2-3-research0007
67. Falnes PO, Johansen RF, Seeberg E. AlkB-mediated oxidative demethylation reverses DNA damage in Escherichia coli. *Nature* (2002) 419(6903):178–82. doi: 10.1038/nature01048
68. Trewick SC, Henshaw TF, Hausinger RP, Lindahl T, Sedgwick B. Oxidative demethylation by Escherichia coli AlkB directly reverts DNA base damage. *Nature* (2002) 419(6903):174–8. doi: 10.1038/nature00908
69. Yu B, Edstrom WC, Benach J, Hamuro Y, Weber PC, Gibney BR, et al. Crystal structures of catalytic complexes of the oxidative DNA/RNA repair enzyme AlkB. *Nature* (2006) 439(7078):879–84. doi: 10.1038/nature04561
70. Klose RJ, Kallin EM, Zhang Y. JmjC-domain-containing proteins and histone demethylation. *Nat Rev Genet* (2006) 7(9):715–27. doi: 10.1038/nrg1945
71. Imai Y, Matsuo N, Ogawa S, Tohyama M, Takagi T. Cloning of a gene, YT521, for a novel RNA splicing-related protein induced by hypoxia/reoxygenation. *Brain Res Mol Brain Res* (1998) 53(1-2):33–40. doi: 10.1016/S0169-328X(97)00262-3
72. Hartmann AM, Nayler O, Schwaiger FW, Obermeier A, Stamm S. The interaction and colocalization of Sam68 with the splicing-associated factor YT521-B in nuclear dots is regulated by the Src family kinase p59(fyn). *Mol Biol Cell* (1999) 10(11):3909–26. doi: 10.1091/mbc.10.11.3909
73. Stoilov P, Rafalska I, Stamm S. YTH: a new domain in nuclear proteins. *Trends Biochem Sci* (2002) 27(10):495–7. doi: 10.1016/S0968-0004(02)02189-8
74. Nayler O, Hartmann AM, Stamm S. The ER repeat protein YT521-B localizes to a novel subnuclear compartment. *J Cell Biol* (2000) 150(5):949–62. doi: 10.1083/jcb.150.5.949
75. Xu C, Wang X, Liu K, Roundtree IA, Tempel W, Li Y, et al. Structural basis for selective binding of m6A RNA by the YTHDC1 YTH domain. *Nat Chem Biol* (2014) 10(11):927–9. doi: 10.1038/nchembio.1654
76. Zhu T, Roundtree IA, Wang P, Wang X, Wang L, Sun C, et al. Crystal structure of the YTH domain of YTHDF2 reveals mechanism for recognition of N6-methyladenosine. *Cell Res* (2014) 24(12):1493–6. doi: 10.1038/cr.2014.152
77. Xiao W, Adhikari S, Dahal U, Chen YS, Hao YJ, Sun BF, et al. Nuclear m(6)A Reader YTHDC1 Regulates mRNA Splicing. *Mol Cell* (2016) 61(4):507–19. doi: 10.1016/j.molcel.2016.01.012
78. Roundtree IA, Luo G-Z, Zhang Z, Wang X, Zhou T, Cui Y, et al. YTHDC1 mediates nuclear export of N-methyladenosine methylated mRNAs. *Elife* (2017) 6. doi: 10.7554/eLife.31311
79. He Y, Smith R. Nuclear functions of heterogeneous nuclear ribonucleoproteins A/B. *Cell Mol Life Sci CMLS* (2009) 66(7):1239–56. doi: 10.1007/s00018-008-8532-1
80. Alarcón CR, Goodarzi H, Lee H, Liu X, Tavazoie S, Tavazoie SF. HNRNPA2B1 Is a Mediator of m(6)A-Dependent Nuclear RNA Processing Events. *Cell* (2015) 162(6):1299–308. doi: 10.1016/j.cell.2015.08.011
81. Wu B, Su S, Patil DP, Liu H, Gan J, Jaffrey SR, et al. Molecular basis for the specific and multivariant recognitions of RNA substrates by human hnRNP A2/B1. *Nat Commun* (2018) 9(1):420. doi: 10.1038/s41467-017-02770-z
82. Liu N, Zhou KI, Parisien M, Dai Q, Diatchenko L, Pan T, et al. N6-methyladenosine alters RNA structure to regulate binding of a low-complexity protein. *Nucleic Acids Res* (2017) 45(10):6051–63. doi: 10.1093/nar/gkx141
83. Zhou KI, Shi H, Lyu R, Wylder AC, Matuszek Ż, Pan JN, et al. Regulation of Co-transcriptional Pre-mRNA Splicing by mA through the Low-Complexity Protein hnRNPG. *Mol Cell* (2019) 76(1). doi: 10.1016/j.molcel.2019.07.005
84. Luo S, Tong L. Molecular basis for the recognition of methylated adenines in RNA by the eukaryotic YTH domain. *Proc Natl Acad Sci U S A* (2014) 111(38):13834–9. doi: 10.1073/pnas.1412742111
85. Theler D, Dominguez C, Blatter M, Boudet J, Allain FHT. Solution structure of the YTH domain in complex with N6-methyladenosine RNA: a reader of methylated RNA. *Nucleic Acids Res* (2014) 42(22):13911–9. doi: 10.1093/nar/gku1116
86. Patil DP, Pickering BF, Jaffrey SR. Reading mA in the Transcriptome: mA-Binding Proteins. *Trends Cell Biol* (2018) 28(2):113–27. doi: 10.1016/j.tcb.2017.10.001
87. Wang X, Lu Z, Gomez A, Hon GC, Yue Y, Han D, et al. N6-methyladenosine-dependent regulation of messenger RNA stability. *Nature* (2014) 505(7481):117–20. doi: 10.1038/nature12730
88. Du H, Zhao Y, He J, Zhang Y, Xi H, Liu M, et al. YTHDF2 destabilizes m(6)A-containing RNA through direct recruitment of the CCR4-NOT deadenylase complex. *Nat Commun* (2016) 7:12626. doi: 10.1038/ncomms12626
89. Ries RJ, Zaccara S, Klein P, Olarerin-George A, Namkoong S, Pickering BF, et al. mA enhances the phase separation potential of mRNA. *Nature* (2019) 571(7765):424–8. doi: 10.1038/s41586-019-1374-1
90. Wang X, Zhao BS, Roundtree IA, Lu Z, Han D, Ma H, et al. N(6)-methyladenosine modulates messenger RNA translation efficiency. *Cell* (2015) 161(6):1388–99. doi: 10.1016/j.cell.2015.05.014
91. Li A, Chen Y-S, Ping X-L, Yang X, Xiao W, Yang Y, et al. Cytoplasmic mA reader YTHDF3 promotes mRNA translation. *Cell Res* (2017) 27(3):444–7. doi: 10.1038/cr.2017.10
92. Shi H, Wang X, Lu Z, Zhao BS, Ma H, Hsu PJ, et al. YTHDF3 facilitates translation and decay of N-methyladenosine-modified RNA. *Cell Res* (2017) 27(3):315–28. doi: 10.1038/cr.2017.15
93. Zaccara S, Jaffrey SR. A unified model for the function of YTHDF proteins in regulating mA-modified mRNA. *Cell* (2020) 181(7):1582–95.e18. doi: 10.1016/j.cell.2020.05.012

94. Mao Y, Dong L, Liu X-M, Guo J, Ma H, Shen B, et al. mA in mRNA coding regions promotes translation via the RNA helicase-containing YTHDC2. *Nat Commun* (2019) 10(1):5332. doi: 10.1038/s41467-019-13317-9
95. Hsu PJ, Zhu Y, Ma H, Guo Y, Shi X, Liu Y, et al. Ythdc2 is an N-methyladenosine binding protein that regulates mammalian spermatogenesis. *Cell Res* (2017) 27(9):1115–27. doi: 10.1038/cr.2017.99
96. Zhou B, Liu C, Xu L, Yuan Y, Zhao J, Zhao W, et al. N-methyladenosine reader protein Ythdc2 suppresses liver steatosis via regulation of mRNA stability of lipogenic genes. *Hepatol (Baltimore Md)* (2020). doi: 10.1002/hep.31220
97. Nielsen J, Christiansen J, Lykke-Andersen J, Johnsen AH, Wewer UM, Nielsen FC. A family of insulin-like growth factor II mRNA-binding proteins represses translation in late development. *Mol Cell Biol* (1999) 19 (2):1262–70. doi: 10.1128/MCB.19.2.1262
98. Huang H, Weng H, Sun W, Qin X, Shi H, Wu H, et al. Recognition of RNA N-methyladenosine by IGF2BP proteins enhances mRNA stability and translation. *Nat Cell Biol* (2018) 20(3):285–95. doi: 10.1038/s41556-018-0045-z
99. Zhang F, Kang Y, Wang M, Li Y, Xu T, Yang W, et al. Fragile X mental retardation protein modulates the stability of its m6A-marked messenger RNA targets. *Hum Mol Genet* (2018) 27(22):3936–50. doi: 10.1093/hmg/ddy292
100. Wu R, Li A, Sun B, Sun JG, Zhang J, Zhang T, et al. A novel mA reader Prrc2a controls oligodendroglial specification and myelination. *Cell Res* (2019) 29(1):23–41. doi: 10.1038/s41422-018-0113-8
101. Lin S, Choe J, Du P, Triboulet R, Gregory RI. The m(6)A methyltransferase METTL3 promotes translation in human cancer cells. *Mol Cell* (2016) 62 (3):335–45. doi: 10.1016/j.molcel.2016.03.021
102. Choe J, Lin S, Zhang W, Liu Q, Wang L, Ramirez-Moya J, et al. mRNA circularization by METTL3-eIF3h enhances translation and promotes oncogenesis. *Nature* (2018) 561(7724):556–60. doi: 10.1038/s41586-018-0538-8
103. Adams JM, Cory S. Modified nucleosides and bizarre 5'-termini in mouse myeloma mRNA. *Nature* (1975) 255(5503):28–33. doi: 10.1038/255028a0
104. Furuichi Y, Morgan M, Shatkin AJ, Jelinek W, Salditt-Georgieff M, Darnell JE, et al. Methylated, blocked 5 termini in HeLa cell mRNA. *Proc Natl Acad Sci U S A* (1975) 72(5):1904–8. doi: 10.1073/pnas.72.5.1904
105. Wei C, Gershowitz A, Moss B. N6, O2'-dimethyladenosine a novel methylated ribonucleoside next to the 5' terminal of animal cell and virus mRNAs. *Nature* (1975) 257(5523):251–3. doi: 10.1038/257251a0
106. Akichika S, Hirano S, Shichino Y, Suzuki T, Nishimasu H, Ishitani R, et al. Cap-specific terminal -methylation of RNA by an RNA polymerase II-associated methyltransferase. *Science (New York NY)* (2019) 363(6423). doi: 10.1126/science.aav0080
107. Wei CM, Gershowitz A, Moss B. 5'-Terminal and internal methylated nucleotide sequences in HeLa cell mRNA. *Biochemistry* (1976) 15(2):397–401. doi: 10.1021/bi00647a024
108. Liu JE, Li K, Cai J, Zhang M, Zhang X, Xiong X, et al. Landscape and Regulation of mA and mAm Methylome across Human and Mouse Tissues. *Mol Cell* (2020) 77(2):426–40.e6. doi: 10.1016/j.molcel.2019.09.032
109. Boulias K, Toczydłowska-Socha D, Hawley BR, Liberman N, Takashima K, Zaccara S, et al. Identification of the mAm Methyltransferase PCIF1 Reveals the Location and Functions of mAm in the Transcriptome. *Mol Cell* (2019) 75(3):631–43.e8. doi: 10.1016/j.molcel.2019.06.006
110. Ringeard M, Marchand V, Decroly E, Motorin Y, Bennasser Y. FTSJ3 is an RNA 2'-O-methyltransferase recruited by HIV to avoid innate immune sensing. *Nature* (2019) 565(7740):500–4. doi: 10.1038/s41586-018-0841-4
111. Liang H, Jiao Z, Rong W, Qu S, Liao Z, Sun X, et al. 3'-Terminal 2'-O-methylation of lung cancer miR-21-5p enhances its stability and association with Argonaute 2. *Nucleic Acids Res* (2020) 48(13):7027–40. doi: 10.1093/nar/gkaa504
112. Sun H, Zhang M, Li K, Bai D, Yi C. Cap-specific, terminal N-methylation by a mammalian mAm methyltransferase. *Cell Res* (2019) 29(1):80–2. doi: 10.1038/s41422-018-0117-4
113. Fan H, Sakuraba K, Komuro A, Kato S, Harada F, Hirose Y. PCIF1, a novel human WW domain-containing protein, interacts with the phosphorylated RNA polymerase II. *Biochem Biophys Res Commun* (2003) 301(2):378–85. doi: 10.1016/S0006-291X(02)03015-2
114. Goh YT, Koh CWQ, Sim DY, Roca X, Goh WSS. METTL4 catalyzes m6Am methylation in U2 snRNA to regulate pre-mRNA splicing. *Nucleic Acids Res* (2020) 48(16):9250–61. doi: 10.1093/nar/gkaa684
115. Mauer J, Luo X, Blanjoie A, Jiao X, Grozhik AV, Patil DP, et al. Reversible methylation of mA in the 5' cap controls mRNA stability. *Nature* (2017) 541 (7637):371–5. doi: 10.1038/nature21022
116. Zhang X, Wei LH, Wang Y, Xiao Y, Liu J, Zhang W, et al. Structural insights into FTO's catalytic mechanism for the demethylation of multiple RNA substrates. *Proc Natl Acad Sci U S A* (2019) 116(8):2919–24. doi: 10.1073/pnas.1820574116
117. Wei J, Liu F, Lu Z, Fei Q, Ai Y, He PC, et al. Differential mA, mA, and mA Demethylation Mediated by FTO in the Cell Nucleus and Cytoplasm. *Mol Cell* (2018) 71(6):973–85.e5. doi: 10.1016/j.molcel.2018.08.011
118. Sendinc E, Valle-Garcia D, Dhall A, Chen H, Henriques T, Navarrete-Perea J, et al. PCIF1 Catalyzes m6Am mRNA Methylation to Regulate Gene Expression. *Mol Cell* (2019) 75(3):620–30.e9. doi: 10.1016/j.molcel.2019.05.030
119. Dunn DB. The occurrence of 1-methyladenine in ribonucleic acid. *Biochim Biophys Acta* (1961) 46:198–200. doi: 10.1016/0006-3002(61)90668-0
120. Macon JB, Wolfenden R. 1-Methyladenosine. Dimroth rearrangement and reversible reduction. *Biochemistry* (1968) 7(10):3453–8. doi: 10.1021/bi00850a021
121. El Yacoubi B, Bailly M, de Crécy-Lagard V. Biosynthesis and function of posttranscriptional modifications of transfer RNAs. *Annu Rev Genet* (2012) 46:69–95. doi: 10.1146/annurev-genet-110711-155641
122. Sharma S, Watzinger P, Kötter P, Entian KD. Identification of a novel methyltransferase, Bmt2, responsible for the N-1-methyl-adenosine base modification of 25S rRNA in Saccharomyces cerevisiae. *Nucleic Acids Res* (2013) 41(10):5428–43. doi: 10.1093/nar/gkt195
123. Dominissini D, Nachtergaele S, Moshitch-Moshkovitz S, Peer E, Kol N, Ben-Haim MS, et al. The dynamic N(1)-methyladenosine methylome in eukaryotic messenger RNA. *Nature* (2016) 530(7591):441–6. doi: 10.1038/nature16998
124. Li X, Xiong X, Wang K, Wang L, Shu X, Ma S, et al. Transcriptome-wide mapping reveals reversible and dynamic N(1)-methyladenosine methylome. *Nat Chem Biol* (2016) 12(5):311–6. doi: 10.1038/nchembio.2040
125. Li X, Xiong X, Zhang M, Wang K, Chen Y, Zhou J, et al. Base-resolution mapping reveals distinct mA methylome in nuclear- and mitochondrial-encoded transcripts. *Mol Cell* (2017) 68(5):993–1005.e9. doi: 10.1016/j.molcel.2017.10.019
126. Safra M, Sas-Chen A, Nir R, Winkler R, Nachshon A, Bar-Yaacov D, et al. The m1A landscape on cytosolic and mitochondrial mRNA at single-base resolution. *Nature* (2017) 551(7679):251–5. doi: 10.1038/nature24456
127. Chujo T, Suzuki T. Trmt61B is a methyltransferase responsible for 1-methyladenosine at position 58 of human mitochondrial tRNAs. *RNA (New York NY)* (2012) 18(12):2269–76. doi: 10.1261/rna.035600.112
128. Ozanick S, Krecic A, Andersland J, Anderson JT. The bipartite structure of the tRNA m1A58 methyltransferase from S. cerevisiae is conserved in humans. *RNA (New York NY)* (2005) 11(8):1281–90. doi: 10.1261/rna.5040605
129. Vilardo E, Nachbagauer C, Buzet A, Taschner A, Holzmann J. A subcomplex of human mitochondrial RNase P is a bifunctional methyltransferase–extensive moonlighting in mitochondrial tRNA biogenesis. *Nucleic Acids Res* (2012) 40(22):11583–93. doi: 10.1093/nar/gks910
130. Scheitl CPM, Ghaem Maghami M, Lenz AK, Höbartner C, et al. Site-specific RNA methylation by a methyltransferase ribozyme. *Nature* (2020) 587 (7835):663–7. doi: 10.1038/s41586-020-2854-z
131. Liu F, Clark W, Luo G, Wang X, Fu Y, Wei J, et al. ALKBH1-Mediated tRNA Demethylation Regulates Translation. *Cell* (2016) 167(3):1897. doi: 10.1016/j.cell.2016.09.038
132. Aas PA, Otterlei M, Falnes PO, Vågbø CB, Skorpen F, Akbari M, et al. Human and bacterial oxidative demethylases repair alkylation damage in both RNA and DNA. *Nature* (2003) 421(6925):859–63. doi: 10.1038/nature01363
133. Ougland R, Zhang C-M, Liiv A, Johansen RF, Seeberg E, Hou YM, et al. AlkB restores the biological function of mRNA and tRNA inactivated by chemical methylation. *Mol Cell* (2004) 16(1):107–16. doi: 10.1016/j.molcel.2004.09.002
134. Parsyan A, Svitkin Y, Shahbazian D, Gkogkas C, Lasko P, Merrick WC, et al. mRNA helicases: the tacticians of translational control. *Nat Rev Mol Cell Biol* (2011) 12(4):235–45. doi: 10.1038/nrm3083

135. Sonenberg N, Hinnebusch AG. Regulation of translation initiation in eukaryotes: mechanisms and biological targets. *Cell* (2009) 136(4):731–45. doi: 10.1016/j.cell.2009.01.042
136. Zheng Q, Gan H, Yang F, Yao Y, Hao F, et al. Cytoplasmic mA reader YTHDF3 inhibits trophoblast invasion by downregulation of mA-methylated IGF1R. *Cell Discov* (2020) 6:12. doi: 10.1038/s41421-020-0144-4
137. Seo KW, Kleiner RE. YTHDF2 Recognition of N-Methyladenosine (mA)-Modified RNA Is Associated with Transcript Destabilization. *ACS Chem Biol* (2020) 15(1):132–9. doi: 10.1021/acschembio.9b00655
138. He L, Li H, Wu A, Peng Y, Shu G, Yin G, et al. Functions of N6-methyladenosine and its role in cancer. *Mol Cancer* (2019) 18(1):176. doi: 10.1186/s12943-019-1109-9
139. Yue B, Yue B, Song C, Yang L, Cui R, Cheng X, Zhang Z, et al. METTL3-mediated N6-methyladenosine modification is critical for epithelial-mesenchymal transition and metastasis of gastric cancer. *Mol Cancer* (2019) 18(1):142. doi: 10.1186/s12943-019-1065-4
140. Wang Q, Chen C, Ding Q, Zhao Y, Wang Z, Chen J, et al. METTL3-mediated mA modification of HDGF mRNA promotes gastric cancer progression and has prognostic significance. *Gut* (2019) 69(7):1193–205. doi: 10.1136/gutjnl-2019-319639
141. He H, Wu W, Sun Z, Chai L, et al. MiR-4429 prevented gastric cancer progression through targeting METTL3 to inhibit mA-caused stabilization of SEC62. *Biochem Biophys Res Commun* (2019) 517(4):581–7. doi: 10.1016/j.bbrc.2019.07.058
142. Liu T, Yang S, Sui J, Xu SY, Cheng YP, Shen B, et al. Dysregulated N6-methyladenosine methylation writer METTL3 contributes to the proliferation and migration of gastric cancer. *J Cell Physiol* (2020) 235 (1):548–62. doi: 10.1002/jcp.28994
143. Yang D-D, Chen Z-H, Yu K, Lu JH, Wu QN, Wang Y, et al. METTL3 Promotes the Progression of Gastric Cancer via Targeting the MYC Pathway. *Front Oncol* (2020) 10:115. doi: 10.3389/fonc.2020.00115
144. Zhu L, Zhu Y, Han S, Chen M, Song P, Dai D, et al. Impaired autophagic degradation of lncRNA ARHGAP5-AS1 promotes chemoresistance in gastric cancer. *Cell Death Dis* (2019) 10(6):383. doi: 10.1038/s41419-019-1585-2
145. Li T, Hu PS, Zuo Z, Lin JF, Li X, Wu QN, et al. METTL3 facilitates tumor progression via an mA-IGF2BP2-dependent mechanism in colorectal carcinoma. *Mol Cancer* (2019) 18(1):112. doi: 10.1186/s12943-019-1038-7
146. Liu X, Liu L, Dong Z, Li J, Yu Y, Chen X, et al. Expression patterns and prognostic value of mA-related genes in colorectal cancer. *Am J Trans Res* (2019) 11(7):3972–91.
147. Peng W, Li J, Chen R, Gu Q, Yang P, Qian W, et al. Upregulated METTL3 promotes metastasis of colorectal Cancer via miR-1246/SPRED2/MAPK signaling pathway. *J Exp Clin Cancer Res CR* (2019) 38(1):393. doi: 10.1186/s13046-019-1408-4
148. Shen C, Xuan B, Yan T, Ma Y, Xu P, Tian X, et al. mA-dependent glycolysis enhances colorectal cancer progression. *Mol Cancer* (2020) 19(1):72. doi: 10.1186/s12943-020-01190-w
149. Zhu W, Si Y, Xu J, Lin Y, Wang J-Z, Cao M, et al. Methyltransferase like 3 promotes colorectal cancer proliferation by stabilizing CCNE1 mRNA in an m6A-dependent manner. *J Cell Mol Med* (2020) 24(6):3521–33. doi: 10.1111/jcmm.15042
150. Deng R, Cheng Y, Ye S, Zhang J, Huang R, Li P, et al. mA methyltransferase METTL3 suppresses colorectal cancer proliferation and migration through p38/ERK pathways. *OncoTarg Ther* (2019) 12:4391–402. doi: 10.2147/OTT.S201052
151. Uddin MB, Roy KR, Hosain SB, Khiste SK, Hill RA, Jois SD, et al. An N-methyladenosine at the transited codon 273 of p53 pre-mRNA promotes the expression of R273H mutant protein and drug resistance of cancer cells. *Biochem Pharmacol* (2019) 160:134–45. doi: 10.1016/j.bcp.2018.12.014
152. Boumahdi S, Driessens G, Lapouge G, Rorive S, Nassar D, Le Mercier M, et al. SOX2 controls tumour initiation and cancer stem-cell functions in squamous-cell carcinoma. *Nature* (2014) 511(7508):246–50. doi: 10.1038/nature13305
153. Guan K, Liu X, Li J, Ding Y, Li J, Cui G, et al. Expression Status And Prognostic Value Of M6A-associated Genes in Gastric Cancer. *J Cancer* (2020) 11(10):3027–40. doi: 10.7150/jca.40866
154. Li H, Su Q, Li B, Lan L, Wang C, Li W, et al. High expression of WTAP leads to poor prognosis of gastric cancer by influencing tumour-associated T lymphocyte infiltration. *J Cell Mol Med* (2020) 24(8):4452–65. doi: 10.1111/jcmm.15104
155. Su Y, Huang J, Hu J. mA RNA Methylation regulators contribute to malignant progression and have clinical prognostic impact in gastric cancer. *Front Oncol* (2019) 9:1038. doi: 10.3389/fonc.2019.01038
156. Zhang C, Zhang M, Ge S, Huang W, Lin X, Gao J, et al. Reduced m6A modification predicts malignant phenotypes and augmented Wnt/PI3K-Akt signaling in gastric cancer. *Cancer Med* (2019) 8(10):4766–81. doi: 10.1002/cam4.2360
157. Yang X, Zhang S, He C, Xue P, Zhang L, He Z, et al. METTL14 suppresses proliferation and metastasis of colorectal cancer by down-regulating oncogenic long non-coding RNA XIST. *Mol Cancer* (2020) 19(1):46. doi: 10.1186/s12943-020-1146-4
158. Chen D-L, Chen LZ, Lu YX, Zhang DS, Zeng ZL, Pan ZZ, et al. Long noncoding RNA XIST expedites metastasis and modulates epithelial-mesenchymal transition in colorectal cancer. *Cell Death Dis* (2017) 8(8): e3011. doi: 10.1038/cddis.2017.421
159. Chen X, Xu M, Xu X, Zeng K, Liu X, Sun L, et al. METTL14 Suppresses CRC progression via regulating N6-methyladenosine-dependent primary miR-375 processing. *Mol Ther J Am Soc Gene Ther* (2020) 28(2):599–612. doi: 10.1016/j.ymthe.2019.11.016
160. Li Y, Zheng D, Wang F, Xu Y, Yu H, Zhang H. Expression of demethylase genes, FTO and ALKBH1, is associated with prognosis of gastric cancer. *Digest Dis Sci* (2019) 64(6):1503–13. doi: 10.1007/s10620-018-5452-2
161. Zhao Y, Zhao Q, Kaboli PJ, Shen J, Li M, Wu X, et al. m1A regulated genes modulate PI3K/AKT/mTOR and ErbB pathways in gastrointestinal cancer. *Trans Oncol* (2019) 12(10):1323–33. doi: 10.1016/j.tranon.2019.06.007
162. Zhang J, Guo S, Piao HY, Wang Y, Wu Y, Meng XY, et al. ALKBH5 promotes invasion and metastasis of gastric cancer by decreasing methylation of the lncRNA NEAT1. *J Physiol Biochem* (2019) 75(3):379–89. doi: 10.1007/s13105-019-00690-8
163. Wu Y, Yang X, Chen Z, Tian L, Jiang G, Chen F, et al. m6A-induced lncRNA RP11 triggers the dissemination of colorectal cancer cells via upregulation of Zeb1. *Mol Cancer* (2019) 18(1):87. doi: 10.1186/s12943-019-1014-2
164. Relier S, Ripoll J, Guillorit H, Amalric A, Boissière F, Vialaret J, et al. FTO-mediated cytoplasmic m6Am demethylation adjusts stem-like properties in colorectal cancer cell. *bioRixv* (2020). doi: 10.1101/2020.01.09.899724
165. Wang Y, Lu JH, Wu QN, Jin Y, Wang DS, Chen YX, et al. LncRNA LINRIS stabilizes IGF2BP2 and promotes the aerobic glycolysis in colorectal cancer. *Mol Cancer* (2019) 18(1):174. doi: 10.1186/s12943-019-1105-0
166. Ni W, Yao S, Zhou Y, Liu Y, Huang P, Zhou A, et al. Long noncoding RNA GAS5 inhibits progression of colorectal cancer by interacting with and triggering YAP phosphorylation and degradation and is negatively regulated by the mA reader YTHDF3. *Mol Cancer* (2019) 18(1):143. doi: 10.1186/s12943-019-1079-y
167. Bai Y, Yang C, Wu R, Huang L, Song S, Li W, et al. YTHDF1 regulates tumorigenicity and cancer stem cell-Like activity in human colorectal carcinoma. *Front Oncol* (2019) 9:332. doi: 10.3389/fonc.2019.00332
168. Chen R-X, Chen X, Xia LP, Zhang JX, Pan ZZ, Ma XD, et al. N-methyladenosine modification of circNSUN2 facilitates cytoplasmic export and stabilizes HMGA2 to promote colorectal liver metastasis. *Nat Commun* (2019) 10(1):4695. doi: 10.1038/s41467-019-12651-2
169. Tian J, Ying P, Ke J, Zhu Y, Yang Y, Gong Y, et al. ANKLE1 N -Methyladenosine-related variant is associated with colorectal cancer risk by maintaining the genomic stability. *Int J Cancer* (2020) 146(12):3281–93. doi: 10.1002/ijc.32677
170. Huang Y, Yan J, Li Q, Li J, Gong S, Zhou H, et al. Meclofenamic acid selectively inhibits FTO demethylation of m6A over ALKBH5. *Nucleic Acids Res* (2015) 43(1):373–84. doi: 10.1093/nar/gku1276
171. Su R, Dong L, Li C, Nachtergaele S, Wunderlich M, Qing Y, et al. R-2HG Exhibits anti-tumor activity by targeting FTO/mA/MYC/CEBPA signaling. *Cell* (2018) 172(1-2):90–105.e23. doi: 10.1016/j.cell.2017.11.031
172. Huang Y, Su R, Sheng Y, Dong L, Dong Z, Xu H, et al. Small-molecule targeting of oncogenic FTO demethylase in acute myeloid leukemia. *Cancer Cell* (2019) 35(4):677–91.e10. doi: 10.1016/j.ccell.2019.03.006
173. Su R, Dong L, Li Y, Gao M, Han L, Wunderlich M, et al. Targeting FTO suppresses cancer stem cell maintenance and immune evasion. *Cancer Cell* (2020) 38(1):79–96.e11. doi: 10.1016/j.ccell.2020.04.017
174. Zhao J, Li B, Ma J, Jin W, Ma X. Photoactivatable RNA N-methyladenosine editing with CRISPR-Cas13. *Small (Weinheim An Der Bergstrasse Germany)* (2020) 16(30):e1907301. doi: 10.1002/smll.201907301
175. Li J, Chen Z, Chen F, Xie G, Ling Y, Peng Y, et al. Targeted mRNA demethylation using an engineered dCas13b-ALKBH5 fusion protein. *Nucleic Acids Res* (2020) 48(10):5684–94. doi: 10.1093/nar/gkaa269

176. Wilson C, Chen PJ, Miao Z, Liu DR. Programmable mA modification of cellular RNAs with a Cas13-directed methyltransferase. *Nat Biotechnol* (2020) 38(12):1431–40. doi: 10.1038/s41587-020-0572-6

Conflict of Interest: The authors declare that the research was conducted in the absence of any commercial or financial relationships that could be construed as a potential conflict of interest.

frontiers in Oncology

ORIGINAL RESEARCH
published: 23 February 2021
doi: 10.3389/fonc.2021.560506

Analysis and Validation of circRNA-miRNA Network in Regulating m^{6}A RNA Methylation Modulators Reveals CircMAP2K4/miR-139-5p/YTHDF1 Axis Involving the Proliferation of Hepatocellular Carcinoma

Fanwu Chi[1], *Yong Cao*[1*] *and Yuhan Chen*[2*]

[1] Cardiovascular Surgery Department, The People's Hospital of Gaozhou, Gaozhou, China, [2] Department of Radiation Oncology, Nanfang Hospital, Southern Medical University, Guangzhou, China

The m^{6}A RNA methylation modulators play a crucial role in regulating hepatocellular carcinoma (HCC) progression. The circular RNA (circRNA) regulatory network in regulating m^{6}A RNA methylation modulators in HCC remains largely unknown. In this study, 5 prognostic m^{6}A RNA methylation modulators in HCC were identified from The Cancer Genome Atlas (TCGA) and International Cancer Genome Consortium (ICGC) projects. The differentially expressed microRNAs (DEmiRNAs) and circRNAs (DEcircRNAs) between paired tumor and normal tissues were screened out from TCGA and or Gene Expression Omnibus (GEO) database to construct the circRNA-miRNA- m^{6}A RNA methylation modulator regulatory network, which included three m^{6}A RNA methylation modulators (HNRNPC, YTHDF1, and YTHDF2), 11 DEmiRNAs, and eight DEcircRNAs. Among the network, hsa-miR-139-5p expression was negatively correlated with YTHDF1. Hsa-miR-139-5p low or YTHDF1 high expression was correlated with high pathological grade, advanced stage and poor survival of HCC. Additionally, cell cycle, base excision repair, and homologous recombination were enriched in YTHDF1 high expression group by GSEA. A hub circRNA regulatory network was constructed based on hsa-miR-139-5p/YTHDF1 axis. Furthermore, hsa_circ_0007456(circMAP2K4) was validated to promote HCC cell proliferation by binding with hsa-miR-139-5p to promote YTHDF1 expression. Taken together, we identified certain circRNA regulatory network related to m^{6}A RNA methylation modulators and provided clues for mechanism study and therapeutic targets for HCC.

Keywords: circular RNA, microRNA, m^{6}A RNA methylation modulator, regulatory network, hepatocellular carcinoma

OPEN ACCESS

Edited by:
Xiangqian Zheng,
Tianjin Medical University Cancer Institute and Hospital, China

Reviewed by:
Rongquan He,
Guangxi Medical University, China
Jiheng Xu,
New York University, United States

****Correspondence:***
Yuhan Chen
cspnr1@126.com
Yong Cao
wildness@163.com

Specialty section:
This article was submitted to Cancer Genetics, a section of the journal Frontiers in Oncology

Received: *08 September 2020*
Accepted: *07 January 2021*
Published: *23 February 2021*

Citation:
Chi F, Cao Y and Chen Y (2021) Analysis and Validation of circRNA-miRNA Network in Regulating m^{6}A RNA Methylation Modulators Reveals CircMAP2K4/miR-139-5p/YTHDF1 Axis Involving the Proliferation of Hepatocellular Carcinoma. Front. Oncol. 11:560506. doi: 10.3389/fonc.2021.560506

INTRODUCTION

Hepatocellular carcinoma (HCC) is one of the most common malignant tumors worldwide, accounting for 75%–85% of primary liver cancer (1). Despite advances in diagnosis and therapeutic strategies in recent years, the prognosis of HCC is still not ideal. Therefore, there exists an urgent need to identify sensitive and specific biomarkers and therapeutic targets for the early diagnosis and treatment of HCC (2).

Among the chemical modification of RNA, N6-methyladenosine (m^6A) methylated at the N6 position of adenosine is viewed as the most common, abundant and conservative internal transcriptional modification for various kinds of RNA. The m^6A modifications are involved in RNA processing, transporting, translation and metabolism (3). Based on the different functions of m^6A RNA methylation modulators, they are usually classified into "writers", "erasers", and "readers" (4). The "writers" catalyze the formation of m^6A, including Methyltransferase-like 3 (METTL3) (5), METTL14 (6), Wilms tumor 1-associated protein (WTAP) (7), RNA Binding Motif Protein 15 (RBM15) (8) and KIAA1429 (9). The "erasers", removing m^6A modification from RNA, compose of fat mass and obesity-associated protein (FTO) (10) and alkB homologue 5 (ALKBH5) (11). The m^6A readers YT521-B homology (YTH) domain-containing proteins (YTHDF1/2 and YTHDC1/2) function as m^6A binding proteins that recognize m^6A methylation and generate a functional signal (12). Accumulating evidence has demonstrated that m^6A modifications participate in the progression of cancers, such as glioma, breast cancers and hepatocellular carcinoma (HCC) (13).

Circular RNA (circRNA) is a class of covalently closed single-stranded circular RNA molecules formed by back-splicing. CircRNA is considered as the RNA with tissue-, developmental stage- and disease-specificity (14). Notably, it is well documented that circRNAs play crucial roles in cancer by acting as microRNA (miRNA) sponge to modulate the miRNA-mRNA regulatory axis, thereby affecting the initiation and progression of cancer (15). However, whether circRNAs can serve as miRNA sponge to affect the miRNA in the regulation of m^6A RNA methylation modulators in HCC has not been reported yet.

The flowchart of this study design was shown in **Figure S1**. Briefly, we identified prognostic m^6A RNA methylation modulators in HCC patients from The Cancer Genome Atlas (TCGA) and International Cancer Genome Consortium (ICGC) projects. According to the differentially expressed (DE) circRNAs and miRNAs between paired normal and tumor tissues, the circRNA-miRNA-mRNA regulatory network was constructed based on the m^6A RNA methylation modulators. Among the 3 co-expressed miRNA-m^6A RNA methylation modulators pairs, hsa-miR-139-5p low or YTHDF1 high expression was significantly correlated with high pathological grade, advanced stage and poor survival of HCC. Therefore, a hub circRNA regulatory network was constructed based on hsa-miR-139-5p/YTHDF1 axis. Among this hub network, circMAP2K4 was validated to promote HCC cell proliferation by binding with hsa-miR-139-5p to promote YTHDF1 expression. These findings indicate certain circRNA regulatory network is involved in the regulation of m^6A RNA methylation modulators and provide clues for mechanism study and therapeutic strategy development for HCC.

MATERIAL AND METHODS

Data Collection

Regarding the expression data of m6A RNA methylation modulators, we obtained transcriptome data of TCGA-LIHC project from TCGA data portal (https://tcga-data.nci.nih.gov/tcga/) and ICGC-LIRI-JP project from ICGC data portal (https://dcc.icgc.org/), respectively. Regarding the miRNA data, in order to maintain the consistency of data sources, we downloaded miRNA-seq data from the TCGA-LIHC project for subsequent difference and co-expression analysis. For the verification of the prognostic value of miRNA, we searched the Gene Expression Omnibus (GEO) database (http://www.ncbi.nlm.nih.gov/gds/) with "microRNA", "hepatocellular carcinoma", and "survival" as keywords. In order to ensure the reliability of the results, we only selected datasets with more than 100 cases for analysis, and finally included the GSE31384 into this study. Regarding the circRNA data, we searched the GEO database with "circular RNA", "hepatocellular carcinoma", and "microarray" as keywords, and finally included GSE94508, GSE97332 and GSE78520 into this study. Criteria for study inclusion were: 1) The disease was diagnosed as HCC. 2) HCC caused by different etiologies was acceptable. 3) The case had a complete expression profile. 4) The case had clinical information. Criteria for study exclusion were: 1) The survival data was unknown or survival time was less than 30 days. 2) The clinical staging and or pathological grade was unknown. The analysis flowchart of HCC cases with complete expression data was shown in **Figure S2**.

Identification of DERNAs

The mRNA expression level of 13 m^6A RNA methylation modulators were compared between 50 or 199 paired tumor and non-tumor samples from TCGA and ICGC projects by Mann-Whitney-Wilcoxon Test, respectively. And the prognostic value of the m^6A RNA methylation modulators in both TCGA and ICGC were further assessed by univariate Cox regression survival analyses. Finally, those prognostic m^6A RNA methylation modulators in both TCGA and ICGC were identified for the following network construction. The DEmiRNAs were screened out from 49 paired tumor and non-tumor samples from TCGA by using R package "Bioconductor Limma". The adjusted P value (false discovery rate, FDR) of each gene was calculated by Benjamini Hochberg method and the threshold for DEmiRNA selection was FDR <0.05 and $|\log2FC| > 1$. Finally, DEmiRNA is visualized by volcano graph and fold change (FC) filtering. According to the significance scores <0.01 and $|\log2FC| > 2$, the DEcircRNAs between tumor and non-tumor cases from multiple studies was determined by a robust rank aggregation method (16). And the DEcircRNAs were visualized by heatmap.

Construction of CircRNA-miRNA Network Involved in Regulating m^{6}A RNA Methylation Modulators

The miRNAs potentially targeting m^{6}A RNA methylation regulators were predicted by microRNA Data Integration Portal (miRDIP), which integrated more than 20 miRNA related databases for miRNA target or miRNA prediction (17). Among the DEmiRNAs, the potential miRNAs targeting m^{6}A RNA methylation regulators were selected with the very high score (top 1%) in miRDIP. Next, the DEcircRNAs targeted miRNAs were predicted by Cancer-Specific CircRNA Database (CSCD, https://http://gb.whu.edu.cn/CSCD/). As the sponge of miRNA, the expression level of circRNA usually does not influence the expression of miRNA. In addition, some miRNAs may inhibit highly expressed mRNA in a compensatory elevated expression manner (18). Therefore, the selection of circRNA-miRNA or miRNA-mRNA pairs was not limited by their expression patterns that must be reversed. Finally, the circRNA-miRNA-mRNA regulatory network was constructed after taking the intersection of DEcircRNA-miRNA pairs and DEmiRNA–m^{6}A RNA methylation regulator pairs. The regulatory network was visualized using Cytoscape 3.4.0 (http://cytoscape.org/).

Gene Set Enrichment Analysis (GSEA)

The HCC samples from TCGA or ICGC were divided into high- and low-expression groups according to the expression level of YTHDF1, respectively. GSEA (http://software.broadinstitute.org/gsea/index.jsp) was carried out to compare the potential biological pathways between two groups. The annotated gene set list c2.cp.kegg. v5.2.symbols.gmt was utilized as the reference gene set. The cut-off criteria were defined as FDR < 0.25 and a nominal $P < 0.01$. The gene sets with top 5 normalized enrichment score (NES) in high- and low-expression groups were selected for visualization.

Cell Culture and Transfection

Human HCC cell lines Huh7, Hep3B, MHCC97H, HCCLM3, and normal LO2 cells were gained from Shanghai Advanced Research Institute, Chinese Academy of Sciences. Cells were cultured in Dulbecco's Modified Eagle's Medium (DMEM) (pH 7.4) supplemented with 10% (v/v) fetal bovine serum (Gibco). YTHDF1 siRNA, hsa-miR-139-5p mimics, circRNA overexpressing plasmid and their corresponding negative control were purchased from GenePharma (Shanghai, China). The cells in 24-well plates were transfected with 1ug plasmid, 50 nM mimics or siRNA by using Lipofectamine 3000 reagent (Invitrogen) according to the manufacturer's recommendation. The specific siRNA sequences for YTHDF1 were provided in the **Table S1**. Three independent experiments were carried out for cell transfection.

Quantitative Reverse Transcription Polymerase Reaction (qRT-PCR) Analysis

Total RNA were isolated from cells using TRIzol reagent (Invitrogen) and cDNA were synthesized by utilizing the Prime Script RT reagent kit (Takara Bio, Shiga, Japan). The SYBR® Premix Ex Taq™ (Takara) were used for qRT-PCR detection through real-time detection system (ABI7500, USA). The primer sequences for detection were provided in **Table S2**. GAPDH was used as an internal standard control. Gene expression level was quantified using $2^{-\triangle\triangle Ct}$ method. The results were obtained from three independent experiments.

Western Blot

Protein was extracted using RIPA (Beyotime, China) and separated on 10% SDS-PAGE gels and transferred onto polyvinylidene fluoride membranes (Millipore, USA). The primary antibodies of anti-YTHDF1 (#86463) and anti-GAPDH (#2118) were purchased from Cell Signaling Technology (Danvers, MA, USA). After incubating with the primary antibodies at 4°C overnight, the membranes were then subjected to HRP-conjugated secondary antibody (Cell Signaling Technology, USA) at room temperature for 1 h. The blots were visualized using an imaging system (Bio-Rad, USA).

Agarose Gel Electrophoresis Analysis

Total RNA isolation and cDNA synthesis were mentioned as above. Total DNA was extracted using the SteadyPure Universal Genomic DNA Extraction Kit (Accurate Biology Co. Ltd., Changsha, China). The specific divergent primers and convergent primers for circMAP2K4 were used for amplification. The primer sequences were listed in **Table S2**. Then the amplification products were detected in 2% agarose gel electrophoresis. And those products amplified by divergent primers were used for Sanger sequencing to detect the junction site of circMAP2K4. Three independent experiments were carried out for agarose gel electrophoresis analysis.

Cell Proliferation Assay

The transfected cells were seeded in 96-well plates at a density of 2,000 cells per well. Cell viability was accessed from 12 to 120 h by using the Cell Counting Kit-8 (CCK-8) according to the manufacturer's recommendation (Dojindo, Kumamoto, Japan). The optical density (OD) was recorded at 450 nm by an automatic microplate reader (Synergy4; BioTek, Winooski, VT, USA). The results were obtained from three independent experiments.

Luciferase Reporter Assay

The wild type or mutated circRNA sequence containing hsa-miR-139-5p binding site, the wild type or the mutated 3' untranslated region (UTR) of YTHDF1, were respectively synthesized and inserted into pmiR-RB-REPORT™ vector (RIBOBIO, Guangzhou, China). The above vectors and hsa-miR-139-5p mimics or negative control were co-transfected into cells using Lipofectamine3000 (Invitrogen). 48 h after transfection, the cells were harvested for firefly and renilla luciferase activities detection by using the dual-luciferase reporter assay system (Promega, Massachusetts, USA). Renilla luciferase served as the internal control for luciferase activity. The results were obtained from three independent experiments.

Statistical Analysis

OS differences between high and low expression groups were evaluated by Kaplan-Meier survival analysis and log-rank test.

The differences of gene expression between each clinicopathological characteristics were evaluated by Mann-Whitney-Wilcoxon Test. Data differences between in-vitro experimental groups were analyzed by Student's t-test or one-way analysis of variance (ANOVA). All tests were analyzed using R software version 3.4.2 and $P < 0.05$ was considered statistically significant.

RESULTS

Most m^{6}A RNA Methylation Modulators Are Up-Regulated and Correlated With the Prognosis of HCC

In TCGA project, all m^{6}A RNA methylation modulators were up-regulated in HCC, but the expression difference of METL14 and ZC3H13 were not statistically significant (**Figure 1A**). In ICGC project, most m^{6}A RNA methylation modulators except ZC3H13 were up-regulated in HCC, but the up-regulation of METTL14 was not statistically different (**Figure 1B**). Next, we analyzed the prognostic values of 11 commonly DE m^{6}A RNA methylation modulators in both TCGA and ICGC. High expression of YTHDF2, YTHDF1, KIAA1429, HNRNPC, WTAP, METTL3, or RBM15 was correlated with the poor survival of HCC in TCGA project by univariate Cox regression survival analysis (**Figure 1C**). While in ICGC project, high expression of METTL3, YTHDF2, HNRNPC, YTHDF1, YTHDC2, RBM15, or ALKBH5 was associated with poor survival of HCC (**Figure 1D**). Thus, the commonly prognostic m^{6}A RNA methylation modulators, namely METTL3, YTHDF2, HNRNPC, YTHDF1 and RBM15, in both TCGA and ICGC were used for the following study.

Construction of CircRNA-miRNA- m^{6}A RNA Methylation Modulator Regulatory Network in HCC

By screening of miRNA-seq data from paired tumor and adjacent non-tumor tissues in TCGA HCC cases, a total of 121 DEmiRNAs (29 up and 92 down) were obtained (**Figure 2A**). From the circRNA microarray data of paired tumor and adjacent non-tumor tissues in 3 GEO datasets, a total of 22 DEcircRNAs (eight up and 14 down) were identified (**Figure 2B**). 209 miRNA-m^{6}A RNA methylation modulators pairs and 1260 circRNA-miRNA pairs were predicted by miRDIP and CSCD, respectively. After taking the intersection of these RNA pairs, 3 m^{6}A RNA methylation modulators (HNRNPC, YTHDF1, and YTHDF2), 11 DEmiRNAs, and eight DEcircRNAs were utilized to construct a circRNA-miRNA-m^{6}A RNA methylation modulator regulatory network. This network contained 16 circRNA-miRNA pairs and 11 miRNA-mRNA pairs (**Figure 2C**). In order to verify the expression stability of DEmiRNAs and DEmRNAs in the regulatory network, we further analyzed the expression of DEmiRNAs in HCC by using dbDEMC 2.0, a database of differentially expressed miRNAs in human cancers (19) and the expression of DEmRNAs in HCC by using HCCDB, a database of hepatocellular carcinoma expression atlas (20), respectively. The results showed that most DEmiRNAs had the same expression trend in multiple GEO datasets, which were consistent with the

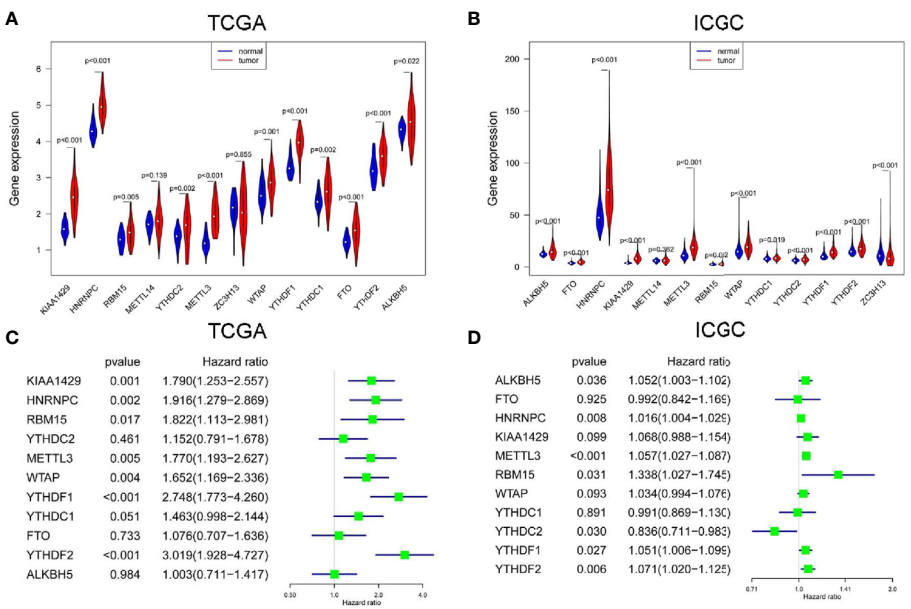

FIGURE 1 | The expression and prognostic value of m6A RNA methylation modulators in HCC. The expression of m6A RNA methylation modulators in paired hepatocellular carcinoma (HCC) and normal tissues from The Cancer Genome Atlas (TCGA) **(A)** and International Cancer Genome Consortium (ICGC) **(B)**. The univariate Cox regression analysis of m6A RNA methylation modulators for OS of HCC cases from TCGA **(C)** and ICGC **(D)**.

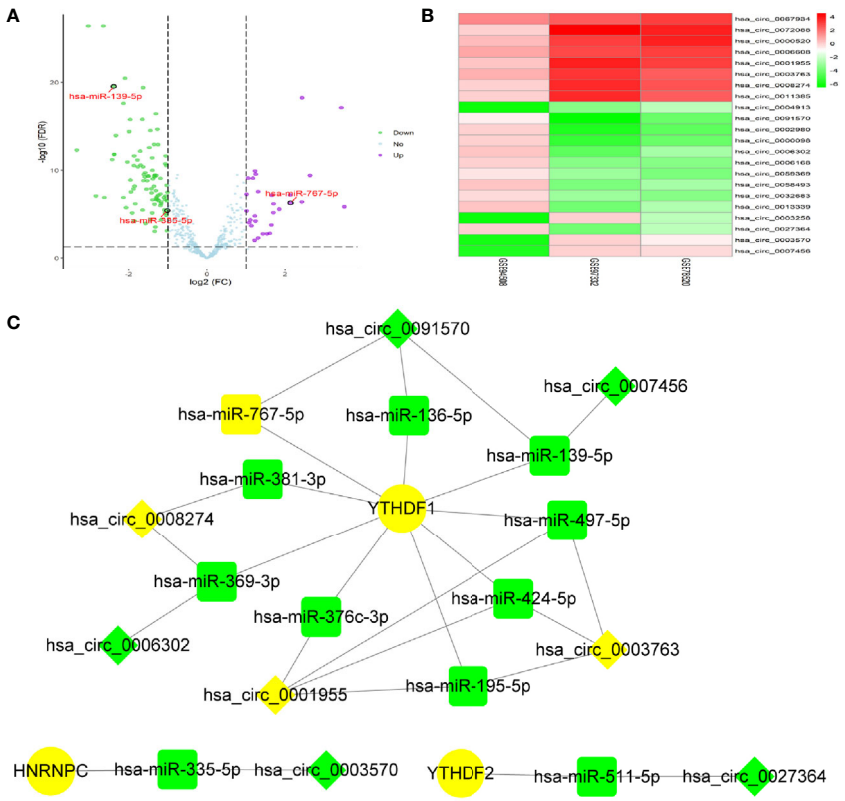

FIGURE 2 | Identification of DEmiRNAs and DEcircRNAs for network construction. **(A)** The DEmiRNAs were screened out from The Cancer Genome Atlas (TCGA). **(B)** The DEcircRNAs were screened out from three GEO datasets. **(C)** Construction of circRNA-miRNA-mRNA network based on m6A RNA methylation modulators with prognostic value. The diamond, rectangle and ellipse indicated circRNA, miRNA, and mRNA, respectively. Yellow and light green represented up- and down-regulated, respectively.

results from TCGA and ICGC (**Table S3**). Especially, hsa-miR-139-5p was down-regulated in HCC tissues from even six datasets. Similarly, in accordance with the TCGA and ICGC results, the expression of YTHDF1, HNRNPC or YTHDF2 was up-regulated in HCC from seven, six, or four datasets, respectively (**Table S4**).

Co-Expression and Clinicopathological Characteristics Correlation Analysis of miRNA

In order to identify the most potentially interactive miRNA-mRNA pairs, co-expression status between 11 DEmiRNAs and 3 m^6A RNA methylation modulators were performed by Pearson correlation analysis. Three co-expressed miRNA-m^6A RNA methylation modulator pairs were identified. As shown in **Figure 3A**, hsa-miR-139-5p expression was negatively correlated with YTHDF1 (r=-0.399, P<0.001), while hsa-miR-335-5p was positively correlated with HNRNPC (r=0.189, P<0.001) and hsa-miR-767-5p was positively correlated with YTHDF1 (r=0.224, P<0.001). Additionally, high expression of hsa-miR-139-5p but neither hsa-miR-335-5p nor hsa-miR-767-5p was significantly correlated with the low pathological grade in TCGA project (**Figure 3B**). Similarly, the higher the hsa-miR-139-5p expression, the earlier the TNM stage (**Figure 3C**).

Clinicopathological Characteristics Correlation and GSEA of m^6A RNA Methylation Modulators

In accordance with the negative correlation of hsa-miR-139-5p and YTHDF1 expression, the expression of YTHDF1 were higher in high pathological grade and advanced TNM stage in TCGA project (**Figure 4A**). While the expression of HNRNPC were significant different between different pathological grades but not between early and advanced TNM stage in TCGA project (**Figure 4B**). The relationships between YTHDF1 or HNRNPC expression and clinicopathological characteristics could not be fully investigated due to the lack of data about pathological grade in ICGC project. The expression of YTHDF1 or HNRNPC was significantly higher in the advanced TNM stage of HCC from ICGC project (**Figure S3A**). Based on the clinical significance of YTHDF1 in both TCGA and ICGC, we further performed GSEA to explore whether biological pathways differ between high and low YTHDF1 expression groups. Among top five gene sets based

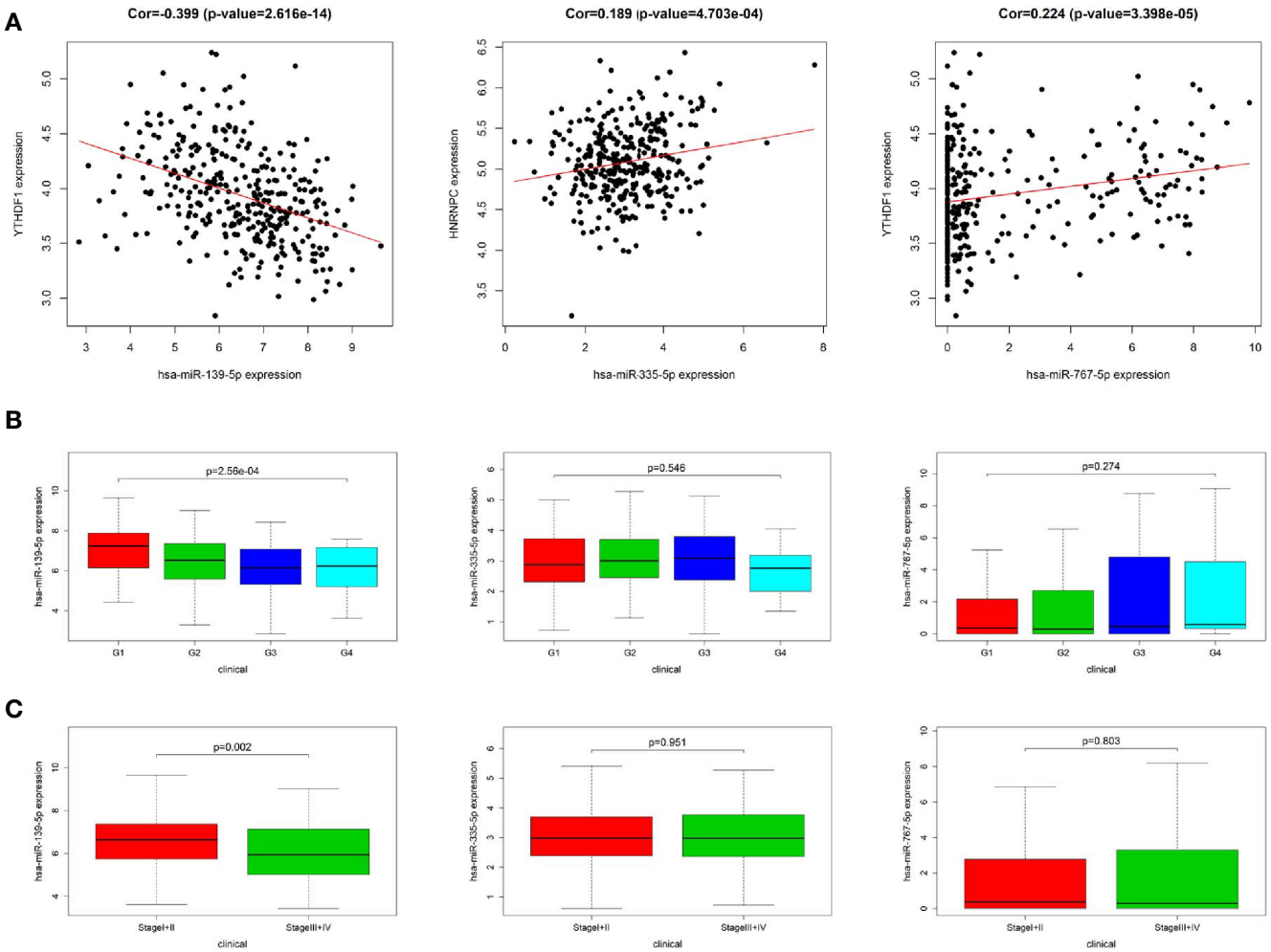

FIGURE 3 | Relationship between miRNAs and m6A RNA methylation modulators as well as clinicopathological characteristics in The Cancer Genome Atlas (TCGA). **(A)** Co-expression analysis between three miRNAs and two m6A RNA methylation modulators. **(B)** Comparison of three miRNAs expression level between different pathological grades. **(C)** Comparison of three miRNAs expression level between different stages.

on NES, cell cycle, base excision repair and homologous recombination were enriched in YTHDF1 high expression group in both TCGA and ICGC (**Figure 4C**, **Figure S3B**). While fatty acid metabolism, retinol metabolism, complement and coagulation cascades were enriched in YTHDF1 low expression group in both TCGA and ICGC (**Figure 4C**, **Figure S3B**).

Prognostic Value of the hsa-miR-139-5p and YTHDF1 Signature and Hub circRNA Network Construction

Based on the co-expressed results of miRNA and m^{6}A RNA methylation modulators, we further explored the prognostic value of 3 miRNA. Survival analysis revealed that only the hsa-miR-139-5p expression status was correlated with the OS for HCC patients (**Figure 5A**). Similar results were observed in GSE31384 (**Figure 5B**). According to the results that hsa-miR-139-5p high or YTHDF1 low expression was associated with the better OS of HCC, we further evaluated the prognosis of HCC patients with hsa-miR-139-5p high and YTHDF1 low expression. The results showed that HCC patients with hsa-miR-139-5p high and YTHDF1 low expression had longer OS time than those with contrast expression level (**Figure 5C**). Based on the clinical significance of hsa-miR-139-5p and YTHDF1, a hub circRNA-miRNA-mRNA regulatory network was constructed finally. This hub network contained two regulatory axes, namely hsa_circ_0007456/hsa-miR-139-5p/YTHDF1 and hsa_circ_0091570/hsa-miR-139-5p/YTHDF1 (**Figure 5D**).

CircMAP2K4 Promotes HCC Proliferation by Modulating hsa-miR-139-5p/YTHDF1

Two potentially dysregulated circRNAs were predicted to involve in regulating hsa-miR-139-5p/YTHDF1 axis in this study. We further analyzed the potential interaction of circRNA and

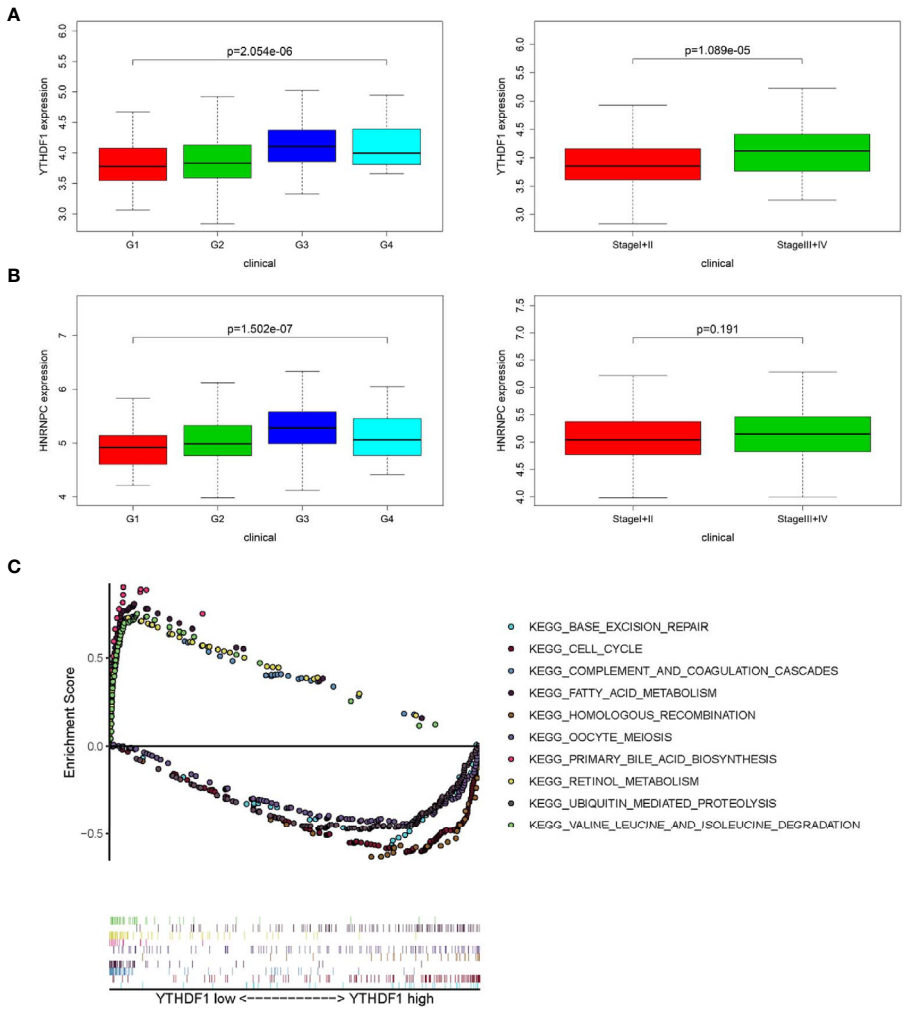

FIGURE 4 | Relationship between m6A RNA methylation modulators and clinicopathological characteristics and gene set enrichment analysis (GSEA) in The Cancer Genome Atlas (TCGA). **(A)** Comparison of YTHDF1 expression level between different pathological grades and stages. **(B)** Comparison of HNRNPC expression level between different pathological grades and stages. **(C)** GSEA results showing the top five gene sets based on normalized enrichment score in YTHDF1 high or low expression groups.

miRNA through miRanda v3.3a, a microRNA target scanning algorithm. The result showed that hsa_circ_0007456 is predicted to has a score of 140 and energy of -19.98 kCal/Mol to interact with hsa-miR-139-5p, which is favorable for hsa_circ_0007456 serving as hsa-miR-139-5p sponge. But no predicting results were provided for the interaction of hsa_circ_0091570 and hsa-miR-139-5p. Thus, we selected the hsa_circ_0007456 for the following study. Hsa_circ_0007456 (circMAP2K4) derived from mitogen activated protein kinase kinase 4 (MAP2K4) gene and its position is located in chr17:11984672-12016677. The expression of circMAP2K4 or hsa-miR-139-5p was the highest in Huh7; moderate in Hep3B and MHCC97H; and lowest in HCCLM3 (**Figure S4A**). In contrast, the mRNA and protein expression of YTHDF1 were the highest in HCCLM3; moderate in Hep3B and MHCC97H; and lowest in Huh7 (**Figure S4A**). Agarose gel electrophoresis results showed that the amplified product of divergent primers for circMAP2K4 could be detected in cDNA but not in gDNA. (**Figure S4B**). Sanger sequencing also confirmed the junction site of circMAP2K4 provided by Circular RNA Interactome (**Figure S4C**). These results indicated that circMAP2K4 was a covalently closed-loop RNA. In order to explore the function of YTHDF1, two siRNAs were designed to knockdown the expression of YTHDF1 in MHCC97H and HCCLM3 cells. The results showed that these two siRNAs could effectively decrease the mRNA and protein expression of YTHDF1 in MHCC97H and HCCLM3 cells (**Figure S4D**). Transfection of YTHDF1 siRNAs significantly inhibited the proliferation of MHCC97H and HCCLM3 cells (**Figure 6A**). Next, we explored the function of circMAP2K4 on regulating hsa-miR-139-5p/YTHDF1 axis. Transfection of hsa-miR-139-5p mimics or circMAP2K4 expressing plasmid could effectively increase the expression of hsa-miR-139-5p (**Figure S4E**) or

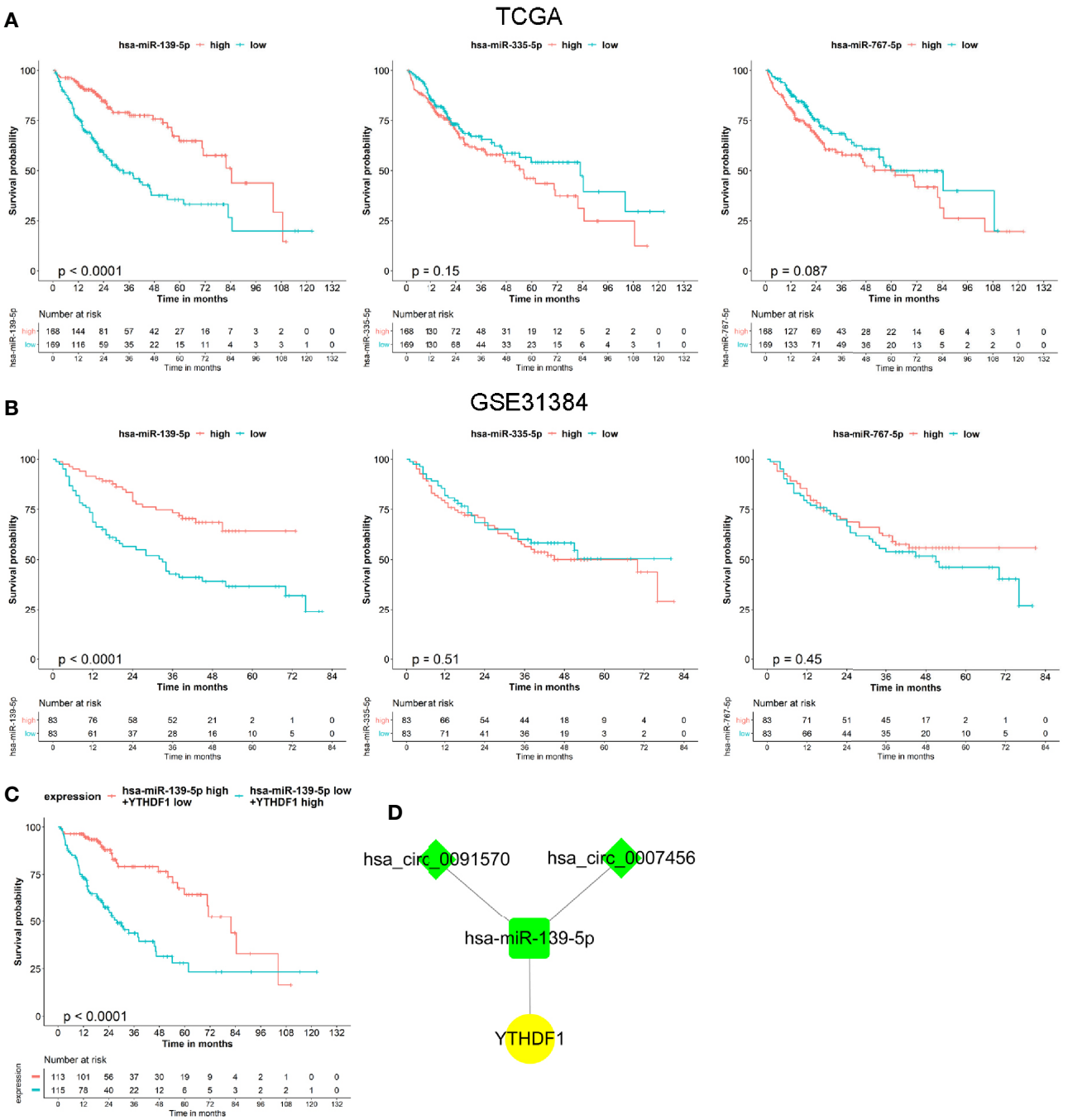

FIGURE 5 | The prognostic value of miRNAs and hub circRNA regulatory network construction in hepatocellular carcinoma (HCC). **(A)** The Kaplan–Meier survival analysis of HCC cases with different miRNA expression level in The Cancer Genome Atlas (TCGA). **(B)** The Kaplan–Meier survival analysis of HCC cases with different miRNA expression level in GSE31384. **(C)** The Kaplan–Meier survival analysis of HCC cases with different expression level of hsa-miR-139-5p and YTHDF1 in TCGA. **(D)** Construction of hub circRNA regulatory network based on hsa-miR-139-5p/YTHDF1 axis. The diamond, rectangle and ellipse indicated circRNA, miRNA, and mRNA, respectively. Yellow and light green represented up- and down-regulated, respectively.

circMAP2K4 (**Figure S4F**), respectively. The luciferase assay showed that the luciferase activity was inhibited when co-transfection of hsa-miR-139-5p mimics and reporter plasmids containing circMAP2K4 wide type sequence with hsa-miR-139-5p binding site. While the luciferase activity had no obvious change when co-transfection of hsa-miR-139-5p mimics and reporter plasmids containing circMAP2K4 mutant sequence (**Figure S4G**). Using the miRanda algorithm, we found that

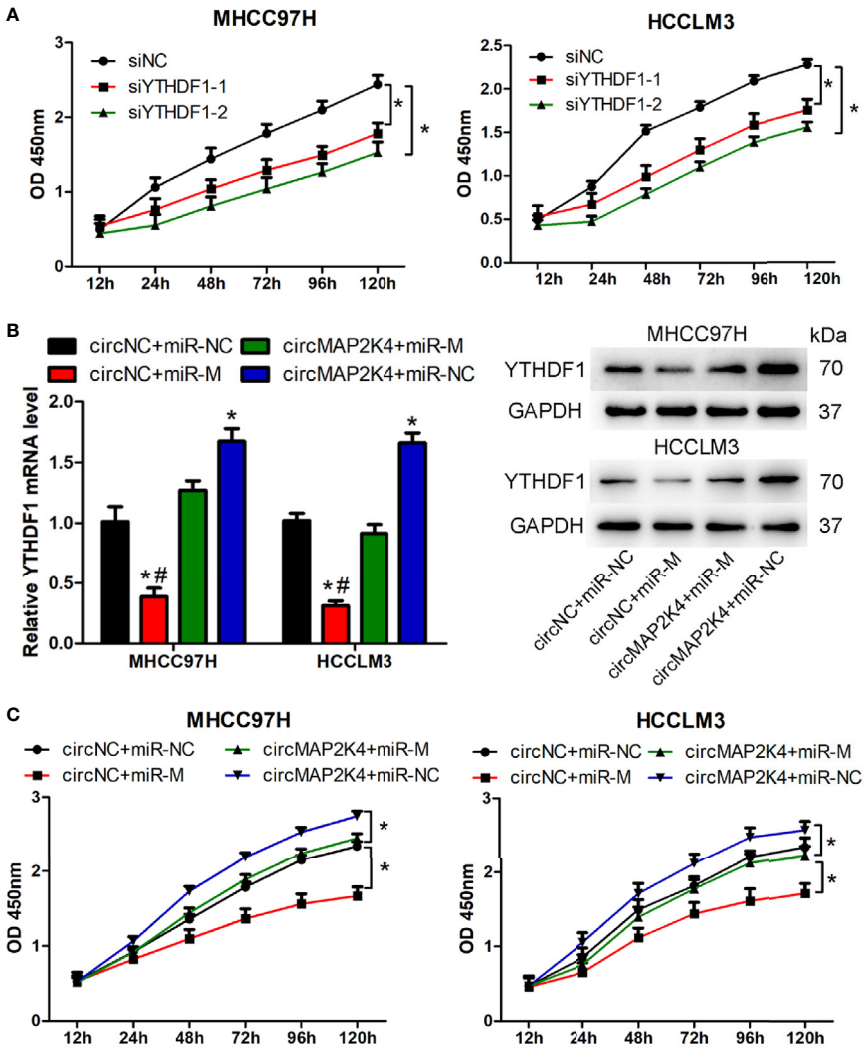

FIGURE 6 | Overexpression of hsa_circ_007456(circMAP2K4) reverses the inhibitory effects of miR-139-5p on the proliferation of hepatocellular carcinoma (HCC) cells. **(A)** CCK8 assay showed the proliferation of HCC cells transfected with YTHDF1 siRNAs or negative control. *$P < 0.05$ vs. negative control. **(B)** qRT-PCR and western blot analysis of YTHDF1 in HCC cells at 24 h after transfection with circMAP2K4 expressing plasmid and or miR-139-5p mimics. *$P < 0.05$ vs. negative control, #$P < 0.05$ vs. circMAP2K4+miR-M group. **(C)** CCK8 assay showed the proliferation of HCC cells transfected with circMAP2K4 expressing plasmid and or miR-139-5p mimics. siNC, siRNA negative control for YTHDF1; siYTHDF1: siRNA specifically against YTHDF1, miR-NC: miRNA negative control, miR-M: miRNA mimics, circNC: negative control for circMAP2K4 expressing plasmid. *$P < 0.05$ vs. negative control.

YTHDF1 contains miRNA response element of hsa-miR-139-5p. Similarly, the luciferase activity of YTHDF1 wide type reporter plasmids was significantly inhibited by transfection of hsa-miR-139-5p mimics (**Figure S4G**). Transfection of hsa-miR-139-5p mimics significantly down-regulated the mRNA and protein expression of YTHDF1 in HCC cells, whereas these effects were reversed by circMAP2K4 overexpression (**Figure 6B**). Moreover, enforced hsa-miR-139-5p expression significantly inhibited the proliferation of HCC cells. However, additive circMAP2K4 overexpression partly abrogated the inhibitory effect of hsa-miR-139-5p on cell proliferation (**Figure 6C**). These results suggested that circMAPK4 acts as has-miR-139-5p sponge to regulate the expression and activity of YTHDF1.

DISCUSSION

The m^{6}A RNA modification is a dynamic and reversible process, which is related to various diseases such as obesity, infertility and cancer (21). Numerous studies have confirmed that circRNAs act as miRNA sponges to modulate the pathogenesis of cancer, which facilitates them to serve as diagnostic and prognostic biomarkers and even therapeutic targets for tumors, including HCC (22). In the present study, we demonstrated that most m^{6}A RNA methylation modulators are up-regulated and correlated with the prognosis of HCC. Based on the prognostic m^{6}A RNA methylation modulators, a circRNA-miRNA-mRNA regulatory network was constructed. Among this network, hsa-miR-139-

5p/YTHDF1 axis was illustrated to be associated with clinicopathological characteristics and prognosis of HCC. Moreover, circMAP2K4 could serve as the hsa-miR-139-5p sponge to up-regulate YTHDF1 expression and promote HCC proliferation.

In this study, METTL3, YTHDF2, HNRNPC, YTHDF1, and RBM15 were identified as the commonly prognostic m^6A RNA methylation modulators for HCC in both TCGA and ICGC projects. Finally, 3 m^6A RNA methylation modulators, namely HNRNPC, YTHDF1, and YTHDF2, were included for the construction of circRNA regulatory network. Our findings were consistent with previous reports that high expression of YTHDF1, HNRNPC, or METTL3 is related to the poor prognosis of HCC (23–25). While high level of METTL3 or YTHDF2 can be used as the poor prognostic factor for hepatoblastoma (26). In addition, the combination of YTHDF1 and METTL3 can reflect the malignant degree and evaluate the prognosis of HCC (27). Combining the biomarkers reported in the previous reports and the prognostic m^6A RNA methylation modulators found in this study, we may try to construct a predictive signature related to the prognosis of HCC in the future study. This may be more beneficial to the evaluation of the prognosis of patients with HCC.

Accumulating evidence revealed that m^6A writers, erasers, and readers participate in the development and progression of HCC by targeting various tumor-related genes. For example, overexpression of METTL3 promotes cell proliferation, migration, and clonal formation by inhibiting suppressor of cytokine signaling 2 mRNA expression in a m^6A-YTHDF2-dependent manner (28). RAD52 motif 1 (RDM1) binds to the tumor suppressor p53 and enhances its stability, while METTL3 overexpression can significantly reduce the expression of RDM1 mRNA through m^6A modification (24). In addition, knockdown of METTL3 results in the down-regulation of Snail, a key transcription factor of epithelial-mesenchymal transition (EMT), thereby reducing the invasion and EMT of HCC cell lines (29). As an m^6A reader, YTHDF is also involved in the occurrence of HCC. YTHDF1 promotes HCC progression by enhancing FZD5 mRNA translation or AKT/GSK-3β/β-catenin signaling activation (30, 31). YTHDF2 is involved in the decay of IL11 and Serpine2 mRNA, which are important genes that regulate the normalization and inflammation of vessels (32). The expression of YTHDF2 in HCC is specifically induced by hypoxia, and overexpression of YTHDF2 inhibits cell proliferation, tumor growth and the activation of MEK and ERK. Mechanistically, YTHDF2 can bind to the 3′UTR m^6A modification site of EGFR, and down-regulate the expression of EGFR mRNA in HCC cells (33). However, the specific mechanisms of HNRNPC in the development of HCC remain unclear. In this study, GSEA results showed that cell cycle, base excision repair and homologous recombination were enriched in YTHDF1 high expression group. Emerging studies had showed that cell cycle dysregulation and DNA damage repair are involved in HCC progression (34, 35), which indicates that high expression of YTHDF1 may promote the progression of HCC by regulating cell cycle progression and DNA damage repair. We also confirmed that knockdown the expression of YTHDF1 could inhibit the proliferation of HCC. These findings explain to some extent the reasons for high YTHDF1 expression was associated with high pathological grade, advanced TNM stage and poor survival of HCC in both TCGA and ICGC project. Combining the reported results with our findings indicate that m^6A RNA methylation modulators play important roles in the occurrence and development of HCC.

Previous studies have demonstrated that some miRNAs participate in the regulation of RNA methylation modulators. For instance, hsa-miR-145 and YTHDF2 mRNA levels were negatively correlated in HCC tissues and overexpression of hsa-miR-145 could down-regulate the expression of YTHDF2, thereby increasing the mA level in HCC cells (36). In hepatoblastoma, METTL3 is identified as a direct target of hsa-miR-186, and the hsa-miR-186/METTL3 axis participates in the progress of hepatoblastoma through the Wnt/β-catenin signaling pathway (26). In this study, YTHDF1 was predicted to be the target gene of hsa-miR-139-5p and hsa-miR-767-5p with a co-expression relationship, and HNRNPC was co-expressed with and predicted to be targeted by hsa-miR-335-5p. There are no reports about these miRNAs acting on these m^6A regulators right now. However, all three miRNAs have been shown to be involved in the development of HCC. For example, high expression of hsa-miR-139-5p and hsa-miR-335-5p can inhibit the proliferation and invasion of HCC cells and induce tumor shrinkage (37, 38). While HCC cells with hsa-miR-767-5p overexpression have significantly higher proliferation, migration and invasion potential (39). In addition, many studies have confirmed that high expression of hsa-miR-139-5p is associated with a better prognosis of HCC (37, 40). Different from previous studies, we firstly found that hsa-miR-139-5p could act on m^6A RNA methylation modulator to regulate the progress of HCC. The present study demonstrated that the expression of hsa-miR-139-5p is negatively correlated with YTHDF1. High expression of hsa-miR-139-5p is associated with a lower grade, an earlier clinical stage, and a better prognosis of HCC, while high expression of YTHDF1 shows the contrast relationship. Moreover, in-vitro experiments also demonstrated that overexpression of hsa-miR-139-5p could inhibit the proliferation of HCC by targeting YTHDF1. These findings suggest that hsa-miR-139-5p/YTHDF1 regulatory axis play an important role in the development of HCC.

According to the important role of hsa-miR-139-5p/YTHDF1 regulatory axis in the progression of HCC, we further evaluated the candidate circRNAs involving in regulating hsa-miR-139-5p and hsa_circ_0007456 and hsa_circ_0091570 were identified finally. As for hsa_circ_0091570, it serves as hsa-miR-1307 sponge and its inhibition promotes HCC cell proliferation, migration and tumor growth in the mouse xenograft model (41). However, to date, the function of hsa_circ_0007456 (circMAP2K4) has not been reported in HCC, which encourages us to test whether circMAP2K4 can also function as miRNA sponge like hsa_circ_0091570 in regulating the proliferation of HCC. We firstly demonstrated that circMAP2K4, hsa-miR-139-5p and YTHDF1 participate in

regulating the proliferation of HCC. Importantly, we validated that circMAP2K4 has the bind site for hsa-miR-139-5p and could reverse the repression of hsa-miR-139-5p on YTHDF1, thus eliminating the inhibitory effect of hsa-miR-139-5p on cell proliferation. YTHDF1 high expression was correlated with high pathological grade and advanced stage, which indicates YTHDF1 may be involved in the migration and metastasis of HCC. Indeed, previous studies have confirmed that upregulation of YTHDF1 improve the migratory and invasive capabilities of HCC cells (30, 31), which provide clues for the investigation of circMAP2K4/miR-139-5p/YTHDF1 axis in the migration and metastasis of HCC in our future study.

There are several limitations in this study. First, the datasets included in this study were from different sources, in which the circRNA data were obtained from the microarray data of GEO, while the data of miRNA and m^6A RNA methylation modulators were obtained from the sequencing data of TCGA or ICGC. Different data sources may affect the reliability of the conclusions to a certain extent. There was no survival information related to the circRNA microarray of HCC in GEO database and due to our lack of HCC tissues, we were unable to evaluate the prognostic value of circRNAs for HCC. Second, due to the limited datasets included in this study, it may lead to that these identified DERNAs were not the most representative although we have verified the expression status of DERNAs through different databases. Moreover, with the advancement of technology and research, more and more m^6A RNA methylation modulators are discovered. In this study, only 13 m^6A RNA methylation modulators were included for analysis, and the threshold for circRNA selection was relatively strict, which may lead to the loss of some DEcircRNAs and m^6A RNA methylation modulators.

In conclusion, we utilize the m^6A RNA methylation modulators with prognostic value combined with DEcircRNAs and DEmiRNAs to construct a circRNA regulatory network in HCC. Among this network, the expression of hsa-miR-139-5p was negatively correlated with YTHDF1. hsa-miR-139-5p low or YTHDF1 high expression was illustrated to be associated with high grade, advanced stage and poor prognosis of HCC. The hub circRNA regulatory network was constructed based on hsa-miR-139-5p/YTHDF1 axis. In the hub network, circMAP2K4 could serve as the hsa-miR-139-5p sponge to up-regulate YTHDF1 expression and promote HCC proliferation. Our findings indicate that certain circRNA regulatory network is involved in the regulation of m^6A RNA methylation modulators and provide a novel insight into mechanism study and therapeutic targets for HCC.

DATA AVAILABILITY STATEMENT

Publicly available data sets were analyzed in this study. These data can be found here: TCGA; ICGC; GSE31384; GSE94508; GSE97332; GSE78520.

AUTHOR CONTRIBUTIONS

YuC designed the study and conducted the experiment. FC performed the specific procedures and wrote the manuscript. YoC analyzed the data and made the pictures and graphs. All the authors have read and approved the manuscript. All authors contributed to the article and approved the submitted version.

FUNDING

This study was supported by Natural Science Foundation of Guangdong Province (grant no. 2019A1515011652), Outstanding Youth Development Scheme of Nanfang Hospital, Southern Medical University (grant no. 2019J006), President Foundation of Nanfang Hospital, Southern Medical University (grant no. 2018C001), and National Natural Science Foundation of China (grant no. 81903132).

SUPPLEMENTARY MATERIAL

The Supplementary Material for this article can be found online at: https://www.frontiersin.org/articles/10.3389/fonc.2021.560506/full#supplementary-material

REFERENCES

1. Bray F, Ferlay J, Soerjomataram I, Siegel RL, Torre LA, Jemal A. Global cancer statistics 2018: GLOBOCAN estimates of incidence and mortality worldwide for 36 cancers in 185 countries. *CA: Cancer J Clin* (2018) 68(6):394–424. doi: 10.3322/caac.21492
2. Yang JD, Hainaut P, Gores GJ, Amadou A, Plymoth A, Roberts LR. A global view of hepatocellular carcinoma: trends, risk, prevention and management. *Nat Rev Gastroenterol Hepatol* (2019) 16(10):589–604. doi: 10.1038/s41575-019-0186-y
3. Roundtree IA, Evans ME, Pan T, He C. Dynamic RNA Modifications in Gene Expression Regulation. *Cell* (2017) 169(7):1187–200. doi: 10.1016/j.cell.2017.05.045
4. He L, Li H, Wu A, Peng Y, Shu G, Yin G. Functions of N6-methyladenosine and its role in cancer. *Mol Cancer* (2019) 18(1):176. doi: 10.1186/s12943-019-1109-9
5. Zeng C, Huang W, Li Y, Weng H. Roles of METTL3 in cancer: mechanisms and therapeutic targeting. *J Hematol Oncol* (2020) 13(1):117. doi: 10.1186/s13045-020-00951-w
6. Weng H, Huang H, Wu H, Qin X, Zhao BS, Dong L, et al. METTL14 Inhibits Hematopoietic Stem/Progenitor Differentiation and Promotes Leukemogenesis via mRNA m(6)A Modification. *Cell Stem Cell* (2018) 22 (2):191–205.e9. doi: 10.1016/j.stem.2017.11.016
7. Ping XL, Sun BF, Wang L, Xiao W, Yang X, Wang WJ, et al. Mammalian WTAP is a regulatory subunit of the RNA N6-methyladenosine methyltransferase. *Cell Res* (2014) 24(2):177–89. doi: 10.1038/cr.2014.3
8. Xie Y, Castro-Hernández R, Sokpor G, Pham L, Narayanan R, Rosenbusch J, et al. RBM15 Modulates the Function of Chromatin Remodeling Factor BAF155 Through RNA Methylation in Developing Cortex. *Mol Neurobiol* (2019) 56(11):7305–20. doi: 10.1007/s12035-019-1595-1
9. Hu Y, Ouyang Z, Sui X, Qi M, Li M, He Y, et al. Oocyte competence is maintained by m(6)A methyltransferase KIAA1429-mediated RNA metabolism during mouse follicular development. *Cell Death Differ* (2020) 27(8):2468–83. doi: 10.1038/s41418-020-0516-1
10. Mathiyalagan P, Adamiak M, Mayourian J, Sassi Y, Liang Y, Agarwal N, et al. FTO-Dependent N(6)-Methyladenosine Regulates Cardiac Function During

Remodeling and Repair. *Circulation* (2019) 139(4):518–32. doi: 10.1161/circulationaha.118.033794
11. Zhang S, Zhao BS, Zhou A, Lin K, Zheng S, Lu Z, et al. m(6)A Demethylase ALKBH5 Maintains Tumorigenicity of Glioblastoma Stem-like Cells by Sustaining FOXM1 Expression and Cell Proliferation Program. *Cancer Cell* (2017) 31(4):591–606.e6. doi: 10.1016/j.ccell.2017.02.013
12. Liu S, Li G, Li Q, Zhang Q, Zhuo L, Chen X, et al. The roles and mechanisms of YTH domain-containing proteins in cancer development and progression. *Am J Cancer Res* (2020) 10(4):1068–84.
13. Lan Q, Liu PY, Haase J, Bell JL, Huttelmaier S, Liu T. The Critical Role of RNA m(6)A Methylation in Cancer. *Cancer Res* (2019) 79(7):1285–92. doi: 10.1158/0008-5472.Can-18-2965
14. Jeck WR, Sorrentino JA, Wang K, Slevin MK, Burd CE, Liu J, et al. Circular RNAs are abundant, conserved, and associated with ALU repeats. *RNA (New York NY)* (2013) 19(2):141–57. doi: 10.1261/rna.035667.112
15. Lei K, Bai H, Wei Z, Xie C, Wang J, Li J, et al. The mechanism and function of circular RNAs in human diseases. *Exp Cell Res* (2018) 368(2):147–58. doi: 10.1016/j.yexcr.2018.05.002
16. Kolde R, Laur S, Adler P, Vilo J. Robust rank aggregation for gene list integration and meta-analysis. *Bioinf (Oxford Engl)* (2012) 28(4):573–80. doi: 10.1093/bioinformatics/btr709
17. Tokar T, Pastrello C, Rossos AEM, Abovsky M, Hauschild AC, Tsay M, et al. mirDIP 4.1-integrative database of human microRNA target predictions. *Nucleic Acids Res* (2018) 46(D1):D360–d70. doi: 10.1093/nar/gkx1144
18. Chen Y, Yuan B, Chen G, Zhang L, Zhuang Y, Niu H, et al. Circular RNA RSF1 promotes inflammatory and fibrotic phenotypes of irradiated hepatic stellate cell by modulating miR-146a-5p. *J Cell Physiol* (2020) 235(11):8270–82. doi: 10.1002/jcp.29483
19. Yang Z, Wu L, Wang A, Tang W, Zhao Y, Zhao H, et al. dbDEMC 2.0: updated database of differentially expressed miRNAs in human cancers. *Nucleic Acids Res* (2017) 45(D1):D812–d8. doi: 10.1093/nar/gkw1079
20. Lian Q, Wang S, Zhang G, Wang D, Luo G, Tang J, et al. HCCDB: A Database of Hepatocellular Carcinoma Expression Atlas. *Genomics Proteomics Bioinf* (2018) 16(4):269–75. doi: 10.1016/j.gpb.2018.07.003
21. Frye M, Harada BT, Behm M, He C. RNA modifications modulate gene expression during development. *Science (New York NY)* (2018) 361(6409):1346–9. doi: 10.1126/science.aau1646
22. Fu L, Jiang Z, Li T, Hu Y, Guo J. Circular RNAs in hepatocellular carcinoma: Functions and implications. *Cancer Med* (2018) 7(7):3101–9. doi: 10.1002/cam4.1574
23. Tremblay MP, Armero VE, Allaire A, Boudreault S, Martenon-Brodeur C, Durand M, et al. Global profiling of alternative RNA splicing events provides insights into molecular differences between various types of hepatocellular carcinoma. *BMC Genomics* (2016) 17:683. doi: 10.1186/s12864-016-3029-z
24. Chen SL, Liu LL, Wang CH, Lu SX, Yang X, He YF, et al. Loss of RDM1 enhances hepatocellular carcinoma progression via p53 and Ras/Raf/ERK pathways. *Mol Oncol* (2020) 14(2):373–86. doi: 10.1002/1878-0261.12593
25. Zhao X, Chen Y, Mao Q, Jiang X, Jiang W, Chen J, et al. Overexpression of YTHDF1 is associated with poor prognosis in patients with hepatocellular carcinoma. *Cancer Biomarkers section A Dis Markers* (2018) 21(4):859–68. doi: 10.3233/cbm-170791
26. Cui X, Wang Z, Li J, Zhu J, Ren Z, Zhang D, et al. Cross talk between RNA N6-methyladenosine methyltransferase-like 3 and miR-186 regulates hepatoblastoma progression through Wnt/beta-catenin signalling pathway. *Cell Proliferation* (2020) 53(3):e12768. doi: 10.1111/cpr.12768
27. Zhou Y, Yin Z, Hou B, Yu M, Chen R, Jin H, et al. Expression profiles and prognostic significance of RNA N6-methyladenosine-related genes in patients with hepatocellular carcinoma: evidence from independent datasets. *Cancer Manage Res* (2019) 11:3921–31. doi: 10.2147/cmar.S191565
28. Chen M, Wei L, Law CT, Tsang FH, Shen J, Cheng CL, et al. RNA N6-methyladenosine methyltransferase-like 3 promotes liver cancer progression through YTHDF2-dependent posttranscriptional silencing of SOCS2. *Hepatol (Baltimore Md)* (2018) 67(6):2254–70. doi: 10.1002/hep.29683
29. Lin X, Chai G, Wu Y, Li J, Chen F, Liu J, et al. RNA m(6)A methylation regulates the epithelial mesenchymal transition of cancer cells and translation of Snail. *Nat Commun* (2019) 10(1):2065. doi: 10.1038/s41467-019-09865-9
30. Liu X, Qin J, Gao T, Li C, He B, Pan B, et al. YTHDF1 Facilitates the Progression of Hepatocellular Carcinoma by Promoting FZD5 mRNA Translation in an m6A-Dependent Manner. *Mol Ther Nucleic Acids* (2020) 22:750–65. doi: 10.1016/j.omtn.2020.09.036
31. Bian S, Ni W, Zhu M, Song Q, Zhang J, Ni R, et al. Identification and Validation of the N6-Methyladenosine RNA Methylation Regulator YTHDF1 as a Novel Prognostic Marker and Potential Target for Hepatocellular Carcinoma. *Front Mol Biosci* (2020) 7:604766. doi: 10.3389/fmolb.2020.604766
32. Hou J, Zhang H, Liu J, Zhao Z, Wang J, Lu Z, et al. YTHDF2 reduction fuels inflammation and vascular abnormalization in hepatocellular carcinoma. *Mol Cancer* (2019) 18(1):163. doi: 10.1186/s12943-019-1082-3
33. Zhong L, Liao D, Zhang M, Zeng C, Li X, Zhang R, et al. YTHDF2 suppresses cell proliferation and growth via destabilizing the EGFR mRNA in hepatocellular carcinoma. *Cancer Lett* (2019) 442:252–61. doi: 10.1016/j.canlet.2018.11.006
34. Zhang L, Huo Q, Ge C, Zhao F, Zhou Q, Chen X, et al. ZNF143-mediated H3K9 trimethylation upregulates CDC6 by activating MDIG in hepatocellular carcinoma. *Cancer Res* (2020) 80(12):2599–611. doi: 10.1158/0008-5472.Can-19-3226
35. Chen CC, Chen CY, Ueng SH, Hsueh C, Yeh CT, Ho JY, et al. Corylin increases the sensitivity of hepatocellular carcinoma cells to chemotherapy through long noncoding RNA RAD51-AS1-mediated inhibition of DNA repair. *Cell Death Dis* (2018) 9(5):543. doi: 10.1038/s41419-018-0575-0
36. Yang Z, Li J, Feng G, Gao S, Wang Y, Zhang S, et al. MicroRNA-145 Modulates N(6)-Methyladenosine Levels by Targeting the 3'-Untranslated mRNA Region of the N(6)-Methyladenosine Binding YTH Domain Family 2 Protein. *J Biol Chem* (2017) 292(9):3614–23. doi: 10.1074/jbc.M116.749689
37. Hua S, Lei L, Deng L, Weng X, Liu C, Qi X, et al. miR-139-5p inhibits aerobic glycolysis, cell proliferation, migration, and invasion in hepatocellular carcinoma via a reciprocal regulatory interaction with ETS1. *Oncogene* (2018) 37(12):1624–36. doi: 10.1038/s41388-017-0057-3
38. Wang F, Li L, Piontek K, Sakaguchi M, Selaru FM. Exosome miR-335 as a novel therapeutic strategy in hepatocellular carcinoma. *Hepatol (Baltimore Md)* (2018) 67(3):940–54. doi: 10.1002/hep.29586
39. Zhang L, Geng Z, Wan Y, Meng F, Meng X, Wang L. Functional analysis of miR-767-5p during the progression of hepatocellular carcinoma and the clinical relevance of its dysregulation. *Histochem Cell Biol* (2020) 154(2):231–43. doi: 10.1007/s00418-020-01878-6
40. Wang X, Gao J, Zhou B, Xie J, Zhou G, Chen Y. Identification of prognostic markers for hepatocellular carcinoma based on miRNA expression profiles. *Life Sci* (2019) 232:116596. doi: 10.1016/j.lfs.2019.116596
41. Wang YG, Wang T, Ding M, Xiang SH, Shi M, Zhai B. hsa_circ_0091570 acts as a ceRNA to suppress hepatocellular cancer progression by sponging hsa-miR-1307. *Cancer Lett* (2019) 460:128–38. doi: 10.1016/j.canlet.2019.06.007

Conflict of Interest: The authors declare that the research was conducted in the absence of any commercial or financial relationships that could be construed as a potential conflict of interest.

frontiers in Oncology

ORIGINAL RESEARCH
published: 23 February 2021
doi: 10.3389/fonc.2021.624395

Comprehensive Analysis of Expression Regulation for RNA m6A Regulators With Clinical Significance in Human Cancers

Xiaonan Liu[1,2†], *Pei Wang*[1,3†], *Xufei Teng*[1,3†], *Zhang Zhang*[1,2,3,4*] *and Shuhui Song*[1,3,4*]

[1] National Genomics Data Center, Beijing Institute of Genomics (China National Center for Bioinformation), Chinese Academy of Sciences, Beijing, China, [2] School of Future Technology, University of Chinese Academy of Sciences, Beijing, China, [3] College of Life Sciences, University of Chinese Academy of Sciences, Beijing, China, [4] CAS Key Laboratory of Genome Sciences and Information, Beijing Institute of Genomics, Chinese Academy of Sciences, Beijing, China

Background: N6-methyladenosine (m6A), the most abundant chemical modification on eukaryotic messenger RNA (mRNA), is modulated by three class of regulators namely "writers," "erasers," and "readers." Increasing studies have shown that aberrant expression of m6A regulators plays broad roles in tumorigenesis and progression. However, it is largely unknown regarding the expression regulation for RNA m6A regulators in human cancers.

Results: Here we characterized the expression profiles of RNA m6A regulators in 13 cancer types with The Cancer Genome Atlas (TCGA) data. We showed that *METTL14*, *FTO*, and *ALKBH5* were down-regulated in most cancers, whereas *YTHDF1* and *IGF2BP3* were up-regulated in 12 cancer types except for thyroid carcinoma (THCA). Survival analysis further revealed that low expression of several m6A regulators displayed longer overall survival times. Then, we analyzed microRNA (miRNA)-regulated and DNA methylation-regulated expression changes of m6A regulators in pan-cancer. In total, we identified 158 miRNAs and 58 DNA methylation probes (DMPs) involved in expression regulation for RNA m6A regulators. Furthermore, we assessed the survival significance of those regulatory pairs. Among them, 10 miRNAs and 7 DMPs may promote cancer initiation and progression; conversely, 3 miRNA/mRNA pairs in kidney renal clear cell carcinoma (KIRC) may exert tumor-suppressor function. These findings are indicative of their potential prognostic values. Finally, we validated two of those miRNA/mRNA pairs (hsa-miR-1307-3p/*METTL14* and hsa-miR-204-5p/*IGF2BP3*) that could serve a critical role for potential clinical application in KIRC patients.

Conclusions: Our findings highlighted the importance of upstream regulation (miRNA and DNA methylation) governing m6A regulators' expression in pan-cancer. As a result, we identified several informative regulatory pairs for prognostic stratification. Thus, our study provides new insights into molecular mechanisms of m6A modification in human cancers.

Keywords: N6-methyladenosine, microRNA, DNA methylation, The Cancer Genome Atlas, prognosis

OPEN ACCESS

Edited by:
Shicheng Guo,
University of Wisconsin-Madison, United States

Reviewed by:
Jian Zhang,
University of Texas Health Science Center at Houston, United States
Wei Zhao,
Chengdu Medical College, China
Xin Zhang,
Jiangmen Central Hospital, China
Vaibhav Shukla,
Manipal Academy of Higher Education, India
Nan Lin,
Regeneron Genetic Center, United States

****Correspondence:***
Shuhui Song
songshh@big.ac.cn
Zhang Zhang
zhangzhang@big.ac.cn

[†]These authors have contributed equally to this work

Specialty section:
This article was submitted to Cancer Genetics, a section of the journal Frontiers in Oncology

Received: *31 October 2020*
Accepted: *06 January 2021*
Published: *23 February 2021*

Citation:
Liu X, Wang P, Teng X, Zhang Z and Song S (2021) Comprehensive Analysis of Expression Regulation for RNA m6A Regulators With Clinical Significance in Human Cancers. Front. Oncol. 11:624395. doi: 10.3389/fonc.2021.624395

INTRODUCTION

N6-methyladenosine (m6A) is the most abundant modification on eukaryotic mRNA. It plays crucial roles in various biological processes, including neuronal development, spermatogenesis, immune response, cell fate transition, and tumorigenesis (1–5). Dynamic m6A modification is regulated by RNA m6A regulators including methyltransferases, demethylases, and binding proteins, also known as "writers," "erasers," and "readers." METTL3, METTL14, and WTAP are core components of m6A methyltransferase complex (6–8). In addition to the core components, other associated regulatory subunits were also reported in succession, including KIAA1429, ZFP217, RBM15, RBM15B, and CBLL1 (9–11). The m6A demethylases FTO and ALKBH5 can remove m6A mark in the nucleus (2, 12). Several m6A binding proteins have been identified, such as YTH family proteins (YTHDF1/2/3, YTHDC1/2) (13–15) and IGF2BP family proteins (IGF2BP1/2/3) (16–18). Moreover, HNRNPC, HNRNPA2B1, and EIF3A also function as "readers" (19, 20). Overall, it is of great significance to elucidate the potential molecular mechanisms of m6A regulators in distinct biological contexts.

Studies have revealed that m6A modification is of essence in tumorigenesis and progression (e.g., bladder cancer, gliomas, ovarian carcinoma, colorectal carcinoma, hepatocellular carcinoma, clear cell renal cell carcinoma, endometrial cancer, breast cancer, and non-small cell lung cancer) (21–29) by controlling distinct oncogenic pathways. In addition, it has been discovered that m6A regulators have widespread genetic alterations and transcriptional dysregulation in pan-cancer, which can disturb a large number of cancer-related molecular pathways (30). Although the role of m6A modification in oncogenic pathways has been extensively documented in previous studies, the molecular determinants responsible for transcriptional dysregulation of RNA m6A regulators remain unclear. Thus, a deeper understanding is urgently needed.

As known, gene expression is regulated at multiple levels, such as epigenetics, transcription, post-transcription, and post-translation. Among them, microRNA (miRNA) and DNA methylation were widely studied for gene expression regulation (31, 32). Accumulating evidences imply that miRNA can affect the expression of oncogenes and tumor suppressor genes (33–35). For example, hsa-miR-140-5p influences cervical cancer growth and metastasis by targeting *IGF2BP1* (36). In addition, aberrant DNA methylation patterns can also alter gene expression during cancer onset and progression (37–39). For example, hypomethylation of *IGF2BP3* can result in its overexpression in breast cancer (40). Therefore, comprehensive analysis of RNA m6A regulators transcriptional dysregulation from miRNA and DNA methylation levels would be desirable to better understand the underlying mechanisms of m6A expression regulation.

In this study, we first profiled the expression variation map of RNA m6A regulators in multiple cancers. Then, we explored the regulatory roles of miRNA and DNA methylation in m6A regulators transcriptional changes. Moreover, we uncovered several key miRNAs and DNA methylation probes (DMPs). They could not only alter the expression of their corresponding m6A regulators but also act as prognostic predictors. Further analysis of these identified miRNA/mRNA regulatory pairs in kidney renal clear cell carcinoma (KIRC) clearly depicted their associations with cancer progression. Overall, our integrative analysis revealed the upstream regulatory landscape of m6A regulators, which may provide new insights into molecular mechanisms of m6A modification in human cancers and help researchers develop novel targets for cancer diagnosis and treatment.

Abbreviations: BRCA, breast invasive carcinoma; COAD, colon adenocarcinoma; HNSC, head and neck squamous cell carcinoma; KICH, kidney chromophobe; KIRC, kidney renal clear cell carcinoma; KIRP, kidney renal papillary cell carcinoma; LIHC, liver hepatocellular carcinoma; LUAD, lung adenocarcinoma; LUSC, lung squamous cell carcinoma; PRAD, prostate adenocarcinoma; STAD, stomach adenocarcinoma; THCA, thyroid carcinoma; UCEC, uterine corpus endometrial carcinoma; m6A, N6-methyladenosine; TCGA, The Cancer Genome Atlas; DMPs, DNA methylation probes; ssGSEA, single sample gene set enrichment analysis; KEGG, Kyoto Encyclopedia of Genes and Genomes.

MATERIALS AND METHODS

A bioinformatics pipeline was developed to identify upstream regulatory factors of m6A regulators (**Figure S1**). The detailed methods and tools were described as follows.

Data Collection and Processing

Multidimensional omics data (including mRNA expression, miRNA expression, and DNA methylation) of The Cancer Genome Atlas (TCGA) cancers and the corresponding clinical data were downloaded from the Broad GDAC Firehose (Stddata_2016_01_28 version, http://gdac.broadinstitute.org/). The mRNA expression data at level 3 in RNA-Seq by expectation maximization (RSEM) format, miRNA expression data in normalized reads per million (RPM) format, 450K DNA methylation array data in β-value format, as well as clinical data at level 4 were used for further analysis. To increase the credibility of comparison between tumor and normal samples, primary solid cancers with more than 25 normal samples were retained. The details of all collected datasets used in this study were summarized in **Table S1**.

Integrative Analysis of miRNA and mRNA Expression Profiles

For miRNA-regulated m6A regulators analysis, the regulatory pairs were downloaded from TargetScan (v7.0, http://www.targetscan.org/) (41) and miRTarBase (v8.0, http://mirtarbase.mbc.nctu.edu.tw/) (42). Thus, for each miRNA/mRNA pair, Spearman correlation analysis was performed using normalized expression values of mRNA-seq and miRNA-seq data. Anti-correlated miRNA/mRNA regulatory pairs (Spearman correlation coefficient (r) < 0, p-value < 0.05) were identified in tumor and normal samples, respectively (43, 44). Furthermore, the Wilcoxon rank sum test was used to identify differentially expressed miRNAs and genes (adjusted p-value < 0.05), separately. The p-value was adjusted by the false discovery rate (FDR) method. The definition of up-regulation (or down-regulation) was that the average expression value of tumor

samples was greater (or lower) than that of normal samples. All regulatory pairs, consisting of an up-regulated (or down-regulated) miRNA and its target, a down-regulated (or up-regulated) gene, were screened to build a network with the igraph package in R. The network allowed identifying hub nodes. The nodes with connections greater than or equal to 4 in each cancer were defined as hub genes. The definition of hub miRNA was that the connection of the node was not less than 2 in one cancer. Specifically, the disease and pathway enrichment analyses were performed with the online tool miEAA (v2.0, http://www.ccb.uni-saarland.de/mieaa_tool/) (45). The miRNAs from the network were picked to run miEAA using the miRNA enrichment analysis, in which two categories (disease items from the MNDR database and pathway items from the miRWalk database) were selected with default parameters' setting. The ggplot2 package in R was used for visualization.

Integrative Analysis of DNA Methylation and Gene Expression Profiles

To determine the regulation of DNA methylation on m6A regulators, DMPs in the promoter regions (TSS200 and TSS1500) of m6A regulators were selected. Spearman correlation analysis was performed on m6A regulators and their corresponding DMPs (46). As those DMPs are negatively regulating their target genes, anti-correlated regulator pairs ($r < 0$, p-value < 0.05) in tumor and normal samples were obtained. Afterward, differential methylation analysis was performed on DMPs using the ChAMP package in R. The DMPs were defined as hypermethylation (or hypomethylation) when the average β value of tumor samples was greater (or lower) than that of normal samples. Only those DMPs satisfying the criteria of FDR < 0.05 were considered as statistically significant (47). All these regulatory pairs were used to construct a biological network. The igraph package in R was used to visualize the regulatory network.

Identification of Potential Prognostic Regulatory Pairs From the Network

To assess the regulatory pairs with survival outcomes, patients were divided into two groups according to the median value of gene expression or methylation. Patients were defined as high expression or hypermethylation group if their expression or methylation values were greater than the median value. Otherwise, patients were defined as low expression or hypomethylation group. Patient survival between the two groups was assessed via Cox regression analysis. The significance of survival differences was estimated in terms of p-value. The regulatory pairs will be considered to have an impact on the prognosis of patients if both p-values were lower than 0.05. Kaplan-Meier survival curves were plotted using two R packages (survminer and survival).

Construction of Prognostic Risk Prediction Model

To acquire the main factors with better prediction effect, the least absolute shrinkage and selection operator (LASSO) Cox regression algorithm was implemented on four potential prognostic regulatory pairs in KIRC with paired miRNA-seq and mRNA-seq data from TCGA. The patients were randomly divided into training dataset ($n = 200$) and test dataset ($n = 49$). The survival and glmnet packages in R were utilized to determine key factors. The risk model was constructed by the following formula:

$$\text{RiskScore} = \sum_1^n r_i \, Exp \quad (i)$$

where r_i is regression coefficient, and $Exp(i)$ is the expression value of the corresponding factor. According to the median value of risk scores, patients were divided into high-risk and low-risk groups respectively. The LASSO regression factor was selected by the minimum value of partial likelihood binomial deviance.

GO and KEGG Enrichment Analysis

Differentially expressed genes (DEGs) between the high-risk and low-risk groups were determined utilizing the Wilcoxon rank sum test. The functional enrichment analysis of DEGs was performed using DAVID (48). Those terms with p-value lower than 0.05 were selected for subsequent analysis. The ggplot2 package was used to visualize the enrichment analysis results. The similarity of these enriched terms was measured with the R package GOSemSim (49).

Protein-Protein Interaction (PPI) Network Construction

The PPI network was constructed on STRING (v11.0, https://string-db.org/). The key different modules were selected using MCODE in Cytoscape (v3.7.0).

Immune Infiltration Analysis

The ESTIMATE algorithm was used to calculate the immune score, stromal score, and tumor purity. The marker genes of each immune cell type were collected from previous studies (50). The ssGSEA method (51) was applied to quantify the infiltration degrees of 28 immune cell types in the tumor microenvironment.

RESULTS

Comprehensive Expression Analysis Revealed the Prognostic Values of m6A Regulators in Cancers

The dynamic m6A modification is regulated by m6A "writers," "erasers," and "readers" (**Figure 1A**). We totally obtained 21 RNA m6A regulators including 8 "writers," 2 "erasers," and 11 "readers" through literature curation. We first elucidated the expression characteristics of these regulators in a pan-cancer context (**Figure 1B**): (i) Expression changes of some clusters (*YTHDF* family, *IGF2BP* family, *METTL14*, *FTO*, and *ALKBH5*) were consistent in selected cancers. For example, *YTHDF1* and *IGF2BP3* were up-regulated in 11 cancer types except for THCA. *METTL14* was down-regulated in all 11 cancer types while *FTO* and *ALKBH5* were down-regulated in most cancer types except for KIRC. (ii) Expression alterations of m6A regulators in THCA

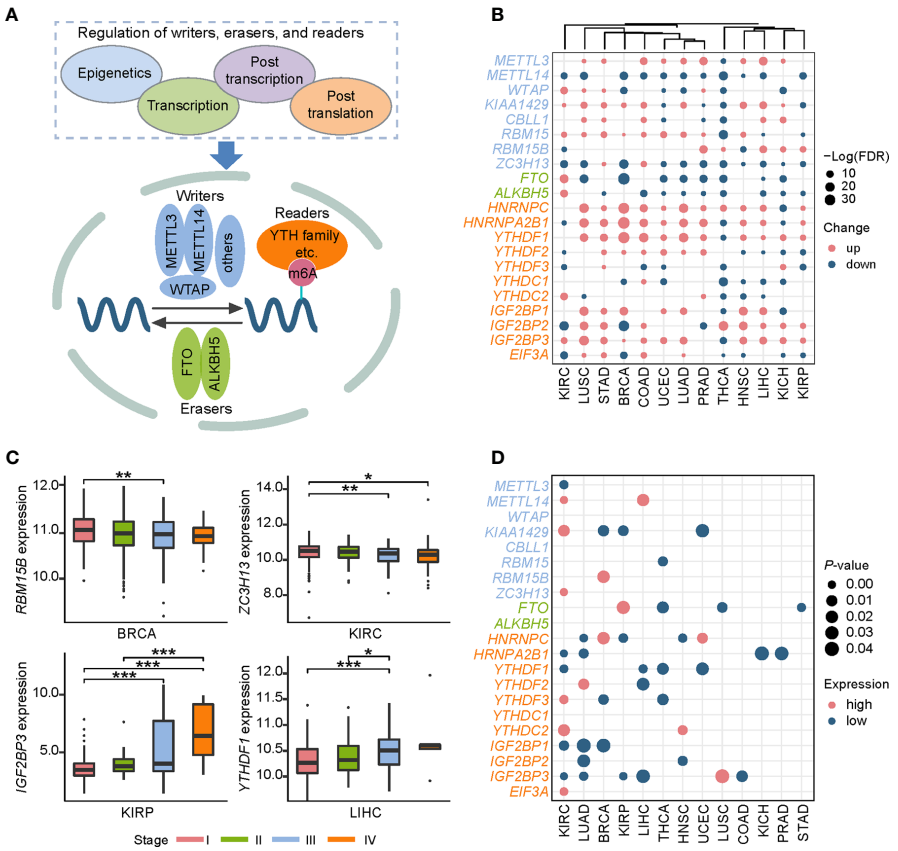

FIGURE 1 | Pan-cancer expression alterations and prognostic values of m6A regulators. **(A)** RNA m6A modification is regulated by RNA m6A regulators, including "writers"-methyltransferase, "erasers"-demethylase, and "readers"-RNA m6A binding proteins. "Writers" consist of core components *METTL3, METTL14, WTAP* and other factors (*KIAA1429, ZFP217, RBM15, RBM15B, and CBLL1*). *FTO* and *ALKBH5* are two "erasers." "Readers" include *HNRNPC, HNRNPA2B1, YTHDF1, YTHDF2, YTHDF3, YTHDC1, YTHDC2, IGF2BP1, IGF2BP2, IGF2BP3*, and *EIF3A*. **(B)** Expression profiles of RNA m6A regulators in 13 cancer types. Up represents higher expression and down represents lower expression. The circle size represents the statistical significance after controlling FDR. **(C)** Representative examples of expression patterns of m6A regulators across four cancer stages. *P < 0.05, **P < 0.01, and ***P < 0.001. **(D)** Overview of prognostic effects of m6A regulators. High represents the patients with better prognosis when gene expression level is high, and low represents the patients with better prognosis when gene expression level is low.

exhibited a specific pattern among all 13 cancers. Most RNA m6A regulators were significantly down-regulated in THCA except for *RBM15B*, *HNRNPC*, and *IGF2BP2*. These findings suggest that there are multiple mechanisms capable of controlling gene expression of m6A regulators in distinct cancers.

Combined with clinical data, we further investigated expression patterns of all m6A regulators in four different cancer stages (stage I, stage II, stage III, and stage IV), a widely used signature for predicting the outcomes of patients (**Table S2**). Two patterns significantly associated with cancer staging were observed: a decreased expression level of *RBM15B* in breast invasive carcinoma (BRCA) and *ZC3H13* in KIRC was accompanied by the progression of cancer stages, while *YTHDF1* in liver hepatocellular carcinoma (LIHC) and *IGF2BP3* in kidney renal papillary cell carcinoma (KIRP) showed the increased expression pattern (**Figure 1C**). Since cancer staging is primarily defined by clinicopathologic features, these observations suggest that m6A regulators may influence patients' survival. Furthermore, we depicted a landscape for strongly survival-related genes across 13 cancer types, and then identified several potential oncogenes and tumor suppressor genes (**Figure 1D**). For instance, *IGF2BP1* and *IGF2BP3* showed an oncogenic role in KIRC and lung adenocarcinoma (LUAD). While *METTL14* and *YTHDC2* functioned as tumor suppressors in KIRC. Both the IGF2BP family proteins, METTL14, and YTHDC2 can function in cancers through directing m6A-modified mRNAs. Together, these results indicate that m6A regulators can be used to develop novel treatment strategies.

Identification of miRNAs Targeting m6A Regulators in Pan-Cancer

As mentioned above, the expression of m6A regulators had a significant difference between tumor and normal samples. Thus, in what follows, we aimed to investigate their upstream regulatory factors that can regulate the expression of these genes. From 1,255 predicted and experimentally confirmed

miRNA/mRNA regulatory pairs, 629 regulatory pairs showing negative correlation (r < 0) across 12 cancer types were selected for further analysis. Among them, 45% (282 out of 629) significantly differentially expressed (*p*-value < 0.05; tumor vs normal) pairs (consisting of 158 miRNAs and 20 m6A regulators) (**Table S3**) were used to construct a pan-cancer miRNA-gene regulatory network (**Figure 2A**). The network showed some observations: i) *RBM15*-associated regulatory pairs were only identified in BRCA. ii) *HNRNPC*-associated regulatory pairs were presented in 11 cancer types, of which BRCA had the most 9 regulatory pairs. iii) *HNRNPA2B1* had the maximum connection. The hsa-miR-195-5p and hsa-miR-326 regulating *HNRNPA2B1* were found in more than one cancer type (**Figure 2B**). Next, we picked out all the hub miRNAs and genes (see methods for details) involving in the transcriptional regulatory network. A case in point is hsa-miR-181a-5p belonging to miR-181 family can target several m6A regulators in BRCA, LIHC, LUSC, and UCEC (**Figure 2C**). The hsa-miR-181a-5p has been reported to be associated with acute myeloid leukemia, papillary thyroid cancer, endometrial carcinoma and so on (52–54). Some m6A regulators, such as *HNRNPC*, *HNRNPA2B1*, and *FTO*, can also be targeted by several miRNAs (**Figure 2D**). In addition, statistical analysis of the network showed that 159 regulatory pairs were found in only

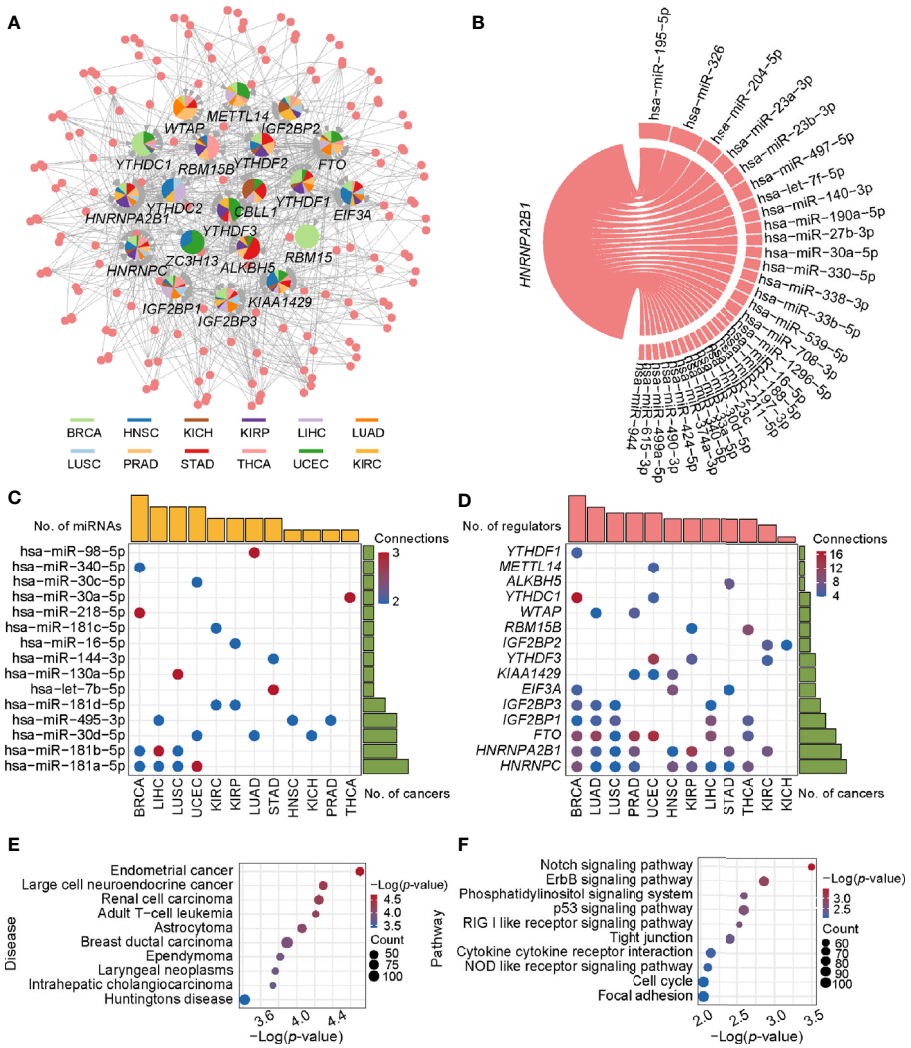

FIGURE 2 | The regulatory network and enriched pathways of miRNA-m6A regulators. **(A)** The regulatory network of miRNAs and m6A regulators in pan-cancer. In the pie chart, different colors represent different cancers, and size reflects the number of regulatory pairs. The circle represents miRNAs. The m6A regulators' names were labeled. **(B)** The *HNRNPA2B1* associated regulatory pairs in the pan-cancer network. The line width represents the number of cancers with this regulatory pair. **(C)** Statistics of hub miRNAs in 12 cancer types. When the connection of miRNA node in the network is greater than or equal to 2, the node is defined as hub miRNA. The top bar out of chart represents the number of hub miRNAs for each cancer and the right bar indicates the number of cancers for each miRNA. The redder the color, the more the connections. **(D)** Statistics of hub genes in 12 cancer types. When the connection of gene node is greater than or equal to 4, the node is defined as hub gene. The top bar out of chart is the number of hub regulators for each cancer. The right bar presented the number of cancers for each regulator. **(E)** Disease enrichment analysis of miRNAs. **(F)** Pathway enrichment analysis of miRNAs.

one cancer type and 13 regulatory pairs were found in at least 5 cancer types (**Table S4**). These results indicate that these miRNAs may play important roles in expression alterations of m6A regulators.

To further understand the functional characteristic of miRNAs in the regulatory network, we performed miRNA enrichment analysis. Among disease ontology items, they were significantly associated with several cancers (such as endometrial cancer, renal cell carcinoma, and breast ductal carcinoma) (**Figure 2E**). In addition, results from miEAA revealed that the candidate set of miRNAs was enriched in some pathways associated with cancer, immune and cellular processes, such as p53 signaling pathway, RIG I like receptor signaling pathway, and cell cycle (**Figure 2F**). More importantly, 13 of the above regulatory pairs have been reported in published studies (**Table 1**). For example, hsa-miR-145 could regulate the expression of *YTHDF2* in hepatocellular carcinoma, which further affected the m6A modification and promoted the disease progression (33). Another example, hsa-miR-188 could inhibit the proliferation, migration and invasion of glioma by suppressing the expression of *IGF2BP2* (55).

Survival analysis identified some miRNA/mRNA regulatory pairs with prognostic value (**Figures S2–S4**). Taken the hsa-miR-204-5p/*IGF2BP3* pair in KIRC for example, low expression of *IGF2BP3* and high expression of hsa-miR-204-5p exhibited a favorable outcome. Therefore, this regulatory pair was defined as a tumor-promoting pair. As for hsa-miR-96-5p/*YTHDC2*, high expression of *YTHDC2* and hsa-miR-96-5p exhibited favorable and opposite outcome respectively, which was thus defined as a tumor-antagonizing pair. Totally, 12 prognosis-related miRNA/mRNA regulatory pairs (9 tumor-promoting and 3 tumor-antagonizing pairs) in four cancer types were finally obtained (**Figure 3**). Besides, several miRNAs including hsa-miR-204-5p, hsa-miR-1307-3p, hsa-miR-96-5p, and hsa-miR-106b-5p may affect the survival and prognosis of patients by regulating the expression of *IGF2BP3*, *METTL14*, *YTHDC2*, and *YTHDF3*, respectively, in KIRC; hsa-let-7c-5p may target multiple m6A regulator genes (including *IGF2BP1* and *IGF2BP3*) in LUAD. Together, those identified miRNAs can account for the differential expression of m6A regulators, and they can serve as potential targets for cancer therapy.

DNA Methylation Probes (DMPs) Targeting m6A Regulators Are Predictive of Patients' Outcome

DNA methylation, an extensively studied epigenetic mark, can affect transcriptional dysregulation in cancers (56). Then, we addressed the effect of DNA methylation on m6A regulators transcriptional dysregulation. Spearman correlation analysis showed that DMPs were negatively correlated with their target genes in most cancers (**Figure 4A**), except that THCA exhibited minor differences between positive and negative correlations in both tumor and normal tissues. Totally, we identified 154 regulatory pairs showing the negative correlation across 11 cancer types. Among the 154 regulatory pairs, 58 unique DMPs were differential methylation. We detected much more frequent hypermethylation than hypomethylation in most cancers (**Figure 4B**). Collectively, most DMPs were hyper-methylated and negatively regulated their target genes (m6A regulators) in a pan-cancer layer. These results indicate that DNA methylation can also account for m6A expression alterations in cancers.

To show a landscape for all potential DMP/gene regulatory pairs across 11 cancer types, we further built a regulatory network (**Figure 4C**) using 100 anti-correlated regulatory pairs, involving 58 differentially methylated DMPs and 13 differentially expressed m6A regulators (**Table S5**). The network showed that *METTL14* was targeted by multiple DMPs in most cancer types. Oppositely, *KIAA1429*, *YTHDC2*, and *EIF3A* associated pairs were only found in one cancer. Based on statistical analysis of the network, we found that 33 regulatory pairs occurred only in one cancer, and 13 regulatory pairs presented in at least three cancer types (**Table S6**). In addition, we also found that *IGF2BP3* and *YTHDF2* were regulated by eight different DMPs across six cancers (**Figure 4D**). Subsequent survival analysis identified seven regulatory relationships, which may serve as tumor-promoting regulatory pairs (**Figure 5**). For example, *IGF2BP3* targeted by cg02860543 and cg07297397 could affect the survival and prognosis of patients in LIHC. Two methylation probes (cg03711622 and cg17671317) could target *HNRNPA2B1* in KIRC. The Kaplan-Meier curves showed that the expression and methylation levels of patients with better outcome were the opposite (**Figure S5**). Our findings indicate

TABLE 1 | Regulatory relationships with literature evidence.

miRNA	Gene	PMID	Journal	Disease	TCGA	m6A
hsa-miR-497	*EIF3A*	28322466	J Cell Biochem.	Pulmonary fibrosis	LIHC	–
hsa-miR-30b-5p	*FTO*	31728912	J Physiol Sci.	Hypoglycemia-associated autonomic failure	KICH, STAD, UCEC	–
hsa-miR-495	*FTO*	31709454	Pflugers Arch.	Type 2 diabetes	KIRC, STAD	–
hsa-miR-30a-5p	*FTO*	31728912	J Physiol Sci.	Hypoglycemia-associated autonomic failure	KIRP	–
hsa-miR-491-5p	*IGF2BP1*	27158341	Am J Transl Res.	Non-small cell lung cancer	LIHC	–
hsa-miR-150	*IGF2BP1*	26561465	Tumour Biol.	Osteosarcoma	KIRP	–
hsa-miR-150	*IGF2BP1*	30220021	Pathol Oncol Res.	Osteosarcoma	KIRP	–
hsa-miR-98-5p	*IGF2BP1*	28244848	Oncol Res.	Hepatocellular carcinoma	LIHC	–
hsa-miR-140-5p	*IGF2BP1*	27588393	Oncotarget.	Cervical cancer	KIRP	–
hsa-let-7b	*IGF2BP2*	27513293	Exp Dermatol.	Wound healing	HNSC, LUSC, STAD	–
hsa-miR-188	*IGF2BP2*	28901413	Mol Med Rep.	Glioma	KIRC	–
hsa-miR-145	*YTHDF2*	28104805	J Biol Chem.	Hepatocellular carcinoma	BRCA, THCA	m6A
hsa-miR-106b-5p	*YTHDF3*	30341748	Breast Cancer.	Breast cancer	KICH, LUSC, UCEC	–

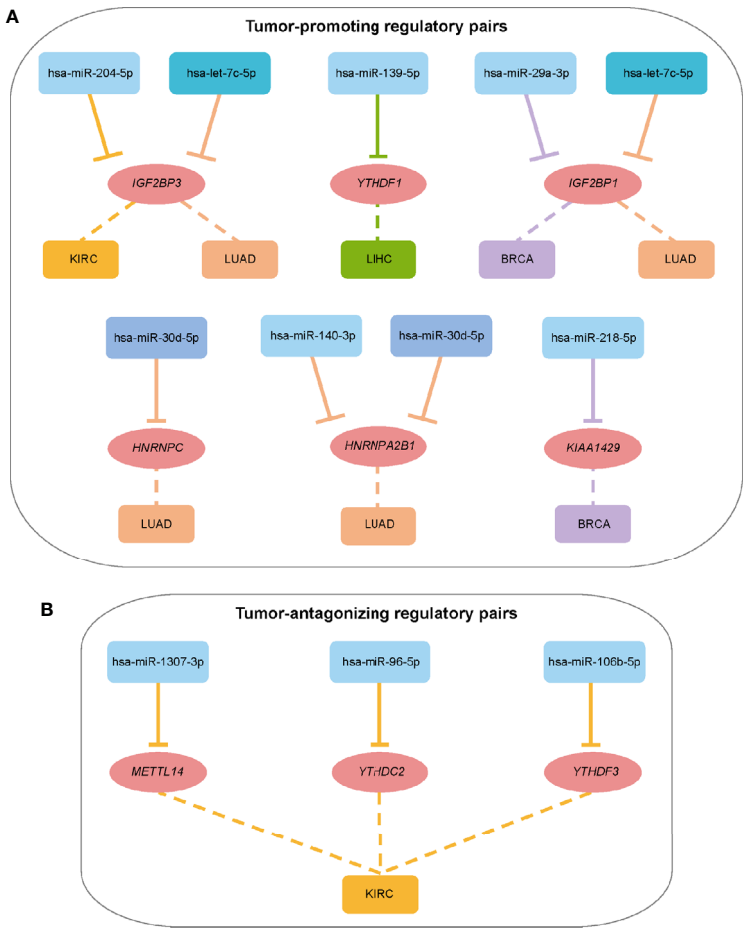

FIGURE 3 | Summary of regulatory relationships between miRNAs and m6A regulators that potentially function as tumor-promoting **(A)** and tumor-antagonizing regulatory pairs **(B)**. Lines of the same color represent the same type of cancer.

that m6A regulators with clinical significance in human cancers can be influenced by dynamic DNA methylation.

Potential Application of miRNA-m6A Regulator Pairs in KIRC Prognosis

To further explore the potential application of miRNA/mRNA regulatory pairs, subsequent in-depth analyses were focused on KIRC. We wonder whether there are any key regulators in specific cancer type. Based on 4 regulatory pairs (hsa-miR-1307-3p/*METTL14*, hsa-miR-106b-5p/*YTHDF3*, hsa-miR-96-5p/*YTHDC2*, and hsa-miR-204-5p/*IGF2BP3*) identified above in KIRC, we screened prognostic regulatory pairs that could best separate risk groups using LASSO regression analysis (**Figure 6A**). The most appropriate number of factors was 4 when the partial likelihood binomial deviance reached the minimum value. Then the four factors (hsa-miR-1307-3p, *METTL14*, hsa-miR-204-5p, and *IGF2BP3*, composed two regulatory pairs hsa-miR-1307-3p/*METTL14* and hsa-miR-204-5p/*IGF2BP3*) were selected to construct the prediction model (see details in *Materials and Methods*). Next, patients' risk score was imputed by the expression values and regression coefficients of these 4 factors. The risk score was used to divide the patients into high-risk and low-risk groups, of which the low-risk group was associated with better survival (p-value < 0.0001). Similar findings were also observed in additional validation dataset (**Figures S6**). These results disclose that expression profiles of hsa-miR-1307-3p/*METTL14* and hsa-miR-204-5p/*IGF2BP3* pairs can well characterize the survival status of patients in KIRC.

We further identified 1,314 DEGs in high-risk group against the low-risk group, including 267 up-regulated and 1047 down-regulated genes. KEGG pathway enrichment analysis of these DEGs detected multiple immune-related pathways (including complement and coagulation cascades, hematopoietic cell lineage, and chemokine signaling pathway) (**Figure 6B**). In addition, pathways related to signal transduction were enriched, such as cytokine-cytokine receptor interaction, neuroactive ligand-receptor interaction, and cell adhesion molecules, etc. Meanwhile, Gene Ontology (GO) enrichment analysis also showed that these DEGs were related to immunity and signal transduction, such as immune response, cell-cell signaling, chemokine-mediated signaling pathway, and inflammatory response (**Figure 6C).** The similarity matrix of enriched terms (**Figure 6D**) further confirmed that

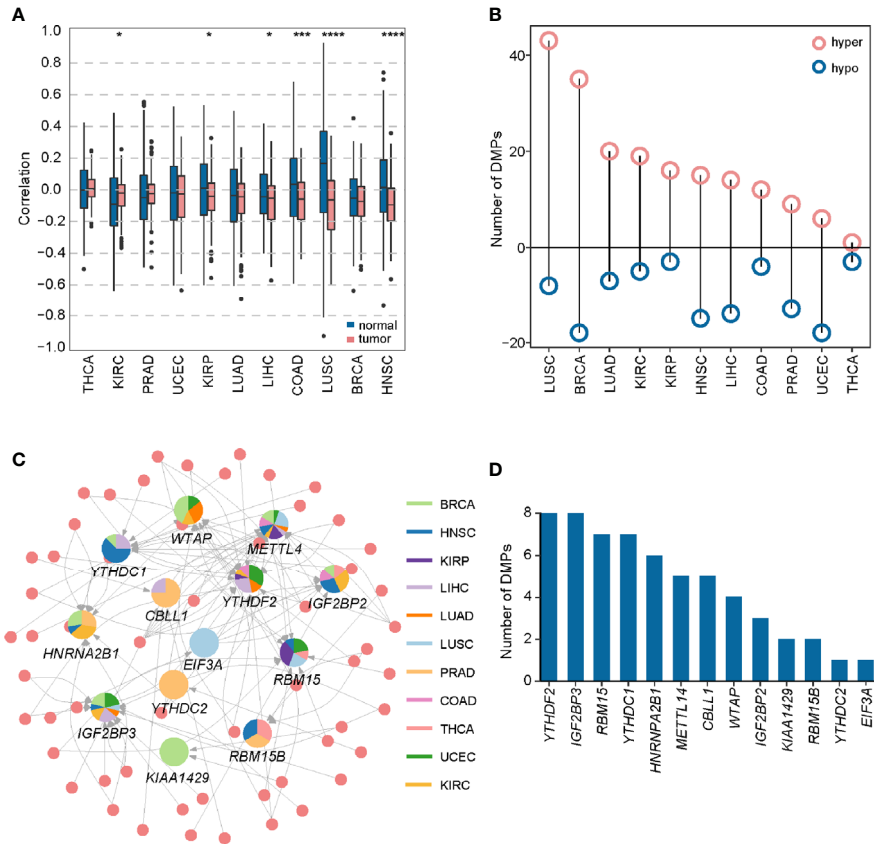

FIGURE 4 | Construction of DMP-mRNA regulatory network. **(A)** Boxplot of Spearman's correlation between DNA methylation data and mRNA-seq data across 11 cancer types. *P < 0.05, ***P < 0.001, and ****P < 0.0001. **(B)** The number of differentially methylated probes in different cancer types. **(C)** The regulatory network of DNA methylation probes and m6A regulators in pan-cancer. In the pie chart, different colors represent different cancers, and size reflects the number of regulatory pairs. The circle represents DMPs. **(D)** Statistics of the number of DMPs regulating m6A regulators in the pan-cancer regulatory network.

immune-related terms presented high similarities with those terms related to signal transduction or other processes, such as immune response and cytokine-cytokine receptor interaction. Moreover, we constructed the PPI network for DEGs with clinical significance and identified four important modules (**Figure S7A**). Of note, several immune-related genes were found in those PPI modules, such as chemokine family (*CXCL8*, *CXCL4*, *CXCL6*, *CCL5*, and *C3*), interleukin (*IL1A* and *IL6*) and so on. These results indicate that these regulatory pairs may function through immune-related mechanisms.

As the functional classes of DEGs were mainly related to immunity, we further calculated the immune score, stromal score, and tumor purity of samples belonging to each risk group. It is worth mentioning that the high-risk group had higher immune score and lower tumor purity by comparison with the low-risk group (**Figure S7B**). Recent studies found that m6A regulators were closely correlated with immune infiltration in glioma and gastric cancer (57, 58), and thus we wondered whether the immune infiltration was different between the two groups. Most immune cells have significantly higher infiltration score in the high-risk group than low-risk group (**Figure 6E**). From the correlation analysis between m6A regulators' expression and immune cell infiltration score (**Table S7**), we found that the expression of *IGF2BP3* was positively correlated with the infiltration scores across 11 immune cells, suggesting that highly expressed *IGF2BP3* may contribute strong immune infiltration and poor survival. In short, we speculate that hsa-miR-204-5p may affect the immune-related processes and immune infiltration by regulating *IGF2BP3*. Such a regulatory axis may promote the occurrence and development of KIRC.

DISCUSSION

With more effective sequencing technologies and tools (59–61), how dysregulated m6A is involved in cancer pathogenesis and progression has attracted much more attention than ever. Here, we profiled the expression variation map of RNA m6A regulators in multiple cancers and explored the upstream regulation of m6A regulators from miRNA and DNA methylation. Furthermore, we identified the potential miRNA-regulated and DNA methylation-regulated regulatory pairs and investigated the effects of miRNA/mRNA regulatory pairs on patients in KIRC.

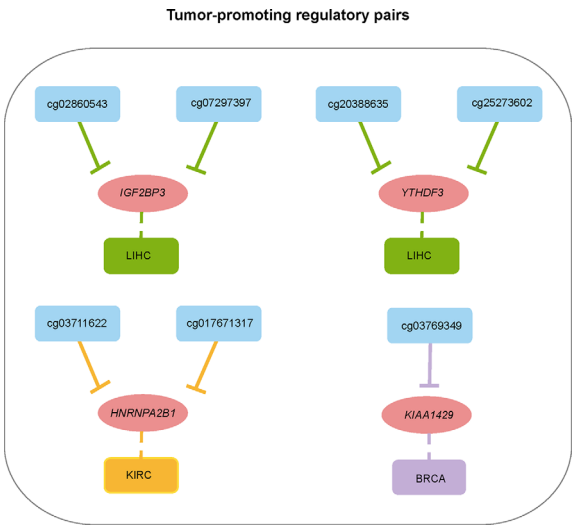

FIGURE 5 | Summary of regulatory relationships between DNA methylation probes and m6A regulators that potentially affect patients prognosis in cancers.

Till now, a few of studies have showed that transcriptional dysregulation of m6A regulators in pan-cancer (30). Here we reported the altered expression of RNA m6A regulators across 13 cancer types in comparison with normal samples, revealing two rules in expression dynamics: the expression of "reader" proteins IGF2BP family and YTHDF family were up-regulated in most cancers, while methyltransferase METTL14, demethylase FTO and ALKBH5 were down-regulated in most cancers. Besides, these varied expression levels were correlated with survival advantages or disadvantages. Although some of them have been reported to play an oncogenic or tumor-suppressive role in different cancers, the role of m6A regulators was only involved in the regulation of cancer-related gene expression (62). The reasons of m6A regulators dysregulation were unclear. As we know, miRNA (63) and DNA methylation (64) are two essential modulation for controlling gene expression, and a large amount of miRNA and DNA methylation sequencing data have been generated. Correlation analysis was first performed on individual m6A regulators for methylation and expression. Then, differential expression and methylation analysis were performed on individual miRNA and DMP. We built regulatory networks with identified potential miRNA/gene and DMP/gene regulatory pairs, in which some pairs had been reported to exert positive effect on cancer pathogenesis and progression. For example, hsa-miR-150/*IGF2BP1* regulatory pair was reported to be a novel potential therapeutic target for osteosarcoma treatment (65), and *IGF2BP1* was identified as a novel target gene of hsa-miR-98-5p in hepatocellular carcinoma (66). Similarly, the DNA demethylation in the promoter region of *IGF2BP3* could influence the progression of G-CIMP gliomas (67), and cg07166550/*ALKBH5* could be used as prognostic biomarkers in prostate cancer (68). Finally, we identified some regulatory pairs with prognostic significance in several cancers. Moreover, studies have reported that differential expression or methylation is highly related with tumorigenesis through regulating gene expression (69–72). Our study identified miRNAs/probes that were differentially expressed/methylated between tumor and normal samples, indicating their potential association with tumorigenesis. Based on four cancer stages, we found that two miRNAs and one probe were relevant to tumor progression (**Figure S8**). Among them, a decreased expression of hsa-miR-204-5p in KIRC and cg03769349 in LIHC was accompanied by the progression of cancer stages, while hsa-miR-106b-5p in KIRC showed the opposite pattern. These findings suggest that miRNA or DNA methylation can affect the tumorigenesis and progression. In addition, when searching for BBcancer (http://bbcancer.renlab.org/; 73), we found that each member of *YTHDC2*/hsa-miR-96-5p regulatory pair had higher expression abundance in peripheral blood. This finding suggests that this regulatory pair can serve as a biomarker for early diagnosis of cancers. All these studies indicate that the detailed mechanisms of miRNA-mRNA and DMP-mRNA regulatory pairs in human cancers warrant further investigation.

Renal cell carcinoma (RCC) is the most lethal urogenital tumor, among which clear cell RCC (ccRCC, also known as KIRC) constitutes 70% to 80% of all RCCs. Few studies found that the prognostic value of some m6A regulators in KIRC (74), but the detailed mechanisms remained unclear. Here we totally identified four miRNA/mRNA regulatory pairs (hsa-miR-1307-3p/*METTL14*, hsa-miR-106b-5p/*YTHDF3*, hsa-miR-96-5p/*YTHDC2*, and hsa-miR-204-5p/*IGF2BP3*) in KIRC. For the four regulatory pairs, we verified the expression relationship of these regulatory pairs using an independent dataset from GEO. As a result, we did find hsa-miR-106b-5p/*YTHDF3* regulatory pair in GSE16441. This finding makes our analysis more credible. To explore the potential application of them in KIRC prognosis. We first performed LASSO Cox regression analysis and identified two regulatory pairs (including hsa-miR-1307-3p/*METTL14* and hsa-miR-204-5p/*IGF2BP3*) in KIRC as significant prognosis-related pairs. The role of *METTL14* and *IGF2BP3* in human cancers was studied before. The promotion function by *METTL14* in pancreatic cancer was uncovered (75) and *IGF2BP3* was found to be a potential prognosis marker and therapeutic target of colon cancer (76). Yet the miRNA-mediated mechanisms of *METTL14* and *IGF2BP3*, if any, remain unclear. According to the expression level of these two pairs, we built a risk model to divide the patients into high-risk and low-risk groups. We found that DEGs between high-risk and low-risk groups were enriched in immune-related biological processes. Moreover, the infiltration score of 28 kinds of immune cells in tumor tissues showed statistically different patterns in the two risk groups. Notably, the expression level of *IGF2BP3* had a strong positive correlation with the infiltration scores of multiple immune cells, suggesting that different features of tumor infiltration may contribute by the expression change of *IGF2BP3*.

In summary, our study demonstrated that miRNA- or DNA methylation- regulated m6A regulators expression involved in tumor progression and strongly correlated with patients' prognosis. Although three types of sequencing data (miRNA-seq, mRNA-seq, and methylation array data) from TCGA were used in our study, a large-scale and multi-omics (such as CNV,

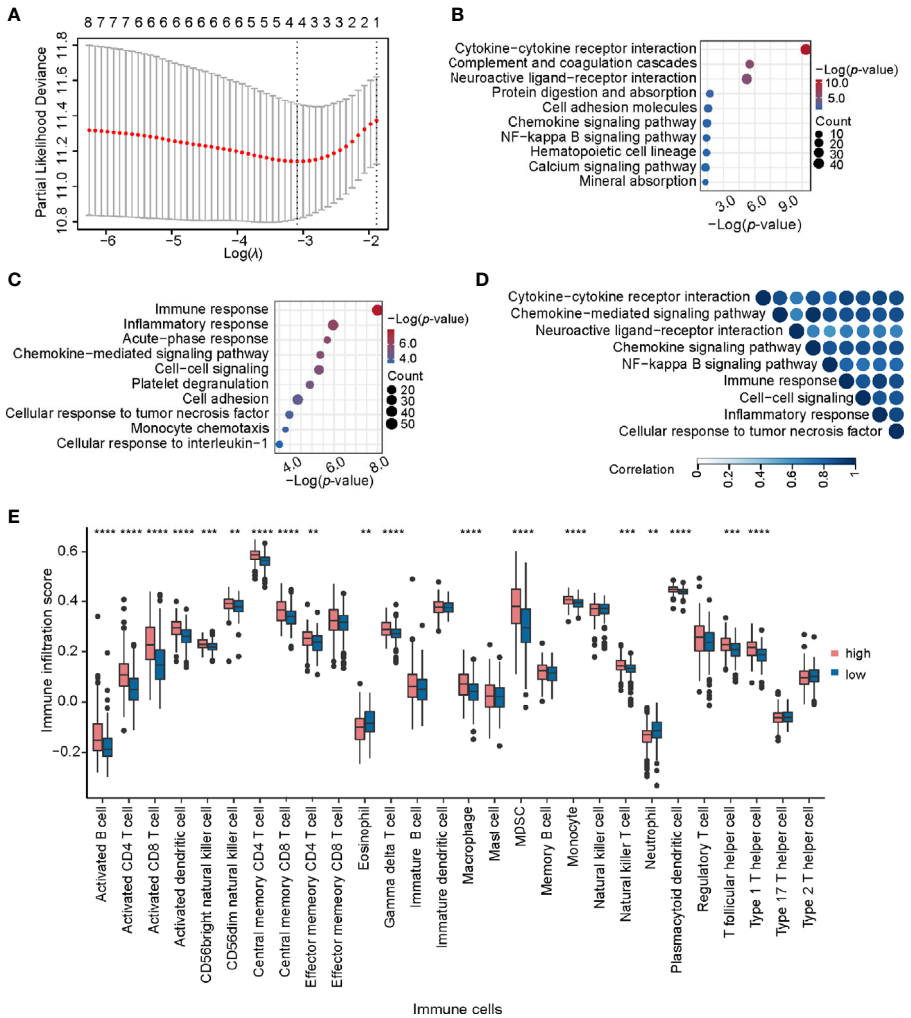

FIGURE 6 | Identification and analysis of key regulatory pairs in KIRC. **(A)** The process of building the signature using LASSO regression algorithm. **(B)** Biological process enrichment analysis of differentially expressed genes between high-risk and low-risk groups. **(C)** KEGG pathway enrichment analysis of differentially expressed genes in high-risk and low-risk groups. **(D)** Functional similarity analysis of gene sets in terms of biological processes. The order of enrichment items in the upper part of triangle is consistent with that of the left side. **(E)** Comparison of infiltration scores of 28 immune cell types between high-risk and low-risk groups. **P < 0.01, ***P < 0.001, and ****P < 0.0001.

lncRNA, and proteomic data) integrative analysis would be desirable as future directions. Furthermore, validation experiments are highly needed to convince our results in the future. Accordingly, all these data should be integrated to build a multi-dimensional regulatory network for better understanding the complex mechanisms of m6A regulators in cancers.

DATA AVAILABILITY STATEMENT

The original contributions presented in the study are included in the article/**Supplementary Material**. Further inquiries can be directed to the corresponding authors.

AUTHOR CONTRIBUTIONS

SS: conception and design. SS, ZZ, and XT: writing—review and editing. XL, PW, and XT: methodology. XL and PW: formal analysis. XL and XT: writing—original draft. All authors contributed to the article and approved the submitted version.

FUNDING

SS received funding support from The Youth Innovation Promotion Association of Chinese Academy of Science (2017141). The Strategic Priority Research Program of the Chinese Academy of Sciences (Grant No. XDA19090116 to SS, Grant No. XDA19050302 to ZZ).

ACKNOWLEDGMENTS

We thank Yamei Niu, Lina Ma, Lili Hao, Lin Liu, Lin Yang, Zhiwei Zhang, and Chunhui Ma for their valuable suggestions and discussions on this work.

SUPPLEMENTARY MATERIAL

The Supplementary Material for this article can be found online at: https://www.frontiersin.org/articles/10.3389/fonc.2021.624395/full#supplementary-material

REFERENCES

1. Ma CH, Chang MQ, Lv HY, Zhang ZW, Zhang WL, He X, et al. RNA m 6 A methylation participates in regulation of postnatal development of the mouse cerebellum. *Genome Biol* (2018) 19:68. doi: 10.1186/s13059-018-1435-z
2. Zheng GQ, Dahl JA, Niu YM, Fedorcsak P, Huang CM, Li CJ, et al. ALKBH5 is a mammalian RNA demethylase that impacts RNA metabolism and mouse fertility. *Mol Cell* (2013) 49:18–29. doi: 10.1016/j.molcel.2012.10.015
3. Winkler R, Gillis E, Lasman L, Safra M, Geula S, Soyris C, et al. m6A modification controls the innate immune response to infection by targeting type I interferons. *Nat Immunol* (2019) 20:173–82. doi: 10.1038/s41590-018-0275-z
4. Batista PJ, Molinie B, Wang J, Qu K, Zhang JJ, Li LJ, et al. m(6)A RNA modification controls cell fate transition in mammalian embryonic stem cells. *Cell Stem Cell* (2014) 15:707–19. doi: 10.1016/j.stem.2014.09.019
5. Vu LP, Pickering BF, Cheng YM, Zaccara S, Nguyen D, Minuesa G, et al. The N 6-methyladenosine (m 6 A)-forming enzyme METTL3 controls myeloid differentiation of normal hematopoietic and leukemia cells. *Nat Med* (2017) 23:1369–76. doi: 10.1038/nm.4416
6. Bokar JA, Shambaugh ME, Polayes D, Matera AG, Rottman FM. Purification and cDNA cloning of the AdoMet-binding subunit of the human mRNA (N6-adenosine)-methyltransferase. *RNA* (1997) 3:1233–47.
7. Liu JZ, Yue YN, Han DL, Wang X, Fu Y, Zhang L, et al. A METTL3-METTL14 complex mediates mammalian nuclear RNA N6-adenosine methylation. *Nat Chem Biol* (2014) 10:93–5. doi: 10.1038/nchembio.1432
8. Zhong SL, Li HY, Bodi Z, Button J, Vespa L, Herzog M, et al. MTA is an Arabidopsis messenger RNA adenosine methylase and interacts with a homolog of a sex-specific splicing factor. *Plant Cell* (2008) 20:1278–88. doi: 10.1105/tpc.108.058883
9. Patil DP, Chen CK, Pickering BF, Chow A, Jackson C, Guttman M, et al. m(6) A RNA methylation promotes XIST-mediated transcriptional repression. *Nature* (2016) 537:369–73. doi: 10.1038/nature19342
10. Knuckles P, Lence T, Haussmann IU, Jacob D, Kreim N, Carl SH, et al. Zc3h13/Flacc is required for adenosine methylation by bridging the mRNA-binding factor Rbm15/Spenito to the m(6)A machinery component Wtap/Fl (2)d. *Genes Dev* (2018) 32:415–29. doi: 10.1101/gad.309146.117
11. Yue YN, Liu J, Cui XL, Cao J, Luo GZ, Zhang ZZ, et al. VIRMA mediates preferential m(6)A mRNA methylation in 3'UTR and near stop codon and associates with alternative polyadenylation. *Cell Discovery* (2018) 4:10. doi: 10.1038/s41421-018-0019-0
12. Jia GF, Fu Y, Zhao X, Dai Q, Zheng GQ, Yang Y, et al. N6-methyladenosine in nuclear RNA is a major substrate of the obesity-associated FTO. *Nat Chem Biol* (2011) 7:885–7. doi: 10.1038/nchembio.687
13. Wang X, Zhao BS, Roundtree IA, Lu Z, Han D, Ma HH, et al. N(6)-methyladenosine Modulates Messenger RNA Translation Efficiency. *Cell* (2015) 161:1388–99. doi: 10.1016/j.cell.2015.05.014
14. Shi HL, Wang X, Lu ZK, Zhao BS, Ma HH, Hsu PJ, et al. YTHDF3 facilitates translation and decay of N6-methyladenosine-modified RNA. *Cell Res* (2017) 27:315–28. doi: 10.1038/cr.2017.15
15. Li A, Chen YS, Ping XL, Yang X, Xiao W, Yang Y, et al. Cytoplasmic m6A reader YTHDF3 promotes mRNA translation. *Cell Res* (2017) 27:444–7. doi: 10.1038/cr.2017.10
16. Muller S, Glass M, Singh AK, Haase J, Bley N, Fuchs T, et al. IGF2BP1 promotes SRF-dependent transcription in cancer in a m6A- and miRNA-dependent manner. *Nucleic Acids Res* (2019) 47:375–90. doi: 10.1093/nar/gky1012
17. Li T, Hu PS, Zuo Z, Lin JF, Li X, Wu QN, et al. METTL3 facilitates tumor progression via an m6A-IGF2BP2-dependent mechanism in colorectal carcinoma. *Mol Cancer* (2019) 18:112. doi: 10.1186/s12943-019-1038-7
18. Wang SF, Chim B, Su YJ, Khil P, Wong M, Wang XT, et al. Enhancement of LIN28B-induced hematopoietic reprogramming by IGF2BP3. *Genes Dev* (2019) 33:1048–68. doi: 10.1101/gad.325100.119
19. Zhou J, Wan J, Gao XG, Zhang XQ, Jaffrey SR, Qian SB. Dynamic m(6)A mRNA methylation directs translational control of heat shock response. *Nature* (2015) 526:591–4. doi: 10.1038/nature15377
20. Alarcon CR, Goodarzi H, Lee H, Liu XH, Tavazoie S, Tavazoie SF. HNRNPA2B1 Is a Mediator of m(6)A-Dependent Nuclear RNA Processing Events. *Cell* (2015) 162:1299–308. doi: 10.1016/j.cell.2015.08.011
21. Cheng MS, Sheng L, Gao Q, Xiong QC, Zhang HJ, Wu MQ, et al. The m(6)A methyltransferase METTL3 promotes bladder cancer progression via AFF4/NF-kappaB/MYC signaling network. *Oncogene* (2019) 38:3667–80. doi: 10.1038/s41388-019-0683-z
22. Chai RC, Wu F, Wang QX, Zhang S, Zhang KN, Liu YQ, et al. m6A RNA methylation regulators contribute to malignant progression and have clinical prognostic impact in gliomas. *Aging (Albany NY)* (2019) 11:1204–25. doi: 10.18632/aging.101829
23. Hua WF, Zhao YZ, Jin XH, Yu DY, He J, Xie D, et al. METTL3 promotes ovarian carcinoma growth and invasion through the regulation of AXL translation and epithelial to mesenchymal transition. *Gynecol Oncol* (2018) 151:356–65. doi: 10.1016/j.ygyno.2018.09.015
24. Bai Y, Yang CX, Wu RL, Huang LH, Song SL, Li WW, et al. YTHDF1 Regulates Tumorigenicity and Cancer Stem Cell-Like Activity in Human Colorectal Carcinoma. *Front Oncol* (2019) 9:332. doi: 10.3389/fonc.2019.00332
25. Chen YH, Peng CH, Chen JR, Chen DY, Yang B, He B, et al. WTAP facilitates progression of hepatocellular carcinoma via m6A-HuR-dependent epigenetic silencing of ETS1. *Mol Cancer* (2019) 18:127. doi: 10.1186/s12943-019-1053-8
26. Zhou JC, Wang JY, Hong BA, Ma KF, Xie HB, Li L, et al. Gene signatures and prognostic values of m6A regulators in clear cell renal cell carcinoma - a retrospective study using TCGA database. *Aging (Albany NY)* (2019) 11:1633–47. doi: 10.18632/aging.101856
27. Liu J, Eckert MA, Harada BT, Liu SM, Lu ZK, Yu KK, et al. m(6)A mRNA methylation regulates AKT activity to promote the proliferation and tumorigenicity of endometrial cancer. *Nat Cell Biol* (2018) 20:1074–83. doi: 10.1038/s41556-018-0174-4
28. Zhang CZ, Samanta D, Lu HQ, Bullen JW, Zhang HM, Chen I, et al. Hypoxia induces the breast cancer stem cell phenotype by HIF-dependent and ALKBH5-mediated m(6)A-demethylation of NANOG mRNA. *Proc Natl Acad Sci U S A* (2016) 113:E2047–2056. doi: 10.1073/pnas.1602883113
29. Shi HJ, Zhao JP, Han LZ, Xu M, Wang KJ, Shi JJ, et al. Retrospective study of gene signatures and prognostic value of m6A regulatory factor in non-small cell lung cancer using TCGA database and the verification of FTO. *Aging (Albany NY)* (2020) 12:17022–37. doi: 10.18632/aging.103622
30. Li YS, Xiao J, Bai J, Tian Y, Qu YW, Chen X, et al. Molecular characterization and clinical relevance of m(6)A regulators across 33 cancer types. *Mol Cancer* (2019) 18:137. doi: 10.1186/s12943-019-1066-3
31. Lee TJ, Yuan XY, Kerr K, Yoo JY, Dong DHK, Kaur B, et al. Strategies to Modulate MicroRNA Functions for the Treatment of Cancer or Organ Injury. *Pharmacol Rev* (2020) 3:639–67. doi: 10.1124/pr.119.019026
32. Urbano A, Smith J, Weeks RJ, Chatterjee A. Gene-Specific Targeting of DNA Methylation in the Mammalian Genome. *Cancers (Basel)* (2019) 10:1515. doi: 10.3390/cancers11101515
33. Yang Z, Li J, Feng GX, Gao S, Wang Y, Zhang SQ, et al. MicroRNA-145 Modulates N(6)-Methyladenosine Levels by Targeting the 3'-Untranslated mRNA Region of the N(6)-Methyladenosine Binding YTH Domain Family 2 Protein. *J Biol Chem* (2017) 292:3614–23. doi: 10.1074/jbc.M116.749689
34. Cai XL, Wang X, Cao C, Gao Y, Zhang SQ, Yang Z, et al. HBXIP-elevated methyltransferase METTL3 promotes the progression of breast cancer via inhibiting tumor suppressor let-7g. *Cancer Lett* (2018) 415:11–9. doi: 10.1016/j.canlet.2017.11.018

35. Du YZ, Hou GF, Zhang HL, Dou JZ, He JF, Guo YM, et al. SUMOylation of the m6A-RNA methyltransferase METTL3 modulates its function. *Nucleic Acids Res* (2018) 46:5195–208. doi: 10.1093/nar/gky156
36. Su YL, Xiong J, Hu JY, Wei X, Zhang XL, Rao LJ. MicroRNA-140-5p targets insulin like growth factor 2 mRNA binding protein 1 (IGF2BP1) to suppress cervical cancer growth and metastasis. *Oncotarget* (2016) 42:68397–411. doi: 10.18632/oncotarget.11722
37. Spainhour JC, Lim HS, Yi SV, Qiu P. Correlation Patterns Between DNA Methylation and Gene Expression in The Cancer Genome Atlas. *Cancer Inform* (2019) 18:1176935119828776. doi: 10.1177/1176935119828776
38. Cheng J, Wei D, Ji Y, Chen L, Yang L, Li G, et al. Integrative analysis of DNA methylation and gene expression reveals hepatocellular carcinoma-specific diagnostic biomarkers. *Genome Med* (2018) 10:42. doi: 10.1186/s13073-018-0548-z
39. Wang LB, Wang B, Quan ZX. Identification of aberrantly methylateddifferentially expressed genes and gene ontology in prostate cancer. *Mol Med Rep* (2020) 21:744–58. doi: 10.3892/mmr.2019.10876
40. Scott CM, Wong EM, Joo JE, Dugué PA, Jung CH, O'Callaghan N, et al. Genome-wide DNA methylation assessment of 'BRCA1-like' early-onset breast cancer: Data from the Australian Breast Cancer Family Registry. *Exp Mol Pathol* (2018) 3:404–10. doi: 10.1016/j.yexmp.2018.11.006
41. Agarwal V, Bell GW, Nam JW, Bartel DP. Predicting effective microRNA target sites in mammalian mRNAs. *Elife* (2015) 4:e05005. doi: 10.7554/eLife.05005
42. Hsu SD, Tseng YT, Shrestha S, Lin YL, Khaleel A, Chou CH, et al. miRTarBase update 2014: an information resource for experimentally validated miRNA-target interactions. *Nucleic Acids Res* (2014) 42:D78–85. doi: 10.1093/nar/gkt1266
43. Wei X, Yu LL, Kong XB. miR-488 inhibits cell growth and metastasis in renal cell carcinoma by targeting HMGN5. *Onco Targets Ther* (2018) 11:2205–16. doi: 10.2147/OTT.S156361
44. Dyskova T, Fillerova R, Novosad T, Kudelka M, Zurkova M, Gajdos P, et al. Correlation Network Analysis Reveals Relationships between MicroRNAs, Transcription Factor T-bet, and Deregulated Cytokine/Chemokine-Receptor Network in Pulmonary Sarcoidosis. *Mediators Inflamm* (2015) 2015:121378. doi: 10.1155/2015/121378
45. Kern F, Fehlmann T, Solomon J, Schwed L, Grammes N, Backes C, et al. miEAA 2.0: integrating multi-species microRNA enrichment analysis and workflow management systems. *Nucleic Acids Res* (2020) 48:W521–8. doi: 10.1093/nar/gkaa309
46. Bailey AM, Zhan L, Maru D, Shureiqi I, Pickering CR, Kiriakova G, et al. FXR silencing in human colon cancer by DNA methylation and KRAS signaling. *Am J Physiol Gastrointest Liver Physiol* (2014) 306:G48–58. doi: 10.1152/ajpgi.00234.2013
47. Li ZF, Zhang RQ, Yang XL, Zhang DD, Li BR, Zhang D. et.al. Analysis of gene expression and methylation datasets identified ADAMTS9, FKBP5, and PFKBF3 as biomarkers for osteoarthritis. *J Cell Physiol* (2019) 234:8908–17. doi: 10.1002/jcp.27557
48. Huang DW, Sherman BT, Lempicki RA. Systematic and integrative analysis of large gene lists using DAVID bioinformatics resources. *Nat Protoc* (2009) 4:44–57. doi: 10.1038/nprot.2008.211
49. Yu GC, Li F, Qin YD, Bo XC, Wu YB, Wang SQ. GOSemSim: an R package for measuring semantic similarity among GO terms and gene products. *Bioinformatics* (2010) 26:976–8. doi: 10.1093/bioinformatics/btq064
50. Charoentong P, Finotello F, Angelova M, Mayer C, Efremova M, Rieder D, et al. Pan-cancer Immunogenomic Analyses Reveal Genotype-Immunophenotype Relationships and Predictors of Response to Checkpoint Blockade. *Cell Rep* (2017) 18:248–62. doi: 10.1016/j.celrep.2016.12.019
51. Barbie DA, Tamayo P, Boehm JS, Kim SY, Moody SE, Dunn IF, et al. Systematic RNA interference reveals that oncogenic KRAS-driven cancers require TBK1. *Nature* (2009) 462:108–12. doi: 10.1038/nature08460
52. Seipel K, Messerli C, Wiedemann G, Bacher U, Pabst T. MN1, FOXP1 and hsa-miR-181a-5p as prognostic markers in acute myeloid leukemia patients treated with intensive induction chemotherapy and autologous stem cell transplantation. *Leuk Res* (2020) 89:106296. doi: 10.1016/j.leukres.2020.106296
53. Zhang C, Bo CR, Guo LH, Yu PY, Miao SS, Gu X. BCL2 and hsa-miR-181a-5p are potential biomarkers associated with papillary thyroid cancer based on bioinformatics analysis. *World J Surg Oncol* (2019) 17:221. doi: 10.1186/s12957-019-1755-9
54. He SM, Zeng SM, Zhou ZW, He ZX, Zhou SF. Hsa-microRNA-181a is a regulator of a number of cancer genes and a biomarker for endometrial carcinoma in patients: a bioinformatic and clinical study and the therapeutic implication. *Drug Des Devel Ther* (2015) 9:1103–75. doi: 10.2147/DDDT.S73551
55. Ding L, Wang L, Guo F. microRNA−188 acts as a tumor suppressor in glioma by directly targeting the IGF2BP2 gene. *Mol Med Rep* (2017) 16:7124–30. doi: 10.3892/mmr.2017.7433
56. Wang ZS, Yin JQ, Zhou WW, Bai J, Xie YJ, Kang XU, et al. Complex impact of DNA methylation on transcriptional dysregulation across 22 human cancer types. *Nucleic Acids Res* (2020) 48:2287–302. doi: 10.1093/nar/gkaa041
57. Lin SJ, Xu HS, Zhang AK, Meng T, Xu YZ, Ren J, et al. m6A signature and tumour immune microenvironment for predicting prognostic value in gliomas. (2020). doi: 10.2139/ssrn.3523837
58. Zhang B, Wu Q, Li B, Wang DF, Wang L, Zhou YL. m(6)A regulator-mediated methylation modification patterns and tumor microenvironment infiltration characterization in gastric cancer. *Mol Cancer* (2020) 19:53. doi: 10.1186/s12943-020-01170-0
59. Meng J, Lu ZL, Liu H, Zhang L, Zhang SW, Chen YD, et al. A protocol for RNA methylation differential analysis with MeRIP-Seq data and exomePeak R/Bioconductor package. *Methods* (2014) 69:274–81. doi: 10.1016/j.ymeth.2014.06.008
60. Zhang Y, Liu T, Meyer CA, Eeckhoutem J, Johnson DS, Bernstein BE, et al. Model-based analysis of ChIP-Seq (MACS). *Genome Biol* (2008) 9:R137. doi: 10.1186/gb-2008-9-9-r137
61. Li YL, Song SH, Li CP, Yu J. MeRIP-PF: an easy-to-use pipeline for high-resolution peak-finding in MeRIP-Seq data. *Genomics Proteomics Bioinf* (2013) 11:72–5. doi: 10.1016/j.gpb.2013.01.002
62. He LE, Li HY, Wu AG, Peng YL, Shu G, Yin G. Functions of N6-methyladenosine and its role in cancer. *Mol Cancer* (2019) 1:176. doi: 10.1186/s12943-019-1109-9
63. Cui XL, Liu Y, Sun W, Ding J, Bo XC, Wang HY. Comprehensive analysis of miRNA-gene regulatory network with clinical significance in human cancers. *Sci China Life Sci* (2020) 8:1201–12. doi: 10.1007/s11427-019-9667-0
64. Spainhour JC, Lim HS, Yi SV, Qiu P. Comparative pan-cancer DNA methylation analysis reveals cancer common and specific patterns. *Brief Bioinform* (2017) 5:761–73. doi: 10.1093/bib/bbw063
65. Wang L, Aireti A, Aihaiti A, Li K. Expression of microRNA-150 and its Target Gene IGF2BP1 in Human Osteosarcoma and their Clinical Implications. *Pathol Oncol Res* (2019) 25:527–33. doi: 10.1007/s12253-018-0454-0
66. Jiang TH, Li MF, Li QY, Guo ZQ, Sun XJ, Zhang XF, et al. MicroRNA-98-5p Inhibits Cell Proliferation and Induces Cell Apoptosis in Hepatocellular Carcinoma via Targeting IGF2BP1. *Oncol Res* (2017) 7:1117–27. doi: 10.3727/096504016X14821952695683
67. Nomura M, Saito K, Aihara K, Nagae G, Yamamoto S, Tatsuno K, et al. DNA demethylation is associated with malignant progression of lower-grade gliomas. *Sci Rep* (2019) 1:1903. doi: 10.1038/s41598-019-38510-0
68. Zhao SS, Geybels MS, Leonardson A, Rubicz R, Kolb S, Yan QX, et al. Epigenome-Wide Tumor DNA Methylation Profiling Identifies Novel Prognostic Biomarkers of Metastatic-Lethal Progression in Men Diagnosed with Clinically Localized Prostate Cancer. *Clin Cancer Res* (2017) 1:311–9. doi: 10.1158/1078-0432.CCR-16-0549
69. Sun Y, Li SH, Cheng JW, Chen G, Huang ZG, Gu YY, et al. Downregulation of miRNA-205 Expression and Biological Mechanism in Prostate Cancer Tumorigenesis and Bone Metastasis. *BioMed Res Int* (2020) 2020:6037434. doi: 10.1155/2020/6037434
70. Li SL, Sui Y, Sun J, Jiang TQ, Dong G. Identification of tumor suppressive role of microRNA-132 and its target gene in tumorigenesis of prostate cancer. *Int J Mol Med* (2018) 41:2429–33. doi: 10.3892/ijmm.2018.3421
71. Lapthanasupkul P, Klongnoi B, Mutirangura A, Kitkumthorn N. Investigation of PTEN promoter methylation in ameloblastoma. *Med Oral Patol Oral Cir Bucal* (2020) 25:e481–7. doi: 10.4317/medoral.23498
72. Lv LT, Cao LY, Hu GN, Shen QY, Wu JZ. Methylation-Driven Genes Identified as Novel Prognostic Indicators for Thyroid Carcinoma. *Front Genet* (2020) 11:294. doi: 10.3389/fgene.2020.00294
73. Zuo ZX, Hu HJ, Xu QX, Luo XT, Peng D, Zhu KY, et al. BBCancer: an expression atlas of blood-based biomarkers in the early diagnosis of cancers. *Nucleic Acids Res* (2020) 48:D789–96. doi: 10.1093/nar/gkz942

74. Rini BI, Campbell SC, Escudier B. Renal cell carcinoma. *Lancet* (2009) 373:1119–32. doi: 10.1016/S0140-6736(09)60229-4
75. Wang M, Liu J, Zhao Y, He RZ, Xu XD, Guo XJ, et al. Upregulation of METTL14 mediates the elevation of PERP mRNA N 6 adenosine methylation promoting the growth and metastasis of pancreatic cancer. *Mol Cancer* (2020) 19:130. doi: 10.1186/s12943-020-01249-8
76. Yang Z, Wang TF, Wu DJ, Min ZJ, Tan JY, Yu B. RNA N6-methyladenosine reader IGF2BP3 regulates cell cycle and angiogenesis in colon cancer. *J Exp Clin Cancer Res* (2020) 1:203. doi: 10.1186/s13046-020-01714-8

Conflict of Interest: The authors declare that the research was conducted in the absence of any commercial or financial relationships that could be construed as a potential conflict of interest.

frontiers in Oncology

REVIEW
published: 24 February 2021
doi: 10.3389/fonc.2021.611660

m^{6}A Modifications Play Crucial Roles in Glial Cell Development and Brain Tumorigenesis

Jing Wang[1,2], *Yongqiang Sha*[1] *and Tao Sun*[1]*

[1] Center for Precision Medicine, School of Medicine and School of Biomedical Sciences, Huaqiao University, Xiamen, China, [2] College of Materials Science and Engineering, Huaqiao University, Xiamen, China

RNA methylation is a reversible post-transcriptional modification to RNA and has a significant impact on numerous biological processes. N^6-methyladenosine (m^{6}A) is known as one of the most common types of eukaryotic mRNA methylation modifications, and exists in a wide variety of organisms, including viruses, yeast, plants, mice, and humans. Widespread and dynamic m^{6}A methylation is identified in distinct developmental stages in the brain, and controls development of neural stem cells and their differentiation into neurons, glial cells such as oligodendrocytes and astrocytes. Here we summarize recent advances in our understanding of RNA methylation regulation in brain development, neurogenesis, gliogenesis, and its dysregulation in brain tumors. This review will highlight biological roles of RNA methylation in development and function of neurons and glial cells, and provide insights into brain tumor formation, and diagnostic and treatment strategies.

Keywords: N^6-methyladenosine (m^{6}A), brain development, neural stem cell, glial cell, brain tumor, glioma

OPEN ACCESS

Edited by:
Shicheng Guo,
University of Wisconsin-Madison,
United States

Reviewed by:
Huabing Li,
Shanghai Jiao Tong University School of Medicine, China
Kai Li,
Peking-Tsinghua Center for Life Sciences, China
Briana Prager,
Cleveland Clinic, United States

***Correspondence:**
Tao Sun
taosun@hqu.edu.cn

Specialty section:
This article was submitted to Cancer Genetics, a section of the journal Frontiers in Oncology

Received: *29 September 2020*
Accepted: *11 January 2021*
Published: *24 February 2021*

Citation:
Wang J, Sha Y and Sun T (2021) m^{6}A Modifications Play Crucial Roles in Glial Cell Development and Brain Tumorigenesis. Front. Oncol. 11:611660. doi: 10.3389/fonc.2021.611660

INTRODUCTION

N^6-methyladenosine (m^{6}A) is the most common and abundant methylation modification in RNA molecules present in eukaryotes (1, 2). More than 150 distinct chemical marks on cellular RNAs have been identified to date, and m^{6}A modifications account for over 80% of all RNA methylations (3). High-throughput m^{6}A sequencing studies have shown that thousands of mRNAs and non-coding RNAs are modified by m^{6}A, which in turn affects gene expression, participates in animal development and pathogenesis of human diseases (4, 5). m^{6}A is the most prevalent internal mRNA modification, with an average of one to three modifications per transcript, and potentially regulates every step in mRNA metabolism to some extent (6).

m^{6}A methylation is catalyzed by an m^{6}A methyltransferase complex (MTC) composed of methyltransferase-like 3 and 14 (METTL3 and METTL14) and their cofactors such as Wilms tumor 1-associated protein (WTAP), termed as "writer" (7–9). Removal of m^{6}A is facilitated by Fat mass and obesity-associated (FTO) and AlkB homolog H5 (ALKBH5), two m^{6}A demethylases that recognize distinct sets of target mRNAs, termed as "eraser" (10, 11). YTHDF1/2/3 and YTHDC1, members of the YT521-B homology (YTH) domain family proteins, are m^{6}A direct "readers," which affect translation, stability, and splicing of target mRNAs (12) (**Figure 1**). m^{6}A modification has emerged as a multifaceted controller for gene expression regulation, mediated through its effector proteins—writers, readers, and erasers (6).

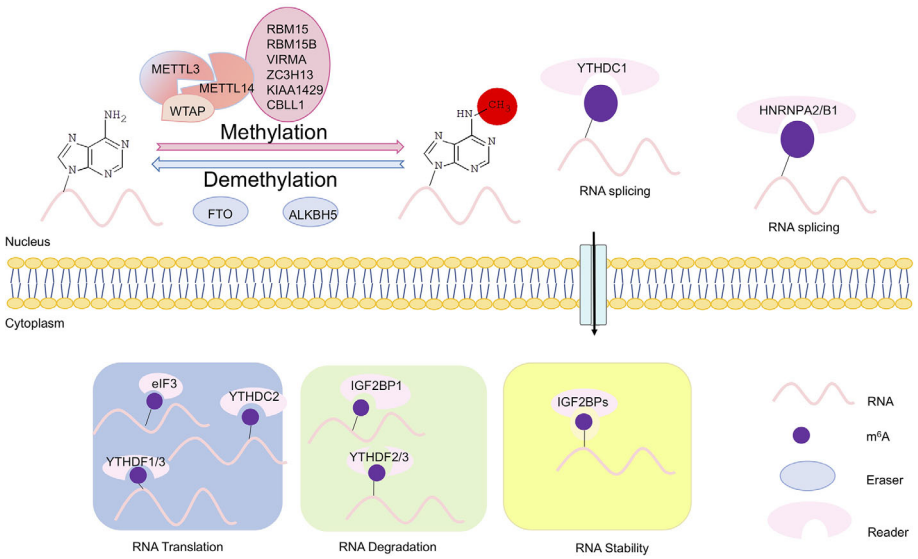

FIGURE 1 | Scheme of m^{6}A modifications. The writers, erasers, and readers of *N*6-methyladenosine (m^{6}A). The m^{6}A writer complex, which comprises the core methyltransferase-like protein 3 (METTL3) and its adaptors, is located in the nucleus. m^{6}A demethylation is executed by two demethylases FTO and ALKBH5. The m^{6}A erasers also are localized in the nucleus. In the nucleus, m^{6}A can bind specific nuclear reader proteins such as YTHDC1 and HNRNPA2/B1, which may affect RNA splicing and mRNA export. Upon mRNA being exported to the cytoplasm, m^{6}A binds to specific reader proteins, which affects stability, translation and/or localization of mRNAs. In the cytoplasm, translation of m^{6}A modified mRNAs is mediated by the m^{6}A readers YTHDF1, YTHDF3, and YTHDC2, the eukaryotic translation initiation factor eIF3, and METTL3. YTHDF2 and YTHDF3 regulate degradation of m^{6}A modified mRNAs, while the insulin-like growth factor 2 mRNA-binding proteins (IGF2BPs) enhances stability m^{6}A modified mRNAs.

m^{6}A modifications in mRNAs or non-coding RNAs play important roles in virtually all types of bioprocesses including tissue development, self-renewal and differentiation of stem cells, heat shock response, circadian clock control, DNA damage response, and maternal-to-zygotic transition (8, 12). m^{6}A is an important epitranscriptomic mark with high abundance in the central nervous system (CNS), and plays a crucial role in neural development and function (13). Dysregulation of m^{6}A modifications also is associated with tumorigenesis of various cancers, such as gliomas (14).

In this review, we first summarize the recent advance in our understanding of biological functions and underlying molecule mechanisms of m^{6}A regulation in neural development, with an emphasis in neurons and glial cells. We then highlight m^{6}A regulatory roles in formation of brain tumors.

N^6-METHYLADENOSINE (m^{6}A) MODIFICATIONS

As the most common and prevalent internal modification in eukaryotic mRNAs, m^{6}A methylation has a significant impact on various physiological events (6, 15).

Components and Functions of m^{6}A Modifications

Modification of m^{6}A on mRNAs is post-transcriptionally installed, erased, and recognized by m^{6}A methyltransferases, demethylases and m^{6}A-specific binding proteins, respectively. Methyltransferases include METTL3/14, WTAP, RBM15/15B, and KIAA1429, also termed as "writers" (1, 7, 9) (**Figure 1**). METTL3 is the catalytic subunit, and METTL14 is an essential component to facilitate RNA binding (16). m^{6}A methyltransferase is widely conserved among eukaryotic species that range from yeast, plants, and flies to mammals (17, 18). Demethylases consist of FTO and ALKBH5, termed as "erasers" (10, 11, 19). And m^{6}A-specific binding proteins include YTHDF1/2/3 and IGF2BP1, termed as "readers" (20) (**Figure 1**).

In mammals, m^{6}A is widely distributed in multiple tissues, with a higher expression in the liver, kidney, and brain than in other tissues (21). In the rodent brain, the global level of m^{6}A is developmentally regulated, with expression peaking in the adult brain (22). Studies of m^{6}A modifications have revealed m^{6}A binding sites in over 25% of human transcripts, with enrichment in long exons, near stop codon and 3′ untranslated terminal region (3'-UTR) (2, 21, 22).

m^{6}A modification in eukaryotic mRNAs exhibits substantial contributions to post-transcriptional gene expression regulation, and plays crucial and evolutionarily conserved roles in fundamental cellular processes such as meiosis and cell differentiation in yeast, plants, and mammals (18). m^{6}A methyltransferase is crucial for yeast meiosis, differentiation of mouse embryonic stem cells, and viability of human cells (18, 23, 24). Depletion of the METTL3 homologs in yeast and flies leads to developmental arrest and defects in gametogenesis (18, 25). The m^{6}A demethylase AlkBH5 deficient male mice are characterized by impaired fertility, resulting

from apoptosis that affects meiotic metaphase-stage spermatocytes (19). Moreover, m^{6}A modifications improve the stability of mRNAs and can control protein production (15, 26). For example, YTHDF1/2/3 exhibit 5- to 20-fold higher binding affinity for methylated RNAs compared to unmethylated RNAs (12). YTHDF1 and YTHDF3 bind m^{6}A at the 3′ end of transcripts and increase their cap-dependent translation, possibly through a looping interaction with eukaryotic elongation factor 3 (eIF3) (15, 27). And the mRNA-binding protein IGF2BP1 enhances stability and translation of oncogenic mRNAs, including c-Myc, and in turn promotes cell proliferation and tumorigenesis (28).

m^{6}A Modifications in mRNAs

m^{6}A modification appears to directly affect biological activities of RNAs with unclear molecular mechanisms (**Figure 1**). m^{6}A modification directly recruits m^{6}A-specific proteins of the YTH domain family (29). These proteins contribute methyl-selective RNA binding with an amount of cellular processes, and produce m^{6}A-dependent regulation of pre-mRNA processing, microRNA (miRNA) processing, translation initiation, and mRNA decay (5). Mature mRNAs with m^{6}A methylation are regulated in the cytoplasm by the YTH family proteins. YTHDF1 is associated with initiating ribosomes, and delivers its target mRNAs for enhanced translation efficiency in HeLa cells (15). A second YTH family protein, YTHDF2, directly recruits the CCR4-NOT deadenylase complex and accelerates degradation of methylated transcripts (12, 30).

Moreover, some RNA transcripts exhibit increased half-lives upon m^{6}A methylation. The well-established RNA stabilizer protein (HuR)/microRNA pathway mediates m^{6}A-upregulated RNA stability (8). m^{6}A modifications can assist protein binding either by destabilizing the helix around it, in turn allowing protein access, or by causing a conformation change to place m^{6}A in a single-stranded context (31).

m^{6}A Modifications in Translational Regulations

Interestingly, the methyltransferase complex may also function as a protein scaffold in RNA-processing and metabolism (19, 32). Translation regulation by m^{6}A occurs during initiation and elongation. Sequences in the 5'-UTR of mRNAs are important for ribosome recruitment and translation initiation (33). m^{6}A residues within 5'-UTR can act as an m^{6}A-induced ribosome engagement site (MIRES), which promotes cap-independent translation of mRNAs (34). Moreover, eukaryotic elongation factor 3 family (eIF3a/b/h) can function as m^{6}A readers, and physically interact with METTL3 to enhance translation by forming densely packed polyribosomes through recognizing m^{6}A modifications at the 5'-UTR of mRNAs (35, 36). METTL3, independent of METTL14, is associated with chromatin and localized to the transcriptional start sites of active genes that have the CAATT-box binding protein CEBPZ present. Promoter-bound METTL3 can induce m^{6}A modifications within the coding region of the associated mRNA transcript, and enhance its translation by relieving ribosome stalling (34, 37). In addition, METTL13-mediated methylation of eukaryotic elongation factor 1A (eEF1A) increases translation elongation and enhances protein synthesis to promote tumorigenesis (38).

Based on above biochemical and genetic evidence, m^{6}A methylation plays a broad role in many aspects of bioprocesses by direct modifications on mRNAs, and through regulating RNA transcription and translation.

m^{6}A MODIFICATIONS IN NERVOUS SYSTEM DEVELOPMENT

Proper development of the brain is critical for its function. Deficits in neural development have been implicated in many brain disorders. In the adult mouse brain, almost half of stably expressed RNAs are methylated, indicating important roles of m^{6}A in brain development and function.

m^{6}A Modifications in Development of the Cerebral Cortex

The cerebral cortex controls social interactions, decision-making, behavioral output, and other complex cognitive behaviors (39). In the developing cortex, m^{6}A modifications are enriched in transcripts involved in neurogenesis and neuronal differentiation (40, 41). Studies have shown that *Mettl14* deletion leads to a significant reduction of m^{6}A levels in cortical mRNAs *in vivo* and in cultured cortical neural progenitors (40). *Mettl14* deletion in the embryonic mouse brain causes prolonged cell cycle in cortical radial glia cells (RGCs), results in delayed neurogenesis and gliogenesis (40) (**Figure 2**).

Moreover, *Fto* knockout mice show a significant increase of m^{6}A levels in transcripts of hippocampus (42). Altered expression of genes with m^{6}A modifications contributes to impaired adult neurogenesis (42, 43). In addition, conditional depletion of *Ythdf2* in mice causes decreased self-renewal of neural stem/progenitor cells (NSPCs) and defects in spatiotemporal generation of neurons in the embryonic cortex (44). *Ythdf1* knockout mice exhibit impaired hippocampal synaptic transmission and long-term potentiation (13). *Ythdf1* re-expression in hippocampus in adult *Ythdf1* knockout mice rescues behavioral and synaptic defects, while hippocampus-specific acute knockdown of *Ythdf1* or *Mettl3* recapitulates the hippocampal deficiency (13) (**Figure 2**).

m^{6}A Modifications in Cerebellar Development

Studies have shown that m^{6}A levels are higher in the cerebellum than in the cerebral cortex, and a substantial number of cerebellar RNAs exhibits developmentally regulated methylation (45). m^{6}A writers (METTL3, METTL14, and WTAP) and erasers (ALKBH5 and FTO) are highly expressed at the early stage of cerebellar development by postnatal day 7 (P7), and show a gradual reduction towards the maturation of cerebellar neurons by P60 (45). From P7 to P60, numbers of temporal-specific m^{6}A peaks in start codon regions of RNA transcripts are greatly increased, while they are decreased in the coding sequence (CDS) and stop codon regions, which suggests that m^{6}A

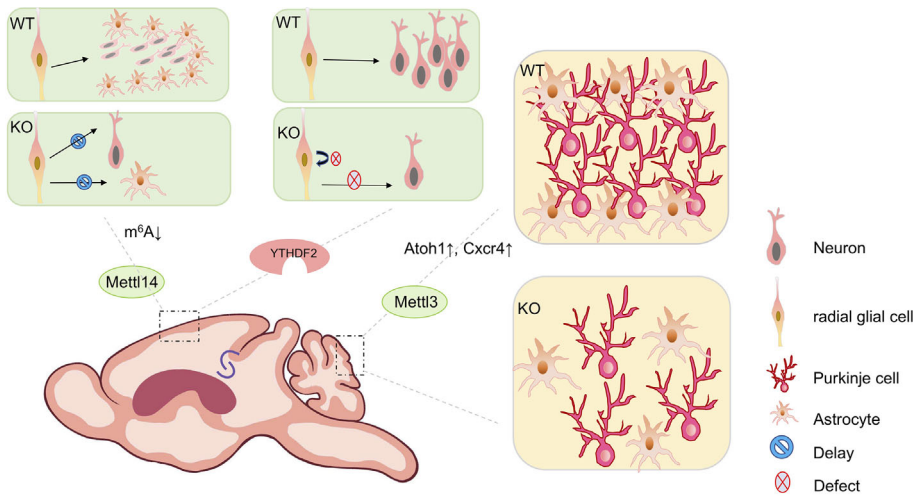

FIGURE 2 | The biological impact of m^{6}A modifications in mouse brain development. m^{6}A modifications play a key role throughout brain development during mouse embryonic and postnatal stages. *Mettl14* conditional knockout mouse (cKO) in the mouse embryonic brain causes prolonged cell cycle in cortical radial glial cells, results in delayed neurogenesis and gliogenesis, compared to wild type (WT) mice. Conditional depletion of *Ythdf2* in mice causes decreased self-renewal of neural stem/progenitor cells (NSPCs) and defects in spatiotemporal generation of neurons in the embryonic cortex. Knocking out *Mettl3* in the mouse embryonic brain causes cerebellar hypoplasia. Ectopic expression of *Mettl3* leads to a disorganized laminal structure of both Purkinje cells and glial cells. Key developmental genes such as *Atoh1* and *Cxcr4* are abnormally upregulated due to the extended mRNA half-lives induced by m^{6}A depletion.

modification status might be associated with cerebellar development (45).

Knocking out *Mettl3* in the mouse embryonic brain causes cerebellar hypoplasia, due to drastically enhanced apoptosis of newborn cerebellar granule cells (CGCs) in the external granular layer (EGL) (46) (**Figure 2**). Key developmental genes such as *Atoh1* and *Cxcr4* are abnormally upregulated due to the extended mRNA half-lives induced by m^{6}A depletion (46). Ectopic expression of *Mettl3* leads to a disorganized laminal structure of both Purkinje cells and glial cells (45). Moreover, deletion of the eraser gene *Alkbh5* causes increased nuclear export of hypermethylated RNAs, and abnormal proliferation and differentiation in the cerebellum (45). In addition, the cerebellum of *Fto*-deficient mouse is smaller than that of wild-type mouse (42).

m^{6}A Modifications in Synaptogenesis and Axon Guidance

m^{6}A modifications also contribute to neuronal growth and regeneration as well as to the local regulation of synaptic functions (22, 47). Synaptic m^{6}A epitranscriptome (SME), which is functionally enriched in synthesis and modulation of tripartite synapses, has been identified in mouse adult forebrains using low-input m^{6}A-sequencing of synaptosomal RNAs (48). The synaptic m^{6}A peak distribution along mRNAs shows characteristic accumulation at the stop codon (22, 40).

Increased adenosine methylation in a subset of mRNAs important for neuronal signaling, including many in the dopaminergic (DA) signaling pathway has been found in the midbrain and striatum of *Fto*-knockout mice (43). Inhibition of FTO leads to increased m^{6}A modifications and decreased local translation of axonal *GAP-43* mRNA, which eventually represses axon elongation (49). Moreover, knockdown of *Ythdf1* in hippocampal neurons reduces the cell surface expression of AMPA receptor subunit GluA1 and causes altered spine morphology and reduced excitatory synaptic transmission (48). Mutation of m^{6}A sites in *Robo3.1* mRNA or *YTHDF1* knockdown or knockout leads to reduction of Robo3.1 protein, but not *Robo3.1* mRNA, indicating that YTHDF1-mediated translation of m^{6}A-modified *Robo3.1* mRNA controls pre-crossing of axon guidance in the spinal cord (50). In addition, *YTHDF3*-knockdown neurons display a decreased percentage of spines containing a postsynaptic density (PSD) and surface GluA1 expression, indicating synaptic deficits in both structure and transmission (48).

In summary, these studies demonstrate important functions of m^{6}A modifications in the nervous system. Mechanistic roles of m^{6}A in regulating proliferation and differentiation of neural progenitors remain unclear. Whether such a mechanism is widespread within the brain will be an important area of future research.

m^{6}A MODIFICATIONS IN GLIAL CELL DEVELOPMENT

Glial cells, including oligodendrocytes and astrocytes, which are derived from the neuroepithelium in the CNS, and microglia, which are derived from mesodermal hematopoietic cells, make up 10–20% of the cells in the *Drosophila* nervous system and at least 50% of the cells in the human brain (51).

m^{6}A Regulations in Gliogenesis

Embryonic neurogenesis and gliogenesis involve NSC proliferation, differentiation of NSCs into various neural and glial cell types, and their migration to their final destinations in the nervous system.

In the developing mouse cortex, NSCs or RGCs initially give rise to neurons in embryonic stages, and later switch to produce glial cells in early postnatal stages (52). Recent studies have shown that epigenetic mechanisms are involved in the precise spatiotemporal gene expression program, which controls transition in the developmental competence of progenitor cells in the sequential generation of neural and glial progeny and the maintenance of their differentiated identities (53). Several studies have investigated the mechanisms by which m^{6}A regulates RGC differentiation. Reduction of m^{6}A level decreases RGC proliferation, resulting in delayed neurogenesis and gliogenesis (40). *Mettl3* depletion not only inhibits neuronal proliferation and differentiation, but also interferes differentiation of NSCs towards the glial lineage (54).

m^{6}A Regulation of Oligodendrocytes

Transcripts that encode a number of histone modifiers are dynamically marked by m^{6}A in oligodendrocytes precursor cells (OPCs) and oligodendrocytes, suggesting that m^{6}A RNA modifications may play a role in regulating the expression of epigenetic modifiers in distinct oligodendrocyte lineages (55). Inactivating an m^{6}A writer component METTL14 results in unchanged numbers of OPCs, decreased numbers of oligodendrocytes and hypomyelination in the CNS (56). A number of RNA transcripts that encode transcription factors implicated in oligodendrocytes lineage progression is dynamically marked by m^{6}A at different stages of the oligodendrocyte lineage. *Mettl14* ablation disrupts postmitotic oligodendrocyte maturation and has distinct effects on transcriptomes of OPCs and oligodendrocytes (56). Moreover, loss of *Mettl14* in oligodendrocyte lineage cells causes aberrant splicing of myriad RNA transcripts, including those that encode the essential paranodal component neurofascin 155 (NF155) (56). These results indicate a time-specific post-transcriptional regulatory role of m^{6}A in OPCs and oligodendrocytes.

Moreover, studies have shown that m^{6}A reader PRRC2A controls OPC generation, proliferation, and fate determination. Deletion of *Prrc2a* in mouse OPCs leads to hypomyelination and consequent locomotive and cognitive defects, without affecting neurogenesis (57). PRRC2A binds and stabilizes the methylated transcript of oligodendrocyte transcription factor 2 (*Olig2*), a key oligodendroglial lineage determination transcription factor, in an m^{6}A-dependent manner (57).

m^{6}A Regulation of Astrocytes

Studies have shown that astrocytes and neurons are derived from a common neuroepithelial precursor (58). *Mettl3* regulates lineage commitment during NSC differentiation, with a preference towards a neuronal fate. Mettl3-mediated m^{6}A modification reduces the percentage of new born astrocytes (54). Knockout of *Mettl14* in the mouse developing nervous system results in a significant decrease in the number of S100b$^+$ astrocytes (40). Knocking down *Mettl3* causes reduced astrocyte numbers in the developing cerebellum (45). *Alkbh5* deficiency leads to reduced dendritic arborization of Purkinje cells, concomitant with an increase in disorganization of the radial fibers in astrocytes (45).

In summary, these results indicate that m^{6}A modifications are critical for proper temporal progression of gliogenesis including oligodendrocytes and astrocytes.

m^{6}A MODIFICATIONS IN PRIMARY BRAIN TUMORS

Brain tumors are categorized into various types based on their nature, origin, rate of growth, and progression stage (59). Primary brain tumors can be broadly classified as malignant or non-malignant (benign) tumors, and graded from I to IV using a classification scheme specified by the World Health Organization (WHO) (60). Glioblastoma (GBM), a grade IV glioma, is the most prevalent (80% of all brain tumors) malignant and lethal intrinsic tumor in the CNS (61, 62).

RNA modifications, especially m^{6}A modifications, have been shown to be essential for tumor development (63, 64). In particular, m^{6}A modifications seem to play pivotal roles since both m^{6}A writers and erasers contribute to the tumorigenesis of glioblastoma, especially glioma stem cells (GSCs) (62). Studies have shown that as the WHO grade is increased, the expression of WTAP, RBM15, YTHDF, and ALBKH5 is increased, while the expression of FTO is decreased in glioma (65).

m^{6}A Writers Play an Oncogenic Role in Glioblastoma

Studies have shown that high expression of *METTL3* is associated with clinical aggressiveness of malignant gliomas. METTL3 plays an oncogenic role by modulating nonsense-mediated mRNA decay (NMD) of splicing factors and alternative splicing of *BCLX* and *NCOR2* isoform switches in glioblastoma (66). Silencing *METTL3* or overexpressing dominant-negative mutant form of *METTL3* suppresses growth and self-renewal of GSCs. METTL3 maintains the stability of a specific set of transcripts, such as apoptosis pathways and glial differentiation genes including *SRSF1/2/3/6/11*, *CASP3/7*, *CASPB*, *DFFB*, *BMP2*, *LIF*, *IL1B*, and *HES1* in glioblastoma (66) (**Figure 3**). It appears that the oncogenic ability of METTL3 is dependent upon its methyltransferase catalytic domain. Knockdown of METTL14 expression reduces m^{6}A levels in transcripts in GSCs, however, knockout of *METTL14* has no effect on tumorigenesis of glioblastoma, suggesting that catalytic activity in METTL3 might be crucial in tumorigenesis (21, 67).

In addition, low levels of METTL3 or METTL14 lead to decreased m^{6}A modifications on *ADAM19* and increased level of *ADAM19* in GSCs, ultimately causing glioma (67). The elevated sphere-formation rate induced by knockdown of *Mettl3* or *Mettl14* in GSCs can be reversed by knockdown of *ADAM19*, suggesting

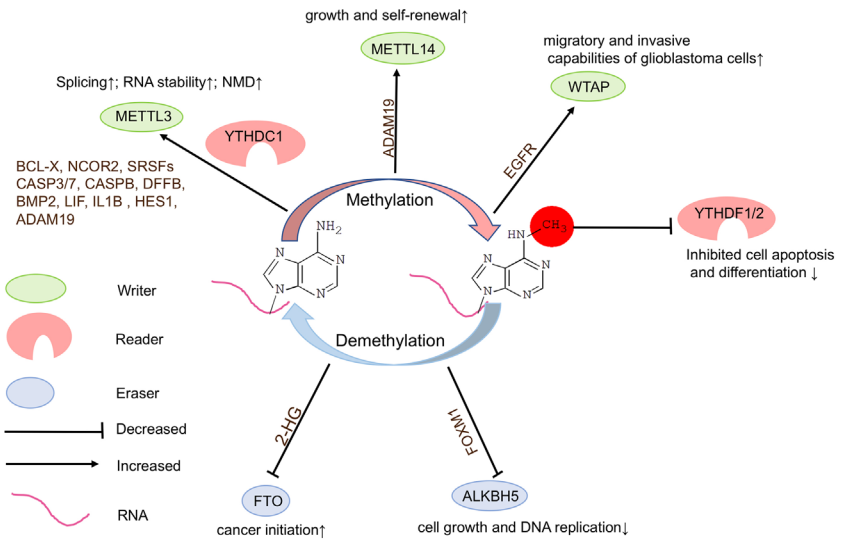

FIGURE 3 | Functions of m^{6}A modifications in brain tumors. *N*6-methyladenosine (m^{6}A) modifications play a crucial role in brain tumorigenesis. Inadequate or dysregulated expression of writers, erasers, and readers of m^{6}A is associated with brain tumor formation.

that *ADAM19* acts as a target of m^{6}A RNA methylation to regulate GSC self-renewal. It appears that knockdown of *Mettl3* or *Mettl14* dramatically promotes human GSC growth, self-renewal, and tumorigenesis (67). These controversial discoveries suggest that the role of METTL3 in glioblastoma requires further studies based on large amount of tumor samples and well-designed experimental systems.

Moreover, WTAP, an important component of the m^{6}A methyltransferase complex, can regulate migratory and invasive capabilities of glioblastoma cells by increasing expression of epidermal growth factor receptor (*EGFR*) (68) (**Figure 3**).

Suppressing m^{6}A Erasers May Inhibit Tumorigenesis

In glioma, mutations occur only in 0.1% of cases for m^{6}A ereasers ALKBH5 and no mutations have been reported in FTO (69). Knockdown of *Alkbh5* inhibits cell growth and decreased DNA replication in GSCs, and causes decreased *Foxm1* transcription, and extended survival with a lower rate of tumor formation in mice (70) (**Figure 3**). These results demonstrate that the demethylation activity of ALKBH5 is critical to represses GSC-induced tumorigenesis.

Moreover, mutation of isocitrate dehydrogenase 1 (*IDH1*) occurs frequently, which results in accumulation of the metabolic byproduct 2-hydroxy-glutarate (2-HG) in glioma. 2-HG can inhibit FTO activity, and in turn increase global m^{6}A modifications and contribute to cancer initiation (66) (**Figure 3**). In addition, treatment of GSCs with an FTO inhibitor MA2 suppresses GSC-initiated tumorigenesis and prolongs the lifespan of GSC-engrafted mice (67). Studies also have shown that FTO may play an oncogenic role *via* maintaining the stability of transcripts of avian myelocytomatosis viral oncogene homolog (c-Myc) and CCAAT enhancer binding protein alpha (CEBPA) in glioma, especially IDH1/2 mutant glioma (71).

m^{6}A Readers Promote Progression of Glioblastoma

Studies have shown that *YTHDF1* and *YTHDF2* mRNA expression levels are positively correlated with malignancy of gliomas, with significant increases in higher grade gliomas, suggesting a role for these m^{6}A readers in glioma progression (65, 69) (**Figure 3**). YTHDF2 may recognize specific methylated mRNAs, lead to their decay and subsequently to decreased cell apoptosis and differentiation, and in turn promote glioblastoma growth and de-differentiation, and also stabilize *MYC* and *VEGFA* transcripts in GSCs in an m^{6}A-dependent manner (12, 72).

Moreover, a major splicing factor serine and arginine rich splicing factor 3 (SRSF3) is frequently upregulated in clinical glioma specimens (73). Knockdown of *YTHDC1* leads to accumulation of NMD of *SRSF3* mRNAs in glioblastoma cells, which can accelerate the proliferation of tumor cells (66).

In summary, altered m^{6}A modifications are associated with the occurrence and development of glioblastoma, likely through regulating self-renewal of glioma stem cells. It appears that both m^{6}A writers and erasers play an oncogenic role, and m^{6}A readers function in progression in development of glioblastoma. However, inconsistent results indicate complicity of m^{6}A modifications in brain tumor formation, likely through regulating distinct downstream genes.

CONCLUSIONS AND PERSPECTIVES

Brain development is based on coordinated spatiotemporal cell fate decisions, and tightly regulated gene expression.

Accumulating studies have shown that m^{6}A methylation plays an important role in brain development and even in brain tumorigenesis. A major challenge is to identify specific target RNAs for m^{6}A modifications in specific cell types and at different developmental stages. Recent improvements to m^{6}A mapping methods will undoubtedly facilitate studies of activity-dependent changes to the epitranscriptome within distinct RNA populations in the brain. Moreover, an interesting research will be to determine whether changes to the mRNA modification landscape are causing factors or a consequence of activity-dependent regulation of gene expression.

How m^{6}A methylation regulates brain tumor formation remains obscure. Taking the advantage of technical development of m^{6}A methylation analysis at the single-cell level, mechanistic understanding of RNA methylation in different cell types will be revealed. Interestingly, in the late stage of glioma, high m^{6}A modification levels may increase epigenetic reprogramming of non-GSCs into GSCs, whereas knockdown of *METTL3* may reduce the ratio of GSCs in glioblastoma (66). Thus, a more profound breakthrough in the role of m^{6}A methylation in brain tumor diagnostics and treatment strategy also should be developed.

AUTHOR CONTRIBUTIONS

JW and TS wrote the manuscript and produced figures. YQS modified the manuscript. TS edited the manuscript. All authors contributed to the article and approved the submitted version.

FUNDING

This work was supported by the Scientific Research Funds of Huaqiao University (Z16Y0017, TS), and the National Natural Science Foundation of China (31771141 and 81701132).

REFERENCES

1. Schwartz S, Mumbach MR, Jovanovic M, Wang T, Maciag K, Bushkin GG, et al. Perturbation of m6A writers reveals two distinct classes of mRNA methylation at internal and 5' sites. *Cell Rep* (2014) 8(1):284–96. doi: 10.1016/j.celrep.2014.05.048
2. Li J, Yang X, Qi Z, Sang Y, Liu Y, Xu B, et al. The role of mRNA m(6)A methylation in the nervous system. *Cell Biosci* (2019) 9(1). doi: 10.1186/s13578-019-0330-y
3. Boccaletto P, Machnicka MA, Purta E, Piatkowski P, Baginski B, Wirecki TK, et al. MODOMICS: a database of RNA modification pathways. 2017 update. *Nucleic Acids Res* (2018) 46(D1):D303–7. doi: 10.1093/nar/gkx1030
4. Hsu PJ, Shi H, He C. Epitranscriptomic influences on development and disease. *Genome Biol* (2017) 18(1):197. doi: 10.1186/s13059-017-1336-6
5. Roundtree IA, Evans ME, Pan T, He C. Dynamic RNA Modifications in Gene Expression Regulation. *Cell* (2017) 169(7):1187–200. doi: 10.1016/j.cell.2017.05.045
6. Shi H, Wei J, He C. Where, When, and How: Context-Dependent Functions of RNA Methylation Writers, Readers, and Erasers. *Mol Cell* (2019) 74(4):640–50. doi: 10.1016/j.molcel.2019.04.025
7. Liu J, Yue Y, Han D, Wang X, Fu Y, Zhang L, et al. A METTL3-METTL14 complex mediates mammalian nuclear RNA N6-adenosine methylation. *Nat Chem Biol* (2014) 10(2):93–5. doi: 10.1038/nchembio.1432
8. Wang Y, Li Y, Toth JI, Petroski MD, Zhang Z, Zhao JC. N6-methyladenosine modification destabilizes developmental regulators in embryonic stem cells. *Nat Cell Biol* (2014) 16(2):191–8. doi: 10.1038/ncb2902
9. Ping XL, Sun BF, Wang L, Xiao W, Yang X, Wang WJ, et al. Mammalian WTAP is a regulatory subunit of the RNA N6-methyladenosine methyltransferase. *Cell Res* (2014) 24(2):177–89. doi: 10.1038/cr.2014.3
10. Zhao BS, Roundtree IA, He C. Post-transcriptional gene regulation by mRNA modifications. *Nat Rev Mol Cell Biol* (2017) 18(1):31–42. doi: 10.1038/nrm.2016.132
11. Jia G, Fu Y, Zhao X, Dai Q, Zheng G, Yang Y, et al. N6-methyladenosine in nuclear RNA is a major substrate of the obesity-associated FTO. *Nat Chem Biol* (2011) 7(12):885–7. doi: 10.1038/nchembio.687
12. Wang X, Lu Z, Gomez A, Hon GC, Yue Y, Han D, et al. N6-methyladenosine-dependent regulation of messenger RNA stability. *Nature* (2014) 505(7481):117–20. doi: 10.1038/nature12730
13. Shi H, Zhang X, Weng YL, Lu Z, Liu Y, Lu Z, et al. m(6)A facilitates hippocampus-dependent learning and memory through YTHDF1. *Nature* (2018) 563(7730):249–53. doi: 10.1038/s41586-018-0666-1
14. Deng X, Su R, Weng H, Huang H, Li Z, Chen J. RNA N(6)-methyladenosine modification in cancers: current status and perspectives. *Cell Res* (2018) 28(5):507–17. doi: 10.1038/s41422-018-0034-6
15. Wang X, Zhao BS, Roundtree IA, Lu Z, Han D, Ma H, et al. N(6)-methyladenosine Modulates Messenger RNA Translation Efficiency. *Cell* (2015) 161(6):1388–99. doi: 10.1016/j.cell.2015.05.014
16. Wang X, Feng J, Xue Y, Guan Z, Zhang D, Liu Z, et al. Corrigendum: Structural basis of N(6)-adenosine methylation by the METTL3-METTL14 complex. *Nature* (2017) 542(7640):260. doi: 10.1038/nature21073
17. Horowitz S, Horowitz A, Nilsen TW, Munns TW, Rottman FM. Mapping of N6-methyladenosine residues in bovine prolactin mRNA. *Proc Natl Acad Sci U S A* (1984) 81(18):5667–71. doi: 10.1073/pnas.81.18.5667
18. Yue Y, Liu J, He C. RNA N6-methyladenosine methylation in post-transcriptional gene expression regulation. *Genes Dev* (2015) 29(13):1343–55. doi: 10.1101/gad.262766.115
19. Zheng G, Dahl JA, Niu Y, Fedorcsak P, Huang CM, Li CJ, et al. ALKBH5 is a mammalian RNA demethylase that impacts RNA metabolism and mouse fertility. *Mol Cell* (2013) 49(1):18–29. doi: 10.1016/j.molcel.2012.10.015
20. Muller S, Glass M, Singh AK, Haase J, Bley N, Fuchs T, et al. IGF2BP1 promotes SRF-dependent transcription in cancer in a m6A- and miRNA-dependent manner. *Nucleic Acids Res* (2019) 47(1):375–90. doi: 10.1093/nar/gky1012
21. Meyer KD, Patil DP, Zhou J, Zinoviev A, Skabkin MA, Elemento O, et al. 5' UTR m(6)A Promotes Cap-Independent Translation. *Cell* (2015) 163(4):999–1010. doi: 10.1016/j.cell.2015.10.012
22. Meyer KD, Saletore Y, Zumbo P, Elemento O, Mason CE, Jaffrey SR. Comprehensive analysis of mRNA methylation reveals enrichment in 3' UTRs and near stop codons. *Cell* (2012) 149(7):1635–46. doi: 10.1016/j.cell.2012.05.003
23. Schwartz S, Agarwala SD, Mumbach MR, Jovanovic M, Mertins P, Shishkin A, et al. High-resolution mapping reveals a conserved, widespread, dynamic mRNA methylation program in yeast meiosis. *Cell* (2013) 155(6):1409–21. doi: 10.1016/j.cell.2013.10.047
24. Geula S, Moshitch-Moshkovitz S, Dominissini D, Mansour AA, Kol N, Salmon-Divon M, et al. Stem cells. m6A mRNA methylation facilitates resolution of naïve pluripotency toward differentiation. *Science (New York NY)* (2015) 347(6225):1002–6. doi: 10.1126/science.1261417
25. Hongay CF, Orr-Weaver TL. Drosophila Inducer of MEiosis 4 (IME4) is required for Notch signaling during oogenesis. *Proc Natl Acad Sci U S A* (2011) 108(36):14855–60. doi: 10.1073/pnas.1111577108
26. Wang X, He C. Dynamic RNA modifications in posttranscriptional regulation. *Mol Cell* (2014) 56(1):5–12. doi: 10.1016/j.molcel.2014.09.001

27. Shi H, Wang X, Lu Z, Zhao BS, Ma H, Hsu PJ, et al. YTHDF3 facilitates translation and decay of N(6)-methyladenosine-modified RNA. *Cell Res* (2017) 27(3):315–28. doi: 10.1038/cr.2017.15
28. Huang H, Weng H, Sun W, Qin X, Shi H, Wu H, et al. Recognition of RNA N (6)-methyladenosine by IGF2BP proteins enhances mRNA stability and translation. *Nat Cell Biol* (2018) 20(3):285–95. doi: 10.1038/s41556-018-0045-z
29. Dominissini D, Moshitch-Moshkovitz S, Schwartz S, Salmon-Divon M, Ungar L, Osenberg S, et al. Topology of the human and mouse m6A RNA methylomes revealed by m6A-seq. *Nature* (2012) 485(7397):201–6. doi: 10.1038/nature11112
30. Du H, Zhao Y, He J, Zhang Y, Xi H, Liu M, et al. YTHDF2 destabilizes m(6)A-containing RNA through direct recruitment of the CCR4-NOT deadenylase complex. *Nat Commun* (2016) 7:12626. doi: 10.1038/ncomms12626
31. Roost C, Lynch SR, Batista PJ, Qu K, Chang HY, Kool ET, et al. Structure and thermodynamics of N6-methyladenosine in RNA: a spring-loaded base modification. *J Am Chem Soc* (2015) 137(5):2107–15. doi: 10.1021/ja513080v
32. Xiao W, Adhikari S, Dahal U, Chen YS, Hao YJ, Sun BF, et al. Nuclear m(6)A Reader YTHDC1 Regulates mRNA Splicing. *Mol Cell* (2016) 61(4):507–19. doi: 10.1016/j.molcel.2016.01.012
33. Xue S, Tian S, Fujii K, Kladwang W, Das R, Barna M. RNA regulons in Hox 5' UTRs confer ribosome specificity to gene regulation. *Nature* (2015) 517 (7532):33–8. doi: 10.1038/nature14010
34. Zhang C, Fu J, Zhou Y. A Review in Research Progress Concerning m6A Methylation and Immunoregulation. *Front Immunol* (2019) 10:922. doi: 10.3389/fimmu.2019.00922
35. Choe J, Lin S, Zhang W, Liu Q, Wang L, Ramirez-Moya J, et al. mRNA circularization by METTL3-eIF3h enhances translation and promotes oncogenesis. *Nature* (2018) 561(7724):556–60. doi: 10.1038/s41586-018-0538-8
36. Lin S, Choe J, Du P, Triboulet R, Gregory RI. The m(6)A Methyltransferase METTL3 Promotes Translation in Human Cancer Cells. *Mol Cell* (2016) 62 (3):335–45. doi: 10.1016/j.molcel.2016.03.021
37. Barbieri I, Tzelepis K, Pandolfini L, Shi J, Millán-Zambrano G, Robson SC, et al. Promoter-bound METTL3 maintains myeloid leukaemia by m(6)A-dependent translation control. *Nature* (2017) 552(7683):126–31. doi: 10.1038/nature24678
38. Liu S, Hausmann S, Carlson SM, Fuentes ME, Francis JW, Pillai R, et al. METTL13 Methylation of eEF1A Increases Translational Output to Promote Tumorigenesis. *Cell* (2019) 176(3):491–504.e421. doi: 10.1016/j.cell.2018.11.038
39. Boles NC, Temple S. Epimetronomics: m6A Marks the Tempo of Corticogenesis. *Neuron* (2017) 96(4):718–20. doi: 10.1016/j.neuron.2017.11.002
40. Yoon K-J, Ringeling FR, Vissers C, Jacob F, Pokrass M, Jimenez-Cyrus D, et al. Temporal Control of Mammalian Cortical Neurogenesis by m6A Methylation. *Cell* (2017) 171(4):877–89.e817. doi: 10.1016/j.cell.2017.09.003
41. Du K, Zhang L, Lee T, Sun T. m(6)A RNA Methylation Controls Neural Development and Is Involved in Human Diseases. *Mol Neurobiol* (2019) 56 (3):1596–606. doi: 10.1007/s12035-018-1138-1
42. Li L, Zang L, Zhang F, Chen J, Shen H, Shu L, et al. Fat mass and obesity-associated (FTO) protein regulates adult neurogenesis. *Hum Mol Genet* (2017) 26(13):2398–411. doi: 10.1093/hmg/ddx128
43. Hess ME, Hess S, Meyer KD, Verhagen LA, Koch L, Bronneke HS, et al. The fat mass and obesity associated gene (Fto) regulates activity of the dopaminergic midbrain circuitry. *Nat Neurosci* (2013) 16(8):1042–8. doi: 10.1038/nn.3449
44. Li M, Zhao X, Wang W, Shi H, Pan Q, Lu Z, et al. Ythdf2-mediated m(6)A mRNA clearance modulates neural development in mice. *Genome Biol* (2018) 19(1):69. doi: 10.1186/s13059-018-1436-y
45. Ma C, Chang M, Lv H, Zhang ZW, Zhang W, He X, et al. RNA m(6)A methylation participates in regulation of postnatal development of the mouse cerebellum. *Genome Biol* (2018) 19(1):68. doi: 10.1186/s13059-018-1435-z
46. Wang CX, Cui GS, Liu X, Xu K, Wang M, Zhang XX, et al. METTL3-mediated m6A modification is required for cerebellar development. *PloS Biol* (2018) 16 (6):e2004880. doi: 10.1371/journal.pbio.2004880
47. Flamand MN, Meyer KD. The epitranscriptome and synaptic plasticity. *Curr Opin Neurobiol* (2019) 59:41–8. doi: 10.1016/j.conb.2019.04.007
48. Merkurjev D, Hong WT, Iida K, Oomoto I, Goldie BJ, Yamaguti H, et al. Synaptic N(6)-methyladenosine (m(6)A) epitranscriptome reveals functional partitioning of localized transcripts. *Nat Neurosci* (2018) 21(7):1004–14. doi: 10.1038/s41593-018-0173-6
49. Yu J, Chen M, Huang H, Zhu J, Song H, Zhu J, et al. Dynamic m6A modification regulates local translation of mRNA in axons. *Nucleic Acids Res* (2018) 46(3):1412–23. doi: 10.1093/nar/gkx1182
50. Zhuang M, Li X, Zhu J, Zhang J, Niu F, Liang F, et al. The m6A reader YTHDF1 regulates axon guidance through translational control of Robo3.1 expression. *Nucleic Acids Res* (2019) 47(9):4765–77. doi: 10.1093/nar/gkz157
51. Rowitch DH, Kriegstein AR. Developmental genetics of vertebrate glial-cell specification. *Nature* (2010) 468(7321):214–22. doi: 10.1038/nature09611
52. Yao B, Christian KM, He C, Jin P, Ming GL, Song H, et al. Epigenetic mechanisms in neurogenesis. *Nat Rev Neurosci* (2016) 17(9):537–49. doi: 10.1038/nrn.2016.70
53. Chang M, Lv H, Zhang W, Ma C, He X, Zhao S, et al. Region-specific RNA m(6)A methylation represents a new layer of control in the gene regulatory network in the mouse brain. *Open Biol* (2017) 7(9):170166. doi: 10.1098/rsob.170166
54. Chen J, Zhang YC, Huang C, Shen H, Sun B, Cheng X, et al. m(6)A Regulates Neurogenesis and Neuronal Development by Modulating Histone Methyltransferase Ezh2. *Genomics Proteomics Bioinformatics* (2019) 17 (2):154–68. doi: 10.1016/j.gpb.2018.12.007
55. Zhou H, Wang B, Sun H, Xu X, Wang Y. Epigenetic Regulations in Neural Stem Cells and Neurological Diseases. *Stem Cells Int* (2018) 2018:6087143. doi: 10.1155/2018/6087143
56. Xu H, Dzhashiashvili Y, Shah A, Kunjamma RB, Weng YL, Elbaz B, et al. m(6)A mRNA Methylation Is Essential for Oligodendrocyte Maturation and CNS Myelination. *Neuron* (2020) 105(2):293–309 e295. doi: 10.1016/j.neuron.2019.12.013
57. Wu R, Li A, Sun B, Sun JG, Zhang J, Zhang T, et al. A novel m(6)A reader Prrc2a controls oligodendroglial specification and myelination. *Cell Res* (2019) 29(1):23–41. doi: 10.1038/s41422-018-0113-8
58. Rasband MN. Glial Contributions to Neural Function and Disease. *Mol Cell Proteomics* (2016) 15(2):355–61. doi: 10.1074/mcp.R115.053744
59. Johnson DR, Guerin JB, Giannini C, Morris JM, Eckel LJ, Kaufmann TJ. 2016 Updates to the WHO Brain Tumor Classification System: What the Radiologist Needs to Know. *Radiographics* (2017) 37(7):2164–80. doi: 10.1148/rg.2017170037
60. Ostrom QT, Gittleman H, Truitt G, Boscia A, Kruchko C, Barnholtz-Sloan JS. CBTRUS Statistical Report: Primary Brain and Other Central Nervous System Tumors Diagnosed in the United States in 2011-2015. *Neuro-oncology* (2018) 20(suppl_4):iv1–iv86. doi: 10.1093/neuonc/noy131
61. Ostrom QT, Cioffi G, Gittleman H, Patil N, Waite K, Kruchko C, et al. CBTRUS Statistical Report: Primary Brain and Other Central Nervous System Tumors Diagnosed in the United States in 2012-2016. *Neuro-oncology* (2019) 21(Suppl 5):v1–v100. doi: 10.1093/neuonc/noz150
62. Dong Z, Cui H. The Emerging Roles of RNA Modifications in Glioblastoma. *Cancers (Basel)* (2020) 12(3):736. doi: 10.3390/cancers12030736
63. Huang H, Weng H, Chen J. m(6)A Modification in Coding and Non-coding RNAs: Roles and Therapeutic Implications in Cancer. *Cancer Cell* (2020) 37 (3):270–88. doi: 10.1016/j.ccell.2020.02.004
64. Thapar R, Bacolla A, Oyeniran C, Brickner JR, Chinnam NB, Mosammaparast N, et al. RNA Modifications: Reversal Mechanisms and Cancer. *Biochemistry* (2019) 58(5):312–29. doi: 10.1021/acs.biochem.8b00949
65. Chai RC, Wu F, Wang QX, Zhang S, Zhang KN, Liu YQ, et al. m(6)A RNA methylation regulators contribute to malignant progression and have clinical prognostic impact in gliomas. *Aging* (2019) 11(4):1204–25. doi: 10.18632/aging.101829
66. Li F, Yi Y, Miao Y, Long W, Long T, Chen S, et al. N(6)-Methyladenosine Modulates Nonsense-Mediated mRNA Decay in Human Glioblastoma. *Cancer Res* (2019) 79(22):5785–98. doi: 10.1158/0008-5472.can-18-2868
67. Cui Q, Shi H, Ye P, Li L, Qu Q, Sun G, et al. m(6)A RNA Methylation Regulates the Self-Renewal and Tumorigenesis of Glioblastoma Stem Cells. *Cell Rep* (2017) 18(11):2622–34. doi: 10.1016/j.celrep.2017.02.059
68. Jin DI, Lee SW, Han ME, Kim HJ, Seo SA, Hur GY, et al. Expression and roles of Wilms' tumor 1-associating protein in glioblastoma. *Cancer Sci* (2012) 103 (12):2102–9. doi: 10.1111/cas.12022
69. Ceccarelli M, Barthel Floris P, Malta Tathiane M, Sabedot Thais S, Salama Sofie R, Murray Bradley A, et al. Molecular Profiling Reveals Biologically Discrete Subsets and Pathways of Progression in Diffuse Glioma. *Cell* (2016) 164(3):550–63. doi: 10.1016/j.cell.2015.12.028

70. Zhang S, Zhao BS, Zhou A, Lin K, Zheng S, Lu Z, et al. m(6)A Demethylase ALKBH5 Maintains Tumorigenicity of Glioblastoma Stem-like Cells by Sustaining FOXM1 Expression and Cell Proliferation Program. *Cancer Cell* (2017) 31(4):591–606.e596. doi: 10.1016/j.ccell.2017.02.013
71. Su R, Dong L, Li C, Nachtergaele S, Wunderlich M, Qing Y, et al. R-2HG Exhibits Anti-tumor Activity by Targeting FTO/m6A/MYC/CEBPA Signaling. *Cell* (2018) 172(1-2):90–105.e123. doi: 10.1016/j.cell.2017.11.031
72. Dixit D, Prager BC, Gimple RC, Poh HX, Wang Y, Wu Q, et al. The RNA m6A reader YTHDF2 maintains oncogene expression and is a targetable dependency in glioblastoma stem cells. *Cancer Discov* (2020). doi: 10.1158/2159-8290.cd-20-0331
73. Song X, Wan X, Huang T, Zeng C, Sastry N, Wu B, et al. SRSF3-Regulated RNA Alternative Splicing Promotes Glioblastoma Tumorigenicity by Affecting Multiple Cellular Processes. *Cancer Res* (2019) 79(20):5288–301. doi: 10.1158/0008-5472.can-19-1504

Conflict of Interest: The authors declare that the research was conducted in the absence of any commercial or financial relationships that could be construed as a potential conflict of interest.

frontiers in Oncology

MINI REVIEW
published: 25 February 2021
doi: 10.3389/fonc.2020.612337

The Impact of m6A RNA Modification in Therapy Resistance of Cancer: Implication in Chemotherapy, Radiotherapy, and Immunotherapy

Omprakash Shriwas[1,2], *Pallavi Mohapatra*[1,3], *Sibasish Mohanty*[1,3] *and Rupesh Dash*[1]*

[1] Institute of Life Sciences, Bhubaneswar, India, [2] Manipal Academy of Higher Education, Manipal, India, [3] Regional Center for Biotechnology, Faridabad, India

OPEN ACCESS

Edited by:
Shicheng Guo,
University of Wisconsin-Madison,
United States

Reviewed by:
Huabing Li,
Shanghai Jiao Tong University School of Medicine, China
Jinkai Wang,
Sun Yat-Sen University, China
Fan Shen,
University of Alberta, Canada

***Correspondence:**
Rupesh Dash
rupesh.dash@gmail.com;
rupeshdash@ils.res.in

Specialty section:
This article was submitted to Cancer Genetics, a section of the journal Frontiers in Oncology

Received: 30 September 2020
Accepted: 11 December 2020
Published: 25 February 2021

Citation:
Shriwas O, Mohapatra P, Mohanty S and Dash R (2021) The Impact of m6A RNA Modification in Therapy Resistance of Cancer: Implication in Chemotherapy, Radiotherapy, and Immunotherapy. Front. Oncol. 10:612337. doi: 10.3389/fonc.2020.612337

m6A RNA methylation, which serves as a critical regulator of transcript expression, has gathered tremendous scientific interest in recent years. From RNA processing to nuclear export, RNA translation to decay, m6A modification has been studied to affect various aspects of RNA metabolism, and it is now considered as one of the most abundant epitranscriptomic modification. RNA methyltransferases (writer), m6A-binding proteins (readers), and demethylases (erasers) proteins are frequently upregulated in several neoplasms, thereby regulating oncoprotein expression, augmenting tumor initiation, enhancing cancer cell proliferation, progression, and metastasis. Though the potential role of m6A methylation in growth and proliferation of cancer cells has been well documented, its potential role in development of therapy resistance in cancer is not clear. In this review, we focus on m6A-associated regulation, mechanisms, and functions in acquired chemoresistance, radioresistance, and resistance to immunotherapy in cancer.

Keywords: m6A methylation, cisplatin, PD-1, METTL3, YTHDF1, ALKBH5

INTRODUCTION

Cancer remains a key public health concern posing a major threat to the world's population. According to Siegel et al. each year approximately1,806,590 new cases of cancer are being diagnosed and around 606,520 people lose their life to cancer alone in the United States (1). The most frequently used therapeutic regimens for cancer include surgery, chemotherapy, radiotherapy, and more recently immunotherapy (2, 3). Although there have been breakthroughs and successes in treating specific types of cancer, most strategies have not proven as efficacious as hoped or predicted. One of the major causes of failure to treat cancer is a lack of understanding of the molecular mechanism behind the therapy resistance. Chemoresistance is one of the major factors for treatment failure in cancer. The chemotherapy drugs efficiently eradicates the rapidly dividing cells but poorly eliminates the slow dividing cells, particularly when lower dose of drug is provided to balance its cytotoxic effect on normal or non-transformed cells. This population of cells, which partially responds to chemotherapy drug, contributes to development of chemoresistance. Ultimately, the patients experience tumor relapse, which culminates with continued tumor growth and metastatic

spread (4). The chemoresistance can be divided into two categories: "intrinsic chemoresistance" where cancer cells are inherently resistant prior to chemotherapy and "acquired chemoresistance" where cancer cells acquire resistance during prolonged treatment with agents that they initially displayed sensitivity. The chemoresistant phenotype of cancer cells can be attributed due to impaired apoptosis, altered cellular metabolism, decreased drug accumulation, reduced drug-target interactions, and increased populations of cancer stem cells (2). However, these are the endpoint events and the causative factors responsible for acquired chemoresistance is yet to be known. Similarly, cancer cells develop resistance against ionizing radiation (radioresistance) by enhancing DNA damage response, altering the expression of oncogene/tumor supressors, manipulating the tumor microenvironment, and by regulating the cell cycle (5). Understanding the molecular mechanisms behind the therapy resistance will enable us to overcome the drug resistance in cancer.

With the discovery of methylation of O6-methylguanine-DNA methyltransferase (MGMT) that sensitizes glioblastoma multiforme (GBM) cells to temozolomide, epigenetic alterations have been extensively studied to uncover the molecular mechanism behind therapy resistance (6, 7). Approximately 100 different types of modifications can be observed at RNA level, but m6A modification of RNA has gathered much attention. Since then, researchers pushed their focus and discovered Writer, Reader, and Erasers for RNA modification (8). Advancement of techniques like high throughput sequencing enabled the scientific community to uncover m6A enrichment at RNA. Modification of m6A in transcriptome is not random, but happens at a consensus sequences like DRACH (D = G, A, or U; R = G or A; H = A, C, or U), which are enriched mostly in CDS as well as 3'UTR region (9, 10). RNA methylation occurs on several sites including 5-methylcytosine (m5 C), 7-methylguanosine (m7 G), m1 G, m2 G, m6 G, N1 - methyl adenosine (m1 A), and m6 A (11). The m6A modification occurs *via* "writers" (i.e., m6A methyltransferases), recognized by "readers" (i.e., m6A-binding proteins), and removed by "erasers" (i.e., m6A demethylases) in eukaryotes (12). Methyltransferase-like 3 (METTL3), METTL14, Wilms tumor 1-associated protein (WTAP), KIAA1429, RNA-binding motif protein 15 (RBM15), and zinc finger CCCH domain-containing protein 13 (ZC3H13) forms the "writer" complex that initiates the m6A modification (13, 14). YT521-B homology(YTH) proteins, insulin-like growth factor 2 mRNA binding proteins (IGF2BPs), eukaryotic initiation factor 3 (eIF3), heterogeneous nuclear ribonucleoproteins (HNRNPs), and fragile X mental retardation proteins (FMRPs) are included under "reader" complex that recognizes the m6A RNA modification and initiates downstream signaling (13). Obesity-associated protein (FTO) and alkB homolog 5 (ALKBH5) stimulate the demethylation process and are included under "eraser" complex (15, 16). Extensive studies on m6A modification indicated toward its contribution in regulation of mRNA (17), long non-coding RNA (lncRNA) (18), microRNA (19), and circular RNA (circRNA) (20). m6A modification being an important RNA regulatory mechanism has been proved to play a critical role in regulating RNA processing, transportation, translation, and decay. Methyltransferase-like 3 (METTL3) methylates pri-miRNAs, enabling them to be recognized by RNA-binding protein DGCR8 and thereby leading to miRNA maturation (21). The global RNA modification study suggests that RNA demethylase FTO was found to regulate pre-mRNA processing including alternative splicing and 3′ UTR processing (22). Studies also revealed that m6A is added to exons in nascent pre-mRNA and its addition in the nascent transcript is a determinant of cytoplasmic mRNA stability (22). Interestingly, selective down regulation of METTL3 reduces the translation of mRNAs bearing 5' UTR methylation. In this study, it was found that ABCF1 coordinates with METTL3 in m6A-facilitated and eIF4F independent mRNA translation (23), demonstrating the role of m6A methylation in mRNA translation. m6A-binding protein YTHDC1 mediates export of methylated mRNA from the nucleus to the cytoplasm, demonstrating the potential role of m6A modification in RNA translocation (24). There is emerging evidence indicating that m6A modification is strongly associated with acquired therapy resistance in cancer. In this review, we have focused on the mechanisms of RNA m6A modification-associated therapy resistance and possible approaches to overcome it.

IMPLICATION IN CHEMORESISTANCE

Reprogramming chemoresistant cells to undergo drug induced apoptosis is a viable approach to treat recurrent neoplastic diseases. This can be achieved by selective downregulation of anti-apoptotic factors or activation of pro-apoptotic factors in tumor cells (2). Among several novel approaches, modulation of N6-methyladenosine(m6A) RNA modification was found to be an important strategy in various types of cancer cells to overcome drug induced cell death. Various studies indicate that m6A modification confers drug resistance by regulating ABC transporters directly on transcript level or *via* upstream signaling pathways (19). Similarly, studies suggested that m6A modification affects the expression of BCL-2 with variable outcomes depending on the different cancer types (25, 26). Recent studies indicate that the m6A modification is involved in the maintenance of CSCs in tumors, leading to drug resistance and recurrence. Considering the potential role of m6A RNA modification in development of chemoresistance, it can be a viable therapeutic target to overcome chemoresistance.

Cisplatin Resistance and m6A Modification

Cisplatin is the first line of treatment for several neoplasms. In 1965, Barnett Rosenberg accidently discovered the role of cisplatin in cell division. Further studies substantiated that it is the most promising agent for treatment of cancer (27). Writer protein METTL3 is involved in acquired cisplatin resistance by regulating TRIM11 expression. Methylated RNA immunoprecipitation (Me-RIP) study suggests that TRIM11 m6A level was higher in cisplatin resistant cells compared to sensitive cells in nasopharyngeal carcinoma (NPC) lines. Depletion of METTL3 results in reduced TRIM11 expression that sensitizes NPC lines to cisplatin (28). Similarly, METTL3

enhances the YAP1 m6A methylation at mRNA level and stabilize its expression in human lung cancer lines. The elevated YAP1 mediates cisplatin resistance in NSCLC (19). Reader protein YTHDF1 depletion mediates cisplatin resistance in NSLCC through KEAP1/NRF2/AKR1C1 axis and higher expression of YTHDF1 showed better clinical outcome of NSCLC patient (29). Erasers also play an important role in acquired cisplatin resistance in several neoplasms. FTO demethylates β-catenin mRNA and stabilizes the β-catenin in cervical squamous cell carcinoma, thereby inducing chemo-radio therapy resistance (30). In our study, we found that ALKBH5 is directly regulated by human RNA helicase DDX3, which leads to decreased m6A methylation in FOXM1 and NANOG nascent transcript that contribute to cisplatin resistance in OSCC (31).

Kinase Inhibitor and m6A Modification

Kinase inhibitors have emerged as a potential strategy for treatment of cancer. Currently, several FDA approved kinase inhibitors are being evaluated in different phases of clinical trials to treat cancer (32). m6A RNA modifications play an important role in acquiring resistance against kinase inhibitors. A comparative study in NSCLC cell lines suggests that higher m6A enrichment scores can be found in afatinib resistant lines as compared with sensitive cells (33). Similarly, RNA methylation status was compared between TKI (tyrosine kinase inhibitor) resistant and sensitive cells and it was found that cells having hypomethylation showed greater tolerance for TKI and better growth rate. FTO- enhances mRNA stability of prosurvival transcripts and further induces resistance to tyrosine kinase inhibitors (TKIs) in leukaemia cells (26). Depletion of METTL3 induces sorafenib resistance in human liver cancer lines. Mechanistically, it was found that depletion of METTL3 reduces the stabilization of FOXO3 mRNA and ectopic overexpression of FOXO3 restores sorafenib sensitivity (34).

5-Fluorouracil Resistance and m6A Modification

5-Fluorouracil (5FU) is a widely used anticancer drug in many cancers. It is an analogue of uracil, which gets incorporated into nucleic acids and interfere with nucleotide metabolism (35, 36). For treatment of several neoplasms, the common chemotherapy regimen involves TPF (Taxol, Platinum, and Fluorouracil) or FOLFOX (Folinic acid, Fluorouracil and Oxaliplatin) (37). The role of m6A in 5 FU resistance is not well studied except few reports, which indicates m6A RNA modification augments the chemosensitivity of 5 FU. METTL3 knockdown increases the 5FU sensitivity in pancreatic ductal adeno carcinomas (38). Similarly, reader protein YTHDF1 knockdown results in enhanced 5FU sensitivity in colorectal cancer (39).

PARP Inhibitor and m6A Modification

DNA damage is a common mode of action for most of the anticancer drugs and absence of an efficient DNA repair system in cancer cells leads to drug induced death. PARP (poly (ADP-ribose) polymerase) is a key enzyme that plays important roles in DNA damage response. PARP1 identifies and interacts with single stranded DNA damage through its DNA binding domain. Further, PARP1 synthesizes poly(ADP) ribose (PAR) and transfers it to acceptor proteins. PAR recruits repair proteins to the damaged DNA site. Henceforth, PARP1 has been established as an important target for cancer therapy. As many as 8 different PARP inhibitors are in different phases of clinical trial against various neoplasms (40–42). PARP inhibitors generally bind to the cofactor and catalytic domain and inhibits its enzyme activity (43). The most commonly used PARP1 inhibitors are Olaparib, Rucaparib, Niraparib, and Talazoparib (44). Olaparib is the first inhibitor used for clinical trial in BRCA 1 mutant solid tumor (45). Only few studies with m6A modification and PARP1i resistance are available in literature. Fukumoto et al. (2019) performed a global m6A modification profiling and found that in BRCA-mutated lines, m6A modification stabilizes the expression of FZD10 mRNA, which ultimately contributes to PARP inhibitor resistance. Mechanistically it was found that enhanced expression of *FZD10* leads to activation of Wnt/β-Catenin signalling. ALKBH5 and FTO knockdown decreased FZD10 mRNA stability and sensitize the cell to PARP inhibitor (46). This study clearly indicated that m6A modification plays a crucial role during the development of PARPi resistance.

Gemcitabine and m6A Modification

Gemcitabine, a pyrimidine analogue, is used as chemotherapeutic regimen in several neoplasms including pancreatic, ovarian, breast, bladder, and small lung carcinoma. Moreover, Gemcitabine enhances the survival rate of pancreatic cancer patients up to 20% (47). Interestingly, Gemcitabine decreased the expression of ALKBH5 in PDAC xenografts. Ectopic overexpression of ALKBH5 sensitizes PDAC lines to Gemcitabine. On the other hand, knockdown of ALKBH5 in PDAC lines enhanced cell growth, proliferation, and migration. RNA immunoprecipitation followed by sequencing data suggests that in ALKBH5 knock down cells, increased m6A modification at the 3′ UTR region of the WIF-1 (Wnt inhibitory factor 1) mRNA can be observed. Henceforth, the expression of WIF-1 is down regulated in ALKBH5 KD cells, which in turns activate Wnt pathway and enhances the expression of Wnt target genes like C-MYC, Cyclin D1, and MMP-2 (48). On the contrary, knock down of METTL3 enhanced the sensitivity towards many chemotherapeutic drugs including gemcitabine (38).

IMPLICATION IN IMMUNOTHERAPY

Interestingly, m6A RNA modification also plays an important role in regulating immune response in cancer patients. He et al. analyzed the RNA sequencing data of 24 different m6A regulators in 775 breast cancer patients from TCGA database and categorized them in two subgroups. One group had a lower RNA methylation status (RM1) and other had a high methylation status (RM2). The RM1 group showed shorter overall survival rate and higher enrichment of PI3K and KRAS signalling. On the other hand, the RM2 group showed higher numbers of tumor-infiltrating CD8+ T cells, helper T cells, and activated NK cells, but lower expressions of PD-L1, PD-L2,

TIM3, and CCR4 than RM1 group (49). Similarly, the study by Winkler et al. suggested that m6A modifications serve as a negative regulator of interferon response by modulating the turnover of interferon mRNAs (50). Writer, reader, and erasers play important roles in immune surveillance. Rubio et al. suggest that writer METTL14 depletion induces IFNβ1 production, whereas ALKBH5 depletion reduces IFNβ1 production (51). T cell homeostasis is very important for any kind of defense balance, but depletion of writer METTL3 in CD4 cells hampered the homeostasis of T cells (52). METTL3 depletion in dendritic cells resulted in impaired maturation of dendritic cell and led to weak costimulatory signal by CD40-CD80 as well as exerted reduced T cell stimulation (53).The reader protein YTHDF1 regulates immune response in melanoma cancer. YTHDF1 deletion in mice showed slower growth of melanoma and higher survival rate compared to WT YTHDF1 by enhancing antigen specific CD8+ T cell antitumor response. With depletion of YTHDF1 in dendritic cells, increased cross-presentation of tumor antigens and the cross-priming of CD8+ T cells was observed *in vivo*. It was found that lysosomal protease enzyme in dendritic cells with m6A was recognized by YTHDF1 (54).

After landmark discovery of PD1/PD-L1 and its role in immune evasion of cancer cells, the immune check point inhibitors (PD-1 inhibitors) have been established as potential anti-tumor agents. Immunotherapy has contributed immensely in terms of survival and quality of life in addition to chemoradiotherapy. The m6A modifications are also reported to play a key role in acquiring therapy resistance against checkpoint inhibitors. FTO inhibition suppresses melanoma tumorigenicity and increased the m6A methylation in PD-1, CXCR1, and SOX10 mRNA, henceforth enhancing the decay of mRNA by YTHDF2. Selective blocking of FTO restores IFN-γ response and sensitizes anti-PD-1 treatment *in vivo* (55). A study by Yi L et al. (56) suggest that m6A regulators are upregulated in HNSCC as compared to normal counterpart. Further they have demonstrated that m6A regulators show positive correlation with PDL-1 in tumor immune microenvironment (TIME), hence presenting the m6A regulators as viable therapeutic targets in HNSCC (56). Zhang et al. (57) suggested that low m6A scores activate immune cells to infiltrate TIME and increases the survival rate of gastric cancer patient compared with high m6A score with low survival rate. Low m6A score increased the neoantigen load as well as sensitized anti PDL-1 immunotherapy. Eraser protein ALKBH5 modulates TIME, deletion of ALKBH5 in colon and melanoma syngeneic tumor model enhances the immune cells infiltration in TIME. Mechanistically ALKBH5 modulates Mct4/Slc16a3 expression and lactate content in TIME, which ultimately suppressed the Treg and myeloid derived Cell. Deletion of ALKBH5 sensitizes the tumor against the anti PD-1 treatment and GVAX vaccine (58). Overall, these studies suggest that m6A methylation is a major regulator of immune response in tumor cells and TIME.

IMPLICATION IN RADIOTHERAPY

Other than chemotherapy, radiation therapy is a major treatment regimen for cancer patients that target cancer cells by damaging the DNA. The concurrent chemo radio therapy is the most common

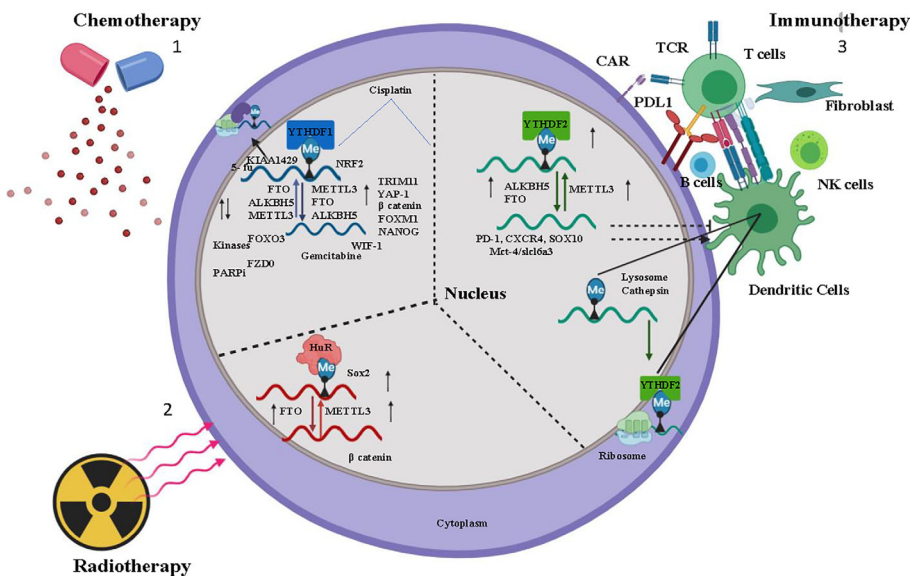

FIGURE 1 | Overview of m6A regulation in Chemotherapy, Immunotherapy, and Radiotherapy- 1) Chemotherapeutic drugs Cisplatin, Kinase inhibitor modulates m6A regulator (Writer-METTL3, Raeder-YTHDF1, Eraser-ALKBH5, FTO) stabilizes the oncogene mRNA and induces chemoresistance. 2) Tumor immuno microenvironment (TIME) (B cells, dendritic cells, T cells, NK cells, fibroblast) activated by m6A regulator and induces immunotherapy resistance for cancer cells. 3) Radiation induces m6a regulator and stabilizes mRNA of cancer stem cell. In the figure, the small upward black arrow indicates "upregulation" and the downward black arrow indicates "down regulation".

TABLE 1 | Summary of m6A RNA modification in therapy resistant cancer cells.

Sr No.	Resistance	Cancer	m6A regulator	Onco/tumor suppressor	Ref
1	Cisplatin	CSCC	FTO	Oncogene	(30)
2	Cisplatin	Nasopharyngeal	METTL3	Oncogene	(28)
3	Cisplatin	NSCLC	METTL3	Oncogene	(19)
4	Cisplatin	NSCLC	YTHDF1	Tumor suppressor	(29)
5	Cisplatin	OSCC	ALKBH5	Oncogene	(31)
6	Cisplatin	Pancreatic cancer	METTL3	Oncogene	(38)
7	Cisplatin	NKTCL	WTAP	Oncogene	(61)
8	Cisplatin	Ovarian Cancer	YTHDF1	Oncogene	(62)
7	oxaliplatin	Colorectal cancer	YTHDF1	Oncogene	(39)
9	Doxorubicin	Osteosarcoma	m6A	Oncogene	(63)
10	Sorafenib	Hepatocellular carcinoma	METTL3	Tumor suppressor	(34)
11	Sorafenib	hepatocellular carcinoma	m6A	Oncogene	(64)
12	Afatinib	NSCLC	m6A	Oncogene	(33)
13	Crizotinib	NSCLC	METTL3/WTAP	Oncogene	(65)
14	Gefitinib	NSCLC	METTL3	Oncogene	(66)
15	5-Fu	Pancreatic Cancer	METTL3	Oncogene	(38)
16	5-Fu	Colorectal cancer	YTHDF1	Oncogene	(39)
17	Olaparib	Ovarian cancer	FTO/ALKBH5	Oncogene	(46)
18	Everolimus	Gastric cancer	METTL3	Tumor Suppressor	(67)
17	Tamoxifen	Breast Cancer	m6A	Oncogene	(68)
19	Y- Irradiation	GBM	METTL3	Oncogene	(60)
20	Y- Irradiation	Pancreatic cancer	METTL3	Oncogene	(38)
21	Y- Irradiation	CSCC	FTO	Oncogene	(30)
22	Anti PD1	Melanoma	FTO/YTHDF2	Oncogene	(55)
23	Anti PD1	Melanoma/colorectal	ALKBH5	Oncogene	(58)
24	PDL1	HNSCC	m6A	Oncogene	(56)

therapeutic regimen followed by surgery (59). Radiation in GBM (glioblastoma) cells enhances the METTL3 expression and it increases the stability of SOX2 by recruiting hUR (human antigen R) and induces resistance against radiation (60). Similarly, selective knock down of METTL3 results in sensitizing pancreatic cancer lines to radiotherapy (38). Eraser protein FTO also induces chemo radio resistance in cervical squamous carcinoma by demethylation of β-catenin mRNA, which stabilizes its expression (30).

CONCLUSION

Therapy resistance in cancer is a consequence of multiple factors such as individual variability in sensitivity to the drug, location of the tumor, tissue lineage, tumor aggressiveness, and intracellular molecular alteration. As discussed earlier, deciphering the consequences of m6A modification on selective transcripts can lead to understanding the molecular mechanism of the therapy resistance (**Figure 1** and **Table 1**), thereby enabling us to optimize the combination therapy of existing drugs or to design specific drugs to overcome resistance property. However, the disadvantage lies on the insufficient studies regarding the selectivity of target mRNA by m6A methyltransferases, demethylases, and binding reader proteins. Along with that localization of m6A modified target transcripts, target specificity of m6A writer, reader, and eraser protein and their varied mode of action in different neoplasms remain unclear.

AUTHOR CONTRIBUTIONS

OS and RD designed the content of this review. OS, PM, and RD wrote the first draft of the manuscript. SM wrote sections of the manuscript. All authors contributed to the article and approved the submitted version.

FUNDING

This work is supported by Institute of Life Sciences, Bhubaneswar intramural support, ICMR (5/13/9/2019-NCD-III) and SERB (CVD/2020/000154). OS is a UGC-SRF. PM is CSIR-JRF, and SM is UGC-JRF.

REFERENCES

1. Siegel RL, Miller KD, Jemal A. Cancer statistics, 2020. *CA Cancer J Clin* (2020) 70:7–30. doi: 10.3322/caac.21590
2. Maji S, Panda S, Samal SK, Shriwas O, Rath R, Pellecchia M, et al. Bcl-2 Antiapoptotic Family Proteins and Chemoresistance in Cancer. *Adv Cancer Res* (2018) 137:37–75. doi: 10.1016/bs.acr.2017.11.001
3. Esfahani K, Roudaia L, Buhlaiga N, Del Rincon SV, Papneja N, Miller WHJr. A review of cancer immunotherapy: from the past, to the present, to the future. *Curr Oncol* (2020) 27:S87–97. doi: 10.3747/co.27.5223
4. D'Alterio C, Scala S, Sozzi G, Roz L, Bertolini G. Paradoxical effects of chemotherapy on tumor relapse and metastasis promotion. *Semin Cancer Biol* (2020) 60:351–61. doi: 10.1016/j.semcancer.2019.08.019

5. Tang L, Wei F, Wu Y, He Y, Shi L, Xiong F, et al. Role of metabolism in cancer cell radioresistance and radiosensitization methods. *J Exp Clin Cancer Res* (2018) 37:87. doi: 10.1186/s13046-018-0758-7
6. Berdasco M, Esteller M. Clinical epigenetics: seizing opportunities for translation. *Nat Rev Genet* (2019) 20:109–27. doi: 10.1038/s41576-018-0074-2
7. Hegi ME, Diserens AC, Gorlia T, Hamou MF, de Tribolet N, Weller M, et al. MGMT gene silencing and benefit from temozolomide in glioblastoma. *N Engl J Med* (2005) 352:997–1003. doi: 10.1056/NEJMoa043331
8. Fu Y, Dominissini D, Rechavi G, He C. Gene expression regulation mediated through reversible m(6)A RNA methylation. *Nat Rev Genet* (2014) 15:293–306. doi: 10.1038/nrg3724
9. Dominissini D, Moshitch-Moshkovitz S, Schwartz S, Salmon-Divon M, Ungar L, Osenberg S, et al. Topology of the human and mouse m6A RNA methylomes revealed by m6A-seq. *Nature* (2012) 485:201–6. doi: 10.1038/nature11112
10. Meyer KD. DART-seq: an antibody-free method for global m(6)A detection. *Nat Methods* (2019) 16:1275–80. doi: 10.1038/s41592-019-0570-0
11. Lan Q, Liu PY, Haase J, Bell JL, Huttelmaier S, Liu T. The Critical Role of RNA m(6)A Methylation in Cancer. *Cancer Res* (2019) 79:1285–92. doi: 10.1158/0008-5472.CAN-18-2965
12. Shi H, Wei J, He C. Where, When, and How: Context-Dependent Functions of RNA Methylation Writers, Readers, and Erasers. *Mol Cell* (2019) 74:640–50. doi: 10.1016/j.molcel.2019.04.025
13. Zaccara S, Ries RJ, Jaffrey SR. Reading, writing and erasing mRNA methylation. *Nat Rev Mol Cell Biol* (2019) 20:608–24. doi: 10.1038/s41580-019-0168-5
14. Warda AS, Kretschmer J, Hackert P, Lenz C, Urlaub H, Hobartner C, et al. Human METTL16 is a N(6)-methyladenosine (m(6)A) methyltransferase that targets pre-mRNAs and various non-coding RNAs. *EMBO Rep* (2017) 18:2004–14. doi: 10.15252/embr.201744940
15. Jia G, Fu Y, Zhao X, Dai Q, Zheng G, Yang Y, et al. N6-methyladenosine in nuclear RNA is a major substrate of the obesity-associated FTO. *Nat Chem Biol* (2011) 7:885–7. doi: 10.1038/nchembio.687
16. Zheng G, Dahl JA, Niu Y, Fedorcsak P, Huang CM, Li CJ, et al. ALKBH5 is a mammalian RNA demethylase that impacts RNA metabolism and mouse fertility. *Mol Cell* (2013) 49:18–29. doi: 10.1016/j.molcel.2012.10.015
17. Roignant JY, Soller M. m(6)A in mRNA: An Ancient Mechanism for Fine-Tuning Gene Expression. *Trends Genet* (2017) 33:380–90. doi: 10.1016/j.tig.2017.04.003
18. Yi YC, Chen XY, Zhang J, Zhu JS. Novel insights into the interplay between m(6)A modification and noncoding RNAs in cancer. *Mol Cancer* (2020) 19:121. doi: 10.1186/s12943-020-01233-2
19. Jin D, Guo J, Wu Y, Du J, Yang L, Wang X, et al. m(6)A mRNA methylation initiated by METTL3 directly promotes YAP translation and increases YAP activity by regulating the MALAT1-miR-1914-3p-YAP axis to induce NSCLC drug resistance and metastasis. *J Hematol Oncol* (2019) 12:135. doi: 10.1186/s13045-019-0830-6
20. Zhou C, Molinie B, Daneshvar K, Pondick JV, Wang J, Van Wittenberghe N, et al. Genome-Wide Maps of m6A circRNAs Identify Widespread and Cell-Type-Specific Methylation Patterns that Are Distinct from mRNAs. *Cell Rep* (2017) 20:2262–76. doi: 10.1016/j.celrep.2017.08.027
21. Alarcon CR, Lee H, Goodarzi H, Halberg N, Tavazoie SF. N6-methyladenosine marks primary microRNAs for processing. *Nature* (2015) 519:482–5. doi: 10.1038/nature14281
22. Bartosovic M, Molares HC, Gregorova P, Hrossova D, Kudla G, Vanacova S. N6-methyladenosine demethylase FTO targets pre-mRNAs and regulates alternative splicing and 3'-end processing. *Nucleic Acids Res* (2017) 45:11356–70. doi: 10.1093/nar/gkx778
23. Coots RA, Liu XM, Mao Y, Dong L, Zhou J, Wan J, et al. m(6)A Facilitates eIF4F-Independent mRNA Translation. *Mol Cell* (2017) 68:504–14.e507. doi: 10.1016/j.molcel.2017.10.002
24. Roundtree IA, Luo GZ, Zhang Z, Wang X, Zhou T, Cui Y, et al. YTHDC1 mediates nuclear export of N(6)-methyladenosine methylated mRNAs. *Elife* (2017) 6. doi: 10.7554/eLife.31311
25. Wang H, Xu B, Shi J. N6-methyladenosine METTL3 promotes the breast cancer progression via targeting Bcl-2. *Gene* (2020) 722:144076. doi: 10.1016/j.gene.2019.144076
26. Yan F, Al-Kali A, Zhang Z, Liu J, Pang J, Zhao N, et al. A dynamic N(6)-methyladenosine methylome regulates intrinsic and acquired resistance to tyrosine kinase inhibitors. *Cell Res* (2018) 28:1062–76. doi: 10.1038/s41422-018-0097-4
27. Gomez-Ruiz S, Maksimovic-Ivanic D, Mijatovic S, Kaluderovic GN. On the discovery, biological effects, and use of Cisplatin and metallocenes in anticancer chemotherapy. *Bioinorg Chem Appl* (2012) 2012:140284. doi: 10.1155/2012/140284
28. Zhang R, Li SW, Liu L, Yang J, Huang G, Sang Y. TRIM11 facilitates chemoresistance in nasopharyngeal carcinoma by activating the beta-catenin/ABCC9 axis via p62-selective autophagic degradation of Daple. *Oncogenesis* (2020) 9:45. doi: 10.1038/s41389-020-0229-9
29. Shi Y, Fan S, Wu M, Zuo Z, Li X, Jiang L, et al. YTHDF1 links hypoxia adaptation and non-small cell lung cancer progression. *Nat Commun* (2019) 10:4892. doi: 10.1038/s41467-019-12801-6
30. Zhou S, Bai ZL, Xia D, Zhao ZJ, Zhao R, Wang YY, et al. FTO regulates the chemo-radiotherapy resistance of cervical squamous cell carcinoma (CSCC) by targeting beta-catenin through mRNA demethylation. *Mol Carcinog* (2018) 57:590–7. doi: 10.1002/mc.22782
31. Shriwas O, Priyadarshini M, Samal SK, Rath R, Panda S, Das Majumdar SK, et al. DDX3 modulates cisplatin resistance in OSCC through ALKBH5-mediated m(6)A-demethylation of FOXM1 and NANOG. *Apoptosis* (2020) 25:233–46. doi: 10.1007/s10495-020-01591-8
32. Kannaiyan R, Mahadevan D. A comprehensive review of protein kinase inhibitors for cancer therapy. *Expert Rev Anticancer Ther* (2018) 18:1249–70. doi: 10.1080/14737140.2018.1527688
33. Meng Q, Wang S, Zhou S, Liu H, Ma X, Zhou X, et al. Dissecting the m(6)A methylation affection on afatinib resistance in non-small cell lung cancer. *Pharmacogenom J* (2020) 20:227–34. doi: 10.1038/s41397-019-0110-4
34. Lin Z, Niu Y, Wan A, Chen D, Liang H, Chen X, et al. RNA m(6) A methylation regulates sorafenib resistance in liver cancer through FOXO3-mediated autophagy. *EMBO J* (2020) 39:e103181. doi: 10.15252/embj.2019103181
35. Rutman RJ, Cantarow A, Paschkis KE. Studies in 2-acetylaminofluorene carcinogenesis. III. The utilization of uracil-2-C14 by preneoplastic rat liver and rat hepatoma. *Cancer Res* (1954) 14:119–23.
36. Noordhuis P, Holwerda U, Van der Wilt CL, Van Groeningen CJ, Smid K, Meijer S, et al. 5-Fluorouracil incorporation into RNA and DNA in relation to thymidylate synthase inhibition of human colorectal cancers. *Ann Oncol* (2004) 15:1025–32. doi: 10.1093/annonc/mdh264
37. Xie H, Lu Q, Wang H, Zhu X, Guan Z. Two postoperative chemotherapies for gastric cancer: FOLFOX4 vs. *TPF Oncol Lett* (2019) 17:933–6. doi: 10.3892/ol.2018.9695
38. Taketo K, Konno M, Asai A, Koseki J, Toratani M, Satoh T, et al. The epitranscriptome m6A writer METTL3 promotes chemo- and radioresistance in pancreatic cancer cells. *Int J Oncol* (2018) 52:621–9. doi: 10.3892/ijo.2017.4219
39. Nishizawa Y, Konno M, Asai A, Koseki J, Kawamoto K, Miyoshi N, et al. Oncogene c-Myc promotes epitranscriptome m(6)A reader YTHDF1 expression in colorectal cancer. *Oncotarget* (2018) 9:7476–86. doi: 10.18632/oncotarget.23554
40. Pines A, Mullenders LH, van Attikum H, Luijsterburg MS. Touching base with PARPs: moonlighting in the repair of UV lesions and double-strand breaks. *Trends Biochem Sci* (2013) 38:321–30. doi: 10.1016/j.tibs.2013.03.002
41. Bryant HE, Petermann E, Schultz N, Jemth AS, Loseva O, Issaeva N, et al. PARP is activated at stalled forks to mediate Mre11-dependent replication restart and recombination. *EMBO J* (2009) 28:2601–15. doi: 10.1038/emboj.2009.206
42. Gibson BA, Kraus WL. New insights into the molecular and cellular functions of poly(ADP-ribose) and PARPs. *Nat Rev Mol Cell Biol* (2012) 13:411–24. doi: 10.1038/nrm3376
43. Lord CJ, Ashworth A. PARP inhibitors: Synthetic lethality in the clinic. *Science* (2017) 355:1152–8. doi: 10.1126/science.aam7344
44. Sachdev E, Tabatabai R, Roy V, Rimel BJ, Mita MM. PARP Inhibition in Cancer: An Update on Clinical Development. *Targ Oncol* (2019) 14:657–79. doi: 10.1007/s11523-019-00680-2
45. Fong PC, Boss DS, Yap TA, Tutt A, Wu P, Mergui-Roelvink M, et al. Inhibition of poly(ADP-ribose) polymerase in tumors from BRCA mutation carriers. *N Engl J Med* (2009) 361:123–34. doi: 10.1056/NEJMoa0900212

46. Fukumoto T, Zhu H, Nacarelli T, Karakashev S, Fatkhutdinov N, Wu S, et al. N(6)-Methylation of Adenosine of FZD10 mRNA Contributes to PARP Inhibitor Resistance. *Cancer Res* (2019) 79:2812–20. doi: 10.1158/0008-5472.CAN-18-3592
47. Heinemann V. Gemcitabine: progress in the treatment of pancreatic cancer. *Oncology* (2001) 60:8–18. doi: 10.1159/000055290
48. Tang B, Yang Y, Kang M, Wang Y, Wang Y, Bi Y, et al. m(6)A demethylase ALKBH5 inhibits pancreatic cancer tumorigenesis by decreasing WIF-1 RNA methylation and mediating Wnt signaling. *Mol Cancer* (2020) 19:3. doi: 10.1186/s12943-019-1128-6
49. He X, Tan L, Ni J, Shen G. Expression pattern of m(6)A regulators is significantly correlated with malignancy and antitumor immune response of breast cancer. *Cancer Gene Ther* (2020). doi: 10.1038/s41417-020-00208-1
50. Winkler R, Gillis E, Lasman L, Safra M, Geula S, Soyris C, et al. m(6)A modification controls the innate immune response to infection by targeting type I interferons. *Nat Immunol* (2019) 20:173–82. doi: 10.1038/s41590-018-0275-z
51. Rubio RM, Depledge DP, Bianco C, Thompson L, Mohr I. RNA m(6) A modification enzymes shape innate responses to DNA by regulating interferon beta. *Genes Dev* (2018) 32:1472–84. doi: 10.1101/gad.319475.118
52. Li HB, Tong J, Zhu S, Batista PJ, Duffy EE, Zhao J, et al. m(6)A mRNA methylation controls T cell homeostasis by targeting the IL-7/STAT5/SOCS pathways. *Nature* (2017) 548:338–42. doi: 10.1038/nature23450
53. Wang H, Hu X, Huang M, Liu J, Gu Y, Ma L, et al. Mettl3-mediated mRNA m(6)A methylation promotes dendritic cell activation. *Nat Commun* (2019) 10:1898. doi: 10.1038/s41467-019-09903-6
54. Han D, Liu J, Chen C, Dong L, Liu Y, Chang R, et al. Anti-tumour immunity controlled through mRNA m(6)A methylation and YTHDF1 in dendritic cells. *Nature* (2019) 566:270–4. doi: 10.1038/s41586-019-0916-x
55. Yang S, Wei J, Cui YH, Park G, Shah P, Deng Y, et al. m(6)A mRNA demethylase FTO regulates melanoma tumorigenicity and response to anti-PD-1 blockade. *Nat Commun* (2019) 10:2782. doi: 10.1038/s41467-019-10669-0
56. Yi L, Wu G, Guo L, Zou X, Huang P. Comprehensive Analysis of the PD-L1 and Immune Infiltrates of m(6)A RNA Methylation Regulators in Head and Neck Squamous Cell Carcinoma. *Mol Ther Nucleic Acids* (2020) 21:299–314. doi: 10.1016/j.omtn.2020.06.001
57. Zhang B, Wu Q, Li B, Wang D, Wang L, Zhou YL. m(6)A regulator-mediated methylation modification patterns and tumor microenvironment infiltration characterization in gastric cancer. *Mol Cancer* (2020) 19:53. doi: 10.1186/s12943-020-01170-0
58. Li N, Kang Y, Wang L, Huff S, Tang R, Hui H, et al. ALKBH5 regulates anti-PD-1 therapy response by modulating lactate and suppressive immune cell accumulation in tumor microenvironment. *Proc Natl Acad Sci U S A* (2020) 117:20159–70. doi: 10.1073/pnas.1918986117
59. Domina EA, Philchenkov A, Dubrovska A. Individual Response to Ionizing Radiation and Personalized Radiotherapy. *Crit Rev Oncog* (2018) 23:69–92. doi: 10.1615/CritRevOncog.2018026308
60. Visvanathan A, Patil V, Arora A, Hegde AS, Arivazhagan A, Santosh V, et al. Essential role of METTL3-mediated m(6)A modification in glioma stem-like cells maintenance and radioresistance. *Oncogene* (2018) 37:522–33. doi: 10.1038/onc.2017.351
61. Ma H, Shen L, Yang H, Gong H, Du X, Li J. m6A methyltransferase Wilms' tumor 1-associated protein facilitates cell proliferation and cisplatin resistance in NK/T cell lymphoma by regulating dual-specificity phosphatases 6 expression via m6A RNA methylation. *IUBMB Life* (2020). doi: 10.1002/iub.2410
62. Hao L, Wang JM, Liu BQ, Yan J, Li C, Jiang JY, et al. m6A-YTHDF1-mediated TRIM29 upregulation facilitates the stem cell-like phenotype of cisplatin-resistant ovarian cancer cells. *Biochim Biophys Acta Mol Cell Res* (2021) 1868:118878. doi: 10.1016/j.bbamcr.2020.118878
63. Wang Y, Zeng L, Liang C, Zan R, Ji W, Zhang Z, et al. Integrated analysis of transcriptome-wide m(6)A methylome of osteosarcoma stem cells enriched by chemotherapy. *Epigenomics* (2019) 11:1693–715. doi: 10.2217/epi-2019-0262
64. Xu J, Wan Z, Tang M, Lin Z, Jiang S, Ji L, et al. N(6)-methyladenosine-modified CircRNA-SORE sustains sorafenib resistance in hepatocellular carcinoma by regulating beta-catenin signaling. *Mol Cancer* (2020) 19:163. doi: 10.1186/s12943-020-01281-8
65. Ding N, You A, Tian W, Gu L, Deng D. Chidamide increases the sensitivity of Non-small Cell Lung Cancer to Crizotinib by decreasing c-MET mRNA methylation. *Int J Biol Sci* (2020) 16:2595–611. doi: 10.7150/ijbs.45886
66. Liu S, Li Q, Li G, Zhang Q, Zhuo L, Han X, et al. The mechanism of m(6)A methyltransferase METTL3-mediated autophagy in reversing gefitinib resistance in NSCLC cells by beta-elemene. *Cell Death Dis* (2020) 11:969. doi: 10.1038/s41419-020-03148-8
67. Sun Y, Li S, Yu W, Zhao Z, Gao J, Chen C, et al. N(6)-methyladenosine-dependent pri-miR-17-92 maturation suppresses PTEN/TMEM127 and promotes sensitivity to everolimus in gastric cancer. *Cell Death Dis* (2020) 11:836. doi: 10.1038/s41419-020-03049-w
68. Liu X, Gonzalez G, Dai X, Miao W, Yuan J, Huang M, et al. Adenylate Kinase 4 Modulates the Resistance of Breast Cancer Cells to Tamoxifen through an m(6)A-Based Epitranscriptomic Mechanism. *Mol Ther* (2020). doi: 10.1016/j.ymthe.2020.09.007

Conflict of Interest: The authors declare that the research was conducted in the absence of any commercial or financial relationships that could be construed as a potential conflict of interest.

frontiers in Oncology

ORIGINAL RESEARCH
published: 12 April 2021
doi: 10.3389/fonc.2021.592107

Identification of Expression Patterns and Potential Prognostic Significance of m^{5}C-Related Regulators in Head and Neck Squamous Cell Carcinoma

Zhenyuan Han[1,2†], *Biao Yang*[3†], *Yu Wang*[1,2], *Xiuxia Zeng*[4] *and Zhen Tian*[1*]

[1] Department of Oral Pathology, Shanghai Ninth People's Hospital, Shanghai Jiao Tong University School of Medicine, Shanghai, China, [2] National Clinical Research Center for Oral Diseases, Shanghai, China, [3] Department of Neurosurgery, Huashan Hospital of Fudan University, Shanghai, China, [4] Department of Stomatology, Putian Hanjiang Hospital, Putian, China

5-Methylcytosine (m^{5}C) methylation is a major epigenetic technique of RNA modification and is dynamically mediated by m^{5}C "writers," "erasers," and "readers." m^{5}C RNA modification and its regulators are implicated in the onset and development of many tumors, but their roles in head and neck squamous cell carcinoma (HNSCC) have not yet been completely elucidated. In this study, we examined expression patterns of core m^{5}C regulators in the publicly available HNSCC cohort *via* bioinformatic methods. The differentially expressed m^{5}C regulators could divide the HNSCC cohort into four subgroups with distinct prognostic characteristics. Furthermore, a three-gene expression signature model, comprised of NSUN5, DNMT1, and DNMT3A, was established to identify individuals with a high or low risk of HNSCC. To explore the underlying mechanism in the prognosis of HNSCC, screening of differentially expressed genes, followed by the analysis of functional and pathway enrichment, from individuals with high- or low-risk HNSCC was performed. The results revealed a critical role for m^{5}C RNA modification in two aspects of HNSCC: (1) dynamic m^{5}C modification contributes to the regulation of HNSCC progression and (2) expression patterns of NSUN5, DNMT1, and DNMT3A help to predict the prognosis of HNSCC.

Keywords: head and neck squamous cell carcinoma, m^{5}C RNA methylation, prognostic signature, TCGA, expression pattern

OPEN ACCESS

Edited by:
Zhifu Sun,
Mayo Clinic, United States

Reviewed by:
Prashanth N. Suravajhala,
Birla Institute of Scientific Research, India
Shulan Tian,
Mayo Clinic, United States

****Correspondence:***
Zhen Tian
tianzhen_256@126.com

† These authors have contributed equally to this work and share first authorship

Specialty section:
This article was submitted to Cancer Genetics, a section of the journal Frontiers in Oncology

Received: *06 August 2020*
Accepted: *15 February 2021*
Published: *12 April 2021*

Citation:
Han Z, Yang B, Wang Y, Zeng X and Tian Z (2021) Identification of Expression Patterns and Potential Prognostic Significance of m^{5}C-Related Regulators in Head and Neck Squamous Cell Carcinoma. Front. Oncol. 11:592107. doi: 10.3389/fonc.2021.592107

INTRODUCTION

According to the most recent report, head and neck squamous cell carcinoma (HNSCC) is a relatively lethal type of cancer, and HNSCC ranks among the top six in terms of incidence and mortality, seriously threatening public health and the quality of life of patients with HNSCC worldwide (1). Despite consecutive forms of treatment, namely, surgery, chemotherapy, and radiotherapy, and considerable advancement in the therapeutic schedule for HNSCC, the 5-year survival rate of patients with HNSCC remains far from satisfactory, owing to end-stage diagnosis, rapid development, high recurrence rate, and induction of metastasis to distant sites (2). Mounting evidence has demonstrated that molecular markers hold a promising function not only because of their prognostic value but also because of their role as molecular targets. For example, HNSCC therapy has undergone a significant change in recent years with the

development of precision medicines, such as bevacizumab, against vascular endothelial growth factor (VEGF)/VEGF receptor (VEGFR) based on the special gene expression signature, and prognostic outcomes in HNSCC (3–5). More recently, increasing knowledge has brought into focus the features of several macromolecules (protein, RNA, DNA, and sugar) that are involved in tumorigenesis and progression, especially in epigenetic modifications; and the value of these features as prognostic indicators and potential therapeutic targets has been gradually recognized (6–8). To date, the molecular mechanism of HNSCC occurrence and development has not yet been completely elucidated. Therefore, it is imperative to gain a deeper insight into the molecular mechanism of carcinogenesis of HNSCC and thereby provide valuable detection and effective targets for patients with HNSCC.

To date, RNA modification methods have become prominent because of the development of detection technologies and the realization that RNA not only serves as the intermediate molecule for translation or as an auxiliary function for protein synthesis (rRNA and tRNA) but also acts as a functional regulator for the transmission of genetic signals (lncRNA and miRNA) (9, 10). Among these methods, RNA methylation is one of the most common techniques in the epigenetic modification of posttranscriptional RNA, even though extensive effort has been made on studying protein and DNA modifications (11). Generally, RNA methylation predominantly includes m^{6}A, m^{5}C, m^{1}A, and m^{7}G, among which m^{6}A and m^{5}C modification techniques are two of the most major and most representative types of posttranscriptional RNA modification in over 170 chemical modification schemes (12–15). The m^{6}A modification technique has been predominantly studied in HNSCC, but that of m^{5}C does not attract much attention since the current knowledge of its functions is limited to regulation of the exportation of mRNA and the maintenance of the structure and stability of mRNA (12, 16–18). Its modulating effects have been characterized to be reversible and dynamic, similar to those of histone and DNA modification methods, owing to the involvement of m^{5}C writers, erasers, and readers (19, 20). Taking these regulators further, m^{5}C was established by adding the methyl group through a number of methyl transferases (NOP2, NSUN2, NSUN3, NSUN4, NSUN5, NSUN6, NSUN7, TRDMT1, DNMT3A, DNMT3B, and DNMT1), was removed by demethylase (TET2 and TET3), and was recognized by binding proteins (ALYREF and YBX1), which were jargonized as "writers," "erasers," and "readers," respectively (12, 13, 21–23).

At present, accumulating evidence has demonstrated that the aberrant expression of m^{5}C RNA regulators and specific methylated genes is involved in the pathogenesis of abnormal differentiation in progenitors, fertility damage in males, and cancer oncogenesis (24–27). For instance, DNMT1- and EZH2-mediated epigenetic silencing promotes the progression of glioblastoma and gastric cancer (28). Furthermore, NSUN6 promotes the activation of breast cancer metastasis by incorporating the adaptor proteins, LLGL2, and lncRNA MAYA, to accumulate YAP1 in the nucleus for transcriptional activation (29). In addition, one of the main m^{5}C RNA writers, NSUN2, was also noted to be overexpressed in different types of cancer and was deemed an effective prognostic biomarker (25, 27). However, the gene features and prognostic values of m^{5}C-related regulators in HNSCC remain obscure and need in-depth investigation.

In this study, we systematically analyzed and evaluated the expression patterns of 15 widely studied m^{5}C-related regulators in 501 tumor and 44 normal control tissues and the association between clinicopathological and survival parameters from The Cancer Genome Atlas (TCGA) database.

MATERIALS AND METHODS

HNSCC Dataset Acquisition and Bioinformatic Analysis

The transcriptome TCGA-HNSCC datasets and the corresponding clinical features applied in this study were obtained from the TCGA database *via* the GDC Data Portal, as described earlier (https://portal.gdc.cancer.gov/) (30). In total, 501 tumor and 44 normal control datasets from 527 patients were available for further experimental procedure. In addition, the mutation data and the expression values in the pan-cancer analysis of three selected risk genes were obtained from the cBioPortal database (https://www.cbioportal.org/) and the Gene Expression Profiling Interactive Analysis 2 (GEPIA2) database (http://gepia2.cancer-pku.cn/) (31–33). The differentially expressed genes (DEGs) were generated by the R (3.6.0) package "limma," the heat map by "pheatmap," the volcano plots and the bubble plots by "ggplot2," and the chord plots by "GOplot."

Landscape of m^{5}C RNA Methylation Regulators

In total, 15 m^{5}C-associated regulators composed of 11 writers (NOP2, NSUN2, NUSN3, NSUN4, NSUN5, NSUN6, NSUN7, DNMT1, DNMT3A, DNMT3B, and TRDMT1), two erasers (TET2 and TET3), and two readers (ALYREF and YBX1) were retrieved from the published literature. The expression profile of these 15 regulators, accompanied by clinicopathological parameters, was then systematically extracted and analyzed in patients with HNSCC.

Consensus Clustering of m^{5}C-Related Regulators

To better investigate and construct the distinct classification model, the 13 selected m^{5}C-related regulators were screened out to primarily conduct the consensus clustering analysis using the "ConsensusClusterPlus" package of R (3.6.0) (34). Furthermore, the survival analysis of different clusters was performed to determine the best clustering in HNSCC samples.

Construction of Prognostic Prediction Model

To obtain a better prediction of m^{5}C RNA methylation regulators in HNSCC, first, we calculated the hazard ratio (HR), which indicates the result of comparing the hazard function between individuals who are exposed to the hazard function and those who are not, and 95% confidence interval

(CI) of the m^{5}C-related regulators to identify the appropriate candidate genes by univariate Cox regression analysis. Second, the appropriate candidate m^{5}C-related regulators were assigned and built for potential HNSCC prognostic signatures using LASSO Cox regression, which was calculated with the formula described below:

$$Risk\ Score = \sum_{i=1}^{n} coefi \times x_i$$

where n represents the number of module RNAs, *coefi* is the coefficient, and x_i denotes the z-score-transformed relative expression level ($\log_2$ (FPKM + 1)) for each gene. Then, the HNSCC cohort from TCGA was divided into two subgroups, high risk and low risk, on account of the median risk score. The Kaplan–Meier survival analysis/risk prediction model was applied to estimate the prognostic values of the candidate risk genes.

Protein-Protein Interactions and Functional Annotations Analysis

Protein-protein interactions (PPIs) of the 15 m^{5}C-related regulators with a combined confidence score > 0.4 and the DEGs between the two risk subgroups were evaluated *via* the STRING database (https://string-db.org/) and visualized using Cytoscape (3.7.1) (35, 36). The Reactome (https://reactome.org/), the Kyoto Encyclopedia of Genes and Genomes (KEGG), and the Annotation, Visualization, and Integrated Discovery (DAVID) databases (https://david.ncifcrf.gov/) were used to evaluate the enriched functional annotations (37–41).

Immunofluorescence Analysis

Following the guidelines set by the Research Ethics Committee of the Shanghai Ninth People's Hospital, which is affiliated to the Shanghai Jiao Tong University School of Medicine, 10 pairs of tumors, in which the pathological results revealed HNSCC, were selected for this study. Normal human oral mucosal epithelial tissues obtained from the oral mucosa during the surgical resection of HNSCC were used as a control. Paraffin-embedded samples corresponding to the most representative tumor area on H&E-stained slides were selected for performing the IF assay. Briefly, the original fresh-frozen IF sections with a thickness of 6 μm were acquired through cryosection, air-dried for 10 min, fixed with acetone, washed with phosphate buffered saline (PBS) (1×), and incubated at room temperature for 2 h with NSUN5 (Proteintech Group, Rosemont, IL, USA, 1:50), DNMT1 (Bioworld Technology, Inc., St. Louis Park, MN, USA, 1:50), and DNMT3A (Novus Biologicals, Littleton, CO, USA, 1:170) primary antibodies. The sections were rinsed with sterile PBS (1×) and then incubated with a Goat Anti-Rabbit IgG secondary antibody (Abcam, Cambridge, UK, 1:200) protected from light. Next, the nuclei of the sections were counterstained with DAPI (Beyotime, Shanghai, China). Primary antibodies were replaced with PBS as a negative control.

Statistical Analysis

Statistical analysis was conducted using R software (3.6.0). Moreover, the DEGs between the two groups were analyzed by the Student's t-test. $p < 0.05$ was deemed statistically significant.

RESULTS

Expression Patterns of m^{5}C RNA Methylation Regulators in HNSCC

The overall flowchart of the procedure that was applied to in this study and that elucidated the risk score for investigating the prognostic values of HNSCC is summarized in **Figure 1**. To decipher the expression of essential biological functions of m^{5}C-related regulators in HNSCC, we first downloaded and extracted the efficacious gene expression data from the TCGA database. Expression levels of the individual m^{5}C RNA methylation catalase in HNSCC and control samples are presented in the heat map (**Figure 2A**). Among the 545 cases, 14 of the 15 m^{5}C methylation regulatory genes were differentially expressed between tumors and healthy samples, with $p < 0.05$. Specifically, NOP2, NSUN2, NSUN3, NSUN4, NSUN5, NSUN6, NSUN7, DNMT1, DNMT3A, DNMT3B, TET2, TET3, ALYREF, and YBX1 exhibited different expression patterns. However, no distinct discrepancies in the TRDMT1 ($p = 0.83$) expression were analyzed in HNSCC tissues when compared with normal tissues (**Figure 2B**). Of these 14 genes, the majority of writers (NOP2, NSUN2, NSUN3, NSUN4, NSUN5, NSUN6, DNMT3A, DNMT3B, and DNMT1) were more substantially upregulated in the HNSCC samples compared with normal tissues, with the exception of NSUN7, which showed an opposite expression trend with the other 9 m^{5}C writers ($p < 0.05$). In addition, in HNSCC tumor tissues, the expression level of the m^{5}C eraser TET3 was significantly elevated, while that of TET2 was downregulated. Similarly, the readers ALYREF and YBX1 showed a higher expression level in HNSCC compared to normal tissues. In summary, we concluded that m^{5}C RNA methylation regulators had distinct expression changes in HNSCC and corresponding normal tissues.

Interaction and Correlation Patterns Among the m^{5}C RNA Methylation Regulators in HNSCC

To investigate the associations between the main m^{5}C RNA methylation regulators, we built a PPI network. The interactions among the 15 m^{5}C-related regulators are shown in **Figure 2C**. TRDMT1 appeared to be the hub gene of the interaction network and was predominantly associated with most of the m^{5}C RNA methylation regulators, except for ALYREF and YBX1. Since the PPI network did not provide details of correlation, we performed a further correlation analysis on HNSCC, as shown in **Figure 2D**. There was a close correlation between TET2 and TET3, two members of the TET gene family. Except for NSUN5 and DNMT3B, NSUN6 was correlated with the other 12 m^{5}C RNA methylation regulators. Moreover, the expression of DNMT1 was positively related to the other m^{5}C-related methylation genes but not to TRDMT1 and NSUN5. Similarly, NSUN4 also

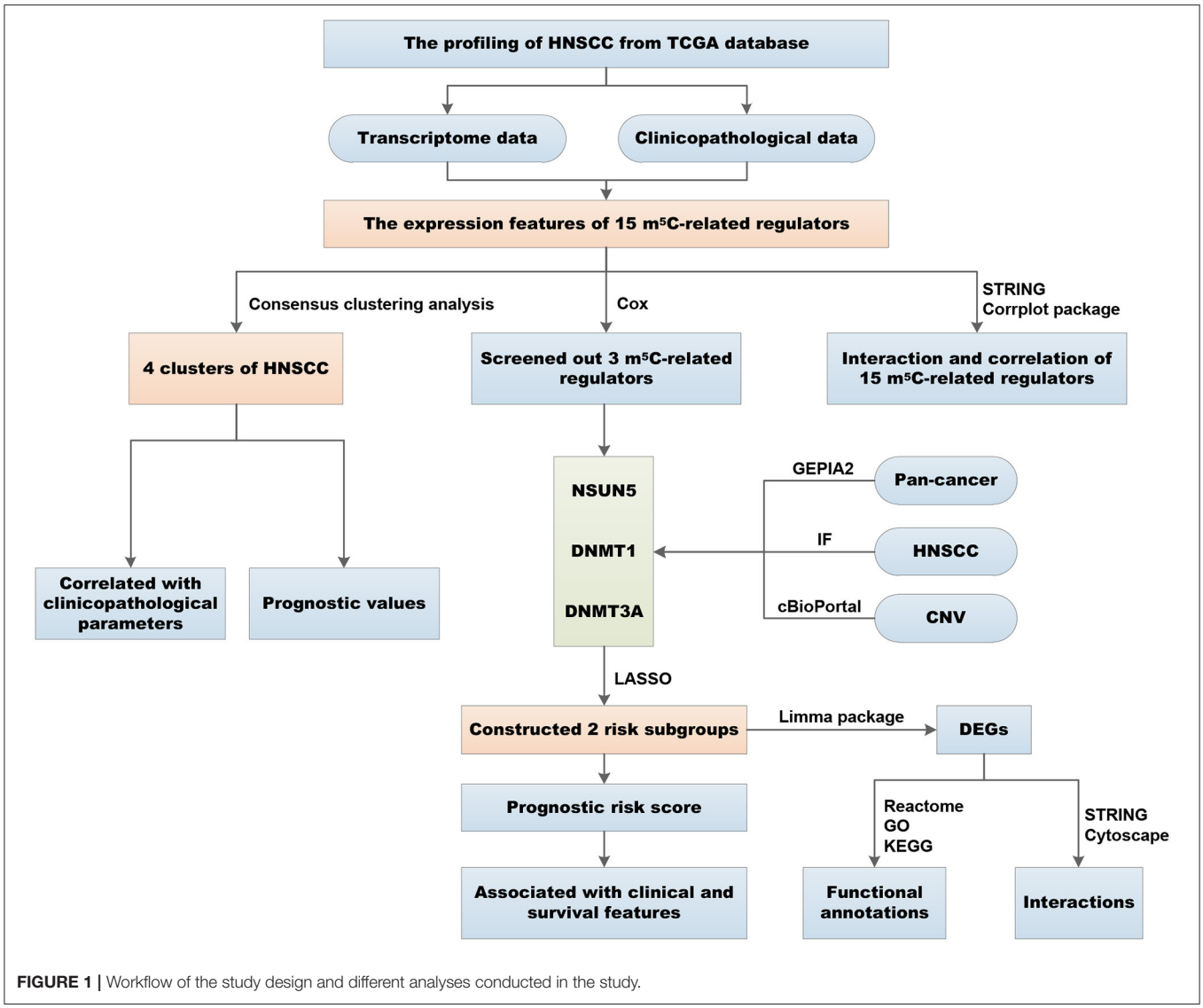

FIGURE 1 | Workflow of the study design and different analyses conducted in the study.

shows a positive relationship with other m^{5}C-related methylation regulators except for NSUN5 and DNMT3B. Furthermore, it is worthwhile to note that both erasers, TET2 and TET3, were most negatively correlated with NSUN5 among all the correlations of m^{5}C RNA methylation regulators with the Pearson's correlation coefficient of −0.34 and −0.19, respectively.

Identification of Four Clusters of HNSCC Samples With Different Clinical Outcomes and Characteristics

Transcriptome data of 545 HNSCC samples from the TCGA database were used for consensus clustering analysis. From the differentially expressed m^{5}C-related methylation regulators described above, we used 13 m^{5}C-related genes (NOP2, NSUN2, NSUN3, NSUN4, NSUN5, NSUN6, DNMT1, DNMT3A, DNMT3B, TET2, TET3, ALYREF, and YBX1) for further research. Based on the expression similarity profiling of the 13 m^{5}C-related regulators combined with consensus clustering cumulative distribution function (CDF) and relative change in the area under the CDF curve, as shown in **Figures 3A,B**, $k = 4$ was deemed as the appropriate number of clusters when the clustering stability datasets varied from $k = 2$ to $k = 10$ (**Figures 3C,D**). Then, the HNSCC samples with survival parameters were classified accordingly into four groups. A noticeably shorter overall survival (OS) was observed in HNSCC cases in cluster 1 compared with the other clusters. We highly postulate that the expression of these 13 m^{5}C-related genes can divide the HNSCC samples into four groups with distinct prognoses (**Figure 3E**). Additionally, to better predict the clinicopathological characteristics of HNSCC with these four subgroups, a heat map was applied to present the significant difference in grade and survival condition with both $p < 0.01$, while no huge difference was witnessed with other features, such as TNM classification, gender, age, and clinical stage (**Figure 3F**). Overall, we can conclude that the expression features of the 13m^{5}C-related genes were associated with the grade and survival condition of patients with HNSCC.

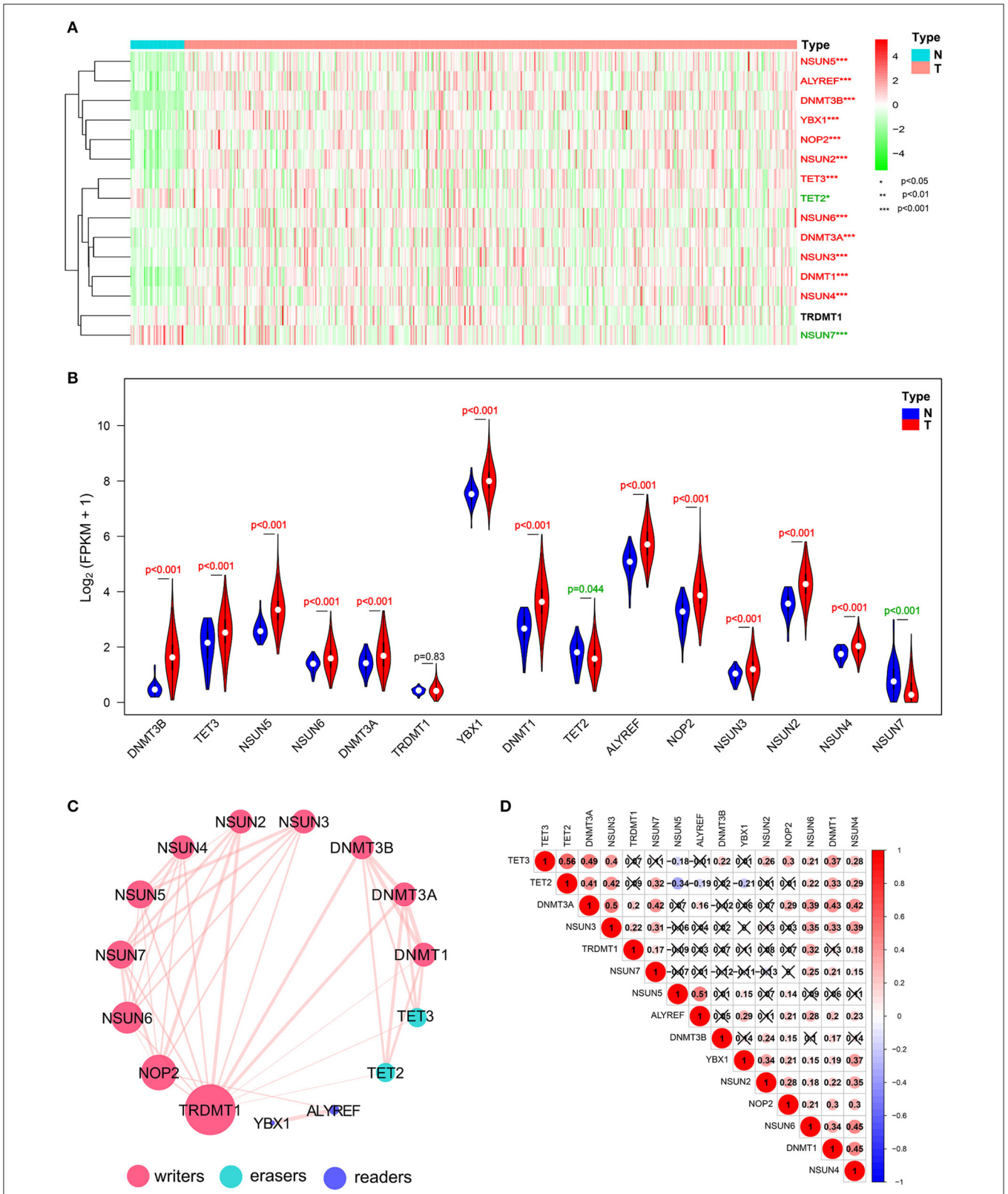

FIGURE 2 | Expressional and interactive landscape of the m^{5}C modification signature in head and neck squamous cell carcinoma (HNSCC). **(A)** The heat map shows the expression levels of 15 m^{5}C RNA decoration regulators in each clinical sample (N, normal; T, tumor; $^*p < 0.05$; $^{**}p < 0.01$; $^{***}p < 0.001$). **(B)** A violin plot was

(Continued)

FIGURE 2 | applied to demonstrate the significantly differentially expressed m^{5}C RNA modification regulators between tumor tissues and those of normal control. **(C)** The protein–protein interaction (PPI) network of 15 m^{5}C-related regulators was constructed to visualize the interaction (the size of the node is applied to reflect the degree of regulator; the size of the line is applied to denote the combined_score). **(D)** Pearson correlation analysis was delineated to determine the correlation among 15 selected m^{5}C-related regulators in The Cancer Genome Atlas (TCGA) HNSCC cohort.

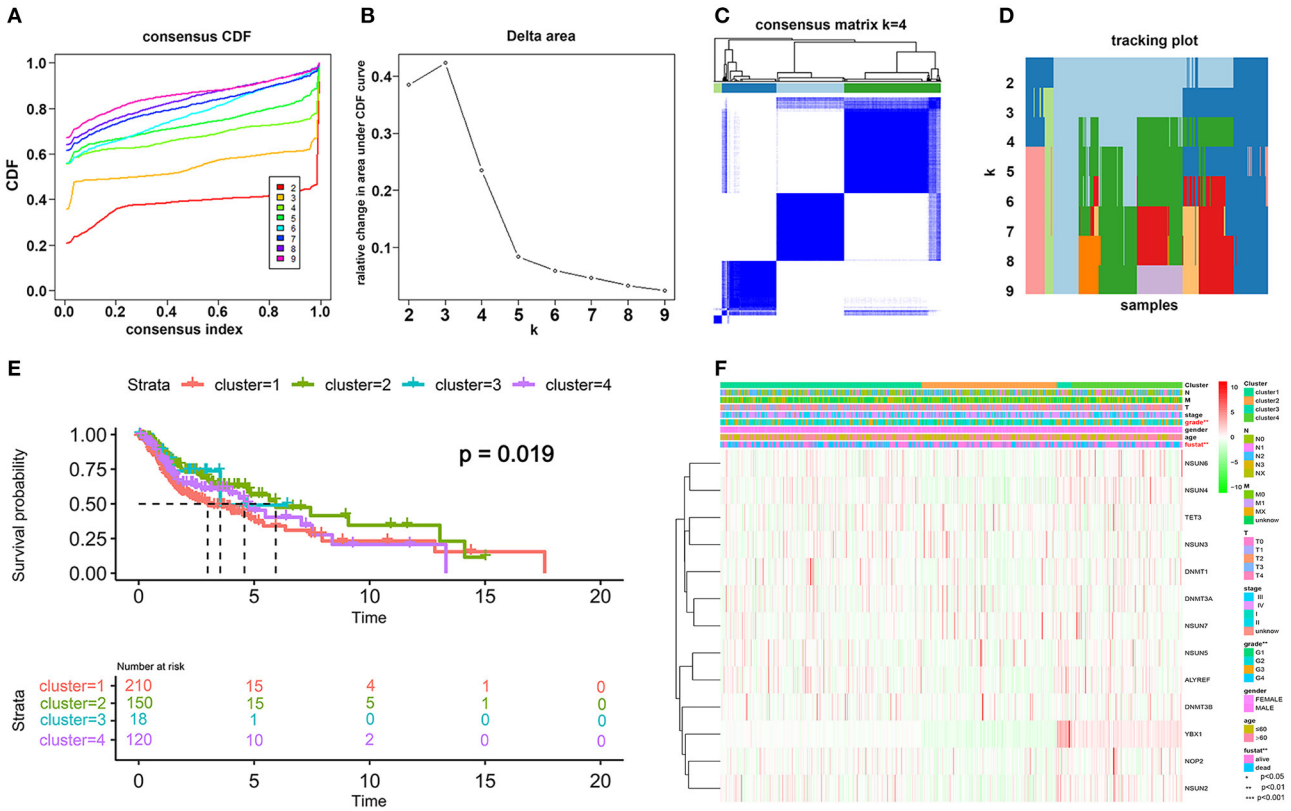

FIGURE 3 | Differential patterns of expressional and clinical features of patients with TCGA HNSCC in cluster 1–4 subgroups. **(A)** Consensus clustering cumulative distribution function (CDF) and **(B)** relative change in the area under the CDF curve from $k = 2$ to $k = 9$. **(C)** Consensus clustering matrix was assessed by $k = 4$. **(D)** The tracking plot of the HNSCC samples. **(E)** The survival analysis for the four clusters by the Kaplan–Meier method. **(F)** The clinicopathological characteristics of the four clusters were determined by coexpression patterns of the consensus expression of 13 selected m^{5}C-related regulators (*$p < 0.05$; **$p < 0.01$; ***$p < 0.001$).

Construction of a Three-Gene Risk Signature With Distinct Prognostic Value

To investigate the prognostic role of m^{5}C RNA methylation regulators in HNSCC, univariate Cox regression analysis was applied to the 13 m^{5}C-related gene expression profiles. According to the details contained in these results (**Figure 4A**), three (NSUN5, DNMT1, and DNMT3A) of the 13 genes that presented a significant prognostic value ($p < 0.1$) were specifically selected to establish the risk signature. Among these three selected genes, DNMT1 and DNMT3A were protective genes with HR < 1, while NSUN5 served as a risk factor with HR > 1.

Then the three screened genes with prognostic values were applied to build the survival risk model using LASSO Cox regression. The coefficients of individual candidate genes were generated based on the minimum criteria (**Figure 4B**). Subsequently, the risk score of each patient with HNSCC from the TCGA database was calculated as follows: risk score = (−0.029572) ∗expression of DNMT1 + (−0.038603) ∗expression of DNMT3A + (0.021496) ∗expression of NSUN5 (**Figure 4C**). Afterward, patients with HNSCC were divided into two subgroups, low risk and high risk, according to the median bound. It was observed that patients in the high-risk subgroup had a significantly shorter OS than patients in the low-risk subgroup (**Figure 4D**, $p < 0.05$). Taken together, these results suggest that the three risk genes can be used as a predictor for the clinical outcomes of HNSCC.

The Prognostic Patterns of Signature-Based Risk Scores Were Associated With Clinical Features in HNSCC

To evaluate the clinical parameters with the three selected m^{5}C methylation regulators in the two subgroups, a heat map was

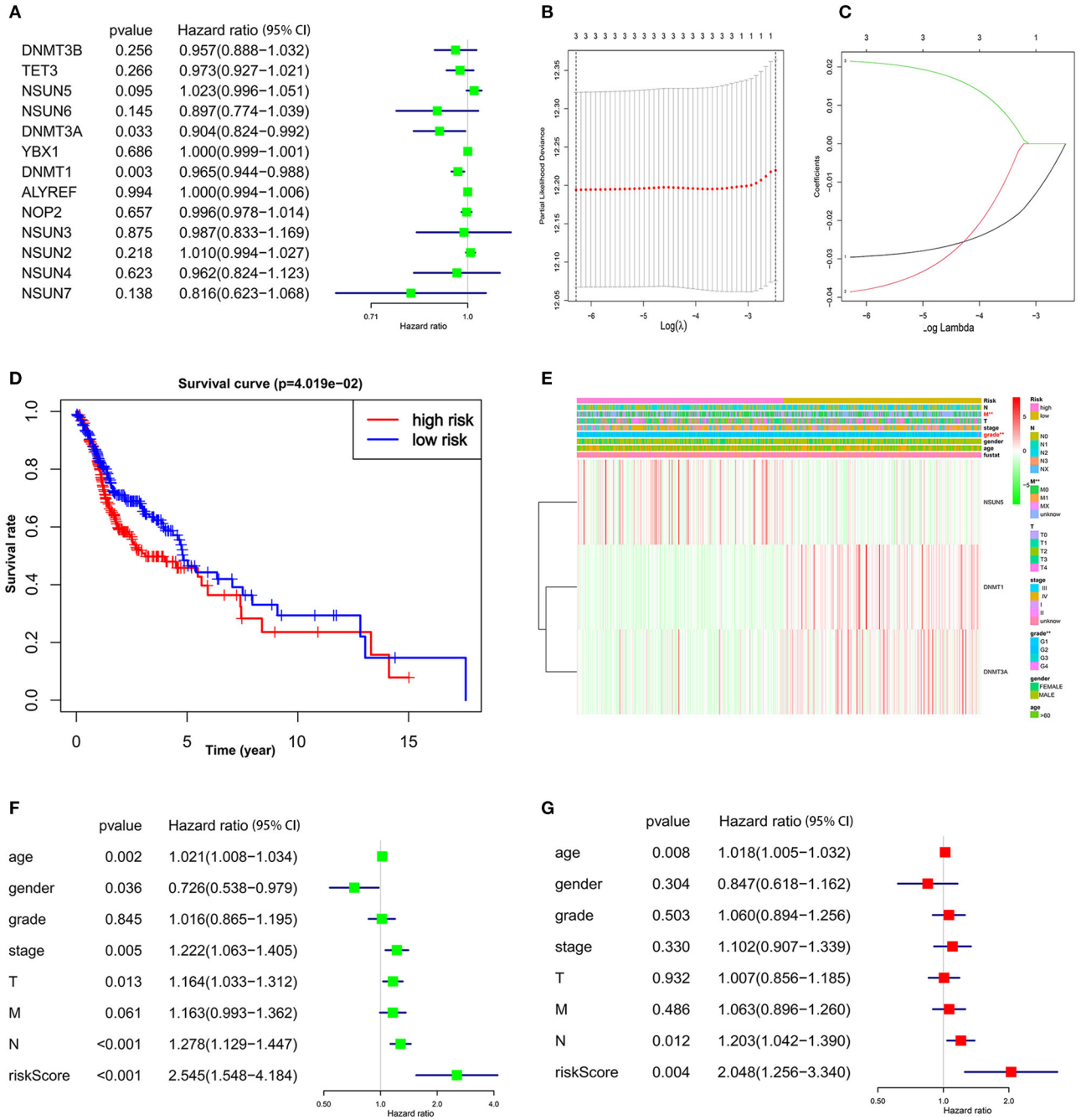

FIGURE 4 | The prognostic risk signature was created with the three m^{5}C RNA methylation regulators. **(A)** The process of analyzing the signature regulators by the univariate Cox regression model. **(B,C)** LASSO Cox regression analysis shows the coefficients of the three selected regulators (NSUN5, DNMT1, and DNMT3A). **(D)** The Kaplan–Meier overall survival analysis of the two subgroups of TCGA HNSCC cohorts assigned to high- and low-risk groups followed by risk scores. **(E)** Significant differences were observed in the area of M stage and grade across the high- and low-risk subgroups. **(F)** Univariate and **(G)** multivariate Cox regression showed the relationship between clinicopathological features and the risk score.

generated to visualize the relationship pattern. The expression of DNMT1 and DNMT3A was high in the low-risk subgroup, whereas, the expression of NSUN5 mainly emerged in the high-risk subgroup. Furthermore, significant differences were disclosed in this heat map concerning the M stage and grade (**Figure 4E**, $p < 0.01$).

Next, we further performed univariate and multivariate Cox regression analyses to confirm whether the risk signature was an

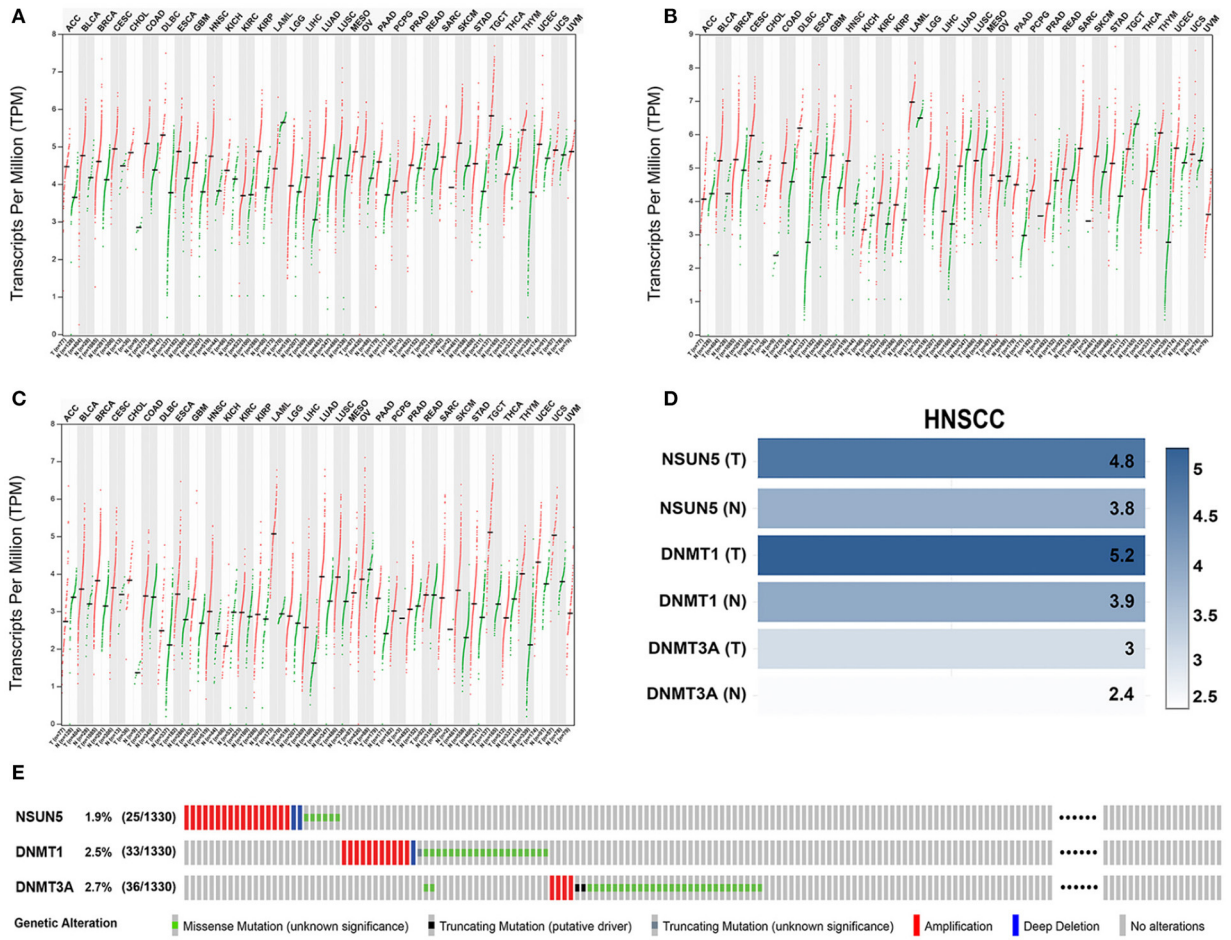

FIGURE 5 | The expression and genetic alteration patterns of three risk genes of various types of cancer in human. The expression values of **(A)** NSUN5, **(B)** DNMT1, and **(C)** DNMT3A in pan-cancers and corresponding normal tissues. **(D)** Expression levels of three risk genes in HNSCC and normal controls based on the GEPIA2 database. **(E)** The profiling of the expression alterations of the three genes in the HNSCC sample (n = 1,332) from TCGA datasets.

independent prognostic element. Remarkably, age (p = 0.002, HR = 1.021, 95% CI = 1.008–1.034), gender (p = 0.036, HR = 0.726, 95% CI = 0.538–0.979), T stage (p = 0.013, HR = 1.164, 95% CI = 1.033–1.312), N stage (p < 0.001, HR = 1.278, 95% CI = 1.129–1.447), and the risk score (p < 0.001, HR = 2.545, 95% CI = 1.548–4.184) were determined to be independent prognostic factors from univariate analysis (**Figure 4F**), while these parameters were calculated by the multivariate Cox regression model. The valuable factors was reduced to age (p = 0.008, HR = 1.018, 95% CI = 1.005–1.032), N stage (p = 0.012, HR = 1.203, 95% CI = 1.042–1.390), and the risk score (p = 0.004, HR = 2.048, 95% CI = 1.256–3.340) (**Figure 4G**).

External Confirmation of the Expression Patterns and Genetic Alterations of Three Risk Signature Genes in HNSCC

To better explore the expression profiles of NSUN5, DNMT1, and DNMT3A in human organs and corresponding tumors, the GEPIA2 database was utilized to investigate the distinct organ expression features of these three prognostic markers. As shown in **Supplementary Figure 1** and **Supplementary Table 1**, these three markers were almost overexpressed in tumors compared with normal organs in 26 pairs of comparison. Next, further comparison of the three genes at the transcriptional level among the 31 human pan-cancer samples was conducted, and an almost identical result was obtained from these contrasts. This validation indicates that NSUN5, DNMT1, and DNMT3A were nearly overexpressed in human tumors compared with normal samples (**Figures 5A–C**).

Considering the complexity of the posttranscriptional regulation and the protein expression, we further employed the GEPIA2 database and IF at the protein level to evaluate and verify the expression of three m^{5}C signature writers. The GEPIA2 database contains TCGA and Genotype-Tissue Expression (GTEx) data with a larger sample population, which may increase the statistical confidence in a precise estimate. The mRNA expression profiles illustrate that all the three risk signature genes were upregulated in GEPIA2, and similar

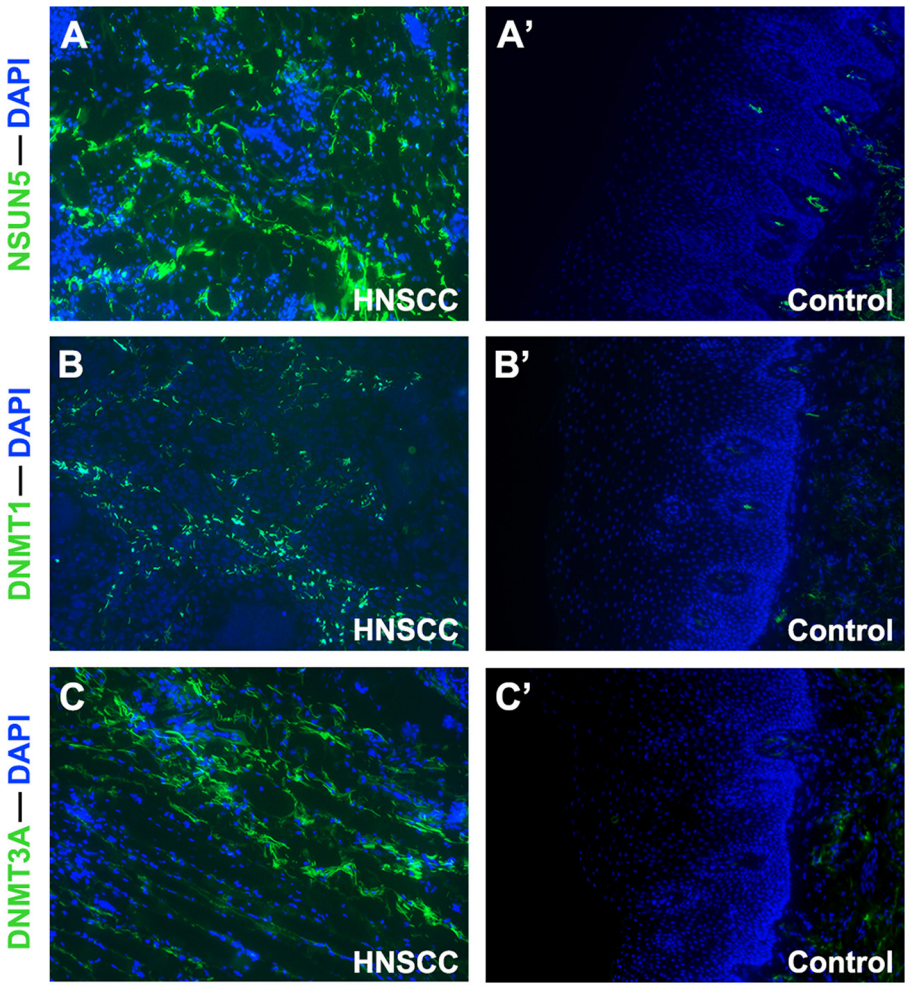

FIGURE 6 | Immunofluorescence analysis of NSUN5, DNMT1, and DNMT3A in tissues of HNSCC tumors and normal oral epithelium (×100). Compared with oral epithelium controls **(A'–C')**, a higher expression of **(A)** NSUN5, **(B)** DNMT1, and **(C)** DNMT3A was detected in HNSCC tumor tissues.

results were obtained from IF (**Figures 5D**, **6**). Among the 1,330 patients with HNSCC, 92 patients (7.1%) had genetic mutations of NSUN5, DNMT1, or DNMT3A (**Figure 5E**).

Functional Annotation and Pathways of Two Risk Subgroups Determined by Three Prognostic Genes

The results mentioned above suggest that the two risk subgroups may be closely related to the prognostic capacity of patients with HNSCC. Next, we sought to explore the potential markers targeting the two subgroups and identified the involved biological functions. In total, 725 DEGs, with 359 being upregulated ($p < 0.05$, $\log_2$FC > 0.5) and 366 being downregulated ($p < 0.05$, $\log_2$FC < -0.5), were screened in the high-risk subgroup by the limma package ($p < 0.05$). Among them, we ranked the DEGs followed by $\log_2$FC. From a total of 20 polar DEGs, 10 upregulated mRNAs (KRT83, BPIFA1, KRT79, FABP4, LOR, LINC01214, FLG2, IGFL2, DSC1, and S100A12) and 10 downregulated mRNAs (PRR27, NPS, STATH, DEFA6, FGF3, TKTL1, BPIFA2, IGKV2D-28, PIP, and ZG16B), were found to be at the top of rankings with the highest $|\log_2$FC$|$ (**Figure 7A**). To better understand the interactions between the upregulated and downregulated genes, we also evaluated the PPIs *via* the STRING database and visualized them by Cytoscape (**Supplementary Figures 2**, **3**). In addition, to better summarize the function of DEGs, Reactome, GO, and KEGG analyses were performed to illustrate the functional annotations of DEGs using the GOplot and ggplot2 packages.

The GOplot and ggplot2 data of the relationship between the listed 359 upregulated and 366 downregulated genes and their corresponding metabolic pathways in the Reactome database, together with the $\log_2$FC of the two-part genes, are presented in **Figures 7B–E** ($p < 0.05$). Furthermore, we also applied ggplot2 to demonstrate the functional annotations in the GO database. The leading highly enriched GO terms of biological process (BP), cellular component (CC), and molecular function (MF) in the high-risk subgroup were "translation," "cytoplasm," and

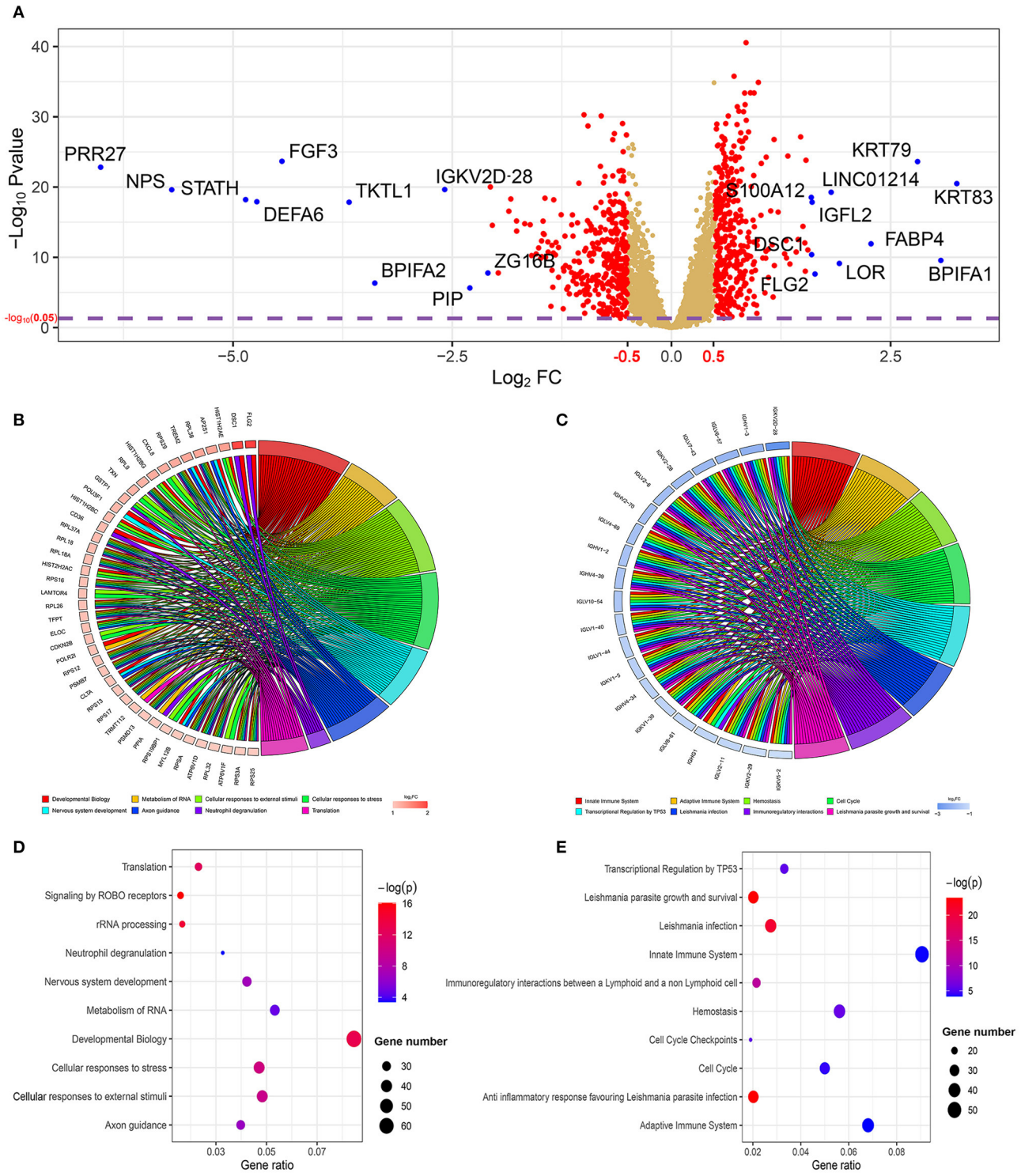

FIGURE 7 | The profiling of differentially expressed genes (DEGs) and their functional annotations from the two risk subgroups. **(A)** The volcano plot shows the DEGs in the two subgroups. The top 10 upregulated and downregulated genes with the highest $|\log_2 FC|$ value are labeled with blue dots. Significantly enriched the Reactome pathway analysis of **(B)** 359 upregulated genes and **(C)** 366 downregulated genes was visualized using the package GOplot in R. The plot includes eight Reactome pathway terms. The genes with at least two terms and the terms that included at least eight genes are demonstrated in this plot. $\log_2 FC$ represents the difference between the high- and low-risk subgroups. The bubble chart shows the top 10 significant enrichment terms of **(D)** 359 upregulated genes and **(E)** 366 downregulated genes in the Reactome database.

"protein binding," respectively (**Figures 8A–E**, $p < 0.05$). On the other hand, in the low-risk subgroup, the principal terms of these three aspects degenerated into "positive regulation of transcription from RNA polymerase II promoter," "plasma membrane," and "ATP binding" (**Figures 8B–F**, $p < 0.05$). Moreover, the enriched signaling cascade for the 359 upregulated and 366 downregulated genes identified by the analysis of the KEGG pathway was selected according to $\log_2$FC ($p < 0.05$). In the high-risk subgroup, the top-ranking terms were associated with "ribosome," "oxidative phosphorylation," "non-alcoholic fatty liver disease," and "synaptic vesicle cycle," and so on ($p < 0.05$); among them, "oxidative phosphorylation" was testified to be related to larger tumor size of HNSCC (**Figure 8G**) (42). Verification of the low-risk subgroup with KEGG analysis also revealed that "cell cycle" and "HTLV-infection" were linked with these genes (**Figure 8H**).

DISCUSSION

Recently, increasing evidence has demonstrated that HNSCC is a complex and heterogeneous disease that is attributed to the combination of virus infection, environmental risk factors, and genetic predisposition. Of note, tobacco smoking and alcohol abuse are considered to be the leading carcinogenic factors for HNSCC (43). In addition, m^{5}C RNA modification in HNSCC has garnered substantial attention among researchers worldwide. Its functions should include numerous BPs, such as mRNA export, RNA stability, translation, and alternative splicing (12, 17, 18, 44–47). m^{5}C RNA modification can be detected in most types of RNA and is associated with a wide range of disorders (13, 48). In particular, abnormal m^{5}C methylation has been implicated in the development of many malignant tumors, namely human skin squamous cell carcinomas and breast cancer (8). Although, Xue et al. (49) reported that the gene significance of m^{5}C regulators can predict the prognosis of patients with HNSCC, the role of m^{5}C modification in HNSCC is still obscure, and in-depth investigations in the field are urgent. In this study, we analyzed the expression patterns of 15 m^{5}C regulators in HNSCC and constructed a three-gene risk signature to predict the prognosis of patients with HNSCC.

Because of the advancements in sensitive, quantitative, and specific technologies, the identification of modification techniques on the low abundance RNA m^{5}C regulators has been brought into focus. Mounting evidence has shown that these regulators, namely m^{5}C "writers," "erasers," and "readers," modulate the occurrence and progression of tumors primarily through their methylation function. For example, the well-identified "writer" NSUN5 exhibits tumor-suppressing characteristics in gliomas. DNA methylation-associated epigenetic silencing of NSUN5 is observed in human gliomas, and it helps glioma cells overcome hostile stress conditions (50). Chen et al. (21) revealed that YBX1 is an m^{5}C "reader" that recognizes m^{5}C-modified mRNAs in human urothelial carcinoma of the bladder (UCB) and maintains the stability of its target mRNAs. Moreover, YBX1 targets the m^{5}C methylation site in the HDGF 3′ untranslated region to drive UCB pathogenesis (21). Notably, most m^{5}C regulators have been reported to participate in cancer pathogenesis *via* non-methylated pathways. Xu et al. revealed the critical role of YBX1 in modulating abnormal ubiquitination in hepatocellular carcinoma (HCC). Protection of YBX1 from PRP19-mediated ubiquitination degradation by circRNA-SORE, a newly discovered circRNA highly expressed in HCC, increases sorafenib resistance in patients with HCC (51).

In this study, we intend to investigate the expression profile of 15 m^{5}C-related regulators in HNSCC. Analysis of the TCGA HNSCC cohort revealed that 14, namely, NOP2, NSUN2, NSUN3, NSUN4, NSUN5, NSUN6, NSUN7, DNMT1, DNMT3A, DNMT3B, TET2, TET3, ALYREF, and YBX1, out of 15 m^{5}C-related RNA regulators exhibited different expression hallmarks among tumors and normal controls. Considering that m^{5}C regulators are differentially expressed in other tumors and involved in the regulation of their pathogenesis, interpretation of the analyzed results somewhat indicates that the differentially expressed regulators may affect HNSCC development and therapy. For example, the levels of DNMT3B, NSUN2, DNMT3A, NOP2, DNMT1, NSUN4, NSUN5, and ALYREF were upregulated in lung adenocarcinoma (52). Zhang et al. (53) have found that DNMT1 could enhance the radiosensitivity of HPV-positive HNSCC through suppressor of morphogenesis in genitalia 1 (SMG1). The NSUN family member, NSUN2, is found to be implicated in regulating cell cycles and accumulates in a variety of tumor lesions compared with normal samples (25, 54). Therefore, it seems valuable to further investigate the role of m^{5}C regulators in HNSCC.

This study attempted to uncover the prognostic effects of m^{5}C RNA methylation regulators in HNSCC. We identified four subgroups of HNSCC based on m^{5}C RNA methylation regulators by means of consensus clustering and found that the classification was related to OS and tumor grade, implying that the expression pattern of m^{5}C-related genes was positively correlated with the malignant process and prognosis of HNSCC. A previous study divided the TCGA HNSCC cohort into two subgroups depending on the 13 m^{6}A RNA methylation regulators and applied consensus clustering (55). The OS and tumor grade of patients were also found to be strongly different between two identified subgroups. Taken together, these results indicate that RNA methylation regulators (m^{6}A, m^{5}C) might be associated with the prognosis of HNSCC.

Afterward, the prognostic three-gene risk signature, comprised of NSUN5, DNMT1, and DNMT3A, was built to effectively distinguish between patients with high risk and patients with low risk and robustly predict OS in the subgroups of HNSCC. Specifically, we observed that low NSUN5, together with high DNMT1 and DNMT3A levels, were positively associated with favorable functional outcomes in patients with HNSCC. Besides, both univariate and multivariate Cox analyses revealed that the risk score could act as an independent prognostic factor in HNSCC, implying that NSUN5, DNMT1, and DNMT3A could be involved in tumor oncogenes and suppressors. It is noteworthy that all three risk genes were m^{6}A "writers," though they showed the opposite effect on survival in HNSCC, which may hint that the NSUN

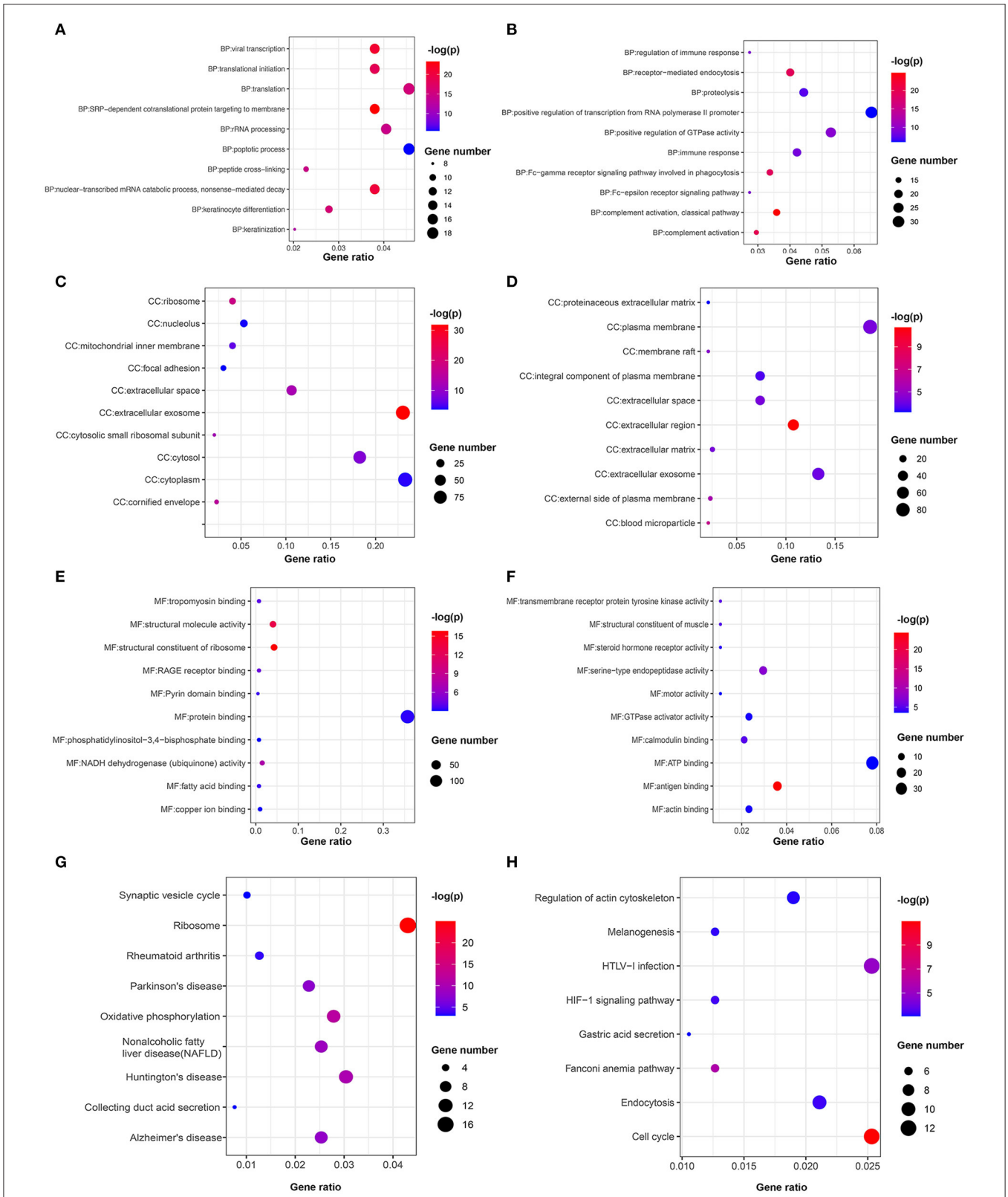

FIGURE 8 | Bubble chart of the enriched terms in GO and KEGG. Functional annotations of upregulated genes in the high-risk subgroup and low-risk subgroup are analyzed by **(A,B)** GO biological processes, **(C,D)** cellular component, **(E,F)** molecular function, and **(G,H)** KEGG pathways.

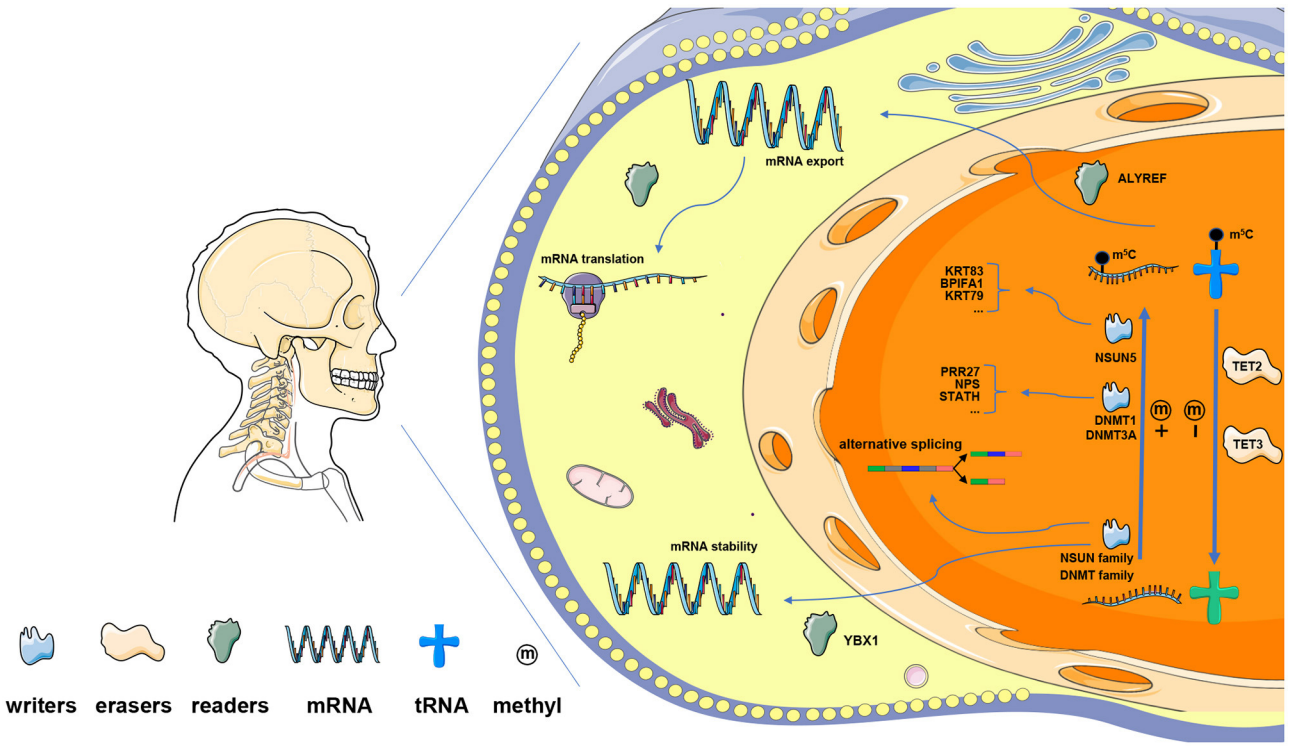

FIGURE 9 | The presumptive outline of m^{5}C RNA modification in HNSCC. Methyltransferases of the NSUN family and DNMT family are the main m^{5}C "writers." Among them, NSUN5 is predicted to methylate KRT83, KRT79, and BPIFA1; whereas DNMT1 and DNMT3A target PRR27, NPS, and STATH. TET2 and TET3 serve as m^{5}C "erasers," which regulate RNA m^{5}C dynamics together with "writers" in the nucleus. m^{5}C readers bind m^{5}C-modified RNA and modulate the processes of mRNA translation, alternative splicing, and RNA decay. Specifically, ALYREF functions in the nucleus and regulates mRNA export, while YBX1 maintains mRNA stability in the cytoplasm.

and DNMT family proteins affect the OS in HNSCC with diverse impacts.

Currently, the roles of NSUN5, DNMT1, and DNMT3A in tumors have been widely explored. NSUN5 was reported to be responsible for modifying the second m^{5}C position in eukaryotic rRNA and maintaining global protein synthesis and normal growth in mice (56, 57). Another study demonstrated that NSUN5 epigenetic inactivation is a hallmark of long-term survival for patients with glioma (50). Additionally, emerging research has indicated that DNMT1 and DNMT3A share oncogene affections (58, 59). These results agree well with the constructed risk model using the three risk genes. Taken together, the risk model offers a basis for further studies of pathogenesis, and for the determination of the novel classification and construction of the prognosis model of HNSCC.

Moreover, the m^{5}C-related risk model was found to be associated with the signaling pathways and biological functions of HNSCC. The role of m^{5}C RNA regulators was discovered not so long ago. Thus, we identified several functional annotations and signaling pathways related to the two risk subgroups. In the high-risk subgroup, the translation, protein binding, and oxidative phosphorylation terms were enriched by the Reactome, the GO, and the KEGG databases, which were ascertained to be correlated with tumorigenesis (60–62). On the other hand, the top 20 DEGs identified in the two risk groups are probably associated with a high likelihood of underregulation by the three m^{5}C writers (NSUN5, DNMT1, and DNMT3A). In detail, the results suggest an m^{5}C-regulated mechanism in HNSCC, by which NSUN5 might target KRT83, KRT79, and BPIFA1, while DNMT1 and DNMT3A methylate PRR27, NPS, and STATH. Consistent with these m^{5}C "writers," m^{5}C "readers" ALYREF and YBX1 might be implicated in HNSCC by functioning as mediators of the mRNA output from the nucleus and by maintaining the stability of their target mRNAs (12, 21). Based on this, the hypotheses on the role of m^{5}C in HNSCC initiation and progression through its internal interactions and signaling pathways have been proposed (**Figure 9**). Besides, the IF analysis revealed that NSUN5, DNMT1, and DNMT3A were similarly overexpressed at the protein level, which was concordant with the transcriptomic level. This is the first characteristic for detecting RNA methylation regulators using IF. These findings, if verified in a larger cohort of prospective clinical cases combined with prognostic data, might be precise for the forecasting and management of patients with HNSCC. In addition to this shortcoming, we also need to acknowledge another limitation that we came across. Whether m^{5}C decoration on RNA was associated with HNSCC prognosis was not directly proven.

CONCLUSION

In summary, we systematically illustrated the expression profile, biological function, and clinical prognostic value of m^{5}C regulators in HNSCC. The association between m^{5}C-related genes and HNSCC progression has been identified. Furthermore, a 3-m^{5}C-related gene-based risk score model was built using NSUN5, DNMT1, and DNMT3A, hinting at a prognostic value in HNSCC.

DATA AVAILABILITY STATEMENT

The publicly available datasets were analyzed in this study. All of the raw data can be found in The Cancer Genome Atlas (TCGA), the Gene Expression Profiling Interactive Analysis 2 (GEPIA2), and the cBioPortal databases.

ETHICS STATEMENT

The studies involving human participants were reviewed and approved by the Ethics Committee of Shanghai Ninth People's Hospital affiliated to Shanghai Jiao Tong University, School of Medicine. The patients/participants provided their written informed consent to participate in this study.

AUTHOR CONTRIBUTIONS

ZT conceived and developed the outline of the study. ZH and BY downloaded the data and performed the statistical study. ZH and XZ generated figures and tables and wrote the manuscript. YW revised the paper. All of the authors read and approved the final manuscript.

FUNDING

This work was supported by the Natural Science Foundation of Shanghai (Grant No. 18ZR1422200).

ACKNOWLEDGMENTS

The authors would like to thank Yuanming Lei and Qin Wang for their valuable assistance and instructions to improve this study.

SUPPLEMENTARY MATERIAL

The Supplementary Material for this article can be found online at: https://www.frontiersin.org/articles/10.3389/fonc.2021.592107/full#supplementary-material

REFERENCES

1. Zhou C, Parsons JL. The radiobiology of HPV-positive and HPV-negative head and neck squamous cell carcinoma. *Expert Rev Mol Med*. (2020) 22:e3. doi: 10.1017/erm.2020.4
2. Huang F, Xin C, Lei K, Bai H, Li J, Chen Q. Non-coding RNAs in oral premalignant disorders and oral squamous cell carcinoma. *Cell Oncol (Dordr)*. (2020) 43:763–77. doi: 10.1007/s13402-020-00521-9
3. Qi Y, Li W, Kang S, Chen L, Hao M, Wang W, et al. Expression of BDNF, TrkB, VEGF and CD105 is associated with pelvic lymph node metastasis and prognosis in IB2-stage squamous cell carcinoma. *Exp Ther Med*. (2019) 18:4221–30. doi: 10.3892/etm.2019.8100
4. Ahn PH, Machtay M, Anne PR, Cognetti D, Keane WM, Wuthrick E, et al. Phase I trial using induction ciplatin, docetaxel, 5-FU and erlotinib followed by cisplatin, bevacizumab and erlotinib with concurrent radiotherapy for advanced head and neck cancer. *Am J Clin Oncol*. (2018) 41:441–6. doi: 10.1097/COC.0000000000000317
5. Argiris A, Li S, Savvides P, Ohr JP, Gilbert J, Levine MA, et al. Phase III Randomized Trial of Chemotherapy With or Without Bevacizumab in Patients With Recurrent or Metastatic Head and Neck Cancer. *J Clin Oncol*. (2019) 37:3266–74. doi: 10.1200/JCO.19.00555
6. Zhou X, Han J, Zhen X, Liu Y, Cui Z, Yue Z, et al. Analysis of genetic alteration signatures and prognostic values of m6A regulatory genes in head and neck squamous cell carcinoma. *Front Oncol*. (2020) 10:718. doi: 10.3389/fonc.2020.00718
7. Deng X, Jiang Q, Liu Z, Chen W. Clinical significance of an m6A reader gene, IGF2BP2, in head and neck squamous cell carcinoma. *Front Mol Biosci*. (2020) 7:68. doi: 10.3389/fmolb.2020.00068
8. Barbieri I, Kouzarides T. Role of RNA modifications in cancer. *Nat Rev Cancer*. (2020) 20:303–22. doi: 10.1038/s41568-020-0253-2
9. Yao RW, Wang Y, Chen LL. Cellular functions of long non-coding RNAs. *Nat Cell Biol*. (2019) 21:542–51. doi: 10.1038/s41556-019-0311-8
10. Gebert LFR, MacRae IJ. Regulation of microRNA function in animals. *Nat Rev Mol Cell Biol*. (2019) 20:21–37. doi: 10.1038/s41580-018-0045-7
11. Zhang J, Yang PL, Gray NS. Targeting cancer with small molecule kinase inhibitors. *Nat Rev Cancer*. (2009) 9:28–39. doi: 10.1038/nrc2559
12. Yang X, Yang Y, Sun BF, Chen YS, Xu JW, Lai WY, et al. 5-methylcytosine promotes mRNA export - NSUN2 as the methyltransferase and ALYREF as an m(5)C reader. *Cell Res*. (2017) 27:606–25. doi: 10.1038/cr.2017.55
13. Bohnsack KE, Höbartner C, Bohnsack MT. Eukaryotic 5-methylcytosine (m5C) RNA Methyltransferases: Mechanisms, Cellular Functions, and Links to Disease. *Genes*. (2019) 10:102. doi: 10.3390/genes10020102
14. Boccaletto P, Machnicka MA, Purta E, Piatkowski P, Baginski B, Wirecki TK, et al. MODOMICS: a database of RNA modification pathways. 2017 update. *Nucleic Acids Res*. (2018) 46:D303–7. doi: 10.1093/nar/gkx1030
15. Andersen NM, Douthwaite S. YebU is a m5C methyltransferase specific for 16 S rRNA nucleotide 1407. *J Mol Biol*. (2006) 359:777–86. doi: 10.1016/j.jmb.2006.04.007
16. Ban Y, Tan P, Cai J, Li J, Hu M, Zhou Y, et al. LNCAROD is stabilized by m6A methylation and promotes cancer progression *via* forming a ternary complex with HSPA1A and YBX1 in head and neck squamous cell carcinoma. *Mol Oncol*. (2020) 14:1282–96. doi: 10.1002/1878-0261.12676
17. Trixl L, Lusser A. The dynamic RNA modification 5-methylcytosine and its emerging role as an epitranscriptomic mark. *Wiley Interdiscip Rev RNA*. (2019) 10:e1510. doi: 10.1002/wrna.1510
18. Zhang X, Liu Z, Yi J, Tang H, Xing J, Yu M, et al. The tRNA methyltransferase NSun2 stabilizes p16INK4 mRNA by methylating the 3'-untranslated region of p16. *Nat Commun*. (2012) 3:712. doi: 10.1038/ncomms1692
19. Dor Y, Cedar H. Principles of DNA methylation and their implications for biology and medicine. *Lancet*. (2018) 392:777–86. doi: 10.1016/S0140-6736(18)31268-6
20. Kouzarides T. Chromatin modifications and their function. *Cell*. (2007) 128:693–705. doi: 10.1016/j.cell.2007.02.005
21. Chen X, Li A, Sun BF, Yang Y, Han YN, Yuan X, et al. 5-methylcytosine promotes pathogenesis of bladder cancer through stabilizing mRNAs. *Nat Cell Biol*. (2019) 21:978–90. doi: 10.1038/s41556-019-0361-y
22. Fu L, Guerrero CR, Zhong N, Amato NJ, Liu Y, Liu S, et al. Tet-mediated formation of 5-hydroxymethylcytosine in RNA. *J Am Chem Soc*. (2014) 136:11582–5. doi: 10.1021/ja505305z
23. Yang Y, Wang L, Han X, Yang WL, Zhang M, Ma HL, et al. RNA 5-Methylcytosine Facilitates the Maternal-to-Zygotic

Transition by Preventing Maternal mRNA Decay. *Mol Cell*. (2019) 75:1188–202.e11. doi: 10.1016/j.molcel.2019.06.033
24. Flores JV, Cordero-Espinoza L, Oeztuerk-Winder F, Andersson-Rolf A, Selmi T, Blanco S, et al. Cytosine-5 RNA methylation regulates neural stem cell differentiation and motility. *Stem Cell Reports*. (2017) 8:112–24. doi: 10.1016/j.stemcr.2016.11.014
25. Frye M, Watt FM. The RNA methyltransferase Misu (NSun2) mediates Myc-induced proliferation and is upregulated in tumors. *Curr Biol*. (2006) 16:971–81. doi: 10.1016/j.cub.2006.04.027
26. Harris T, Marquez B, Suarez S, Schimenti J. Sperm motility defects and infertility in male mice with a mutation in Nsun7, a member of the Sun domain-containing family of putative RNA methyltransferases. *Biol Reprod*. (2007) 77:376–82. doi: 10.1095/biolreprod.106.058669
27. Jhiang SM, Yaneva M, Busch H. Expression of human proliferation-associated nucleolar antigen p120. *Cell Growth Differ*. (1990) 1:319–24.
28. Ning X, Shi Z, Liu X, Zhang A, Han L, Jiang K, et al. DNMT1 and EZH2 mediated methylation silences the microRNA-200b/a/429 gene and promotes tumor progression. *Cancer Lett*. (2015) 359:198–205. doi: 10.1016/j.canlet.2015.01.005
29. Li C, Wang S, Xing Z, Lin A, Liang K, Song J, et al. A ROR1-HER3-lncRNA signalling axis modulates the Hippo-YAP pathway to regulate bone metastasis. *Nat Cell Biol*. (2017) 19:106–19. doi: 10.1038/ncb3464
30. Mounir M, Lucchetta M, Silva TC, Olsen C, Bontempi G, Chen X, et al. New functionalities in the TCGAbiolinks package for the study and integration of cancer data from GDC and GTEx. *PLoS Comput Biol*. (2019) 15:e1006701. doi: 10.1371/journal.pcbi.1006701
31. Cerami E, Gao J, Dogrusoz U, Gross BE, Sumer SO, Aksoy BA, et al. The cBio cancer genomics portal: an open platform for exploring multidimensional cancer genomics data. *Cancer Discov*. (2012) 2:401–4. doi: 10.1158/2159-8290.CD-12-0095
32. Tang Z, Kang B, Li C, Chen T, Zhang Z. GEPIA2: an enhanced web server for large-scale expression profiling and interactive analysis. *Nucleic Acids Res*. (2019) 47:W556–60. doi: 10.1093/nar/gkz430
33. Gao J, Aksoy BA, Dogrusoz U, Dresdner G, Gross B, Sumer SO, et al. Integrative analysis of complex cancer genomics and clinical profiles using the cBioPortal. *Sci Signal*. (2013) 6:pl1. doi: 10.1126/scisignal.2004088
34. Wilkerson MD, Hayes DN. ConsensusClusterPlus: a class discovery tool with confidence assessments and item tracking. *Bioinformatics*. (2010) 26:1572–3. doi: 10.1093/bioinformatics/btq170
35. Shannon P, Markiel A, Ozier O, Baliga NS, Wang JT, Ramage D, et al. Cytoscape: a software environment for integrated models of biomolecular interaction networks. *Genome Res*. (2003) 13:2498–504. doi: 10.1101/gr.1239303
36. Szklarczyk D, Gable AL, Lyon D, Junge A, Wyder S, Huerta-Cepas J, et al. STRING v11: protein-protein association networks with increased coverage, supporting functional discovery in genome-wide experimental datasets. *Nucleic Acids Res*. (2019) 47:D607–13. doi: 10.1093/nar/gky1131
37. Jassal B, Matthews L, Viteri G, Gong C, Lorente P, Fabregat A, et al. The reactome pathway knowledgebase. *Nucleic Acids Res*. (2020) 48:D498–503. doi: 10.1093/nar/gkz1031
38. Ashburner M, Ball CA, Blake JA, Botstein D, Butler H, Cherry JM, et al. Gene ontology: tool for the unification of biology. The Gene Ontology Consortium. *Nat Genet*. (2000) 25:25–9. doi: 10.1038/75556
39. Huang da W, Sherman BT, Lempicki RA. Bioinformatics enrichment tools: paths toward the comprehensive functional analysis of large gene lists. *Nucleic Acids Res*. (2009) 37:1–13. doi: 10.1093/nar/gkn923
40. Huang da W, Sherman BT, Lempicki RA. Systematic and integrative analysis of large gene lists using DAVID bioinformatics resources. *Nat Protoc*. (2009) 4:44–57. doi: 10.1038/nprot.2008.211
41. Kanehisa M, Goto S. KEGG: kyoto encyclopedia of genes and genomes. *Nucleic Acids Res*. (2000) 28:27–30. doi: 10.1093/nar/28.1.27
42. Qin T, Koneva LA, Liu Y, Zhang Y, Arthur AE, Zarins KR, et al. Significant association between host transcriptome-derived HPV oncogene E6* influence score and carcinogenic pathways, tumor size, and survival in head and neck cancer. *Head Neck*. (2020) 42:2375–89. doi: 10.1002/hed.26244
43. Plzák J, Bouček J, Bandúrová V, Kolár M, Hradilová M, Szabo P, et al. The head and neck squamous cell carcinoma microenvironment as a potential target for cancer therapy. *Cancers*. (2019) 11:440. doi: 10.3390/cancers11040440
44. Chernyakov I, Whipple JM, Kotelawala L, Grayhack EJ, Phizicky EM. Degradation of several hypomodified mature tRNA species in Saccharomyces cerevisiae is mediated by Met22 and the 5'-3' exonucleases Rat1 and Xrn1. *Genes Dev*. (2008) 22:1369–80. doi: 10.1101/gad.1654308
45. Courtney DG, Tsai K, Bogerd HP, Kennedy EM, Law BA, Emery A, et al. Epitranscriptomic addition of m(5)C to HIV-1 transcripts regulates viral gene expression. *Cell Host Microbe*. (2019) 26:217–27.e6. doi: 10.1016/j.chom.2019.07.005
46. Hoernes TP, Clementi N, Faserl K, Glasner H, Breuker K, Lindner H, et al. Nucleotide modifications within bacterial messenger RNAs regulate their translation and are able to rewire the genetic code. *Nucleic Acids Res*. (2016) 44:852–62. doi: 10.1093/nar/gkv1182
47. Sharma S, Lafontaine DLJ. 'View from a bridge': a new perspective on eukaryotic rRNA base modification. *Trends Biochem Sci*. (2015) 40:560–75. doi: 10.1016/j.tibs.2015.07.008
48. Guo G, Wang H, Shi X, Ye L, Yan K, Chen Z, et al. Disease activity-associated alteration of mRNA m(5) C methylation in CD4(+) T cells of systemic lupus erythematosus. *Front Cell Dev Biol*. (2020) 8:430. doi: 10.3389/fcell.2020.00430
49. Xue M, Shi Q, Zheng L, Li Q, Yang L, Zhang Y. Gene signatures of m5C regulators may predict prognoses of patients with head and neck squamous cell carcinoma. *Am J Transl Res*. (2020) 12:6841–52.
50. Janin M, Ortiz-Barahona V, de Moura MC, Martínez-Cardús A, Llinàs-Arias P, Soler M, et al. Epigenetic loss of RNA-methyltransferase NSUN5 in glioma targets ribosomes to drive a stress adaptive translational program. *Acta Neuropathol*. (2019) 138:1053–74. doi: 10.1007/s00401-019-02062-4
51. Xu J, Ji L, Liang Y, Wan Z, Zheng W, Song X, et al. CircRNA-SORE mediates sorafenib resistance in hepatocellular carcinoma by stabilizing YBX1. *Signal Transduct Target Ther*. (2020) 5:298. doi: 10.1038/s41392-020-00375-5
52. Sun L, Liu WK, Du XW, Liu XL, Li G, Yao Y, et al. Large-scale transcriptome analysis identified RNA methylation regulators as novel prognostic signatures for lung adenocarcinoma. *Ann Transl Med*. (2020) 8:751. doi: 10.21037/atm-20-3744
53. Zhang C, Mi J, Deng Y, Deng Z, Long D, Liu Z. DNMT1 enhances the radiosensitivity of HPV-positive head and neck squamous cell carcinomas *via* downregulating SMG1. *Onco Targets Ther*. (2020) 13:4201–11. doi: 10.2147/OTT.S227395
54. Hussain S, Benavente SB, Nascimento E, Dragoni I, Kurowski A, Gillich A, et al. The nucleolar RNA methyltransferase Misu (NSun2) is required for mitotic spindle stability. *J Cell Biol*. (2009) 186:27–40. doi: 10.1083/jcb.200810180
55. Zhao X, Cui L. Development and validation of a m(6)A RNA methylation regulators-based signature for predicting the prognosis of head and neck squamous cell carcinoma. *Am J Cancer Res*. (2019) 9:2156–69.
56. Heissenberger C, Liendl L, Nagelreiter F, Gonskikh Y, Yang G, Stelzer EM, et al. Loss of the ribosomal RNA methyltransferase NSUN5 impairs global protein synthesis and normal growth. *Nucleic Acids Res*. (2019) 47:11807–25. doi: 10.1093/nar/gkz1043
57. Schosserer M, Minois N, Angerer TB, Amring M, Dellago H, Harreither E, et al. Methylation of ribosomal RNA by NSUN5 is a conserved mechanism modulating organismal lifespan. *Nat Commun*. (2015) 6:6158. doi: 10.1038/ncomms7158
58. Xu SF, Zheng Y, Zhang L, Wang P, Niu CM, Wu T, et al. Long non-coding RNA LINC00628 interacts epigenetically with the LAMA3 promoter and contributes to lung adenocarcinoma. *Mol Ther Nucleic Acids*. (2019) 18:166–82. doi: 10.1016/j.omtn.2019.08.005
59. Zhang J, Yang C, Wu C, Cui W, Wang L. DNA methyltransferases in cancer: biology, paradox, aberrations, and targeted therapy. *Cancers*. (2020) 12:2123. doi: 10.3390/cancers12082123
60. Diamantopoulou Z, Castro-Giner F, Aceto N. Circulating tumor cells: Ready for translation? *J Exp Med*. (2020) 217:e20200356. doi: 10.1084/jem.20200356
61. Ghosh P, Guo Y, Ashrafi A, Chen J, Dey S, Zhong S, et al. Oxygen-enhanced optoacoustic tomography reveals the effectiveness of targeting heme and oxidative phosphorylation at normalizing tumor vascular oxygenation. *Cancer Res*. (2020) 80:3542–55. doi: 10.1158/0008-5472.CAN-19-3247
62. Kang YT, Purcell E, Palacios-Rolston C, Lo TW, Ramnath N, Jolly S, et al. Isolation and profiling of circulating tumor-associated exosomes

using extracellular vesicular lipid-protein binding affinity based microfluidic device. *Small*. (2019) 15:e1903600. doi: 10.1002/smll.201903600

Conflict of Interest: The authors declare that the research was conducted in the absence of any commercial or financial relationships that could be construed as a potential conflict of interest.

frontiers in Oncology

ORIGINAL RESEARCH
published: 01 June 2021
doi: 10.3389/fonc.2021.648794

Correlation Analysis Between *MTHFR C677T* Polymorphism and Uterine Fibroids: A Retrospective Cohort Study

Jiahui Shen[1†], Yanhui Jiang[2†], Fengzhi Wu[1†], Hui Chen[1], Qiujing Wu[1], Xiaoxiao Zang[1], Le Chen[1], Yong Chen[2*] and Qiwen Yuan[1*]*

[1] Department of Obstetrics, The Fifth Affifiliated Hospital of Sun Yat-sen University, Zhuhai, China, [2] Department of Gynecology, The Fifth Affifiliated Hospital of Sun Yat-sen University, Zhuhai, China

OPEN ACCESS

Edited by:
Shenying Fang, University of Texas MD Anderson Cancer Center, United States

Reviewed by:
Andrea Tinelli, Moscow Institute of Physics and Technology, Russia
Renjie Wang, Fudan University, China

***Correspondence:**
Qiwen Yuan
yhj6621563@163.com
Yong Chen
cy840508@163.com
Le Chen
kenpig120608@163.com

[†]These authors have contributed equally to this work

Specialty section:
This article was submitted to Cancer Genetics, a section of the journal Frontiers in Oncology

Received: *02 January 2021*
Accepted: *28 April 2021*
Published: *01 June 2021*

Citation:
Shen J, Jiang Y, Wu F, Chen H, Wu Q, Zang X, Chen L, Chen Y and Yuan Q (2021) Correlation Analysis Between MTHFR C677T Polymorphism and Uterine Fibroids: A Retrospective Cohort Study. Front. Oncol. 11:648794. doi: 10.3389/fonc.2021.648794

Background: Uterine fibroids(UF) are the most common benign tumors in women, with high incidence and unknown causes. We aimed to explore the correlation between Methylenetetra-hydrofolate reductase (*MTHFR*) *C677T* polymorphism and UF.

Methods: This is a retrospective cohort study. Data were collected from 2411 women detected for *MTHFR C677T* polymorphism in the Fifth Affiliated Hospital of Sun Yat-sen University from 2018 to 2020. B-ultrasound (BU) and the first page of medical records were used to analyze whether they had ever been diagnosed with UF. The collected data were analyzed. Using the chi-square test and regression analysis to explore the correlation, and the risk factors was screened by multifactor logistic regression analysis.

Results: A total of 2411 pregnant women were in the *MTHFR C677T* polymorphism detection. Among them, 226(9.37%) were diagnosed as UF by BU or clinical diagnosis. The allele and genotype of *MTHFR C677T* were significantly different between the case and control group ($p<0.05$), and the distribution of the allele was following Hardy-Weinberg (H-W) equilibrium. Comparing with the wild-type (*C/C*), the mutant group (*C/T+T/T*) was more likely to form UF(OR,1.43;OR95%CI,1.07-1.89). After adjusting for confoundings, the heterozygous mutant (*C/T*) was more susceptible to UF than the wild-type (aOR,1.41; aOR95%CI,1.41-1.91). In the case group, BMI, gravidity and parity were not associated with the size and number of UF and the *MTHFR C677T* polymorphism ($p>0.05$). However, older maternal age was associated with the incidence of UF, especially the multiple UF ($p<0.05$).

Conclusion: Our results found that *MTHFR C677T* polymorphism was associated with UF occurrence for the first time. This could imply that it may increase the risk of forming UF in women of gestational age.

Keywords: uterine fibroids, UF, Methylenetetrahydrofolate reductase, MTHFR, heritability

INTRODUCTION

Uterine fibroids (UF), originating from the Smooth muscle layer of the uterus and are composed of Smooth muscle cells (SMC) and connective tissue, are the most common benign tumour in gynecology with specific hereditary characteristics (1). They are highly prevalent, the incidence is as high as 70% and more common in women of childbearing age, and most of them are asymptomatic, and the rate of malignant degeneration is low. However, it often causes abnormal uterine bleeding, secondary anemia, pelvic organ pressure, infertility and pregnancy. It may even appear during pregnancy with severe complications such as red degeneration and is one of the main diseases leading to hysterectomy (2). With the development of ultrasound technology, the incidence of UF infertile women has increased from about 35% (clinically diagnosed only) to about 50% (ultrasono-graphy) (3). Moreover, the annual treatment cost is high that imposes a considerable burden on medical resources and poses a severe threat to women's physical and mental health by the end of their reproductive years. With the opening of China's two-child policy, more attention had paid to the impact of UF on women of childbearing age (4). It has a significant impact on the preparation, process and outcome of pregnancy on women of childbearing age that increasing the incidence of adverse pregnancy outcomes and maternal mortality to a certain extent. Therefore, it is crucial to identify the risk factors for UF and long-term quality of life in young women of childbearing age.

However, the widespread prevalence of the disease and the mechanisms involved in its growth are largely unknown, leading to slow progress in developing effective treatment options (5). Most previous studies have shown that UF are related to the level of sexual arousal in women and the number of hormone receptors expressed on the myometrium's surface, but the cause and mechanism of action are still unclear that the treatment means are limited (6). Recently, an increasingly popular view suggested that UF may result from a consequence of a chronically active inflammatory immune system that secreted related inflammatory factors as mediators of sexual steroids and involved in UF's formation and proliferation fibrosis and angiogenesis (7). Therefore, It is defined by the accumulation of excess extracellular matrix (ECM) components. Its occurrence may be related to the imbalance of the inflammatory process, oxidative stress (OS), and the differential expression of various growth factors involved in angiogenesis. At the same time, hormones may promote fibroids' growth by activating fibroblasts, but the mechanism is not certain (8). Reactive oxygen species (ROS) is the main source of superoxide and subsequent oxidative stress. Folic acid (FA) is an antioxidant that can reduce the production of ROS (9). Recent studies have shown that FA supplementation can reverse the disease by reducing oxidative stress and fibrosis (10), and high homocysteine(Hcy) can up-regulate vascular endothelial growth factor(VEGF) promoting the occurrence and development of the disease.

MTHFR plays a key role in the enzymatic process in the folate metabolism pathway, and its principal function is to convert 5,10-methylenetetrahydrofolate to 5-methy- ltetrahydrofolate with biological functions, and then participate in DNA synthesis, modification and methylation (11). The *MTHFR* gene is composed of 11 exons and located on the short arm of chromosome1(1p36.3) (12). It is one of the most common mutations at position 677 in exon 4 that the cytosine (*C*) was replaced by the thymine (*T*) (13). Its 222nd amino acids in the protein alanine into valine and eventually leads to the decrease of *MTHFR* activity, the increase of Hcy level, and the decrease of DNA synthesis and methylation (14). Numerous epidemiological studies have shown that abnormal folate metabolism and high Hcy are resulting in abnormal DNA methylation, vascular endothelial cell injury and dysfunction of blood coagulation, and causing many systems many kinds of diseases, such as the tumors of gynecology, digestive system and nervous system, cardiovascular diseases and systemic diseases (15). At present, there are no relevant reports on UF and *MTHFR C677T* polymorphism, and the correlation between them remains unclear. *MTHFR C677T* polymorphism mostly leads to abnormal FA metabolism and increased Hcy level, while FA supplementation can significantly reduce the Hcy content in tissues (16). At the same time, studies have shown that UF has a specific genetic correlation (10), but there have been no reports on the *MTHFR C677T* polymorphism and UF's occurrence and development, and its effect on the occurrence and development of UF is unknown.

The authors undertook a retrospective study to analyze the correlation between *MTHFR C677T* polymorphism and UF to explore UF's pathogenesis factors and that will be a promising intervent approach for the prevention and treatment of UF.

MATERIALS AND METHODS

Patient Enrollment

This study's subjects were women aged 20-45 years of childbearing age who visited the Fifth Affiliated Hospital of Sun Yat-sen University and underwent the *MTHFR C677T* polymorphism detection between 2018 and 2020. Considering *MTHFR C677T* genotypes can differ depending on ethnicity and smoking incidence, and ethnicity or maternal smoking may be a confounding factors. Our study's ethnicity is Han, and the women with a history of smoking was excluded. The first page of the medical record and B-ultrasound system were used to screen the diagnosis of UF. Relevant data obtained through the outpatient medical record system, examination system, ultrasonic examination system, and inpatient electronic medical record system, and these data were analyzed retrospectively. Subjects were separated into the case group and the control the control group based on the diagnosis of UF.

Abbreviations: UF, Uterine fibroids; *MTHFR*, Methylenetetrahydrofolate reductase; BU, B-ultrasound; H-W, Hardy-Weinberg; SMC, Smooth muscle cells; ECM, extracellular matrix; OS, oxidative stress; ROS, Reactive oxygen species; FA, Folic acid; Hcy, homocysteine; VEGF, vascular endothelial growth factor; UNG, uracil- N-glycosylase; OR, odd rate; CI, confidence interval; PPV, positive predictive values; NPV, negative predictive values; P-ENOS, phosphorylated-endothelial nitric oxide synthase.

MTHFR A1298C and *C677T* mutations are associated with folate metabolism, however, it is common to detect *MTHFR C677T* polymorphism in our hospital. The number of cases detected by *MTHFR A1298C* polymorphism is still too small to be included in the study, so our study has not been included in the analysis.

Inclusion criteria were as follows: (1) All women are Han women, and women had detected the *MTHFR C677T* polymorphism in our hospital; (2) She had B-ultrasound examination in our hospital and indicated or not that she had uterine fibroids. (3) She had hospitalized in our hospital or another hospital for UF.

Exclusion criteria: (1) women who had the detection of the *MTHFR A1298C* polymorphism but without the detection of *MTHFR C677T* polymorphism, (2) women who had the detection of the *MTHFR C677T* polymorphism in our hospital, but they never had the B-ultrasound examination in our hospital or outside the hospital. (3) other minority women. (4) women with a history of smoking. (5) women who had the detection of the *MTHFR A1298C* polymorphism.

The Review Committee of the Fifth Affiliated Hospital of Sun Yat-sen University approved the study. Considering that our study was retrospective, no informed consent is required.

Genotyping Methods

The *MTHFR C677T* polymorphism was detected in the Molecular Biology Laboratory of the Fifth Affiliated Hospital of Sun Yat-sen University. And the PCR reaction solution of the *MTHFR C677T* Polymorphism Detection Kit contains (Wuhan Youzhiyou, China, batch number: C12Q1/68): PCR buffer, dNIPS, specific probe (*MTHFR 677C*:5'-FAM-GTGTCTGCGGGAGCCG-NFQ-MGB-3' and *MTHFR 677T*: 5'-VIC-GTGTCTGCGGGAGTCG-NFQ-MGB-3'), internal standard primers(F sequence of forward internal standard primer:5'-CGCGAACTCCGT-3' and R sequence of reverse internal standard primer:5'-CACTAGGCGCTCACTGT-3'), internal Standard Probe (ROX-5'-CACCTTCCCCATGG TGTCT-3' -BHQ2), Taq enzyme,uracil- N-glycosylase (UNG) enzyme, positive control solution (plasmid DNA mixture of *MTHFR 677C* and *MTHFR 677T*) and blank control solution (Tris-HCl buffer (10mM))

Genomic DNA Extraction from Peripheral Blood Samples: Whole anticoagulant blood of 200 μL EDTA was extracted from the subjects' peripheral veins, and genomic DNA was extracted according to the instructions of the blood genome extraction kit. Tia Namp Blood DNA Kit (DP348, Beijing Tiangen Biochemical Technology Co, Ltd.). Genomic DNA concentration was detected by Nano Drop, and the genomic DNA was stored at -80°C.

Detection of *MTHFR C677T* polymorphism(PCR fluorescence probe): the genomic DNA of the samples to be tested, the positive control and the blank control were added into the reaction tube with the PCR reaction solution at the addition amount of 2μl, and then water was added to form the reaction system of 25μL.Procedures for quantitative fluorescence PCR reaction under the real-time quantitative fluorescence PCR instrument (AB 7500): treatment at 37°C for 10min, pre-denaturation at 95°C for 5min, 40 cycles were performed according to the following procedure: 95°C for 15s, 60°C for 1min.

MTHFR genotyping: According to the amplification curve, the appropriate baseline (starting set at 3, ending set at 15) and fluorescence threshold were determined to obtain Ct values of different ROX channels after PCR amplification. Then, according to the Ct value of ROX channel, genotypes can be distinguished as follows: wild-type(*C/C*): FAM channel acuities were 36 Ct values, VIC channel Ct value >36 or without Ct value; heterozygous mutant (*C/T*): FAM channel Ct value ≤36, VIC channel Ct value ≤36; homozygous mutations (*T/T*): FAM channel Ct value > 36 or no Ct, VIC channel Ct value does not exceed 36.

UF diagnosed by BU was obtained by the BU examination system and diagnosed by the clinical obtained by the first page of our hospital's medical records. Specific clinical characteristics (such as age, height, weight, BMI, number of pregnancies, number of births, size and number of UF) were obtained by the examination system, outpatient and inpatient medical records system. And the height and weight measurements was taken by the health care provider in our hospital. Considering the age, BMI, and gestational history may have an effect on UF, so will be discrete as classification variables for analysis.

Statistical Analysis

Epidada software was used to establish a database, and statistical software SPSS 25.0 was used to analyze and process the data. The counting data were expressed by mean ± SD (Standard deviation), and the composition ratio expressed the measurement data. The allele frequencies were calculated by the gene frequency counting method, and H-W equilibrium was tested by goodness-fit chi-square test. Genotype and gene frequency were compared between the two groups by the chi-square test, and the relative risk was estimated by the odd rate (OR) value and its 95% confidence interval(CI). A bilateral p value <0.05 was considered statistically significant.

RESULTS

Study Characteristics

In this study, a total of 2411 women were detected for peripheral blood *MTHFR C677T* polymorphism and 226(9.73%) women who had been clinically and ultrasonically diagnosed with UF. The mean age when the UF was first detected was (30.9 ± 4.37) years. Relevant demographic characteristics (such as age, height, weight, BMI, parity and gravidity) and UF (size and number of fibroids) in the case and control groups were shown in **Table 1**. There were no statistically significant differences in height, weight, BMI, parity and gravidity, frequency of UF, or distribution of *MTHFR C677T* polymorphism between the case and control groups (p>0.05).In terms of age, older maternal age women were more likely to develop UF(p<0.05). The size and number of UF correlated with *MTHFR C677T* polymorphism (p<0.05).

TABLE 1 | General characteristics of study subjects.

Variable	group		P value	Genotype		P value
	Controls n=2185	Cases n=226		*C/C* n=1072	*C/T+T/T* n=1339	
Age(y,mean ± SD)	29.83 ± 4.25	32.56 ± 4.73	0.00	29.77 ± 4.36	30.34 ± 4.37	0.75
<35	1863(92.3)	156(7.7)	0.00	908(45.0)	1111(55.0)	0.25
≥35	322(82.1)	70(17.9)		164(41.8)	228(58.2)	
Height(cm,mean ± SD)	159.84 ± 5.35	159.64 ± 4.78	0.69	159.65 ± 4.87	159.96 ± 5.62	0.06
weight(kg,mean ± SD)	54.60 ± 9.20	55.45 ± 7.96	0.53	54.22 ± 8.93	55.05 ± 9.20	0.06
BMI(kg/m^2,mean ± SD)	21.41 ± 4.48	21.74 ± 2.87	0.44	21.28 ± 3.39	21.58 ± 4.99	0.07
<18.5	326(92.4)	27(7.6)	0.28	159(45.0)	194(55.0)	0.13
18.5-25	1610(90.6)	167(9.4)		804(45.2)	973(54.8)	
≥25	249(88.6)	32(11.4)		109(38.8)	172(61.2)	
Gravidity(n,mean ± SD)	1.94 ± 1.07	2.08 ± 1.23	0.27	1.92 ± 1.09	1.99 ± 1.09	0.83
1	923(90.3)	99(9.7)	0.66	471(46.1)	551(53.9)	0.17
≥2	1261(90.9)	127(9.1)		601(43.3)	787(56.7)	
Parity(n,mean ± SD)	1.43 ± 0.58	1.42 ± 0.62	0.23	1.43 ± 0.57	1.44 ± 0.59	0.40
unipara	1258(90.4)	137(9.6)	0.60	630(44.3)	792(55.7)	0.85
pluripara	900(91.0)	89(9.0)		442(44.7)	547(55.3)	
size(mm,mean ± SD)	–	–		22.12 ± 9.03	29.33 ± 10.40	0.02
number						<0.05
single	–	–		71	123	
multiple	–	–		12	20	

BMI, Body Mass Index; SD, Standard deviation.

Correlation Analysis Between UF and *MTHFR C677T* Polymorphism

The incidence of UF was 9.73%(226/2411), which was correlated with *MTHFR C677T* polymorphism (p<0.05). The allele distribution in the case group and the control group was equal to the H-W equilibrium(p>0.05). The incidence of UF for mutations group(*C/T+T/T*)(12.0%,143/1196) is higher than wild-type(*C/C*)(8.4%,83/989). Regression analysis showed that the mutant group (*C/T+T/T*) had a higher risk of UF than the wild-type group(*C/C*)(OR,1.43;OR95%CI,1.07-1.89). After adjusting for age, height, weight, BMI, parity, and gravidity, heterozygous mutant(*C/T*) incidence was still higher than wild-type(*C/C*) (aOR,1.41;aOR95%CI,1.41-1.91) (**Table 2**).

The Predictive Value of *MTHFR C677T* Polymorphism in the Diagnosis of UF

The positive predictive values(PPV) of the allele and gene mutation for UF were 10.4%[173/(1494 + 173)] and 10.7% [143/(143 + 1196)], and the negative predictive values(NPV) were 91.2% [2876/(2876 + 279)] and 93.3% [989/(989 + 83)]. The allele sensitivity was 38.3%[173/(173 + 279)], and the specificity was 65.8%[2876/(2876 + 1494)]. Mutation genotype of sensitivity was 63.3% [143/(83 + 143)], and the specificity was 45.3% [989/(989 + 1196)].

Correlation Analysis Between *MTHFR C677T* Polymorphism and the Size and Number in the Case Group

Table 3 showed that the incidence of single UF in the case group was 84.51%(191/226), and the incidence of multiple UF was 15.49%(35/226). The number of UF and the distribution difference of *MTHFR C677T* polymorphism were statistically significant (p<0.05) in the mutant group (*C/T+T/T*). The probability of occurrence of a single UF was relatively high (85.3%). However, there were no significant differences between *MTHFR C677T* polymorphism and the size distribution of UF(p>0.05).

TABLE 2 | Correlation analysis between UF and *MTHFR C677T* polymorphism.

MTHFR	Controls	Cases	χ^2 value	P value	OR95%CI	
	n	n			Unadjusted	adjusted
Allele			3.03	0.08		
C	2876	279			1	–
T	1494	173			0.84(0.69-1.02)	–
Genotype			7.25	0.03		
C/C	989	83			1	
C/T	898	113			1.50(1.11-2.02)*	1.41(1.04-1.91)*
T/T	298	30			1.20(0.78-1.86)	1.01(0.64-1.58)
C/T+T/T	1196	143	6.05	0.01	1.43(1.07-1.89)*	1.31(0.98-1.75)

**P value <0.05, the different was considered statistically significant. OR, odd rate; CI, confidence interval.*

TABLE 3 | Correlation analysis between *MTHFR C677T* polymorphism and the size and number in the case group.

	Single n (%)	Multiple n (%)	P value	OR95%CI	≤40mm n (%)	>40mm n (%)	P value	OR95%CI
MTHFR			0.04				0.54	
C/C	69(83.1)	14(16.9)		1	64(77.1)	19(22.9)		1
C/T	101(89.4)	12(10.6)		0.59(0.26-1.34)	90(79.6)	23(20.4)		0.86(0.43-0.71)
T/T	21(70.0)	9(30.0)		2.11(0.80-5.57)	26(86.7)	4(13.3)		0.52(0.16-1.67)
C/T+T/T	122(85.3)	21(14.7)	0.66	0.20(0.41-1.77)	116(81.1)	27(18.9)	0.47	0.30(0.41-1.52)

OR, odd rate; CI, confidence interval.

The Influence of Different Demographic Characteristics on the Incidence of UF in the Case Group

In the case group, the distribution between BMI, age, parity and gravidity, the size and number of UF and *MTHFR C677T* polymorphism was shown in **Table 4**. There was no correlation between them. But age was associated with the number of UF, and older maternal age were more likely to have multiple UF ($p<0.05$).

DISCUSSION

As the most common benign tumor of the female genital tract, UF seriously affects women's health. Currently, UF etiology has been reported that it is related to genetic factors, fibrosis, OS, and hormone levels. Nevertheless, the specific etiology of that is still unclear. For the first time, our study found that UF incidence was related to *MTHFR C677T* polymorphism, but was not related to the size and number of UF, which may be involved in the occurrence of UF in some way.

Previous studies have shown that the genetic alteration and epigenetic mechanism of leiomyoma are involved in UF occurrence, but the specific mechanism is unclear (1). Maekawa and Tamura et al. found the X chromosome's abnormal DNA hypomethylation in UF through whole genome DNA methylation analysis (17). Sato found that the UF samples had the hypomethylation of TSPYL2. And the expression of some genes decreased related to X chromosome inactivation (18). Their study suggests that a specific UF type may be associated with abnormal DNA hypomethylation of chromosomes. As a key enzyme in folate metabolism, *MTHFR* is involved in DNA synthesis, modification and methylation (19). The gene mutation may lead to the decrease of related to DNA methylation, which leads to related chromosomal abnormalities and contributes to UF occurrence. A retrospective study of UF showed significant genomic heterogeneity in leiomyoma lesions and identified gene mutations associated with intercellular interaction and extracellular matrix remodeling (20). However, there is no report about the relation of *MTHFR C677T* mutation and UF. Moreover, whether it involves in UF occurrence is unclear. *MTHFR* gene detection in UF samples should further explore.

Fibrosis is a pathological feature of many chronic inflammatory diseases caused by the accumulation of excessive ECM (7). The ECM of UF is mainly composed of collagen, fibronectin and proteoglycan, 50% more than the corresponding myometrium, and is generally considered as a fibrosis disease (21). An animal study showed that FA supplementation significantly reduced blood sugar levels and Hcy levels of heart tissue in mice, thereby reducing myocardial fibrosis and reversing cardiac dysfunction caused by a high-fat diet (9). Another clinical study showed a higher frequency of vitamin B_{12} and FA deficiency in patients with oral submucosal fibrosis (22). These findings suggest that low FA levels are associated

TABLE 4 | The influence of different demographic characteristics on the incidence of UF in the case group (n=226).

Variable	number		P value	size		P value	Genotype		P value
	Single n=191	Multiple n=35		≤40mm n=180	>40mm n=46		*C/C* n=83	*C/T+T/T* n=143	
Age(y)			<0.01			0.79			0.61
<35	139(89.1)	17(10.9)		125(80.1)	31(19.9)		59(37.8)	97(62.2)	
≥35	52(74.3)	18(25.7)		55(78.6)	15(21.4)		24(34.3)	46(65.7)	
BMI(kg/m^2)			0.40			0.72			0.33
<18.5	25(92.6)	2(7.4)		22(81.5)	5(18.5)		10(37.0)	17(63.0)	
18.5-25	139(83.2)	28(16.8)		131(78.4)	36(21.6)		65(38.9)	102(61.1)	
≥25	27(84.4)	5(15.6)		27(84.4)	5(15.6)		8(25.0)	24(75.0)	
parity			0.65			0.16			0.45
unipara	117(85.4)	20(14.6)		105(76.6)	32(23.4)		53(38.7)	84(61.3)	
multiple	74(83.1)	15(16.9)		75(84.3)	14(15.7)		30(33.7)	59(66.3)	
gravidity			0.22			0.05			0.20
1	87(87.9)	12(12.1)		73(73.7)	26(26.3)		41(41.4)	58(58.6)	
≥2	104(81.9)	23(18.1)		107(84.3)	20(15.7)		42(33.1)	85(66.9)	

BMI, Body Mass Index.

with fibrosis and may promote the formation of fibrosis. Recent studies have shown that ECM's deposition, cell proliferation, and angiogenesis are critical cellular events associated with leiomyoma growth (7). In this study, it found that the incidence of UF in the mutant group (*CT+TT*) was higher than that in the wild type (*C/C*), and heterozygous mutation (*C/T*) was still a risk factor for UF after the correction of mixed ligation factors. Moreover, the sensitivity of genotype mutation to the occurrence prediction of UF is as high as 63.3%. BU still has a certain rate of missed diagnosis of UF, and its combination with BU is helpful for the diagnosis of UF. But its specificity is low, easy to lead to over-examination. A multi-center randomized control analysis was still needed in clinical practice that will be our future research plan.

Previous studies showed that the overall *677T* allele frequency was 36.9% in China, which exceeds that of many other countries (23), Our study found that the ratio of heterozygous mutations (*C/T*)(1011/2411) was higher than that of homozygous mutations (*T/T*)(328/2411). As a key enzyme in folate metabolism, *MTHFR* gene mutation may reduce the activity of folate metabolizing enzymes and increase the concentration of plasma Hcy, leading to oxidative stress and promoting the deposition of extracellular matrix in fibroids. Therefore, the heterozygous mutations (*C/T*) may give the most significant phenotype. There is no relevant research, which may need to be further proved by basic experiments.

FA is an antioxidant that reduces the production of reactive oxygen species. Previous studies have shown that FA supplementation can reduce cardiac dysfunction caused by the OS during ischemia (24). Fibroid cells are characterized by a unique NOX profile, which was the primary source of superoxide and subsequent OS to promote severe prooxidant states (25). And NOX derivative of ROS is SMC proliferation, a vital part of the signal transduction pathways (8). It suggests that OS may be an essential factor in UF formation. The mutation of the *MTHFR C677T* gene leads to the disorder of folate metabolism, the decrease of antioxidant capacity, the increase of uterine related ROS, and the proliferation of uterine smooth muscle cells, thus leading to the formation of UF. Besides, this study found no statistically significant difference between *MTHFR C677T* polymorphism and the size and number of UF, which may only be involved in UF formation. Studies have shown that estrogen promotes UF proliferation by activating fibroblasts, so its size may be correlated with hormone levels (10, 26), but not with *MTHFR C677T* polymorphism. How the gene mutation regulates the signaling pathway of the OS and thus promotes UF occurrence has not been studied yet, which needs to explore later further.

Recently, some emerging ideas have suggested that UF is the result of the chronic active inflammatory immune system, and their occurrence may be related to inflammatory disorders. As mediators of sex steroids, relevant inflammatory factors are involved in the formation and proliferation of UF, fibrosis, and angiogenesis (9). Studies have shown that hyperhomocysteine unregulated the protein expression of mesenteric VEGF. Moreover, phosphorylated-endothelial nitric oxide synthase (P-ENOS) and FA treatment can reverse these effects (16). Studies have shown differential expression of various growth factors involved in angiogenesis in leiomyomas, such as VEGF, basic fibroblast growth factor, activin A and TGF-β, Etc. *MTHFR C677T* polymorphism was associated with increasing Hcy levels (8). The incidence of UF was higher in the homozygous mutation (*C/T*) (**Table 3**). Whether the *MTHFR C677T* polymorphism leads to folate metabolism disorder which in turn leads to increased Hcy levels, promotes the secretion of VEGF, and is involved in the formation of UF. A case-control study proved that eating fruits and green vegetables had a protective effect on UF occurrence (27).

Advantages and disadvantages: Our study found that *MTHFR C677T* polymorphism was associated with UF incidence for the first time and was accorded with H-W balance in the case and control groups. It causes mutations, maybe by reducing DNA methylation, promoting UF fibrosis, promote the secretion of OS and abnormal growth factor mediating the happening of the UF, and provide clues for the mechanism of UF. However, this study focused on the relationship between *MTHFR C677T* polymorphism and UF. FA, Hcy, estrogen, progesterone, and related receptors were not included in the analysis, so its promoting effect on UF occurrence could not be excluded. Meanwhile, this study's number of case groups was still small, and multi-center randomized control analysis was still needed. In the meantime, in clinical practice, the cost of detecting and obtaining mRNA gene expression value is high, and some patients cannot afford the related costs, leading to the delay of diagnosis and treatment of related diseases and adverse outcomes. The same is true for other diseases or tumors. The detecting of mRNA gene expression value has not been widely used in clinical practice.

Prior research has not yet found that the correlation of *MTHFR C677T* polymorphism and uterine fibroids. Here, we observed through PCR-RFLP that the *MTHFR C677T* polymorphism is associated with the onset of UF. A study in the future, we will further test the mutation of *MTHFR C677T* in the myometrium tissue and compare to the difference of peripheral blood and local tissue and the case and control tissue, and further explore the mechanism of *MTHFR C677T* polymorphism participate in forming UF.

In conclusion, The results show that *MTHFR C677T* polymorphism was associated with the occurrence of UF. A broader assessment of this association is necessary to provide a reference for exploring UF's pathogenesis and address additional genetic variation in FA metabolism pathways. The report suggests that using the larger study populations with prospective sampling in the future to minimize other factors' opportunities and influence on possible survival advantages.

DATA AVAILABILITY STATEMENT

The data analyzed in this study is subject to the following licenses/restrictions: The data can be made available by the

corresponding author upon reasonable request. Requests to access these datasets should be directed to Jiahui Shen,18718804918@163.com.

AUTHORS CONTRIBUTIONS

QY, JS, and YJ: Conceptualization, Methodology, Software. FW, YC, and HC: Data curation, Writing-Original draft preparation. JS, LC, and YC: Visualization, Investigation. QY and XZ: Supervision. HC, LC, and XZ: Software, Validation: QY, JS, and YJ: Writing-Reviewing and Editing. The United laboratory of SYSU The Fifth Affiliated Hospital-BGI provides the Detection Report of *MTHFR C677T* polymorphism and database. All authors contributed to the article and approved the submitted version.

ACKNOWLEDGMENTS

The detection of *MTHFR C677T* polymorphism is a cooperation between the Fifth Affiliated Hospital of Sun Yat-sen University (SYSU) and Beijing Genomics institution (BGI). This institution has reached an agreement with the United laboratory of SYSU The Fifth Affiliated Hospital-BGI, and the *MTHFR C677T*gene detection has become one of the examination items in our antenatal clinic.

REFERENCES

1. Islam MS, Protic O, Giannubilo SR, Toti P, Tranquilli AL, Petraglia F, et al. Uterine Leiomyoma: Available Medical Treatments and Newpossibletherapeutic Options. *J Clin Endocrinol Metab* (2013) 98(3):921–34. doi: 10.1210/jc.2012-3237
2. Commandeur AE, Styer AK, Teixeira JM. Epidemiological and Genetic Clues for Molecular Mechanisms Involved in Uterine Leiomyoma Development and Growth. *Hum Reprod Update* (2015) 21(5):593–615. doi: 10.1093/humupd/dmv030
3. Manta L, Suciu N, Toader O, Purcărea RM, Constantin A, Popa F. The Etiopathogenesis of Uterine Fibromatosis. *J Med Life* (2016) 9(1):39–45. Available at: https://medandlife.org/all-issues/2016/issue-1-2016/article/the-etiopathogenesis-of-uterine-fibromatosis/.
4. Cardozo ER, Clark AD, Banks NK, Henne MB, Stegmann BJ, Segars JH. Theestimated Annual Cost of Uterine Leiomyomata in the United States. *Am J Obstet Gynecol* (2012) 206(3):211.e1–9. doi: 10.1016/j. ajog.2011.12.002
5. Downes E, Sikirica V, Gilabert-Estelles J, Bolge SC, Dodd SL, Maroulis C, et al. The Burden of Uterine Fibroids in Five European Countries. *Eur J Obstet Gynecol Reprod Biol* (2010) 152:96–102. doi: 10.1016/j.ejogrb.2010.05.012
6. Rafnar T, Gunnarsson B, Stefansson OA, Sulem P, Ingason A, Frigge ML, et al. Variants Associating With Uterine Leiomyoma Highlight Genetic Background Shared by Various Cancers and Hormone-Related Traits. *Nat Commun* (2018) 9(1):3636. doi: 10.1038/s41467-018-05428-6
7. Islam MS, Akhtar MM, Ciavattini A, Giannubilo SR, Protic O, Janjusevic M, et al. Use of Dietary Phytochemicals to Target Inflammation, Fibrosis, Proliferation, and Angiogenesis in Uterine Tissues: Promising Options for Prevention and Treatment of Uterine Fibroids? *Mol Nutr Food Res* (2014) 58 (8):1667–84. doi: 10.1002/mnfr.201400134
8. Mesquita FS, Dyer SN, Heinrich DA, Bulun SE, Marsh EE, Nowak RA. Reactive Oxygen Species Mediate Mitogenic Growth Factor Signaling Pathways in Humanleiomyoma Smooth Muscle Cells. *Biol Reprod* (2010) 82(2):341–51. doi: 10.1095/biolreprod.108.075887
9. Wang YP, Wu YC, Cheng SJ, Chen HM, Sun A, Chang JY. High Frequencies Ofvitamin B12 and Folic Acid Deficiencies and Gastric Parietal Cell Antibody Positivity in Oral Submucous Fibrosis Patients. *J Formos Med Assoc* (2015) 114(9):813–9. doi: 10.1016/j.jfma.2015.05.011
10. Reis FM, Bloise E, Ortiga-Carvalho TM. Hormones and Pathogenesis of Uterine Fibroids. *BestPract Res Clin Obstet Gynaecol* (2016) 34:13–24. doi: 10.1016/j.bpobgyn.2015.11.015
11. Coppede F, Stoccoro A, Tannorella P, Gallo R, Nicoli V, Migliore L. Association of Polymor-phisms in Genes Involved in One-Carbon MetabolismwithMTHFRMethylation Levels. *Int J Mol Sci* (2019) 20 (15):3754. doi: 10.3390/ijms20153754
12. Goyette P, Pai A, Milos R, Frosst P, Tran P, Chen Z, et al. Genestructure of Human and Mouse Methylenetetrahydrofolate Reductase (MTHFR). *Mamm Genome* (1998) 9(8):652–6. doi: 10.1007/s003359900838
13. Gong M, Dong W, He T, Shi Z, Huang G, Ren R, et al. Mthfr 677c > T Polymorphism Increases the Male Infertility Risk: A Metaanalysis Involving 26 Studies. *PloS One* (2015) 10(3):e0121147. doi: 10.1371/journal.pone.0121147
14. Steluti J, Carvalho AM, Carioca AAF, Miranda A, Gattas GJF, Fisberg RM, et al. Genetic Variants Involved in One-Carbon Metabolism: Polymorphism Frequencies and Differences in Homocysteine Concentrations in Thefolic Acid Fortification Era. *Nutrients* (2017) 9(6):539. doi: 10.3390/nu9060539
15. McNulty H, Strain JJ, Hughes CF, Ward M. Riboflavin, MTHFR Genotype and Blood Pressure: A Personalized Approach to Prevention and Treatment of Hypertension. *Mol Aspects Med* (2017) 53:2–9. doi: 10.1016/j.mam.2016.10.002
16. Ho HL, Tsai MH, Hsieh YH, Huo TI, Chang CC, Lee FY, et al. Folic Acid Ameliorates Homocysteine-Induced Angiogenesis and Porto-Systemic Collaterals in Cirrhotic Rats. *Ann Hepatol* (2019) 18(4):633–9. doi: 10.1016/j.aohep.2018.12.008
17. Maekawa R, Tamura I, Shinagawa M, Mihara Y, Sato S, Okada M, et al. Genome-Wide DNA Methylation Analysis Revealed stableDNA Methylation Status During Decidualization in Human Endometrial Stromalcells. *BMC Genomics* (2019) 20(1):324. doi: 10.1186/s12864-019-5695-0
18. Sato S, Maekawa R, Yamagata Y, Asada H, Tamura I, Lee L, et al. Potential Mechanisms of Aberrant DNA Hypomethylation on the X-Chromosome in Uterine Leiomyomas. *J Reprod Dev* (2014) 60(1):47–54. doi: 10.1262/jrd.2013-095
19. Hiraoka M, Kagawa Y. Genetic Polymorphisms and Folate Status. *CongenitAnom (Kyoto)* (2017) 57(5):142–9. doi: 10.1111/cga.12232
20. Yatsenko SA, Mittal P, Wood-Trageser MA, Jones MW, Surti U, Edwards RP, et al. Highly Heterogeneous Genomic Landscape of Uterineleiomyomas By Whole Exome Sequencing and Genome-Wide Arrays. *Fertil Steril* (2017) 107 (2):457–466.e9. doi: 10.1016/j.fertnstert.2016.10.035
21. Fujita M. Histological and Biochemical Studies of Collagen in Human Uterineleiomyomas. *Hokkaido Igaku Zasshi* (1985) 60(4):602–15.
22. Mahamid M, Mahroum N, Bragazzi NL, Shalaata K, Yavne Y, Adawi M, et al. Folate and B12 Levels Correlate With Histological Severity Innashpatients. *Nutrients* (2018) 10(4):440. doi: 10.3390/nu10040440
23. ALFRED. *The ALlele Frequency Database.* Available at: http://alfred.med.yale.edu/alfred/SiteTable1A_working.asp?siteuid=SI001032G (Accessed onApril 26, 2015).
24. Li W, Tang R, Ouyang S, Ma F, Liu Z, Wu J. Folic Acid Prevents Cardiac Dysfunction and Reduces Myocardial Fibrosis in a Mouse Model of High-Fat-Diet-Induced Obesity. *Nutr Metab (Lond)* (2017) 14:68. doi: 10.1186/s12986-017-0224-0
25. Fletcher NM, Saed MG, Abuanzeh S, Abu-Soud HM, Al-Hendy A, Diamond MP, et al. Nicotinamide Adenine Dinucleotide Phosphate Oxidase is Differentially Regulated in Normal Myometrium Versus Leiomyoma. *Reprod Sci* (2014) 21(9):1145–52. doi: 10.1177/1933719114522552
26. Luo N, Guan Q, Zheng L, Qu X, Dai H, Cheng Z. Estrogen-Mediated Activation of Fibroblasts and its Effects on the Fibroid Cell Proliferation. *Transl Res* (2014) 163(3):232–41. doi: 10.1016/j.trsl.2013.11.008
27. Parazzini F, Di Martino M, Candiani M, Viganò P. Dietary Components and Uterine Leiomyomas: A Review of Published Data. *Nutr Cancer* (2015) 67 (4):569–79. doi: 10.1080/01635581.2015.1015746

Conflict of Interest: The authors declare that the research was conducted in the absence of any commercial or financial relationships that could be construed as a potential conflict of interest.

Advantages of publishing in Frontiers

OPEN ACCESS
Articles are free to read for greatest visibility and readership

FAST PUBLICATION
Around 90 days from submission to decision

HIGH QUALITY PEER-REVIEW
Rigorous, collaborative, and constructive peer-review

TRANSPARENT PEER-REVIEW
Editors and reviewers acknowledged by name on published articles

Frontiers
Avenue du Tribunal-Fédéral 34
1005 Lausanne | Switzerland

Visit us: www.frontiersin.org
Contact us: frontiersin.org/about/contact

REPRODUCIBILITY OF RESEARCH
Support open data and methods to enhance research reproducibility

DIGITAL PUBLISHING
Articles designed for optimal readership across devices

FOLLOW US
@frontiersin

IMPACT METRICS
Advanced article metrics track visibility across digital media

EXTENSIVE PROMOTION
Marketing and promotion of impactful research

LOOP RESEARCH NETWORK
Our network increases your article's readership